

The identification of *Panicum miliaceum* in archaeology:
A molecular, isotopic, and experimental investigation

Edward Alexander Standall

PhD in Archaeology

University of York
Department of Archaeology

August 2021

Abstract

The investigation of broomcorn millet (*Panicum miliaceum*) is an enticing subject of archaeological research that has garnered greater interest in recent years. The cereal was domesticated in Northeast China and translocated across varied environments and among diverse cultures and communities of Northern Eurasia during prehistory. Theoretical discussions have examined the potential motives, methods, and significance of its translocation and use, yet few archaeological studies have attempted to investigate and understand the role of *P. miliaceum* among past populations. An emergent method of investigation utilises molecular and isotopic techniques to analyse archaeological food residues and understand the role and significance of *P. miliaceum* in culinary contexts. However, neither the accuracy, reliability, nor interpretive potential of this method has been assessed, despite widespread application to new archaeological contexts and research questions.

This thesis presents the first in-depth molecular and isotopic investigation of organic residues comprising *P. miliaceum*. The analysis of reference, experimental, and archaeological materials provides an opportunity to assess and refine criteria used in the identification and interpretation of archaeological residues comprising *P. miliaceum*. Furthermore, application of refined criteria, to archaeological materials, enables a greater understanding of the uses and significance of *P. miliaceum* to past populations.

The analysis of reference materials assesses the accuracy and reliability of molecular analysis, while experiments demonstrate the extent to which *P. miliaceum* may be recognised by molecular and isotopic analysis of food residues. Intensive analysis of archaeological foodcrusts and ceramic-absorbed residues from Bruszczewo, Poland, provides an opportunity to comprehensively understand evidence for *P. miliaceum* processing at one site. Finally, the analysis of ceramic-absorbed residues from 12 sites in Northern Greece and Bulgaria provides an opportunity to conduct a spatiotemporal investigation of *P. miliaceum* introduction and use, across a broad region, that is integrated with established ceramic studies.

Contents

List of Figures	7
List of Tables	14
Acknowledgements	16
Declaration	18
Chapter 1: Introduction	19
The investigation of <i>P. miliaceum</i> in archaeology	19
The investigation of <i>P. miliaceum</i> by organic residue analysis	20
Expansion of ORA to detect <i>P. miliaceum</i>	21
Research aims and objectives	21
Thesis structure	23
Chapter 2: Organic residues and isotopes	25
Natural abundance of lipids and isotopes	25
Lipids	25
Isotopes	26
ORA: residue formation, alteration, degradation and contamination	31
Formation	31
Alteration	33
Degradation	34
Contamination	35
SIA: material formation, alteration, degradation and contamination	36
Formation	36
Alteration	38
Preservation	38
Contamination	39
Extraction and analysis	40
ORA	40
Bulk isotopes	41
GC-MS	42
IRMS	43
The detection of plant and animal product processing in archaeological residues	43
Plant products	43
Animal products	58
Compound specific carbon isotope mixing models	62
Conclusion	63
Chapter 3: The domestication and translocation of <i>Panicum miliaceum</i> in Northern Eurasia	65
Introduction	65
What is a millet?	65

Identification of <i>P. miliaceum</i> and <i>S. italica</i>	66
Macro remains	66
Micro remains	69
Molecular and isotopic analysis	69
Domestication of <i>P. miliaceum</i> in China	70
Why move starchy cereals?	74
<i>P. miliaceum</i> in Central and West Asia	77
<i>P. miliaceum</i> in Europe	80
Contentious early European evidence	81
Earliest evidence for <i>P. miliaceum</i> in Europe	83
The dispersal of <i>P. miliaceum</i> in Europe	90
Assessing and improving the detection of <i>P. miliaceum</i>	91
Conclusion	92
Chapter 4: Miliacin and Millets	94
Introduction	94
Miliacin standard experiment results	95
Discussion	98
Assessing the natural abundance of triterpenes in millets	100
Analysis	102
Results	102
Discussion	111
Conclusion	116
Chapter 5: Experiments investigating the molecular and isotopic composition of <i>P. miliaceum</i> residues	118
Introduction	118
Understanding ceramic absorption of miliacin	118
Understanding the bulk and compound-specific carbon isotope composition of <i>P. miliaceum</i> residues	119
Experimental research questions	120
Experimental method	120
Experimental ingredients and materials	123
Bulk isotope analysis results	125
Formulating bulk $\delta^{13}\text{C}$, $\delta^{15}\text{N}$, and C/N values from cooking liquid samples	125
Unmixed ingredient experiments	127
Beef and wheat experiments	129
Millet and beef experiments	130
Wheat and millet experiments	131
Discussion of bulk isotope data	132
Ceramic-absorbed residue results and discussion	136
Unmixed ingredient experiments	136
Wheat and millet experiments	138

Beef and wheat experiments _____	138
Millet and beef experiments _____	138
Discussion of ceramic-absorbed residue data _____	139
Conclusion _____	141
<i>Chapter 6: ORA investigations at Bruszczewo _____</i>	<i>144</i>
Introduction _____	144
Research questions _____	144
Site location and regional context _____	145
Chronology of Bruszczewo _____	145
EBA site layout and function _____	147
LBA/EIA site layout and function _____	149
The ceramic assemblages _____	150
The faunal assemblage _____	154
The archaeobotanical assemblage _____	156
Evidence for <i>P. miliaceum</i> in Poland _____	157
Sampling strategy _____	161
Results _____	161
Bulk isotope analysis _____	161
Molecular analysis _____	165
GC-C-IRMS _____	175
Discussion and conclusion _____	184
<i>Chapter 7: ORA investigations in North Greece and Bulgaria _____</i>	<i>189</i>
Introduction _____	189
Evidence for <i>P. miliaceum</i> in Northern Greece _____	190
Evidence for <i>P. miliaceum</i> in Bulgaria _____	194
The archaeological sites _____	196
Lete I (Central Macedonia, Greece) _____	196
Dikili Tash (East Macedonia, Greece) _____	197
Archondiko (West Macedonia, Greece) _____	198
Angelochori (West Macedonia, Greece) _____	199
Olympus sites: Valtos-Leptokarya, Trimpina, Pigi Artemidos and Rema Xydias (Northern Greece) _____	200
Petko Karavelovo (North Bulgaria) _____	200
Avren (North East Bulgaria) _____	201
Sokol (Central Bulgaria) _____	201
Chokoba (Central Bulgaria) _____	201
Sampling and ORA strategy _____	201
Results and discussion _____	202
Lipid recovery rates and yields _____	202
Contamination _____	204
Lete I _____	207

Dikili Tash _____	208
Archondiko _____	210
Angelochori _____	215
Olympus _____	221
Petko Karavelovo _____	223
Avren and Sokol _____	225
Chokoba _____	226
Summary and discussion of <i>P. miliaceum</i> in SE Europe _____	228
Conclusion _____	233
Chapter 8: Conclusion _____	235
Research aims and objectives _____	235
Revised identification criteria _____	235
Archaeological research outcomes _____	237
Suggestions for future research _____	238
Reference materials and experiments _____	238
Archaeological investigations _____	238
New methods of identifying <i>P. miliaceum</i> residues _____	240
Microscopy _____	240
Pyrolysis _____	241
Proteomics _____	241
Final statement _____	242
References _____	244
Appendix One: Methods _____	283
Cleaning _____	283
Sampling _____	283
Ceramics _____	283
Foodcrusts _____	283
Millets _____	283
Cooking liquids _____	284
Lipid Extraction _____	284
Acid methanol _____	284
Solvent _____	284
Bulk Isotope Sample Preparation _____	285
Analysis _____	285
EA-IRMS _____	285
Gas Chromatography - Mass Spectrometry _____	285
Gas Chromatography - Combustion - Isotope Ratio Mass Spectrometry _____	286
Appendix Two: Triterpene Identification (Chapter 4) _____	288
Appendix Three: Bruszczewo Dataset (Chapter 6) _____	293
Appendix Four: Greece and Bulgaria Dataset (Chapter 7) _____	300
Appendix Five: Modern Reference and Mixing Model Data _____	312

List of Figures

Figure 1. Example skeletal structure of an alkylresorcinol (AR23). _____	46
Figure 2. Example skeletal structure of (n) 17-Dotriacontanol. _____	48
Figure 3. Skeletal structure of miliacin. _____	49
Figure 4. Skeletal structure of palmitone. _____	53
Figure 5. Skeletal structure of dehydroabietic acid (left), 7-oxodehydroabietic acid (middle), and retene (right), detailing degradation from abietic acid in Pinaceae resins. _	57
Figure 6. Skeletal structure of 4,8,12-TMTD (top), pristanic (middle), and phytanic (bottom) acids. _____	59
Figure 7. Microscope image in plan of <i>Setaria italica</i> (A) and <i>Panicum miliaceum</i> (B). ____	67
Figure 8. Spatiotemporal distribution of 184 directly dated millet remains from Central and East Asia organised by region, in addition to sites presenting early microbotanical evidence for <i>P. miliaceum</i> , including: 1 Nanzhuangtou, 2 Donghulin, 3 Cishan, 4 Xinglonggou, 5 Yuezhuang, 6 Zhuzhai, 7 Xiaohu, 8 Tianshanbeilu. A Topographical location. B Longitudinal distribution of median dates (Leipe et al. 2019 2). _____	71
Figure 9. Distribution of human isotope studies demonstrating the spread and extent of millet consumption across Central and East Asia in the second millennium BCE. The figure indicates that many Central Asian communities did not consume significant quantities of <i>P. miliaceum</i> , even a thousand years after its introduction, although limited evidence could also reflect the limitations of isotope analysis in identifying C ₄ cereal consumption (Wang et al. 2017 1029). _____	73
Figure 10. Sample location of all directly dated early European millet caryopses, including those discussed in this thesis; 1 Vynohradyni Sad (3275 ±35), 2 Fajsz (3214 ±36), 3 Lavagnone (3208 ±26), 4 Lipnik (3040 ±35), 5 Lutomiersk-Koziówki (2810 ±35), 6 Assiros Toumba (3071 ±12), 7 Cornești (3087 ±22) (Filipovic et al. 2020 3). _____	81
Figure 11. Chronological division at 100 year intervals of the earliest directly dated European millet caryopses. Symbol size corresponds to the relative probability that a sample is of the stated interval (Filipovic et al. 2020 7). _____	82
Figure 12. Human bulk isotope values of individuals from the Great Hungarian Plain (Gamarra et al. 2018 11). _____	86
Figure 13. Bulk isotope data of humans from Northern Italy and Croatia. Blue and orange points represent EBA and MBA/LBA individuals respectively. Data obtained from Varalli et al. (2016a, 2016b); Tafuri et al. (2018); Masotti et al. (2019). _____	89
Figure 14. Partial TIC of an AM-extracted miliacin standard heated at 70°C for, A two, B four, C six, and D eight, hours. Peak II is miliacin $\Delta^{18(19)}$ and peaks I $\Delta^{13(18)}$ and III $\Delta^{12(13)}$ are alteration products produced during acid isomerisation. Peaks marked with a star are internal n-alkane standards C ₃₄ and C ₃₆ respectively. _____	96
Figure 15. Skeletal structure of miliacin, olean-18-en-3 β -ol methyl ether (left). Skeletal structure demonstrating a double bond migration, from $\Delta^{18(19)}$ to $\Delta^{13(18)}$ and $\Delta^{12(13)}$, that occurs during thermally-assisted acid isomerisation of miliacin (right). _____	97
Figure 16. Mass spectra of peaks I, II and III from Figure 15, representing $\Delta^{13(18)}$, $\Delta^{18(19)}$ and $\Delta^{12(13)}$ -oleanenes discussed in this section. _____	97

Figure 17. The relative abundance of miliacin (yellow), δ -amyrin ME (green), and β -amyrin ME (blue), in AM extracted samples of a miliacin standard heated for two, four, six and eight hours. Crosses of corresponding colours represent the average relative abundance of these compounds in archaeological samples subjected to the standard four-hour method.	98
Figure 18. Partial TIC of the AM (top) and solvent (bottom) extracts of <i>D. sanguinalis</i> . Numerals relate to compounds listed in the text and Appendix 2 and the star indicates a C ₃₆ alkane standard.	104
Figure 19. Partial TIC of the AM (top) and solvent (bottom) extracts of <i>D. exilis</i> . Numerals relate to compounds listed in the text and Appendix 2 and the star indicates a C ₃₆ alkane standard.	105
Figure 20. Partial TIC of the AM (top) and solvent (bottom) extracts of <i>P. sonorum</i> . Numerals relate to compounds listed in the text and Appendix 2 and the star indicates a C ₃₆ alkane standard.	107
Figure 21. Partial TIC of the AM (top) and solvent (bottom) extracts of <i>P. sumatrense</i> . Numerals relate to compounds listed in the text and Appendix 2 and the star indicates a C ₃₆ alkane standard.	108
Figure 22. Partial TIC of the AM (top) and solvent (bottom) extracts of <i>Echinochloa colona</i> (<i>E. Frumentacea</i> dom.). Numerals relate to compounds listed in the text and Appendix 2.	109
Figure 23. Partial TIC of the AM (top) and solvent (bottom) extracts of <i>Sorghum bicolor</i> r. <i>durra</i> . Numerals relate to compounds listed in the text and Appendix 2 and the star indicates a C ₃₆ alkane standard.	111
Figure 24. Demonstration of the equipment setup used during this experiment. A pilot experiment with 500 mL of water proved to be insufficient for one hour of cooking. Therefore, 900 mL of water was used in the actual experiments.	121
Figure 25. Photograph demonstrating the separation of lower and upper layers and fatty cap layer in freeze dried liquid samples. In this sample, the fatty cap has fallen to the bottom of the vial (bottom right of the image).	123
Figure 26. Example of the briquettes used in these experiments.	124
Figure 27. Bulk $\delta^{13}\text{C}$ and $\delta^{15}\text{N}$ values of beef (circles), wheat (squares), and millet (triangles). Open shapes represent liquid samples obtained during cooking. Filled shapes are values of each ingredient when raw.	128
Figure 28. Bulk $\delta^{15}\text{N}$ (left) and $\delta^{13}\text{C}$ (right) values of liquid samples obtained from cooking beef (circles), wheat (squares) and millet (triangles).	128
Figure 29. Bulk $\delta^{15}\text{N}$ (left) and $\delta^{13}\text{C}$ (right) values of liquid samples obtained from cooking beef + wheat. The solid, dashed, and dotted lines represent, B75+W25, B50+W50 and B25+W75 respectively.	129
Figure 30. Bulk $\delta^{15}\text{N}$ (left) and $\delta^{13}\text{C}$ (right) values of liquid samples obtained from cooking millet + beef. The solid, dashed, and dotted lines represent, M75+B25, M50+B50, and M25+B75 respectively.	131
Figure 31. Bulk $\delta^{15}\text{N}$ (left) and $\delta^{13}\text{C}$ (right) values of liquid samples obtained from cooking wheat + millet. The solid, dashed, and dotted lines represent, W75+M25, W50+M50, and W25+M75 respectively.	132

Figure 32. Bulk $\delta^{15}\text{N}$ (left) and $\delta^{13}\text{C}$ (right) values of liquid samples obtained from cooking beef + wheat (black), millet + beef (green), and wheat + millet (orange). The solid, dashed, and dotted lines represent, a75+b25, a50+b50, and a25+b75 respectively, with a and b representing the first and second ingredient respectively. _____	133
Figure 33. Bulk $\delta^{15}\text{N}$ and $\delta^{13}\text{C}$ values of liquid samples obtained from cooking beef + wheat (black), millet + beef (green), and wheat + millet (orange), plotted with 1σ confidence ellipses. Points annotated with B, W, and M mark the average values of unmixed beef, wheat, and millet cooking liquid samples respectively. _____	134
Figure 34. Bulk $\delta^{15}\text{N}$ and C/N values of liquid samples obtained from cooking beef + wheat (black), millet + beef (green), and wheat + millet (orange). Points annotated with B, W, and M mark the average values of unmixed beef, wheat, and millet cooking liquid samples respectively. _____	134
Figure 35. EBA sites in the Kościan region. 1 Osieczna-Kleszczewo, 2 Granowo-Granowo, 3 Granowo-Granowko, 4 Szcodrowo, 5 Kościan-Kokorzyn, 6 Naclaw, 7 Prysieka Polska, 8 Stare Bojanowo, 9 Prysieka Stara, 10 Kamieniec-Plastowo, 11 Kościan, 12 Kamieniec-Parzezewo, 13 Grodzisk Wielkopolski, 14 Włoozakowice, 15 Czempin, 16 Piotrkowice, 17 Przemęt-Starkowo, 18 Steszew, 19 Krzywín-Nowy Dwór. Filled black square (fortified settlement) is Bruszczewo (Müller and Kneisel 2010 761). _____	146
Figure 36. Summed probability plot of EBA (n= 112) and LBA/EIA (n= 3) radiocarbon dates. Two dates from LBA/EIA contexts overlap with the Hallstatt plateau, a flattening-out of the calibration curve, providing broad, low probability, and ultimately useless dates for the end of Lusatian Culture occupation (Czebreszuk et al. 2015b 40). _____	147
Figure 37. Bruszczewo site plans. A Trench 30, 31, and 52, from which material was analysed, are highlighted within black boxes. B House structures highlighted (Müller and Kneisel 2010 753, 761). _____	148
Figure 38. Representative developmental phases of Únětice Culture ceramics at Bruszczewo (Müller and Kneisel 2010 777). _____	151
Figure 39. Sherd F3102ID4632 (Br 114) with millet caryopsis impressions scattered randomly across the internal surface. _____	153
Figure 40. Sherd F3102ID4632 (Br 114) with millet caryopsis impressions in the area under the vessel wall. _____	154
Figure 41. Areas of Bruszczewo examined during assessment of the faunal assemblage, including the central mineralised zone, around central area, fortifications, and peat north and south areas (Makowiecki 2015 55). _____	155
Figure 42. Bulk isotope data of humans from Poland. Blue and orange points represent pre-MBA and MBA/LBA individuals respectively. Data obtained from: Pokoutta and Howcroft (2015); Pokoutta et al. (2015); Mnich et al. (2020); Pospieszny et al. (2021). _____	160
Figure 43. Bulk $\delta^{13}\text{C}$ and $\delta^{15}\text{N}$ values of all charred crusts from Bruszczewo. _____	162
Figure 44. $\delta^{15}\text{N}$ against C:N ratios of the complete Bruszczewo dataset. A significant, moderately negative, relationship exists between $\delta^{15}\text{N}$ and C:N values of EBA samples ($r(27) = .46, p < .02$) but the relationship between $\delta^{15}\text{N}$ and C:N values of LBA/EIA samples is not significant ($r(25) = .35, p > .05$). _____	163
Figure 45. $\delta^{13}\text{C}$ and $\delta^{15}\text{N}$ values of the complete EBA and LBA/EIA Bruszczewo dataset plotted against reference ellipses (1σ) of cooking mixtures outlined in Chapter 5. _____	164

Figure 46. Partial TIC of sample Br 104 I, highlighting the contribution of Pinaceae resin degradation products. IS = Internal Standard. _____	168
Figure 47. Partial TIC of Br 005 F highlighting the relative abundance of phytosterols. IS = Internal Standard. _____	169
Figure 48. P:S plotted against E:H ratios of EBA (black) and LBA/EIA (green) charred crusts (left) and ceramics (right). _____	171
Figure 49. $\delta^{13}\text{C}$ and $\delta^{15}\text{N}$ values of the complete Bruszczewo dataset plotted against reference ellipses (1σ) of cooking mixtures outlined in Chapter 5. EBA + and LBA + samples were analysed by GC-MS. M = miliacin present. _____	172
Figure 50. Partial Extracted Ion Chromatograms (EICs) of m/z 189 from the same vessel demonstrate the absence of miliacin in the crust. Br109 F (charred crust, top) and Br 109 I (absorbed residue, bottom). _____	174
Figure 51. Plot of $\delta^{13}\text{C}_{16:0}$ and $\delta^{13}\text{C}_{18:0}$ values from EBA samples against reference ellipses (1σ) of, Left domesticated and Right wild animals. D = dairy, P = porcine, Pl = C ₃ plant, R = ruminant, WN-R = wild non-ruminant, WR = wild ruminant. Circles and diamonds represent ceramic and charred crust samples respectively. Reference data is presented in Appendix 5. _____	177
Figure 52. Plot of $\delta^{13}\text{C}_{16:0}$ and $\delta^{13}\text{C}_{18:0}$ values from EBA samples against ellipses (1σ) of Polish Neolithic CP = Cooking pots and S = sieves (Salque et al. 2013). _____	177
Figure 53. Plot of $\delta^{13}\text{C}_{16:0}$ and $\delta^{13}\text{C}_{18:0}$ values (Left) and plot of $\delta^{13}\text{C}_{16:0}$ and $\Delta^{13}\text{C}$ ($\delta^{13}\text{C}_{18:0} - \delta^{13}\text{C}_{16:0}$) values (Right). Filled and open shapes represent ceramic and charred crust samples respectively. _____	179
Figure 54. E/H values plotted against $\delta^{13}\text{C}$ values of C _{16:0} from EBA (black) and LBA/EIA (green) charred crusts. _____	179
Figure 55. Plot of $\delta^{13}\text{C}_{16:0}$ and $\delta^{13}\text{C}_{18:0}$ values from LBA/EIA samples from Bruszczewo (green) and Vix-Mont Lassois (red, Rageot et al. 2019a). Circles and triangles represent ceramic and charred crust samples respectively. Shapes with a fill contain miliacin. ____	181
Figure 56. Left Plot of $\delta^{13}\text{C}_{16:0}$ and $\delta^{13}\text{C}_{18:0}$ values from LBA/EIA samples against reference ellipses (1σ) and theoretical mixing lines of modern-carbon corrected foodstuffs. Right Plot of $\delta^{13}\text{C}_{16:0}$ and $\Delta^{13}\text{C}$ ($\delta^{13}\text{C}_{18:0} - \delta^{13}\text{C}_{16:0}$) values from LBA/EIA samples against theoretical mixing lines of modern-carbon corrected foodstuffs. D = dairy, P = porcine, Pl = C ₃ plant, R = ruminant, M = P. miliaceum. Shapes with a fill contain miliacin. Reference data and mixing model presented in Appendix 5. _____	182
Figure 57. Bulk isotope data of Neolithic humans from northern Greece. Blue and orange points represent coastal and inland individuals respectively (Data from Papathanasiou 2003; Triantaphyllou 2015). _____	191
Figure 58. Bulk isotope data of EBA and MBA humans from northern Greece. Blue and orange points represent coastal and inland individuals respectively (Data from Vika 2011; Triantaphyllou et al. 2008; Nitsch et al. 2017). _____	192
Figure 59. Bulk isotope data of LBA humans from northern Greece. Blue and orange points represent coastal and inland individuals respectively (Data from Petroutsas et al. 2009; Petroutsas and Manolis 2010; Triantaphyllou 2015). _____	194
Figure 60. Map of sites examined in this chapter. 1 Olympus sites, 2 Angelochori, 3 Archondiko, 4 Lete I, 5 Dikili Tash, 6 Chokoba, 7 Petko Karavelovo, 8 Sokol, 9 Avren. ____	197

Figure 61. Mass spectra comparison between compound identified as octocrylene in archaeological samples (top) and octocrylene in the NIST 17 MSD (bottom). _____ 205

Figure 62. Compound specific carbon isotope data from Lete I (orange circles) and Lete III (grey dots, Whelton et al. 2018). Left: Plot of $\delta^{13}\text{C}_{16:0}$ and $\delta^{13}\text{C}_{18:0}$ values against reference ellipses (1σ) of modern-carbon corrected foodstuffs. D = dairy, P = porcine, PI = C3 plant, R = domesticated ruminant adipose, M = P. miliaceum. Reference data is presented in Appendix 5. Right: Plot of $\delta^{13}\text{C}_{16:0}$ and $\Delta^{13}\text{C}$ ($\delta^{13}\text{C}_{18:0} - \delta^{13}\text{C}_{16:0}$) values. _____ 208

Figure 63. Compound specific carbon isotope data from Dikili Tash (blue circles) and Neolithic sites in Northern Greece (grey dots, Whelton et al. 2018). Left: Plot of $\delta^{13}\text{C}_{16:0}$ and $\delta^{13}\text{C}_{18:0}$ values against reference ellipses (1σ) of modern-carbon corrected foodstuffs. D = dairy, P = porcine, PI = C3 plant, R = domesticated ruminant adipose, M = P. miliaceum. Reference data is presented in Appendix 5. Right: Plot of $\delta^{13}\text{C}_{16:0}$ and $\Delta^{13}\text{C}$ ($\delta^{13}\text{C}_{18:0} - \delta^{13}\text{C}_{16:0}$) values. _____ 209

Figure 64. Partial TIC of Ar 14 demonstrating high long chain alkane abundance and plasticiser contamination (). _____ 210

Figure 65. Partial TIC (top) and m/z 189 EIC (bottom) of Ar 16, demonstrating the three distinct AM alteration products of miliacin. 1 δ -Amyrin ME, 2 Miliacin, 3 β -Amyrin ME. 211

Figure 66. Compound specific carbon isotope data from Archondiko. Filled circle represents sample Ar 16 that contains miliacin. Left: Plot of $\delta^{13}\text{C}_{16:0}$ and $\delta^{13}\text{C}_{18:0}$ values against reference ellipses (1σ) of modern-carbon corrected foodstuffs. D = dairy, P = porcine, PI = C3 plant, R = domesticated ruminant adipose, M = P. miliaceum. Reference data is presented in Appendix 5. Right: Plot of $\delta^{13}\text{C}_{16:0}$ and $\Delta^{13}\text{C}$ ($\delta^{13}\text{C}_{18:0} - \delta^{13}\text{C}_{16:0}$) values. _____ 213

Figure 67. Plot of $\delta^{13}\text{C}_{16:0}$ and $\Delta^{13}\text{C}$ ($\delta^{13}\text{C}_{18:0} - \delta^{13}\text{C}_{16:0}$) values of samples from Archondiko against theoretical mixing lines of modern-carbon corrected foodstuffs, at 10% increments, including P. miliaceum mixed with C₃-fed porcine, domesticated ruminant adipose, and dairy products. Filled circle represents sample Ar 16 that contains miliacin. Reference and mixing model data are presented in Appendix 5. _____ 213

Figure 68. Plot of $\delta^{13}\text{C}_{16:0}$ and $\Delta^{13}\text{C}$ ($\delta^{13}\text{C}_{18:0} - \delta^{13}\text{C}_{16:0}$) values of samples from Archondiko highlighting the difference between houses. Yellow = House B, Blue = House E, Black = House Z, and Red = House Σ T. _____ 215

Figure 69. Partial TIC of Ang 14 SE demonstrating the extent of lipid preservation. _____ 216

Figure 70. Partial TIC of Ang 1 AE highlighting abundant long chain fatty acids, indicative of beeswax and miliacin. _____ 216

Figure 71. Partial TIC of Ang 1 SE highlighting the presence of compounds derived from beeswax. _____ 217

Figure 72. Compound specific carbon isotope data from Angelochori. Filled circles represent samples that contain miliacin. Left: $\delta^{13}\text{C}_{16:0}$ and $\delta^{13}\text{C}_{18:0}$ values plotted against 1σ reference ellipses of modern-carbon corrected foodstuffs. P = porcine, PI = C₃ plants, R = domestic ruminant adipose, D = dairy and M = P. miliaceum. Right: $\delta^{13}\text{C}_{16:0}$ and $\Delta^{13}\text{C}$ ($\delta^{13}\text{C}_{18:0} - \delta^{13}\text{C}_{16:0}$) values. Reference data is presented in Appendix 5. _____ 218

Figure 73. Compound specific isotope data from Angelochori highlighting difference between houses. Yellow = House A and Blue = House D. Filled diamonds contain miliacin. Left: $\delta^{13}\text{C}_{16:0}$ and $\delta^{13}\text{C}_{18:0}$ values. Right: $\delta^{13}\text{C}_{16:0}$ and $\Delta^{13}\text{C}$ ($\delta^{13}\text{C}_{18:0} - \delta^{13}\text{C}_{16:0}$) values. _____ 219

- Figure 74. Reconstruction diagram of a pyraunos vessel (Deliopoulos 2007, See Valamoti 2016 55). _____ 221
- Figure 75. Compound specific isotope data from Olympus. Left: $\delta^{13}\text{C}_{16:0}$ and $\delta^{13}\text{C}_{18:0}$ values plotted against 1σ reference ellipses of modern-carbon corrected foodstuffs. P = porcine, PI = C_3 plants, R = domestic ruminant adipose, D = dairy, and M = P. miliaceum. Right: $\delta^{13}\text{C}_{16:0}$ and $\Delta^{13}\text{C}$ ($\delta^{13}\text{C}_{18:0} - \delta^{13}\text{C}_{16:0}$) values. Reference data is presented in Appendix 5. 223
- Figure 76. Compound specific isotope data from Petko Karavelovo. Left: $\delta^{13}\text{C}_{16:0}$ and $\delta^{13}\text{C}_{18:0}$ values plotted against 1σ reference ellipses of modern-carbon corrected foodstuffs. P = porcine, PI = C_3 plants, R = domestic ruminant adipose, D = dairy, and M = P. miliaceum. Right: $\delta^{13}\text{C}_{16:0}$ and $\Delta^{13}\text{C}$ ($\delta^{13}\text{C}_{18:0} - \delta^{13}\text{C}_{16:0}$) values. Reference data is presented in Appendix 5. _____ 224
- Figure 77. Partial TIC of PK 3 AE highlighting abundant compounds indicative of plant products. _____ 224
- Figure 78. Compound specific isotope data from Avren (pink circles) and Sokol (black circles). Left: $\delta^{13}\text{C}_{16:0}$ and $\delta^{13}\text{C}_{18:0}$ values plotted against 1σ reference ellipses of modern-carbon corrected foodstuffs. P = porcine, PI = C_3 plants, R = domestic ruminant adipose, D = dairy, and M = P. miliaceum. Right: $\delta^{13}\text{C}_{16:0}$ and $\Delta^{13}\text{C}$ ($\delta^{13}\text{C}_{18:0} - \delta^{13}\text{C}_{16:0}$) values. Reference data is presented in Appendix 5. _____ 225
- Figure 79. Compound specific isotope data from Chokoba. Left: $\delta^{13}\text{C}_{16:0}$ and $\delta^{13}\text{C}_{18:0}$ values plotted against 1σ reference ellipses of modern-carbon corrected foodstuffs. P = porcine, PI = C_3 plants, R = domestic ruminant adipose, D = dairy, and M = P. miliaceum. Right: $\delta^{13}\text{C}_{16:0}$ and $\Delta^{13}\text{C}$ ($\delta^{13}\text{C}_{18:0} - \delta^{13}\text{C}_{16:0}$) values. Reference data is presented in Appendix 5. 227
- Figure 80. Plots of Left: $\delta^{13}\text{C}_{16:0}$ and $\delta^{13}\text{C}_{18:0}$ values and Right: $\delta^{13}\text{C}_{16:0}$ and $\Delta^{13}\text{C}$ ($\delta^{13}\text{C}_{18:0} - \delta^{13}\text{C}_{16:0}$) values of samples, from Chokoba, against 1σ reference ellipses and theoretical mixing lines of modern-carbon corrected foodstuffs, at 10% increments, of P = porcine, R = domestic ruminant adipose, D = dairy, with M = P. miliaceum. PI = C_3 plants. Reference and mixing model data are presented in Appendix 5. _____ 227
- Figure 81. Plots of Left $\delta^{13}\text{C}_{16:0}$ and $\delta^{13}\text{C}_{18:0}$ values and Right $\delta^{13}\text{C}_{16:0}$ and $\Delta^{13}\text{C}$ ($\delta^{13}\text{C}_{18:0} - \delta^{13}\text{C}_{16:0}$) values of samples from Neolithic Greece and Chalcolithic Bulgaria. Orange = Lete I, blue = Dikili Tash, green = Petko Karavelovo, and pink = Avren. _____ 229
- Figure 82. Human bulk isotope values of individuals from E-MBA (green) and LBA (red) Greece, demonstrating no ^{13}C enrichment in the E-MBA and substantial enrichment ($\delta^{13}\text{C}$ values $> -18\text{‰}$) in several LBA individuals. _____ 230
- Figure 83. Plots of Left $\delta^{13}\text{C}_{16:0}$ and $\delta^{13}\text{C}_{18:0}$ values and Right $\delta^{13}\text{C}_{16:0}$ and $\Delta^{13}\text{C}$ ($\delta^{13}\text{C}_{18:0} - \delta^{13}\text{C}_{16:0}$) values of samples from LBA Greece and Bulgaria. Black = Angelochori, yellow = Olympus, and blue = Chokoba. Filled circles contain miliacin. _____ 232

Appendix Two

- Figure A2. 1. Mass spectra and identified/proposed structure of compounds observed in solvent and acid methanol extracts of millets discussed in Chapter 4. I δ -amyrin ME, II miliacin, III β -amyrin ME, IV δ -amyrin, V germanicol. _____ 288

Figure A2. 2. Mass spectra and identified/proposed structure of compounds observed in solvent and acid methanol extracts of millets discussed in Chapter 4. VI β -amyrin, VII β -amyrin, VIII compound unknown, IX germanicol TMS, X δ -amyrin acetate?. _____289

Figure A2. 3. Mass spectra and identified/proposed structure of compounds observed in solvent and acid methanol extracts of millets discussed in Chapter 4. XI β -amyrin acetate?, XII β -amyrin acetate?, XIII sawamilletin, XIV compound unknown, XV compound unknown. _____290

Figure A2. 4. Mass spectra and identified/proposed structure of compounds observed in solvent and acid methanol extracts of millets discussed in Chapter 4. XVI compound unknown, XVII compound unknown, XVIII lupeol acetate, XIX friedelin. _____291

Figure A2. 5. Mass spectra and identified/proposed structure of compounds observed in solvent and acid methanol extracts of millets discussed in Chapter 4. XX bauerenol ME and XXI compound unknown. _____292

List of Tables

Table 1. Reference collection list of millet species analysed. _____	102
Table 2. The abundance ($\mu\text{g g}^{-1}$) of miliacin (II), δ -amyrin ME (I), β -amyrin ME (III), δ -amyrin (IV), germanicol (V), and β -amyrin (VI), in each species analysed in this study that produces miliacin. Values are primarily from AM extracts, data from solvent extracts are denoted by ^{SE} and * represents an average value published by Bossard et al. (2013). __	103
Table 3. Mixture combinations and sampling times used during cooking experiments. _____	123
Table 4. Average bulk $\delta^{13}\text{C}$ (corrected) and $\delta^{15}\text{N}$ values of ingredients used in the cooking experiment. _____	125
Table 5. Table of $\delta^{13}\text{C}$ values of CL samples from each experiment. Values represent an average of non-fat layers. Values with * incorporate a 2.5% contribution of the $\delta^{13}\text{C}$ value from the fatty cap to account for separation during storage ($(0.02564 * \delta^{13}\text{C}_{\text{fatty-cap}}) + ((\text{average } \delta^{13}\text{C} \text{ of non-fat layers}))$). This equates to a 2.4999% contribution of carbon from the fatty cap. _____	126
Table 6. Table of $\delta^{15}\text{N}$ values of liquid samples from each experiment. Values are an average of lower layers. Values in red are derived from samples that contained an average nitrogen content < 1%. _____	126
Table 7. Table of C/N values of liquid samples from each experiment. Values represent an average of non-fat layers. Values with * incorporate a 2.5% contribution of the C% value from the fatty cap, to account for separation during storage. A contribution of N% values from the fatty cap samples were not included as they contained < 1% nitrogen and produced a broad range of $\delta^{15}\text{N}$ values (> 15‰), indicating that they are not accurate. Values in red are derived from samples that contained an average nitrogen content < 1%. _____	127
Table 8. TLE yield of ceramic absorbed residues $\mu\text{g g}^{-1}$. _____	137
Table 9. Miliacin yield of ceramic absorbed residues ng g^{-1} . _____	137
Table 10. Summary of the most abundant archaeobotanical remains from Bruszczewo ordered by Horizon and two LBA/EIA features (Kroll 2010). _____	157
Table 11. Summary of $\delta^{13}\text{C}$ and $\delta^{15}\text{N}$ values of the complete Bruszczewo dataset. _____	162
Table 12. Number of samples analysed by GC-MS from each trench. _____	165
Table 13. TLE yield summary of ceramic samples from Bruszczewo. _____	166
Table 14. TLE yield summary of charred crusts from Bruszczewo. _____	166
Table 15. Contribution of Pinaceae biomarker compounds to ceramic TLE. _____	168
Table 16. Mean and range of E/H C ₁₈ APAA isomer values from Bruszczewo samples. _	171
Table 17. Mean, standard deviation and range of miliacin content in LBA/EIA samples presented as percentage of TLE. _____	172
Table 18. Miliacin contribution (sum of δ -amyrin ME, miliacin, and β -amyrin), bulk and compound specific $\delta^{13}\text{C}$ values of LBA/EIA charred crusts. _____	173
Table 19. Summary of compound specific $\delta^{13}\text{C}$ values from EBA and LBA/EIA ceramics analysed in this study and by Heron et al. (2016). _____	175
Table 20. Summary of compound specific $\delta^{13}\text{C}$ values from EBA and LBA/EIA charred crusts analysed in this study and by Heron et al. (2016). _____	175

Table 21. Percentage contribution of miliacin (sum of δ -amyrin ME, miliacin, and β -amyrin) to the TLE of ceramic samples subjected to compound specific isotope analysis.	180
Table 22. Summary of Greek and Bulgarian sites and ceramic samples discussed in this chapter.	196
Table 23. Vessel types analysed from Greek and Bulgarian sites studied in this chapter.	202
Table 24. Number of samples that produced appreciable lipid yields, by AM and solvent extraction, in addition to number of AM extracts comprising sufficient quantities of palmitic and stearic acid for GC-C-IRMS analysis.	203
Table 25. Acid methanol extraction yield and summarised compound specific carbon isotope values of material presented in this chapter.	204

Appendix Three

Table A3. 1. Contextual information for samples from Bruszczewo.	293
Table A3. 1. Continued.	294
Table A3. 2. Details of ceramic sherds sampled from Bruszczewo.	295
Table A3. 2. Continued.	296
Table A3. 3. TLE yield and compound identification of samples from Bruszczewo.	297
Table A3. 3. Continued.	298
Table A3. 4. List of compound specific carbon and bulk carbon and nitrogen isotope values of all samples from Bruszczewo analysed in this study.	299

Appendix Four

Table A4. 1. Bulgarian sherd type and contextual information.	300
Table A4. 2. Greek sherd type and contextual information.	301
Table A4. 2. Continued.	302
Table A4. 2. Continued.	303
Table A4. 3. TLE yield and compound identification of AM extracts from Bulgarian samples.	304
Table A4. 4. TLE yield and compound identification of AM extracts from Greek samples.	305
Table A4. 4. Continued.	306
Table A4. 4. Continued.	307
Table A4. 4. Continued.	308
Table A4. 5. TLE yield and compound identification of solvent extracts from Greek samples.	309
Table A4. 6. Compound specific carbon isotope values of Bulgarian samples.	310
Table A4. 7. Compound specific carbon isotope values of Greek samples.	311

Appendix Five

Table A5. 1. Modern reference $\delta^{13}\text{C}_{16}$ and $\delta^{13}\text{C}_{18}$ values.	312
Table A5. 2. Theoretical mixing model data of <i>P. miliaceum</i> (millet) with average DRA, DRM, and DP $\delta^{13}\text{C}_{16}$ and $\delta^{13}\text{C}_{18}$ values (Table A5. 1.).	317

Acknowledgements

This thesis is the culmination of almost four years of research, during which the trials and tribulations of academia and life have been compounded by a global pandemic. This work would not have been possible without the help, support, contributions, and dedication of a great many people, some of whom I know and others that do not. Herein, I name the people who have been most influential in my work, yet I am also grateful for the efforts of everyone that made this research, and life in general, possible over these turbulent years.

Firstly, I wish to thank Carl Heron, who provided me with the opportunity to undertake this project in the Scientific Research department at the British Museum. The experiences that I have had and knowledge that I have gained from yourself and colleagues in the department has been exceptional. Thank you for always being approachable and offering considered advice. Secondly, I wish to thank Oliver Craig, who has been an excellent supervisor ever since I undertook my MSc at The University of York many years ago. The hard work, dedication, and openness of the organic residue team at York is a reflection on yourself and has been an exceptional example. I thank you both for the opportunities that you have provided, constant support and direction that you have given, and patience that you have shown over the past four years as my supervisors.

This research was made possible as the result of funding by the Wellcome Trust Grant Number 097365/Z/11/Z. Thank you to everyone involved for your dedication in funding, conducting, and promoting research.

I am extremely grateful for the generosity of Dorian Fuller, of UCL, in providing access to the expansive archaeobotanical reference collection that he has spent many years developing. The investigation of millets has become a passion of mine and I hope to work with you again in the future.

I am happy to have worked with and visited Jutta Kneisel, of University of Kiel, Germany, and grateful that I have been able to access and sample outstanding material from Bruszczewo. Thanks also go to everyone else involved in the excavation and investigation of this site, I have thoroughly enjoyed reading all of your reports. I hope you will appreciate the addition of my research to yours when we publish these results.

I am also happy to have worked with and visited Sultana Valamoti and Anastasia Dimoula, of Aristotle University of Thessaloniki, and grateful that I have been able to conduct research as part of the Plant Cult project (ERC Grant Agreement No 682529). Thanks also go to everyone else involved in this project and the investigation of all the sites that have been examined. The material and results have been better than I could have hoped for and I look forward to publishing them with you in the future.

Thank you Sushma Jansari and Andrew Shapland of the British Museum for providing access to the exceptional collections under your care. Working with you both, no matter how brief, was a great experience.

Thank you Steve Wood, of Doves Farm, for your generosity in providing a large sample of emmer wheat free of charge and without being asked.

I would like to thank Helen Talbot, Alexandre Lucquin, Matthew von Tersch, and Chris Mussell for your efforts in maintaining the laboratories at the British Museum and University of York. The equipment may have failed me, but you never did. In addition, thank you for running samples when I could not and giving advice whenever I asked.

Throughout the journey of this PhD I have had the pleasure of meeting and working with great people who helped me develop as a researcher and a person. Thank you Blandine Courel, Kate Fulcher, Akshyeta Suryanarayan and Adrià Breu Barcons for sharing your exceptional knowledge and being great friends. In addition, thank you Antony Simpson for the conversations that helped the days pass a little quicker and all my friends and colleagues at the British Museum and University of York that have made my life better and research easier with their support and friendship.

Finally, I would like to thank members of my family for their unwavering support and encouragement. Thank you, Hollie Standall for being a wonderful sister who has offered great support and advice on all things. Thank you, Bryan Standall for being a brilliant father who has always offered encouragement, support, and asked questions that have made me think. Last but certainly not least, thank you Angela Standall for being an excellent mother, who gave me my passion for food, has always supported me in my work, and helped me through difficult times. I would not have achieved all that I have achieved if it was not for you three. I am eternally grateful.

Declaration

I declare that this thesis is a presentation of original work and I am the sole author. This work has not previously been presented for an award at this, or any other, University. All sources are acknowledged as References.

Chapter 1: Introduction

The investigation of *P. miliaceum* in archaeology

Broomcorn millet (*Panicum miliaceum*) is an uncommon cereal in present-day Europe. Traditionally associated with lower socioeconomic status, *P. miliaceum* has been replaced over the past two centuries, in European cuisine, by new cereals, such as maize (*Zea mays*) (Boutard 2012 11; Jaybhaye *et al.* 2014; Sõukand *et al.* 2015). In 2019 production of *P. miliaceum* in Europe was < 0.1% of total cereal output (FAOSTAT 2019). The rarity of *P. miliaceum* in subsistence strategies and culinary mindsets of present-day Europeans provides an explanation as to why the cereal has, until recently, been subject to limited archaeological investigation and discussion in the region. As such, the significance of this species is poorly understood and often underappreciated. However, interest in *P. miliaceum* has increased substantially in the past decade.

P. miliaceum was independently domesticated in NE China, ca. 6000 BCE, where it played a pivotal role in the establishment of large-scale, complex societies (Zhao 2011; Wang *et al.* 2017; Leipe *et al.* 2019). It was rapidly translocated beyond China, in the third and second millennia BCE, and disrupted the agropastoral systems of Eurasia (Frachetti *et al.* 2010; Valamoti 2016; Kaptcia and Mueller-Bieniek 2019; Mueller-Bieniek *et al.* 2019; Filipovic *et al.* 2020). Researchers have begun to demonstrate the prevalence and abundance of *P. miliaceum* in prehistoric European contexts (Gyulai 2014; Valamoti 2016), prompting reconsideration and refinement of translocation chronologies, via direct radiocarbon dating programmes (Motuzaitė-Motuzėviciute *et al.* 2013; Filipovic *et al.* 2020). Isotopic analyses have increasingly been applied to the identification and investigation of *P. miliaceum* consumption, as the cereal is a C₄ plant and, therefore, isotopically distinct from many other foodstuffs in Northern Eurasia (Lightfoot *et al.* 2013; Wang *et al.* 2017; Hermes *et al.* 2019). In addition, considerable theoretical debate has focused on the economic, social, and cultural significance of this crop to past populations. These discussions have primarily examined the motives for translocating *P. miliaceum* among communities that already possessed starchy cereals (Jones *et al.* 2011; Boivin *et al.* 2012; Lightfoot *et al.* 2013). However, few archaeological investigations have attempted to explore the social and cultural significance of *P. miliaceum*. Indeed, one may

question whether these factors may be explored by either archaeobotanical or isotopic analyses alone.

The investigation of *P. miliaceum* by organic residue analysis

An emergent method of investigating both the presence and significance of *P. miliaceum*, in archaeological material, is organic residue analysis (ORA). The social and cultural significance of foodstuffs may be understood from their use in culinary contexts, e.g. when processed in ceramic vessels, as choices made in the selection, preparation, and consumption of foods are outward displays of individual, social, and cultural identity (Samuel 1996). The inclusion and exclusion of specific products in individual meals, subsistence strategies, and ceremonial activities, may be identified by the analysis of ceramic-absorbed organic residues (Roffet-Salque *et al.* 2017a). Subsequently, patterns of product use may be directly associated with material culture, enabling intricate inference of significance, by integrating organic residue data with established ceramic studies.

Miliacin (olean-18-en-3 β -ol methyl ether) is a pentacyclic triterpene methyl ether (PTME) compound observed at a high abundance in *P. miliaceum* caryopses (Bossard *et al.* 2013). The compound has been employed as a sedimentary biomarker for *P. miliaceum* in restricted archaeological contexts, as production of miliacin is not limited to this species (Jacob *et al.* 2005; Bossard *et al.* 2013). Developing on the use of miliacin as a sedimentary biomarker (Jacob *et al.* 2008a), Heron *et al.* (2016) successfully demonstrated the mobilisation and absorption of miliacin, from caryopsis to ceramic fabric, when boiling *P. miliaceum* caryopses in experimental ceramic vessels. This observation subsequently enabled the identification of *P. miliaceum* in archaeological organic residues, extracted from charred 'foodcrusts' and ceramics, by ORA (Heron *et al.* 2016). Criteria employed by Heron *et al.* (2016) in the identification of *P. miliaceum* residues include:

1. The identification of miliacin in either charred crust or ceramic-absorbed residues
2. The observation of ^{13}C enrichment in bulk carbon isotope values of charred crusts
3. The observation of ^{13}C enrichment in compound specific carbon isotope values of palmitic and stearic acids from charred crust and ceramic-absorbed residues

Expansion of ORA to detect *P. miliaceum*

Following the publication of Heron *et al.* (2016), researchers have attempted to characterise *P. miliaceum* residues in new archaeological contexts and sought to answer novel research questions (e.g. Rageot *et al.* 2019a and Junno *et al.* 2020). However, these studies have exclusively utilised the presence of miliacin to characterise *P. miliaceum* residues. Furthermore, researchers have neither investigated nor developed the accuracy and reliability of either molecular or isotopic identification criteria when applied to different regions and novel research questions. Critical assessment of previously published studies, which is developed in later chapters, provides an opportunity to highlight and contextualise research aims and objectives addressed during this thesis.

Junno *et al.* (2020), Chakraborty *et al.* (2020), and Suryanarayan *et al.* (2021) utilised the detection of miliacin to determine the processing of *P. miliaceum* in Japan and India, yet the production of this compound, by other plant species, has not been investigated in either region. Therefore, without the analysis of local reference materials, the potential exists for false positive identification of the cereal.

Ganzarolli *et al.* (2018) noted a high concentration of miliacin in one ceramic-absorbed residue, relative to 26 others containing miliacin, from Padova, Italy. However, there is no explanation for this difference, as neither the development nor preservation of *P. miliaceum* residues has been investigated by experiments.

Rageot *et al.* (2019a) employed molecular and isotopic analysis in the characterisation of ceramic-absorbed residues from Vix-Mont Lassois, France. While miliacin was identified in several samples, none demonstrated compound specific carbon isotope enrichment, presenting conflicting evidence for the processing of *P. miliaceum*. This observation raises questions as to the accuracy, reliability, and interpretive potential of molecular and isotopic criteria used in the identification and interpretation of *P. miliaceum* residues.

Research aims and objectives

It is imperative that the criteria employed in the identification of *P. miliaceum* residues are evaluated and tested before they are applied to additional archaeological contexts, as there is significant potential for misinterpretation. The primary aim of this

thesis is to address three issues regarding the identification and characterisation of *P. miliaceum* residues outlined in the previous section. These include to:

1. Understand the presence, absence, and abundance of miliacin in commonly exploited plant species.
2. Understand ceramic absorption of miliacin.
3. Understand the bulk and compound-specific carbon isotope composition of *P. miliaceum* residues.

Comprehensive analysis of reference materials and undertaking of thorough experiments are necessary objectives to achieve these aims.

The secondary aim of this thesis is to demonstrate and test the application and usefulness of enhanced identification criteria in the characterisation and understanding of archaeological residues derived from *P. miliaceum*. This aim is achieved by the completion of two objectives:

1. To assess and develop previous identification and characterisation of charred foodcrusts from Bruszczewo, Poland, undertaken by Heron *et al.* (2016). This will be achieved by increased sampling of foodcrusts, in addition to large-scale sampling, for the first time, of ceramic-absorbed residues.
2. To detect and examine the introduction and exploitation of *P. miliaceum* in Northern Greece and Bulgaria by conducting ORA on ceramic-absorbed residues from 12 Neolithic-Bronze Age sites.

In completing these aims and objectives, this thesis will improve the reliability of ORA in identifying *P. miliaceum* residues and further elucidating its role and significance to past populations. Subsequently, future researchers will be able to confidently apply the methods and criteria developed in this thesis to explore and answer novel research questions.

Thesis structure

This thesis commences with a detailed introduction to organic residue and isotope analysis, outlining the basic principles of each technique and presenting methods and criteria used in the identification of plant and animal products relevant to this thesis (Chapter 2). Subsequently, Chapter 3 provides a comprehensive review of the material theme of this thesis, *P. miliaceum*. In this chapter, *P. miliaceum* is defined and methods of identification, in archaeological contexts, are presented, followed by a detailed summary of domestication and translocation, between China and Europe, up to the Late Bronze Age.

The following four chapters present original research conducted during this project. Each chapter has its own aims and objectives that are outlined and discussed in full before commencing with the next chapter. The first two of these chapters present experimental research that is subsequently applied to the following two chapters examining archaeological material.

Chapter 4 begins by examining the effect that ORA extraction methodologies have on the integrity of miliacin and the impact that isomerisation of the biomarker may have on archaeological investigations. The chapter then examines the extent of miliacin production, and composition of the PTME fraction, in 20 species of millet, by employing two different ORA extraction methodologies. Therefore, this chapter addresses the first aim of this thesis.

Chapter 5 presents a series of experiments designed to examine the effect that cooking *P. miliaceum*, with beef and wheat, has on the development of ceramic-absorbed and foodcrust residues over time. Ceramic absorption of miliacin and the carbon isotope composition of residues are investigated by molecular and bulk isotopic techniques, addressing the second and third aims of this thesis.

Chapter 6 presents ORA investigations at Bruszczewo. The chapter begins by posing five methodological and site-specific research questions, that test and develop on the identification of *P. miliaceum* by Heron *et al.* (2016) and further explore culinary practices at the site. The archaeological context of the site is then presented, followed by an overview of evidence for *P. miliaceum* in Poland. This is followed by a presentation of

results, with close integration of experimental data from Chapter 5, and a discussion focused on research questions posed at the start of the chapter.

Chapter 7 presents a broad spatiotemporal investigation of organic residues from 12 Neolithic, Chalcolithic, Early and Late Bronze Age sites in Northern Greece and Bulgaria. An overview of evidence for *P. miliaceum* in the region is detailed before brief background information is presented for each site. A site by site presentation of results is given, followed by a discussion of results in the context of the entire region.

Chapter 8 concludes this thesis by summarising the primary research aims and objectives of this study. New, refined criteria for the investigation of *P. miliaceum* are presented, drawing on the main research achievements of this study. Subsequently, the main archaeological research outcomes are summarised. This is followed by ten suggestions for future reference, experimental, and archaeological research that will improve the identification and interpretation of archaeological *P. miliaceum* residues and further elucidate the uses and significance of this species in the past. Chapter 8 concludes by examining several novel methods of identifying *P. miliaceum*, which may prove useful and be applied to archaeological contexts in the future, followed by a final statement on the investigation of *P. miliaceum* by ORA.

Chapter 2: Organic residues and isotopes

This chapter begins by outlining the principles of ORA and stable isotope analysis (SIA). The formation, alteration, degradation, and contamination of archaeological materials, to which ORA and SIA are applied, are discussed, followed by a summary of sample preparation and analytical methods used in the analysis of different materials. These methods are assessed for their usefulness in identifying different and specific foodstuffs. This chapter concludes with a detailed summary of the criteria employed in the identification of different plant and animal products by ORA and SIA. Greater emphasis is placed on the discussion of materials, methods, and products that are analysed, used, and identified, in this thesis. In addition, the discussion of *P. miliaceum* develops on previous archaeological investigations by incorporating research beyond the field of archaeology, with the aim of improving understanding in the subsequent reference material study.

Natural abundance of lipids and isotopes

Lipids

A variety of organic compounds are preserved in archaeological materials, including proteins, carbohydrates, and lipids (Evershed 1993; Hendy *et al.* 2018). Molecular investigations in ORA are focused on the identification of lipids, primarily due to their abundance in living organism and greater survival potential (Evershed 1993; Evershed 2008a). Lipids predominantly comprise carbon, hydrogen and oxygen, and to a lesser extent phosphorus, nitrogen and sulphur (Evershed 1993). They are generally hydrophobic and soluble in organic solvents (Fahy *et al.* 2005); characteristics that are crucial to the success of ORA.

The exploitation of lipid-rich organic products by humans results in a significant transference of lipids to archaeological materials and contexts. Characteristic lipids include acylglycerols, fatty acids, alkanes and alkenes, alcohols, ketones, wax esters, sterols, and terpenes, that are produced by living organisms, anthropogenic alteration processes, and degradation (Evershed 2008b; Roffet-Salque *et al.* 2017a). Some lipids, such as fatty acids, are ubiquitous, yet others are produced by either a narrower range of organisms or processes, enabling more precise and detailed interpretation. Indeed, lipids

may be restricted to either species, genera, or families. These limited compounds are classified as biomarkers, although their specificity and utility often rely on archaeological and geographical constraints, as many spatiotemporally separated species produce the same compound, e.g. miliacin (Bossard *et al.* 2013). Biomarkers have also been identified for specific alteration and degradation processes of specific compounds, although distinction between anthropogenic and natural activity may be difficult to determine, e.g. dehydroabiatic acid and 7-oxodehydroabiatic acid from degraded Pinaceae resin (Connan and Nissenbaum 2003). It is important to note that ubiquitous lipids, specifically fatty acids, are not without utility in determining biological origin, as their isotopic composition is somewhat distinctive, enabling broad characterisation of archaeological residues.

Isotopes

An isotope is an atomic variant of an element containing a fixed number of protons and a variable number of neutrons. They may be either stable, radioactive, or radiogenic and occur naturally within the environment, with stable isotopes persisting and radioactive isotopes decaying over time. The range and abundance of stable isotopes of each element varies, with atmospheric carbon comprising approximately 98.9% ^{12}C and 1.1% ^{13}C and nitrogen comprising approximately 99.6% ^{14}N and 0.4% ^{15}N (O'Leary 1988; De Laeter *et al.* 2003). An increase in the number of neutrons present within an isotope results in increased atomic mass, imparting different physical properties. Isotopic fractionation occurs due to two sets of physical effects, kinetic and thermodynamic, both of which relate to limiting factors imparted by the physical interaction of lighter and heavier isotopes. Thermodynamic effects are distinguished from kinetic effects as they do not relate to the formation or breaking of bonds, e.g. diffusion (Meier-Augenstein 2002).

Before discussing the natural abundance and fractionation of isotopes further, it is important to outline the method by which isotope measurements are made and reported. Using carbon as an example, the ^{13}C content of a sample is determined as a ratio of the heavier to lighter isotope:

$$R = {}^{13}\text{C}/{}^{12}\text{C}$$

In natural materials R is approximately 0.0112, with only the last digit varying (O'Leary 1988). In order to improve accuracy, compensate for fluctuation of isotopic

abundance over time, and variance between instruments, the ratio of a sample is reported, relative to a standard, as δ values (Meier-Augenstein 1999). The current standard is the Vienna Pee Dee Belemnite (VPDB) (Coplen 1995).

$$\delta^{13}\text{C} = 1000(R_{\text{Sample}} - R_{\text{Standard}})/R_{\text{Standard}}$$

As R values are small, $\delta^{13}\text{C}$ values are reported 'per mil' (‰) for convenience and to better reflect variation in the relative abundance of isotopes between samples. Samples with high $\delta^{13}\text{C}$ values are enriched in ^{13}C compared to samples with low $\delta^{13}\text{C}$ values, which are depleted in ^{13}C . These calculations may be applied to isotopes of other elements by substituting the heavier and lighter isotopes and standard.

Carbon Isotope Fractionation

The carbon isotope composition of an organism reflects its primary carbon source, metabolic pathways, and the environmental conditions in which it developed (Regert 2011). A significant difference is observed in $\delta^{13}\text{C}$ values of primary carbon sources, enabling the distinction between isotopically different products, e.g. marine products in a terrestrial environment (Meier-Augenstein 1999).

Atmospheric CO_2 has a $\delta^{13}\text{C}$ value of approximately -8‰ (Keeling *et al.* 1989). Terrestrial plants source carbon from atmospheric CO_2 but produce lower $\delta^{13}\text{C}$ values due to discrimination against the heavier ^{13}C isotope that forms stronger bonds and is slower to diffuse than the lighter ^{12}C isotope (O'Leary 1988). The degree of discrimination is primarily influenced by the photosynthetic pathway employed by a plant. Most plants, including wheat, rice, barley, and oats, employ the Calvin-Benson cycle photosynthetic pathway, producing a C_3 3-phosphoglycerate (3-PGA), that is commonly referred to as the C_3 pathway. This method is relatively inefficient and highly discriminatory against ^{13}C , producing $\delta^{13}\text{C}$ values between -35‰ and -21‰ (Tieszen 1991; Ripley *et al.* 2007). A substantial number of plants, including millets, maize, sorghum, and sugarcane, employ the Hatch-Slack photosynthetic pathway, producing a C_4 carboxylic acid, that is commonly referred to as the C_4 pathway. This method utilises carbon concentration mechanisms, making the process more efficient, and produces $\delta^{13}\text{C}$ values between -16‰ and -9‰ (Tieszen 1991; Ripley *et al.* 2007). Aquatic plants predominantly employ C_3

photosynthesis, yet $\delta^{13}\text{C}$ values exhibit a large range, between -39‰ and -11‰, due to differences in carbon source (O'Leary 1988; Farquhar *et al.* 1989). For instance, marine plants sourcing carbon from dissolved bicarbonate have $\delta^{13}\text{C}$ values around -20‰ (DeNiro 1987).

Various physiological and environmental factors, including temperature, water, and light exposure, further influence the fractionation of carbon isotopes within plants, thus explaining the range of $\delta^{13}\text{C}$ values within each photosynthetic pathway (O'Leary 1988; Farquhar *et al.* 1989; Meier-Augenstein 1999; Ripley *et al.* 2007; Wallace *et al.* 2013; An *et al.* 2015; Wallace *et al.* 2015). Furthermore, $\delta^{13}\text{C}$ values among a single species, grown under controlled conditions, may vary up to 3‰ (Tieszen 1991), and those grown in a single field further still (O'Leary 1988; Heaton *et al.* 2009). The $\delta^{13}\text{C}$ value of wheat caryopses, from the same plant, may demonstrate up to 0.6‰ and 0.7‰ variation within and between ears respectively. Variation in $\delta^{13}\text{C}$ values between grains in a spikelet is minimal, but greatest between the first and last grains of an ear, indicating that variation is the result of a change in growing conditions and carbon source throughout ear formation. During periods of stress, plants may prioritise caryopsis growth and utilise earlier assimilated carbon, explaining variation within an ear as grains develop at different times (Heaton *et al.* 2009).

Compounds within a plant exhibit a broad range of $\delta^{13}\text{C}$ values, with lignin depleted in ^{13}C , relative to the whole plant, and cellulose slightly enriched (Tieszen 1991). Within grains, proteins and carbohydrates are enriched in ^{13}C , relative to cellulose, and lipids are heavily depleted, relative to bulk plant material (O'Leary 1988; Tieszen 1991; Kanstrup *et al.* 2011). The degree of ^{13}C depletion in lipids of C_3 and C_4 plants may be up to 9‰ and 14‰ respectively (Ballentine *et al.* 1998). However, a significant difference is observed in lipids produced by plant species between photosynthetic groups, allowing source distinction (Bernreuther *et al.* 1990). Lipid $\delta^{13}\text{C}$ values are subject to a similar degree of variation as bulk carbon (Woodbury *et al.* 1995). Furthermore, a lipid produced by multiple species may produce drastically different $\delta^{13}\text{C}$ values, as is observed in miliacin, a compound produced by both C_3 and C_4 plants (Jacob *et al.* 2008b).

Dietary carbon determines the carbon isotope baseline of consumers, with ^{13}C enrichment of bulk carbon around 1‰, although, within species variation may differ up to 2‰ (DeNiro and Epstein 1978). A direct relationship between carbon source and $\delta^{13}\text{C}$

values has been clearly demonstrated across species, diets, and environments, of wild and farmed salmon (Aursand *et al.* 2000), freshwater and marine seals (Smith *et al.* 1996), and foddered domesticates (Stott *et al.* 1997; Craig *et al.* 2005). However, the carbon isotope composition of compounds produced by an animal vary due to differences in carbon source, e.g. lipids, acetate and glucose, for each compound, and the biosynthetic pathways employed in their production (Spangenberg *et al.* 2006). Analysis of fatty acids in redhead duck fat demonstrated significant enrichment in ^{13}C , from dietary fatty acids, indicating significant synthesis of fatty acids from more enriched compound classes, such as proteins and carbohydrates (Hammer *et al.* 1998). Furthermore, synthesis of lipids and proteins in animals results in depletion and enrichment of ^{13}C respectively. Therefore, lipids are depleted relative to collagen by around 5‰, irrespective of C_3 and C_4 plant contribution to diet (Stott *et al.* 1997). Utilisation of multiple dietary carbon sources and employment of various biosynthetic pathways, by animals, results in significant fractionation of carbon isotopes and measurable differences in carbon isotope composition (Spangenberg *et al.* 2006). Relevant examples are discussed further in later sections on the identification of porcine, ruminant and dairy products.

Nitrogen Isotope Fractionation

The $\delta^{15}\text{N}$ composition of natural materials is highly variable due to nitrogen isotope fractionation in many biogeochemical processes (Handley *et al.* 1999). Indeed, the $\delta^{15}\text{N}$ baseline in many environments differ considerably, relating to mean annual temperature, precipitation, vegetation, and microbial action, in addition to anthropogenic intervention in the nitrogen cycle (Amundson *et al.* 2003; Fraser *et al.* 2011). The nitrogen composition of animals is predictable and consistent, with stepwise increase of approximately 3-5‰ associated with trophic level (Minagawa and Wada 1984). However, plants are subject to more complex biogeochemical processes promoting both enrichment and depletion of ^{15}N (Szpak *et al.* 2014).

Physiological processes employed in routing nitrogen may significantly influence nitrogen isotopic composition in plants. However, $\delta^{15}\text{N}$ values are primarily indicative of nitrogen source, i.e. soil $\delta^{15}\text{N}$ values (Styring *et al.* 2016). Increased temperature and decreased precipitation raise $\delta^{15}\text{N}$ values of soils as a result of biogeochemical processes preferentially removing lighter nitrogen isotopes from the soil. Therefore, plants in these

environments are also enriched in ^{15}N (Szpak *et al.* 2014; Styring *et al.* 2019). Such processes are also applicable to water stressed plants in temperate climates. However, anthropogenic intervention in the nitrogen cycle may also result in comparable increases in $\delta^{15}\text{N}$ values of soils and plants. The use of either cattle manure or slash and burn agriculture may increase $\delta^{15}\text{N}$ values between 2-8‰ (Kanstrup *et al.* 2011; Szpak *et al.* 2014). Furthermore, the application of other animal manures may increase $\delta^{15}\text{N}$ values of soils by as much as 40‰, depending on the quantity and duration of manuring (Szpak *et al.* 2014). Differentiation between climatic and anthropogenic activity and the quantification of manuring is potentially achievable within archaeological environments (Styring *et al.* 2019). However, relevant environmental and experimental data is rare for many archaeological sites and contexts.

Minor variation is observed in $\delta^{15}\text{N}$ values of plants grown under the same conditions, relative to field grown plants (Bogaard *et al.* 2007; Fraser *et al.* 2011; Kanstrup *et al.* 2011; Fraser *et al.* 2013). Different tissues and compounds within a plant exhibit depletion and enrichment of ^{15}N . Proteins are enriched in ^{15}N , relative to other compounds, yet protein concentration in caryopses does not increase their $\delta^{15}\text{N}$ values. The production of grains and fruits may result in nitrogen being routed from other areas of the plant, applying a second stage of fractionation. Therefore, caryopses are depleted in ^{15}N relative to the leaves, stems and shoots (Szpak *et al.* 2014). However, experiments have demonstrated that grains are significantly enriched from straw (Kanstrup *et al.* 2011), potentially due to the depletion of ^{15}N in stems during the drying process and harvesting times.

While stepwise increase of $\delta^{15}\text{N}$ values, between consumers, is predictable and consistent, the nitrogen isotopic baseline of an environment is not. Establishing the $\delta^{15}\text{N}$ baseline of domestic crops is essential for the interpretation of faunal and human isotopic data (Szpak *et al.* 2014). Deconvolution of $\delta^{15}\text{N}$ data requires further experimentation, although further discussion of factors relating to the analysis of nitrogen isotopes goes beyond the remit of this section and thesis.

Applying reference isotope data

It is important to note several factors that limit the application of modern reference data to archaeological material. Firstly, $\delta^{13}\text{C}$ values of modern material must be

corrected to account for the Suess effect (Friedli *et al.* 1986; Roberts *et al.* 2018). Secondly, modern synthesised fertilisers reduce $\delta^{15}\text{N}$ values of soil and plants (Kanstrup *et al.* 2011). Thirdly, unknown quantities of resource input and natural variation of isotope baselines introduce significant bias in the interpretation of archaeological material (Roberts *et al.* 2018). These factors should be considered in the interpretation of archaeological material where they cannot be accurately accounted for.

ORA: residue formation, alteration, degradation and contamination

Formation

Charred foodstuffs, ceramic-absorbed residues, adhesives, sealants, and sediments are commonly subject to ORA investigations (Regert 2011). This technique is also infrequently applied to well preserved and charred botanical remains (Copley *et al.* 2001; Lu *et al.* 2009a). Material studied in this thesis includes charred crusts and absorbed ceramic residues. Therefore, only these materials will be discussed in detail.

Ceramics are the most common archaeological materials to which ORA is applied. The ceramic matrix is permeable and porous, enabling the absorption of organic compounds, particularly lipids, into the fabric of a pot. Absorbed lipids are trapped within micro-pores and potentially bind to the metal ions in the ceramic matrix, allowing retention over long periods (Craig *et al.* 2004; Correa-Ascencio and Evershed 2014a). Increased porosity of a ceramic matrix is beneficial to lipid absorption (Evershed 1993; Charters *et al.* 1997; Raven *et al.* 1997). However, increased pore size results in significant loss of absorbed lipids. Pores $< 1 \mu\text{m}$ provide the best preservation conditions for lipids, due to restricted access by microorganisms, water leaching, and potentially the effects of chemical degradation (Drieu *et al.* 2019). The encapsulation of lipids within micro-pores of charred crusts is believed to be the basis of their survival in a relatively exposed material (Oudemans and Boon 1991; Evershed 1993; Oudemans and Boon 1993). Vessel porosity is reduced by high vitrification but may be either increased or decreased, depending on the temper used (Correa-Ascencio and Evershed 2014). It is important to note that organic compounds present within the clay matrix prior to firing are unlikely to survive (Johnson *et al.* 1988), although lipids may transfer from fuel to ceramic during the firing process (Reber *et al.* 2019).

Organic and inorganic treatments are applied to vessel walls in order to reduce permeability and porosity (Reber and Hart 2008) and are understood to be highly effective in improving the water retention functionality of vessels during boiling (Charters *et al.* 1997). The application of organic sealants may complicate archaeological interpretations of absorbed ceramic residues (Heron and Evershed 1993). The application of a glaze to vessel walls was initially believed to make vessels impermeable, resulting in few studies of more modern ceramics (Evershed 1993; Charters *et al.* 1997). However, recent experiments and analysis demonstrate significant absorption of lipids in glazed ceramics, likely due to imperfections and cracks in the glaze, developed during production and use (Pecci *et al.* 2015; 2016).

Lipid accumulation down the profile of ceramic vessels has been demonstrated experimentally and archaeologically, with higher concentrations in the higher wall/rim section and decreasing quantities in the lower wall and base (Charters *et al.* 1993a; 1997). However, this pattern of lipid accumulation is only indicative of boiling, whereby hydrophobic lipids accumulate on the surface of the liquid and are absorbed at the water line at the top of the vessel. Other methods of cooking, such as roasting may produce different concentration profiles in vessels (Charters *et al.* 1993a). The mode of cooking is rarely considered in ORA, presumably due to the limited availability of samples, expense and effort required to sample higher and lower sections, yet it should be considered in interpretation. A concentration gradient through the ceramic wall has also been demonstrated in archaeological vessels, indicating permeation through the fabric and concentration in the top layer of the internal surface (Stern *et al.* 2000). These two characteristics of lipid accumulation dictate current ceramic sampling methods in ORA.

Ceramic-absorbed residues represent the accumulation of lipids throughout the life-use of a vessel and may contain lipids from multiple sources, processed either concurrently or sequentially (Charters *et al.* 1996; Mottram *et al.* 1999; Copley *et al.* 2003; Copley *et al.* 2005; Oudemans and Boon 2007). However, charred crusts are generally formed during single events, enabling the identification of vessels used to process different products and ability to distinguish between meals and average cuisine (Oudemans and Boon 2007; Miller *et al.* 2020).

A method by which the life use of a vessel may be extended is through repair (Heron and Evershed 1993). The addition of organic adhesives, such as resins, may

introduce significant quantities of lipids to ceramic fabrics (Charters *et al.* 1993b), although, repair residues are generally visible upon inspection of a sherd surface (Charters *et al.* 1993b; Regert 2004).

Alteration

Chemical alteration of lipids occurs during the heating of products in ceramic vessels. Thermally assisted oxidation of lipids is a major cause of alteration in ceramics and charred crusts, particularly in areas that are exposed to high temperatures and oxygen. Regert *et al.* (1998) noted increased oxidation in the rims of vessels, due to exposure to air, following evaporation of the cooking liquid. Therefore, this section of a vessel may produce the highest yield of lipids but also an abundance of alteration products. Charred crusts, especially those on external surface of vessels, are also subjected to the same thermal alteration processes (Yoneda *et al.* 2019).

Long-chain ketones are naturally present within some plants and have been suggested as potential biomarkers (Evershed *et al.* 1992). However, they are also formed via decarboxylation and dehydration of free fatty acids and acyl lipids, at temperatures > 300°C, when mediated by inorganic salts in the ceramic matrix. Formation also occurs in the absence of ceramics (Evershed *et al.* 1995; Raven *et al.* 1997). As acyl lipids, which contain fatty acids, are the primary component of fats, the potential for ketone formation during food processing is high. Long-chain ketones formed through alteration, and those naturally present in plants, may be distinguished by compound specific carbon isotope analysis, but only if the $\delta^{13}\text{C}$ values of the two source materials are sufficiently different (Evershed *et al.* 1995).

Unsaturated fatty acids oxidise readily when heated, specifically when burnt. However, in anaerobic conditions, when oxidation is limited, ω -(*o*-alkylphenyl)alkanoic acids (APAAs) are readily formed from unsaturated fatty acids. The formation of APAAs is increased with the degree of unsaturation of the fatty acid and in the presence of the ceramic matrix (Evershed *et al.* 2008a). However, they are observed in a high abundance in charred crusts (Hansel *et al.* 2004; Craig *et al.* 2007) and have been demonstrated to form in the absence of ceramic fabric (Bondetti *et al.* 2021). This alteration process requires temperatures > 120°C, although a significantly greater range and abundance of APAAs is formed at 270°C (Bondetti *et al.* 2021). As these compounds are not naturally occurring, they are employed as evidence of heating and may support the identification

of aquatic product processing (Hansel *et al.* 2004). Furthermore, the relative abundance of C₁₈ APAA isomers may enable broad distinction of different plant and animal products (Bondetti *et al.* 2021). However, the absence of these alteration markers in many archaeological contexts raises questions as to their production and preservation, which remain to be explored.

Conifer resin primarily comprises diterpenoid compounds with abietane skeletons. Retene and methyl dehydroabietate are thermal degradation markers, of conifer products, identified in pitch/tar (Colombini *et al.* 2005; Connan and Nissenbaum 2003; Charrié-Duhaut *et al.* 2013). Retene may be produced through the protracted heating of conifer resin at high temperatures. However, methyl dehydroabietate is only produced by the destructive distillation of conifer wood. When heated in a low oxygen environment, conifer wood releases methanol that reacts with compounds in the resin, forming methyl dehydroabietate (Colombini *et al.* 2005; Hjulström *et al.* 2006). Therefore, it is not only possible to identify the production of conifer tar but also the method by which it was produced.

Other abietane derived compounds are also produced during the heating of pine resin. However, these compounds may also be produced through natural degradation over time (Colombini *et al.* 2000; 2005). Indeed, the oxidation of sterols is significantly increased in the presence of high temperatures, as are other fats, and degradation markers exist, but it is not possible to distinguish between the application of heat and oxidation over time (Evershed *et al.* 1992; Regert 2011).

Degradation

The hydrophobic nature of lipids limits their transfer from ceramics and charred crusts to soils and *vice versa* (Heron *et al.* 1991). As previously discussed, the ceramic matrix may prevent degradation of some lipids, encapsulated in micro-pores, by water leaching, microbial degradation and potentially chemical alteration. However, a significant quantity of absorbed lipids are exposed to these sources of degradation.

Triacylglycerols (TAGs), the main constituent of fats, comprising three fatty acids attached to a glycerol backbone, are abundant in plant and animal products. However, they are rarely recovered in archaeological contexts in significant quantities due to rapid and near complete loss by hydrolysis (Dudd *et al.* 1998). Indeed, their loss in oxic and anoxic environments is significantly higher than waxes, despite their higher relative

abundance before degradation (Evershed 2008a). Hydrolysis of TAGs produces di- and monoacylglycerols (DAGs and MAGs), in addition to free fatty acids, which may be retained within the ceramic matrix. Fatty acids, specifically palmitic and stearic acid, are often the most abundant compounds remaining, partially due to their dominant abundance in plant and animal products. However, oxidative reactions significantly reduce the abundance of unsaturated, especially polyunsaturated, fatty acids. Therefore, their abundance in archaeological residues is as much a reflection of taphonomic processes as the original composition of a residue (Evershed *et al.* 1992; Dudd *et al.* 1998). A decreased degree of saturation and chain length increases the solubility of fatty acids, resulting in substantial loss by water leaching (Evershed *et al.* 1999). Degradation of short chain fatty acids is rapid following cleavage from the parent TAG. Furthermore, TAGs containing short chain fatty acids (< C₄₄) degrade more rapidly than those containing longer chain fatty acids (Dudd *et al.* 1998).

Microorganisms present within the burial environment degrade lipids through enzymatic hydrolysis, oxidation, and structural alteration of compounds, limiting their recovery in oxic environments, where microorganisms thrive (Evershed *et al.* 1992). Experimental degradation of fats demonstrates the limitations of microbial activity in anoxic environments, in which lipids are significantly better preserved (Dudd *et al.* 1998, Evershed 2008a). Arid environments also limit microbial activity, in addition to water leaching, and may produce well preserved residues, specifically of compounds with high water solubility, although oxidation is potentially increased (Colombini *et al.* 2005).

Dicarboxylic acids (diacids) are formed by oxidative cleavage of the double bond in an unsaturated fatty acid, with chain length dependent on the position of the double bond and direction of cleavage (Regert *et al.* 1998). The range and abundance of diacids may be indicative of a precursor product and heating is understood to accelerate diacid formation (Colombini *et al.* 2005; Copley *et al.* 2005). However, it is not possible to distinguish between extensive natural degradation and protracted heating. Furthermore, diacids are highly soluble and susceptible to water leaching, and may be contaminants from bog and peat environments (Colombini *et al.* 2005).

Contamination

A major concern in ORA is the contamination of archaeological residues by lipids in the burial environment. Analysis of ceramic and associated soil samples identified

relatively distinct residue profiles, with ceramics generally containing a more limited range of compounds and greater variability between samples. Conversely, soil samples are dominated by lipids derived from plants and animals that are generally not present in archaeological materials. In addition, the abundance of lipids within ceramics is generally significantly higher than in associated soils, providing two measures of distinction (Heron *et al.* 1991). Studies of contamination in charred crusts are generally restricted to issues impacting bulk isotope analysis. The exposed nature of these charred materials is a source of concern during analysis (Evershed *et al.* 2008a). However, as distinct residue profiles are observed between charred crusts and the soil samples described, it may be presumed that charred crusts suffer little contamination (Oudemans and Boon 1993). Limited migration of lipids is presumed to relate to their hydrophobic nature, preventing transfer to archaeological materials (Evershed 1993). As discussed, microbial action has the potential to degrade original residues, yet they may also introduce lipids to a residue. Branched-chain fatty acids may be indicative of bacterial contamination but are also present in ruminant products. Therefore, the presence and absence of branched-chain fatty acids can neither confirm nor rule out either origin. A general rule in ORA is that samples containing yields $< 5\mu\text{ g}^{-1}$ should not be considered to be of archaeological origin, as the potential influence of contamination is high.

Post-excavation activity, including handling, storage, and poor laboratory practice, are potentially a greater source of contamination. Human derived compounds, such as squalene and cholesterol may be transferred to samples through handling. Squalene is easily discounted due to its rapid degradation in archaeological material, yet cholesterol is much longer lived and may be misinterpreted as ancient (Evershed 1993; Roffet-Salque *et al.* 2017a). Additional contaminants include plasticisers that may leach from storage material and laboratory equipment. Plasticisers are easily recognised and discounted, yet they may coelute with other important compounds and hinder interpretation (Stern *et al.* 2000).

SIA: material formation, alteration, degradation and contamination

Formation

Stable isotope analysis may be applied to human, floral, and faunal remains, amorphous charred materials, and single compounds (DeNiro 1987). However, only

charred caryopses, amorphous remains, and single compounds are analysed in this study. Therefore, only these materials are discussed herein.

Charred crusts, formed by excess heating of consumable products, may comprise varying proportions of proteins, carbohydrates, and lipids. For instance, the lipid component of charred crusts ranges between 0.01 and 5.00% of total material weight (Craig *et al.* 2007). There may be a significant disparity between bulk and single compound isotope measurements, depending on the composition of a crust, given that each compound exhibits a different degree of isotopic enrichment (Miller *et al.* 2020). Therefore, careful consideration of multiple datasets is necessary to accurately characterise charred crusts. Interpretation is further complicated when one considers the likelihood of multiple products forming charred crusts. Experimental studies have demonstrated a nonlinear relationship between the percentage contribution of products, to a cooked mixture, and the isotope values that are obtained during analysis of charred crusts. Furthermore, the release of material from processed products is not consistent over time (Hart *et al.* 2007; 2009). Hart *et al.* (2009) demonstrate that a contribution of up to 80% maize kernels, to a mixture containing a minimum of 20% C₃ products, does not exceed the established -22‰ threshold used to characterise a C₄ plant contribution to charred crusts, after 60 minutes of cooking. Their research also demonstrates that different pre-processing methods, e.g. milling, have a significant impact on the ability to detect maize, and presumably other products, with an increased surface area to volume ratio benefiting the identification of a product. Similar difficulties have been outlined for the detection of marine (C₄) products in bulk isotope data, although molecular and compound specific isotope analysis may aid their identification, due to the abundance of lipids in marine products (Craig *et al.* 2007; Heron and Craig 2015). There is no experimental data available to determine whether the release and entrapment of lipids, from maize to charred crusts, is comparable to bulk material. Therefore, further analysis is necessary to understand whether maize, and other cereals, are equally unrecognisable by compound specific isotope analysis. Only a limited dataset exists to assess the comparability of bulk and ceramic absorbed compound specific (lipid) isotope data (Miller *et al.* 2020). Therefore, substantially more research is necessary to investigate the accuracy and reliability of any relationships between these datasets.

Alteration

The impact of charring on $\delta^{13}\text{C}$ values of caryopses is not significant and is inconsistent, with cereals demonstrating shifts of $0.0 \pm 0.3\text{‰}$, broad beans $-0.1 \pm 0.4\text{‰}$, and lentils $-0.1 \pm 0.1\text{‰}$ (Fraser *et al.* 2013). The charring of foxtail and common millets resulted in $+0.2\text{‰}$ and -0.2‰ shifts in $\delta^{13}\text{C}$ values respectively (An *et al.* 2015). Therefore, the alteration in bulk carbon isotope values of charred caryopses is within the range of natural variation and analytical error. Conversely, $\delta^{15}\text{N}$ values of cereals and pulses demonstrate a consistent positive increase of $1.0 \pm 0.4\text{‰}$ when charred. An increase in $\delta^{15}\text{N}$ values is attributed to the loss of nitrogen containing volatiles from caryopses. (Fraser *et al.* 2013). As such, charred caryopses are determined to be reliable and accurate records of past crop bulk isotopic content.

Lipids from charred plants may exhibit a significant shift in carbon isotope composition. Aerosolised fatty acids extracted from C_3 plants charred under laboratory conditions exhibited 2 - 7‰ enrichment, yet C_4 plants exhibited 2 - 6‰ depletion, relative to those of unburnt plants (Ballentine *et al.* 1998). Whether this alteration is reflected in charred material is presently unexplored. Presumably, the lipids remaining in the charred material would demonstrate an inverse alteration in $\delta^{13}\text{C}$ values, although this may be insignificant depending on the quantity of aerosolised lipids released. Further experimentation is required in order to resolve the alteration of compound specific $\delta^{13}\text{C}$ values of plants. The bulk $\delta^{13}\text{C}$ and $\delta^{15}\text{N}$ values of processed plant material may vary by $\pm 3\text{‰}$ when charred (De Niro 1987) suggesting that other compounds present within plant matter are not affected uniformly.

Preservation

The isotopic composition of charred caryopses and absorbed residues is maintained during deposition, with no significant degradation observed (De Niro 1987; Charters 1996; Evershed 2008a). In addition, while the isotopic composition of charred crusts before and after deposition has not been assessed experimentally, the preservation of polysaccharides, proteins, and lipids indicates maintenance of the original components and potentially their original isotopic composition (Oudemans and Boon 1991). Degradation experiments are required to corroborate this hypothesis.

Contamination

Contamination of archaeological materials by isotopically distinct compounds is potentially the greatest factor impacting the accuracy of stable isotope data. The addition of carbon from fuel, during the formation of charred materials, has been suggested as a potential first source of contamination in charred material, with external charred crusts, close to the fuel source, demonstrating greater variability in $\delta^{13}\text{C}$ values (Yoneda *et al.* 2019), although this is yet to be experimentally tested. A potentially greater degree of contamination originates in the burial environment, with carbonates, nitrates, and humic acids infiltrating charred materials (Fraser *et al.* 2013; Vaiglova *et al.* 2014). These contaminants may affect bulk but not compound specific analysis, as this technique allows for their separation from targeted compounds. In different environments, carbonates may return $\delta^{13}\text{C}$ values $\leq 2\%$ and nitrates may return $\delta^{15}\text{N}$ values $\leq 8\%$. Humic acids can be produced when processing plants, therefore, they may be either endogenous or exogenous and isotopically similar or distinct (Vaiglova *et al.* 2014). Despite the potential for contamination, deposition of charred cereals and pulses for two years demonstrated no significant change in either $\delta^{13}\text{C}$ and $\delta^{15}\text{N}$ values or the % carbon and nitrogen content of samples (Fraser *et al.* 2013). The same experiment placed charred millet caryopses in soils containing isotopically distinct humic acids. After six months, a significant $+0.5\%$ shift in $\delta^{13}\text{C}$ values occurred and was maintained for the following 18 months. Contamination by the humic acids present would have resulted in a negative shift, therefore it can be assumed that the charred millet caryopses were not contaminated by these compounds (Fraser *et al.* 2013). Nonetheless, the potential for contamination remains in certain environments, requiring the application of removal methods (Fraser *et al.* 2013; Vaiglova *et al.* 2014; Brinkkamper *et al.* 2018).

It is not possible to determine contamination of a single, isotopically distinct compound, by exogenous post-depositional organisms and materials, via ORA and compound specific isotope analysis. However, as previously discussed, the contamination of lipids is understood to be negligible (Heron *et al.* 1991). Post-excavation contamination is a greater cause for concern due to the high abundance of compounds, investigated by isotope analysis, in the modern environment. Therefore, exceptional sample collection and processing methods are necessary to limit contamination and provide accurate data.

Extraction and analysis

ORA

Extraction methods applied to archaeological materials exploit the solvent soluble nature of lipids and endeavour to maximise the quantity of lipids extracted while maintaining residue quality. However, achieving both is often impractical and, in some cases, unachievable, consequently compromises are made. Two extraction methods currently dominate archaeological research, due to their ease of application and utility. Solvent extraction (SE) recovers a broad range of compounds, including alkanes, alkenes, ketones, fatty acids, acylglycerols, wax esters, and sterols, that possess a range of polarities and volatilities. Extracted compounds containing carboxyl and hydroxy groups are derivatised, to decrease their polarity and increase their volatility, making them amenable to analysis by GC-MS (Regert 2011). Silylation and methylation are the most common derivatisation methods employed in ORA. Silylation employs BSTFA (N,O-Bis(trimethylsilyl) trifluoroacetamide), yet the addition of three carbon atoms reduces the accuracy of compound specific carbon isotope analysis by increasing the sample-to-derivative carbon molar ratio (Evershed 2009 401). Therefore, methylation, of a separate fraction of the solvent extract, must be undertaken for compound specific isotope analysis (Evershed 1994). Early papers noted the limited extraction potential of the SE method and the potential for bound lipids to remain in the insoluble fraction, resulting in low yields (Regert *et al.* 1998; Stern *et al.* 2000; Correa-Ascencio and Evershed 2014). Alkaline hydrolysis of the insoluble fraction, followed by derivatisation, releases these compounds. However, this requires an additional step, adding to the overall method time.

The demand for more efficient extraction methods, that produce significantly higher lipid yields, resulted in the development of the acidified methanol (AM) extraction method (Correa-Ascencio and Evershed 2014). This method enables one-step extraction and derivatisation of lipids, in a shorter time frame than SE, in addition to extraction of bound lipids. Furthermore, samples that contain no extractable lipids when employing SE may produce appreciable yields by AM extraction, due to the release of bound lipids (Reber 2021). One-step methylation of lipids enables direct analysis of fatty acids by compound specific isotope analysis, without an additional derivatisation step (Correa-Ascencio and Evershed 2014).

Compositional information is lost during AM extraction, by the hydrolysis of acylglycerols and wax esters to their fatty acid and alcohol constituents. The presence of wax esters may be inferred from a high abundance of alcohols but it is not possible to infer the composition of acylglycerols, as their fatty acid constituents are methylated and incorporated into the free fatty acid fraction. However, the loss of acylglycerols is not always significant, given their low abundance in archaeological materials, following extensive degradation in the burial environment (Correa-Ascencio and Evershed 2014). Furthermore, the increased abundance of FFAs is highly beneficial to compound specific isotope analysis and outweighs the interpretive potential of TAGs.

Bulk isotopes

A range of pre-treatment methods have been developed and applied to charred materials, prior to bulk isotope analysis, to remove contaminants. Carbonates, nitrates, and humic acids are soluble in acids, water, and alkali respectively. A combination of acid-base-acid (ABA) treatments are proposed to remove these contaminants (Vaiglova *et al.* 2014). The acid treatment removes carbonates, the base removes humic acids, and the final acid treatment removes CO₂ absorbed during the base step (Fraser *et al.* 2013). The application of pre-treatment methods stemmed from radiocarbon dating methodologies, that contend with significantly less ¹⁴C content in samples. However, the necessity of pre-treatment was initially overestimated, with recent studies highlighting inconsistent δ¹³C offsets, between untreated and treated samples, of only ±1‰ in 96% of samples. In addition, δ¹⁵N offsets of ±1.5‰ were recorded in 96% of samples (Brinkkamper *et al.* 2018). Several studies have also observed a significant decrease in sample mass due to the loss of material during treatment methods (Vaiglova *et al.* 2014; Brinkkamper *et al.* 2018). In one study, charred millet caryopses samples were reduced by 51.9% and 98.4%, during acid and ABA methods respectively (Brinkkamper *et al.* 2018). Therefore, even gentle pre-treatment methods may result in a degree of sample loss that is unacceptable for precious archaeological material. Fourier transform infrared spectroscopy (FTIR) has been employed in pre-screening samples prior to pre-treatment, to assess the type and degree of contamination, with limited success and a high rate of false positives (Vaiglova *et al.* 2014; Brinkkamper *et al.* 2018). Present research indicates that water-washed samples provide accurate and reliable bulk isotope data in most environments (Brinkkamper *et al.* 2018). Pre-treatment methods have been sporadically applied to

charred crusts subjected to bulk isotope analysis, as experimental research is primarily limited to charred botanical remains (Craig *et al.* 2007; Heron and Craig 2015; Heron *et al.* 2016; Yoneda *et al.* 2019). From the present state of research, further experiments appear unnecessary.

GC-MS

Gas chromatography-mass spectrometry (GC-MS) combines the separation potential of a Gas Chromatograph (GC) with the high identification sensitivity of a Mass Spectrometer (MS). The GC is a programmable oven containing a capillary column, with one end attached to an injection port and the other to the MS. The capillary column is lined with a thin siloxane stationary phase through which a carrier gas, the mobile phase, flows. The purpose of the GC is to separate complex mixtures of compounds, preventing coelution into the MS where they are ionised and identified. Samples are injected into the GC and are passed onto the column by several methods (e.g. on-column, PTV) depending on the GC setup. The GC oven is set to run a specified temperature ramp during which compounds injected into the column volatilise and are carried by the mobile phase, through the column, to the MS. Compounds interact with the stationary phase of the column during transit. Those with a higher affinity to the stationary phase pass more slowly through the column, resulting in a longer retention time. Molecular mass, structure, and functional group of compounds dictate their elution time. For instance, higher molecular weight compounds require increasing temperatures to volatilise and enter the mobile phase. The choice of stationary phase within a column, flow rate of the carrier gas, and temperature program must match the compounds and degree of separation required for the sample. Compounds pass from the GC into the ion source of the MS from which they are sent to a detector via an ion beam. The MS restricts ions sent to the detector according to their mass-to-charge ratio (m/z). The MS may be run in two modes, selected ion monitoring (SIM) and scan. In SIM mode, the MS will only detect specified m/z values, that are often limited, to increase sensitivity, due to down time as the detector alternates between detecting each m/z value. Scan mode detects a broader range of m/z values but is less sensitive. Generally, scan mode is applied to unknown archaeological mixtures and SIM mode is applied when there is a specific research question. The identification of compounds is made by comparison of distinctive

fragmentation patterns to established databases, such as NIST, and retention time, relative to internal standards and elution of compounds in a homologous series.

IRMS

Isotope Ratio Mass Spectrometry (IRMS) enables high precision measurements of isotopic abundance. Measurement of a sample is always made relative to an internationally recognised isotopic standard, accounting for fluctuations in isotopic abundance over time and variance between instruments. The MS in IRMS is more precise and sensitive than those attached to GCs, aiming to detect subtle differences in the isotopic abundance of CO₂ and N₂. In order to obtain these gases, samples are combusted and filtered, prior to being routed to the IRMS. Bulk samples are processed using an elemental analyser (EA) interface, producing average measurements of the whole sample (Muccio and Jackson 2009). Limited sample preparation is required for bulk analysis, with pre-treatment often unnecessary. However, this process does not allow measurements of each constituent compound in the sample. By combining the separation potential of GC, with the precision and sensitivity of an IRMS, it is possible to measure the isotopic abundance of single compounds. Compound specific isotope analysis utilises a GC interface, with eluted compounds directed to a combustion oven, that is linked to an IRMS (GC-C-IRMS) (Meier-Augenstein 1999; 2002; Muccio and Jackson 2009; Regert 2011). Of great importance in the analysis of single compounds is correction for each carbon added during derivatisation, thus explaining why methylation is preferable to silylation (Meier-Augenstein 1999).

The detection of plant and animal product processing in archaeological residues

Plant products

At the broadest scale, plant product processing may be recognised in archaeological residues when phytosterols are observed. Campesterol, sitosterol, and stigmasterol are present in low abundance (around 1% of total lipid content) in a wide variety of plants (Heron and Evershed 1993). In general, plant products contain a higher abundance of palmitic (C_{16:0}) than stearic (C_{18:0}) acid, in addition to significant quantities of even-numbered long-chain (C_{20:0} - C_{28:0}) fatty acids. Unsaturated fatty acids of varying chain length are abundant in plant products (Dubois *et al.* 2007), as opposed to terrestrial animal products, wherein saturated fatty acids dominate. While the fatty acid profiles of

fresh plant and aquatic animal products differ, profiles observed in archaeological material bear strong similarities. Degraded fatty acid profiles of aquatic animal products contain a higher proportion of monounsaturated fatty acids, than is present in fresh material, due to preferential and rapid degradation of polyunsaturated fatty acids during deposition. Therefore, degraded aquatic residues overlap with plant fatty acid profiles (Reber and Evershed 2004). In addition, as monounsaturated fatty acids are more susceptible to degradation than saturated compounds, degraded plant products can resemble terrestrial animal products. Therefore, distinction between terrestrial animal, plant, and aquatic animal products, based on fatty acid profiles, is unreliable.

Recent experimental research indicates that it may be possible to broadly distinguish certain product types, including cereals, non-leafy vegetables, and animal products, according to the proportion of E and H C₁₈ APAA isomers formed during heating of stearic acid (Bondetti *et al.* 2021). While the formation of APAA isomers requires further investigation, the E/H ratio of these product types appear to be maintained during short-term deposition, although burial over longer periods and under different conditions may have an adverse effect, necessitating further experiments. Furthermore, additional experiments are necessary to assess the effect that mixing different products may have on the E/H ratio (Bondetti *et al.* 2021).

Compound specific carbon isotope analysis is not especially useful in the identification of plant products. In plants, palmitic acid is generally depleted in ¹³C, relative to stearic acid, enabling limited distinction from other product types (Spangenberg *et al.* 2006). For instance, lipid rich plant products, e.g. acorns, may be tentatively identified by compound specific carbon isotope analysis (Lucquin *et al.* 2016a). However, two factors limit the identification of plant products by this technique. Firstly, the range of palmitic and stearic $\delta^{13}\text{C}$ values of plant products is broad and overlaps with various animal products. As such, freshwater fish and ruminant animals exhibit $\delta^{13}\text{C}$ values similar to C₃ plants, whereas marine animals and C₄-fed terrestrial animals may produce $\delta^{13}\text{C}$ values similar to C₄ plants (Craig *et al.* 2005; Jacob *et al.* 2008b; Craig *et al.* 2011; Horiuchi *et al.* 2015; Lucquin *et al.* 2016b). Secondly, most plant products are not lipid rich, relative to animal products, and comprise small quantities of palmitic and stearic acid, relative to other lipids. Indeed, repeat processing of cereals has demonstrated minimal lipid accumulation in ceramics (Hammann and Cramp 2018).

Therefore, while plant products, specifically cereals, may form the bulk of human subsistence, they contribute small quantities of lipids to organic residues. Cereals may contribute greater quantities of lipids to residues when processed with lipid rich products, i.e. meat, yet these residues are dominated by the lipid rich product (Hammann and Cramp 2018), making the identification of the plant product, via compound specific isotope analysis, more difficult. In this instance, an increased cereal component is only recognised by the presence of biomarkers.

Biomarkers are the most effective and accurate means of identifying plant products in archaeological residues, enabling species level identification in certain contexts, although identification may be limited to either genus or family. Observed biomarkers can also aid the interpretation of compound specific isotope data, with the isotopic composition of a known product helping to identify other products in a residue, via theoretical mixing models.

Cereals

Biomarkers of wheat, rye, and barley (Colonese *et al.* 2017), maize (Reber and Evershed 2004), and broomcorn millet (Heron *et al.* 2016) have been identified in archaeological material. However, these biomarkers are observed in a lower abundance and frequency than would be expected for such significant products of human subsistence (Colonese *et al.* 2017; Lucejko *et al.* 2018). A difference in the size, structure, and distribution of lipids among plant caryopses may limit the release of lipids during cooking. In addition, experiments indicate the low extraction efficiency of water limits the transference of cereal biomarkers from caryopses into suspension (Hammann and Cramp 2018). These observations correspond to bulk isotope data, obtained from processing mixtures of maize and wild rice, wherein isotope values were not significantly affected by cereals until the caryopses broke down and released material, primarily carbohydrates, into suspension (Hart *et al.* 2009). Pre-processed products, with a greater surface area, influenced bulk isotope values to a greater degree, in a shorter period of time. However, this does not necessarily correspond to either a greater release of lipids or ceramic-absorption of lipids, as has been demonstrated in experiments using wheat flour (Hammann and Cramp 2018). Ethnographic studies detail the boiling of starch-rich plant products to seal freshly fired ceramics. These products do not contain abundant lipids, as

other organic sealants do, indicating that starch may block pores on the internal ceramic surface and act as a physical barrier to lipid absorption (May and Tuckson 1982 49). This account may provide an explanation as to why low lipid yields are obtained when processing cereal flours. Indeed, experimental data, presented in Chapter 5, demonstrates, for the first time, the effectiveness of this practice. Nonetheless, some cereal lipids are absorbed during cooking, providing a means to identify their use.

Alkylresorcinols

Alkylresorcinols (ARs) are phenolic lipids with an odd-numbered alkyl chain that are observed in a high abundance in wheat and rye bran (Figure 1). They are also observed in lower abundances in other cereals, such as barley, millet, and maize, and are produced by some bacteria. However, it is proposed that the quantity of bacteria required to produce an appreciable yield of ARs makes this origin improbable in archaeological material (Colonese *et al.* 2017). The relative abundance of C₁₇ and C₂₁ ARs is markedly different in wheat and rye caryopses, allowing for their distinction. This ratio is maintained during cooking (Colonese *et al.* 2017), although experiments demonstrate that AR profiles are not uniformly absorbed by ceramics (Hamman and Cramp 2018). Therefore, while the degradation of ARs is uniform under anoxic conditions, it is not possible to distinguish these products in ceramic-absorbed organic residues (Hamman and Cramp 2018). A further consideration of using AR profiles, in other contexts, would be the potential effects of mixing cereals, although this has not been investigated by experiments.

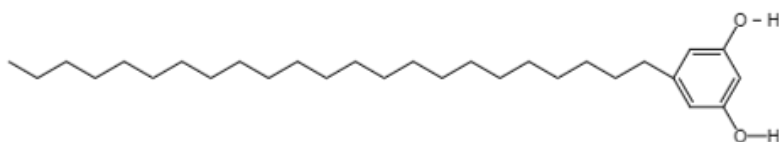


Figure 1. Example skeletal structure of an alkylresorcinol (AR23).

There is no evidence to suggest that ARs are formed during protracted heating of products at high temperatures, unlike long-chain ketones (Evershed *et al.* 1995) and structurally similar ω -(*o*-alkylphenyl)alkanoic acids (APAAs) (Evershed *et al.* 2008a;

Colonese *et al.* 2017; Hammann and Cramp 2018). The distribution of ARs in other domesticates and wild plant species has not been thoroughly investigated and must remain a consideration during ORA investigation. However, complementary studies, including archaeobotanical and proteomic analyses, may limit potential sources of ARs, e.g. Colonese *et al.* (2017). Unfortunately, ARs cannot be extracted using the AM method (Colonese *et al.* 2017), limiting the frequency of their identification in most archaeological studies.

Estolides

Ergot fungi (genus *Claviceps*) are a common cereal pest (Tenberge 1999) that produce distinctive estolide compounds, frequently with ricinoleic acid as a substituent (Lucejko *et al.* 2018). The observation of ricinoleic acid and estolides in large pithoi (storage) vessels, and others presumed to have been used for cooking, have been used to infer cereals as their contents (Lucejko *et al.* 2018). However, the application of this biomarker is of limited use in archaeological research as ergot fungi parasitize over 600 plant species in the families Poaceae, Juncaceae, Cyperaceae (Tenberge 1999). Therefore, the observation of distinctive estolides allows neither the identification of specific cereals, nor the unequivocal identification of cereals, as a wild plant origin and contamination must also be considered. Indeed, questions remain as to the formation and preservation potential of these compounds, within archaeological material, throughout use-life and deposition. In addition, ricinoleic acid is present, at a high abundance (83-89%), in castor oil and beans (Serpico and White 2000) and has been employed in their identification in archaeological materials that are unrelated to cereal storage and processing (Colombini *et al.* 2005). Therefore, while Lucejko *et al.* (2018) employed ricinoleic acid as a selection criterion for further analysis, to identify estolides, there is potential to excessively analyse material when using this criterion.

Maize

A non-specific contextual biomarker, *n*-dotriacontanol (Figure 2), has been utilized in the identification of maize processing in North America (Reber *et al.* 2004; Reber and Evershed 2004). The compound is common in the natural environment, as it is an alcohol derived from waxes that are produced by plants and insects, although it is unlikely to

form during pre- and post-depositional activity (Reber *et al.* 2004). It is abundant in maize, which is the dominant C₄ plant in North America, enabling its use as a biomarker, when compound specific carbon isotope analysis can confirm a C₄ plant source (Reber *et al.* 2004; Reber and Evershed 2004). Investigations of North American ceramic residues indicate that the exploitation of maize was widespread, yet the biomarker is less common and abundant than isotopic analysis of human remains suggests (Reber and Evershed 2004). Compound specific isotope analysis of C_{16:0} and C_{18:0} fatty acids in ceramic residues demonstrated minimal ¹³C enrichment, indicating that absorption and preservation of *n*-dotriacontanol is comparable to other maize lipids (Reber *et al.* 2004; Reber and Evershed 2004). Several authors propose a ceramic processing of maize (Reber and Evershed 2004; Hart *et al.* 2009). However, a preference for the use of maize flour could reduce the absorption of lipids, in accordance with the arguments outlined previously. One must question whether compound specific isotope analysis provides an accurate assessment of lipid contribution from maize, given observations made during bulk isotope experiments (Hart *et al.* 2009), the low lipid content of maize kernels, and the likelihood of lipids from other products overwhelming absorbed residues. Further experimental research is necessary to understand the reliability of *n*-dotriacontanol and compound specific isotope analysis in the detection of maize processing.

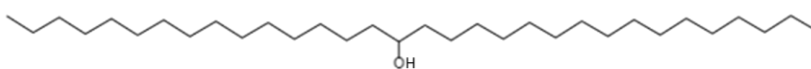


Figure 2. Example skeletal structure of (n) 17-Dotriacontanol.

Panicum miliaceum (broomcorn millet)

Miliacin (olean-18-en-3 β -ol methyl ether, Figure 3) is an oleanane-type pentacyclic triterpene methyl ether (PTME) compound employed as a biomarker for *Panicum miliaceum* (broomcorn millet) in European archaeological contexts (Jacob *et al.* 2008a; Bossard *et al.* 2011; 2013; Heron *et al.* 2016). Pentacyclic triterpenes with an oxygenated group at Δ^3 are widely distributed in the plant kingdom but methyl ethers are relatively uncommon (Jacob *et al.* 2005). Miliacin production is common in the *Panicum* genus, and

uncommon in *Pennisetum*, although species in these genera are mostly limited to tropical and subtropical regions (Connor and Purdie 1981; Wouw *et al.* 2008; Robert *et al.* 2011). Miliacin concentrations range between 3 and 577 $\mu\text{g g}^{-1}$ in *Panicum* and *Pennisetum* species (Bossard *et al.* 2013).

Miliacin is produced by a native European millet species (*Digitaria sanguinalis*), although the concentration of this compound in its caryopses has not been reported (Ohmoto *et al.* 1970; Tutin *et al.* 2000). The species is generally considered a weed and there are no reports of its exploitation in prehistoric European contexts, although it has been infrequently consumed by humans in the recent past (CABI 2019). Therefore, the presence of miliacin in prehistoric European culinary contexts may be attributed to *P. miliaceum*. The presence of miliacin in soils and sediments is more difficult to ascribe to a single species, given the possibility for contamination from other species present in an environment (e.g. Jacob *et al.* 2005; Oyo-Ita *et al.* 2010). Previous studies have suggested that *Chaetomium olivaceum* (a type of mould) and *Setaria italica* (foxtail millet) produce a low abundance of miliacin (Lu *et al.* 2009a). However, subsequent analysis indicates that miliacin is not present in either, suggesting that the presence of miliacin in the former study was due to improper sampling and contamination (Bossard *et al.* 2013).

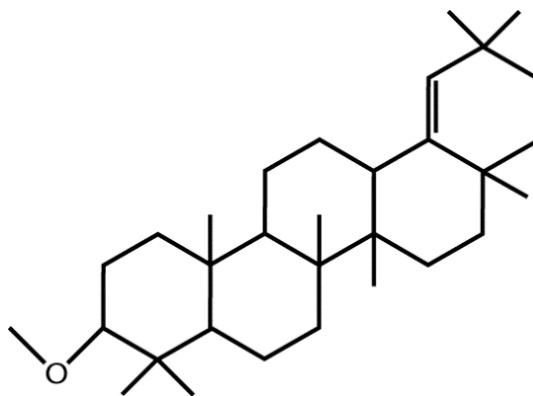


Figure 3. Skeletal structure of miliacin.

Miliacin is present in the caryopses, stem, and leaves of *Panicum miliaceum* plants but not in its roots. Caryopses contain the highest concentration of miliacin, with stems containing half as much, and leaves a negligible quantity. Miliacin is observed in the roots of plants grown in fields, but not those grown hydroponically, indicating contamination by soils containing the compound following years of cultivation (Bossard *et al.* 2013).

Therefore, while the presence of miliacin in sediments and palaeosoils has proven to be a useful marker of *Panicum miliaceum* cultivation in some contexts (Jacob *et al.* 2008a; Motuzaitė-Motuzevičiūtė *et al.* 2016), it poses a potential source of contamination in others (e.g. Kučera *et al.* 2019, Chapter 3). The absence of miliacin in the hull of *Panicum miliaceum* caryopses (Bossard *et al.* 2013) suggests that threshing and winnowing would not lead to large scale contamination of sites where domestic activity took place. Therefore, only soils of either cultivated fields or areas where large quantities of caryopses were deposited would contain miliacin (Courel *et al.* 2017).

The analysis of 20 caryopses from 76 *Panicum miliaceum* (variety sunrise) plants identified three PTMEs, including miliacin (86.5-100%), α -amyrin ME (0-10.5%), and β -amyrin ME (0-7.2%). However, miliacin was the only PTME identified in other varieties studied. Among *Panicum miliaceum* varieties, miliacin abundance ranged between 297 and 476 $\mu\text{g g}^{-1}$ and between 306 and 424 $\mu\text{g g}^{-1}$ in sunrise (Bossard *et al.* 2013). Inter and intra-variety variation in physiology may explain differences in the frequency and abundance of PTMEs, although environmental conditions and stress factors may also influence this, as has been identified in other triterpene producing plants (Gershenzon 1984). The yield of PTMEs in hydroponically grown sunrise plants was greater than plants grown outdoors, perhaps indicating an environmental factor in their production, although the proportion of PTMEs was uniform in both environments, potentially suggesting that a specific PTME is not produced in response to stress. Further experiments and analysis are necessary to understand any variation in PTME production and explore whether environmental conditions may be inferred from the presence of specific PTMEs associated with miliacin.

Presently, only miliacin has been identified in archaeological samples (Heron *et al.* 2016; Ganzarolli *et al.* 2018; Rageot *et al.* 2019). This may indicate that the range of PTMEs identified in the sunrise variety were not present in ancient varieties, although analysis of ancient caryopses would be required to prove this. As the wild progenitor of *P. miliaceum* has not been identified (Hunt *et al.* 2008), it is not possible to infer the range of PTMEs present in ancient cultivated varieties. Another explanation for the sole observation of miliacin may be the complete degradation of minor PTMEs, although further research is necessary to understand the degradation of different PTMEs in archaeological food residues. Miliacin, α -amyrin ME and β -amyrin ME have been

identified in sediment and soil samples, demonstrating their preservation in a variety of archaeological and environmental contexts (Jacob *et al.* 2005; Jacob *et al.* 2008a; Bossard *et al.* 2013). Jacob *et al.* (2005) noted that PTMEs are relatively resistant to degradation and have been shown to survive in sediments for thousands of years (Courel *et al.* 2017). Therefore, the absence of α -amyrin ME and β -amyrin ME in food residues may indicate that they are either lost during processing or not present in high enough abundance to survive.

Thermal alteration of PTMEs may occur during cooking, resulting in the formation of more thermodynamically stable skeletal structures, via thermally assisted acid isomerisation. This process has been identified in geological contexts, contributing to a decrease in the range of PTMEs present in sediments than in the biosphere (ten Haven *et al.* 1992; Rullkötter *et al.* 1994). In addition, it has been proposed that clay minerals may catalyse these reactions (ten Haven *et al.* 1992), potentially making their formation in ceramic vessels more likely. It has been noted that oleanane-type compounds with a double bond at Δ^{18} (e.g. miliacin) are thermodynamically less stable than those with double bonds at Δ^{12} (e.g. β -amyrin ME) and Δ^{13-18} (Rullkötter *et al.* 1994). Therefore, a decrease in the abundance of miliacin and an increase in Δ^{12} and Δ^{13-18} isomers would occur, yet this is not observed in archaeological residues. It is noted that the Δ^{12} and Δ^{18} isomers are equally susceptible to diagenesis via hydrogenation (ten Haven *et al.* 1992). Therefore, assuming the relative abundance of PTMEs in *Panicum miliaceum* is not altered during processing, non-acidic degradation would result in miliacin being the last surviving PTME.

Microbial activity has also been proposed as a potential cause of alteration of PTMEs in sediments (ten Haven *et al.* 1992). The biotransformation of triterpenes by fungi (Bastos *et al.* 2007) and other microorganisms (Muffler *et al.* 2011) highlight the variety of species and chemical processes by which these compounds degrade during processing and deposition. Fermentation, by the propagation of yeast, is an obvious anthropogenically induced microbial action. Analytical investigations have identified the alteration and formation of novel oleanane-type triterpenes in fermented green tea (Huang *et al.* 2014). Therefore, it is possible that fermentation of *P. miliaceum* could result in alteration of its oleanane-type PTMEs, potentially resulting in the formation of novel compounds that could be used as fermentation-specific biomarkers. However,

miliacin is reported to possess anti-microbial/anti-fungal properties (Jacob *et al.* 2008a; Bossard *et al.* 2013), that may either limit or prevent alteration during deposition and fermentation. Whether other triterpenes in *P. miliaceum* are susceptible to microbe-induced alteration is currently unknown. Further experimental research is necessary to understand whether certain triterpenes are susceptible to alteration and if it is possible to distinguish between intentional and unintentional alteration. Inclusion of archaeological data, such as the occurrence of compounds in specific ceramic types, could provide corroboratory evidence of specific activities.

It is possible to distinguish *P. miliaceum* from the predominantly C₃ plant environment of prehistoric Europe, via isotope analysis, as it is a C₄ plant (Jacob *et al.* 2008b; Heron *et al.* 2016), although cautious interpretation of ¹³C enriched residues is necessary in contexts where the processing of either marine or C₄-fed animal products may have occurred. In such contexts, the observation of miliacin is critical to confident identification of *P. miliaceum* processing. *D. sanguinalis* is also a C₄ plant, and could, in theory, complicate the interpretation of isotopic datasets. However, as there is little evidence for the processing and consumption of this species, it may be discounted.

Limited compound specific carbon isotope analysis of palmitic and stearic acids, extracted from eight *P. miliaceum* caryopses, produced an average $\delta^{13}\text{C}_{16:0}$ and $\delta^{13}\text{C}_{18:0}$ value of -18.8‰ and -19.1‰ respectively (Taché *et al.* 2021). Miliacin, extracted from *P. miliaceum* caryopses and archaeological soils, has produced $\delta^{13}\text{C}$ values of -23.5‰ and between -21.3‰ and -21.6‰ respectively (Jacob *et al.* 2008b; Courel *et al.* 2017). However, further analysis of reference materials is necessary to understand the range of compound specific $\delta^{13}\text{C}$ values that may be obtained from different *P. miliaceum* plants, grown under different conditions.

Bulk $\delta^{13}\text{C}$ values of modern *Panicum miliaceum* caryopses ($n= 19$), grown in a variety of environments in China, range from -12‰ to -14.3‰, with a mean of $-12.6 \pm 0.6\%$ (An *et al.* 2015). Charring experiments demonstrate no significant difference between charred and fresh *Panicum miliaceum* caryopses (Yang *et al.* 2011). Archaeological samples are enriched in ¹³C as expected, due to modern release of fossil carbon, with Chinese material ranging between -9.2‰ to -11.9‰ (An *et al.* 2015; Wang *et al.* 2018) and Greek material ranging between -10.3‰ to -10.8‰ (Nitsch *et al.* 2017). The limited range in $\delta^{13}\text{C}$ values obtained from Greek material is potentially due to a small

sample size (n= 8) and a limited number of sites sampled (n= 2). Bulk $\delta^{13}\text{C}$ values of *Panicum miliaceum* do not correlate with annual precipitation. However, up to 1‰ temporal shifts have been observed, highlighting the need for local archaeological sampling for accurate comparison of results between materials (An *et al.* 2015). Furthermore, bulk $\delta^{13}\text{C}$ values of *Panicum miliaceum* plant leaves are depleted in ^{13}C and exhibit a greater range than caryopses (An *et al.* 2015). Therefore, comparison of bulk isotope values of charred plant, faunal, and human remains must consider variations in foddering and consumption patterns. Few stable nitrogen isotope analyses have been reported for *Panicum miliaceum*, with a range of $\delta^{15}\text{N}$ values between 1.6‰ to 7.4‰ published (Nitsch *et al.* 2017).

Vegetables

Vegetable product processing has been proposed following the observation of lipids, derived from epicuticular plant waxes, in archaeological residues. Nonacosane, nonacosan-15-one and nonacosan-15-ol are present in high abundance in *Brassica spp.*, e.g. cabbage and turnip (Evershed *et al.* 1991). In addition, hentriacontane and hentriacontan-16-one are present in high abundance in leek (Evershed *et al.* 1992). While these compounds are abundant in the products listed, they are not exclusive to them. Therefore, these compounds may be employed as broad indicators of leafy vegetable processing but allow no greater interpretation without supporting archaeobotanical evidence (Dunne *et al.* 2019). Palmitone (hentriacontan-16-one, Figure 4) has also been proposed as a potentially more specific sedimentary biomarker for taro in the context of the Pacific island of Vanuatu (Krentscher *et al.* 2019). Extensive sampling of native flora indicates that taro is the only historic plant to produce this compound and environmental sampling produced no evidence for the migration of palmitone in soils (Krentscher *et al.* 2019). As such, this compound may be used as a biomarker of taro processing if observed in archaeological residues. However, any interpretation of ketones must consider the potential for their formation when heating fatty acids (Evershed *et al.* 1995; Raven *et al.* 1997).

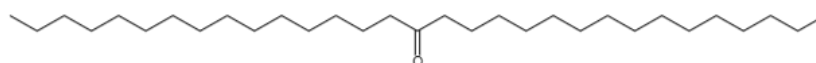


Figure 4. Skeletal structure of palmitone.

Alcohol

The detection of alcohol production and consumption, specifically of wine, has been the subject of great interest in many published studies, yet the application of some extraction methods and identification criteria are not suited to the research question (Drieu *et al.* 2020). Tartaric acid is frequently applied as a 'biomarker' of wine, due to its concentration in grapes, relative to other fruits (Michel *et al.* 1993; McGovern *et al.* 2005; McGovern *et al.* 2017). However, tartaric acid is also synthesized by many other plants, including Chinese hawthorn, and some species of yeast (McGovern *et al.* 2004; Barnard *et al.* 2011). The observation of tartaric, malic, succinic, and citric acids, in residues of vessels presumed to contain wine, have also been used to propose wine production (McGovern *et al.* 2017). However, these compounds are produced by other fruits, including apples, in varying proportions (Barden *et al.* 1997). In addition, in the McGovern *et al.* (2017) study, malic acid was observed in significantly higher abundance than tartaric acid, despite tartaric acid possessing a greater preservation potential than the other acids (Pecci *et al.* 2013). Therefore, an alternative source of these compounds may be suggested, in which malic acid is a greater component. Confirmation bias is a significant issue among many studies, wherein tartaric acid is only searched for in material already believed to contain wine (Drieu *et al.* 2020). Tartaric acid is water soluble and prone to migration in the burial environment, limiting its application in contexts beyond arid environments (Barnard *et al.* 2011; Drieu *et al.* 2020). Analysis of ceramic residues from societies and regions in which viticulture was not practiced identified tartaric acid in variable quantities, demonstrating that this compound may be a marker of fruit but not grapes specifically (Drieu *et al.* 2020).

Phenolic compounds, including flavonoids, anthocyanins, and tannins, are common components of plants, including grapes, apples, and blueberries (Schieber *et al.* 2001; Garnier *et al.* 2003; Zadernowski *et al.* 2005). Malvidin-3-glucoside is the main anthocyanin in grapes and polymerises when aged, forming the red pigment in red wines. The presence of malvidin in archaeological materials may be recognised through alkaline degradation, releasing syringic acid (Guasch-Jané *et al.* 2004; Garnier and Valamoti 2016; Drieu *et al.* 2020). However, blueberries, pomegranates, and a variety of medicinal plants also contain malvidin (Barnard *et al.* 2011; Dall'Asta *et al.* 2012; Huang *et al.* 2014). Furthermore, syringic acid is present in many other products (Ribéreau-Gayon *et al.* 2006;

Srinivasulu *et al.* 2018; Drieu *et al.* 2020) and may be released from other compound sources, e.g. figs (Guasch-Jane *et al.* 2004; Stern *et al.* 2008; Veberic *et al.* 2008). While free syringic acid may be removed from samples, its release from malvidin, derived from another foodstuff, remains an issue to the application of this biomarker.

It is important to note that tartaric acid and phenolic compounds are not markers of fermentation but of fruit products, which may include grapes. Pyruvic and succinic acids are present in fermented grape products and have been identified in archaeological residues (Garnier and Valamoti 2016). However, pyruvic acid is depleted during fermentation and succinic acid is produced by a variety of organisms (Ribéreau-Gayon *et al.* 2006). While methods for the detection of wine are severely limited (Drieu *et al.* 2020), the archaeobotanical evidence proposed by Garnier and Valamoti (2016) supports identification of wine production. Indeed, many studies identifying fermentation rely on the observation of uncommon compounds in association with archaeological evidence, such as macro remains (Garnier and Valamoti 2016), vessel type (Guasch-Jane *et al.* 2004), and associated molecules, e.g. beeswax (McGovern *et al.* 2004).

Indirect evidence of fermentation is potentially identifiable in archaeological material, through the observation of bacterial hopanoids. These compounds are produced by the bacterium *Zymomonas mobilis*, that is believed to have been exploited in the production of alcoholic beverages (Correa-Ascencio *et al.* 2014; Rageot *et al.* 2019a; 2019b). Evolutionary adaptations allow *Z. mobilis* to withstand low pH and ethanol stress encountered during fermentation, with its cell membrane containing the highest abundance of hopanoids presently identified in bacteria (Correa-Ascencio *et al.* 2014). Hopanoids are a common class of compounds present in soils and are regularly assessed during the investigation of bacteria in environments (Quirk *et al.* 1984; Ourisson and Albrecht 1992). Therefore, their utility as a biomarker of fermentation is limited. However, their presence, in association with contextual archaeological data, allows inference of fermentation. For example, the occurrence of hopanoids with resin biomarkers (Correa-Ascencio *et al.* 2014) and in limited vessel types (Rageot *et al.* 2019a). Such interpretation is reliant upon large-scale sampling, although further research is necessary to provide evidence of these compound accumulating in experimental ceramic vessels used for fermentation.

Resins

Resins are water insoluble plant exudates that generally contain a high abundance of di- and triterpenes (Brettell *et al.* 2014), with diterpenes including abietane and pimarane type compounds (Brettell 2015), and triterpenes including oleanane, ursane, lupane, and friedelane type compounds (Burger *et al.* 2009). The occurrence of di- and triterpenes in plants is limited, often to family, due to specific biosynthetic pathways employed in their production. Many species produce these compound classes, yet few do so in high abundance, enabling their use as biomarkers in archaeological contexts (Brettell 2015). The main diterpene producing families are in the order Pinales, of which *Pinaceae* is most relevant to this thesis. Triterpenes are produced by a variety of angiosperms, including *Anacardiaceae*, *Burseraceae*, *Dipterocarpaceae*, *Leguminosae* and *Styraceae* (Burger *et al.* 2009; Brettell *et al.* 2014). Resins are components in the defence mechanisms of many plants, exuded at the site of injury, and have been harvested by humans for numerous purposes, due to their insolubility in water, plasticity, fragrance, aesthetic, and medicinal properties (Burger *et al.* 2011). The term resin should only be used in reference to unmodified materials, with those undergoing anthropogenic thermal alteration being termed either pitch or tar (Connan and Nissenbaum 2003). Resins can be either partially or completely modified by natural and anthropogenic activity, inducing a variety of chemical reactions, although they are relatively resistant to degradation in the burial environment. Degradation products of resins are often distinctive of preservation state, age, and anthropogenic activity (Burger *et al.* 2009; Burger *et al.* 2011; Brettell 2015). Only two resinous products are discussed herein for the sake of brevity and utility in subsequent archaeological interpretations in this thesis. However, it should be noted that extensive exploitation of other resinous products has been reported, including *Pistacia* sp. resin or mastic (Colombini *et al.* 2000; Stern *et al.* 2003; Assimopoulou and Papageorgiou 2005a; 2005b; Brettell *et al.* 2014), frankincense (Mathe *et al.* 2004; 2007; Regert *et al.* 2008; Brettell 2015), copals (Regert *et al.* 2008; Crowther *et al.* 2015), and benzoe/storax (Modugno *et al.* 2006).

Pinaceae (pine, spruce, larch, fir) species produce a diterpenic resin that is commonly used to produce pitches and tars for adhesives and sealants (Colombini *et al.* 2005; Hjulström *et al.* 2006; Romanus *et al.* 2009). The resin primarily comprises abietic and pimaric acids, although they rarely survive in archaeological contexts (Helwig *et al.*

2014). Natural degradation of *Pinaceae* resin results in an increased abundance of dehydroabietic acid and 7-oxodehydroabietic acid (Figure 5), that are employed as biomarkers. These compounds are also produced via protracted heating of the resin, to produce pitch/tar, in addition to retene (Regert 2004). Retene may derive from natural degradation but it is generally only present in low abundance naturally, relative to pitch (Colombini *et al.* 2005). Methyl dehydroabietate may also derive from natural degradation but is more commonly associated with heating resinous wood that releases methanol, which then methylates dehydroabietic acid (Colombini *et al.* 2005). Reactive benzylic positions in dehydroabietic acid may increase its rate of degradation and subsequent loss, with oxygenated functional groups in 7-oxodehydroabietic acid potentially increasing water solubility (Courel *et al.* 2018). These compounds persist in environments over archaeological timescales, especially in areas with dense *Pinaceae* coverage. Therefore, they may be frequent and abundant environmental contaminants (Hjulström *et al.* 2006). Retene is less likely to be a natural contaminant, yet it may be present from the use of *Pinaceae* wood as fuel and is transferred by woodsmoke (Bari *et al.* 2010).

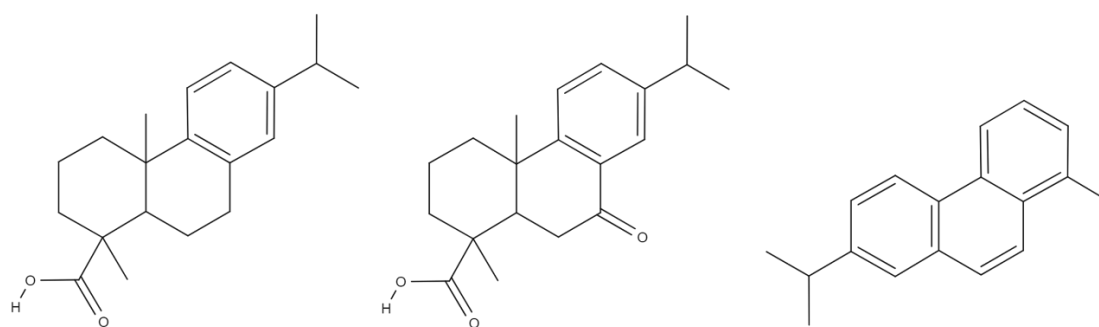


Figure 5. Skeletal structure of dehydroabietic acid (**left**), 7-oxodehydroabietic acid (**middle**), and retene (**right**), detailing degradation from abietic acid in *Pinaceae* resins.

Birch (*Betulaceae*) bark is often subjected to destructive pyrolytic treatment to produce birch bark tar (Urem-Kotsou *et al.* 2002; Regert 2004; Rageot *et al.* 2019c). The fresh exudate primarily comprises betulin and lupeol, although these decrease in abundance, corresponding to an increase of betulone and lupenone, due to oxidative degradation. These products may be formed by either natural or pyrolytic degradation (Regert 2004; Rageot *et al.* 2019c). Compounds exclusive to degraded products include

Lupa-2,20(29)-diene, and others, such as 3-oxoallobetulane, are distinctive of extensive pyrolytic treatment (Courel *et al.* 2018; Rageot *et al.* 2019c). These compounds rarely occur in nature, due to the high temperatures and acidic conditions necessary for their formation. Therefore, they may be employed as biomarkers of anthropogenic processing (Rageot *et al.* 2019c). Rare and unique triterpenoid fatty acyl esters have been observed in archaeological material, resulting from protracted heating of birch bark tar and animal fats. These compounds provide unambiguous evidence of past human activity as they are not present in nature (Dudd and Evershed 1999).

Animal products

In many regions and periods, the exploitation of animals is primarily limited to a narrow range of species, making distinction difficult. Unfortunately, few animal species produce distinctive lipids, that may be utilised as biomarkers, and degradation of lipid profiles, from different animals, generally result in similar residues dominated by ubiquitous fatty acids (Evershed 2008a). The carbon isotope composition of lipids in animals is, in part, derived from diet. However, different biosynthetic and metabolic pathways result in the synthesis of some lipids, producing distinctive $\delta^{13}\text{C}$ values of specific compounds, such as palmitic and stearic acid (Stott *et al.* 1997). Therefore, compound specific carbon isotope analysis is the primary method used by archaeologists to distinguish residues of animal origin. Isotope fractionation is independent of diet; therefore, enrichment and depletion are relative (Stott *et al.* 1997; Craig *et al.* 2005; Roffet-Salque *et al.* 2017b). Modern reference material is primarily derived from C_3 -fed animals and is applicable to most temperate environments. However, this data is less applicable to temperate environments with greater C_4 plant coverage, e.g. North America and China, and in periods when the exploitation of C_4 plants was high.

Aquatic animal products

Distinction between aquatic species is limited due to the absence of specific biomarkers and shared ecology, which limits distinction by isotope analysis. Furthermore, distinctive compounds, present in some aquatic species, are highly susceptible to degradation and are often underrepresented in archaeological residues (Oras *et al.* 2017). Distinction between marine and freshwater resources, via isotopic analysis, is often the limit of distinction, although bulk nitrogen isotope analysis may enable characterisation of

trophic level (Craig *et al.* 2007; 2011; Oras *et al.* 2017). Presently, limited investigation of freshwater resources has been undertaken and there are no well-established criteria for their identification (Heron *et al.* 2015).

Aquatic products contain a high abundance of isoprenoid fatty acids (Figure 6, 4,8,12-trimethyltridecanoic acid (4,8-12-TMTD), 3,7,11,15-tetramethylhexadecanoic acid (phytanic acid), and 2,6,10,14-tetramethylpentadecanoic acid (pristanic acid) (Ackman and Hooper 1968; Lucquin *et al.* 2016a)). However, phytanic and pristanic acid are also present in ruminant animals (Hansel *et al.* 2004; Lucquin *et al.* 2016a). Phytanic acids is produced via the chemical alteration of phytol, a constituent of chlorophyll, in ruminants, zooplankton, and aquatic invertebrates, and may be transmitted through food chains (Lucquin *et al.* 2016a). The relative abundance of two diastereomers of phytanic acid, 3S,7R,11R, 15- and 3R,7R,11R, 15- (SRR and RRR), enables the determination of either aquatic or ruminant origin as the SRR diastereomer is significantly more abundant in aquatic products (mean = 76%). This method of identification has been applied to coastal and inland sites, with corroborating molecular and isotopic investigations, proving its accuracy (Lucquin *et al.* 2016b). However, further research is required to ascertain the abundance of phytanic acid in freshwater species, the alteration and degradation potential of each diastereomer, and the impact of mixed ruminant and aquatic resource processing. Nonetheless, observation of TMTD and a high SRR/RRR ratio provides strong evidence for the processing of aquatic products.

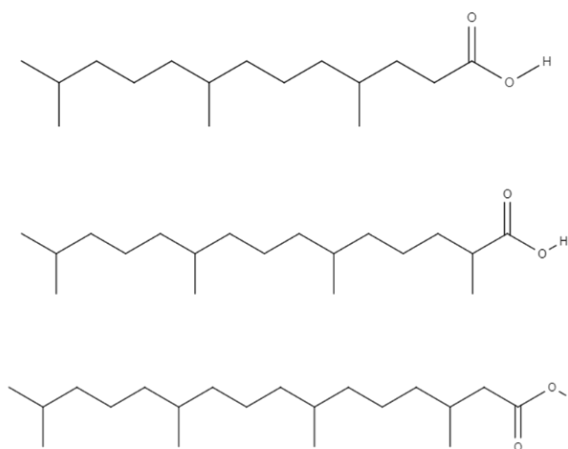


Figure 6. Skeletal structure of 4,8,12-TMTD (top), pristanic (middle), and phytanic (bottom) acids.

Aquatic resources contain a high abundance of long-chain polyunsaturated fatty acids > C₂₀ (Ackman and Hooper 1968). Unsaturated fatty acids may form APAAs during protracted heating; therefore, the presence of > C₂₀ APAAs provides supporting evidence for the processing of aquatic products. However, as plants also contain long-chain unsaturated fatty acids, isoprenoid fatty acids must also be present to attribute > C₂₀ APAAs to aquatic resources (Hansel *et al.* 2004).

When isoprenoid fatty acids are absent, isotope analysis may aid the identification of aquatic resources. The carbon isotope baseline of marine environments is significantly enriched in ¹³C, relative to C₃ terrestrial environments, enabling their distinction in many contexts, although they are not distinguishable when ¹³C enriched, i.e. C₄, plant and terrestrial animal products are also present. Freshwater fish generally produce compound specific δ¹³C values below -30‰, overlapping with C₃ plants and beaver, making their distinction more difficult without supporting evidence. Furthermore, the identification of brackish water species is problematic, due to intermediary δ¹³C values (Craig *et al.* 2007; Oras *et al.* 2017). Bulk carbon isotope values of freshwater and marine organisms are limited to < -28‰ and > -26‰ respectively (Craig *et al.* 2007), although brackish water resources produce intermediary values. Bulk nitrogen isotope analysis enables broad distinction between trophic level, with shellfish and molluscs > 8‰, top carnivores > 18‰, and intermediate species between 11‰ and 16‰ (Craig *et al.* 2007; Yoneda *et al.* 2019). However, depending on the nitrogen isotope baseline of a terrestrial context, and anthropogenic activity, there is potential for higher bulk δ¹⁵N values of some terrestrial animals to overlap lower trophic level marine organisms.

Terrestrial mammals

Terrestrial mammals are divisible into two broad groups, ruminants and non-ruminants, which include wild and domestic species. Non-ruminants are monogastric animals that absorb and synthesise lipids via similar mechanisms. Arguably the most extensively exploited non-ruminant animals are porcine species, including domesticated pigs and wild boar. Feeding experiments demonstrate that pigs synthesise a significant quantity of lipids from whole diet, in addition to the absorption of dietary lipids. As such, the δ¹³C values of porcine C_{16:0} and C_{18:0} fatty acids correspond closely to bulk dietary

carbon, although there is an offset between the two ($\Delta^{13}\text{C} = \delta^{13}\text{C}_{18:0} - \delta^{13}\text{C}_{16:0}$) of $> -1\text{‰}$ (Stott *et al.* 1997; Copley *et al.* 2003).

Ruminant animals, including cattle, sheep, goats, and deer, absorb dietary lipids and synthesise $\text{C}_{16:0}$ and $\text{C}_{18:0}$ de novo. However, they source a greater quantity of $\text{C}_{18:0}$ from the rumen, during the production of adipose fats, which is synthesised by the biohydrogenation of dietary $\text{C}_{18:n}$ (Vernon 1981). Therefore, as lipids are depleted in ^{13}C , $\text{C}_{18:0}$ in ruminant animal adipose is also depleted in ^{13}C , relative to $\text{C}_{16:0}$ in ruminant adipose that is sourced from less depleted compounds. In addition, $\text{C}_{18:0}$ is not synthesised in the mammary gland de novo, requiring greater routing of $\text{C}_{18:0}$ from the rumen and diet in the production of milk. Therefore, $\text{C}_{18:0}$ in dairy fat is further depleted in ^{13}C , relative to $\text{C}_{16:0}$ (Moore and Christie 1981). These two fractionation processes increase the offset between the two fatty acids, below that of porcine products, with $\Delta^{13}\text{C}$ values between -1‰ and -3.3‰ for domestic ruminant adipose and $< -3.3\text{‰}$ for ruminant dairy (Copley *et al.* 2003; Craig *et al.* 2005). However, wild ruminant adipose $\Delta^{13}\text{C}$ values may be $\geq -4.3\text{‰}$, often limiting the identification of dairy fats to those $< -4.3\text{‰}$. Lower $\delta^{13}\text{C}_{18:0}$ values in deer adipose may relate to greater direct routing of the fatty acid from diet, yet this requires further investigation (Craig *et al.* 2012). The SRR/RRR phytanic acid ratio of residues may enable the identification of cheese production when corresponding $\Delta^{13}\text{C}$ values are observed (Lucquin *et al.* 2016a). However, further experiments and analysis is necessary to understand the effects of degradation and mixing on the proportion of phytanic acid diastereomers, in relation to $\Delta^{13}\text{C}$ values of the product. The application of modern dairy $\Delta^{13}\text{C}$ reference ranges requires careful consideration of animal diet. Foddering with high starch and oil rich products disrupts normal synthesis of $\text{C}_{18:0}$ in the rumen, increasing remobilisation of $\text{C}_{18:0}$ from adipose to dairy fats, resulting in dairy $\Delta^{13}\text{C}$ values comparable to ruminant adipose fats (Roffet-Salque *et al.* 2017b). Foddering with products of this nature is unlikely to have occurred in the past, therefore this is not a consideration for the interpretation of archaeological residues.

Molecular analysis does not provide an unambiguous and definitive method of distinguishing ruminant and non-ruminant products. Branched chain fatty acids are observed in ruminant products, potentially enabling their identification, yet they may also be the product of bacterial contamination (Mottram *et al.* 1999). A variety of positional isomers of oleic acid ($\text{C}_{18:1}$) are produced by ruminants but only the Δ^9 isomer is observed

in monogastric animals. Therefore, a residue containing multiple isomers may indicate a ruminant origin, although their absence may result from degradation and not the original components of a residue (Mottram *et al.* 1999). Short chain fatty acids C₄ - C₁₄ may indicate a dairy residue, yet they are susceptible to degradation and loss via water leaching and are infrequently observed in archaeological samples (Dudd *et al.* 1998; Evershed *et al.* 2002). To complicate matters further, the degradation of dairy fats results in a lipid profile resembling ruminant adipose fats, making molecular distinction between the two improbable in many archaeological contexts (Dudd and Evershed 1998).

Beeswax

Beeswax, and the honey it stores, is exploited for a variety of purposes, including illumination, medicine, consumption, and the sealing of ceramic vessels (Evershed *et al.* 1997; Regert *et al.* 2001; Kimpe *et al.* 2002; Parras *et al.* 2015; Rageot *et al.* 2016). While authors have suggested the production of fermented beverages from honey, when beeswax is observed (McGovern and Hall 2016), there is neither molecular nor isotopic evidence to prove such interpretation. Beeswax comprises odd number *n*-alkanes (C₂₁ - C₃₃), with a predominance of odd over even chain lengths, even number FFAs (C₂₂ - C₃₀), and long chain palmitate esters (C₄₀ - C₅₂) (Regert and Rolando 2002; Roffet-Salque *et al.* 2017b). Hydrolytic degradation of wax esters releases abundant free palmitic acid, that is enriched in ¹³C, with the potential to significantly influence compound specific δ¹³C_{16:0} values of mixtures (Evershed *et al.* 1997; Evershed *et al.* 2003). This is critical in AM extraction, as wax esters are hydrolysed. An over-abundance of palmitic acid and long chain alkanes may indicate the presence of waxes in AM extracts, yet small quantities may be misidentified. Therefore, solvent extraction is better suited to the identification of beeswax.

Compound specific carbon isotope mixing models

Theoretical mixing models are employed in the determination of products that contributed palmitic and stearic acids to the formation of a residue and production of δ¹³C_{16:0} and δ¹³C_{18:0} values. Mixing models calculate the δ¹³C_{16:0} and δ¹³C_{18:0} values of a residue by estimating the average abundance and δ¹³C value of each fatty acid in products that contribute to a processed mixture (Woodbury *et al.* 1995; Mukherjee *et al.*

2008). However, the relationship between the proportion of a product processed and its contribution of lipids to a residue is not necessarily linear. Indeed, cooking experiments, analysed via bulk isotope analysis, have demonstrated that different products release compounds in varying quantities and that this release is inconsistent over time (Hart *et al.* 2009). Furthermore, experiments indicate that cereals release a greater quantity of lipids when processed in the presence of a lipid-rich product, i.e. meat (Hamman and Cramp 2018). Therefore, archaeologists must be cautious in the use of mixing models to infer broad culinary trends and use of specific products. It is imperative that experimental research assesses the validity of theoretical mixing models before they are used to address these research areas.

Recent investigation of theoretical mixing models has highlighted that mixing small quantities of C₃ and C₄ plant lipids, with ruminant dairy and adipose lipids, may result in the production of $\Delta^{13}\text{C}$ values indicative of ruminant adipose and dairy lipids respectively (Hendy *et al.* 2018). In addition, it is important to note that a mixture of C₃ plant products and animal adipose cannot produce a $\Delta^{13}\text{C}$ value indicative of dairy. Therefore, in predominantly C₃ plant environments, the identification of dairy is secure, but perhaps less likely to be observed, when vessels are used to process multiple products. However, when C₄ plants are present, $\Delta^{13}\text{C}$ values indicative of dairy are more likely to be observed in mixed use vessels, but this identification is not secure. The validity of this theoretical mixing model requires thorough assessment by experimental investigation.

The interpretation of compound specific carbon isotope data requires careful consideration, as the analysis of region-specific reference material is limited, and few studies have analysed degraded fats, of known origin, for use in interpretation. Models may help archaeologists consider the potential products that contributed to the formation of a residue. However, the observation of biomarkers is necessary to confidently identify specific products.

Conclusion

This chapter provides a comprehensive summary of the principles that underpin the investigation, identification, and interpretation of archaeological organic residues. This knowledge has been applied to various studies of archaeological material, with the

aim of elucidating past culinary and dietary traditions (Lee-Thorp 2008; Evershed 2008b). Indeed, integration of organic residue data, with established ceramic studies, has provided a means to further understand the uses, significance, movement, and chronology of specific products and vessel types on local and regional bases (Roffet-Salque *et al.* 2017a; Whelton *et al.* 2018; Rageot *et al.* 2019a). As such, these methods are applied to the investigation, identification, and interpretation of experimental and archaeological materials throughout this thesis.

Chapter 3: The domestication and translocation of *Panicum miliaceum* in Northern Eurasia

Introduction

This chapter presents the material theme of this thesis, outlining both the botanical and archaeological context of *Panicum miliaceum*, which is the focus of research questions posed in Chapter 1. This chapter begins by providing a definition of millets, demonstrating their geographic and taxonomic range, before focusing on the two earliest and dominant Asian millets, *P. miliaceum* and *Setaria italica*. The methods employed in identifying these morphologically similar species is subsequently provided, before the domestication history of *P. miliaceum* is summarised. The spread of *P. miliaceum* throughout Eurasia is then detailed, with the timing, rate, and mode of uptake discussed. The question of why this species was translocated beyond its domestication centre is discussed, and supporting evidence is provided, after outlining initial exchanges of Eastern and Western Neolithic cultures. A critical assessment of the methods employed in the identification of *P. miliaceum* presence is conducted throughout this chapter with the aim of presenting archaeological material and theories more accurately than in previous publications. This chapter concludes by considering the relative strengths of ORA in identifying and characterising the presence of *P. miliaceum* in archaeological materials.

What is a millet?

Millet is a common term applied to numerous small caryopsis cereals of a broad genetic and geographic origin. Millet caryopses are generally smaller than wheat, barley, oats, rice, and maize. *Sorghum* spp. may be referred to as a millet, despite producing large caryopses. Taxonomically, the term millet includes species primarily in the Panicoid sub-family and Paniceae tribe, but species are also present in the Chloridoid subfamily. Millets have been cultivated and domesticated on almost all continents where prehistoric agriculture was practiced, with the possible exception of Europe, incorporating at least 18 species (Weber and Fuller 2008).

Hairy crabgrass (*Digitaria sanguinalis*) is a millet species native to Europe, yet there is limited evidence for its cultivation in prehistoric contexts and it was not

domesticated (Weber and Fuller 2008). Non-native domesticated millet species, present in prehistoric European contexts, include *P. miliaceum* and foxtail millet (*Setaria italica*).

Genetic analysis has identified the wild progenitor of *S. italica* as *Setaria viridis*, a wild grass species native to Eurasia, with morphological differences between the two species identified in caryopses, starches, and phytoliths (Weber and Fuller 2008; Lu 1998; Hunt *et al.* 2008; Zhang *et al.* 2011; Yang *et al.* 2012a). *P. miliaceum* is an allotetraploid cereal containing genetic material from multiple ancestors, none of which have been conclusively identified (Hunt *et al.* 2018). Indeed, the wild ancestor(s) of *P. miliaceum* may be extinct. A weedy form of *P. miliaceum* is present throughout Eurasia and may harbour ancestral variants of the species. However, it is not certain whether the weedy form is present by either descent from a common wild ancestor, feral mutation of cultivated forms, or introgression between wild and domesticated forms, as there is no reproductive isolation between forms (Hunt *et al.* 2014; Xu *et al.* 2019). Accessions of millets are not well represented in seedbanks, relative to other major domesticated cereals, necessitating further fieldwork and laboratory analysis to determine the ancestry of this species (Hunt *et al.* 2014; 2018).

Early publications proposed a European domestication centre for *P. miliaceum* and *S. italica*, due to their occurrence in Neolithic contexts (Zohary *et al.* 2012). However, recent radiocarbon dating programmes have demonstrated that both species originated in China (Leipe *et al.* 2019; Filipovic *et al.* 2020), where there is substantial supporting evidence for domestication (Zhao 2011; Hunt *et al.* 2018; Leipe *et al.* 2019; Xu *et al.* 2019). As such, European Neolithic observations of these species are deemed erroneous and are not discussed in this chapter.

Identification of *P. miliaceum* and *S. italica*

Macro remains

Differentiation between *P. miliaceum* and *S. italica* caryopses is complicated by similarities in their shape, size, and colour, yet subtle morphological differences exist among mature modern reference material (Figure 7). Analysis of immature reference material demonstrates consistency in morphological traits during caryopsis development (Motuzaitė-Matuzevičiūtė *et al.* 2012; Song *et al.* 2013). However, immature *S. italica* caryopses may be confused with small-grained wild *Digitaria* and *Setaria spp.*, which has

potentially resulted in their overrepresentation in archaeobotanical assemblages. Indeed, immature *S. italica* may even resemble *P. miliaceum* (Song *et al.* 2013).

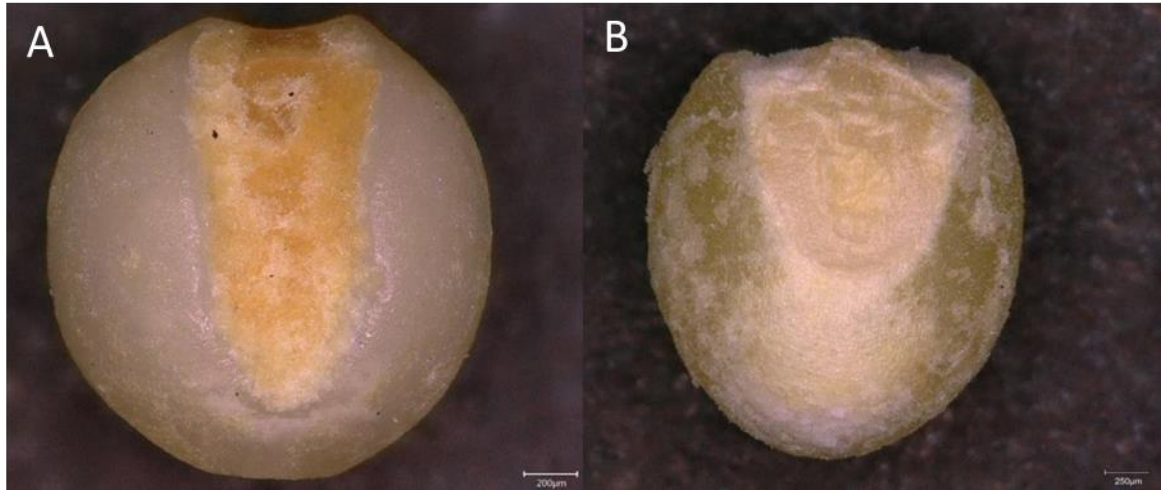


Figure 7. Microscope image in plan of *Setaria italica* (A) and *Panicum miliaceum* (B).

In archaeological contexts, the primary mode of plant remain preservation is carbonisation. However, carbonisation often results in the alteration of morphological characteristics, severely limiting interpretive potential, and in many instances leads to the complete loss of material. During carbonisation, expanding starch breaks through the surface of millet caryopses, potentially destroying characteristic features. The degree of damage incurred differs between species and is dependent upon both temperature and exposure time. Under oxidising conditions, *P. miliaceum* carbonises between 225°C and 400°C over one hour, and 225°C and 335°C over four hours. The carbonisation range of *S. italica*, under oxidising conditions, is between 220°C and 500°C over one hour, and 220°C and 400°C over four hours (Märkle and Rösch 2008). Carbonisation under reducing conditions generally increases the temperature and exposure time a caryopsis can withstand before total loss of morphological characteristics (Boardman and Jones 1990), and *S. italica* demonstrates a marginal increase in these factors. However, a decrease in temperature range is observed in *P. miliaceum*, under reducing conditions, with carbonisation occurring between 270°C and 325°C over one hour, and 245°C and 315°C over four hours (Märkle and Rösch 2008). Both millet species have a lower chance of successful carbonisation than other cereals, due to limited temperature ranges, and *P. miliaceum* is least likely to carbonise successfully (Märkle and Rösch 2008). Compounding

this issue further is that mature *P. miliaceum* caryopses (> 16 days) are completely destroyed at high temperatures and immature caryopses (< 8 days) are friable after carbonisation, to the point that any mechanical action destroys them (Motuzaitė-Matuzevičiute *et al.* 2012). Conversely, immature *S. italica* caryopses carbonise under the same conditions as mature caryopses (Walsh 2017). As both species produce a high percentage of immature caryopses, this is liable to have a detrimental impact on *P. miliaceum* survivability in the archaeological record. It is possible that the underrepresentation of *P. miliaceum* in archaeological contexts is the result of these factors (Märkle and Rösch 2008).

Mechanical action is only briefly referenced here but is no less important in the survivability of small and fragile caryopses during deposition over archaeological timescales (Märkle and Rösch 2008; Weber and Fuller 2008). Indeed, the small size of these grains is an important factor in their limited recovery across archaeological sites, with the recent application of flotation only now increasing their recovery (Weber and Fuller 2008; Marinova and Valamoti 2014). Millet caryopses are easily transferred through and between archaeological contexts, due to their size, and are a common intrusive species in earlier periods than they were actually present (Motuzaitė-Matuzevičiute *et al.* 2013). Formation, preservation, recovery, and identification factors discussed limit an accurate assessment of millet presence, specifically of *P. miliaceum*, in archaeological contexts. Furthermore, variation in these factors across regions prevents supra-regional assessments of millet dispersal, highlighting the limitations of archaeobotanical analysis (Marinova and Valamoti 2014; Brite *et al.* 2017).

In the absence of carbonised macro remains, millet caryopses may be 'preserved' as impressions in ceramics, a feature that has been commonly described in archaeological material (Bakels *et al.* 2003; Moskal-del Hoyo *et al.* 2017; An *et al.* 2019). To accurately assess ceramic impressions, casts must be taken, using either silicone or plasticine, and assessed by microscopy, although this has been infrequently applied to archaeological material. Neither casting material is perfect, as silicon does not always retain subtle characteristics and plasticine is liable to be damaged after casting, removing some subtle characteristics. However, it is possible to obtain a cast capable of differentiating *P. miliaceum* and *S. italica* caryopses from both materials. Impressions may preserve the shape and size of the seed, hilum, and embryo, in addition to surface patterns.

Micro remains

The analysis of plant macro remains, including phytoliths and starch grains, enables the identification of millet species with varying degrees of accuracy. Intra species variation and inter species overlap of phytoliths, and to a greater extent starch grains, limits the interpretive potential of individual micro remains. Furthermore, genetic and environmental factors have a detrimental impact on the study of these materials. For instance, Zhang *et al.* (2011) identified morphological differences between phytoliths of Chinese, Eastern European, and French varieties of *S. italica*, necessitating further analysis of reference material. Indeed, limited assessment of regional varieties of millet species hinders accurate analysis of archaeological phytoliths (Dal Corso *et al.* 2017). Environmental stress and harvesting before full maturation negatively impact the size and morphology of starch grains, yet the range of morphological change requires further analysis before they are accurately considered in microbotanical studies (Yang *et al.* 2012a). Therefore, unambiguous results require an assemblage-based assessment of macro remains, yet these results should be treated with caution in Europe, where fewer studies of local reference material have been conducted (Zhang *et al.* 2011; Yang *et al.* 2012a).

Criteria employed in the identification of millet microremains are not presented in this section as they are not applied in this thesis. Furthermore, few microbotanical studies, focusing on millet, have been conducted beyond China and are, therefore, of limited application to this study. The discrimination between *P. miliaceum*, *S. italica*, and other millet species phytoliths is discussed in detail by Lu *et al.* (2009a), Out and Madella (2016), and Weisskopf and Lee (2016). Importantly, criteria have been established to discriminate between phytoliths of *S. italica* and *S. viridis* (Zhang *et al.* 2011). Less stringent criteria have been described for the distinction between *P. miliaceum*, *S. italica*, and *S. viridis* starch grains by Yang *et al.* (2012a). These criteria rely more heavily on the relative abundance of starch grains of varying size, which are more susceptible to change depending on growing and harvesting conditions.

Molecular and isotopic analysis

Archaeobotanical studies may determine the presence of a species at a site. However, they do not necessarily provide evidence for the extent of cultivation,

processing, and consumption. Molecular analysis of sediments and soils enables the identification of millet cultivation at a localised scale (Jacob *et al.* 2008a; 2008b; 2009; Bossard *et al.* 2011; 2013) and may allow direct radiocarbon dating of molecular markers (Courel *et al.* 2017). In addition, molecular analysis of ceramic residues is an established method of assessing patterns of food product processing. By combining traditional archaeological and molecular analysis of ceramics it is possible to establish relative chronologies, patterns in use, and extent of exploitation of *P. miliaceum* (Ganzarolli *et al.* 2018; Rageot *et al.* 2019a; 2019b). Finally, isotopic analysis of human and animal remains enables inference of diet, although, the sensitivity of isotopic techniques is low and assigning dietary range to only two variables may result in ambiguous results (Lee-Thorp 2008). The biological and chemical principles of molecular and isotopic analysis are presented in Chapter 2, along with a discussion of methods employed in the identification of *P. miliaceum*. No biomarker has been identified for *S. italica*. Both *P. miliaceum* and *S. italica* are C₄ plants that are enriched in ¹³C and are indistinguishable by isotopic analysis.

Domestication of *P. miliaceum* in China

Archaeologists have concluded that *P. miliaceum* was domesticated in China (Motuzaitė-Matuzevičiūtė *et al.* 2013; Wang *et al.* 2017; Leipe *et al.* 2019). However, the origin of domestication in China remains a contentious issue, primarily due to controversial microbotanical studies with methodological limitations and ambiguous chronologies (Zhao 2011; Leipe *et al.* 2019). Yang *et al.* (2012b) propose the earliest evidence for *P. miliaceum* processing at the sites of Nanzhuangtou (10th/9th millennium BC) and Donghulin (9th/8th millennium BC), via the observation of starch grains associated with grinding tools (Figure 8). However, intra- and inter-species variation, environmental conditions, and the harvesting of immature caryopses are cited as potential issues in concluding domesticated *P. miliaceum* processing at these sites (Zhao 2011), in line with those discussed in the preceding section on microbotanical remains. Phytoliths derived from *P. miliaceum* are observed in late occupation phases at Donghulin, potentially corroborating a *P. miliaceum* identification of starch grains (Yang *et al.* 2012b). However, limited sampling of both domestic and wild *P. miliaceum* variety phytoliths, in addition to wild *Panicum spp.* phytolith sampling (Lu *et al.* 2009b; Zhao 2011) makes such conclusions unwise. Long-term trends in starch grain size and morphology at Nanzhuangtou and

Donghulin potentially indicate progress towards domestication at the two sites, yet the starch grain assemblage size is too small to accurately assess long term change (Yang *et al.* 2012b).

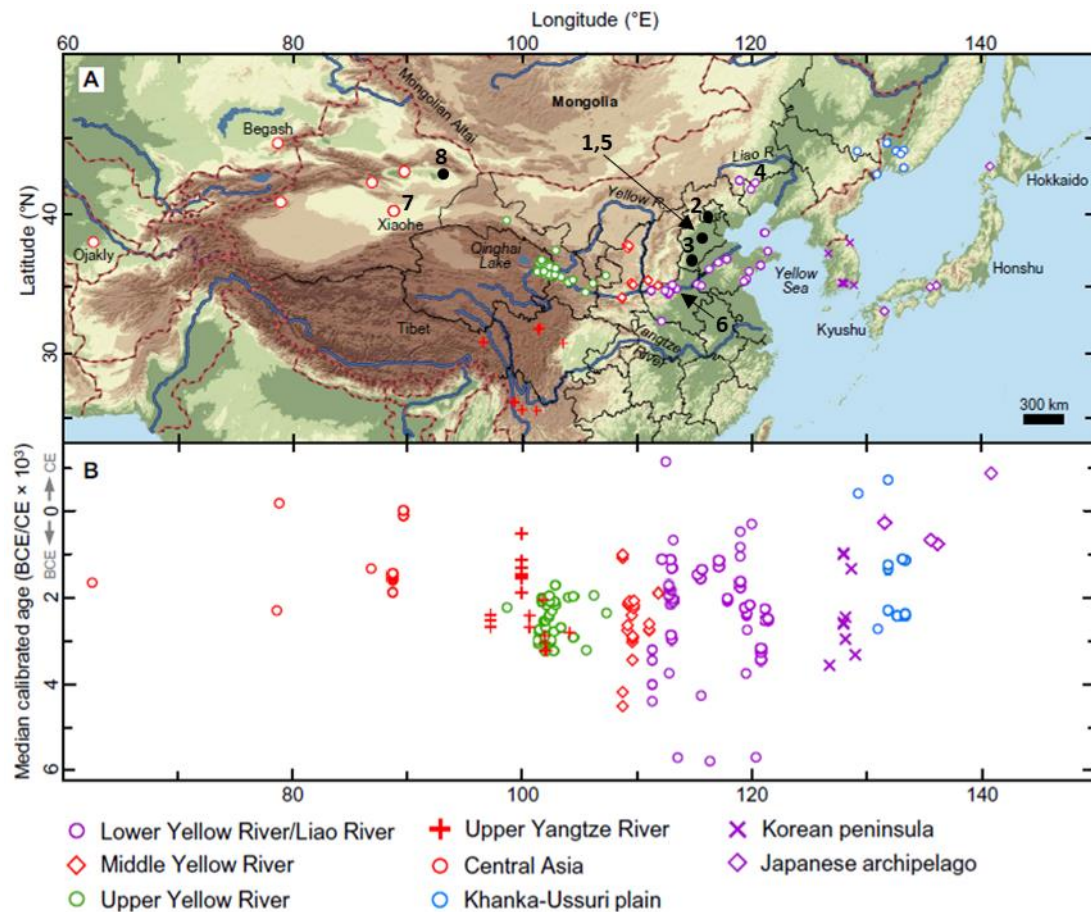


Figure 8. Spatiotemporal distribution of 184 directly dated millet remains from Central and East Asia organised by region, in addition to sites presenting early microbotanical evidence for *P. miliaceum*, including: 1 Nanzhuangtou, 2 Donghulin, 3 Cishan, 4 Xinglonggou, 5 Yuezhuang, 6 Zhuzhai, 7 Xiaohe, 8 Tianshanbeilu. **A** Topographical location. **B** Longitudinal distribution of median dates (Leipe *et al.* 2019 2).

The site of Cishan, North China, has perhaps produced the earliest directly dated evidence of *P. miliaceum*, with phytoliths and miliacin detected in samples from storage pits. According to archaeological reports, macrobotanical remains were observed in the storage pits but rapidly oxidised to ash and were too friable for microscopic analysis. The earliest of the ash samples analysed were dated to 8300-6700 cal BCE (Lu *et al.* 2009b). However, in the absence of clearly defined domestication traits, it is not possible to determine whether the evidence for *P. miliaceum* at Cishan represents either cultivation or domestication. Furthermore, a series of issues in the excavation and sampling

chronology, in addition to the dating programme, raise serious doubts over the accuracy of these results (Zhao 2011). The most accurate method of determining *P. miliaceum* presence is via traditional archaeobotanical analysis of macro remains.

The earliest directly dated domesticated *P. miliaceum* caryopses are from the site of Yuezhuang, in the Lower Yellow / Liao River Region of China, ca. 5779 cal BCE. Two other sites in this region, Zhuzhai and Xinglonggou, produced similarly early dates of ca. 5695 and 5690 cal BCE respectively (Leipe *et al.* 2019). Indeed, radiocarbon dating of 184 Central/East Asian domesticated millet caryopses identify the Chinese Fertile Crescent (CFC), at the lower reaches of the Yellow and Liao Rivers, around the Bohai Sea (Figure 8), as the centre of millet domestication in China ca. 6100-5700 BCE, median 5800 BCE (Leipe *et al.* 2019). From the CFC, millet agriculture spread West to the Middle Yellow River Region ca. 5000-4000 BCE, median 4600 BCE, and into the Upper Yellow River Region ca. 3400-3000 BCE, median 3200 BCE. The SW spread of millet, from the Middle Yellow River Region to the Upper Yangtze River Region, occurred ca. 3700-3100 BCE, median 3400 BCE. Presently, radiocarbon dates demonstrate a significant delay in the first appearance of millet in high altitude upper river regions of China, for which anthropogenic and environmental factors are potential explanations (Leipe *et al.* 2019).

Presently, few millet caryopses from the Xinjiang Region of West China have been directly radiocarbon dated (Figure 8). The earliest occurrence of *P. miliaceum* in this region is ca. 1615 cal BCE, at the site of Xiaohe, although an unidentified domesticated millet caryopsis from the site was dated to ca. 1886 cal BCE (Flad *et al.* 2010; Leipe *et al.* 2019). Radiocarbon dates of *P. miliaceum* caryopses from Xinjiang are later than the earliest directly dated material in Central Asia (Frachetti *et al.* 2010; Spengler *et al.* 2018) and significantly later than the earliest evidence for C₄ plant consumption in Central Asia (Hermes *et al.* 2019). Furthermore, direct radiocarbon dating of early wheat caryopses in the Lower Yellow River Region demonstrate links between East and Central Asian communities from ca. 2600 cal BCE (Long *et al.* 2018). Millet and wheat appear to have spread along the Altai Mountains and the Southern Mongolian Plateau, bypassing Xinjiang and Upper and Middle Yellow River communities, in the third millennium BCE (Long *et al.* 2018; Leipe *et al.* 2019). The later appearance of wheat in Xinjiang ca. 1900 cal BCE, and late arrival of millet, attest to this theory. However, there are currently no directly dated millet finds along the Altai Mountains and there is limited direct

radiocarbon dating of caryopses in the Xinjiang Region, warranting caution in discounting the role of Xinjiang communities in the spread of millet into Central Asia.

It is important to note, for the sake of future discussion, that the first appearance of millet across sites in China did not result in a complete shift in carbon isotope values of humans (Liu *et al.* 2012; Wang *et al.* 2017). In fact, during the second millennium BCE, several thousand years after the introduction of millet, communities in the Upper Yellow River and Xinjiang regions demonstrate mixed C₃ and C₄ diets (Figure 9, Wang *et al.* 2017). This demonstrates that an automatic, large-scale shift in isotope values should not be expected as millet is translocated, even in its domestication centre. Whether this is more significant in communities either transitioning to or with established Neolithic agriculture is debatable and discussions must consider the lifeways of the communities being assessed. Furthermore, the insensitivity of isotopic analysis of human bone collagen is an important factor that must be considered in assessing these data.



Figure 9. Distribution of human isotope studies demonstrating the spread and extent of millet consumption across Central and East Asia in the second millennium BCE. The figure indicates that many Central Asian communities did not consume significant quantities of *P. miliaceum*, even a thousand years after its introduction, although limited evidence could also reflect the limitations of isotope analysis in identifying C₄ cereal consumption (Wang *et al.* 2017 1029).

The sporadic increase in carbon isotope values of individuals across western China raises questions of the importance of millet in terms of subsistence, economy, and culture. Exemplifying these questions is a single individual, among 120 analysed, at the cemetery of Tianshanbeilu, Xinjiang Region, that demonstrates a predominantly C₄ diet. The individual dates to the period of millet introduction to the region, ca. 1850 cal BCE, and is significantly isotopically isolated, in carbon and nitrogen, from other individuals at the cemetery (Wang *et al.* 2017). There is no evidence to suggest this individual was either high or low status, or that they were a migrant from millet consuming communities to the east. Therefore, each option must remain a consideration.

Why move starchy cereals?

Current archaeological evidence indicates that the Neolithic complexes of East and West Asia converged between East Kazakhstan and the Xinjiang Region of China in the third millennium BCE. Interactions between Neolithic complexes resulted in the dispersal of plants, specifically starchy cereals, among communities that already possessed similar products. As plants are moved beyond their natural habitat, they are exposed to novel environmental pressures, including exposure to water, heat, oxygen, and light. Conditions may, to some degree, be managed by humans but seasonal fluctuations present a significant barrier to plant growth (Jones *et al.* 2016). Furthermore, the introduction of new crops interrupts the farming cycles of communities, with western and eastern cereals requiring different management strategies (Liu *et al.* 2019). As such, new cereals are not merely a new foodstuff but a new way of life, seasonal patterns are disrupted, and management strategies are changed. Introduced cereals are neither passive nor mundane and the significance of their movement has resulted in considerable debate from which one question arises. If these communities already possessed starchy cereals, why did they adopt another?

The motives for incorporating a new plant into established agricultural systems have been summarised into three categories, ecological opportunism, economic principles, and cultural identity (Jones *et al.* 2011). The categories are not mutually exclusive and are subject to spatial and temporal variation (Boivin *et al.* 2012). Indeed, ecological niches between sites may influence the exploitation of plants on a highly localised basis (Lightfoot *et al.* 2013).

Ecological opportunism may be applied in two modes, intensification and diversification, both of which may relate to an increase in surplus for either economic gain or risk management (Jones *et al.* 2011; Marston *et al.* 2011). The objective of intensification is to increase the production yield of land, in a given area accessible to a farmer, and may be achieved by either increasing yields per unit of land or the number of units of land exploited in the given area, without diversifying the plant species exploited. For instance, high yield, intensively managed crops enable the former, and lower yield, less intensively managed crops may enable the latter. Furthermore, the selection of a single crop with rapid maturation may enable two consecutive harvests within a growing season. Anthropogenic activities, such as manuring and water management, are also methods of intensification. It is important to note that intensification systems result in a single dominant crop. Diversification achieves similar objectives to intensification, through spatial and temporal changes in land use, by growing multiple crops. For instance, it may be possible to exploit new areas of accessible land by selecting a crop with a specific tolerance to environmental pressures. Furthermore, multi-cropping may enable the harvest of two different crops on the same unit of land, over a yearly cycle, exploiting maturation rates and seasonal fluctuations in environmental conditions. Diversification results in a broader range of species exploited but may still produce a dominant crop, depending on the method and extent to which it is applied. In discussing ecological opportunism, consideration must also be given to the exploitation of domesticated animals and wild resources. The intensification and diversification methods discussed may enable increased production of fodder and the ability to more easily access seasonal resources, which have the potential to significantly impact overall subsistence strategies (Jones *et al.* 2011; Marston *et al.* 2011).

P. miliaceum has the shortest growing season (60-90 days) and, combined with inherent drought and high temperature tolerance, the lowest water requirement of any cereal. The plant may be cultivated in low nutrient, marginal soils, without the need for intensive management and ploughing (Hunt *et al.* 2011; Miller *et al.* 2016; Wang *et al.* 2017). These qualities enable the incorporation of *P. miliaceum* into a variety of agricultural systems seeking to intensify and diversify agricultural output. Rapid maturation and low intensity management are especially beneficial to mobile pastoral groups. Furthermore, the rapid maturation of *P. miliaceum* enables cultivation in

previously unsettled regions with narrow optimal growth seasons (Jones *et al.* 2011; Miller *et al.* 2016; Spengler *et al.* 2016).

Jones *et al.* (2011) argued that ecological opportunism was the driving factor in the spread of *P. miliaceum* across Eurasia. However, Boivin *et al.* (2012) suggest that the delay between evidence for the first appearance and large-scale adoption of *P. miliaceum* across many Eurasian sites is indicative of either its employment as a low-level risk mitigation crop, or, more likely, a crop with economic and cultural significance. Boivin *et al.* (2012) argue that if *P. miliaceum* was introduced primarily for subsistence it would appear in greater frequency and abundance than the current archaeological record indicates. However, such an assessment assumes that current archaeological reports are both accurate and comprehensive, which they are not. This is especially true of Central Asian sites and among pastoral communities that inhabited the Eurasian Steppe (Spengler *et al.* 2016; Hermes *et al.* 2019). Nonetheless, economic and cultural factors are an important consideration in the movement of new crops.

New products may be adopted for curiosity, pleasure, and value beyond economic importance. The diversification of food culture, in periods when there is little diversity of food product processing, is perhaps understated in archaeology (Boivin *et al.* 2012). Therefore, the current perception of cereals as mundane is not necessarily applicable to past cultures. In prehistoric periods, a new cereal may be comparable to the extraordinary features of spices. Furthermore, discussing a plant product in isolation, without considering related processing and consumption practices, ignores a large part of cultural interaction and significance of food (Sherratt 1991; Valamoti *et al.* 2019).

The economic and cultural value of crops are, in some instances, difficult to separate, with complimentary and contradictory values bestowed upon similar products (Boivin *et al.* 2012). New products are often associated with social prestige due to their exotic nature, rarity, and expense, with elite groups drawing in these products to regions and specific sites. Generally, these factors are related to unessential products of little subsistence value, and not cereals that are easily produced in higher quantities. However, incorporation of introduced cereals into established ceremonial, medicinal, and high-status activities, alongside other important and exotic products, may establish significance by association (Boivin *et al.* 2012). The observation of such products within ceremonial and high-status contexts may indicate their economic and cultural significance

to elite groups (Jones *et al.* 2011). However, it must not be assumed that elite groups are the driver of crop introduction and adoption, as a new plant may be perceived as less desirable than established crops. Adoption of new crops by low-status individuals may be driven by high yields being achieved on small and marginal lands and the low economic cost of the crop. The rigidity of elite groups, to economic and cultural norms, and the perception of lower-class tastes may result in initial rejection, yet persistent interaction with low-status groups can result in eventual adoption by elites (Liu and Jones 2014). In either instance, the crop is of cultural significance among certain aspects of communities. The observation of new crops in either centre or periphery sites may enable distinction between introduction processes, and chronological studies may demonstrate adoption processes.

Whether *P. miliaceum* was adopted across Eurasia by the economic and cultural scenarios detailed is considered throughout the following discussion, yet the topic requires thorough investigation beyond the scope of this thesis. It is important to consider that the motive for introduction is not necessarily the same motive for adoption and continued exploitation of a crop. Furthermore, economic and cultural values are subject to significant spatiotemporal change. Therefore, the motives for the introduction and adoption of a crop at one site is not necessarily comparable to another.

***P. miliaceum* in Central and West Asia**

The archaeobotanical record of Central Asia is sparse and macro remains are often observed in fortuitous contexts, i.e. burials, rather than established settlements. Generally, northern communities in Central Asia focused on pastoral subsistence supplemented by wild and domesticated plant and animal resources. Observations of domesticated plants within these northern regions are disputed in earlier periods and authors have questioned the importance of domesticated crops, especially *P. miliaceum*, prior to the end of the second millennium BCE (Ventresca-Miller *et al.* 2014; Lightfoot *et al.* 2015a; Motuzaite-Matuzeviciute *et al.* 2015; Spengler *et al.* 2016; Dong *et al.* 2017; Wang *et al.* 2017). However, the extent of material formation and preservation among mobile pastoral communities, with small deposits scattered across large areas, has been questioned, providing a potential explanation for limited observations of plant cultivation (Jones *et al.* 2011; Spengler *et al.* 2014a; 2016; Hermes *et al.* 2019). Furthermore, limited

archaeological investigations have been conducted in the region to date (Spengler *et al.* 2016). Recently published research from this region has substantially altered perceptions and pushed back introduction chronologies by hundreds of years (Spengler *et al.* 2018; Hermes *et al.* 2019), yet substantial research remains to be undertaken.

The earliest directly dated *P. miliaceum* caryopsis in Central Asia is from the site of Begash, East Kazakhstan, ca. 2390 cal BCE (Frachetti *et al.* 2010). However, faunal and human isotopic evidence from Begash and two regional sites, Tasbas and Dali, demonstrate significant exploitation of C₄ plants, most likely cultivated *P. miliaceum*, from ca. 2700 cal BCE (Hermes *et al.* 2019). The faunal dataset demonstrated significant ¹³C enrichment, depending on species, individual, and season of slaughter, yet a single human individual analysed from Dali, ca. 2635 cal BCE, demonstrated only minor ¹³C enrichment ($\delta^{13}\text{C} = -17.6\text{‰}$, Narasimhan *et al.* 2019). Further analysis is necessary to understand the role and significance of *P. miliaceum* among these communities, specifically whether the cereal was consumed directly by humans or exclusively used as a fodder crop.

The Eurasian Steppe provides a direct route between East Kazakhstan and the earliest directly dated *P. miliaceum* finds in Europe. It is known to have been a route of cultural exchange in later periods, yet it is debated as to when these exchanges began (Narasimhan *et al.* 2019). Isotopic enrichment, potentially indicating *P. miliaceum* consumption, is not observed in West Kazakhstan until ca. 1600 BCE, at the site of Vodokhranilische. However, this reflects the current state of archaeological research in this region and not necessarily the absence of millet. Two individuals from the MBA (ca. 2100-1700 BC) site of Bestamak, N Kazakhstan, demonstrate minor isotopic enrichment, are isotopically separated from the community, and are buried with atypical grave goods, potentially indicating the early movement of *P. miliaceum*, across the Eurasian Steppe, from sites such as Kanai (Ventresca-Miller *et al.* 2014). However, the individuals from Bestamak post-date the southern movement of *P. miliaceum* and there is limited additional evidence for this species in North Kazakhstan. Furthermore, there is no evidence to suggest that *P. miliaceum* was introduced to the NE Caucasus from Kazakhstan.

The prevailing theory for the westward movement of *P. miliaceum* in Central Asia is via the Inner Asian Mountain Corridor (IAMC). The IAMC is an important route of

cultural, material, and genetic exchange, prior to the third millennium BCE (Spengler *et al.* 2014b; Ventresca-Miller and Makarewicz 2019; Narasimhan *et al.* 2019), that potentially established an exchange framework for *P. miliaceum*. A significant node of *P. miliaceum* cultivation, consumption, and perhaps exchange in the IAMC is the Murghab Alluvial Fan region of Turkmenistan. The earliest evidence for *P. miliaceum* in the Murghab region is a directly dated caryopsis from the mobile pastoralist site of Adji Kui 1, ca. 2117 cal BCE (Spengler *et al.* 2018). The date of this find corresponds to isotopic enrichment of two human individuals from the nearby sedentary site of Gonur, ca. 2060 cal BCE (Narasimhan *et al.* 2019). The observation of *P. miliaceum* impressions in a ceramic sherd from Gonur provides further evidence for the prominence of the species (Bakels 2003). The caryopsis from Adji Kui 1 is, presently, the second earliest in Central Asia, predating the previous second-earliest seed, from Ojakly ca. 1660 cal BCE, by approximately 500 years. These two samples represent the westerly extent of published directly dated evidence of *P. miliaceum*, before its earliest appearance in Europe. There is limited evidence to suggest the route by which *P. miliaceum* was translocated from the Murghab region and into Europe. Two potential routes include south and west, through Turkey, and south and north, through the Caucasus.

There are no published early direct dates of *P. miliaceum* caryopses from Turkey. Furthermore, archaeobotanical and isotopic datasets currently suggest that *P. miliaceum* was not present in the region until the end of the second millennium BCE (Nesbitt and Summers 1988; Hunt *et al.* 2008; Ramaroli *et al.* 2010; Marston *et al.* 2011; Lightfoot *et al.* 2013; Miller 2015; Miller *et al.* 2016; Irvine 2017; Irvine *et al.* 2019; Karakaya 2019; Ventresca-Miller and Makarewicz 2019). However, due to the limited spatial and temporal range of these studies, the introduction of *P. miliaceum* to Europe, from Turkey, cannot be discounted. A significantly greater number of studies are necessary to accurately investigate the presence of *P. miliaceum* in this region during the second millennium BCE.

P. miliaceum caryopses found in EBA contexts at sites in the Caucasus have been directly radiocarbon dated but demonstrated later intrusion from LBA and EIA activity (Herrscher *et al.* 2018a). A single *S. italica* seed reportedly dated to the MBA, although the identification of this sample is questionable and is perhaps a wild *Setaria* spp. (Herrscher *et al.* 2018b). These radiocarbon dates have not been satisfactorily reported

and published, preventing an accurate understanding of *P. miliaceum* presence in this region. As such the earliest directly dated *P. miliaceum* caryopsis in the Caucasus is from the site of Guamsky Grot, ca. 1010 cal BCE (Trifonov *et al.* 2017). Isotopic analysis demonstrates significant ^{13}C enrichment from the LBA/EIA, ca. 1100 BCE, corresponding to the current chronology of directly dated caryopses (Hollund *et al.* 2010; Trifonov *et al.* 2017; Herrscher *et al.* 2018a). A small dataset from Klin-Yar cemetery suggests that animals did not consume *P. miliaceum*, at the time of its introduction, whereas humans did (Higham *et al.* 2010). However, further research is necessary to understand the exact nature and significance of direct *P. miliaceum* consumption among this community, i.e. whether cultural, social, or subsistence practices effect its use.

Presently, it is not possible to develop on either the timing, direction, rate, or significance of *P. miliaceum* translocation in Central and West Asia. Extensive archaeobotanical, isotopic, and molecular studies, corroborated with direct radiocarbon dates, are necessary to understand the presence and uses of *P. miliaceum* in these regions. Indeed, until detailed studies have been conducted in Turkey and the Caucasus, it will be difficult to identify the route by which *P. miliaceum* entered Europe.

***P. miliaceum* in Europe**

The timing of *P. miliaceum* introduction to Europe is a contentious issue, with some authors presenting questionable evidence (e.g. Kučera *et al.* 2019) that contradicts the current Eurasian translocation chronology. Recent European radiocarbon dating programmes, incorporating over 100 measurements, demonstrate that early (Neolithic) observations of *P. miliaceum* caryopses derive from later intrusion (Motuzaite Matuzeviciute *et al.* 2013; Filipovic *et al.* 2020). Earlier dates of samples in more westerly European regions, gaps in the Central Asian chronology, and limited sampling in Eastern Europe (Figure 10), present some uncertainty as to the exact timing of *P. miliaceum* introduction to Europe. It is important to note that earlier European dates will almost certainly be reported in the future as sampling increases.

The present European radiocarbon dataset indicates the arrival of *P. miliaceum* in Ukraine prior to 1500 cal BCE, followed by a rapid spread to the Carpathian Basin and Northern Italy in the 16th century BCE (Figure 11). Further analysis is necessary to improve the accuracy of this chronological framework, particularly in areas with limited sampling,

yet the radiocarbon dataset provides a means of calibration for other evidence strands that are often open to uncertainty in dating. Firstly, however, contentious early evidence is briefly discussed and discounted.



Figure 10. Sample location of all directly dated early European millet caryopses, including those discussed in this thesis; **1** Vynohradynl Sad (3275 ± 35), **2** Fajsz (3214 ± 36), **3** Lavagnone (3208 ± 26), **4** Lipnik (3040 ± 35), **5** Lutomiersk-Koziówki (2810 ± 35), **6** Assiros Toumba (3071 ± 12), **7** Cornești (3087 ± 22) (Filipovic *et al.* 2020 3).

Contentious early European evidence

Ceramics are generally perceived as stratigraphically and chronologically reliable forms of evidence. Therefore, the occurrence of ‘millet impression’ in Neolithic ceramic fabrics has, until now, proven troublesome. Thousands of impressions are reportedly observed in ceramic sherds, from hundreds of European sites, dating to before the second millennium BCE. Isolated and concentrated impressions are reported in individual sherds and across entire assemblages, although reporting of distribution and identification is often vague (Hunt *et al.* 2008; An *et al.* 2018; 2019). A large portion of these reports are from eastern Europe, particularly Ukraine and Moldova, where they represent some of the earliest evidence of millet in Europe. However, recent microscopic analysis of ‘millet impressions’ in ceramics from Usatovo sites in Ukraine demonstrated

that none were formed from *P. miliaceum*. Impressions were initially misattributed to *P. miliaceum* due to their small size, rather than any defining characteristics (An *et al.* 2019). Consequently, all early impressions require either reassessment, using microscopic analysis, or supporting archaeological evidence to confirm that they conform to the translocation history and originate from *P. miliaceum*.

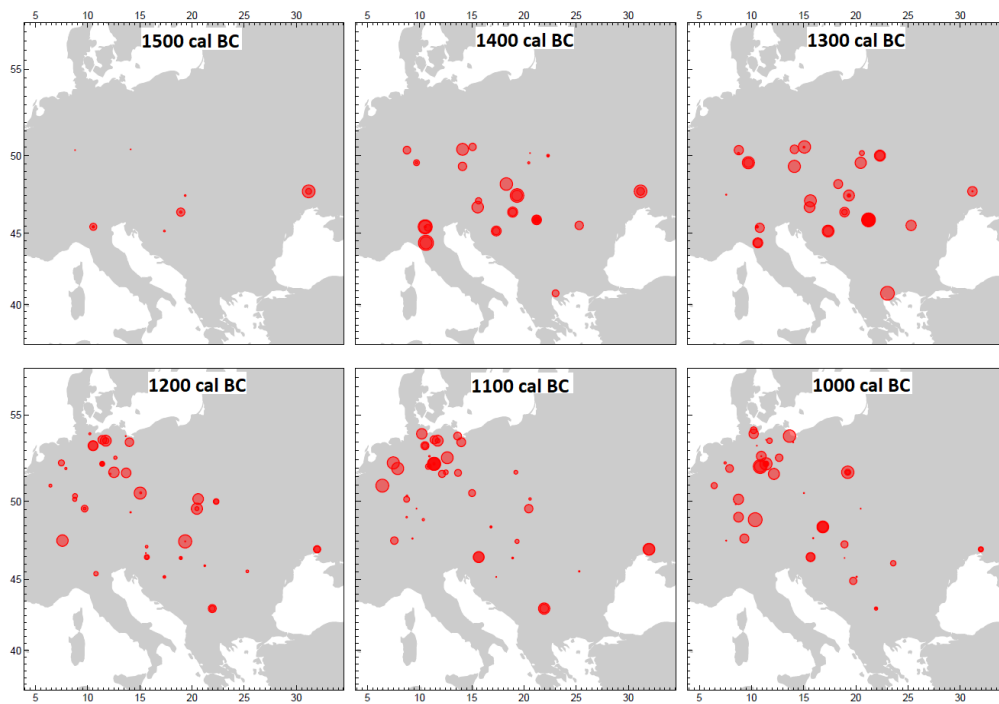


Figure 11. Chronological division at 100 year intervals of the earliest directly dated European millet caryopses. Symbol size corresponds to the relative probability that a sample is of the stated interval (Filipovic *et al.* 2020 7).

Kučera *et al.* (2019) propose the earliest direct evidence of *P. miliaceum* in Europe, ca. 2639 cal BCE, at Držovice, Czech Republic. The soil fill of one complete vessel contained miliacin, although it was not absorbed in the ceramic fabric. Miliacin was not identified in the neck section of the soil fill, potentially indicating that it is not a contaminant from overlying soils. Therefore, the authors concluded that *P. miliaceum* was placed in the vessel as an offering. However, there are several issues with this interpretation. Firstly, prior to the MBA, only single carbonised *P. miliaceum* caryopses are reported at Czech sites (Dreslerová and Kočár 2013). Indeed, no consideration is given to the translocation history of this species, as this observation pre-dates the earliest evidence of *P. miliaceum* West of China. Secondly, no consideration is given to other

miliacin producing species, i.e. *D. sanguinalis*, present in Europe during the third millennium BCE. Thirdly, there is insufficient understanding of miliacin transfer and accumulation, from either *P. miliaceum* or *D. sanguinalis*, to conclusively discount the contamination of this context throughout the course of deposition. The failure of Kučera *et al.* (2019) to consistently sample, analyse, and report results, for each vessel and across the contexts, adds further doubt to the accuracy of their report. Ascertaining the date of the miliacin may be confirmed by radiocarbon dating (Courel *et al.* 2017). However, supporting macro- and microbotanical evidence is necessary to attribute miliacin to *P. miliaceum*.

Stable carbon isotope analyses of human and animal remains have provided contentious data proposed as evidence of early *P. miliaceum* consumption (Lightfoot *et al.* 2013). Goslar *et al.* (2017) propose that a single human individual, that produced a $\delta^{13}\text{C}$ value of -17.9‰, from a fourth to second millennium BCE cemetery in Ukraine, is representative of *P. miliaceum* consumption. However, no supporting evidence is provided for such specific identification and the study ignores other potential sources of enrichment, such as climatic factors and wild C_4 plants. Such minor enrichment is easily discounted, yet $\delta^{13}\text{C}$ values of -16.3‰ observed in an individual from Vertebea Cave and -15.3‰ observed in two individuals at Osipovka, both in Ukraine, require closer scrutiny. The individual from the Neolithic Vertebea Cave site was originally radiocarbon dated to ca. 3266 cal BCE (Nikitin *et al.* 2010). However, following the return of the unusual carbon isotope data, the individual was re-dated, providing a new date of ca. 647 cal BCE (Lillie *et al.* 2017). In addition, the two individuals from the Mesolithic-Neolithic cemeteries of Osipovka were radiocarbon dated to ca. 1000 cal BCE (Lillie and Richards 2000). Such comprehensive radiocarbon dating of remains is uncommon and these results are rather fortuitous. There are a significantly greater number of studies in which radiocarbon dating is not as broadly applied, from which outlier individuals are overinterpreted (Lightfoot *et al.* 2013). These results demonstrate that isotopic outliers should not be relied upon in order to demonstrate *P. miliaceum* consumption without supporting evidence.

Earliest evidence for *P. miliaceum* in Europe

The proceeding sections outline three regions that have produced the earliest and most comprehensive evidence for *P. miliaceum* in Europe. While several *P. miliaceum*

caryopses, from Germany and Italy, have produced earlier radiocarbon dates than are observed in the discussed regions, radiocarbon date ranges are subject to interpretation. Incorporation of other evidence strands and consideration of the most probable trajectory of *P. miliaceum* introduction, i.e. from East to West, suggests that these samples date to the lower range of the date estimate (Filipovic *et al.* 2020 5). However, future research may provide cause to re-evaluate this interpretation.

Evidence for *P. miliaceum* in regions beyond those discussed is fragmentary, sparse, and of limited relevance to archaeological discussions in this thesis. Therefore, many regions have been omitted from this discussion. Furthermore, evidence for *P. miliaceum* in Poland, and Northern Greece and Bulgaria, is discussed in the context archaeological analyses presented in Chapter 6 and 7 respectively.

Southern Ukraine

The earliest directly dated *P. miliaceum* caryopsis in eastern Europe is from Vynohradynl Sad, Ukraine, ca. 1550 cal BCE. Other caryopses from the site date marginally later, ca. 1450 cal BCE (Filipovic *et al.* 2020). Presently, archaeobotanical, isotopic, and environmental research indicates large-scale exploitation of *P. miliaceum* in Ukraine began in the LBA and IA, yet this may reflect limited analysis of EBA and MBA sites (Motuzaitė-Matuzevičiūtė 2012; 2016; Filipovic *et al.* 2020). Given that only one Ukrainian site has produced early direct dates, further research is necessary to determine an accurate chronology of *P. miliaceum* introduction. Furthermore, if one presumes that the species was introduced to Europe via the Caucasus and Ukraine, dates from regions further West should be substantially later. However, direct dates from Hungary are in close proximity to those from Vynohradynl Sad. Therefore, either earlier Ukrainian dates are yet to be discovered or the direction of *P. miliaceum* should be reconsidered.

Significant ^{13}C enrichment is observed in two individuals, with $\delta^{13}\text{C}$ values of -15.4‰ and -14.8‰, from the BA site Glubokoe Ozero II (1400-1100 BC), Ukraine. No enrichment was observed in 68 faunal samples, indicating extensive direct consumption of *P. miliaceum* by some individuals (Lightfoot *et al.* 2013). In the absence of direct radiocarbon dates for these individuals, significant *P. miliaceum* consumption cannot be attributed to either the early or late phase of the site. Therefore, it is not possible to ascertain whether the cereal was cultivated and consumed as either a rare exotic or

staple product, throughout introduction and adoption. Furthermore, limited stable isotope sampling of human remains, at Glubokoe Ozero II and other Ukrainian BA sites, prevents an assessment of the adoption process, e.g. by either elite groups or wider society.

Great Hungarian Plain (Hungary)

The earliest directly dated millet caryopsis in Hungary is from Fajsz 18, ca. 1510 cal BCE, corresponding to the MBA. A second caryopsis from this site produced a later date, ca. 1335 cal BCE, corresponding to the LBA. Interestingly, both were observed within secure Neolithic (5500-4500 BC) contexts, with associated ceramic and lithic artefacts, evidently having intruded from overlying BA layers (Motuzaitė-Matuzevičiūtė *et al.* 2013). Direct dating casts doubt on frequent and abundant *P. miliaceum* caryopses observed in Neolithic contexts (Gyulai 2014). Furthermore, the observation of ^{13}C enrichment, in two EN individuals from Hodmezovasarhely-Kotacpart, is also called into question. Additional isotope analysis of human and animal remains, from this and contemporary sites, demonstrate no ^{13}C enrichment (Figure 12, Pearson and Hedges 2007; Lightfoot *et al.* 2013; Giblin and Yerkes 2016; Gamarra *et al.* 2018). Therefore, it is likely that the two individuals from Hodmezovasarhely-Kotacpart are younger than their apparent context, although radiocarbon dating is necessary to prove this interpretation.

P. miliaceum is infrequent and scarce in Hungarian Chalcolithic contexts, corresponding to human and faunal isotope studies (Giblin and Yerkes 2016; Gamarra *et al.* 2018), that demonstrate no ^{13}C enrichment (Figure 12). The prevalence and abundance of *P. miliaceum* increases significantly during the BA. Several carbonised caryopses are observed at one EBA site, Szigetszentmiklós, although one must consider that they may be intrusive. There is no evidence of ^{13}C enrichment in the EBA, yet only two individuals have been sampled, necessitating further analysis, and small-scale consumption would not result in a significant change of $\delta^{13}\text{C}$ values. Direct dating of caryopses from Szigetszentmiklós is necessary to understand their origin.

In addition to Fajsz 18, two other MBA sites, Bölcske-Vörösgyír and Százhalombatta-Földvár, produce substantial quantities of *P. miliaceum*, although not at an abundance to suggest large scale cultivation and consumption. For instance, 57 *P. miliaceum* caryopses were observed among ca. 7000 cereal grains at Százhalombatta-

Földvár (Stika and Heiss 2013). However, there is no isotopic data from MBA material to confirm whether the cereal was either a rare exotic product or common staple that is poorly represented in the archaeobotanical record. As discussed previously, traces of *P. miliaceum* may be either poorly preserved or difficult to detect in the archaeobotanical record, especially when exploited in low abundance.

The frequency and abundance of *P. miliaceum* is high during the LBA, often representing the third most dominant cereal in archaeobotanical assemblages, at sites including Börcs Paphomlok, Mosonmagyaróvár-Németbánya, Mosonmagyaróvár-Németdűlő and Százhalombatta-Földvár (Gyulia 2014). However, a high abundance is not observed across all sites in the region, e.g., Gőr-Kápolnadomb (Gyulai 2014), potentially indicating either different motives or rates of adoption. The increased prevalence of *P. miliaceum* caryopses in the region corresponds to ^{13}C enrichment observed in most, if not all, LBA individuals presently studied (Figure 12, Gamarra *et al.* 2018). There is no carbon isotope data for animal remains. Therefore, it is not possible to demonstrate whether *P. miliaceum* was either consumed directly by humans or used as fodder for animals.

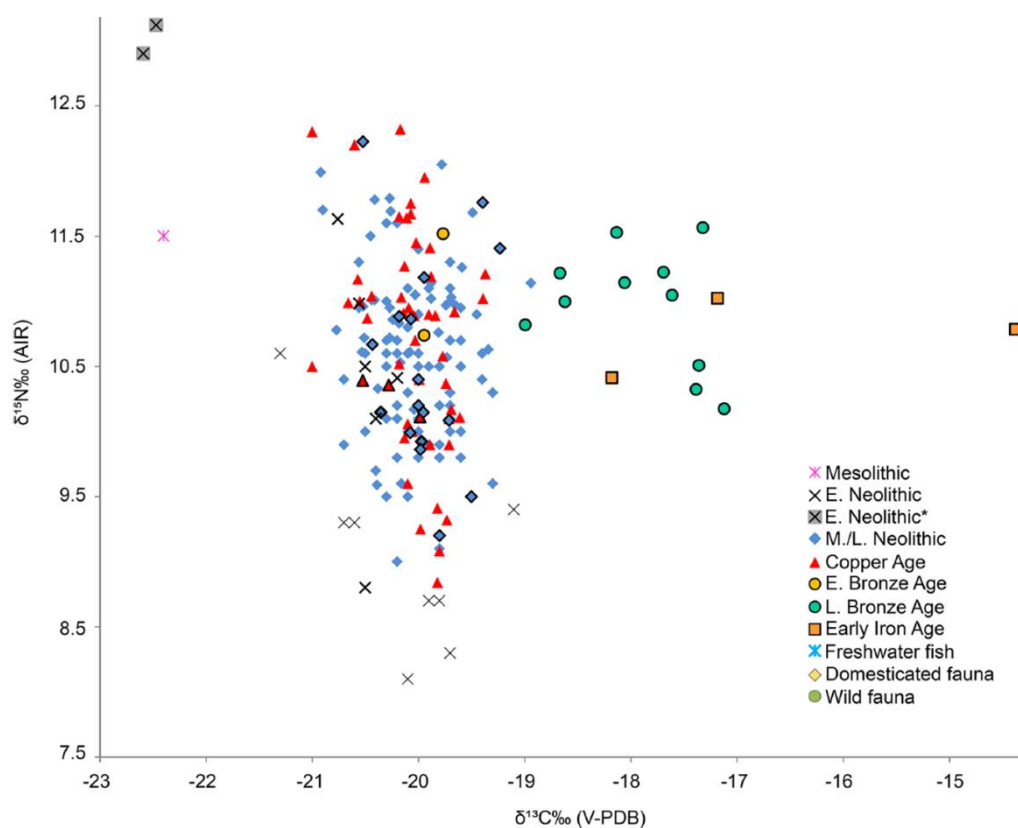


Figure 12. Human bulk isotope values of individuals from the Great Hungarian Plain (Gamarra *et al.* 2018 11).

Genetic analysis of 13 humans from the Great Hungarian Plain demonstrate a significant change in the BA, corresponding to a change in stable carbon isotope values indicative of C₄ plant consumption (Gamba *et al.* 2014; Gamarra *et al.* 2018). Genetic change coincides with the introduction and development of new cultural groups with links to North Pontic and Balkan cultures (Gamba *et al.* 2014), potentially demonstrating the different routes of *P. miliaceum* introduction. Furthermore, differences in 'genetic affiliation' between groups may explain the varied rates of millet adoption across the region. However, the sample size of this genetic study is very small, necessitating further analysis. Furthermore, additional archaeological research, in the North Pontic and Balkan regions, is necessary to accurately investigate any relationship between population movement and translocation of *P. miliaceum*. Multiproxy investigations, focused on a limited number of sites, are necessary to better investigate the introduction, adoption, and use of *P. miliaceum* during the BA in Hungary. In doing so, it may be possible to compare evidence for *P. miliaceum* in this region to others in Europe.

Po Plain (Northern Italy)

The analysis of macro- and microbotanical remains, in addition to human and animal stable isotopes, from Northern Italy provides the most comprehensive early dataset, enabling spatial and temporal analysis of the motives for and methods of *P. miliaceum* introduction and adoption.

Presently, directly dated *P. miliaceum* caryopses cluster either around or just after 1500 cal BCE, corresponding to the MBA in the region. Carbonised caryopses and impressions in ceramics are observed in a limited number of Neolithic contexts, yet their identification is doubtful (Rottoli and Castiglioni 2009; Tafuri *et al.* 2018; An *et al.* 2019). There is no evidence of ¹³C enrichment, that may be unambiguously attributed to *P. miliaceum*, in either humans or animals dating to the Neolithic, demonstrating that even if the cereal was present, which is unlikely, it was not consumed in significant quantities.

Evidence for the exploitation of *P. miliaceum* increases in the BA, with substantial finds observed in MBA and LBA archaeobotanical assemblages. Small quantities of carbonised caryopses are observed in EBA contexts at Canàr, Veneto Region, but are generally rare at other contemporary sites (Perego 2015; Tafuri *et al.* 2018). Except for one individual from Dossetto di Nogara, with a δ¹³C value of -13.5‰, EBA human and

animal remains do not demonstrate ^{13}C enrichment (Figure 13, Varalli *et al.* 2016a, 2016b; Tafuri *et al.* 2018; Masotti *et al.* 2019). As animals did not demonstrate respective enrichment at Dossetto di Nogara, it may be presumed that ^{13}C enriched products were consumed by this individual directly. The consumption of marine products is perhaps unlikely, due to a low $\delta^{15}\text{N}$ value from this individual, although low trophic level organisms, i.e. shellfish, would not necessarily result in substantial ^{15}N enrichment whilst imparting ^{13}C enrichment. The direct consumption of C_4 plants is another explanation for ^{13}C enrichment, although there is no evidence for significant consumption of wild C_4 plants at the site and it is unlikely that *P. miliaceum* was either present or consumed in significant quantities in the EBA. Therefore, one must consider that the Dossetto di Nogara individual is perhaps misattributed to this period (Tafuri *et al.* 2018).

The introduction of *P. miliaceum*, during the MBA, is clearly demonstrated at Lavagnone, where it is absent in EBA contexts but becomes dominant in the MBA, appearing in 90% of contexts and comprising 48% of the cereal assemblage. The cultivation of other cereals, including emmer, barley, and einkorn, persists, demonstrating diversification of cultivated crops, with a heavy reliance of *P. miliaceum* (Perego 2015). Carbonised *P. miliaceum* caryopses, and phytoliths resembling the species, are identified at Fondo Paviani (Dal Corso *et al.* 2017). In addition, *P. miliaceum* appears to have contributed greatly to the diets of pigs at Fondo Paviani, and to a lesser extent cattle, but not sheep. The current faunal database is limited, yet it appears this pattern is observed throughout the region, including at M/LBA Olmo di Nogara (Tafuri *et al.* 2018). Further isotopic investigations of faunal remains are necessary, yet it appears that *P. miliaceum* was incorporated into diverse subsistence strategies that were common across the region.

Stable isotope analysis of MBA human remains demonstrates significant ^{13}C enrichment (Figure 13, Tafuri *et al.* 2009; Tafuri *et al.* 2018). Unfortunately, human and animal remains have been analysed from different sites, in varied proportions, preventing accurate interpretation of *P. miliaceum* exploitation. However, on a regional basis, it appears that both humans and animals consumed the cereal directly, although not necessarily at the same site, indicating varied approaches to *P. miliaceum* exploitation (Tafuri *et al.* 2009; 2018). The MBA human isotope dataset from northern Italy demonstrates a significant difference in $\delta^{13}\text{C}$ and $\delta^{15}\text{N}$ values between males and females,

potentially indicating a difference in diet. The data indicates that males potentially had greater access to animal protein, yet there is no evidence to suggest that *P. miliaceum* was restricted by sex. Furthermore, there is no evidence to suggest that *P. miliaceum* consumption was restricted by status, although the consumption of animal protein, by females, may have been.

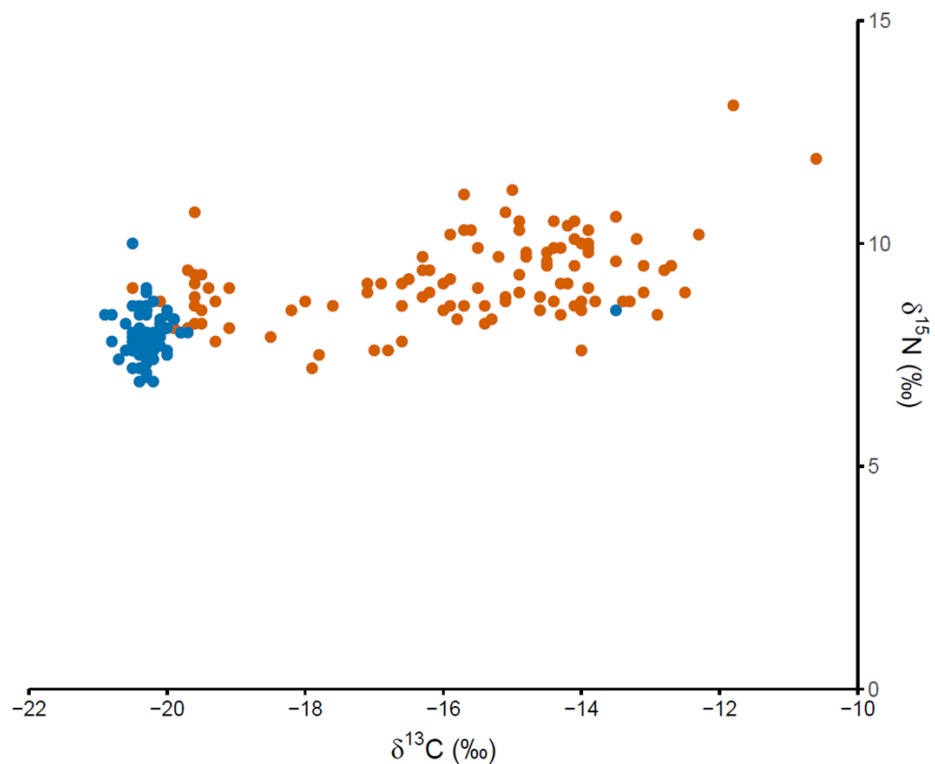


Figure 13. Bulk isotope data of humans from Northern Italy and Croatia. Blue and orange points represent EBA and MBA/LBA individuals respectively. Data obtained from Varalli *et al.* (2016a, 2016b); Tafuri *et al.* (2018); Masotti *et al.* (2019).

The data from northern Italy suggests that *P. miliaceum* was a staple crop from its inception and that no special significance was placed on it, other than its importance to subsistence. Frequent and sometimes abundant ritual deposits of carbonised *P. miliaceum* caryopses, in association with other dominant crop remains, may highlight its importance to subsistence in the Alpine region (Boivin *et al.* 2012; Heiss 2014). Indeed, the cereal is more frequently observed than other species, perhaps highlighting its importance in diversifying and intensifying land use. Furthermore, the high abundance and exclusivity of *P. miliaceum* caryopses in many LBA ritual deposits corresponds to deteriorating climatic conditions and the adoption of drought tolerant crops, potentially

highlighting its role as a risk mitigation crop (Perego 2015; Varalli *et al.* 2016a; 2016b; Tafuri *et al.* 2018; Masotti *et al.* 2019). Northern Italy, specifically the Po Plain, experiences significant demographic pressure at the time of *P. miliaceum* introduction (Dal Corso *et al.* 2017), likely indicating either the need for or result of increased agricultural output.

Present evidence indicates that there is no disparity between the introduction and use of *P. miliaceum*, for either fodder or human consumption, at the sites discussed. However, adoption was discontinuous across the broader region, with sites in the Friuli region providing little evidence of cultivation and the site of Fivavè, a late regional contemporary of Lavagnone, producing no millet (Perego 2015). Human isotope data from M/LBA Monte Orcino/Určín, NW Croatia, which neighbours the Friuli region, demonstrates no ¹³C enrichment (Tafuri *et al.* 2018), although, faunal remains from the site have not been analysed, raising the possibility that *P. miliaceum* was used exclusively for animal fodder. Isotope data from other sites in West Croatia may demonstrate that the region was not a mass adopter of this new crop (Lightfoot *et al.* 2012; 2015b; Zavodney *et al.* 2019), although this is contradictory of archaeobotanical finds (Reed *et al.* 2013; Mareković *et al.* 2015). These observations have led some to suggest that *P. miliaceum* was introduced to northern Italy via Alpine routes (Tafuri *et al.* 2018), yet the present evidence is far too fragmentary and sparse to confirm either possibility.

The dispersal of *P. miliaceum* in Europe

The current European dataset is too fragmentary and sparse to enable either an accurate or reliable interpretation of *P. miliaceum* translocation from region to region. Direct radiocarbon dating currently indicates that the species was introduced to Europe by the 15th C. BCE (Figure 11), before spreading rapidly to the West and South, although northward dispersal may have occurred later (Filipovic *et al.* 2020). It is important to consider that both the point and timing of entry has not been conclusively resolved. Therefore, a discussion of point to point translocation would be premature. In addition, when examining the current radiocarbon dataset, it is important to distinguish between material dating to either the introduction, initial adoption, or mass adoption of the cereal, assuming they occurred separately. Further radiocarbon dating programmes, that critically assess the context of *P. miliaceum* finds, are necessary to identify early occurrences and enable an accurate discussion of *P. miliaceum* dispersal across Europe.

Assessing and improving the detection of *P. miliaceum*

Recently published data, summarised in this chapter, demonstrates concurrent introduction and adoption of *P. miliaceum* across Eurasia. The data suggests that subsistence was the primary motive for *P. miliaceum* translocation, although differences in the rate and degree of adoption, within and between sites, potentially suggest a cultural element in decision making. The research synthesis presented in this chapter arguably provides the most thorough assessment of evidence to date, yet the current dataset is limited.

The limits of *P. miliaceum* macro remain production, preservation, observation, and identification indicate that archaeobotanical analysis may underestimate the significance of *P. miliaceum* exploitation. As such, one may question the accuracy of this technique in identifying and quantifying *P. miliaceum* macro remains, especially during early periods of small-scale exploitation when the potential sample size is reduced. Furthermore, as radiocarbon dating of macro remains is infrequent, one may question the reliability of dates obtained in ascertaining the true timing of first introduction. In addition, qualitative interpretation of *P. miliaceum* macro remains is limited, with overtly ritualistic and ceremonial contexts forming the basis of the few cultural interpretations presently discussed (Frachetti *et al.* 2010; Heiss 2014). There is difficulty in directly associating archaeobotanical data to methods of exploitation, preventing an understanding of the role that a species occupied within cuisine and cultural identity. As Sherratt (1991 50) stated, “people do not eat species, they eat meals”.

Isotope analysis cannot identify small-scale consumption of *P. miliaceum*, although the sensitivity of this technique varies depending on the material studied, e.g. collagen and bone carbonate. In addition, it is difficult, if not impossible, to distinguish the consumption of *P. miliaceum* from other ^{13}C enriched products and nuanced elements of cuisine and consumption are not recognisable. Isotope analysis struggles to associate consumption with material culture, except in a limited number of burials with grave goods. However, in these exceptional contexts, the association between an individual and an artefact may be distinct from the relationship between an individual and *P. miliaceum*. Therefore, the cultural significance of the cereal may be difficult to ascertain.

Archaeobotanical and isotopic analyses currently provide most evidence for *P. miliaceum* translocation and adoption. One must ask whether these techniques are sufficiently sensitive, accurate, and reliable, to enable the identification of *P. miliaceum* exploitation, in archaeological materials, when it was a rare product. In addition, what detail do these techniques provide as to the nuanced uses of this cereal in the past? If these techniques are limited in determining whether the introduction and adoption of *P. miliaceum* occurred concurrently and what it was used for, then it is not possible to fully understand the motives for its translocation and answer the question ‘why move starchy cereals?’ (Lightfoot *et al.* 2013).

Organic residue analysis and the biomarker approach (miliacin) may provide the preservation, specificity, sensitivity, reliability, and comparability necessary to better understand the translocation, adoption, use and significance of *P. miliaceum* in the past. Archaeological organic residues are potentially vast stores of information that provide substantial preservation potential (Chapter 2), with evidence for *P. miliaceum* processing reported in prehistoric contexts across Europe and Asia (Heron *et al.* 2016; Ganzarolli *et al.* 2018; Isaksson and Nilsson 2018; Rageot *et al.* 2019a; 2019b; Junno *et al.* 2020). The processing of *P. miliaceum* may be identified in the absence of archaeobotanical remains, highlighting the sensitivity and specificity of this approach. Furthermore, integration of ORA data with ceramic studies has been demonstrated to provide new insights into the role and significance of this cereal (Rageot *et al.* 2019a; 2019b). However, further analysis of reference and experimental materials is necessary to assess the accuracy and reliability of these studies and the use of ORA to detect traces of *P. miliaceum* processing.

Conclusion

Current evidence for the translocation and exploitation of *P. miliaceum* is sparse and fragmentary, consisting of concentrated regions of research that have not been subjected to unified sampling and analytical strategies. A comprehensive assessment of past activities is not possible, given gaps in research, and compounding limitations of analytical techniques currently applied to archaeological materials. The expansion of archaeobotanical and isotopic analyses would certainly increase the breadth of our understanding, yet one must question the ability of these datasets to elucidate potentially nuanced motives and methods of *P. miliaceum* translocation and exploitation.

Recent research indicates that the analysis of organic residues may provide evidence that has been missing from past discussions.

Chapter 4: Miliacin and Millets

This chapter presents analyses assessing the effect that AM extraction has on the integrity of miliacin and the triterpene fraction of 20 millet species. The chapter begins by outlining the rationale of this research, before presenting an experiment aimed at demonstrating the negative effects of AM extraction on miliacin. The results of this experiment are briefly discussed and interpreted, regarding the use of miliacin as a biomarker, then used as the premise for the analysis of the triterpene fraction from the caryopses of 20 different millet species. Finally, the results of these analyses are discussed in detail and considered in the wider context of identifying *P. miliaceum* and other millet species by AM extraction and ORA.

Introduction

Effective extraction of lipids is critical to the analysis of archaeological residues, that are often degraded and diminished during deposition. The principal extraction methodologies currently employed in ORA studies are discussed in Chapter 2. To summarise, AM extraction provides increased yield and efficiency benefits at the cost of qualitative data. Conversely, SE provides greater qualitative data yet has lower extraction potential, resulting in lower yields and limited effectiveness in many environments with poor preservation (Correa-Ascencio and Evershed 2014). Combined SE and AM extraction has proven effective (Papakosta *et al.* 2015), yet is not routinely applied, likely due to additional cost and time constraints. Therefore, archaeologists must often choose between either SE or AM methodologies, both of which have proven successful in the extraction and identification of miliacin in archaeological residues (Heron *et al.* 2016; Ganzarolli *et al.* 2018). However, no study has assessed the effectiveness of these methodologies in the extraction and identification of miliacin. Indeed, miliacin is generally only discussed in terms of presence and absence. As is noted in Chapter 2, terpenes are susceptible to thermally assisted acid isomerisation, a process that may be catalysed by the presence of clay minerals (ten Haven *et al.* 1992). Therefore, one may question whether exposing miliacin to both a strong acid and high temperatures, during AM extraction, often in the presence of ceramic powder, results in alteration of its molecular structure.

During a pilot study of archaeological material, employing AM extraction, it was noted that two PTMEs, with similar and overlapping retention times, mass spectra, and the same molecular weight (M^+ 440), co-occurred and co-eluted with miliacin. The most abundant of the two compounds is not present in *P. miliaceum* caryopses and the least abundant is not present in *P. miliaceum* caryopses in such quantities (Bossard *et al.* 2013). These compounds may derive from a product, other than *P. miliaceum*, that contributed to the residue. However, neither of these compounds nor this hypothetical product have been identified in previous publications. It was hypothesised, after investigating the mass spectrum of each compound, that the two novel PTMEs were present as the result of acid isomerisation of miliacin. Alteration of miliacin has not been reported previously in AM extracted residues (Heron *et al.* 2016; Isaksson and Nilsson 2018; Junno *et al.* 2020). Therefore, an experiment, using a miliacin standard, was designed to test this hypothesis.

A 10 μ L sample of a pure miliacin standard was subjected to both solvent and AM extraction (Appendix 1), in the absence of a ceramic powder, to establish whether alteration of the compound occurs as a result of the extraction methods used. Three additional AM extractions of the miliacin standard were undertaken, with samples placed in the heating block for different lengths of time, to assess the extent to which alteration may occur and whether optimisation of the AM extraction methodology could improve recovery of miliacin. These samples were heated for two, four (standard extraction method), six, and eight hours. The GC-MS method, used for the archaeological samples, was adapted, lowering the rate of temperature increase, to enable greater separation of the three compounds and prevent co-elution that prevented accurate identification from previously obtained mass spectra.

Miliacin standard experiment results

The solvent extract produced a chromatogram with a single peak, that was identified as miliacin (olean-18-en-3 β -ol ME), confirming the purity of the standard. All AM extracts produced three peaks (Figure 14), one of which was miliacin (Figure 15), corresponding to those observed in archaeological samples. The samples produced clear mass spectra, enabling accurate identification of the two alteration products (Figure 16). The compounds were identified by consulting relevant literature and mass spectra databases, containing oleanane-type triterpenes. Peak II is miliacin, with ions of m/z 177,

189 and 204 derived from a $\Delta^{18(19)}$ double bond. Peak I is δ -amyrin ME, an isomer of miliacin, with a prominent m/z 205 ion, indicative of a $\Delta^{13(18)}$ double bond. Peak III is β -amyrin ME, another isomer, with a dominant m/z 218 ion, indicative of a $\Delta^{12(13)}$ double bond (Sorkina *et al.* 1968). The double bond migration and structure of the alteration products is presented in Figure 15.

The double bond first migrates from the $\Delta^{18(19)}$ position to the $\Delta^{13(18)}$ position, resulting in a rapid increase in the abundance of δ -amyrin ME (Figure 17). The double bond may then migrate to either the $\Delta^{12(13)}$ position, forming β -amyrin ME, or back to the $\Delta^{18(19)}$ position, reforming miliacin. The abundance of β -amyrin ME is initially low but increases as more δ -amyrin ME is formed from miliacin. The abundance of miliacin continues to decrease until chemical equilibrium is reached, between four and eight hours (Figure 17), resulting in a high abundance of δ -amyrin ME and slight preference for β -amyrin ME, as miliacin is less thermodynamically stable. This equates to around 59% δ -amyrin ME, 23% β -amyrin ME, and 18% miliacin.

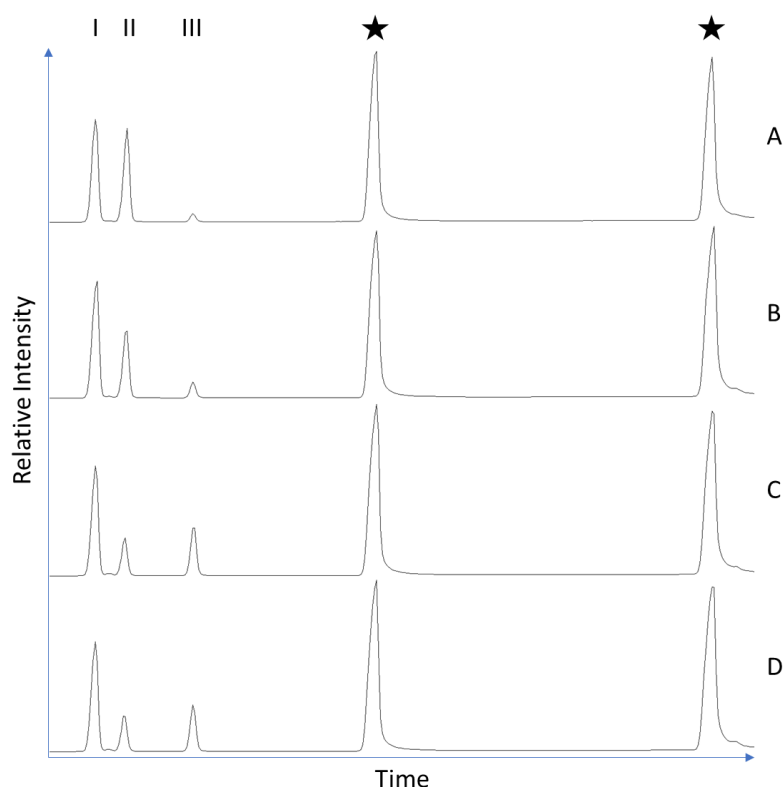


Figure 14. Partial TIC of an AM-extracted miliacin standard heated at 70°C for, **A** two, **B** four, **C** six, and **D** eight, hours. Peak II is miliacin $\Delta^{18(19)}$ and peaks I $\Delta^{13(18)}$ and III $\Delta^{12(13)}$ are alteration products produced during acid isomerisation. Peaks marked with a star are internal *n*-alkane standards C₃₄ and C₃₆ respectively.

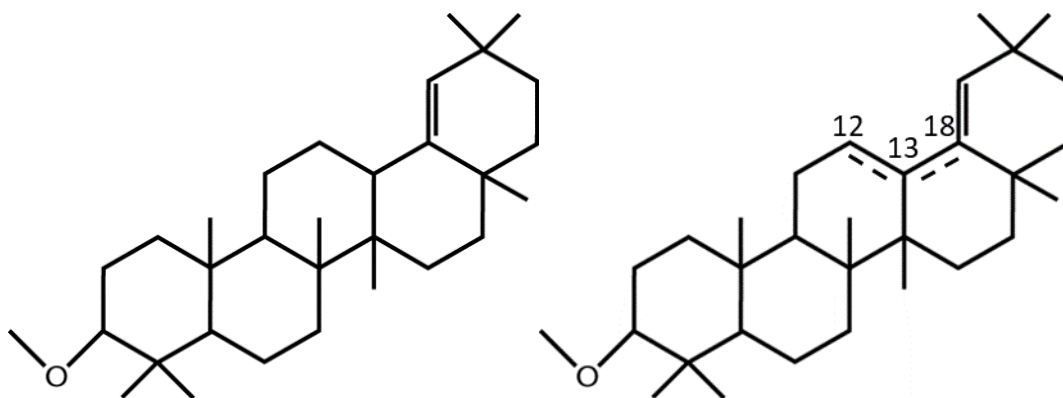


Figure 15. Skeletal structure of miltiacin, olean-18-en-3 β -ol methyl ether (**left**). Skeletal structure demonstrating a double bond migration, from $\Delta^{18(19)}$ to $\Delta^{13(18)}$ and $\Delta^{12(13)}$, that occurs during thermally-assisted acid isomerisation of miltiacin (**right**).

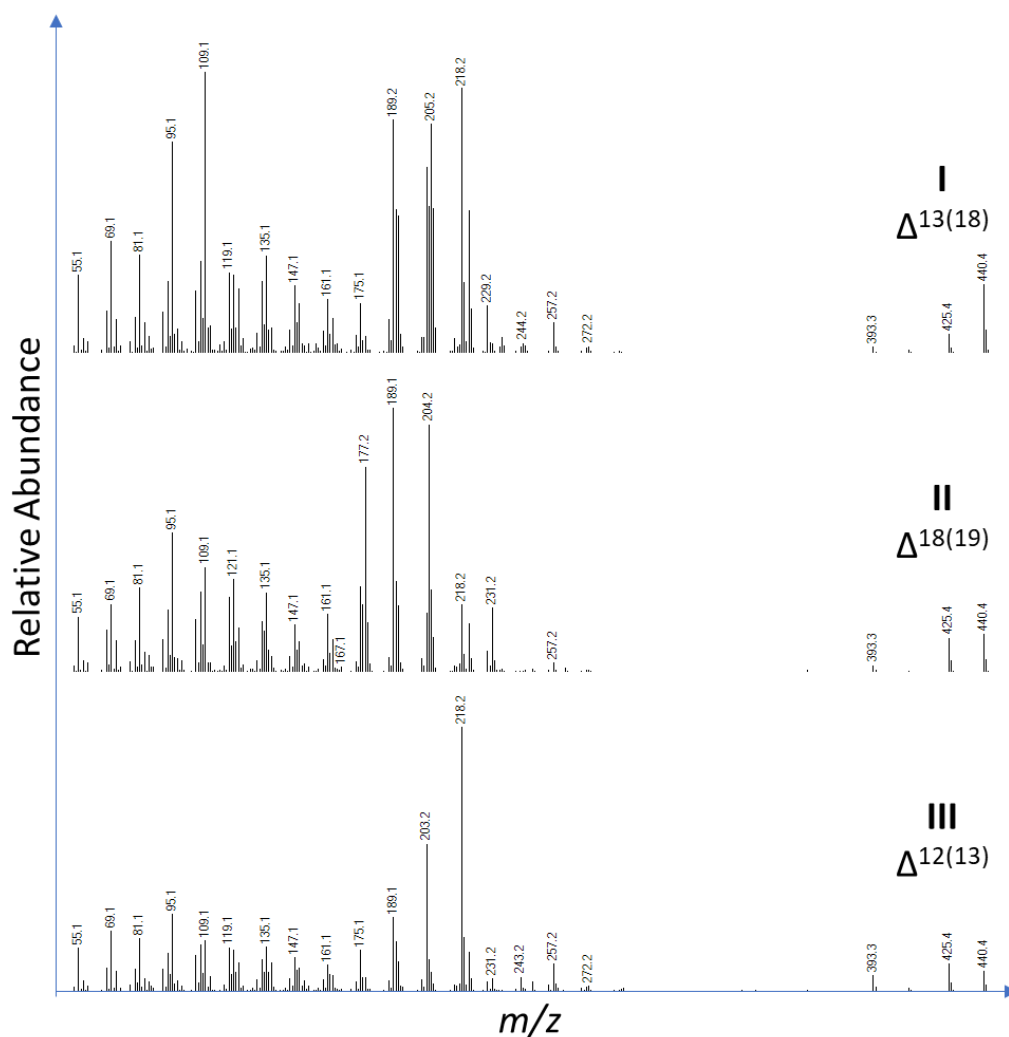


Figure 16. Mass spectra of peaks I, II and III from Figure 15, representing $\Delta^{13(18)}$, $\Delta^{18(19)}$ and $\Delta^{12(13)}$ -oleanenes discussed in this section.

Discussion

The results clearly demonstrate that miliacin is susceptible to double bond migration during AM extraction. Isomerisation does not result in the complete loss of miliacin, but the standard AM method (four hours extraction time) reduces its abundance by 66%. Depending on the initial abundance of miliacin, resolution of the chromatography, and clarity of the mass spectra, isomerisation may lower the abundance of miliacin to below the detection threshold of standard GC-MS scan methods. Therefore, if the compound is not specifically searched for, AM extraction may result in an increased frequency of false negative results. This issue is observed in archaeological samples analysed during this project, where the β -amyrin ME peak is frequently absent, and miliacin peak is either difficult to distinguish from the background or produces a poor mass spectrum, despite attempts to deconvolute the data. Generally, δ -amyrin ME is readily identifiable in the chromatogram and mass spectra data. The use of extracted ion chromatograms is often necessary to identify β -amyrin ME and miliacin, thus highlighting the thorough methods required for the characterisation of broomcorn millet residues in archaeological materials.

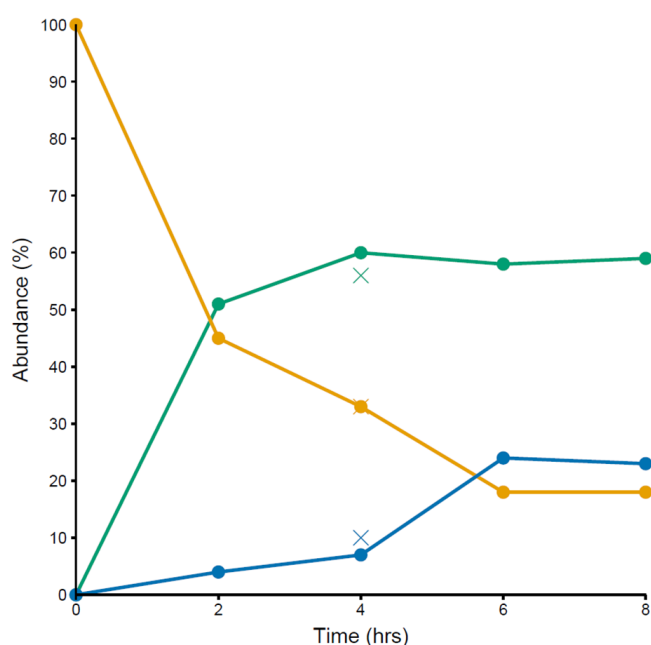


Figure 17. The relative abundance of miliacin (yellow), δ -amyrin ME (green), and β -amyrin ME (blue), in AM extracted samples of a miliacin standard heated for two, four, six and eight hours. Crosses of corresponding colours represent the average relative abundance of these compounds in archaeological samples subjected to the standard four-hour method.

Adaptation of the AM method, by reducing either the time a sample is exposed to H₂SO₄ or a reduction in temperature, reduces the degree of isomerisation. However, this may be at the expense of extracting other compounds. Correa-Ascencio and Evershed (2014) heat samples for one hour, mixing every 5 minutes, whereas Papakosta *et al.* (2015) heat samples for four hours, with no mixing. This experiment demonstrates that the abundance of miliacin is 12% greater at two than four hours, therefore, it is likely that the Correa-Ascencio and Evershed (2014) method would prove a more efficient extraction protocol and result in greater miliacin yields. Presently, there is no evidence to suggest that the presence of either other compounds, ceramic powder, or materials, in archaeological samples from Poland, Greece and Bulgaria, substantially impacts the alteration of miliacin (Figure 17). Therefore, clay mineral catalysts do not appear to be an important consideration for the ceramics/regions assessed in this study, yet this factor should be considered elsewhere. In addition, ceramic catalysts should also be considered if the AM methodology employed in this study is adapted. For instance, mixing samples during extraction may increase interaction between ceramic powder, acid, and miliacin. Therefore, further research is necessary to investigate potential adaptations of the AM extraction method used in this thesis (Appendix 1).

The observation of miliacin isomerisation demonstrates the potential for alteration of this compound when exposed to acidic conditions, during both anthropogenic activity and deposition, as suggested previously (Chapter 2). Weak acidic conditions and low temperatures, achieved during processing and deposition, are perhaps unlikely to result in the degree of alteration observed when miliacin is exposed to concentrated H₂SO₄ and high temperatures during AM extraction. However, over long periods of time and in an amenable burial environment, the degree of alteration could increase significantly. Indeed, repeated activities, e.g. fermentation, that require application of heat and production of an acidic liquid, could result in the production of abundant alteration products. Further experimental research is necessary to investigate whether anthropogenic activities, such as fermentation, and deposition in acidic environments result in recognisable alteration of miliacin and *P. miliaceum* residues. Currently, when applying the AM extraction method, it is important to consider that such nuanced data may be lost. It is important to state, however, that the effectiveness and efficiency of AM extraction is greater than solvent extraction, enabling more frequent and

abundant lipid, including miliacin, extraction in archaeological material (e.g. Chapter 7). Therefore, despite the potential limitations of this method in preserving and identifying miliacin, it remains the primary choice for archaeological investigations.

The usefulness of a biomarker is determined by its abundance and frequency in a given environment. They are preferably concentrated in a single species yet this is not necessary. When examining archaeological residues, produced during food processing, the potential source of a biomarker is limited to products that were consumed in a specific place and period. For instance, although *D. sanguinalis* produces miliacin, it is not known to have been extensively cultivated and consumed in prehistoric Europe. Therefore, archaeological residues containing miliacin may be confidently attributed to *P. miliaceum* (Chapter 2). However, the data presented here complicates this interpretation, as isomerisation is not unidirectional. Miliacin would be observed in AM extracted residues that contain either δ -amyrin ME or β -amyrin ME derived from other species. Although δ -amyrin ME is rare, with no apparent reports of its identification, β -amyrin ME is a common PTME, that is observed in many species (Jacob *et al.* 2005; Oyo-Ita *et al.* 2010; Bossard *et al.* 2013). Therefore, archaeologists must carefully consider species that produce all three PTMEs when interpreting AM extracted archaeological residues.

Assessing the natural abundance of triterpenes in millets

The application of miliacin as a biomarker of *P. miliaceum* is expanding beyond its initial European focus. Junno *et al.* (2020) identified miliacin in one ceramic-absorbed residue from Hamanaka 2, Rebun Island, Japan. The compound was attributed to *P. miliaceum*, despite the species being absent from the archaeobotanical assemblage, as it is known to have been used by contemporary societies in the wider region. However, miliacin may not be limited to *P. miliaceum* in Japanese contexts, making the interpretation of a single sample, without either supporting evidence or analysis of local reference material, contentious. Chakraborty *et al.* (2020) and Saryanarayan *et al.* (2021) note an absence of miliacin in ceramic-absorbed residues from Indus Civilisation pottery in NW India. They conclude that *P. miliaceum* was not processed in the vessels. However, miliacin may also be produced by one of several other millet species present in Indus Civilisation archaeobotanical assemblages. Therefore, the absence of miliacin at these sites, and its presence at other sites, may provide either greater or lesser interpretive

potential than is currently recognised, highlighting the necessity of analysing local reference materials.

Bossard *et al.* (2013) note that miliacin is common in the genus *Panicum*, uncommon in *Pennisetum*, and is observed in some *Digitaria*, *Eragrostis*, and *Paspalum* species. These genera include several important domesticated millet species, including *Panicum sonorum*, *Pennisetum glaucum*, *Digitaria exilis*, *Eragrostis tef*, and *Paspalum scrobiculatum*. Therefore, one must consider whether these domesticated species produce miliacin. Furthermore, as acid isomerisation may produce miliacin during AM extraction, one must also consider the production of other PTMEs among a wider range of species.

The identification of biomarkers in other millet species is of great importance for two principal reasons. Firstly, novel biomarkers would enable molecular investigations of cereal cultivation and consumption in additional archaeological contexts that have not previously been explored. Secondly, understanding the range, prevalence, and abundance of biomarkers in domesticated cereals, specifically millets, would help elucidate potentially conflicting sources of these distinctive compounds. The domestication centres of most millet species do not overlap considerably (Weber and Fuller 2008). However, the domestication centres of *P. glaucum* and *D. exilis* overlap and translocation of *P. miliaceum*, across Eurasia, results in overlapping cultivation with *Panicum sumatrense* in India. Therefore, there is the potential for two domesticated, and widely consumed, miliacin-producing cereals to be present within a single region, at the same time.

The proceeding section details the analysis of millet caryopses, from 19 species, by GC-MS. Of these species, 17 are domesticated and two are wild, although all are understood to have been extensively exploited by humans in the past. Latin and common names are presented in Table 1.

The objectives of this analysis were to:

1. Determine whether other millet species produce miliacin.
2. Identify abundant terpenes that may be used as biomarkers to either identify or distinguish millet species.
3. Investigate the effect of acid isomerisation on the terpene fraction of millets.

Analysis

All species of millet were subject to solvent extraction, as identifying the natural abundance of compounds was the primary objective of this analysis. Limited quantities of *S. pumila*, *S. verticillata*, and *S. viridis*, prevented additional analysis, therefore, only 16 species were subjected to AM extraction. Details of sample preparation, extraction, and analytical methods are detailed in Appendix 1.

Table 1. Reference collection list of millet species analysed.

Latin Name	Common Names
<i>Brachiaria ramosa</i>	Browntop millet, pedda-sama
<i>Digitaria exilis</i>	Fonio, acha, fundi
<i>Digitaria sanguinalis</i>	Hairy crabgrass
<i>Echinochloa colona</i> (<i>E. frumentacea</i> dom.)	Sawa millet
<i>Eleusine coracana</i>	Finger millet
<i>Eragrostis tef</i>	Teff
<i>Panicum sonorum</i>	Sauwi millet, Sonoran millet
<i>Panicum sumatrense</i>	Little millet, samai
<i>Paspalum scrobiculatum</i>	Kodo millet
<i>Pennisetum glaucum</i>	Pearl millet
<i>Setaria italica</i>	Foxtail millet
<i>Setaria palmifolia</i>	Highland pitpit
<i>Setaria pumila</i>	Yellow foxtail millet, korali
<i>Setaria verticillata</i>	Bristly foxtail millet
<i>Setaria viridis</i> (wild)	
<i>Sorghum arundinaceum</i> (wild)	
<i>Sorghum bicolor</i> (r. Bicolor w. Husk)	
<i>Sorghum bicolor</i> (r. Bicolor)	Sorghum, jowra
<i>Sorghum bicolor</i> (r. durra)	
<i>Spodiopogon formosanus</i>	Taiwan hill millet

Results

Triterpenes were observed, in an abundance $> 10 \mu\text{g g}^{-1}$, in eight of the 19 millet species analysed. These species include, *P. sonorum*, *P. sumatrense*, *D. sanguinalis*, *D. exilis*, *E. frumentacea*, *S. bicolor* r. bicolor, *S. bicolor* r. dura, and *S. arundinaceum*. Triterpenes were identified using the NIST mass spectra database, comparison of mass spectra with published studies, and inference from PTME alteration discussed previously. It was not possible to identify all observed triterpenes, although the base skeleton of

compounds could often be inferred. Terpenes were either absent or present in trace quantities in the remaining 11 millets. These compounds are not discussed in greater detail due to their limited interpretive potential. However, it is perhaps important to note that neither miliacin nor any other triterpene was identified in either *S. italica* or *S. viridis*.

Digitaria sanguinalis

Miliacin (II) was observed in the solvent extract of *D. sanguinalis* at an abundance of 781 $\mu\text{g g}^{-1}$ (Table 2). The three isomers, δ -amyrin ME (I), miliacin (II), and β -amyrin ME (III), were observed in the AM extract at an abundance of 980, 633, and 352 $\mu\text{g g}^{-1}$ respectively. This equates to approximately 1956 $\mu\text{g g}^{-1}$ of miliacin extracted by the AM method, as neither alteration product was present in the solvent extract (Figure 18). A difference in the concentration of miliacin in each sample is perhaps the result of a difference between the extraction potential of each method, although a difference in the abundance of miliacin in caryopses and the homogeneity of the samples may have also contributed to the observed variance.

Table 2. The abundance ($\mu\text{g g}^{-1}$) of miliacin (II), δ -amyrin ME (I), β -amyrin ME (III), δ -amyrin (IV), germanicol (V), and β -amyrin (VI), in each species analysed in this study that produces miliacin. Values are primarily from AM extracts, data from solvent extracts are denoted by ^{SE} and * represents an average value published by Bossard *et al.* (2013).

Species	II ^{SE}	I	II	III	IV	V	VI
<i>Digitaria exilis</i>	473	390	109	163	78	31	54
<i>Digitaria sanguinalis</i>	781	980	633	352	235	81	111
<i>Panicum sonorum</i>	1012	148	60	66	0	0	0
<i>Panicum sumatrense</i>	666	517	201	212	28	9	12
<i>Panicum miliaceum</i>	306*	351	97	117	0	0	0

A low abundance (11 $\mu\text{g g}^{-1}$) of germanicol, present as a TMS derivative (IX), was observed in the solvent extract of *D. sanguinalis*. Conversely, a high abundance of δ -amyrin (IV), germanicol (V) and β -amyrin (VI), was observed in the AM extract (Table 2). Germanicol acetate (VII) is present in both the solvent and AM extract, yet it is more abundant in the former extract, therefore, it is proposed that this compound is subject to the loss of its acetyl group and double bond migration, forming relatively high

concentrations of δ -amyrin, germanicol, and β -amyrin in the AM extract. Three other compounds, X, XI, and XII, that have the same molecular weight as germanicol acetate ($M^+ 468$), were identified in the solvent extract, potentially indicating further isomers are present in the caryopsis naturally. However, they are either completely altered or reduced in abundance, below the detection threshold, following AM extraction. These acetates would also increase the relative abundance of germanicol isomers in the AM extract.

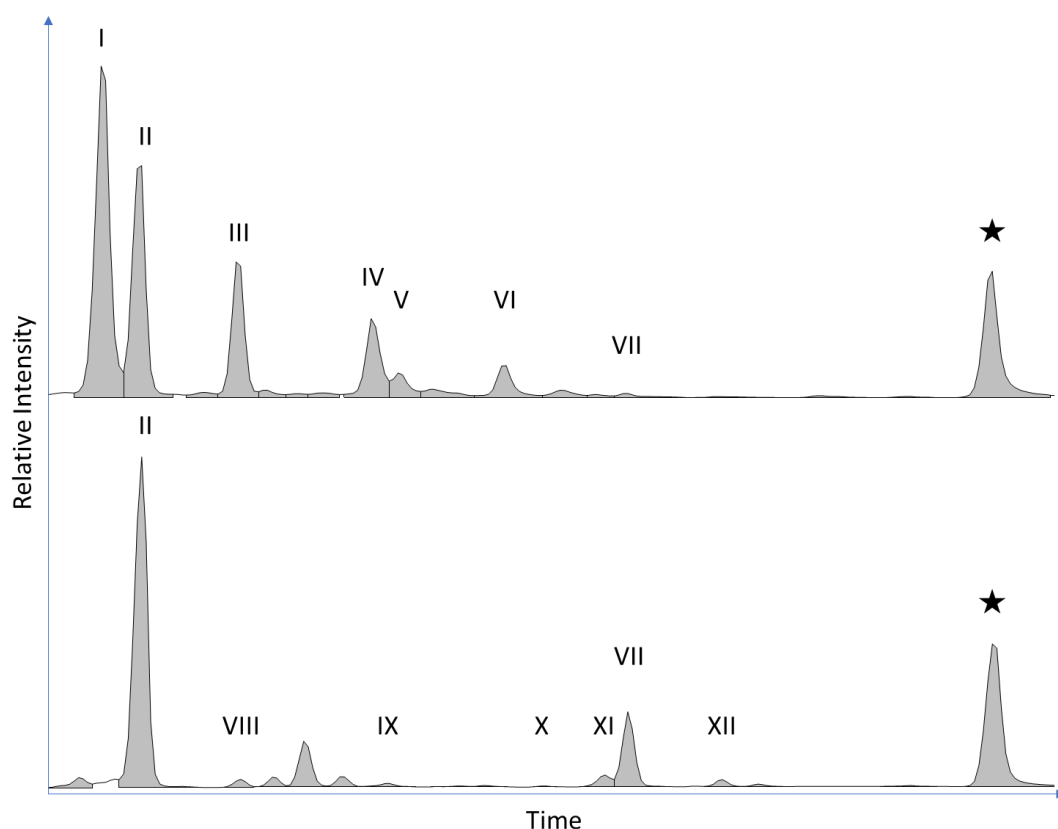


Figure 18. Partial TIC of the AM (**top**) and solvent (**bottom**) extracts of *D. sanguinalis*. Numerals relate to compounds listed in the text and Appendix 2 and the star indicates a C₃₆ alkane standard.

One other compound, VIII, was observed in the solvent extract of *D. sanguinalis*, yet it was unidentifiable from its mass spectra. It has the same molecular weight as miliacin ($M^+ 440$), therefore, it may be a similar oleanane-type PTME with a different double bond position. However, it is either absent, i.e. altered completely by acid

isomerisation, or coelutes with another compound and cannot be identified in the AM extract.

Digitaria exilis

Miliacin (II) was observed in the solvent extract of *D. exilis* at an abundance of 473 $\mu\text{g g}^{-1}$. The three PTME isomers, δ -amyrin ME (I), miliacin (II), and β -amyrin ME (III), were observed in the AM extract, equating to approximately 661 $\mu\text{g g}^{-1}$. A relatively low abundance of germanicol (26 $\mu\text{g g}^{-1}$) was present in the solvent extract as a TMS derivative (IX). However, δ -amyrin (IV), germanicol (V), and β -amyrin (VI), were present in the AM extract in a much higher abundance, totalling 163 $\mu\text{g g}^{-1}$ (Table 2). Germanicol acetate (VII) is observed in the solvent extract of *D. exilis*, but not in the AM extract, therefore, it may be presumed that the compound was completely altered or reduced below the detection threshold of GC-MS, following AM extraction.

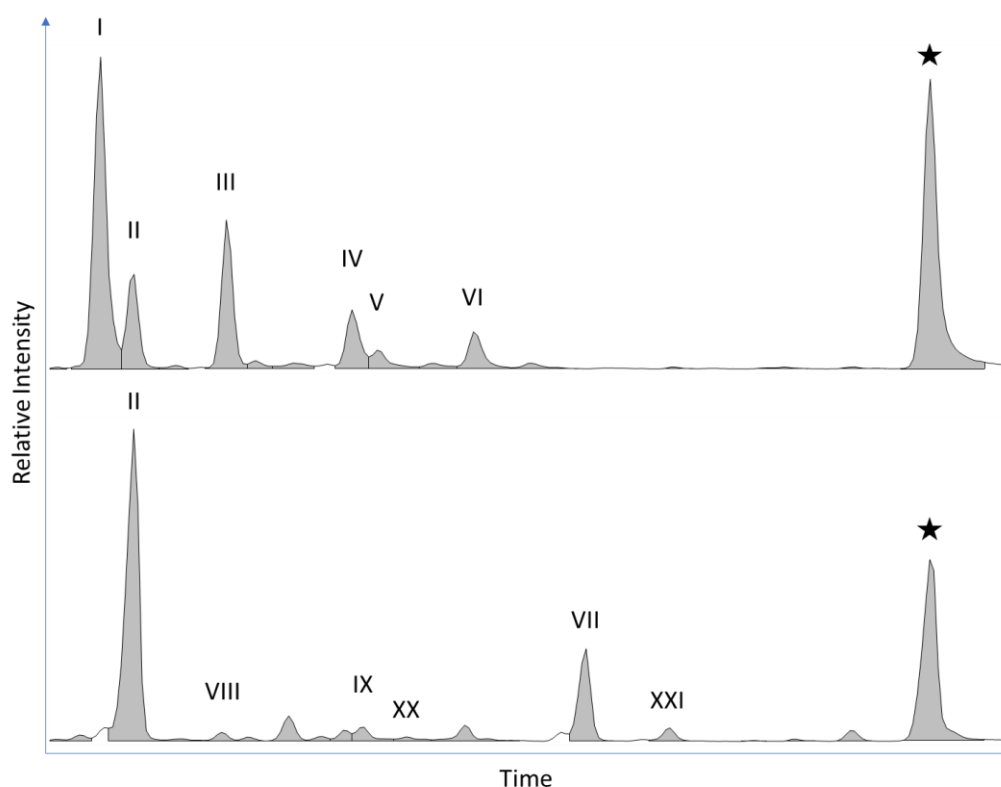


Figure 19. Partial TIC of the AM (**top**) and solvent (**bottom**) extracts of *D. exilis*. Numerals relate to compounds listed in the text and Appendix 2 and the star indicates a C₃₆ alkane standard.

A low abundance of the unidentified compound VIII, with a M^+ of 440, was also present in the solvent extract of *D. exilis* but not the AM extract (Figure 19). Two additional compounds, XX and XXI, were observed in the solvent but not the AM extract of this species. The first compound has been identified as bauerenol ME (XX), a friedelane-type PTME with a double bond on the B ring. The second compound (XXI) has a mass spectra characteristic of a triterpene acetate, similar to those discussed previously, with a M^+ of 468. This compound is potentially a friedelane-type triterpene acetate, which would correspond to the identification of baurenol ME. However, as neither compound is present in a high abundance, they are perhaps unlikely to be useful in the characterisation of archaeological residues.

Panicum sonorum

Miliacin is observed at a high abundance of $1012 \mu\text{g g}^{-1}$ in the solvent extract of *P. sonorum*. However, a relatively low abundance of the PTME isomers, δ -amyrin ME (I), miliacin (II), and β -amyrin ME (III), were observed in the AM extract (Figure 20), equating to approximately $274 \mu\text{g g}^{-1}$ (Table 2). The difference in the abundance of miliacin and its isomers in solvent and AM extracts is contrary to the abundance of these compounds in all other samples, likely indicating that they are not accurate. The sample of *P. sonorum* used for analysis did not comprise many caryopses (< 10). Therefore, it is possible that failure to homogenise the sample exacerbated a broad range of miliacin concentrations in caryopses. Such variance in the concentration of miliacin would be an interesting observation, as triterpenes are often produced in relation to environmental pressures (Phillips *et al.* 2006; Yendo *et al.* 2010), therefore, there may be circumstances in which miliacin is more likely to be observed for this and perhaps other species. However, further analysis is necessary to determine whether these results are inaccurate, and what the cause of any potential inaccuracies may be, before interpretations are made.

Two other triterpenes, VIII and germanicol present as a TMS derivative (IX), were observed at a low abundance in the solvent extract of *P. sonorum* (Figure 20). However, they were absent in the AM extract, likely as a result of alteration and a reduction in abundance below the detection limit of GC-MS.

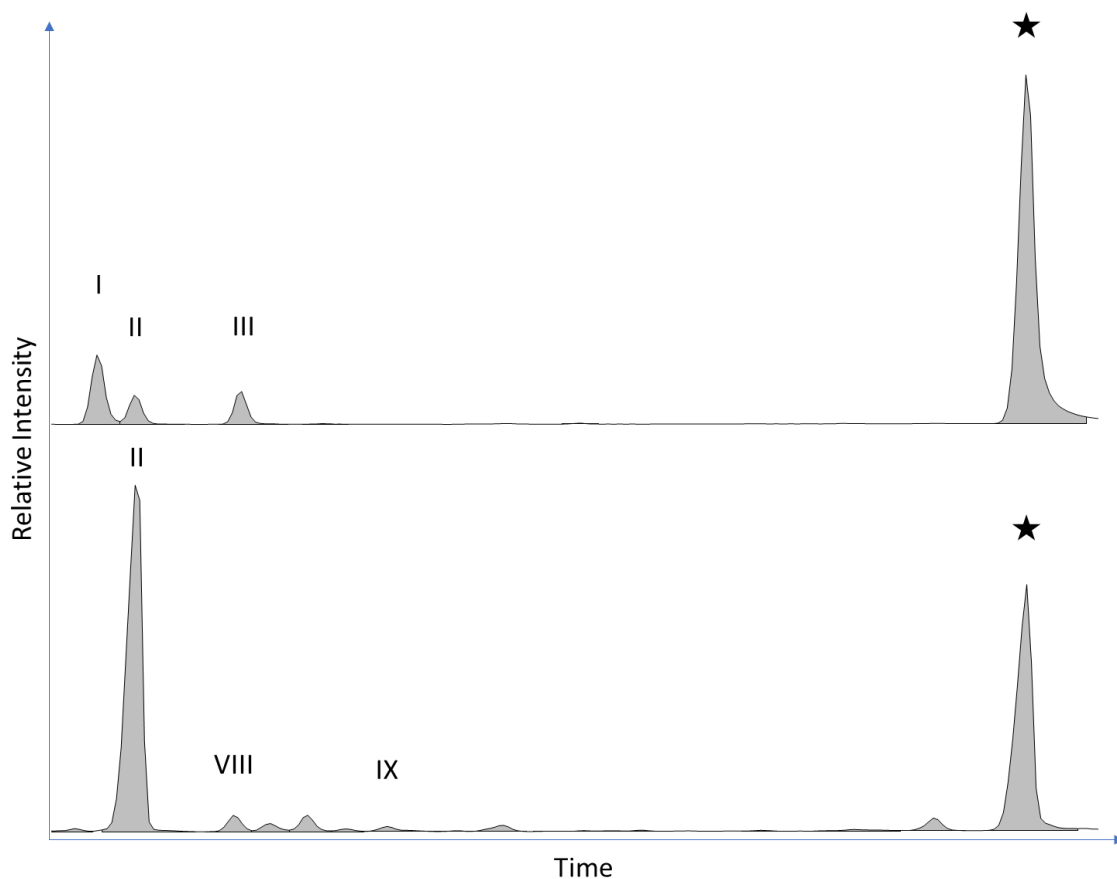


Figure 20. Partial TIC of the AM (**top**) and solvent (**bottom**) extracts of *P. sonorum*. Numerals relate to compounds listed in the text and Appendix 2 and the star indicates a C₃₆ alkane standard.

Panicum sumatrense

Miliacin is observed in the solvent extract of *P. sumatrense* at an abundance of 666 $\mu\text{g g}^{-1}$. The PTME isomers, δ -amyrin ME (I), miliacin (II), and β -amyrin ME (III), were observed in the AM extract (Figure 21), equating to 930 $\mu\text{g g}^{-1}$. A low abundance of δ -amyrin (IV), germanicol (V), and β -amyrin (VI), were also observed in the AM extract, equating to 49 $\mu\text{g g}^{-1}$. A low abundance of germanicol (32 $\mu\text{g g}^{-1}$), present as a TMS derivative (IX), and germanicol acetate (39 $\mu\text{g g}^{-1}$, VII), likely contribute to the formation of the three isomers of germanicol in the AM extract.

The unidentified triterpene, VIII, was also identified in low abundance in the solvent extract of this species but not the AM extract, corresponding to observations in other samples.

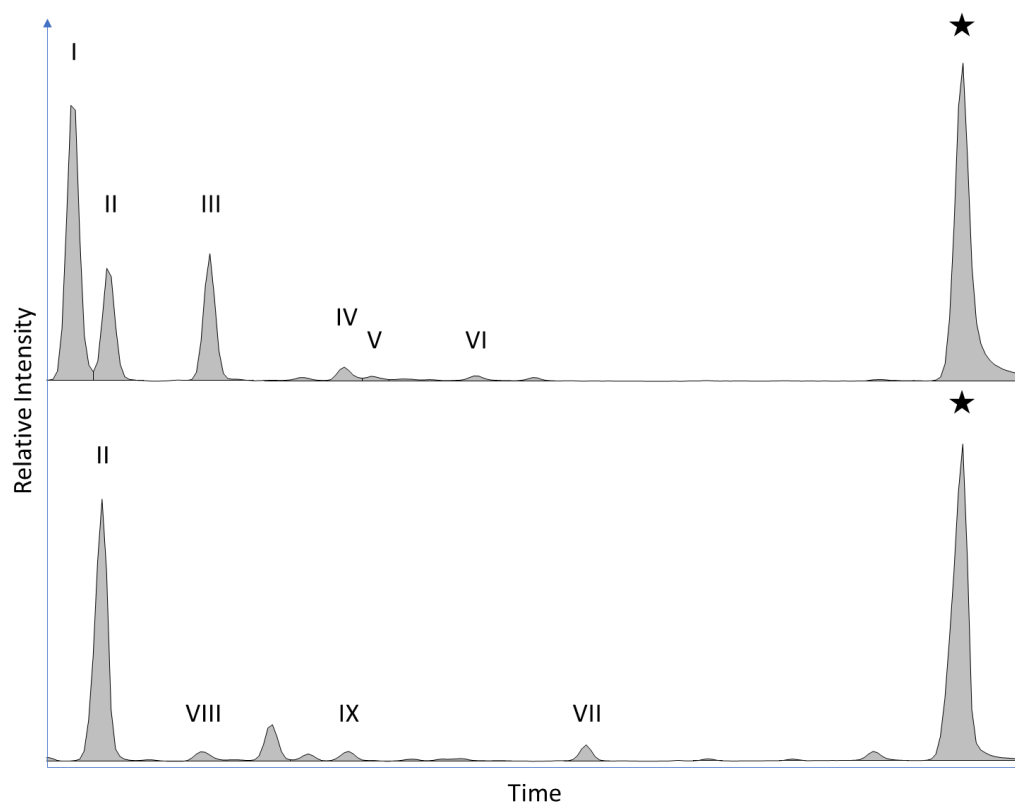


Figure 21. Partial TIC of the AM (**top**) and solvent (**bottom**) extracts of *P. sumatrense*. Numerals relate to compounds listed in the text and Appendix 2 and the star indicates a C₃₆ alkane standard.

Echinochloa colona (*E. Frumentacea* dom.)

Sawamilletin (XIII), an oleanane-type PTME with a 3 β methoxy group and a Δ^{14-15} double bond on the D ring, was identified in the solvent extract of this millet. It is an isomer of miliacin, with a molecular weight of M⁺ 440, and has a dominant ion with *m/z* 204. The compound is present in high abundance, 266 $\mu\text{g g}^{-1}$, in the solvent extract. However, it is absent in the AM extract (Figure 22).

Unlike miliacin, sawamilletin appears to be completely lost via acid isomerisation. Instead, three novel triterpenes, XIV, XV, and XVI, are present in the AM extract. One of these compounds (XVI) may be β -amyrin ME, as it has a similar mass spectrum and retention time, although there is a high degree of background noise in the mass spectrum, making interpretation difficult. Furthermore, one should question, if this compound is β -amyrin ME, why is miliacin not also produced via isomerisation. Peak XIV also has a similar mass spectrum to β -amyrin ME, with dominant ions at *m/z* 218, followed by 203 and 189, yet it elutes earlier. Finally, peak XV does not bear similarities to

any of the previously described compounds. It has a dominant ion at m/z 204, followed by m/z 189, 177, and 119 (Appendix 2). The abundance of the three isomers, XIV, XV, and XVI, is 74, 7, and 12 $\mu\text{g g}^{-1}$ respectively, equating to approximately 93 $\mu\text{g g}^{-1}$. A reduction in the total abundance of the PTME fraction, between the solvent and AM extracts, may relate to either sample homogeneity or the isomerisation process. As these samples are derived from a small number of caryopses, crushed by hand, there is the potential for variation in the abundance of PTME containing tissues in the sample used for solvent and AM extraction. This may be compounded by differences in the concentration of PTMEs in each caryopsis used for the homogenised sample. Therefore, repeat analysis, using a larger sample size is necessary to explore the PTME content of this species more accurately.

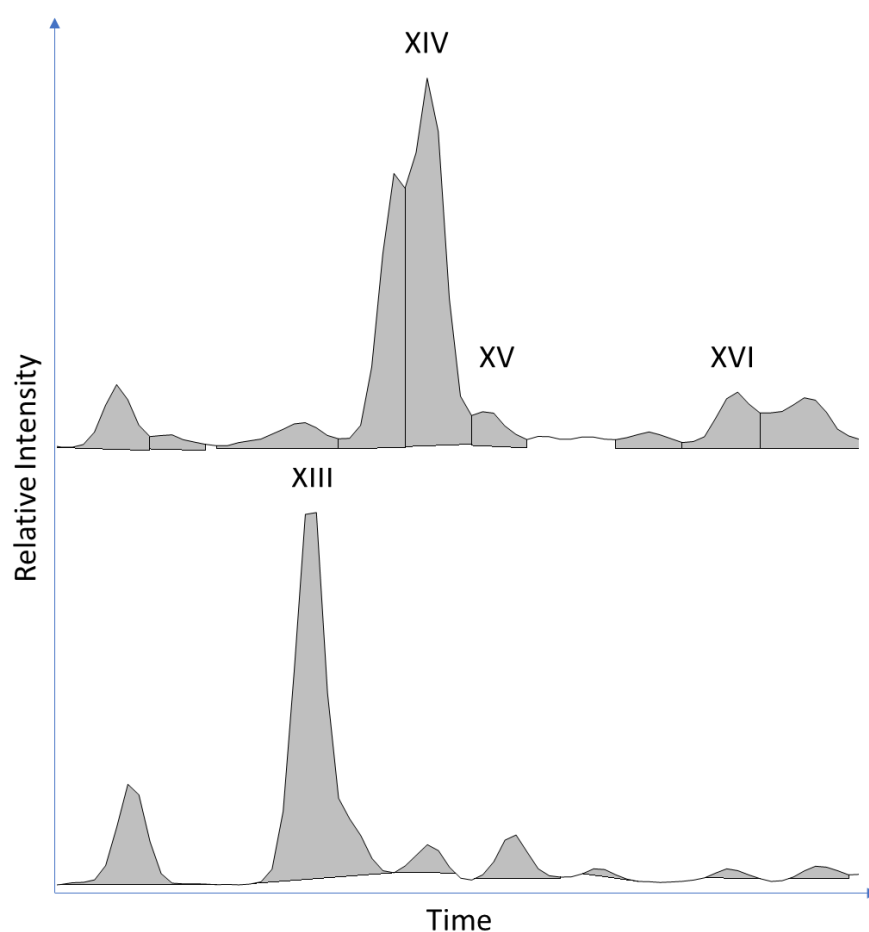


Figure 22. Partial TIC of the AM (**top**) and solvent (**bottom**) extracts of *Echinochloa colona* (*E. Frumentacea* dom.). Numerals relate to compounds listed in the text and Appendix 2.

Isomerisation of sawamilletin (XIII) has not been demonstrated using a pure standard, therefore, it is not possible to state with certainty whether other isomers are produced in a lower abundance that is not recognised in complex samples from caryopses. Nonetheless, the relative abundance of the three isomers is 79%, 7%, and 13%, respectively, which is more heavily weighted to a single isomer than is observed in the alteration of miliacin. Therefore, despite a somewhat low concentration of sawamilletin in this species, the XIV isomer remains abundant and could be used as a biomarker in AM extracts, provided it is restricted in origin.

Sorghum

Lupeol acetate (XVIII), and an unidentified lupeol acetate isomer (XVII), were observed in the solvent extracts of each sorghum (sub-)species analysed, *S. bicolor* r. *bicolor*, *S. bicolor* r. *durra* and *S. arundinaceum* (Figure 23). The abundance of lupeol acetate was 64, 70, and 32 $\mu\text{g g}^{-1}$ in each species, respectively, and the unidentified isomer (XVII) was always present in a low abundance. Neither compound is present in the AM extracts of these species, nor are alteration products derived from either the loss of an acetyl group, methylation, or a double bond shift. Other derivatives of these compounds may be produced during AM extraction, yet their identification would require more thorough investigation of the entire lipid extract, not just the PTME fraction. The loss of lupeol acetate in samples of each species indicates that this observation is not caused by the homogeneity of samples but an action of the extraction process.

A low abundance of friedelin (XIX) was identified in both the solvent (25.6 $\mu\text{g g}^{-1}$) and AM (28.4 $\mu\text{g g}^{-1}$) extracts of *Sorghum bicolor* r. *durra* (Figure 23). As this compound does not possess a carbon-carbon double bond it is not subject to acid isomerisation. Despite its low abundance, friedelin could prove a useful biomarker that may be used to distinguish between sorghum races. *Sorghum bicolor* r. *durra* also contains β -amyrin, but in an abundance that is too low, < 5 $\mu\text{g g}^{-1}$, to prove useful.

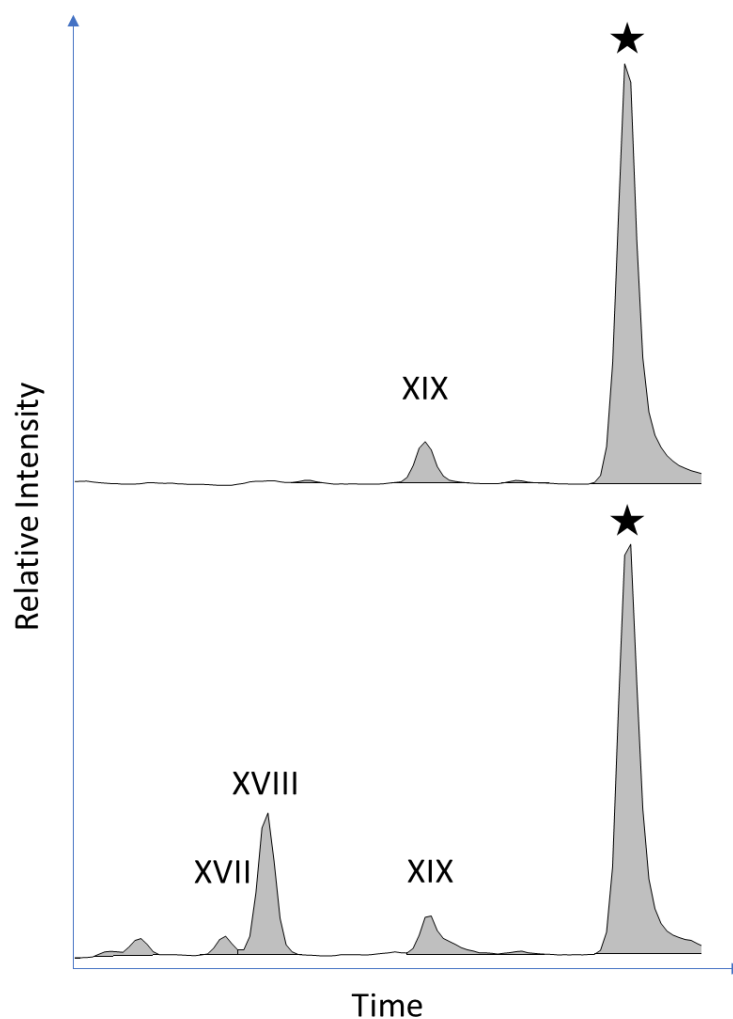


Figure 23. Partial TIC of the AM (**top**) and solvent (**bottom**) extracts of *Sorghum bicolor* r. durra. Numerals relate to compounds listed in the text and Appendix 2 and the star indicates a C₃₆ alkane standard.

Discussion

1. Determine whether other millet species produce miliacin

Miliacin is not an especially rare compound. It is reportedly produced by species from multiple genera that occupy a broad geographical range (Jacob *et al.* 2005; Oyo-Ita *et al.* 2010; Bossard *et al.* 2013). It has previously been identified in two millet species, *P. miliaceum* and *D. sanguinalis* (Ito 1934; Abe 1960; Ohmoto 1970; Bossard *et al.* 2013), and is reportedly common in the *Panicum* genus. It is, therefore, not surprising that miliacin was identified in both panicum species, *P. sonorum* and *P. sumatrense*, analysed in this study. The presence of miliacin in *Digitaria exilis* was not presumed, but is logical,

given previous reports of the compound in *D. sanguinalis*. One wonders whether miliacin is common among the entire *Digitaria* genus, given its close genetic relationship with *Panicum*, although the same could be said for several other genera analysed in this study (Aliscioni *et al.* 2003). Indeed, while several *Pennisetum* species produce miliacin (Bossard *et al.* 2013), and the genera is closely related to *Panicum* (Aliscioni *et al.* 2003), miliacin was not identified in *Pennisetum glaucum*. The absence of miliacin in the *Eragrostis* and *Paspalum* species analysed in this study demonstrate, in part, that the compound is not necessarily ubiquitous in these genera.

The concentration of miliacin in each species analysed in this study is greater than in *P. miliaceum*, except for the AM extract of *P. sonorum*, although, as discussed, the low abundance of miliacin in the AM extract is probably related to the homogeneity of the sample. It is important to consider that this study presents single results, from samples comprising relatively small numbers of caryopses, and that *P. miliaceum* has been studied extensively. Therefore, these results may not be as accurate as those of *P. miliaceum*. Nonetheless, the results of this study demonstrate that miliacin is sufficiently concentrated in five species of domesticated millet to prove useful as a biomarker.

The observation of miliacin in a greater number of species should elicit cautious interpretation of archaeological residues containing the compound. However, the increased prevalence of miliacin among millets is not an issue, at least in early phases of domestication, in most regions. Of the five millets that produce miliacin, *P. sonorum* is native to North America, *D. exilis* to West Africa, *P. sumatrense* to NW India, *D. sanguinalis* to Northern Eurasia, and *P. miliaceum* to NE China (Weber and Fuller 2008). Therefore, there is no overlap in the native range of each species. However, further analysis of reference materials is necessary, especially in North America and West Africa, as wild miliacin-producing species are present in these regions (Oyo-Ita *et al.* 2010; Bossard *et al.* 2013). Furthermore, the translocation and proliferation of cultivation of several species, namely *P. miliaceum* and *P. sumatrense*, may limit the application of miliacin as a biomarker for *P. miliaceum*. For instance, Suryanarayan *et al.* (2021) and Chakraborty *et al.* (2020) examined ceramic-absorbed organic residues from NW India, where various millet species are cultivated, including *P. miliaceum* and *P. sumatrense* (Weber and Fuller 2008). They utilise the absence of miliacin in their characterisation of residues, to determine that *P. miliaceum* was not processed in vessels. Indeed, it is likely,

from the data presented in this study, that neither was *P. sumatrense*. Had miliacin been observed in these samples, it would probably have been used to solely identify *P. miliaceum*, as has been done in other regions (Junno *et al.* 2020).

Unfortunately, it is unlikely that molecular characterisation of residues will provide a method of distinguishing between the two *Panicum* species, as they contain the same compounds. Indeed, none of the miliacin-producing species analysed produced considerably different compounds and what differences are present in the solvent extract are lost in the AM extract. It is also questionable whether triterpenes with either a hydroxyl or acetyl group would survive in the burial environment (Jacob *et al.* 2005). These factors should be a consideration when deciding which extraction methodology to use in regions where several of these millet species were cultivated.

2. Identify abundant terpenes that may be used as biomarkers to either identify or distinguish millet species

Sawamilletin is produced by species from multiple genera that inhabit a broad geographical range (Jacob *et al.* 2005; Oyo-Ita *et al.*; 2010, Schwab *et al.* 2015). It is somewhat common in the *Echinochloa* genera (Nguyen *et al.* 2017) and derives its name from another domesticated millet species, *Echinochloa crus-galli* (sawa millet), that is native to Japan (Obara and Abe 1957). It is, therefore, not unexpected to observe a high concentration of sawamilletin in *Echinochloa colona* (*E. Frumentacea* dom). This compound may be used as a biomarker for either domesticated millet species, as they are cultivated in different regions (Weber and Fuller 2008). Furthermore, the identification of sawamilletin in *Echinochloa colona* (*E. frumentacea* dom) may prove a useful biomarker in archaeological contexts in India, where numerous C₄ plants, including many millets, are consumed, and isotopic distinction is difficult (Suryanarayan *et al.* 2021). Unfortunately, sawamilletin is completely degraded during AM extraction and the resultant PTME isomers have not been identified. Therefore, it is not possible to state whether the alteration products are either restricted in their origin or useful as biomarkers. However, the high concentration of compound XIV does provide hope that the species could be identified in AM extracts of archaeological residues. Further analysis is necessary to characterise these isomers before any attempt is made to infer sawamilletin presence in

AM extracts of archaeological material. Until then, solvent extraction provides the most reliable method of detecting this species.

Acetates are highly susceptible to degradation (hydrolysis) in the burial environment and are unlikely to persist in either old material or unfavourable environments (Oyo-Ita *et al.* 2010). Considering that lupeol acetate was observed in a low abundance in each sorghum species analysed, it is unlikely that the compound would be a useful archaeological biomarker. Furthermore, the compound was completely lost during AM extraction. Lupeol is reportedly extracted by both solvent and AM methods (Reber 2021). Therefore, further investigation is necessary to investigate the reason for the loss of lupeol acetate during AM extraction. Friedelin is likely to be better preserved in archaeological materials than lupeol acetate, although not to the extent of PTMEs. The compound is present in a wide variety of species, including *Sorghum japonicum* (Chandler and Hooper 1979). Therefore, a significant degree of contextual investigation would be necessary for this compound to be a plausible biomarker. However, in certain contexts, it may prove useful to identify *S. bicolor* r. *durra* and to distinguish it from other *Sorghum* species.

3. Investigate the effect of acid isomerisation on the terpene fraction of millets

The miliacin standard experiment, presented at the start of this chapter, demonstrates double bond migration between the Δ^{18} and Δ^{12} position of this oleanane-type PTME, when it is subject to AM extraction. The relative abundance of δ -amyrin ME, miliacin, and β -amyrin ME, is 59, 18, and 23% respectively in the standard. This distribution is comparable to AM extracts of caryopses containing miliacin, except for *D. sanguinalis*, where the isomers are present at 52, 32, and 18% respectively (Table 2). This deviation warrants further consideration of the effects that AM extraction has on the entire triterpene fraction, although relative abundance is unlikely to prove a useful tool in distinguishing different species that produce miliacin.

Germanicol is subject to isomerisation during AM extraction. Double bond migration occurs between the same positions as is observed during the isomerisation of miliacin. Furthermore, the relative abundance of germanicol isomers is comparable to miliacin isomers with the same double bond position (Table 2). Additionally, triterpenes

with hydroxyl groups are not methylated during AM extraction. Therefore, the presence of germanicol in a caryopsis cannot explain an increased relative abundance of miliacin in the AM extract of *D. sanguinalis*.

The data from this analysis demonstrates that germanicol acetate is also subject to isomerisation, and the loss of the acetyl group, during AM extraction. However, there is insufficient data to state with certainty whether germanicol acetate is methylated, following the loss of an acetyl group. A difference in the relative abundance of miliacin, in species that do and do not produce germanicol acetate, could be explained, if methylation occurs either after or at a greater rate than double bond migration. However, this is unlikely, as both *D. sanguinalis* and *D. exilis* caryopses contain germanicol acetate, in proportion with miliacin, yet produce a different relative abundance of miliacin (32% and 16% respectively). Compound specific isotope analysis could demonstrate whether methylation occurs, provided isotopically distinct methanol was used during AM extraction.

The absolute abundance of miliacin in *D. sanguinalis* could explain why the relative abundance of miliacin is so high in the AM extract. The concentration of miliacin, per vial, is $15 \mu\text{g g}^{-1}$, compared to $< 4 \mu\text{g g}^{-1}$ for all other species. Therefore, a rate determining factor of double bond migration would result in the higher relative abundance of miliacin in this sample. Further adapted AM extractions of *D. sanguinalis*, similar to the miliacin standard experiment, would elucidate whether a rate determining factor exists.

Double bond migration is not limited to between the three positions of the miliacin isomers. Sawamilletin, with a double bond in the D ring, produces three novel isomers, with different yet unknown double bond positions. The observed loss of sawamilletin likely demonstrates that the three novel isomers are more thermodynamically stable. However, this potentially poses a problem for the identification of species that produce sawamilletin, as the novel isomers may either be more common in the natural world or overlap with alteration products of other triterpenes.

Oleanane-type triterpenes are unlikely to be the only triterpenes that are subject to double bond migration. However, alteration products of other triterpenes were not observed, due to the low initial abundance of these compounds, e.g. bauerenol ME. It

may be presumed that the alteration products were present but below the detection limit of GC-MS, as was hypothesised previously, although additional analysis, with a larger sample size, is necessary to prove this. The complete loss of lupeol acetate, without any observed derivatives, in sorghum samples, is also concerning and interesting, given the persistence of germanicol from germanicol acetate.

Conclusion

This chapter demonstrates that AM extraction has an impact on the integrity of organic residues containing certain triterpenes. Isomerisation is not limited to miliacin, with double bond migration observed in other triterpenes. This process distributes the initial abundance of a compound across several isomers, in varied proportions, reducing the likelihood of detecting any one compound. Furthermore, there is evidence to suggest that some compounds, i.e. lupeol acetate, are completely degraded and leave no trace of their presence, following AM extraction. These observations challenge the effectiveness of AM extraction in assessing the triterpene fraction of archaeological residues and perhaps the use of triterpenes as biomarkers. A potential benefit of isomerisation is that the fermentation of *P. miliaceum* may be identifiable, by the observation of miliacin isomers in solvent extracted samples. However, this would require rigorous experimentation and further consideration of factors that may induce isomerisation, e.g. deposition in acidic environments. This study demonstrates that archaeologists must weigh the potential advantages and disadvantages of solvent and AM extraction when analysing archaeological materials.

The production of certain triterpenes by multiple species, in addition to the effects of isomerisation, highlight the necessity of rigorous analysis of local flora to avoid false positive identification of *P. miliaceum* in archaeological materials. This study did not demonstrate the formation of miliacin, via isomerisation of either δ -amyrin ME or β -amyrin ME, as no species analysed contained these PTMEs. However, it is likely that miliacin would be formed in such situations. Indeed, the formation of three novel triterpenes from sawamilletin raises the possibility of other PTMEs forming miliacin via acid isomerisation, although this requires further investigation.

This study demonstrates that the observation of miliacin, in archaeological materials, should not be accepted as conclusive evidence for *P. miliaceum*, without a

comprehensive assessment of all potential formation factors. However, it is also important to consider whether other species that produce miliacin, and its isomers, were exploited in culinary contexts. Further research is necessary to understand the usefulness of molecular markers of other millets analysed in this study, yet their identification may enable previously unachievable ORA investigations of understudied cereals and regions.

Chapter 5: Experiments investigating the molecular and isotopic composition of *P. miliaceum* residues

This chapter presents a series of cooking experiments conducted with the objective of producing cooking liquid (CL) samples, which act as proxies of foodcrusts, and ceramic-absorbed lipid residues. The aim of these experiments is to improve the understanding of how processing millet (*P. miliaceum*), in isolation and in mixtures with beef and wheat, affects the development of foodcrusts and ceramic-absorbed residues over time. The development of experimental cooking liquids and absorbed residues are assessed by bulk isotope and molecular (GC-MS) analysis respectively. As such, this study refines criteria employed in the detection and interpretation of archaeological residues comprising *P. miliaceum* (Chapter 1).

Introduction

The release, absorption, and accumulation of molecules, including lipids, carbohydrates, and proteins, from different food products, during cooking, is a complex process that is difficult to predict without undertaking experimental research. When employing molecular and isotopic analyses, Hart *et al.* (2009), Hammann and Cramp (2018), and Miller *et al.* (2020), have demonstrated complex relationships between raw products and cooking residues of spelt, rye, barley, maize, wild rice, beef, milk, and wild deer (Chapter 2). However, while molecular and isotopic techniques are employed in the identification of *P. miliaceum* residues (Heron *et al.* 2016), their reliability and interpretive potential have not been investigated by experiments.

Understanding ceramic absorption of miliacin

In demonstrating ceramic absorption of miliacin, Heron *et al.* (2016) revealed that only a fraction of the miliacin present in *P. miliaceum* caryopses (see Bossard *et al.* 2013) is absorbed by the ceramic matrix during cooking. Ganzarolli *et al.* (2018) identified a low abundance of miliacin, relative to other compounds, in 26 ceramic-absorbed residues from Padova, Italy, conforming to experimental observations made by Heron *et al.* (2016). However, a high concentration of miliacin was observed in one sample, where it dominated the lipid fraction. This contrast may demonstrate a difference in either pre- or post-depositional factors, such as the type of products processed with *P. miliaceum* and

preservation conditions favouring miliacin. For instance, cooking experiments with spelt, rye, and barley have demonstrated increased uptake of alkylresorcinols when they are processed in the presence of lipid-rich products (Hamman and Cramp 2018). However, no experiments have investigated factors that influence ceramic absorption of miliacin.

Understanding the bulk and compound-specific carbon isotope composition of *P. miliaceum* residues

Heron *et al.* (2016) attributed bulk ^{13}C enrichment, in foodcrusts from Bruszczewo, to the processing of *P. miliaceum*, noting that bulk $\delta^{13}\text{C}$ values exceeding -20‰ are consistent with the processing of C_4 plant products. However, previous experiments with maize have demonstrated that there is a non-linear relationship between the quantity of maize processed and $\delta^{13}\text{C}$ values of foodcrusts. Indeed, a contribution of up to 80% maize, to a mixture cooked for 60 minutes, may not produce a foodcrust with a $\delta^{13}\text{C}$ value exceeding -22‰ (Hart *et al.* 2009). Therefore, one must question whether *P. miliaceum* is equally as limited in its influence on bulk $\delta^{13}\text{C}$ values, when processed in mixtures, and if the -22‰ threshold, which is commonly employed in the detection of a C_4 plant contribution to foodcrusts (Hart *et al.* 2009), underestimates past *P. miliaceum* processing. Furthermore, one wonders whether it is possible to quantify the proportion of *P. miliaceum* processed, during the formation of a foodcrust, according to bulk isotope data. The large size and structure of maize kernels limits their breakdown and release of carbon during cooking. Therefore, as *P. miliaceum* caryopses are much smaller, it is hypothesised that they would break down at a greater rate, and influence $\delta^{13}\text{C}$ values when present in a lower abundance, than is observed for maize.

Rageot *et al.* (2019a) identified miliacin in 18 ceramic-absorbed residues from Vix-Mont Lassois, France. The compound is attributed to *P. miliaceum*, although evidence indicates the vessels were used to process multiple products. Compound specific carbon isotope analysis was conducted on eleven samples from the site, six of which contained miliacin. However, all samples were depleted in ^{13}C and there was no distinction between $\delta^{13}\text{C}$ values of residues that did and did not contain miliacin. Therefore, a contribution of ^{13}C enriched lipids, from *P. miliaceum*, was not recognisable in these samples. As such, one may question under what circumstances a contribution of ^{13}C enriched lipids, from *P. miliaceum*, is recognisable by compound specific carbon isotope analysis. This question is directly connected to understanding ceramic-absorption of miliacin, as the

presence/absence criteria currently used to interpret molecular and compound specific isotope datasets do not appear to correlate with one another.

Experimental research questions

An experiment was designed, developing on the methodology of Hart *et al.* (2009), to assess the temporal development of foodcrusts and ceramic-absorbed residues, when beef, wheat, and millet are cooked in isolation and incremental mixtures. Two sample sets were obtained from these experiments, including CL samples and ceramic-absorbed residues. This study addressed four research questions with the aim of refining criteria used to identify and interpret archaeological *P. miliaceum* residues.

1. What proportion of either a beef or wheat mixture must *P. miliaceum* comprise for $\delta^{13}\text{C}$ values of cooking liquid samples to exceed -22‰ ?
2. Is it possible to distinguish cooking liquid samples, derived from processing *P. miliaceum* with either beef or wheat, by bulk isotope analysis?
3. Is it possible to determine the composition of processed mixtures, including *P. miliaceum*, beef, and wheat, by bulk isotope analysis of cooking liquid samples?
4. Does the abundance of miliacin in ceramic-absorbed residues relate to either the type or quantity of products processed with *P. miliaceum*?

Experimental method

The experimental methodology was as follows. A clean 1 L Pyrex jug was filled with approximately 900 mL deionised water and placed on a hotplate. A briquette was submerged in the water, sitting proud of the water line by several millimetres, and held in place by forceps held in a clamp stand (Figure 24). The water was heated to 100°C , taking approximately 21 minutes, and maintained at this temperature throughout the experiment. At 21 minutes, ingredients were added to the boiling water and a timer was set for 20 minutes. After 20 minutes, a section of the briquette was snapped off, allowed to cool, and wrapped in aluminium foil, with the remainder of the briquette staying in place in the cooking liquid. In addition, a 3 mL sample of the cooking liquid, including floating surface material, i.e. lipids, was taken, using a clean glass pipette, and stored in a clean hydrolysis vial. The timer was reset every 20 minutes until 60 minutes was reached,

resulting in three sampling events at 20, 40 and 60 minutes. Samples from each cooking experiment were stored separately in a freezer before analysis.



Figure 24. Demonstration of the equipment setup used during this experiment. A pilot experiment with 500 mL of water proved to be insufficient for one hour of cooking. Therefore, 900 mL of water was used in the actual experiments.

This experiment was conducted under laboratory conditions to minimise the variables, e.g. temperature fluctuation and uneven heating, that affect outdoor cooking experiments. In addition, the methodology enabled increased sampling throughout the cooking event, without additional effort and material costs. To maintain a constant temperature the Pyrex jug was placed on a hotplate and ceramic briquettes were used to collect absorbed lipid residues, acting as a proxy for pottery vessels. There are several benefits to using ceramic briquettes, rather than whole vessels, during cooking experiments. Firstly, briquettes can be easily broken, enabling sampling without disrupting an experiment and wasting material. Secondly, using a briquette concentrates absorbed lipids in a small volume of ceramic fabric. Finally, due to their small size and ease of production, briquettes are much cheaper, allowing more comprehensive experiments to be conducted.

There is potentially a small difference between the $\delta^{13}\text{C}$ values of cooking liquids produced within non-porous glass and porous ceramic vessels, although evidence is limited to two experiments with maize (Hart *et al.* 2009). These results warrant further investigation and consideration of other potential differences that non-authentic experiments may produce. However, in this instance, a proxy for ceramic absorption of lipids and other compounds was used. Therefore, the differences between experiments in this study and authentic cooking events are presumed to be insignificant.

Cooking liquid samples were not charred as part of these experiments as the charring process may result in either a variable change in $\delta^{13}\text{C}$ values or a variable increase in $\delta^{15}\text{N}$ values of foodstuffs (Fraser *et al.* 2013; Miller *et al.* 2020). Therefore, the data obtained in these experiments, from uncharred CL samples, may be directly and unambiguously attributed to processes involved in residue formation.

Between each cooking experiment, the Pyrex jug was emptied, rinsed with water, washed with detergent, rinsed with water several times, and dried with disposable paper towels. The internal surface of the jug was then rinsed three times with DCM. All other equipment was subject to the same cleaning protocol. Clean gloves, glassware, and equipment were used to handle samples and materials for each experiment.

The ingredients used in this experiment include beef skirt, emmer wheat, and broomcorn millet. Fresh (wet) beef was used with dry cereals. In total, 12 cooking events were undertaken, using 100 g of ingredients, including nine events that involved mixing two ingredients, in 25% increments, and three events that did not involve mixing (Table 3). This resulted in the production of 36 liquid samples and 36 ceramic samples, that were analysed by EA-IRMS and GC-MS respectively.

The liquid samples obtained during each experiment separated during storage, resulting in a lower dark layer, upper light layer, and fatty cap layer (Figure 25). The fatty cap was only observed in samples from experiments containing beef. Layers were less distinct in samples from experiments that did not contain millet. The layers were maintained during freeze drying, therefore, material from each layer was analysed in duplicate.

Table 3. Mixture combinations and sampling times used during cooking experiments.

Sample (First + Second)	Time (minutes)	Contribution of ingredients (g)			
		100	75 + 25	50 + 50	25 + 75
Millet + Beef	20				
	40				
	60				
Beef + Wheat	20				
	40				
	60				
Wheat + Millet	20				
	40				
	60				

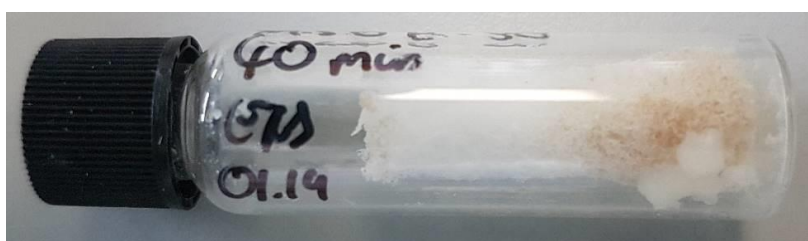


Figure 25. Photograph demonstrating the separation of lower and upper layers and fatty cap layer in freeze dried liquid samples. In this sample, the fatty cap has fallen to the bottom of the vial (bottom right of the image).

Ceramic samples were subject to standard ORA preparation procedures (Appendix 1). When the ceramic sherds were cleaned, by removing the ceramic surface with a drill, it was noted that a thin layer of beige material adhered to the ceramic fabric. This surface deposit was not obvious when looking at the sherd, prior to cleaning, and was only observed on ceramic sherds from cooking events incorporating millet. Lipids were extracted from ceramic samples using AM extraction (Appendix 1).

Experimental ingredients and materials

Organic emmer wheat was obtained from Doves Farm (Hungerford, Berkshire, RG17 0RF, United Kingdom). Emmer wheat was selected for this experiment due to its frequency and abundance in the archaeobotanical record of Bronze Age Europe and its dominance at the archaeological sites examined in this thesis (Chapter 6 and 7). The wheat was supplied as florets and required threshing and winnowing prior to use.

Organic beef skirt was purchased from Longwood Farm (The Green, Tuddenham, IP28 6TB, United Kingdom). Beef was selected due to its availability in the UK and the ability to obtain unpasteurised milk from cattle reared at the same site, although milk was ultimately not used in any of these experiments. Longwood Farm was the only producer, providing these two products, that could confirm their cattle did not consume C₄ plants. Cattle at the farm are pastured on grass in the summer and their diets are supplemented by lucerne (*Medicago sativa*), grown on the same farm, in the winter. The cut of beef was selected due to an even distribution of fat and an approximately average fat content for beef, around 9%.

Broomcorn millet (*P. miliaceum*) was purchased from the Daily Bread Co-operative (Northampton, NN4 7AD, United Kingdom). The millet was grown on a non-organic farm in Poland and imported into the UK, undergoing cleaning and bagging at the wholesaler and distributor.

Ceramic briquettes were purchased from Graham Taylor, of Potted History (Gregory Court, Coplish Lane, Rothbury, Northumberland, NE65 7JP, United Kingdom). The briquettes are formed from standard red clay (Bondetti *et al.* 2021) and were fired at 700°C. The specified dimensions of the briquettes were H 3 x W 8 x D 0.5 cm. However, the shallow depth presented difficulties during production. Therefore, the actual depth of briquettes was variable. Briquettes selected for use in the experiments were of approximately equal dimensions, with an average depth of 0.7 cm. Each briquette was scored across its height, at 2 cm intervals along its width, in order to create a weak point that would allow equal sections to be snapped off during the experiment (Figure 26).



Figure 26. Example of the briquettes used in these experiments.

Bulk isotope analysis results

Bulk carbon and nitrogen isotope analysis was conducted on each ingredient, prior to use in the experiment, to establish their isotopic baseline and ensure that the beef skirt was sourced from a C₃-fed cow. Samples were taken in quadruplicate from two separate samples of beef and duplicate from homogenised cereals. The results of this analysis, presented in Table 4, confirms the carbon source of beef. The low $\delta^{15}\text{N}$ value of wheat, relative to millet, is likely a result of organic farming utilising crop rotation. Conversely, the relatively high $\delta^{15}\text{N}$ value of millet is likely derived from fertilisers used during cultivation.

Table 4. Average bulk $\delta^{13}\text{C}$ (corrected) and $\delta^{15}\text{N}$ values of ingredients used in the cooking experiment.

Ingredient	$\delta^{13}\text{C}$	C %	$\delta^{15}\text{N}$	N %	C/N
Beef	-24.5	48.5	9.0	15.1	3.8
Wheat	-23.0	41.1	0.3	2.3	21.2
Millet	-11.0	48.7	4.7	2.1	27.1

Formulating bulk $\delta^{13}\text{C}$, $\delta^{15}\text{N}$, and C/N values from cooking liquid samples

Bulk $\delta^{13}\text{C}$, $\delta^{15}\text{N}$, and C/N values of CL samples are presented in Table 5, 6, and 7 respectively. All bulk $\delta^{13}\text{C}$ values are corrected to account for the Suess effect, enabling the interpretation of experimental results in the context of archaeological research questions, i.e. the -22‰ threshold for detecting ^{13}C enriched material input from C₄ plants. The $\delta^{13}\text{C}$ value of each sample is calculated as an average of $\delta^{13}\text{C}$ values from each non-fat layer, plus a 2.5% equivalent contribution of the $\delta^{13}\text{C}$ value from the fatty cap (where applicable). The $\delta^{13}\text{C}$ value of the fatty cap is added to the average to account for a separation of lipids, from the non-fat layers, during storage and freeze drying. A contribution of 2.5% is used as an approximate average lipid content of foodcrusts, that may range from 0-5% of the total mass of charred crusts (Craig *et al.* 2007). This calculation is also used to produce the carbon percentage for the C/N ratio. Fatty cap layers did not comprise sufficient quantities of nitrogen for accurate measurement of $\delta^{15}\text{N}$ values. Therefore, only measurements from non-fat layers were used to calculate $\delta^{15}\text{N}$ values.

Table 5. Table of $\delta^{13}\text{C}$ values of CL samples from each experiment. Values represent an average of non-fat layers. Values with * incorporate a 2.5% contribution of the $\delta^{13}\text{C}$ value from the fatty cap to account for separation during storage $((0.02564 * \delta^{13}\text{C}_{\text{fatty-cap}}) + ((\text{average } \delta^{13}\text{C} \text{ of non-fat layers})))$. This equates to a 2.4999% contribution of carbon from the fatty cap.

Sample	Time (minutes)	$\delta^{13}\text{C}$ values (‰)			
		100	75 + 25	50 + 50	25 + 75
Millet + Beef	20	-10.4	-20.0*	-14.7	-21.3
	40	-10.5	-19.6*	-17.5*	-18.7*
	60	-10.3	-12.4*	-12.7*	-17.8*
Beef + Wheat	20	-26.0	-25.2	-28.9*	-28.1*
	40	-26.7*	-27.2*	-27.4*	-25.7*
	60	-26.9*	-28.9	-27.4*	-28.0*
Wheat + Millet	20	-23.7	-13.3	-11.4	-11.0
	40	-23.6	-13.0	-11.2	-10.8
	60	-22.9	-13.6	-10.8	-10.7

Table 6. Table of $\delta^{15}\text{N}$ values of liquid samples from each experiment. Values are an average of lower layers. Values in red are derived from samples that contained an average nitrogen content < 1%.

Sample	Time (minutes)	$\delta^{15}\text{N}$ values (‰)			
		100	75 + 25	50 + 50	25 + 75
Millet + Beef	20	1.2	3.6	6.6	7.8
	40	2.3	3.4	4.8	7.1
	60	0.7	3.3	2.9	7.0
Beef + Wheat	20	8.7	7.7	7.9	6.7
	40	8.7	7.2	6.5	5.1
	60	7.7	7.1	5.4	4.8
Wheat + Millet	20	0.7	2.8	1.4	2.2
	40	0.1	0.3	0.7	1.4
	60	-0.6	-1.2	-4.4	-0.1

A single non-fat layer was obtained from beef + wheat CL samples and two non-fat layers, which demonstrated only minor variance in $\delta^{13}\text{C}$ values (< 1‰), were obtained from wheat + millet CL samples. Two non-fat layers were obtained from millet + beef CL samples, yet they demonstrated substantially different $\delta^{13}\text{C}$ values, up to 10‰, indicating a difference in composition. Lower layers have a greater nitrogen content and generally

produce lower $\delta^{13}\text{C}$ values, likely indicating a higher protein content derived from beef. Conversely, upper layers have a greater carbon content and generally produce higher $\delta^{13}\text{C}$ values, likely indicating a higher carbohydrate content derived from millet. It is presumed that all compounds released into suspension contribute to the formation of foodcrusts in roughly equal proportions, as there was little difference in the abundance of each non-fat layer. Therefore, the averaged isotope values calculated are believed to approximately represent authentic foodcrusts. However, this may be subject to revision if future authentic cooking experiments demonstrate greater variance in the composition of foodcrusts. Presently, the data produced is viewed as a guide and not absolute measure.

Table 7. Table of C/N values of liquid samples from each experiment. Values represent an average of non-fat layers. Values with * incorporate a 2.5% contribution of the C% value from the fatty cap, to account for separation during storage. A contribution of N% values from the fatty cap samples were not included as they contained < 1% nitrogen and produced a broad range of $\delta^{15}\text{N}$ values (> 15‰), indicating that they are not accurate. Values in red are derived from samples that contained an average nitrogen content < 1%.

Sample	Time (minutes)	C/N values			
		100	75 + 25	50 + 50	25 + 75
Millet + Beef	20	68.6	84.9*	21.8	5.6
	40	73.8	94.6*	58.1*	14.6*
	60	94.4	61.6*	38.0*	11.8*
Beef + Wheat	20	5.5	4.9	14.6*	18.7*
	40	4.9*	7.4*	13.1*	12.3*
	60	5.3*	15.1	14.3*	25.3*
Wheat + Millet	20	20.0	28	58.8	48.2
	40	23.4	61.5	60.0	64
	60	26.9	49.4	206.7	86.8

Unmixed ingredient experiments

Bulk $\delta^{13}\text{C}$ and $\delta^{15}\text{N}$ values of raw beef, wheat, and millet, and their respective CL samples, from the unmixed experiments, are plotted in Figure 27 and 28. The data demonstrates that cooking liquids produce distinct and characteristic isotope values by 20 minutes. However, while the release of material from millet and beef was clearly visible within 20 minutes, there was little evidence of a contribution from wheat, to the cooking liquid, until later in the experiment.

The $\delta^{13}\text{C}$ value of beef CL samples demonstrate ^{13}C depletion, $\leq 2.4\text{‰}$, relative to the raw ingredient (Figure 27), with a decrease observed over time indicating preferential release of lipids (Figure 28). A concurrent decrease in $\delta^{15}\text{N}$ values, by $\leq 1.3\text{‰}$ over 60 minutes, indicates fractionation of nitrogen isotopes during cooking, although the nature of this fractionation process is unknown.

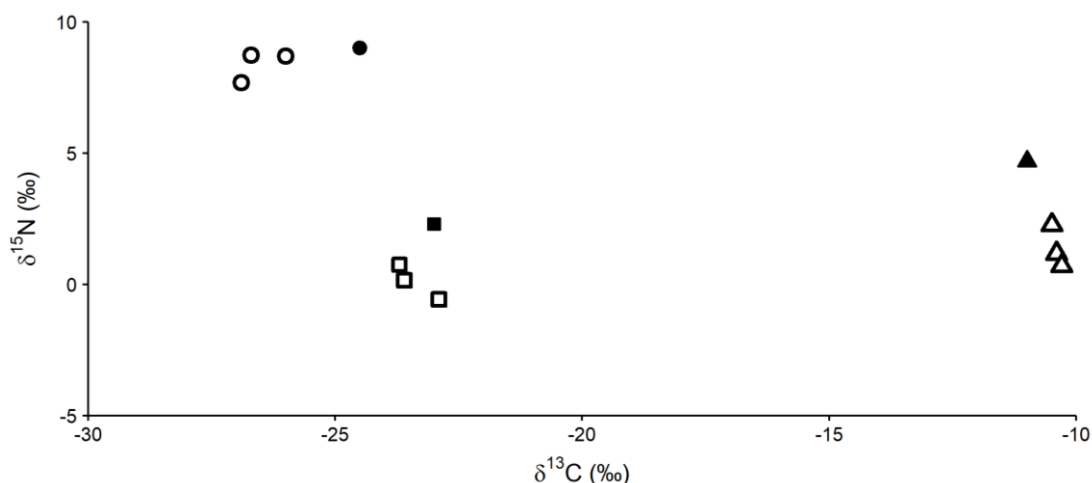


Figure 27. Bulk $\delta^{13}\text{C}$ and $\delta^{15}\text{N}$ values of beef (circles), wheat (squares), and millet (triangles). Open shapes represent liquid samples obtained during cooking. Filled shapes are values of each ingredient when raw.

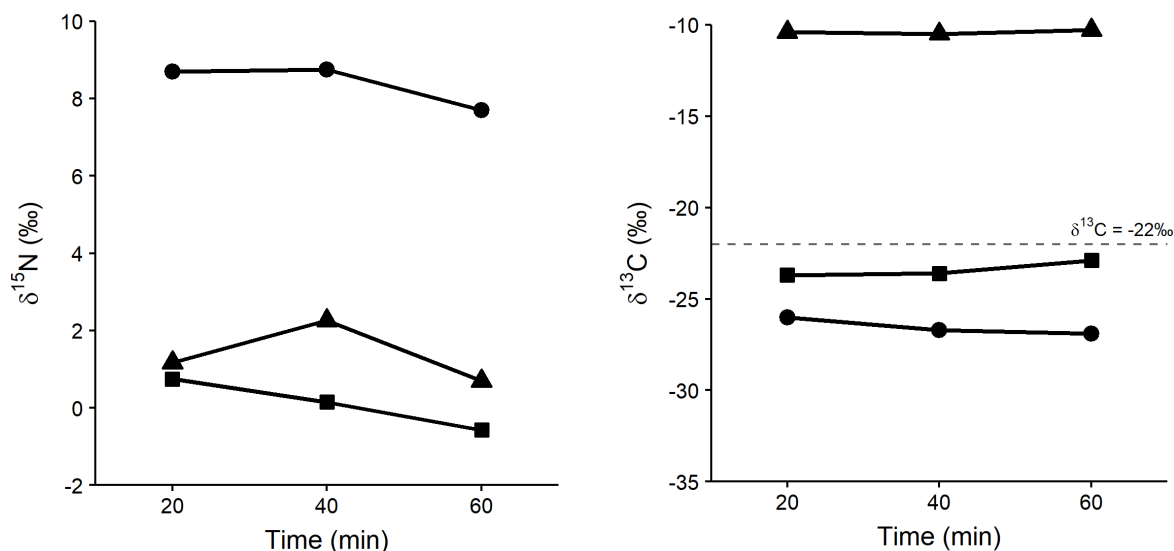


Figure 28. Bulk $\delta^{15}\text{N}$ (left) and $\delta^{13}\text{C}$ (right) values of liquid samples obtained from cooking beef (circles), wheat (squares) and millet (triangles).

The $\delta^{13}\text{C}$ and $\delta^{15}\text{N}$ values of raw and CL samples of wheat vary by $< 1\text{‰}$. However, an increase and decrease are observed in these values respectively during cooking (Figure

28). Increasing C/N values from these samples indicate that higher $\delta^{13}\text{C}$ values result from the release of relatively ^{13}C enriched carbohydrates into suspension (Table 7). Lower $\delta^{15}\text{N}$ values may result from fractionation during cooking.

The $\delta^{13}\text{C}$ values of millet CL samples are consistent throughout cooking, although increasing C/N values indicate the release of carbon, into suspension, over time (Figure 28). The $\delta^{15}\text{N}$ values of all millet CL samples are lower than the raw ingredient and decrease between 20 and 60 minutes, although there is a minor increase at 40 minutes. However, the reliability of this data is questionable, given the low nitrogen content of samples (Table 6).

Beef and wheat experiments

The data from beef + wheat CL samples is presented in Figure 29. All samples produced $\delta^{15}\text{N}$ values lower than unmixed beef, demonstrating a contribution of nitrogen from wheat, with lower $\delta^{15}\text{N}$ values corresponding to an increased proportion of wheat in mixtures. There is a decrease in $\delta^{15}\text{N}$ values of all mixtures over time, although this is greater in samples containing $\geq 50\%$ wheat. This indicates that wheat releases additional nitrogen into suspension after 20 minutes. However, this is not easily recognised in mixtures containing $\leq 25\%$ wheat, as nitrogen released from wheat is overwhelmed by nitrogen released from beef.

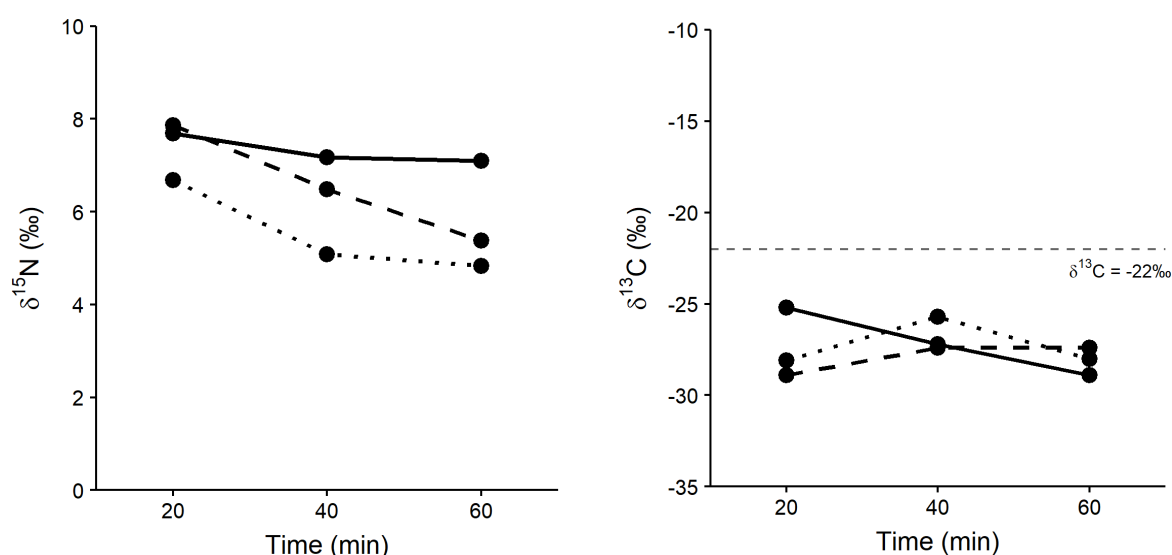


Figure 29. Bulk $\delta^{15}\text{N}$ (left) and $\delta^{13}\text{C}$ (right) values of liquid samples obtained from cooking beef + wheat. The solid, dashed, and dotted lines represent, B75+W25, B50+W50 and B25+W75 respectively.

Mixtures containing $\geq 50\%$ wheat produce lower $\delta^{13}\text{C}$ values at 20 minutes than B75+W25, despite raw beef having a lower $\delta^{13}\text{C}$ value than wheat. This may relate to a difference in the availability of either ^{13}C -depleted lipids or ^{13}C -enriched carbohydrates in the portion of either beef or wheat used in each experiment. The $\delta^{13}\text{C}$ values of B75+W25 decrease over time, indicating the release of lipids. Conversely, there is an overall increase in $\delta^{13}\text{C}$ values from mixtures containing $\geq 50\%$ wheat, indicating the release of ^{13}C -enriched carbohydrates from wheat, corresponding to the release of nitrogen, during cooking. An increase in C/N values of B25+W75 and B75+W25, between 20 and 60 minutes, support the interpretation that greater quantities of carbon are released during cooking, although the C/N value of B50+W50 is relatively stable throughout cooking, warranting further investigation (Table 7). The $\delta^{13}\text{C}$ values of B50+W50 and B25+W75 decrease and increase respectively, at different rates, between 40 and 60 minutes, potentially demonstrating that the release of carbon is not uniform throughout cooking. This likely derives from an increase in the release of ^{13}C depleted lipids from beef, between 40 and 60 minutes, that counteracts the release of ^{13}C enriched carbohydrates from wheat, when beef contributes $\geq 50\%$ to a processed mixture.

Millet and beef experiments

The data from millet + beef CL samples is presented in Figure 30. It is important to note that the nitrogen content of CL samples from M75+B25 were low, potentially resulting in inaccurate $\delta^{15}\text{N}$ values. However, high, intermediate, and low $\delta^{15}\text{N}$ values, from M25+B75, M50+B50, M75+B25 respectively, correspond to the contribution of millet and beef in mixtures. A gradual decrease of $\delta^{15}\text{N}$ values is observed over time in samples from M75+B25 and M25+B75. However, a severe decrease is observed in samples from M50+B50. The data indicates that each ingredient dominates the nitrogen content of samples when they are the primary component of a mixture. However, when their contribution is equal, an initial release of nitrogen from beef is quickly overwhelmed by the release of nitrogen from millet, rapidly lowering $\delta^{15}\text{N}$ values.

The $\delta^{13}\text{C}$ values of CL samples from millet + beef mixtures clearly demonstrate a contribution of ^{13}C enriched carbon from millet, although this does not correspond to the proportion of millet in each mixture. At 20 minutes, both M75+B25 and M25+B75 produce similar $\delta^{13}\text{C}$ values, -20.0‰ and -21.3‰ respectively, while M50+B50 produced a

relatively high $\delta^{13}\text{C}$ value of -14.7‰ . The low $\delta^{13}\text{C}$ and high C/N value of the M75+B25 sample, at 20 minutes, indicates a high contribution of carbon from beef. This, and the unexpectedly high $\delta^{13}\text{C}$ value of M50+B50 at 20 minutes, may reflect inadvertent sampling of concentrated material from beef and millet respectively, warranting repeat experiments and analysis. There is a close concordance between samples at 40 minutes, with M75+B25 producing the lowest $\delta^{13}\text{C}$ value. This may suggest that inadvertent sampling bias is not the issue in this experiment, but that the 25 g portion of beef used was particularly rich in lipids. The $\delta^{13}\text{C}$ values of all mixtures increase between 40 and 60 minutes to a maximum of -12.4‰ .

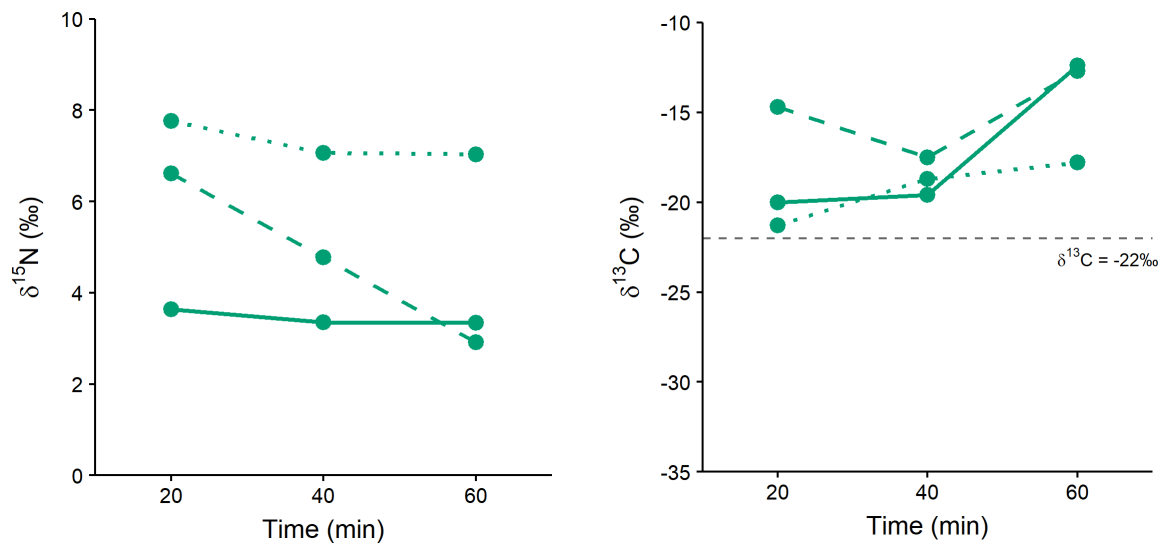


Figure 30. Bulk $\delta^{15}\text{N}$ (left) and $\delta^{13}\text{C}$ (right) values of liquid samples obtained from cooking millet + beef. The solid, dashed, and dotted lines represent, M75+B25, M50+B50, and M25+B75 respectively.

Wheat and millet experiments

The data from wheat + millet CL samples is presented in Figure 31. The nitrogen content in most samples is low, potentially resulting in inaccurate measurement of $\delta^{15}\text{N}$ values. There is only a minor difference in $\delta^{15}\text{N}$ values at 20 and 40 minutes, but there is a greater distinction between samples at 60 minutes, likely as a result of an inaccurate measurement. All $\delta^{15}\text{N}$ values decrease over time, potentially demonstrating increasing release of nitrogen from wheat, which has a lower bulk $\delta^{15}\text{N}$ value than millet. However, this decrease does not correspond to the proportion of wheat in different mixtures.

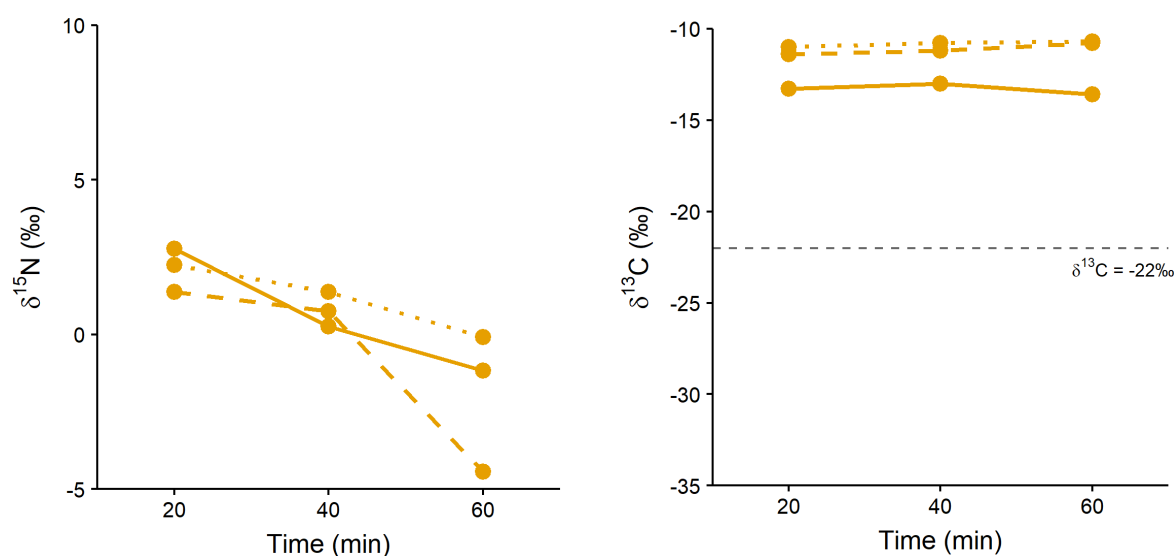


Figure 31. Bulk $\delta^{15}\text{N}$ (left) and $\delta^{13}\text{C}$ (right) values of liquid samples obtained from cooking wheat + millet. The solid, dashed, and dotted lines represent, W75+M25, W50+M50, and W25+M75 respectively.

The $\delta^{13}\text{C}$ value of wheat + millet CL samples are consistently high throughout cooking, demonstrating a dominant contribution of ^{13}C enriched material from millet before 20 minutes. The release of carbon, from millet, is either continuous or sufficient to dominate the cooking liquid over 60 minutes. However, a decrease in the $\delta^{13}\text{C}$ value of W75+M25, between 40 and 60 minutes, may demonstrate a late release of carbon from wheat, which is also observed in beef + wheat mixtures, that is only sufficient in lowering $\delta^{13}\text{C}$ values when millet is a minor constituent of the mixture.

Discussion of bulk isotope data

Bulk isotope data from all mixing experiments are presented in Figure 32, 33, and 34 for ease of comparison.

1. What proportion of either a beef or wheat mixture must *P. miliaceum* comprise for $\delta^{13}\text{C}$ values, of cooking liquid samples, to exceed -22‰?

All CL samples from mixtures comprising *P. miliaceum* produced $\delta^{13}\text{C}$ values that exceeded -22‰, demonstrating that a 25% contribution of the cereal is recognisable by 20 minutes of cooking. As this experiment did not use smaller quantities of *P. miliaceum*,

it is not possible to state a minimum contribution of the cereal necessary to elevate $\delta^{13}\text{C}$ values above -22‰ . However, as the lowest $\delta^{13}\text{C}$ value obtained was -21.3‰ , and that this value was obtained from a 50% contribution of *P. miliaceum*, it is likely that, when accounting for sample variability, a minimum contribution necessary to exceed -22‰ is around 25%. One must also consider that a shorter cooking time would likely result in $\delta^{13}\text{C}$ values below -22‰ , although this requires further investigation. These results are in stark contrast to the limited influence that maize has on $\delta^{13}\text{C}$ values, yet they conform to the hypothesis that smaller grain size is related to the breakdown of cereals and the release of carbon (Hart *et al.* 2009). One may question to what extent different caryopsis structures also influence the release of carbon by cereals. Certainly, the breakdown and release of carbon from *P. miliaceum* was obvious during cooking and increasing C/N values correspond to the proportion of the cereal in each mixture.

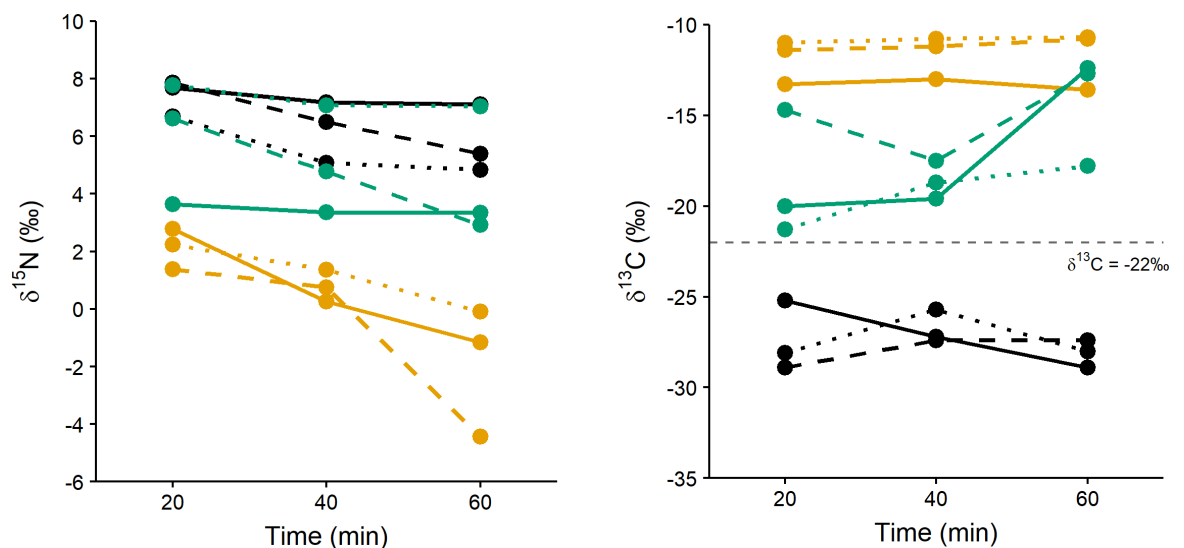


Figure 32. Bulk $\delta^{15}\text{N}$ (left) and $\delta^{13}\text{C}$ (right) values of liquid samples obtained from cooking beef + wheat (black), millet + beef (green), and wheat + millet (orange). The solid, dashed, and dotted lines represent, a75+b25, a50+b50, and a25+b75 respectively, with a and b representing the first and second ingredient respectively.

Given the extent of ^{13}C enrichment in wheat + millet CL samples, one may explore this question from another perspective, asking whether it is possible to distinguish CL samples from wheat + millet and millet processed in isolation. There is a 0.2‰ difference between CL samples of unmixed millet, cooked for 40 minutes, and W25+M75, cooked for 60 minutes, with other wheat + millet CL samples producing similar $\delta^{13}\text{C}$ values. As

this difference is within the analytical error of EA-IRMS, it is possible that a contribution of $\leq 25\%$ wheat may not be recognised when mixed with millet, depending on cooking times. Conversely, there is a $\geq 2\text{‰}$ difference between CL samples from unmixed millet and millet + beef mixtures, indicating that even a small contribution of beef is identifiable when cooked with millet over 60 minutes.

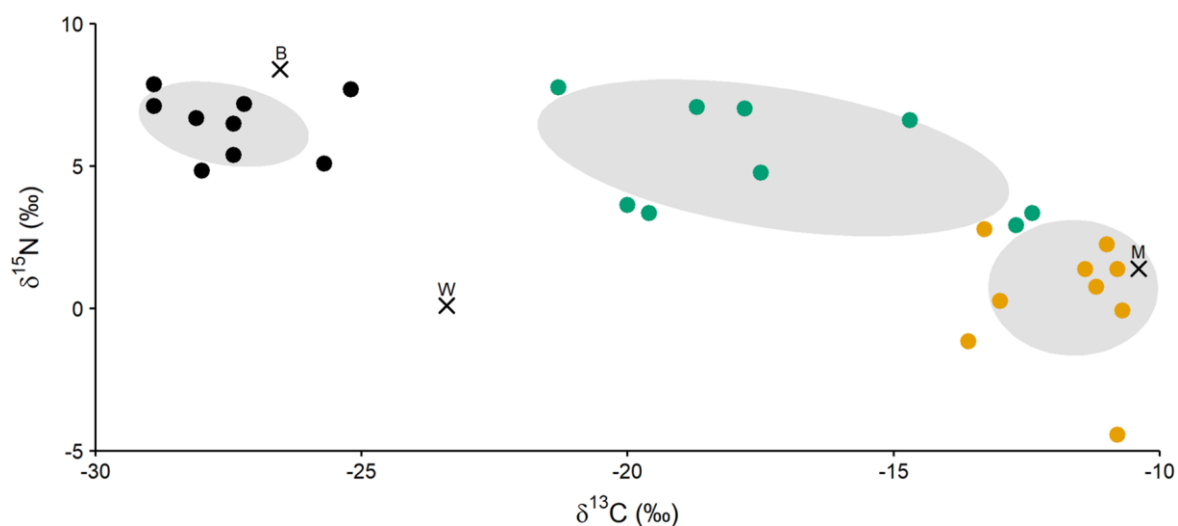


Figure 33. Bulk $\delta^{15}\text{N}$ and $\delta^{13}\text{C}$ values of liquid samples obtained from cooking beef + wheat (**black**), millet + beef (**green**), and wheat + millet (**orange**), plotted with 1σ confidence ellipses. Points annotated with B, W, and M mark the average values of unmixed beef, wheat, and millet cooking liquid samples respectively.

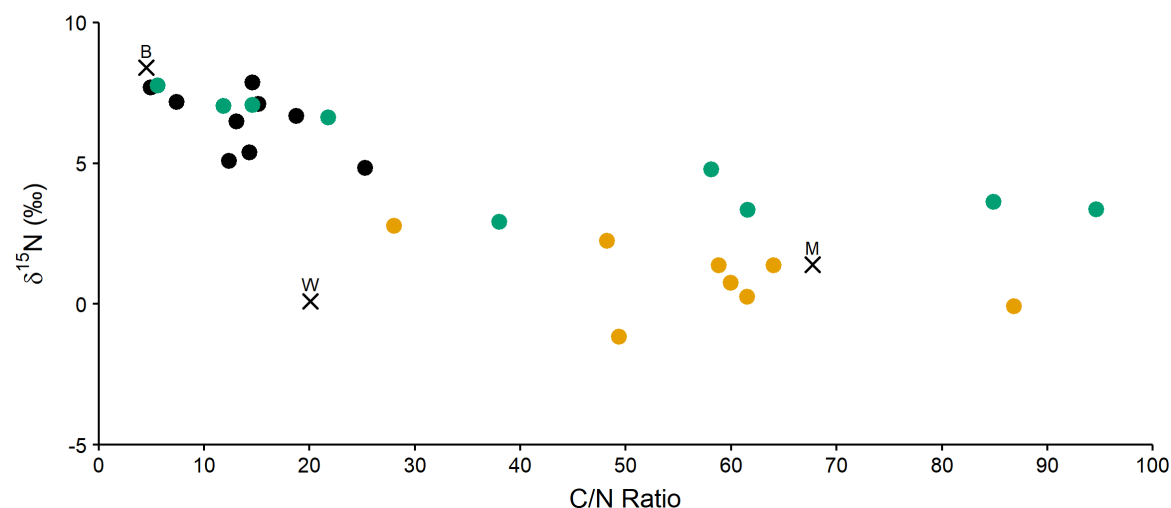


Figure 34. Bulk $\delta^{15}\text{N}$ and C/N values of liquid samples obtained from cooking beef + wheat (**black**), millet + beef (**green**), and wheat + millet (**orange**). Points annotated with B, W, and M mark the average values of unmixed beef, wheat, and millet cooking liquid samples respectively.

2. Is it possible to distinguish cooking liquid samples derived from processing *P. miliaceum*, with either beef or wheat, by bulk isotope analysis?

There is a significant difference between the $\delta^{13}\text{C}$ and $\delta^{15}\text{N}$ values of millet + beef and wheat + millet CL samples (paired t-test, $t = 4.6739$, $df = 8$, $p = .0016$ and $t = 7.1648$, $df = 8$, $p = .0001$ respectively). However, there is overlap between $\delta^{13}\text{C}$ and C/N values, and close similarity between $\delta^{15}\text{N}$ values, when mixtures comprising $\leq 50\%$ beef and $\geq 75\%$ wheat are compared over 60 minutes. The $\delta^{15}\text{N}$ values of all millet + beef and wheat + millet CL samples are $> 2.9\text{‰}$ and $< 2.8\text{‰}$ respectively. However, low nitrogen concentrations in these samples, particularly from wheat + millet experiments, likely make $\delta^{15}\text{N}$ values inaccurate. Furthermore, it is important to consider that charring may result in a variable increase in $\delta^{15}\text{N}$ values (Fraser *et al.* 2013). Therefore, distinction of product source according to such fine margins would likely be unreliable. As such, it may be proposed that CL samples from millet + beef and wheat + millet mixtures, which comprise a high and low contribution of beef and wheat respectively, are broadly distinguishable when examining $\delta^{13}\text{C}$ and $\delta^{15}\text{N}$ values. However, mixtures comprising a similar contribution of each ingredient are not distinguishable, due to the isotopic development of cooking liquids over time.

3. Is it possible to determine the composition of processed mixtures, including *P. miliaceum*, beef, and wheat, by bulk isotope analysis of cooking liquid samples?

There is considerable overlap and similarity between the $\delta^{13}\text{C}$ and $\delta^{15}\text{N}$ values of millet + beef CL samples, although $\delta^{15}\text{N}$ values $\geq 7.0\text{‰}$ may be attributable to a $\geq 75\%$ contribution of beef (Table 5 and 6). It may be possible to approximate the contribution of each ingredient to a mixture by examining C/N values. A dominant contribution of beef may be recognised by C/N values < 21 and values around 39 are indicative of an approximately equal contribution of each ingredient. However, while C/N values > 85 indicate a dominant contribution of millet, in a millet + beef mixture, this figure may also be produced by wheat + millet CL samples. Therefore, as there is also overlap and similarity in $\delta^{13}\text{C}$ and $\delta^{15}\text{N}$ values of M75+B25, M50+B50, and W75+M25 mixtures,

outlined in the previous section, a dominant contribution of millet, to a millet + beef mixture, cannot be reliably identified. Unfortunately, overlap and similarity between $\delta^{13}\text{C}$, $\delta^{15}\text{N}$, and C/N values of all other wheat + millet CL samples also precludes their characterisation (Table 5, 6, and 7).

There is considerable overlap and similarity between the $\delta^{13}\text{C}$ and $\delta^{15}\text{N}$ values of beef + wheat CL samples, although $\delta^{15}\text{N}$ values $\leq 5.1\text{‰}$ may be attributable to a $\geq 75\%$ contribution of wheat (Table 5 and 6). In addition, while beef + wheat CL samples produce a narrow range of C/N values, between 4.9 and 25.3, those < 7.4 and > 18.7 are likely attributable to a dominant ($\geq 50\%$) contribution of beef and wheat respectively (Table 7).

Ceramic-absorbed residue results and discussion

Lipids were successfully extracted from all 36 ceramic samples. The TLE yields of 12 samples were $< 5 \mu\text{g g}^{-1}$ and below the threshold used in the interpretation of archaeological material. However, as the ceramic briquettes were devoid of lipids prior to use, these residues may only have derived from the processed products. Therefore, all residues are considered in this discussion.

A low abundance of $\text{C}_{16:0}$ and $\text{C}_{18:0}$ prevented the application of compound specific carbon isotope analysis to 25 samples, including all those derived from mixtures comprising millet. Therefore, as the aim of these experiments was to understand the development of *P. miliaceum* residues, it was deemed unnecessary to analyse the remaining 12 samples.

No considerable difference was observed in the range and abundance of compounds present in each sample, except for the presence of miliacin. Therefore, this discussion focuses on a comparison of the TLE and miliacin yield of samples. The TLE and miliacin yield of each sample is presented in Table 8 and 9.

Unmixed ingredient experiments

The TLE yield of ceramic-absorbed residues from unmixed beef are consistently low, relative to previously published data (Hamman and Cramp 2018). The fat content of the beef used in these experiments should, in theory, have resulted in greater lipid absorption. Indeed, a large quantity of suspended lipids was observed on the liquid surface during cooking (Figure 25), and $\delta^{13}\text{C}$ values of CL samples decreased over time (Figure 28), demonstrating their release from the beef used. However, in this instance,

lipids do not appear to have transferred to the ceramic fabric in large quantities. Neither the sampling strategy nor variables of this experiment differed from others, therefore it is difficult to explain the inconsistent and low yields obtained from unmixed beef.

Table 8. TLE yield of ceramic absorbed residues $\mu\text{g g}^{-1}$.

Sample	Time (minutes)	TLE yield ($\mu\text{g g}^{-1}$)			
		100	75 + 25	50 + 50	25 + 75
Millet + Beef	20	5.8	4.9	12.0	15.3
	40	4.4	5.6	10.1	5.2
	60	12.0	2.7	9.3	3.4
Beef + Wheat	20	18.8	30.1	24.8	4.8
	40	20.4	72.9	266.5	29.5
	60	15.0	389.2	240.6	78.0
Wheat + Millet	20	7.4	4.1	4.1	6.3
	40	6.2	4.3	3.5	4.0
	60	3.4	4.6	2.8	6.3

Table 9. Miliacin yield of ceramic absorbed residues ng g^{-1} .

Sample	Time (minutes)	Miliacin yield (ng g^{-1})			
		100	75 + 25	50 + 50	25 + 75
Millet + Beef	20	1857	4	600	1907
	40	14	4	626	54
	60	16	0	4	21
Wheat + Millet	20	-	22	6	118
	40	-	14	17	37
	60	-	9	33	673

The TLE yield of ceramic-absorbed residues from unmixed wheat are consistently low, corresponding to previously published experiments (Hamman and Cramp 2018), although they decrease over time. The palmitic/stearic (P/S) values of these samples are < 1 , which is not consistent with the lipid content of wheat caryopses and provides no indication that the residue is formed from processing cereals.

The TLE yield of ceramic-absorbed residues from unmixed millet are also consistently low, corresponding to the abundance of lipids in *P. miliaceum* caryopses and limited transference of lipids observed when boiling other cereals (Hamman and Cramp 2018). The P/S value of these samples is also < 1 , potentially demonstrating that fatty

acids are neither released nor absorbed in proportion to their abundance in wheat and *P. miliaceum*. The miliacin yield of ceramic-absorbed residues from the unmixed millet experiment do not correspond to TLE yields (Table 8 and 9), with a very high miliacin yield at 20 minutes (1857 ng g⁻¹), and very low miliacin yield at 40 (14 ng g⁻¹) and 60 minutes (16 ng g⁻¹), relative to previously published experiments (290ng g⁻¹, Heron *et al.* 2016).

Wheat and millet experiments

The TLE yield of ceramic-absorbed residues from wheat + millet mixtures are consistently low and comparable to samples from both unmixed wheat and millet experiments. While no residue reaches the maximum TLE yield of unmixed millet, higher yields do not correspond to an increased contribution of either wheat or millet. In addition, TLE yields are not consistent throughout cooking (Table 8). The miliacin yield of ceramic-absorbed residues from W75+M25 and W50+M50 are low (< 33 ng g⁻¹), although a broad range of miliacin yields, between 37 and 673 ng g⁻¹, are observed in W25+M75 samples (Table 9). There is a moderate significant relationship between miliacin and TLE yields in samples from wheat + millet mixtures ($r(7) = .677$ $p < .05$).

Beef and wheat experiments

The TLE yield of ceramic-absorbed residues from beef + wheat mixtures range between 4.8 and 389 µg g⁻¹, with a mean of 126 µg g⁻¹, and are significantly different from wheat + millet TLE yields (paired t-test, $t=2.6542$, $df=8$, $p=.0291$). Increased yields demonstrate a significant contribution of lipids from beef that was not observed in samples from the unmixed beef experiment. The TLE yield of each sample increases with cooking time and the proportion of beef in mixtures, although the 40 minute sample of B50+M50 does not conform to this trend and is higher than the 60 minute sample. The data indicates that a substantial quantity of lipids, from beef, are either not released or absorbed until after 20 minutes. This later release of lipids potentially explains a decrease and lower rate of increase in bulk δ¹³C values, of B25+W75 and B50+W50 respectively, between 40 and 60 minutes, although, given the proportion of beef in these experiments, the development of bulk δ¹³C values should be reversed.

Millet and beef experiments

The TLE yield of ceramic-absorbed residues from millet + beef mixtures range between 2.7 and 15.3 µg g⁻¹, with a mean of 7.6 µg g⁻¹. They are not significantly different

from wheat + millet mixtures (paired t-test, $t = 2.1599$, $df = 8$, $p = .0628$) and are significantly different from beef + wheat mixtures (paired t-test, $t = 2.5698$, $df = 8$, $p = 0.0331$). This demonstrates that large quantities of lipids, released from beef, are not absorbed into the ceramic fabric during cooking. However, a higher average TLE yield is observed in these samples, than wheat + millet samples, indicating that beef lipids contribute to ceramic-absorbed residue formation. Higher TLE yields are observed in samples containing $\geq 50\%$ beef, yet they are not consistently higher than the mixture containing 25% beef (Table 7). Interestingly, the TLE yields of M75+B25 samples are lower, in two instances, than respective unmixed millet samples, demonstrating that the absorption of lipids, from beef, is neither consistent nor guaranteed. Contrary to beef + wheat samples, the TLE yield of millet + beef residues decrease with cooking time, although the 40 minute sample of M75+B25 does not conform to this trend and is higher than both the 20 and 60 minute sample. The miliacin yield of ceramic-absorbed residues from millet + beef experiments range between 0 and 1907 ng g^{-1} , demonstrating the highest yield and greatest variability of all samples analysed (Table 9). There is a strong significant relationship between miliacin and TLE yields in samples from millet + beef mixtures ($r(7) = .855$ $p = .00332$). Indeed, failure to detect miliacin in the 60 minute sample from M75+B25 corresponds to the lowest TLE yield of all ceramic-absorbed residues.

Discussion of ceramic-absorbed residue data

One would presume that lipids accumulate in ceramic fabrics, throughout cooking, as they are released by processed products. However, increasing, decreasing, and variable TLE yields are observed across all experiments over time. Natural variation in the abundance and availability of lipids in the ingredients used may explain a difference in the rate of lipid accumulation, but not decreasing yields over time. Constant migration of lipids, between cooking liquids and the ceramic briquette, could result in a reduction in TLE yields over time, especially when limited quantities of lipids are present in processed ingredients. Indeed, mixtures that release a high abundance of lipids into suspension may exceed the rate of reverse migration, from the ceramic fabric to the cooking liquid, resulting in greater accumulation over time, e.g. beef + wheat experiments. However, this would not explain why TLE yields of samples from the unmixed beef experiment are low

and variable. Therefore, the variation observed may also relate to uneven horizontal absorption and distribution of lipids across the briquette. Previous experiments have demonstrated a vertical difference in TLE yields, which is associated with the hydrophobicity of lipids (Charters *et al.* 1993a), yet horizontal variation in sites of lipid absorption have not been investigated. Further research is necessary to understand the exact cause of the variation observed during this experiment and whether, for instance, the use of a coarser ceramic fabric may result in greater variability between samples.

Higher TLE yields from millet + beef residues, at 20 minutes, generally correspond to lower bulk $\delta^{13}\text{C}$ and C/N values, and higher $\delta^{15}\text{N}$ values, of CL samples. Conversely, lower yields, at 40 and 60 minutes, correspond to higher $\delta^{13}\text{C}$ and C/N values, and lower $\delta^{15}\text{N}$ values, of CL samples. Isotopic data indicates that millet releases a greater quantity of material into suspension, between 20 and 60 minutes, than beef. This may explain why TLE yields do not increase throughout cooking, despite the large quantities of lipids released from beef during this timeframe. It is proposed that the thick, carbohydrate-rich liquid, observed during all experiments with millet, blocked pores in the ceramic fabric, preventing the absorption of lipids. This process is indicated by the adhesion of a beige surface coating, to the ceramic fabric, that was observed during sampling. Past researchers have noted ethnographic examples of people processing plant products, which are rich in starch, in ceramic vessels, to seal them (Heron and Evershed 1993). This data provides strong evidence for the effectiveness of such practices, given the difference in TLE yields of millet + beef and beef + wheat samples, and may highlight potential limitations in the formation and detection of meat + millet ceramic-absorbed residues.

4. Does the abundance of miliacin in ceramic-absorbed residues relate to either the type or quantity of products processed with *P. miliaceum*?

There is no significant difference between the miliacin yield of samples from millet + beef and wheat + millet mixtures (paired t-test, $t = 2.1599$, $df = 8$, $p = 0.0628$). This is expected, given the relationship between TLE and miliacin yields in these mixtures, and that there is no significant difference between the TLE yields of the two datasets. This data indicates that ceramic-absorption of miliacin is generally proportional to the absorption of other lipids and explains why a higher average and range of miliacin yields are

observed in millet + beef samples, as they also produce a higher average and range of TLE yields, relative to wheat + millet samples.

A relative increase in the TLE and miliacin yield of ceramic-absorbed residues from millet + beef mixtures, corresponding to an increased contribution of beef, may be explained by the smaller quantity of millet, which releases less material into suspension, being unable to block ceramic pores and limit lipid absorption. However, as beef + wheat experiments demonstrated that wheat does not hinder lipid absorption to the extent of *P. miliaceum*, one may question why a relative increase is not also observed across TLE and miliacin yields of wheat + millet mixtures. It could be proposed that beef promotes lipid absorption, which in turn increases miliacin absorption, given that mixtures comprising 75% beef produced a higher TLE and miliacin yield than mixtures comprising 75% wheat. However, one must then question why the miliacin yield of samples from W25+M75 are higher than M75+B25, despite the same quantity of millet being processed. It would also be difficult to explain why M75+B25 produces lower TLE and substantially lower miliacin yield than unmixed millet samples.

This dataset demonstrates that a substantial quantity of miliacin may be absorbed, by ceramic fabrics, within 20 minutes, when *P. miliaceum* is processed in isolation and with beef and wheat. However, it is not possible to conclude if either the type or quantity of products processed with *P. miliaceum* influence ceramic absorption of miliacin. This is due to contradictions in the dataset and unknown sources of variation, within and between experiments using different mixtures.

Conclusion

This study provides new insights into the release of different compounds, and ceramic absorption of lipids, from *P. miliaceum* caryopses, beef, and wheat, during cooking. The bulk isotope data obtained improves confidence in the application of criteria used to detect *P. miliaceum* in archaeological foodcrusts, in addition to outlining further criteria that may prove useful in broadly distinguishing the products that *P. miliaceum* was processed with and their contribution to a given 'recipe'. As such, this study demonstrates the reliability of bulk carbon isotope analysis in detecting the use of *P. miliaceum*, attests to the accuracy of previous studies (e.g. Heron *et al.* 2016), and has

developed an understanding of scenarios in which past traces of *P. miliaceum* use would not be identified.

The molecular data obtained questions the reliability of miliacin absorption and potentially limits the use of this compound to identifying the presence of *P. miliaceum* processing, rather than either proving its absence or providing a method to quantify its use. Limited use of *P. miliaceum*, in nuanced activities, such as ceremonial and medicinal practices, may not result in a lasting trace of miliacin being transferred to the ceramic matrix, potentially highlighting an issue with the sensitivity of this approach in answering certain archaeological questions. Repeatedly processing *P. miliaceum*, particularly in larger quantities, would likely result in an accumulation of miliacin, leading to its detection in most culinary contexts, although the extent of miliacin accumulation requires further investigation. As such, the observation of high miliacin yields in archaeological material, e.g. Ganzarolli *et al.* (2018), may require alternate explanations and the investigation of different processing methods and preservation conditions. It is important to state, however, that this data does demonstrate that a low concentration of miliacin should not be interpreted as indicating small-scale *P. miliaceum* processing.

Failure to produce sufficient lipid yields from *P. miliaceum* mixtures demonstrated an important limiting factor in the development of ceramic-absorbed residues. The obstruction of ceramic pores, by carbohydrate rich products, has not previously been investigated in ORA literature. However, this observation is a cause for concern, as residues from cooking events incorporating *P. miliaceum* would be underrepresented in accumulated ceramic-absorbed residues. Indeed, in combination with variable miliacin absorption, this observation may explain the apparent lack of ^{13}C enrichment in archaeological ceramic-absorbed lipid residues that contain miliacin (e.g. Rageot *et al.* 2019a). Therefore, determining the products processed with this cereal and understanding its significance to cuisine, culture, and subsistence, would potentially be difficult to examine via GC-C-IRMS analysis of ceramic-absorbed residues.

It is important to consider that this dataset is derived from a limited number of samples, taken from single cooking events. The repetition of experiments, in addition to increased, duplicate sampling, would account for natural variation in the ingredients and materials used, in addition to potential sampling bias, that has been outlined throughout this chapter. Doing so would improve the reliability of these datasets, although future

experiments should also investigate factors that affect the formation of authentic foodcrusts, in addition to lipid absorption and retention, to improve understanding of food residue development.

As stated at the outset of these results, the data produced is a guide and not an absolute measure for the detection and characterisation of *P. miliaceum* residues. The use of either cracked or milled wheat and beef products with different consistencies, e.g. minced meat, would likely drastically influence the data produced (e.g. Hart *et al.* 2009). Concurrent processing with additional ingredients would also have an influence on the data produced, although this is perhaps harder to predict, as the type and quantity of compounds released into suspension varies between products and throughout cooking. As such, further experiments are necessary to gauge the ability of the analytical techniques used to identify and distinguish *P. miliaceum* processing under different conditions.

In planning future experiments, it is important to consider whether the end result of a cooking event is an authentic representation of past human culinary activity. One wonders whether past peoples would have either intended or needed to boil *P. miliaceum* caryopses for 60 minutes, when their structure and texture is severely diminished within 20 minutes. Furthermore, it is conceivable that *P. miliaceum* caryopses may have been added to processed mixtures during the final stages of cooking other ingredients. Therefore, experiments must investigate whether *P. miliaceum* caryopses release material into suspension in a shorter timeframe, than has been investigated here, and whether this may be recognised among material that is released by other products earlier in the cooking process.

Chapter 6: ORA investigations at Bruszczewo

Introduction

Chapter 6 presents EA-IRMS, GC-MS, and GC-C-IRMS analysis of charred crust and ceramic-absorbed residues from Bruszczewo, Poland, developing on previous research conducted by Heron *et al.* (2016). Presently, bulk isotope analysis has demonstrated ^{13}C enrichment in LBA/EIA, but not EBA, charred crusts that corresponded to compound specific carbon isotope analysis of one LBA/EIA and one EBA charred crust. The one LBA/EIA charred crust analysed by GC-MS also contained miliacin, enabling the determination of *P. miliaceum* processing at the site (Heron *et al.* 2016). Heron *et al.* (2016) hypothesised that ^{13}C enrichment in all LBA/EIA charred crusts is derived from *P. miliaceum* processing.

This study assesses and develops on previous analyses by increasing the number of charred crusts analysed by EA-IRMS, GC-MS, and GC-C-IRMS, in addition to applying GC-MS and GC-C-IRMS to ceramic-absorbed residues. Concurrent sampling of charred crusts and ceramic-absorbed residues, in several instances from the same sherd, enables a nuanced understanding of culinary activities and critical assessment of criteria used for the identification of *P. miliaceum* in archaeological residues. In addition, the application of experimental data, presented in Chapter 5, develops understanding of methods used to process the cereal at Bruszczewo. This study is driven by the following research questions.

Research questions

1. Is there evidence of *Panicum miliaceum* processing in the Early Bronze Age?
2. Do charred crusts that produce high bulk $\delta^{13}\text{C}$ values contain miliacin?
3. Is evidence for the processing of *P. miliaceum* comparable between charred crust and ceramic samples?
4. Is *Panicum miliaceum* exclusively associated with either another food product or specific vessel type?
5. What differences in pottery use are observable between the EBA and LBA/EIA?

Site location and regional context

Archaeological excavations at Bruszczewo, conducted by multiple research groups, have taken place sporadically since the 1960s, with monographs published primarily in Polish and German (Czebreszuk and Müller 2004; Müller *et al.* 2010; Silska 2012). The most recent monographs are in English and earlier material has been translated, when necessary, for this study (Czebreszuk and Müller 2015; Czebreszuk *et al.* 2015a).

The archaeological site of Bruszczewo 5 is located in the Samic River Valley of Kościan County, Poland, approximately 60 km south of Poznań (52°00' 47" N, 16°35' 07" E). Bronze Age activity is concentrated on an elevated spur, as the valley floor formed a lake during this period. The Samic River has since changed course and the lake dried, yet low lying areas of Bruszczewo remain waterlogged, resulting in the preservation of organic materials (Czebreszuk and Jager 2015).

An EBA fortified settlement at Bruszczewo is believed to be the centre of development for the Kościan Group, a subset of the Únětice Culture, due to its size and monumental nature. The group is defined by the proximity of sites (Figure 35), presence of elaborate burials (Leki Małe - 15 km and Przysieka Polska - 1.5 km), and common traits observed in archaeological materials across the Kościan region (Müller and Kneisel 2010; Jaeger and Czebreszuk 2011; Jaeger 2016).

The function and extent to which Bruszczewo was used in the LBA/EIA is not presently clear; however, material culture at the site corresponds with the Lusatian Culture. Bruszczewo is on the periphery of the Lusatian Culture and is downstream, figuratively and literally, of the Samic and Oder rivers and major Lusatian Urnfield (LUF) Culture settlement clusters. Development at the site during the LBA/EIA potentially stemmed from contact with Silesian LUF groups through these river networks (Ignaczak 2015).

Chronology of Bruszczewo

In total, 116 radiocarbon dates were obtained from human, faunal, and floral remains from Bruszczewo, including short- and long-lived wooden structures subjected to dendrochronological dating (Czebreszuk *et al.* 2015b). The fortifications in Trench 7 returned the earliest date, ca. 2000 cal BCE (Figure 36), corresponding to environmental and material evidence for the beginning of occupation. The spatial and temporal

development and decline of the settlement is observed in new and renovated wooden structures (Czebreszuk *et al.* 2015b), environmental cores (Jaeger 2016), and the ceramic assemblage (Müller and Kneisel 2010). Peak occupation is identified in Phase 3, ca. 1750-1650 cal. BCE, followed by a rapid decline, beginning in the East of the settlement, and total abandonment around 1500 BCE.

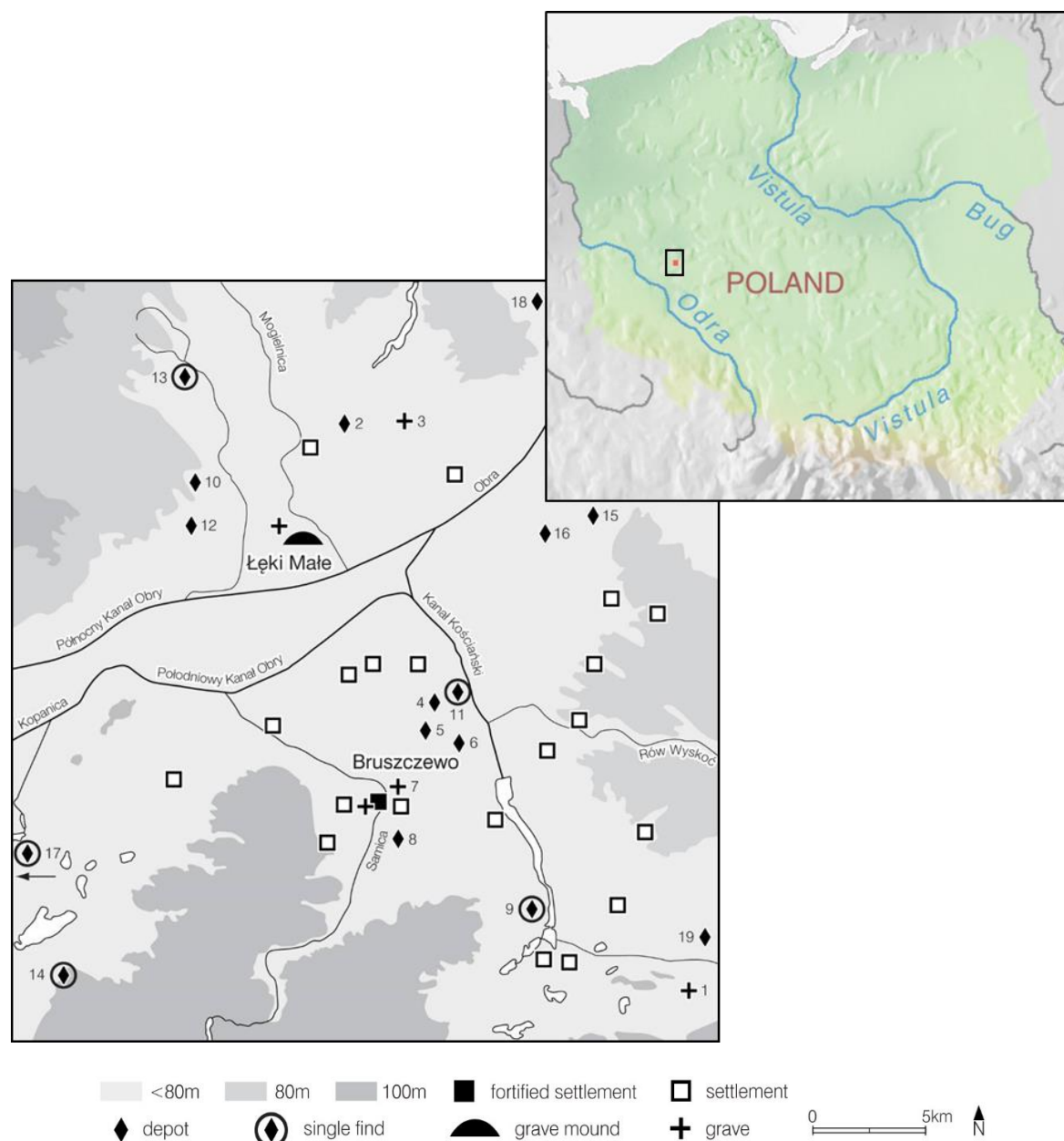


Figure 35. EBA sites in the Kościan region. 1 Osieczna-Kleszczewo, 2 Granowo-Granowo, 3 Granowo-Granowko, 4 Szcodrowo, 5 Kościan-Kokorzyn, 6 Naclaw, 7 Prysieka Polska, 8 Stare Bojanowo, 9 Prysieka Stara, 10 Kamieniec-Plastowo, 11 Kościan, 12 Kamieniec-Parzezewo, 13 Grodzisk Wielkopolski, 14 Włoozakowice, 15 Czempin, 16 Piotrkowice, 17 Przemęt-Starkowo, 18 Steszew, 19 Krzywín-Nowy Dwór. Filled black square (fortified settlement) is Bruszczewo (Müller and Kneisel 2010 761).

Presently, four LBA/EIA samples have been subjected to radiocarbon dating, although one proved to be intrusive from a later context, which was recognised in the archaeological record after sampling (Czebreszuk *et al.* 2015b). Furthermore, two samples returned dates overlapping with the Hallstatt plateau, a flattening of the radiocarbon calibration curve around the LBA/EIA transition (Walanus 2009; Ignaczak 2015; Trias *et al.* 2020). Therefore, only one sample, Ki-5906, provides an accurate date for LBA/EIA activity at the site, ca. 960 cal BCE (Ignaczak 2015). The ceramic assemblage, and other archaeological features, indicate a single phase of LBA/EIA activity, yet the beginning and end points are presently unknown (Ignaczak 2015).

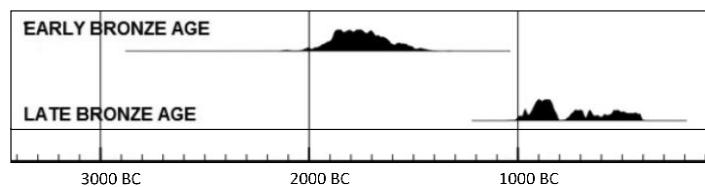


Figure 36. Summed probability plot of EBA (n= 112) and LBA/EIA (n= 3) radiocarbon dates. Two dates from LBA/EIA contexts overlap with the Hallstatt plateau, a flattening-out of the calibration curve, providing broad, low probability, and ultimately useless dates for the end of Lusatian Culture occupation (Czebreszuk *et al.* 2015b 40).

EBA site layout and function

Several structures have been attributed to the EBA settlement, including large-scale fortifications and houses (Figure 37). Houses are interpreted based on sunken features, uniform post holes, building materials, and hearths, that are comparable to contemporary Únětice Culture settlements in Poland and Moravia (Jaeger and Stróżyk 2015). Furthermore, craft workshops have potentially been identified in the east, occurring with material evidence for their use (Müller and Kneisel 2010). Substantial quantities of worked animal bone and antler fragments in Trench 52, and foot bones of large ruminants in Trench 15, indicate the processing of secondary animal products for tools and leather respectively. Abundant glume deposits in Trench 30 indicate this area was used extensively for cereal processing and wood chips in Trench 31 potentially indicate a woodworking area (Müller and Kneisel 2010).

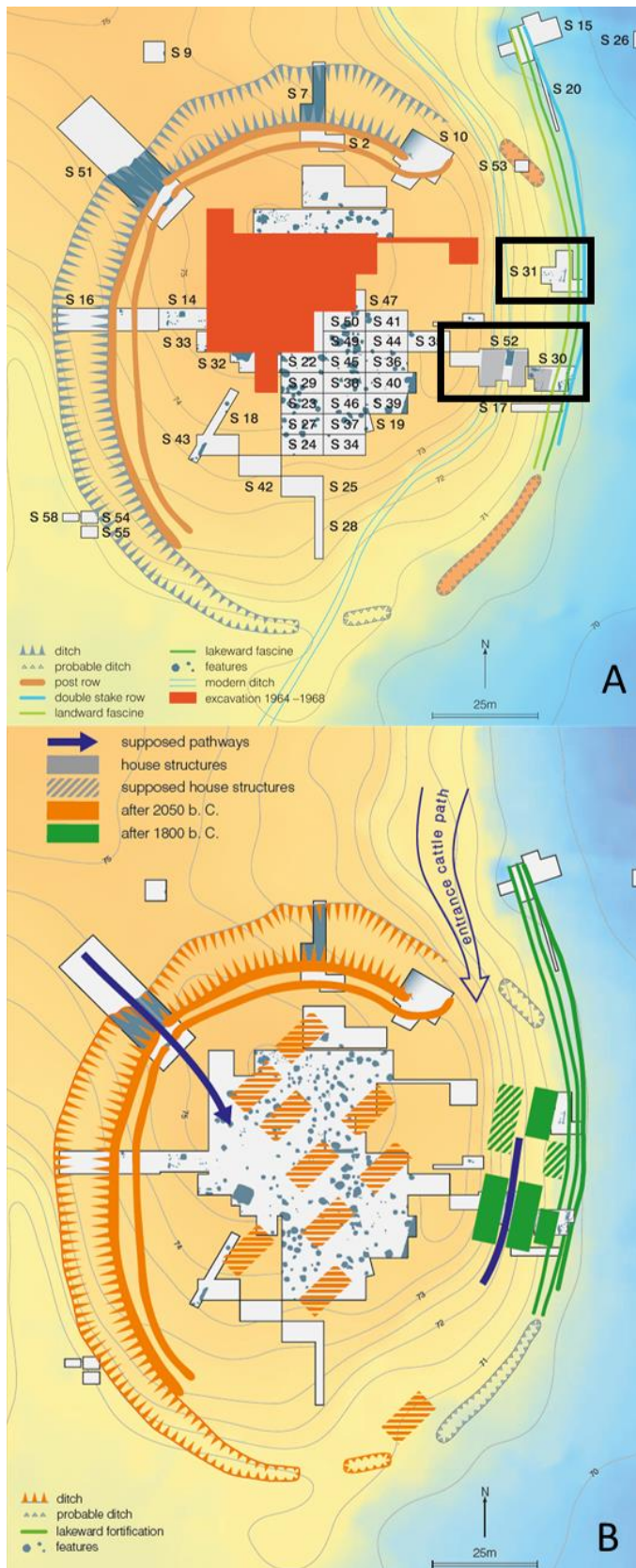


Figure 37. Bruszczewo site plans. **A** Trench 30, 31, and 52, from which material was analysed, are highlighted within black boxes. **B** House structures highlighted (Müller and Kneisel 2010 753, 761).

Bruszczewo is the only site to produce evidence for metalworking in the Koscian Group, suggesting that it may have acted as a regional distribution centre, controlled by an elite metalworking community. The wealth and significance of the site is further demonstrated by the presence of an amber bead, that demonstrates a long-distance exchange connection with Baltic communities and perhaps Carpathian Basin communities, as Bruszczewo lies on a route between the two. Presently, there is no direct evidence for a ceramic production area at Bruszczewo, yet the presence of necessary raw materials makes local production probable (Müller and Kneisel 2010; Kneisel *et al.* 2015). Current theories propose the control of production and exchange of materials and goods by an elite community within Bruszczewo. The spatial distribution of decorated and large storage capacity ceramics, faunal and floral remains, metal objects and metalworking paraphernalia, and amber artefacts, within the settlement, indicate the presence of a high-status group. Indeed, it is suggested that high status individuals from Bruszczewo were likely buried in nearby, structurally and material significant graves, containing amber and metal artefacts, at Leki Małe and Przysieka Polska (Müller *et al.* 2015).

LBA/EIA site layout and function

The LBA/EIA site is enclosed by a ditch and bank that was constructed over the EBA fortification, suggesting that remnants of EBA occupation were preserved and that there was potentially a significance and permanence to the site. The later landscaping would have provided minimal defence; therefore, a non-defensive function is proposed (Ignaczak 2015). A total of 43 features, 37 pits, and 6 post holes are attributed to LBA/EIA activity, limiting interpretation of site layout and function. Two dense clusters of features are observed in the north and south of the site, although material remains are distributed across the site in a single cultural layer. Pit features have generally uniform depths but varied diameters, they were roughly cut and rapidly filled in single events (Ignaczak 2015). It is believed that they would have had wooden superstructures, forming dwellings (Ignaczak 2015), yet there is no archaeological evidence for this, and their function remains unknown. Neither the spatial organisation of features nor the character and distribution of movable finds observed at Bruszczewo conform to normal Lusatian Culture settlement patterns (Ignaczak 2015). Certainly, the site does not resemble the eighth century BCE LUF settlement developments in the nearby Biskupin Settlement Network

that demonstrate uniform rows of large houses, with clear evidence of domestic activity (Czebreszuk 2013). Limited similarities exist between Bruszczewo and the LUF Settlement Powodów Site 2 (Ignaczak 2015). However, reports of the Powodów excavations have not been published, preventing detailed comparison. A notable difference is the absence of definitive settlement features at Bruszczewo. The ceramic assemblage of Bruszczewo is atypical of LUF settlements, indicating a ceremonial and perhaps ritual function of the site, and a nearby contemporary cemetery potentially supports a ceremonial/ritual interpretation, although no direct link is evident between the two. However, the presence of human remains at Bruszczewo complicates a funerary ritual interpretation, as they do not conform to standard LUF burial practices (Czebreszuk 2013). Indeed, the absence of features expected of a ritual site, such as hearths, are not observed at Bruszczewo (Ignaczak 2015). Future excavations at Bruszczewo, and other LUF sites, may provide a more accurate indication of its function in the LBA/EIA.

The ceramic assemblages

Presently, discussion of the ceramic assemblage is limited to material from the fortifications, central area, two pits in the northern ridge, and the north and south peat zones in the east of the site (Müller and Kneisel 2010; Czebreszuk *et al.* 2015c; Ignaczak 2015). It should be noted that similarities between Únětice and Lusatian Culture ceramics, poor stratigraphic separation of deposits, and the present state of radiocarbon dating all limit the interpretation of the ceramic assemblage (Czebreszuk 2015; Ignaczak 2015).

The EBA assemblage is divided into four chronological phases, marking the development and decline of the settlement (Figure 38). The range of vessel types increases between Phase 1-3, when the settlement reaches its peak, and the rate of deposition increases in Phase 2-3, indicating increased production. A change in the range and frequency of vessel types in the East peat zone in Phase 3 suggests a transition from food processing to storage/living space, corresponding to the expansion of human habitation (Figure 37, Müller and Kneisel 2010). However, in Phase 4, the range of vessel types and deposition rate decrease, corresponding to the decline of Bruszczewo.

The EBA assemblage indicates socioeconomic differentiation of groups, with a broader typology and higher abundance of decorated wares observed in the central

mineralised zone, than is observed in the East peat zone (Czebreszuk *et al.* 2015c). Indeed, several pits in the mineralised zone, that are potentially associated with houses, contain more elaborately decorated wares than the entire peat zone. As stylistic developments are unrelated to vessel function, these observations may indicate social differentiation between the two areas (Müller and Kneisel 2010).

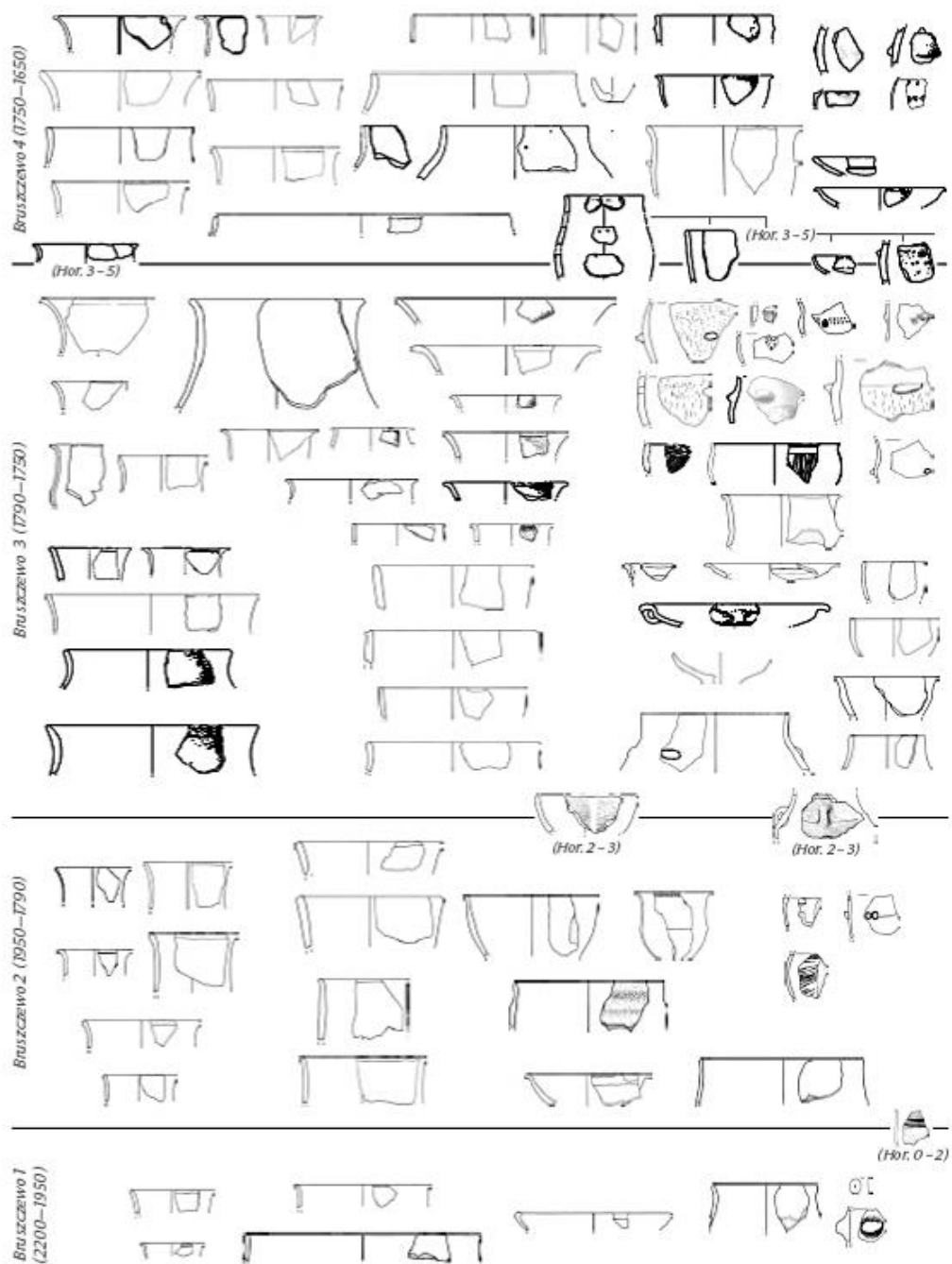


Figure 38. Representative developmental phases of Únětice Culture ceramics at Bruszczevo (Müller and Kneisel 2010 777).

The Lusatian Culture assemblage comprises 9005 sherds, derived exclusively from the mineralised zone, with just over half recovered from the cultural layer and the remainder recovered from Trench 51. The concentration of ceramics in the ditch, intersected by Trench 51, demonstrates heavy and prolonged use as either a refuse dump or feature of ritual significance. The observation of whole vessels and human remains in this feature may indicate the latter, resembling the use of a moat encompassing Powodów Site 2, although the presence of human remains across the cultural layer at Bruszczewo complicates a ritual interpretation and comparison with Powodów Site 2.

The LBA/EIA assemblage is atypical for Lusatian Culture settlements, with bowls, cups, and plates the most common vessel forms, and pots and vases relatively minor components. Jugs are notably absent from the assemblage, despite their frequency at most settlement sites. The range, frequency, and deposition of ceramics are consistent with contemporary Lusatian Culture cemeteries, e.g. Kietrz and Laski, indicating a common function. This distribution of ceramics corresponds to an increase in drinking and feasting activities observed at ceremonial and funerary sites in Europe during the 13th-12th C BCE. The development of standardised drinking vessels, in the LBA/EIA at Bruszczewo, supports an interpretation of common and established activities being undertaken, in either production or use (Ignaczak 2015). It is difficult to accurately interpret the distribution of decorated ceramics across LBA/EIA contexts at Bruszczewo, due to limited excavation and identification of features dating to this period. However, present evidence suggests that decoration is not a significant differentiating factor between contexts.

Comprehensive tables, that include the find location, context description, and associated finds, in addition to sherd size, type, decoration, surface treatment, temper, inclusions, and probable function of material analysed in this study are provided in Appendix 3. Unfortunately, only a limited number of samples possess distinguishing features and there was no evidence that any of these characteristics related to the data obtained from the analysis of either charred crust or ceramic residues. Therefore, inclusion of these tables, at this point, was deemed unnecessary.

Sherds with two distinctive characteristics were identified in the LBA/EIA assemblage. Firstly, one sherd possessed a white layer on its internal surface, that may have either been deliberately applied or built up during use. White surface layers are

characteristic of ceramics produced by Carpathian-Danube LUF and Hallstatt Cultures and were widely traded and reproduced in the 10th - 8th C BCE (KulKova 2020). However, further analysis is required to determine the composition of the white material, as it may be a calcite layer formed during boiling of water (Hendy *et al.* 2018). As no similar observations were made from other sherds, the former explanation is more probable.

Several sherds possessed abundant impressions, that have been confidently attributed to millet (Kroll 2010). While more thorough investigation and microscopic analysis is necessary to identify the millet species that produced these impressions, *P. miliaceum* is the most likely candidate, given its presence at the site. Impressions are distributed randomly across the internal surface of the sherd, including under where the vessel wall would have attached to the base sherd (Figure 39 and 40). Sampling, undertaken during this analysis, demonstrated that impressions were superficial and that millet was not incorporated into the clay fabric as temper, i.e. impressions were made during vessel formation, before the wall was attached to the base. There is no obvious explanation for the presence of these impressions, as they appear to be neither functional nor stylistic, nor do they occur with other distinct features. Indeed, the rarity and randomness of millet impressions makes one question whether production was deliberate. The sherds with impressions originate from Horizon 5, a transgression layer between EBA and LBA/EIA contexts and may derive from either period (Kroll 2010).



Figure 39. Sherd F3102ID4632 (Br 114) with millet caryopsis impressions scattered randomly across the internal surface.

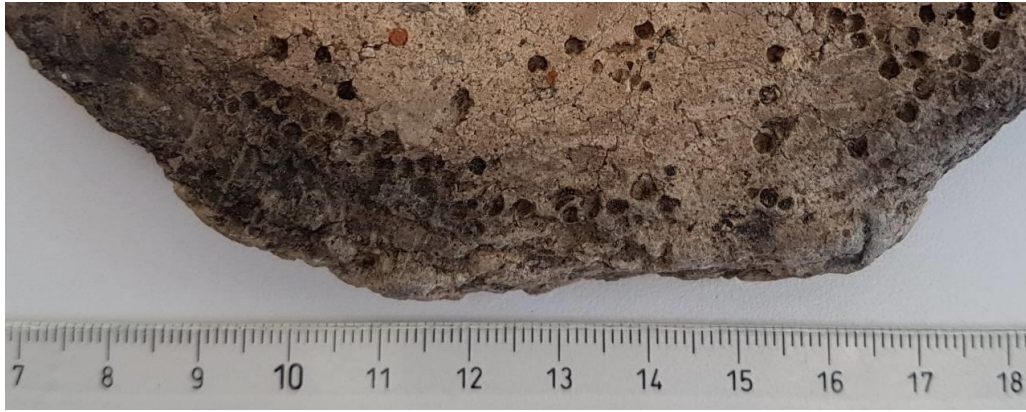


Figure 40. Sherd F3102ID4632 (Br 114) with millet caryopsis impressions in the area under the vessel wall.

The faunal assemblage

The faunal assemblage is limited by varied preservation conditions across the site, in addition to different excavation methods employed between excavation seasons. The waterlogged peat zone (Figure 41) demonstrates a greater degree of preservation, with a higher rate of element identification, than the central mineralised zone (Makowiecki 2015). However, peat staining has diminished the identification of burn and char marks, limiting some interpretive potential (Mikołaj and Marciniak 2015). Flotation was not undertaken during initial excavations, that focused on the central zone, exacerbating preservation issues. Therefore, both fish and bird bones, that are susceptible to degradation and being overlooked, are underrepresented in the earlier central assemblage. Redistribution of bones is evident from the stratigraphy of features and prevalence of gnawing and weathering on bones from the peat zone, further hindering spatial analysis (Mikołaj and Marciniak 2015). Therefore, the abundance of identifiable elements in both the central and peat zones are potentially inaccurate and treated with caution in this study. Furthermore, preferential preservation, number of elements, and ease of identification should be considered when comparing NISP values.

Both the EBA (NISP = 9783) and LBA/EIA (NISP = 2879) faunal assemblages are dominated by domesticated species (79% and 84% respectively), with wild mammals an important component of subsistence (18% and 15% respectively). Fish are a minor component in the EBA assemblage (3%) and are absent in the LBA/EIA assemblage. The presence of fyke traps within EBA layers of the peat zone demonstrate local exploitation

of fish (Müller and Kneisel 2010). However, even when considering preservation and collection biases, it appears that aquatic resources were not extensively exploited. Birds are rare in both periods (Makowiecki 2015), although this could also relate to preservation issues. The two assemblages are broadly comparable, in terms of their potential influence on absorbed residues, comprising of approximately 60% domesticated ruminant, 21% porcine and 11% wild ruminant remains. The presence of freshwater fish is the only difference between the two assemblages.

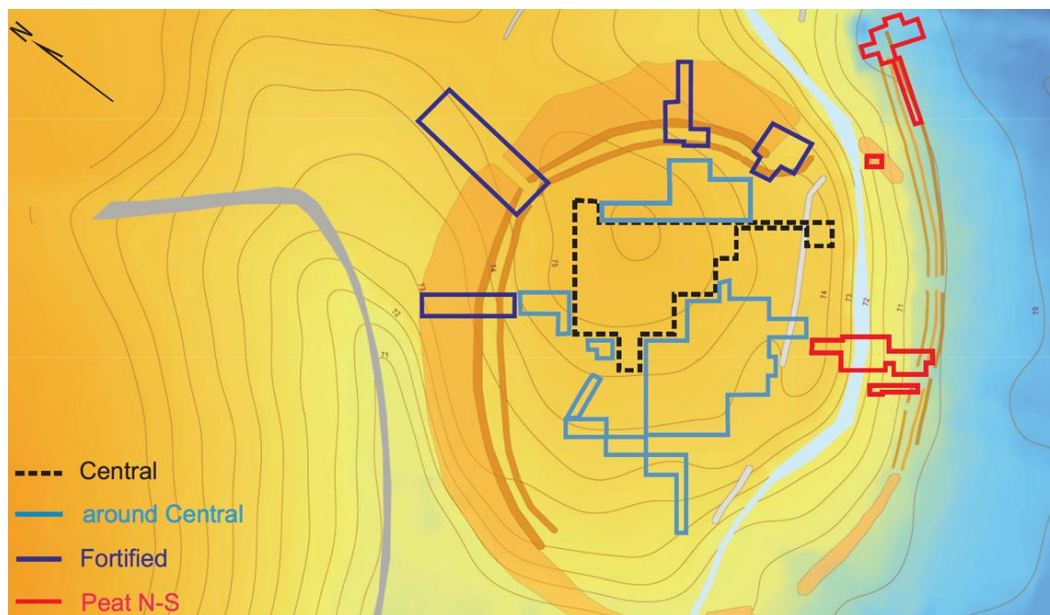


Figure 41. Areas of Bruszczewo examined during assessment of the faunal assemblage, including the central mineralised zone, around central area, fortifications, and peat north and south areas (Makowiecki 2015 55).

Mortality and sex profiles of cattle and sheep from EBA and LBA/EIA assemblages indicate that both species were reared primarily for meat, although milking during lifetime cannot be excluded. Conversely, the mortality and sex profiles of goats, in the EBA assemblage, indicate exploitation for milk. These interpretations correspond to the presence of pathologies related to milking among a limited number of ovicaprids, which are absent among cattle (Makowiecki 2015). However, it is important to note that goat remains are uncommon and dairy products are perhaps unlikely to have contributed significantly to subsistence.

Variation in the abundance of each species is observed between EBA contexts of the central, peat, and around central areas, potentially demonstrating socioeconomic differences. A predominance of ovicaprids and wild mammals in the east peat area may indicate a greater reliance on dairy products and wild resources (Makowiecki 2015). However, it is important to consider potential redepositions of these remains and other associated materials. The prevalence of broken, burnt and charred remains is higher in the east peat area may relate to marrow extraction. However, a high abundance of calcined bones may also demonstrate their use as fuel and indicate secondary deposition from fires (Mikołaj and Marciniak 2015). Furthermore, the use of the east peat area for hide and bone processing may introduce bias to NISP values. For instance, domesticates were butchered within the site and each element is represented proportionally, yet wild species were butchered outside the settlement. As such, the proportion of animal remains within the assemblage cannot be used to refine interpretation of organic residues with great confidence.

The archaeobotanical assemblage

The archaeobotanical assemblage is dominated by domesticated species, with wild species comprising a small but varied component. The range of species exploited varies in accordance with the development and decline of the EBA settlement (Kroll 2010). Barley (*Hordeum vulgare*) dominates in both EBA and LBA/EIA assemblages (Table 10). Emmer (*Triticum dicoccon*) is significantly less abundant but increases in importance in later periods. Spelt (*Triticum spelta*) is frequently observed in low abundance in all periods. In EBA contexts, carbonised peeled acorns (*Quercus spp.*) are observed in substantial quantities, indicating their processing and consumption by humans, yet they are rare in LBA/EIA contexts (Kroll 2010).

The EBA assemblage represents a complex agricultural system to which extensive processing methods were applied. The abundance of emmer, in contexts dominated by barley, varies significantly, indicating that it was deliberately cultivated and not present as a by-grain, yet the presence of einkorn in emmer deposits indicate it was a by-grain (Kroll 2010). Therefore, these cereals were cultivated in different areas. Crops were stored in pits and jars within houses and spatial analysis indicates social differentiation, with those in the central mineralised zone possessing a greater capacity to store surplus (Müller and

Kneisel 2010). A high concentration of quern stones and glume waste in the peat zone indicates decentralised plant product processing. Extensive pre-processing of grains is inferred from concentrated barley, and barley and wheat deposits, that are devoid of weed species (Jaeger 2016).

Table 10. Summary of the most abundant archaeobotanical remains from Bruszczewo ordered by Horizon and two LBA/EIA features (Kroll 2010).

Genus / Species	Horizon						Feature	
	EBA				Trans.	LBA		
	0-2	3	3-4	4	5	6-8	Fl.17	Fl.60
<i>Triticum dicoccon</i>	44	363	2342	110	139	376	13	2
<i>Triticum spelta</i>	65	164	1126	52	82	71	39	
<i>Hordeum vulgare</i>	728	16833	108455	259	351	1779	50	
<i>P. miliaceum</i>			4	1	3	2	131	22
<i>Quercus</i>	3	22	116	2	2	2		

P. miliaceum is observed as isolated grains in late EBA and transgression layer contexts but increases in significance in the LBA/EIA. Evidence for *P. miliaceum*, prior to the LBA/EIA, is likely intrusive, given the regional chronology of *P. miliaceum* introduction (Filipovic *et al.* 2020) and previous isotopic and molecular investigations at Bruszczewo (Heron *et al.* 2016). However, as the present Polish chronology is limited, further investigation is necessary to disprove an early occurrence of *P. miliaceum* at Bruszczewo. *P. miliaceum* caryopses are concentrated in a limited number of LBA/EIA features, such as F17 and F60, where they dominate, but are observed in low abundance in the cultural layer. Overall, the abundance of *P. miliaceum* caryopses suggest limited exploitation, relative to contemporary Lusatian Culture sites (Effenberger 2018; Kacpica and Mueller-Bieniek 2019), although its concentration in certain features may demonstrate a narrow range of specific uses. Unfortunately, the LBA/EIA assemblage has not been thoroughly analysed and published, limiting further discussion of this period.

Evidence for *P. miliaceum* in Poland

Around one quarter of Neolithic sites in Poland produce carbonised *P. miliaceum* caryopses, with relatively rich deposits observed at Olszanica and Zagórze. Ceramic impressions are also observed at Olszanica, although they have not been securely identified (Moskal-del Hoyo *et al.* 2017). The contextual date of the Zagórze deposit is

doubtful as the stratigraphy potentially demonstrates secondary deposition (Lityńska-Zajac *et al.* 2017). The material from Olszanica requires further analysis, as the present chronology of *P. miliaceum* translocation across Eurasia suggests that contextual dating of Neolithic observations in Poland is inaccurate (Filipovic *et al.* 2020).

Six early *P. miliaceum* caryopses have been directly dated, with four in the South and two, from one site, in Central Poland. The earliest is from a MBA context at Lipnik, SE Poland, ca. 1300 cal. BCE (Kapcia and Mueller-Bieniek 2019), with other southern sites producing similar dates (Filipovic *et al.* 2020). These dates correspond to an increase of *P. miliaceum* observations in the region during the MBA, although there is presently no evidence to support the contextual date of a single supposed EBA observation at Trzcinica, SE Poland (Pokutta 2014; Moskal-del Hoyo *et al.* 2015). New settlements, such as Janowice and Wróblowice, were established in the Carpathian foothills of South Poland, during the MBA, by established agricultural communities that possessed *P. miliaceum*. Spelt, an uncommon cereal in Poland during the MBA, is also observed at these sites, potentially indicating the migration of external groups to the region (Moskal-del Hoyo *et al.* 2015). It is not possible to determine the region from which *P. miliaceum* was introduced, due to gaps in the present radiocarbon dataset, although the late occurrence of the species in Poland, relative to neighbouring Ukraine, may suggest that it was not introduced from the East. Further research is necessary to confirm the chronology of *P. miliaceum* at southern sites and investigate the role that migrating groups may have taken in its dispersal.

Wheat is the dominant cereal at Janowice and Wróblowice, where *P. miliaceum* and barley are equally minor crops (Moskal-del Hoyo *et al.* 2015; Mních *et al.* 2020). Cultivation of *P. miliaceum* may have exploited marginal land, in low-intensity, diversified subsistence, given that it requires a different management strategy to other cereals and is present at a low abundance in the assemblages of these sites. Indeed, bulk isotope analysis of carbonised *P. miliaceum* caryopses indicates that the cereal was not manured and was exposed to a limited water supply (Mueller-Bieniek *et al.* 2019), corroborating a low investment, marginal agriculture hypothesis. Conversely, *P. miliaceum* appears to be dominant at Lipnik, where wheat and barley represent minor and minimal elements of subsistence (Kapcia and Mueller-Bieniek 2019). This observation is derived from a single storage pit and should not be overinterpreted, although the absolute abundance of *P.*

miliaceum is substantial for the period, potentially indicating a significant role in subsistence. This observation highlights an important issue in interpreting archaeobotanical deposits that may fortuitously represent a single harvest. This is especially pertinent for *P. miliaceum*, which may be harvested at a different time of the year from other cereals.

Bulk isotope analysis of human remains from Poland is limited, although recent publications have increased the number of BA individuals sampled substantially. Isotopic evidence for the consumption of *P. miliaceum* is absent prior to the EBA, corresponding to archaeobotanical evidence and the absence of miliacin in organic residues from Bruszczewo (Heron *et al.* 2016). Isotopic evidence for the consumption of *P. miliaceum* in the MBA (from the middle 15th C BCE) corresponds to archaeobotanical evidence for its introduction to sites in SE Poland (Figure 42). However, individuals from Central Poland do not demonstrate significant ¹³C enrichment throughout the entire BA (Pospieszny *et al.* 2021). This does not correspond to archaeobotanical evidence for *P. miliaceum* in the region and indicates a difference in either the quantity or nature of *P. miliaceum* consumption among communities and cultures in Central Poland, relative to those in the south. Consumption of *P. miliaceum* was not practiced by all members of communities in SE Poland (Pospieszny *et al.* 2021), suggesting localised attitudes towards the adoption of the cereal. However, there is no evidence to suggest why attitudes differed between and within settlements. Presently, there is no evidence to suggest that animals consumed the cereal, although the current faunal dataset represents limited sampling that requires expansion.

The earliest directly dated *P. miliaceum* caryopsis in Central Poland is from Lutomiersk-Koziówki, ca. 1000 cal BCE, corresponding to the LBA (Mueller-Bieniek *et al.* 2015). The species is not observed in MBA contexts at the site and continuous occupation indicates that the crop was introduced to an established agricultural community, rather than by migrating groups. Interestingly, *P. miliaceum* replaces wheat as the major crop during the LBA, with wheat becoming a significant, albeit minor, crop along with barley (Mueller-Bieniek *et al.* 2015). However, the abundance of *P. miliaceum* at LBA/EIA sites varies significantly, for instance Bruszczewo demonstrates limited exploitation (Kroll 2010) and Ruda demonstrates heavy exploitation (Rembisz *et al.* 2009). Sites in Germany that are culturally and chronologically comparable also demonstrate variable but

significant cultivation (Effenberger *et al.* 2018), suggesting broad acceptance of the cereal but different approaches to its use. Generally, archaeobotanical research in Central Poland is scarce and much post-Neolithic analysis remains unpublished.

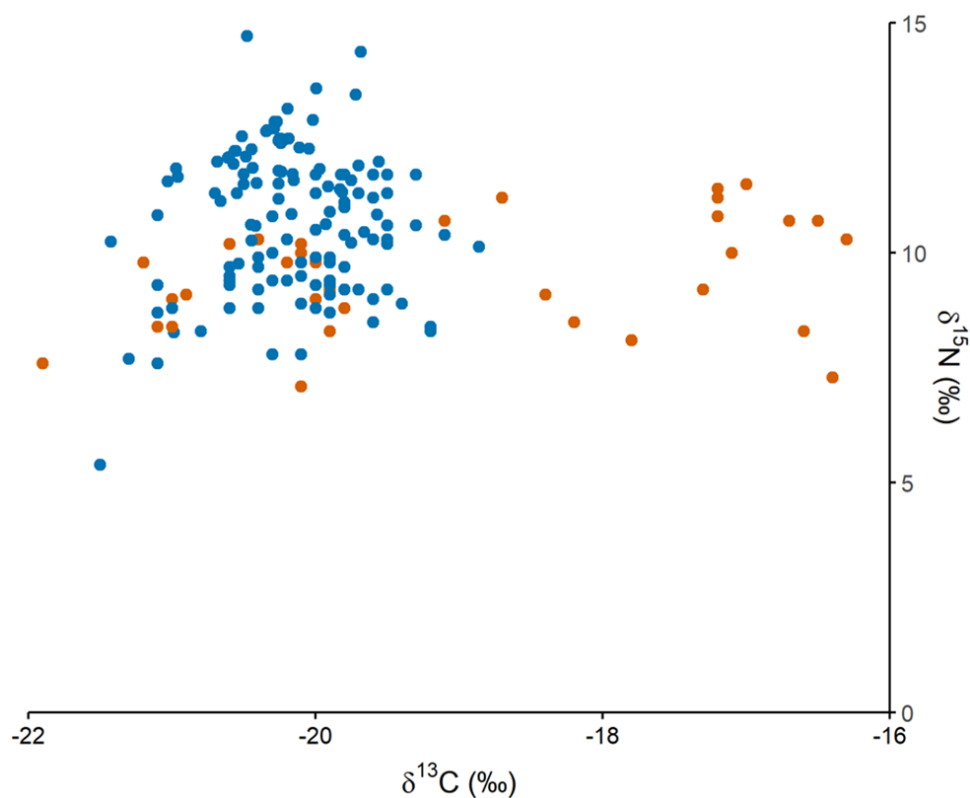


Figure 42. Bulk isotope data of humans from Poland. Blue and orange points represent pre-MBA and MBA/LBA individuals respectively. Data obtained from: Pokoutta and Howcroft (2015); Pokutta *et al.* (2015); Mnich *et al.* (2020); Pospieszny *et al.* (2021).

In addition to ORA evidence from Bruszczewo, miliacin is observed in ceramic-absorbed residues from burial contexts at LBA Maciejowice (Isaksson and Nilsson 2018). This data demonstrates the processing of *P. miliaceum* during domestic and perhaps ceremonial activities, although the precise nature and cultural significance of the Maciejowice material requires further investigation. Motives for the introduction of *P. miliaceum* to SE Poland appear to primarily relate to subsistence, due to the quantity of caryopses recovered and extent of consumption among certain individuals, yet significant questions remain as to how this cereal was exploited among other members of these societies and in other regions. Expansion of molecular and isotopic analysis, combined

with radiocarbon dating, are imperative in elucidating the significance of *P. miliaceum* across BA Poland.

Sampling strategy

A sampling strategy was designed to test the hypotheses of Heron *et al.* (2016) and address the research questions posed at the outset of this chapter. An equal number of samples from secure EBA and LBA/EIA contexts were analysed to ensure the datasets were comprehensive, comparable and not subject to bias, addressing research questions one and five. Repeat and additional charred crust samples were obtained in sufficient quantities for both isotopic and molecular analysis, in order to address research question two, and associated ceramic samples were obtained in order to address research question three. The overlapping and additional sampling of materials enables the incorporation of past results in current interpretations.

Vessels possessing charred crusts were preferentially sampled, with material taken from the rim and wall, to increase the probability of sampling cooking vessels and maximise lipid yield. Material was available from recent excavations conducted in Trench 30, 31, and 52, that are principally located in the east peat zone (Figure 41). A full list of sampled material and relevant contextual information is presented in Appendix 3. Samples were prepared according to methods detailed in Appendix 1.

Results

Bulk isotope analysis

Bulk carbon and nitrogen isotope analysis was conducted on 14 charred crusts, eight from EBA and six from LBA/EIA contexts. Successful results were obtained from five EBA and three LBA/EIA samples. Six samples produced insufficient carbon, < 10% by weight, and were rejected, in line with Heron *et al.* (2016), due to the likelihood of contamination.

New bulk $\delta^{13}\text{C}$ and $\delta^{15}\text{N}$ values of charred crusts are presented with data from Heron *et al.* (2016) in Figure 43 and data is listed in Appendix 3. The combined dataset is representative of all horizons and each trench sampled. The new data conforms to previous results, with minor differences in mean $\delta^{13}\text{C}$ and $\delta^{15}\text{N}$ values and $\delta^{15}\text{N}$ range. Updated mean and range values for each period are presented in Table 11.

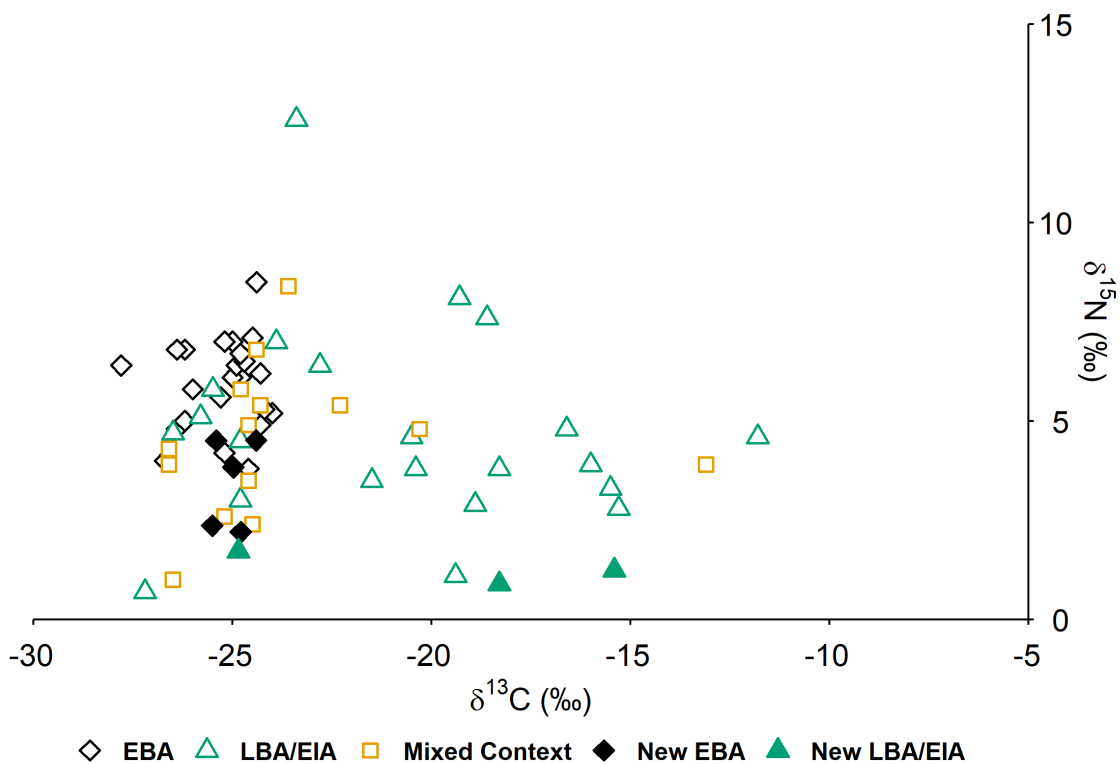


Figure 43. Bulk $\delta^{13}\text{C}$ and $\delta^{15}\text{N}$ values of all charred crusts from Bruszczevo.

Table 11. Summary of $\delta^{13}\text{C}$ and $\delta^{15}\text{N}$ values of the complete Bruszczevo dataset.

	EBA		LBA	
	$\delta^{13}\text{C}$ (‰)	$\delta^{15}\text{N}$ (‰)	$\delta^{13}\text{C}$ (‰)	$\delta^{15}\text{N}$ (‰)
Mean (1 s.d.)	-25.2 ± 0.9	5.5 ± 1.4	-20.5 ± 4.0	4.4 ± 2.5
Range	-24.0 to -27.8	2.2 to 8.5	-11.8 to -27.2	0.9 to 12.6

The difference between $\delta^{15}\text{N}$ values of EBA and LBA/EIA samples is significant (paired t-test, $t=2.9726$, $df=54$, $p=.0044$) when sample F7061ID4765 is removed as an outlier (Z-score = 3.18). This difference may result from a change in either agricultural practices, i.e. manuring, the proportion of products processed, e.g. increased proteinaceous animal products, or type of products processed in vessels. Low $\delta^{15}\text{N}$ values and high C/N values of EBA and LBA/EIA samples indicate the processing of primarily terrestrial plant and animal resources (Figure 44). One LBA/EIA sample, F7061ID4765 ($\delta^{15}\text{N} = 12.6\text{‰}$, $\text{C/N} = 8.7$), probably indicates the processing of aquatic resources, yet the processing of an extremely ^{15}N enriched omnivore could also produce this result. As local $\delta^{15}\text{N}$ baselines and manuring practices in Poland are highly variable (Müller-Bieniek *et al.*

2019), isotopic analysis of botanical and faunal remains from Bruszczewo is necessary to resolve the origin of this sample.

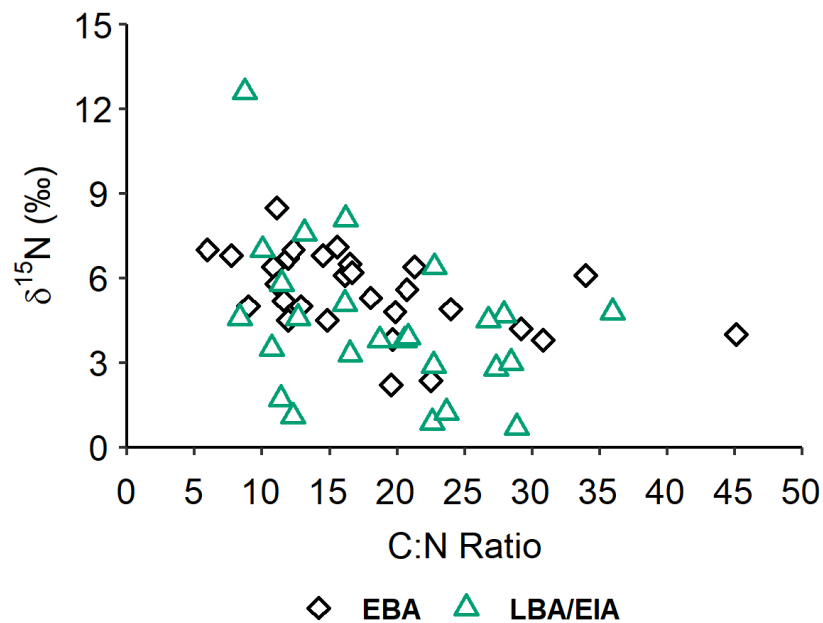


Figure 44. $\delta^{15}\text{N}$ against C:N ratios of the complete Bruszczewo dataset. A significant, moderately negative, relationship exists between $\delta^{15}\text{N}$ and C:N values of EBA samples ($r(27) = .46, p < .02$) but the relationship between $\delta^{15}\text{N}$ and C:N values of LBA/EIA samples is not significant ($r(25) = .35, p > .05$).

The range of $\delta^{13}\text{C}$ values from EBA charred crusts is within that of C_3 products. However, they are significantly different from experimental beef + wheat mixtures (paired t-test, $t=5.7095, df=36, p < .0001$), demonstrating limited overlap and slight ^{13}C enrichment (Figure 45). This may demonstrate either a difference in the isotopic baseline at Bruszczewo, from that of experimental material, or difference in the composition of charred crusts, e.g. greater ^{13}C enriched carbohydrate component. However, there is no evidence to suggest that C_4 plants contributed to the formation of EBA charred crusts. This corresponds to archaeobotanical, zooarchaeological, and isotopic datasets from Bruszczewo and the surrounding region (Kroll 2010; Pokutta and Howcroft 2015; Mnich *et al.* 2020).

The range of $\delta^{13}\text{C}$ values from LBA/EIA charred crusts overlaps with both C_3 and C_4 products and is significantly different from EBA samples (paired t-test, $t=5.4971, df=25, p < .0001$). Significant ^{13}C enrichment demonstrates a contribution of carbon likely derived

from *P. miliaceum*. Most LBA/EIA samples produce $\delta^{13}\text{C}$ values between -22‰ and -15‰ . These charred crusts are perhaps unlikely to form from C_3 and C_4 plant mixtures, although pre-processed C_3 plant products, e.g. wheat flour, could influence $\delta^{13}\text{C}$ values to such a degree (Chapter 5). Most of these samples also produce high $\delta^{15}\text{N}$ values, overlapping with millet + beef mixtures, and low C/N values likely indicating a substantial contribution of animal products. One sample, F5017ID4992, has a $\delta^{13}\text{C}$ value of -11.8‰ and is within the range of wheat + millet mixtures (Figure 45, Heron *et al.* 2016). However, it has a high $\delta^{15}\text{N}$ value of 4.6‰ , relative to wheat + millet mixtures, potentially indicating a contribution of animal protein. Indeed, this sample plots close to the maximum of the M75+B25 mixture. The data potentially suggests that millet was frequently processed with C_3 -fed animal products and perhaps infrequently with C_3 plant products. However, potential differences in isotopic baselines, natural variation of processed products, diagenesis, and a difference in the type, nature, and quantity of products processed, including C_4 -fed animal products, makes interpretation of bulk isotope data difficult.

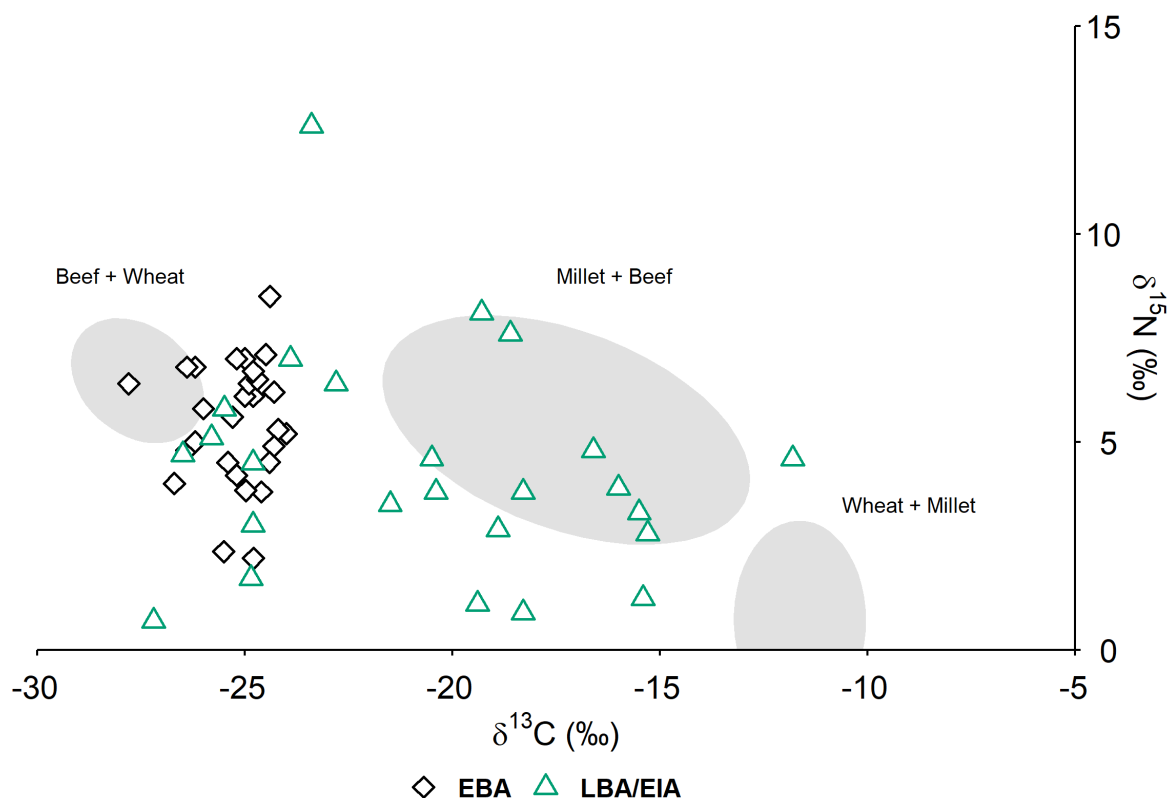


Figure 45. $\delta^{13}\text{C}$ and $\delta^{15}\text{N}$ values of the complete EBA and LBA/EIA Bruszczewo dataset plotted against reference ellipses (1σ) of cooking mixtures outlined in Chapter 5.

Three LBA/EIA samples plot between the upper range of EBA $\delta^{13}\text{C}$ values (-24‰) and the lower range of experimental millet + beef mixtures (-21.3‰), potentially indicating a small (< 25%) contribution of millet to processed mixtures (Chapter 5). Slight ^{13}C enrichment, in addition to a very high $\delta^{15}\text{N}$ value, of F7061ID4765 is likely the result of stepwise enrichment in aquatic food chains and the processing of freshwater fish. However, the other two samples potentially demonstrate the processing of C_4 plants, as they do not produce high $\delta^{15}\text{N}$ values indicative of aquatic resources (Craig *et al.* 2007).. The observation of no ^{13}C enrichment in a minority of LBA/EIA samples suggests that neither C_4 plant nor C_4 -fed animal products were a component of every meal.

Sampling of floral and faunal remains from Bruszczewo is necessary in order to clarify the potential mixtures of products that contribute to charred crusts. The foremost question is whether animals consumed C_4 plants during the LBA/EIA. Establishing the nitrogen isotopic baseline and extent of manuring practices throughout the EBA and LBA/EIA is also of vital importance in the interpretation of these results.

Molecular analysis

Molecular analysis was conducted on 42 sherds, split 20-22, and 20 charred crusts, split 11-9, between the EBA and LBA/EIA respectively. Sampling is representative of all trenches analysed, although a greater proportion of EBA samples are from Trench 52 and most LBA/EIA samples are from Trenches 30 and 31 (Table 12). Therefore, spatial analysis is limited.

Table 12. Number of samples analysed by GC-MS from each trench.

Trench	EBA		LBA/EIA	
	Ceramic	Charred Crust	Ceramic	Charred Crust
30	2	2	11	6
31	3	3	10	3
52	15	6	2	0

TLE Yields

All ceramic samples, and all but one charred crust (B2), produced appreciable quantities of lipid (> 5 $\mu\text{g g}^{-1}$). The TLE yield of each sample is presented in Appendix 3 and the average yields from sherds and charred crusts are presented by period in Table 13

and 14 respectively. A table containing all identified compounds is also presented in Appendix 3.

There is no significant difference between yields of EBA and LBA/EIA ceramics (paired t-test, $t=1.307$, $df=19$, $p > .20$) and charred crusts (paired t-test, $t=1.678$, $df=8$, $p > .13$). High and low yields are observed in sherds from fine wares, cooking vessels, and decorated vessels. There is no indication that food processing was limited to specific vessel types. However, it should be noted that descriptive information for the vessels sampled is limited.

Table 13. TLE yield summary of ceramic samples from Bruszczewo.

	TLE Yield $\mu\text{g g}^{-1}$	
	EBA	LBA/EIA
Mean (1 s.d.)	113 \pm 150	274 \pm 520
Range	16 to 637	14 to 2469

Table 14. TLE yield summary of charred crusts from Bruszczewo.

	TLE Yield $\mu\text{g g}^{-1}$	
	EBA	LBA/EIA
Mean (1 s.d.)	932 \pm 1097	1205 \pm 1114
Range	86.7 to 4049	30 to 3227

Comparable EBA TLE yield data is limited to a single carinated jug from a Únětice Culture barrow grave at Kąty Wrocławskie, Lower Silesia, that produced a yield of $630 \mu\text{g g}^{-1}$ (Pokutta 2015). The yield of the Kąty Wrocławskie sample exceeds all but one EBA sample from Bruszczewo, despite utilising the less efficient solvent extraction method, potentially indicating that the vessel was either subject to heavier use or preservation conditions were preferential at Kąty Wrocławskie. Comparable LBA/EIA data is limited to two sites, Szadek ($n= 2$) and Maciejowice ($n= 12$), that produced average yields of $175 \mu\text{g g}^{-1}$ and $82 \mu\text{g g}^{-1}$ respectively (Szumny *et al.* 2015; Isaksson and Nilsson 2018). The range and average yield of LBA/EIA ceramics from Bruszczewo are greater than both, demonstrating either heavier usage or better preservation. Lower yields observed at Maciejowice may relate to their use as offering vessels in funerary contexts, although this

is yet to be proven conclusively and the observation of scorch marks on these vessels indicates that they were used at least once (Isaksson and Nilsson 2018).

Fatty Acids

A broader range of alkanolic acids is observed in ceramics ($C_{9:0}$ - $C_{34:0}$) than charred crusts ($C_{12:0}$ - $C_{36:0}$), potentially due to greater preservation of short chain length compounds trapped in the ceramic fabric (Evershed 2008a). Monounsaturated alkenolic acids are comparable between ceramics and charred crusts ($C_{16:1}$ - $C_{24:1}$), with shorter chain length compounds, down to $C_{10:1}$, observed in one ceramic sample. A greater number of LBA/EIA samples ($n=8$) contained $C_{18:2}$ than EBA samples ($n=3$), potentially indicating either a change in products processed or increased degradation of polyunsaturated compounds over time (Evershed *et al.* 1999).

Ceramic residues are dominated by $C_{18:0}$, with average palmitic/stearic values around 1, in both EBA and LBA/EIA samples. Conversely, charred crusts are dominated by $C_{16:0}$, with average P/S values of 1.76 and 2.35 in EBA and LBA/EIA samples respectively. These values indicate a greater contribution of plant products to the formation of charred material and potentially a greater degree of plant product processing in the LBA/EIA. However, degradation of $C_{16:0}$ over time, different processing methods, and the processing of different products are also plausible explanations.

Dicarboxylic acids (C_7 - C_{18}) are observed in ceramic and charred crust samples from both periods, demonstrating a high degree of preservation (Regert *et al.* 1998). However, they appear more frequently in LBA/EIA material, potentially demonstrating age-related degradation of unsaturated alkenolic acids. Neither the abundance nor frequency of dicarboxylic acids correspond to either the trench or context from which the material was recovered. Therefore, preservation conditions are judged to be comparable across the area studied, throughout deposition.

Branched chain alkanolic acids (C_{12} - C_{18}) are observed in most samples, potentially indicating the processing of ruminant products. However, microbial contamination is probable, given their ubiquity in this dataset (Dudd *et al.* 1998; Mottram *et al.* 1999).

Pinaceae Markers

Methyl dehydroabietate and 7-oxodehydroabietic acid are observed at low abundance in most ceramic and some charred crust samples, potentially indicating

contamination from either woodsmoke or the burial environment (Brettell *et al.* 2015; Simoneit *et al.* 2000). However, these compounds, in addition to retene, are observed at high abundance in two EBA and two LBA/EIA ceramic samples, indicating either deliberate application of Pinaceae pitch to, or the processing of Pinaceae resin in, these vessels (Table 15, Figure 46).

Table 15. Contribution of Pinaceae biomarker compounds to ceramic TLE.

Sample	Retene		Methyl dehydroabietate		7-oxodehydroabietic acid	
	%	$\mu\text{g g}^{-1}$	%	$\mu\text{g g}^{-1}$	%	$\mu\text{g g}^{-1}$
Br 013	5.9	1.4	2.4	0.6	1.2	0.3
Br 015	4.4	13	10.5	32	9.9	30
Br 104	2.5	10	7.6	30	9.1	36
Br 106	9.4	233	21.3	526	7.7	190

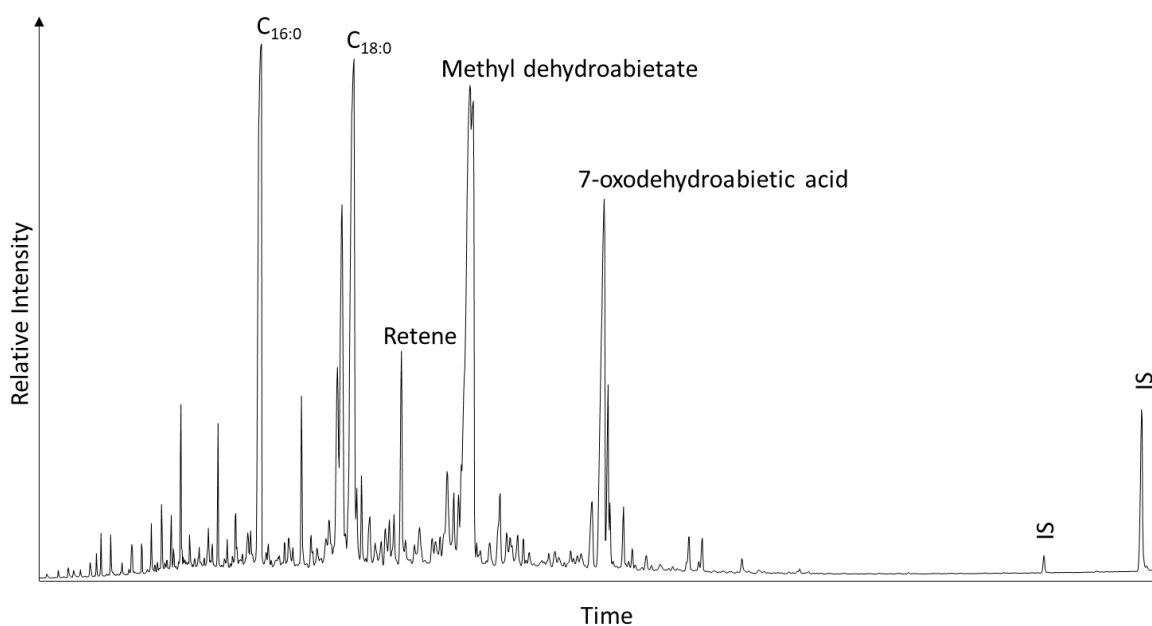


Figure 46. Partial TIC of sample Br 104 I, highlighting the contribution of Pinaceae resin degradation products. IS = Internal Standard.

There is no indication that resinous products were applied during the repair of vessels. The application of resinous products as sealant may explain the presence of these compounds, although contamination during firing could also explain their occurrence in high concentrations (Reber *et al.* 2019). A low abundance of retene observed in samples

Br 002 and Br 102 may result from either the degradation of an applied sealant or environmental contamination. However, the absence of retene in charred crusts may exclude environmental contamination.

Sterols

Cholesterol, phytosterols (sitosterol, stigmasterol, campesterol), and their derivatives are observed in varying abundance in EBA and LBA/EIA ceramic and charred crust samples. Cholesterol is most common in ceramics but at low abundance, potentially as a result of either processing animal products or contamination (Evershed 1993). Conversely, phytosterols are most common in charred crust samples, frequently at high abundance, likely demonstrating a high contribution of plant products to charred materials (Figure 47). Animal and plant sterols are not mutually exclusive, perhaps indicating mixed use of vessels, but observations at low abundance are considered cautiously. Ergosterol is also observed in several samples and may relate to either the processing of fungi or fungal contamination (Weete *et al.* 2010; Hamman and Cramp 2018).

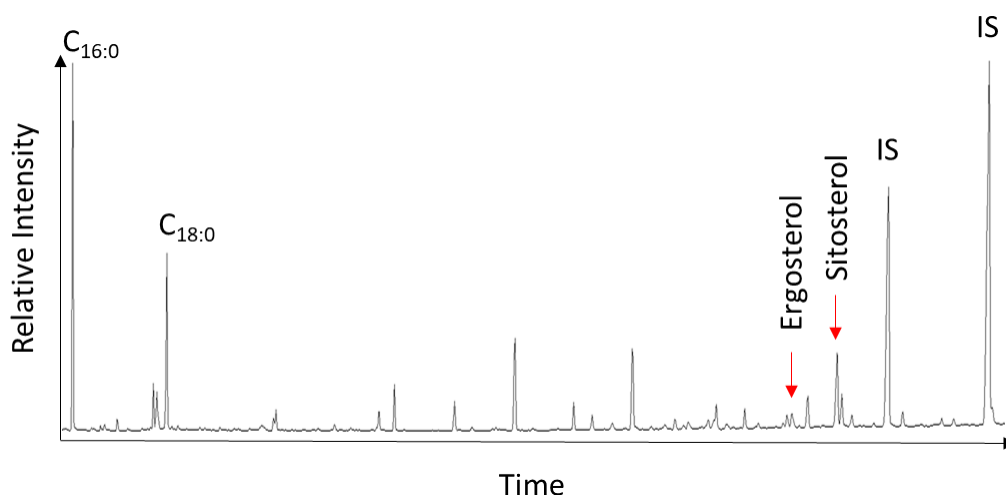


Figure 47. Partial TIC of Br 005 F highlighting the relative abundance of phytosterols. IS = Internal Standard.

APAAs

All samples were analysed by SIM to detect APAAs of C₁₈, C₂₀, and C₂₂ alkanolic acids, in addition to isoprenoid fatty acids, 4,8,12-TMTD, phytanic acid and pristanic acid. Only isomers of C₁₈ APAAs were identified, appearing more frequently and at higher

abundances in charred crusts than ceramic samples. Interestingly, not all charred crusts contained APAAs, potentially demonstrating varied formation processes, at both low and high temperatures (Bondetti *et al.* 2021). The absence of C₂₀₊ APAAs and isoprenoid fatty acids, in addition to generally low bulk $\delta^{15}\text{N}$ values of the crusts, demonstrates limited processing of aquatic resources (Hansel *et al.* 2004; Copley *et al.* 2004; Craig *et al.* 2007; Evershed *et al.* 2008a; Heron and Craig 2015). Unfortunately, sufficient material was not available for analysis from charred crust sample F7061D476, preventing determination of an aquatic product component.

The C₁₈ APAA isomer distribution was assessed for all samples and the mean and range of E/H isomer values are presented in Table 16. Ceramics demonstrate a broader range of E/H values than charred crusts, although the datasets are not significantly different (paired t-test, $t=0.7606$, $df=13$, $p > .4$). Several EBA and LBA/EIA samples produce E/H values > 4 (Figure 48), likely indicating the processing of either cereals, non-leafy vegetables, or fruits, although some porcine and beaver products may also produce such values (Bondetti *et al.* 2021). Furthermore, four samples, Br 013, 015, 104, and 106, contain a high abundance of retene, methyl dehydroabietate, and 7-oxodehydroabietic acid, indicating the protracted heating of *Pinaceae* resin. As *Pinaceae* resin comprises a substantial quantity of unsaturated C₁₈ fatty acids (Arshadi *et al.* 2013), it is possible that its high abundance in these samples may elevate E/H values. However, further experimental research is necessary to demonstrate the production of C₁₈ APAA isomers in *Pinaceae* resin and assess their distribution. The highest E/H value (8.1) was produced by the LBA/EIA sample Br 118, suggesting a substantial plant component, yet this sample also produced a P/S value of 1, suggesting a minimal plant component (Figure 48). As reasonably high temperatures are necessary for APAA formation (Bondetti *et al.* 2021), contradictory E/H and P/S values may derive from different processing methods being applied to different product types, resulting in the absorption of lipids but variable APAA production rates. However, further experimental research is necessary to demonstrate this.

There is a significant positive relationship between E/H and P/S values of all charred crusts ($r(12) = .74$, $p < .003$). This relationship is strong and significant in LBA/EIA samples ($r(4) = .93$, $p < .007$) and moderate but not quite significant in EBA samples ($r(6) = .69$, $p = .058$). Nonetheless, combination of these two ratios provide compelling evidence

for a high contribution of plant products to charred material. There is no relationship between the E/H and P/S values of ceramics, perhaps demonstrating the accumulation of lipids from more varied sources and using different processing methods (Figure 48). Comparison of E/H values to other data, e.g. C/N values, is limited in the current dataset, although this remains a potential area of future investigation to further prove the presence of plant products in charred crusts.

Table 16. Mean and range of E/H C₁₈ APAA isomer values from Bruszczewo samples.

	EBA		LBA	
	Charred Crust	Ceramic	Charred Crust	Ceramic
Mean (1 s.d.)	3.6 ± 1.4	3.0 ± 1.8	3.3 ± 1.3	3.5 ± 1.8
Range	1.6 to 5.5	1.1 to 7.8	1.0 to 5.1	1.1 to 8.1

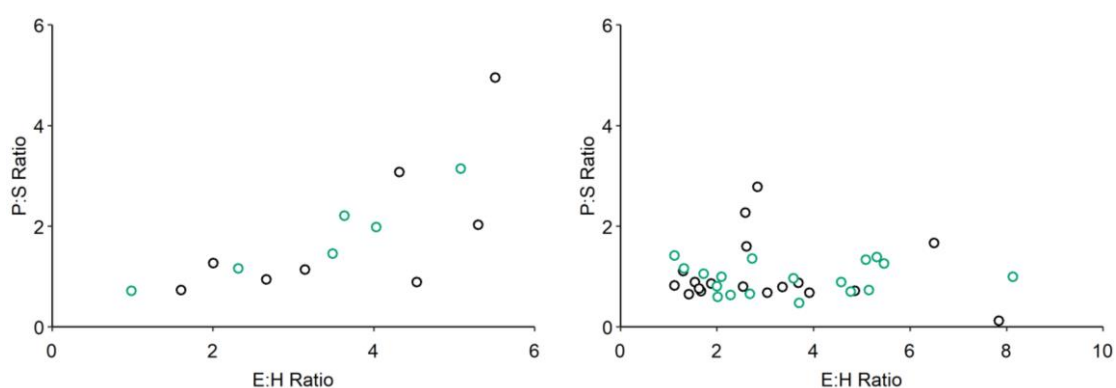


Figure 48. P:S plotted against E:H ratios of EBA (**black**) and LBA/EIA (**green**) charred crusts (**left**) and ceramics (**right**).

Miliacin

Miliacin is absent in all EBA samples, corresponding to bulk $\delta^{13}\text{C}$ values, that demonstrate no significant ^{13}C enrichment, indicating that *P. miliaceum* did not contribute to residue formation. Miliacin is observed in 16/22 ceramic and 6/9 charred crust samples from LBA/EIA contexts. The latter is supported by the enrichment of ^{13}C in the bulk isotope values, demonstrating substantial processing of *P. miliaceum* during this period at Bruszczewo. Miliacin was identified in all charred crusts analysed by GC-MS that demonstrated bulk ^{13}C enrichment. Conversely, all charred crusts analysed by GC-MS

analysis that plotted within the range of C₃ products, did not contain miliacin (Figure 49). This data confirms the observations and hypotheses of Heron *et al.* (2016).

The proportion of LBA/EIA samples containing miliacin is greater than is observed at Macieiwice, 4/12 (Nilsson and Isaksson 2018), potentially demonstrating either a broader use of vessels for, or greater degree of, *P. miliaceum* processing at Bruszczewo. The mean, standard deviation, and range of miliacin yields in LBA/EIA samples is presented in Table 17. Unfortunately, miliacin yields from Macieiwice ceramics are not published, preventing comparison (Nilsson and Isaksson 2018).

Table 17. Mean, standard deviation and range of miliacin content in LBA/EIA samples presented as percentage of TLE.

	Miliacin in TLE (%)	
	Ceramic	Charred Crust
Mean (1 s.d.)	0.51 ± 0.57	3.72 ± 4.00
Range	0.03 to 2.27	0.16 to 10.64

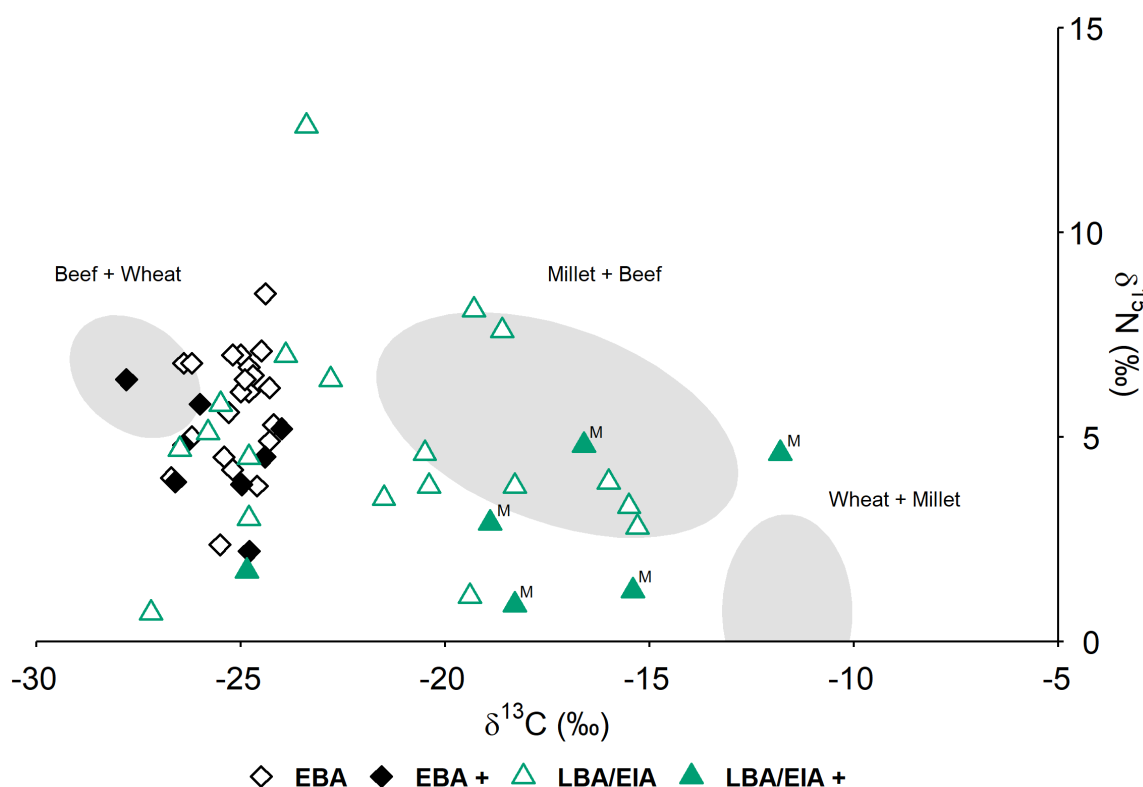


Figure 49. $\delta^{13}\text{C}$ and $\delta^{15}\text{N}$ values of the complete Bruszczewo dataset plotted against reference ellipses (1σ) of cooking mixtures outlined in Chapter 5. **EBA +** and **LBA +** samples were analysed by GC-MS. **M** = miliacin present.

The degree of ^{13}C enrichment observed in bulk $\delta^{13}\text{C}$ values does not correspond to the abundance of miliacin present in charred crusts (Table 18), demonstrating a complex relationship between the two identification criteria. At the extremities of this dataset are samples B3, containing the greatest quantity of miliacin (10.64%) with the lowest bulk $\delta^{13}\text{C}$ value (-18.9‰), and F5017ID4992, producing the highest bulk $\delta^{13}\text{C}$ value (-11.8‰) but containing only trace quantities of miliacin. These results may indicate a source of ^{13}C enrichment other than *P. miliaceum*, such as C_4 -fed animal products. However, a high contribution of non-lipid material, preferential degradation of miliacin, and a complex mechanism of miliacin transference, from caryopsis to charred material, may also result in the observed disparity between datasets. Therefore, additional analysis is necessary to confirm C_4 -fed animal products as a source of ^{13}C enrichment.

Miliacin is observed in samples containing all compound classes discussed previously in this chapter. Miliacin and sitosterol are observed together in all but one charred crust but in none of the ceramic samples analysed. As both compounds are observed in fresh *P. miliaceum*, this observation potentially demonstrates differences in release, absorption, and preservation of the two compounds. Cholesterol is observed in half of the charred crusts analysed, potentially demonstrating the mixing of *P. miliaceum* and animal products, although it is always observed in low abundance and may be derived from contamination.

Table 18. Miliacin contribution (sum of δ -amyrin ME, miliacin, and β -amyrin), bulk and compound specific $\delta^{13}\text{C}$ values of LBA/EIA charred crusts.

Sample ID	Miliacin in TLE %	Bulk $\delta^{13}\text{C}$ ‰	Weighted Average $\delta^{13}\text{C}$ ‰
Br 102 F	0.39	NA	-27.68
Br 113 F	3.64	-18.3	-21.68
Br 121 F	2.13	-15.4	-22.43
B1	5.37	-16.6	-19.5
B3	10.64	-18.9	-23.11
F5017ID4992	Trace	-11.8	-23.7

Ceramic and charred crust samples from Br 109 may demonstrate sequential mixing of *P. miliaceum* and other products, as miliacin is present in the ceramic but not

the charred crust (Figure 50). Had *P. miliaceum* been processed during formation of the charred crust, the release of miliacin, into suspension, would surely have resulted in its incorporation in the charred crust. Unfortunately, there is no corroboratory isotopic data, from the charred crust, to demonstrate the absence of ^{13}C enriched material. Interestingly, miliacin is always present in respective ceramic samples when it is present in the charred crust. Experiments demonstrate variable degrees of miliacin absorption during *P. miliaceum* processing (Chapter 5). Therefore, one may contend that these vessels were used to process *P. miliaceum* on multiple occasions, given consistent co-occurrence in charred crusts and ceramics.

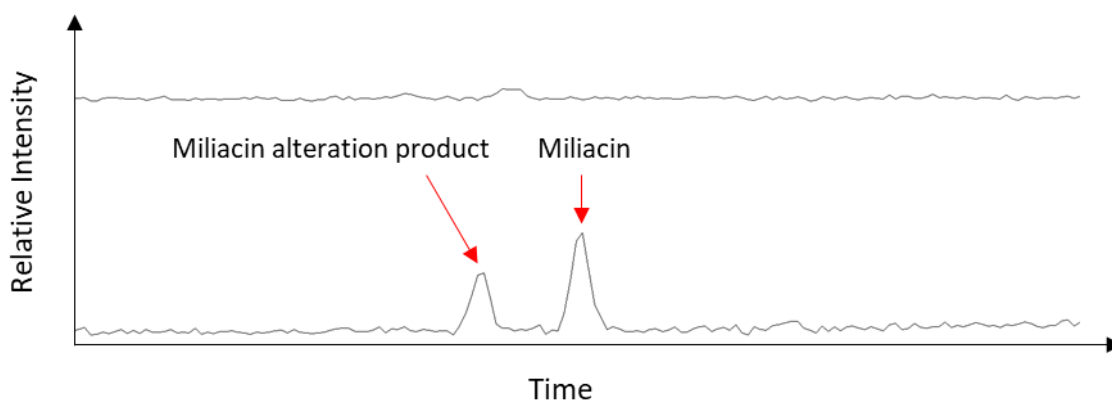


Figure 50. Partial Extracted Ion Chromatograms (EICs) of m/z 189 from the same vessel demonstrate the absence of miliacin in the crust. Br109 F (charred crust, **top**) and Br 109 I (absorbed residue, **bottom**).

The mean TLE yield of LBA/EIA charred crusts that do and do not contain miliacin is $1665 \mu\text{g g}^{-1}$ and $47 \mu\text{g g}^{-1}$ respectively. Experiments demonstrated the release of large quantities of particulate matter into suspension, when processing *P. miliaceum*. Accumulation of this material, on a heated vessel wall, would readily char and entrap suspended lipids, from multiple sources, potentially explaining the stark difference between the two charred crust yields. However, there may also be a difference in the products processed with *P. miliaceum* that result in increased lipid yields. High TLE yields in some EBA charred crusts may be produced by processing resources that result in similarly dense cooking liquids, i.e. wheat flour. However, microscopic analysis of charred crusts is necessary to examine and potentially prove this hypothesis correct, by identifying the type of products forming the charred material.

GC-C-IRMS

Sufficient quantities of C_{16:0} and C_{18:0} fatty acids, > 30 ng per injection, were obtained from 31 sherds, including 13 EBA and 18 LBA/EIA, and 11 charred crusts, including 6 EBA and 5 LBA/EIA. The data is presented in Appendix 3 and the mean, standard deviation, and range of these values are presented in Table 19 and 20, for ceramics and charred crusts respectively.

Table 19. Summary of compound specific $\delta^{13}\text{C}$ values from EBA and LBA/EIA ceramics analysed in this study and by Heron *et al.* (2016).

	EBA		LBA	
	$\delta^{13}\text{C}_{16:0}$ ‰	$\delta^{13}\text{C}_{18:0}$ ‰	$\delta^{13}\text{C}_{16:0}$ ‰	$\delta^{13}\text{C}_{18:0}$ ‰
Mean (1 s.d.)	-29.3 ± 1.3	-30.1 ± 1.5	-28.5 ± 1.3	-29.1 ± 1.2
Range	-26.1 to -31.1	-26.8 to -32.5	-26.5 to -31.6	-26.5 to -31.5

Table 20. Summary of compound specific $\delta^{13}\text{C}$ values from EBA and LBA/EIA charred crusts analysed in this study and by Heron *et al.* (2016).

	EBA		LBA	
	$\delta^{13}\text{C}_{16:0}$ ‰	$\delta^{13}\text{C}_{18:0}$ ‰	$\delta^{13}\text{C}_{16:0}$ ‰	$\delta^{13}\text{C}_{18:0}$ ‰
Mean (1 s.d.)	-30.3 ± 1.8	-30.4 ± 1.8	-23.2 ± 2.3	-22.3 ± 3.1
Range	-27.2 to -33.6	-26.6 to -33.6	-19.7 to -27.3	-19.1 to -28.0

Early Bronze Age

The $\delta^{13}\text{C}_{16:0}$ and $\delta^{13}\text{C}_{18:0}$ values of all EBA samples are within the range of C₃ products. They are depleted from bulk $\delta^{13}\text{C}$ values in line with reference materials (Ballentine *et al.* 1998; Craig *et al.* 2007). A weighted average $\delta^{13}\text{C}$ value was calculated to compare datasets more accurately, by reflecting the proportion of C_{16:0} and C_{18:0} fatty acids in residues. The abundance of each fatty acids is calculated as a percentage of the sum of C_{16:0} and C_{18:0}, before being multiplied by the $\delta^{13}\text{C}$ value of that compound. The two proportional $\delta^{13}\text{C}$ values are then combined to produce a weighted average $\delta^{13}\text{C}$ value that is representative of the contribution of each fatty acid to the residue. The lipid source of residues that are dominated by either compound, e.g. C_{16:0} in charred crust residues, are better reflected by using this measure. Furthermore, this value provides a means to more accurately compare compound specific with bulk isotope data, as bulk

isotope data reflects the average isotopic value of multiple compound classes that have undergone varied fractionation processes (Dunne *et al.* 2016) There is no significant difference between EBA charred crust and ceramic weighted average $\delta^{13}\text{C}$ values (paired t-test, $t=0.6837$, $df=7$, $p > .5$). In addition, there is no significant difference between EBA charred crust and ceramic $\Delta^{13}\text{C}$ values (paired t-test, $t=1.3259$, $df=7$, $p > .2$). Therefore, both materials may be discussed simultaneously.

Most EBA samples plot in the range of C_3 plants and domestic and wild ruminant adipose fats (Figure 51), corresponding to the dominance of C_3 cereals and ruminant animals in the archaeobotanical and zooarchaeological assemblages respectively. The $\delta^{13}\text{C}_{16:0}$ values of ceramic residues from this group are significantly different from the $\delta^{13}\text{C}_{16:0}$ values of Polish Neolithic ceramics, that were reportedly used to process domestic ruminant meat (paired t-test, $t=5.5072$, $df=12$, $p < .0001$, Figure 52, Salque *et al.* 2013). However, $\delta^{13}\text{C}_{18:0}$ values between these two groups are not significantly different (paired t-test, $t=1.1970$, $df=12$, $p > .25$). The depletion of ^{13}C in $\text{C}_{16:0}$ indicates increased processing of C_3 plant products at Bruszczewo, corresponding to elevated bulk $\delta^{13}\text{C}$ and C/N values in EBA charred crusts. Sample Br 007 I plots apart from the main C_3 plant/domestic ruminant adipose group (-30.4‰ , -32.5‰ , Z-score of $\delta^{13}\text{C}_{18:0}$ values = -3.04325), potentially indicating a different source of lipids, i.e. wild ruminant adipose (Figure 51), that was processed less frequently and in separate vessels to domestic ruminant meat. This observation is potentially interesting, as Br 007 is the only EBA sherd with ornamentation (VZ 01 Knob A), warranting further investigation to elucidate any significance placed on wild ruminant products at the site.

Three EBA samples, Br 006 I, Br 017 I, and Br 017 F are distinct from the main C_3 plant/ruminant adipose group, although the sample size is too small to statistically assess a difference. These samples plot either in or near the reference range of porcine products, from which they are likely primarily derived, with a contribution of lipids from C_3 plant and ruminant adipose products. The limited occurrence of these residues corresponds to the low abundance of porcine remains in the zooarchaeological assemblage. Distinction between these two groups of samples may indicate that neither porcine nor ruminant products were regularly processed together, in the same vessel, either concurrently or sequentially, although a greater number of samples is necessary to understand differences in the use of cooking vessels at the site during the EBA.

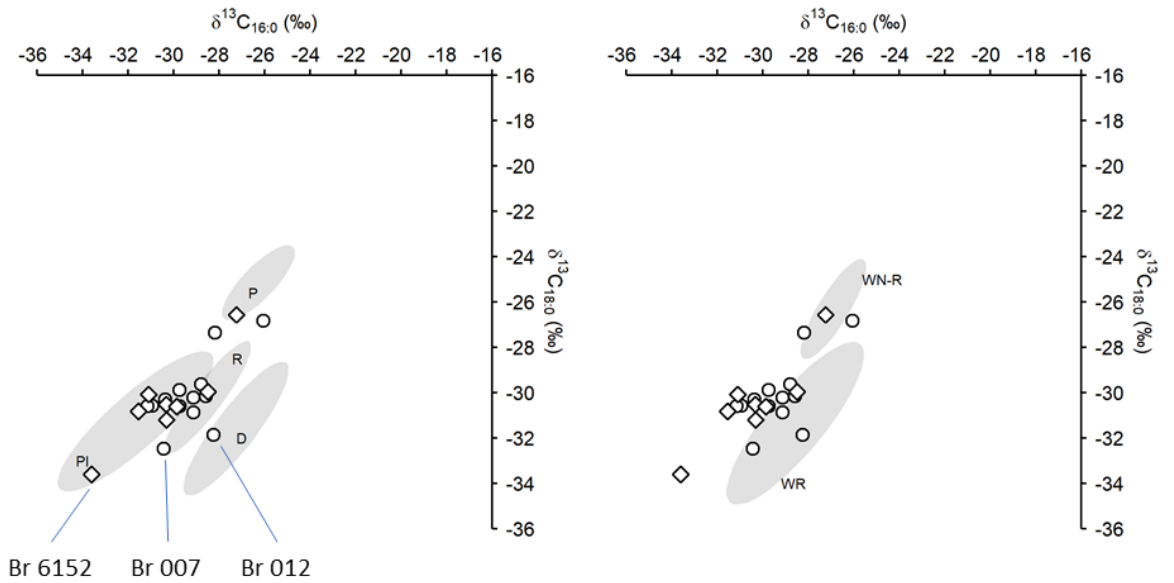


Figure 51. Plot of $\delta^{13}\text{C}_{16:0}$ and $\delta^{13}\text{C}_{18:0}$ values from EBA samples against reference ellipses (1σ) of, **Left** domesticated and **Right** wild animals. **D** = dairy, **P** = porcine, **PI** = C₃ plant, **R** = ruminant, **WN-R** = wild non-ruminant, **WR** = wild ruminant. Circles and diamonds represent ceramic and charred crust samples respectively. Reference data is presented in Appendix 5.

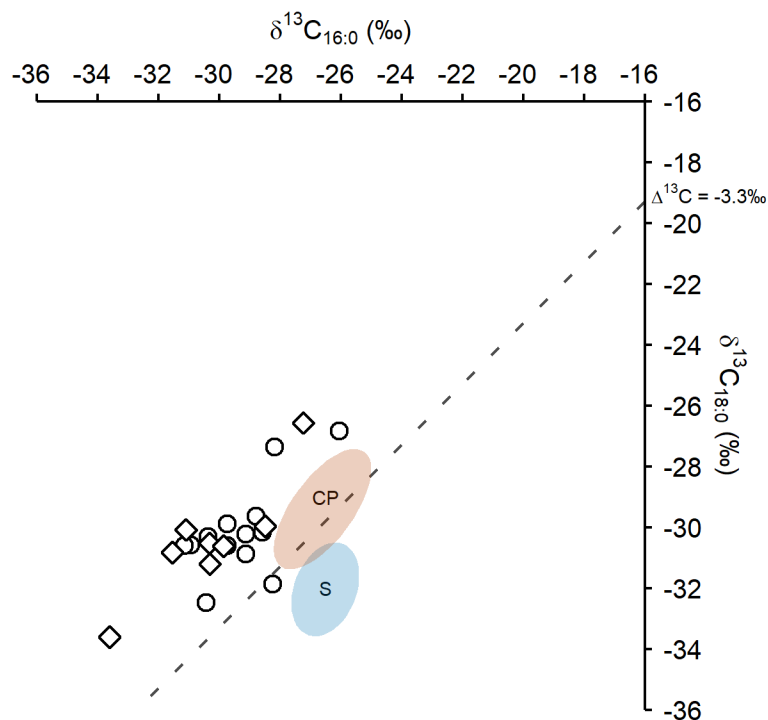


Figure 52. Plot of $\delta^{13}\text{C}_{16:0}$ and $\delta^{13}\text{C}_{18:0}$ values from EBA samples against ellipses (1σ) of Polish Neolithic **CP** = Cooking pots and **S** = sieves (Salque *et al.* 2013).

One sample, Br 012 I, produced a $\Delta^{13}\text{C}$ value of -3.6‰, placing it as an outlier among EBA ceramics (Z-score = 3), indicating either a wild ruminant or dairy origin (Figure 51). However, there is no supporting molecular evidence to suggest which origin is most probable. The sample does not plot within the range of Polish Neolithic ceramic sieves, that were reportedly used for processing dairy products (Figure 52, Salque *et al.* 2013), potentially indicating a wild ruminant origin. However, inter-site variation in environmental conditions could also produce the difference in the $\delta^{13}\text{C}$ values observed between Br 012 I and the sieves (Wallace *et al.* 2013; 2015; An *et al.* 2015). Therefore, a dairy origin cannot be discounted.

The sample size of EBA charred crusts is too small to determine outliers statistically. However, Br 6152 stands out from all other samples as being heavily depleted in ^{13}C . The sample, which plots in the range of plant products (Figure 51), produced a low $\delta^{15}\text{N}$ value (3.8) and high P/S (4.9) and E/H (5.5) values, relative to other EBA charred crusts. Additionally, polyunsaturated fatty acids and a variety of phytosterols were observed, in high abundance, in the TLE, indicating that it is most likely comprised entirely of C_3 plants. Sample Br 6152 is an amorphous charred mass that was recovered free of any ceramic, warranting further microscopic analysis, that may determine whether it is a charred fragment of bread or porridge type product.

Three EBA sherds, Br 001, Br 005 and Br 017, produced ceramic and charred crust samples that contained sufficient quantities of $\text{C}_{16:0}$ and $\text{C}_{18:0}$ fatty acids for compound specific carbon isotope analysis (Figure 53). Therefore, $\delta^{13}\text{C}$ values could be compared between the two materials, to elucidate differences between single event (charred crust) and accumulated, use-life (ceramic) residues.

Charred crusts produce higher $\Delta^{13}\text{C}$ values than respective ceramic samples (Figure 53). Furthermore, there is a significant strong negative correlation between E/H and $\delta^{13}\text{C}$ $\text{C}_{16:0}$ values of EBA charred crusts ($r(3) = -.904$, $p < .00352$) that is likely derived from an increased contribution of $\text{C}_{18:n}$ fatty acids and ^{13}C depleted $\text{C}_{16:0}$ from plant products (Figure 54). This corresponds to a positive relationship between P/S and E/H values of charred crusts, also indicating a higher plant component. This data may demonstrate that plant products were processed during the final use of these vessels, wherein charred crusts were formed, but that vessels were used to process a broader range of products throughout use-life. One may contend that this data demonstrates

different meals and diversity in cuisine and the functional role of ceramics. Furthermore, this data may demonstrate that the contribution of plant lipids, to absorbed ceramic residues, is either limited or difficult to detect. The sample size analysed here precludes a definitive answer and necessitates further investigation to understand whether residues of different meals and use-life may be distinguished.

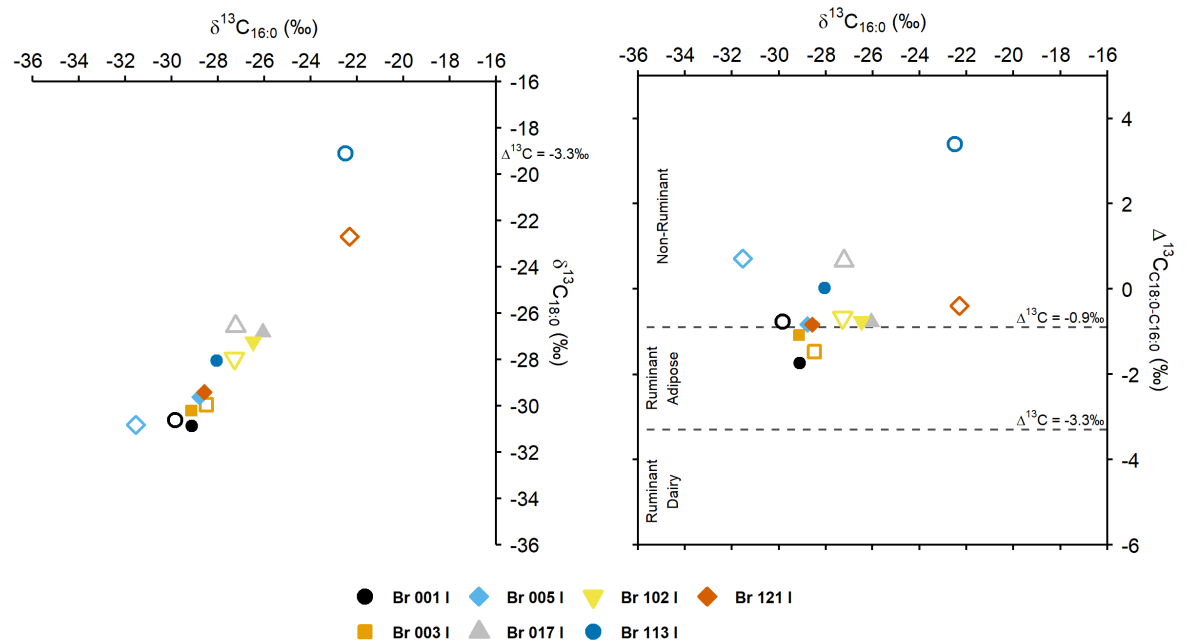


Figure 53. Plot of $\delta^{13}\text{C}_{16:0}$ and $\delta^{13}\text{C}_{18:0}$ values (**Left**) and plot of $\delta^{13}\text{C}_{16:0}$ and $\Delta^{13}\text{C}$ ($\delta^{13}\text{C}_{18:0} - \delta^{13}\text{C}_{16:0}$) values (**Right**). Filled and open shapes represent ceramic and charred crust samples respectively.

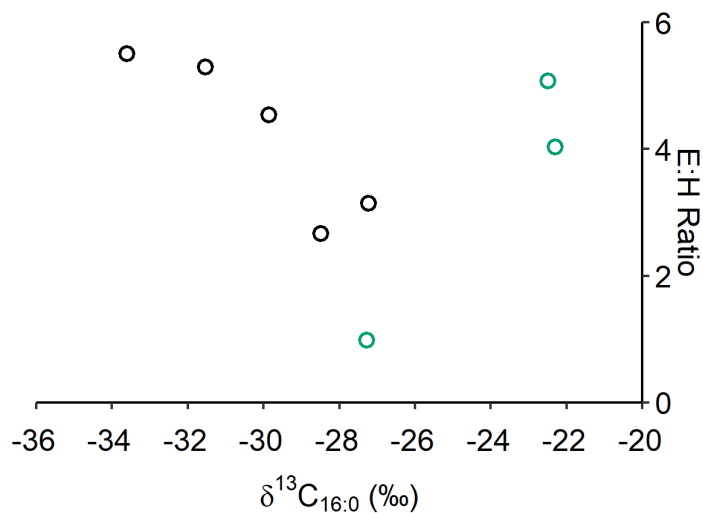


Figure 54. E/H values plotted against $\delta^{13}\text{C}$ values of $\text{C}_{16:0}$ from EBA (**black**) and LBA/EIA (**green**) charred crusts.

Late Bronze Age / Early Iron Age

The difference between the weighted average $\delta^{13}\text{C}$ values of EBA and LBA/EIA ceramics is not significant (paired t-test, $t=2.059$, $df=12$, $p = .0619$). There is $\leq \pm 1\%$ difference in the minimum and maximum range of $\delta^{13}\text{C}$ values of $\text{C}_{16:0}$ and $\text{C}_{18:0}$ between ceramic datasets (Table 19). This data indicates no difference in the carbon source of ceramic residues. However, 14 of 18 ceramic samples analysed by GC-C-IRMS contained miliacin, demonstrating a contribution of ^{13}C enriched plant lipids to ceramic residues. The contribution of miliacin to ceramic TLEs is generally low (Table 17 and 21) and there is no significant relationship between miliacin content and weighted average $\delta^{13}\text{C}$ values of ceramic residues (paired t-test, $t=2.059$, $df=12$, $p = .0619$). These data correspond to experimental observations, wherein the abundance of miliacin is variable but always low in ceramic residues, irrespective of the quantity of *P. miliaceum* processed (Chapter 5). In addition, the LBA/EIA ceramic data from Bruszczevo is comparable to compound specific $\delta^{13}\text{C}$ values of ceramic residues from Iron Age Vix-Mont Lassois, France, that demonstrate *P. miliaceum* processing (Figure 55, Rageot *et al.* 2019a). It is important to note that four LBA/EIA ceramic samples from Bruszczevo, and six from Vix-Mont Lassois, do not contain miliacin, yet they plot within a similar range of miliacin containing samples (Figure 55).

Table 21. Percentage contribution of miliacin (sum of δ -amyrin ME, miliacin, and β -amyrin) to the TLE of ceramic samples subjected to compound specific isotope analysis.

Sample ID	Miliacin in TLE %	Weighted Average $\delta^{13}\text{C}$ ‰
Br 101 I	0.31	-28.68
Br 102 I	0.17	-26.93
Br 105 I	0.55	-29.58
Br 106 I	0.03	-28.83
Br 109 I	0.36	-29.07
Br 110 I	0.92	-31.01
Br 111 I	0.36	-29.64
Br 113 I	2.27	-28.05
Br 114 I	0.5	-29.55
Br 117 I	0.22	-29.6
Br 119 I	0.05	-30.93
Br 120 I	0.07	-27.31
Br 121 I	0.16	-28.93
Br 122 I	0.26	-28.23

Ceramic absorption of miliacin is neither proportional nor consistent when processing *P. miliaceum* (Chapter 5). Furthermore, the survivability of miliacin, relative to other compounds, has not been explored. Therefore, the contribution of an unknown quantity of ^{13}C enriched lipids, to LBA/EIA residues, complicates the interpretation of compound specific isotope data. To better define and distinguish the original components of LBA/EIA residues, theoretical mixing models are applied to the LBA/EIA dataset (Figure 56).

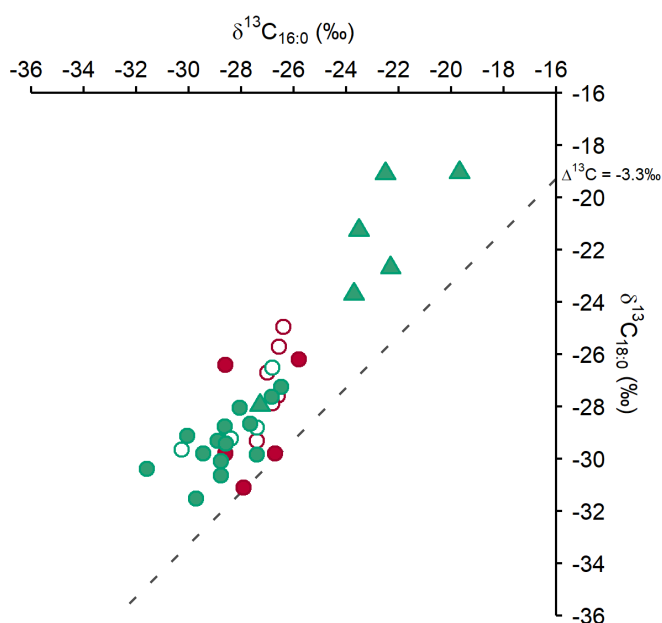


Figure 55. Plot of $\delta^{13}\text{C}_{16:0}$ and $\delta^{13}\text{C}_{18:0}$ values from LBA/EIA samples from Bruszczewo (green) and Vix-Mont Lassois (red, Rageot *et al.* 2019a). Circles and triangles represent ceramic and charred crust samples respectively. Shapes with a fill contain miliacin.

Compound specific $\delta^{13}\text{C}$ values of LBA/EIA ceramic samples plot primarily within the range of ruminant adipose products and, to a lesser extent, C_3 plant products (Figure 56). Processing of *P. miliaceum* with either porcine or ruminant dairy products is unlikely to have been common, although limited processing, in mixed use vessels, cannot be ruled out. The ruminant adipose + *P. miliaceum* mixing model suggests that *P. miliaceum* contributed < 30% of the $\text{C}_{16:0}$ and $\text{C}_{18:0}$ to most residues. This contribution may be higher, if these residues are formed from *P. miliaceum* + C_3 plant mixtures. However, such a contribution is difficult to determine, due to an absence of molecular evidence and

potential variability in the concentration of lipids and $\delta^{13}\text{C}$ values of different plant products. Further research is necessary to understand the persistence and preservation of miliacin, during use and deposition respectively, relative to other lipid constituents of absorbed residues. Subsequently, it may be possible to better quantify the contribution of *P. miliaceum* to residues and understand past processing practices.

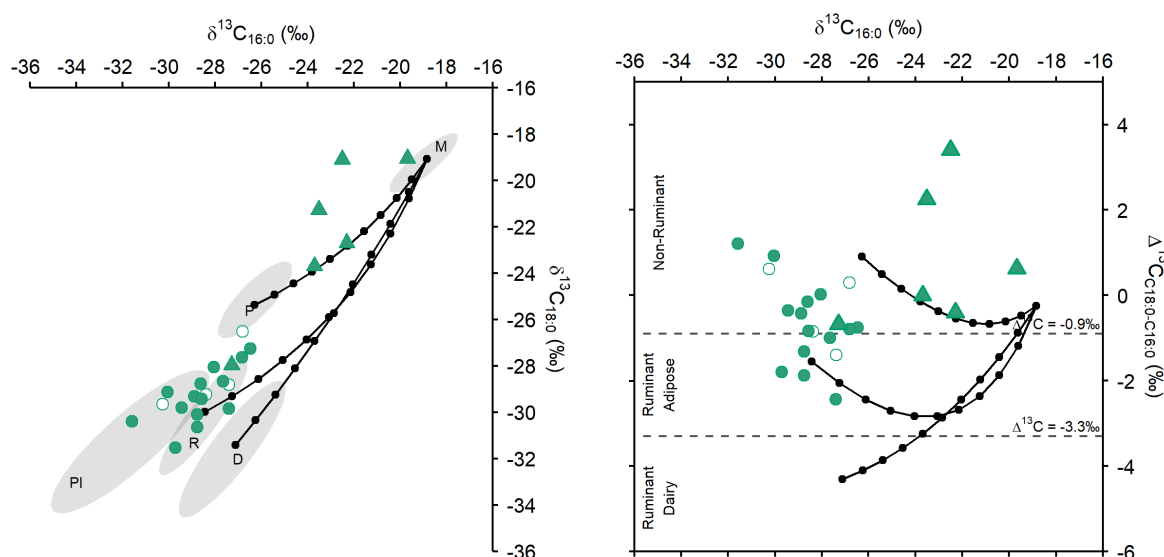


Figure 56. Left Plot of $\delta^{13}\text{C}_{16:0}$ and $\delta^{13}\text{C}_{18:0}$ values from LBA/EIA samples against reference ellipses (1σ) and theoretical mixing lines of modern-carbon corrected foodstuffs. Right Plot of $\delta^{13}\text{C}_{16:0}$ and $\Delta^{13}\text{C}$ ($\delta^{13}\text{C}_{18:0} - \delta^{13}\text{C}_{16:0}$) values from LBA/EIA samples against theoretical mixing lines of modern-carbon corrected foodstuffs. D = dairy, P = porcine, PI = C₃ plant, R = ruminant, M = *P. miliaceum*. Shapes with a fill contain miliacin. Reference data and mixing model presented in Appendix 5.

There is a significant difference between the weighted average $\delta^{13}\text{C}$ values of LBA/EIA charred crusts and ceramics (paired t-test, $t=3.4537$, $df=5$, $p < .02$), with $\delta^{13}\text{C}$ values up to 7.5‰ greater in charred crusts than ceramics, demonstrating a high contribution of ^{13}C enriched lipids to charred material (Table 19 and 20, Figure 55). There is no relationship between bulk and compound specific $\delta^{13}\text{C}$ values (Table 18), demonstrating varied contributions of lipids, carbohydrates, and proteins to charred material, perhaps from different sources. However, bulk-lipid depletion is within the maximum range observed in C₄ plants (Ballentine *et al.* 1998). It is important to consider that charred crusts are heterogeneous and that the fraction analysed by GC-MS may have a different composition to the fraction used for bulk isotope analysis. There does not

appear to be a relationship between miliacin content and lipid ^{13}C enrichment in charred crusts, providing further evidence of varied composition, although there are too few samples to assess a relationship statistically. Therefore, additional sampling and analysis of charred crusts is necessary.

One LBA/EIA charred crust, Br 102 F, plots within the range of C_3 domestic ruminant adipose products, despite containing miliacin (Figure 56). A low abundance of miliacin (0.39% of TLE) and relatively low P/S (0.72) and E/H (0.99) value indicate that *P. miliaceum* lipids are a minor component of this charred crusts. The influence of ^{13}C enriched lipids is demonstrated in the five other charred crusts that contain miliacin and plot either in or towards the range of *P. miliaceum* lipids (Figure 56). Relatively high C/N, P/S and E/H values, and the presence of phytosterols, in several of these charred crusts indicate that ^{13}C enrichment is predominantly derived from *P. miliaceum* processing. However, processing of ^{13}C enriched animal products and *P. miliaceum* cannot be excluded. When examined using theoretical mixing models, it is evident that several charred crusts do not conform to expected mixing lines of the modelled products. This may result from either natural variation in $\Delta^{13}\text{C}$ values or processing of different products, necessitating further isotopic investigation of foodstuffs exploited at Bruszczevo.

A difference is observed in the composition of charred crust and ceramic residues of two LBA/EIA samples, Br 113 and Br 121 (Figure 53). Both charred crust samples are heavily enriched in ^{13}C and demonstrate a strong non-ruminant component, indicative of *P. miliaceum* processing. Both ceramic samples are depleted in ^{13}C , relative to charred crusts, although they are also within the range of non-ruminant products. Conversely, charred crust and ceramic samples from Br 102 are comparable. This data may demonstrate differences between individual meals processed within LBA/EIA vessels at Bruszczevo. This would indicate that, while ceramic vessels were utilitarian in function, cuisine was varied and perhaps complex. However, the disparity between charred crusts and ceramics may also reflect the degree of influence that different plant products have on charred crust and ceramic residue development, as was discussed for EBA material. Further experimental research is necessary to investigate disparities between datasets, as few studies have conducted extensive comparison of these materials (Miller *et al.* 2020).

Discussion and conclusion

1. Is there evidence of *Panicum miliaceum* processing in the Early Bronze Age?

The results clearly demonstrate no evidence for *P. miliaceum* processing during the EBA at Bruszczewo. Bulk isotope analysis conducted by Heron *et al.* (2016) is supplemented by five EBA samples, none of which demonstrated ^{13}C enrichment. No miliacin was observed in 31 ceramic and charred crust samples analysed and GC-C-IRMS analysis of 20 samples demonstrated no ^{13}C enrichment. These results agree with the established chronology of *P. miliaceum* introduction to Europe, and Poland, during the BA (Chapter 3). Therefore, it is likely that individual *P. miliaceum* caryopses observed in EBA contexts at Bruszczewo are intrusive from later periods. Furthermore, sherds with millet impressions observed in the transgression layer between EBA and LBA/EIA contexts are also likely intrusive from LBA/EIA contexts.

2. Do charred crusts that produce high bulk $\delta^{13}\text{C}$ values contain miliacin?

All five LBA/EIA charred crusts, with high $\delta^{13}\text{C}$ values, analysed by GC-MS contained miliacin. Conversely, no charred crusts with low $\delta^{13}\text{C}$ values contained miliacin. The lowest bulk $\delta^{13}\text{C}$ value of a charred crust containing miliacin is -18.3‰, warranting further molecular analysis of charred crusts with lesser ^{13}C enrichment, down to the -22‰ limit often employed in determining the presence of enriched products in charred crusts. As there is no relationship between the abundance of miliacin and bulk $\delta^{13}\text{C}$ values, and C_4 -fed animal product processing cannot be discounted, one must question whether all high bulk $\delta^{13}\text{C}$ values are derived from *P. miliaceum* processing. Additional sampling of charred crusts and faunal remains are necessary to resolve these issues. Further experimental research into the survivability of miliacin, relative to other lipids, is also necessary to understand whether false negative results may also occur.

3. Is evidence for the processing of *P. miliaceum* comparable between ceramic and charred crust samples?

P. miliaceum processing is observable in ceramic samples via the detection of the miliacin biomarker. However, compound specific $\delta^{13}\text{C}$ values of ceramic residues, from Bruszczewo and Vix-Mont Lassois (Rageot *et al.* 2019a), demonstrate the insensitivity of GC-C-IRMS analysis in detecting a contribution of lipids from *P. miliaceum*, as all samples

plot within the range of C₃ plant and animal products. This is, in part, due to the low concentration of lipids in *P. miliaceum*, relative to animal products, but also the limited transference of *P. miliaceum* lipids to the ceramic fabric during cooking (Chapter 5). As a result of these issues, comparison of ceramic data with theoretical mixing models does not enable either unambiguous or quantifiable identification of *P. miliaceum* processing. Conversely, *P. miliaceum* processing is evident, through the observation of miliacin and ¹³C enrichment, in charred crusts. However, compound specific $\delta^{13}\text{C}$ values of charred crusts containing miliacin may be depleted, beyond the point of recognition, if the contribution of *P. miliaceum* to a processed mixture is low.

Experimental research is necessary to identify a minimum contribution of *P. miliaceum*, to a processed mixture, for ¹³C enrichment to be observed in compound specific $\delta^{13}\text{C}$ values of ceramics and charred crusts. Furthermore, the interpretation of ¹³C enrichment, in archaeological material, is complicated by potential sources of carbon other than *P. miliaceum*, warranting further experimental research. Presently, there is no relationship between miliacin abundance and $\delta^{13}\text{C}$ values, although experiments conducted in Chapter 5 do not provide conclusive evidence to support this observation. The miliacin biomarker provides more accurate interpretation, which appears to be reliably observed in archaeological samples, yet questions remain as to the distribution of this compound, and similar PTMEs, among wild flora (Chapter 4).

Discrepancies between ceramic and charred crust datasets enable the inference of sequential and mixed product processing within vessels, that demonstrate significant differences between single event and average use-life processing. Comparison of these data permits greater interpretation of subsistence strategies and food cultures. At Bruszczewo, charred crusts demonstrate a substantial degree of plant product processing that would otherwise be unrecognised in ceramic samples. However, potential under- and overrepresentation of certain products in ceramic and charred crust residues requires further experimental research before conclusions are drawn.

4. Is *Panicum miliaceum* exclusively associated with either another food product or specific vessel type?

There is no evidence to suggest that *P. miliaceum* was an exclusive product at Bruszczewo. The data indicates that it was processed with various plant and animal

products. There is limited evidence to suggest *P. miliaceum* was processed with either porcine or dairy products, yet neither can be excluded conclusively given potential overlap of theoretical mixing lines. Charred crusts likely demonstrate that *P. miliaceum* was processed with other products, during single meals, and sequential processing is demonstrated in Br 109. The observation of miliacin in most ceramic samples analysed indicates that *P. miliaceum* was processed frequently, yet issues regarding the persistence of miliacin in ceramic-absorbed residues, after processing the cereal, limits an assessment of its true importance to subsistence. However, the abundance of charred crusts producing evidence for *P. miliaceum* processing demonstrate that it was an important staple at Bruszczewo. Unrestricted processing of *P. miliaceum* at Bruszczewo corresponds to molecular data for its use at the contemporary cemetery of Maciejowice and archaeobotanical assemblages across Poland, that indicate it was a staple crop at many settlements (Isaksson and Nilsson 2018; Mueller-Bieniek *et al.* 2019). However, as Bruszczewo and Maciejowice are potentially related to ceremonial and ritual activity, future analysis should focus on clearly defined LBA/EIA settlements in this region, to confirm its role in subsistence.

Miliacin is observed in storage, decorated and undecorated, coarse and fine ware vessels, further indicating unrestricted use of the cereal as a staple food at Bruszczewo. The millet impression sherd, Br 114, contained miliacin, that is likely derived from processing *P. miliaceum*, as compounds present in clays and organic tempers are unlikely to survive the firing process (Johnson *et al.* 1988; Heron *et al.* 1991). Neither molecular nor isotopic analysis demonstrate an atypical use of this vessel and there is no evidence to suggest why it was impressed with *P. miliaceum* caryopses. Therefore, one may question whether the impressions are present by mistake or design. The sample from Br 111, the sherd with a white surface layer, also contained miliacin, yet molecular and isotopic data are not atypical of the Bruszczewo dataset. Additional analyses are necessary to characterise the composition of the white surface layer and ascertain whether it could potentially contain other food related compounds, e.g. proteins (Hendy *et al.* 2018). Further analysis would enable better contextualisation of this sherd and determine whether the vessel was either produced on site or imported.

5. What differences in pottery use are observable between the EBA and LBA/EIA?

Ceramic and charred crust samples from EBA material demonstrate the exploitation of a variety of C₃ plant and animal products, with C₃ plants and domestic ruminant adipose dominant. Porcine product processing is uncommon and evidence for dairy products is rare, corresponding proportionally to the occurrence of species in the faunal assemblage. The dominance of cereals, and high abundance of acorns, in the archaeobotanical assemblage potentially provide an explanation for substantial ¹³C depletion in C_{16:0} of EBA residues. Additional solvent extraction of ceramics and charred crusts may identify cereal biomarkers, giving an indication as to their importance to subsistence at the site, although their preservation is not guaranteed. Distinct groups of compound specific $\delta^{13}\text{C}$ values in EBA material potentially indicates a separation of porcine, ruminant adipose, and dairy product processing. Indeed, disparities between $\delta^{13}\text{C}$ values and single event and accumulated residues may demonstrate a complex food culture at Bruszczewo. However, the sample size is too small to assess these patterns accurately. A ceramic processing of foodstuffs is potentially identified in the disassociated charred crust sample Br 6152, that may demonstrate varied approaches to food processing. The relatively small and uneven sample set prevents spatial analysis between trenches and areas of the settlement. Additional analysis, increasing the number of vessels analysed, focusing on specific ceramic types/styles and trenches across the site would enable an accurate assessment of potential socioeconomic differences that are highlighted in other material datasets. The identification of Pinaceae markers in EBA ceramics provides the only evidence for the application of resinous products to ceramics at Bruszczewo and demonstrates a level of technological knowledge previously unidentified at the site and across the region during the BA.

The main difference between EBA and LBA/EIA samples is the high frequency and abundance of miliacin observed in LBA/EIA ceramics and charred crusts associated with ¹³C enrichment. Beyond the introduction of *P. miliaceum* to subsistence strategies, there is limited evidence to suggest a significant difference in subsistence strategies between the two periods. Both C₃ and C₄ plant and domestic ruminant adipose appear to form most LBA/EIA residues. Porcine, dairy, and wild ruminant products do not appear to be a significant element of LBA/EIA residues, yet they cannot be excluded conclusively, due to

the probability of infrequent sequential mixing. As with EBA material, the LBA/EIA dataset and contextual information is too limited to enable accurate material and spatial analysis, warranting additional sampling of specific features and contexts across the site. In addition, isotopic analysis of faunal remains should be prioritised, to further investigate subsistence strategies and clarify the isotopic data presented here. Such analysis would also provide further evidence for the role of the relatively new crop, *P. miliaceum*, as either a food exclusively for humans or also a fodder crop.

The LBA/EIA datasets provide conflicting evidence for the degree of *P. miliaceum* processing at Bruszczewo, with molecular evidence and charred crusts indicating prolific use but compound specific isotope $\delta^{13}\text{C}$ values of ceramics indicating a limited role of the cereal in subsistence. Additional experimental research is necessary to resolve material specific questions, as to the accumulation and persistence of residues during *P. miliaceum* processing, to accurately assess the role of *P. miliaceum* at Bruszczewo. Nonetheless, the data does indicate a far greater role of this cereal than the archaeobotanical assemblage implies. In addition, the prevalence of *P. miliaceum* processing at Bruszczewo exceeds that observed at Maciejowice, warranting further assessment of the role of the cereal in settlement and ceremonial spheres. Future archaeological investigations at Bruszczewo may provide greater clarity as to its function during the LBA/EIA.

A greater number of LBA/EIA ceramic sherds possessed identifiable typological and stylistic characteristics than among EBA samples, although no pattern in vessel use was observed, potentially indicating utilitarian use of vessels during the LBA/EIA. However, the sample size was small and additional analysis is necessary. The identification of Pinaceae markers in ceramic samples demonstrates continuity in the application of technological knowledge that, as with EBA samples, was previously unknown in this region during the BA.

Chapter 7: ORA investigations in North Greece and Bulgaria

Introduction

The point at which *P. miliaceum* entered Europe remains to be identified. The prevailing hypothesis is that the cereal was introduced from the Caucasus, via Ukraine, before dispersing rapidly east to west, with later north to south movement (Chapter 3). However, direct radiocarbon dating has not been extensively applied to *P. miliaceum* caryopses from either Eastern and SE Europe, or the Caucasus and Turkey, preventing translocation routes from being confidently identified (Filipovic *et al.* 2020). Indeed, reliable evidence from regions that border Europe post-date the earliest evidence for *P. miliaceum* in Europe. Therefore, significant scope exists to provide datable, specific, and secure evidence, that may either refine or redefine the chronology of *P. miliaceum* introduction to Europe, by a targeted and large-scale investigation of ceramic-absorbed organic residues. In addition, by examining relatively large sample sizes, from multiple sites, in a restricted region, an ORA investigation has the potential to examine inter and intra-cultural attitudes towards the adoption of this species. Associated ceramic-absorbed residue, ceramic, and spatial data may be cross examined to investigate potential social and cultural differences expressed in cuisine and the consumption of *P. miliaceum*.

This chapter presents the results of molecular and isotopic analysis of ceramic-absorbed residues from Northern Greece and Bulgaria. In total, 113 ceramic sherds were sampled from twelve sites, dating to the Neolithic, Chalcolithic, and Bronze Age. Samples were obtained from recent excavations and museum collections in Greece and Bulgaria and were provided by the Plant Cult project, funded by the European Research Council (ERC Consolidator Grant, GA 682529). The amassed assemblage enables a chronological assessment of the introduction and adoption of *P. miliaceum* in Greece and Bulgaria. Analysis was undertaken in order to address four main research questions.

1. Was *P. miliaceum* processed in either Greece or Bulgaria prior to the BA?
2. Is there evidence to support the observation of *P. miliaceum* in EBA contexts?
3. To what extent was *P. miliaceum* processed in the LBA?
4. Is it possible to identify and characterise the use of *P. miliaceum* in culinary activities, and infer its cultural significance, by the analysis of ceramic-absorbed residues?

Evidence for *P. miliaceum* in Northern Greece

Greece is a significant point of cultural interaction between East and West, with the exchange of crops, technology, and ideas, from Central Europe, Caucasus, and Middle East, evident from the third millennium BCE (Valamoti and Jones 2010). The prominent geographical position of Greece and occurrence of significant deposits of *P. miliaceum* caryopses in EBA contexts warrant investigation of this region as a potential route of *P. miliaceum* introduction to Europe.

Neolithic sites in North Greece, including Argissa, Otzaki Magoula, Limenaria, Agios Ioannis Loukas, Dikili Tash, and Mandalo, have produced isolated and low abundance deposits of carbonised *P. miliaceum* caryopses. However, archaeobotanical assemblages from these sites comprise thousands more caryopses of other cereals and there are many more Neolithic sites where *P. miliaceum* is absent. Furthermore, most Neolithic sites have overlying BA contexts, increasing the probability that Neolithic observations are intrusive (Valamoti 2016; Kotzamani and Livarda 2018). While Neolithic coastal communities exhibit minor ^{13}C enrichment that may be attributed to the consumption of marine products, there is only one Neolithic individual from an inland site, Theoptera, that demonstrates ^{13}C enrichment (Figure 57). This individual may be misattributed to the Neolithic, as the remains have not been directly radiocarbon dated. However, if context-specific dating is accurate, the minor enrichment observed ($\delta^{13}\text{C} - 17.2\%$) may derive from either the consumption of naturally occurring ^{13}C enriched products, e.g. wild C_4 plants and free-browsing animals, or environmental conditions. Micro- and macrobotanical remains of wild *Setaria* spp. are observed at Stavroupoli (Garcia-Granero *et al.* 2018) and macrobotanical remains of *D. sanguinalis* are observed at Revenia (Kotzamani and Livarda 2018). Therefore, wild C_4 species may have been harvested and consumed by humans, although the introduction of these species, to archaeobotanical assemblages, is perhaps more likely to have derived from animals, i.e. the burning of dung. Indeed, isotope analysis of Neolithic animal remains demonstrates ^{13}C enrichment across several species and sites, including cattle at Makriyalos and potentially sheep at Sparta (Vaiglova *et al.* 2018; 2020). Comparable enrichment between domestic and wild herbivores demonstrates the exploitation of environments comprising

a high abundance of ^{13}C enriched plants. Furthermore, the data indicates different management strategies of domestic species within and between sites.

The processing and consumption of ^{13}C enriched animal products, most likely milk, is confirmed by compound specific carbon isotope analysis of ceramic-absorbed residues from Makriyalos and other sites in northern Greece (Evershed *et al.* 2008b; Whelton *et al.* 2018). Miliacin was not reported in these samples, although it is not specified whether the compound was searched for, potentially demonstrating that ^{13}C enrichment was not directly derived from either *P. miliaceum* or *D. sanguinalis*. Indeed, the rarity of wild C_4 plant species in Neolithic archaeobotanical assemblages indicates that they are unlikely to have been harvested, processed, and consumed in significant quantities as to influence $\Delta^{13}\text{C}$ values of ceramic-absorbed residues, and the interpretation of dairy processing, via lipid mixing (e.g. Hendy *et al.* 2018).

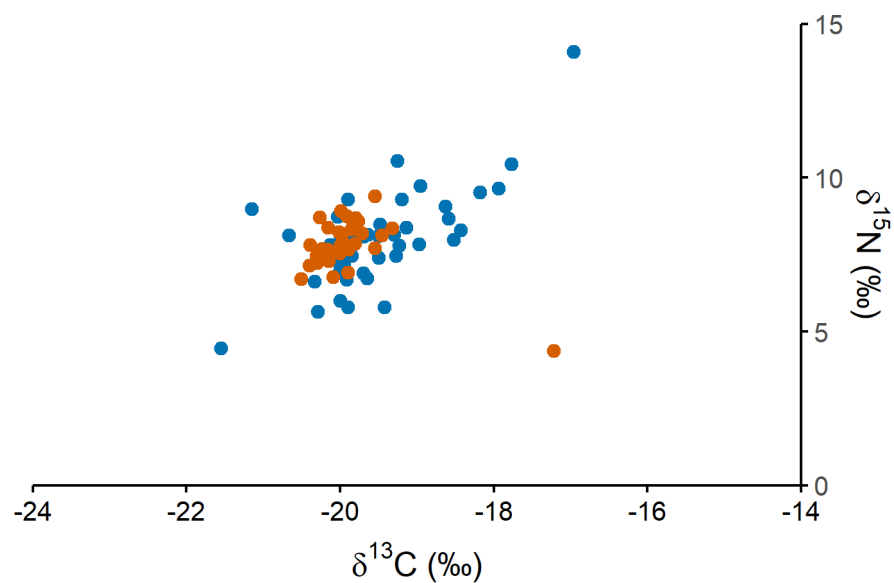


Figure 57. Bulk isotope data of Neolithic humans from northern Greece. Blue and orange points represent coastal and inland individuals respectively (Data from Papathanasiou 2003; Triantaphyllou 2015).

P. miliaceum is observed in EBA contexts (3500-2000 BC) at only two sites in northern Greece, Sitagori (n= 1) and Kastanas (n= 8). However, more abundant and concentrated deposits are observed at two E-MBA transition sites (ca. 2000 BC), Skala Sotiros (n= 367) and Archondiko (n= 40). Individual caryopses, scattered across floor levels, observed at Archondiko potentially indicate intrusion from overlying LBA activity.

Conversely, the deposit at Skala Sotiros is rich and concentrated, the context is believed to be secure, and has been radiocarbon dated, from other plant material, to ca. 2100 cal. BCE (Valamoti 2016). The abundance and proximity of these observations may indicate an earlier introduction of *P. miliaceum* than has previously been considered in Greece and Europe, although additional evidence is necessary to support this hypothesis. A contemporary E-MBA transition site, Agios Athanasios, produced no *P. miliaceum* and the cereal is rare throughout the MBA in Greece, appearing at Agios Mamas (n= 3) but not at Paraskevi and Mitrou (Valamoti 2016). Published archaeobotanical reports for these periods are limited, potentially explaining the low frequency of finds.

Neither EBA nor MBA human remains demonstrate ^{13}C enrichment (Figure 58), including three individuals from Archondiko, corresponding to archaeobotanical data. However, archaeobotanical data indicates small-scale consumption, that would not be recognisable via bulk isotope analysis. Furthermore, archaeobotanical and isotopic datasets represent a limited number of analyses, from different sites. Therefore, these datasets are neither representative nor comparable, necessitating further investigation of EBA and MBA sites and materials.

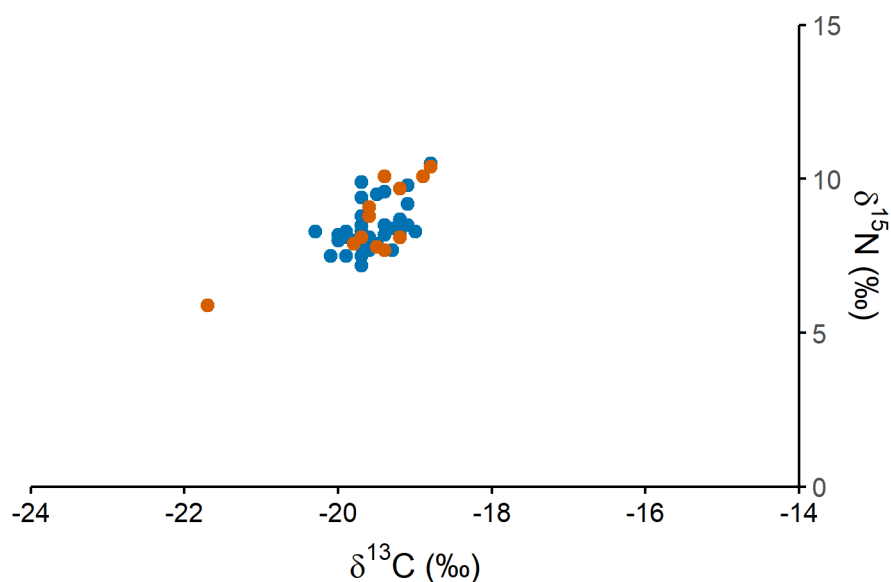


Figure 58. Bulk isotope data of EBA and MBA humans from northern Greece. Blue and orange points represent coastal and inland individuals respectively (Data from Vika 2011; Triantaphyllou *et al.* 2008; Nitsch *et al.* 2017).

The frequency and abundance of *P. miliaceum* increase in the LBA, with rich, pure, and concentrated deposits observed at Archondiko, Kastanas, Agios Mamas, Angelochori, Thessaloniki Toumba, and Assiros Toumba (Marinova and Valamoti 2014; Valamoti 2016). Assiros Toumba provides the only direct date in the region, ca. 1340 cal BCE (Wardle *et al.* 2014).

The exploitation of *P. miliaceum* varies significantly between LBA sites, for instance, representing 5%, 10%, and > 95% of the archaeobotanical assemblage at Angelochori, Agios Mamas, and Kastanas respectively (Valamoti 2016). The species is also absent from some sites, potentially demonstrating that different communities, within a small region, either relied upon, utilised, or rejected the cereal. However, concentrated and pure archaeobotanical deposits may derive from either a single harvest or a storage system wherein cereals were not mixed, potentially introducing bias to the interpretation of subsistence strategies.

Bulk isotope analysis of *P. miliaceum* caryopses from Archondiko and Thessaloniki Toumba potentially indicates manuring during cultivation (Nitsch *et al.* 2017). This corresponds to ^{15}N and ^{13}C enrichment in cattle, relative to wild species, observed at both sites, which may demonstrate the use of *P. miliaceum* as fodder (Nitsch *et al.* 2017). Significant ^{13}C enrichment is also observed in cattle and pig remains from Assiros Toumba, likely demonstrating substantial foddering with *P. miliaceum* (Wardle *et al.* 2014). This data potentially indicates that, while *P. miliaceum* was a minor cereal at Archondiko, and other LBA sites, it may have fulfilled an important role in the intensification and diversification of agricultural practices, perhaps for either risk management or economic gain.

There is poor correspondence between LBA archaeobotanical and human isotope datasets. Furthermore, isotopic studies are limited, preventing thorough examination of individual LBA sites. Significant but varied ^{13}C enrichment is observed at Treis Elies and Thessaloniki Toumba (Figure 59, Triantaphyllou 2015; Nitsch *et al.* 2017). Minor ^{13}C enrichment in most individuals from Thessaloniki Toumba may derive from either small-scale direct consumption of *P. miliaceum* or consumption of ^{13}C enriched animal products (Nitsch *et al.* 2017). Conversely, heavy ^{13}C enrichment in three of six individuals from Treis Elies may indicate substantial direct consumption of either *P. miliaceum* or ^{13}C enriched animal products (Triantaphyllou 2015), although lower $\delta^{15}\text{N}$ values of these individuals

may suggest the former. Bulk isotope analysis of animal remains from the site is necessary to prove this hypothesis.

The LBA dataset indicates that *P. miliaceum* was employed as a minor fodder crop at many sites, although direct consumption by humans likely also occurred. However, isotope analysis is limited in its ability to prove direct consumption of *P. miliaceum* when foddering occurs. It is perhaps likely that any ceremonial significance attributed to this cereal during initial introduction was no longer recognised in the LBA. However, this does not preclude cultural significance. Differences in the degree of ^{13}C enrichment between humans indicates that certain individuals, within and between communities, had either a greater or lesser affinity to, and reliance on, *P. miliaceum*. Further research is necessary to investigate spatial, temporal, cultural, status, and sex-based differences in the consumption of ^{13}C enriched products. For instance, Nitsch *et al.* (2017) propose a potential relationship between *P. miliaceum* consumption and subadults at Thessaloniki Toumba, yet the sample size is too small to assess the accuracy of this hypothesis.

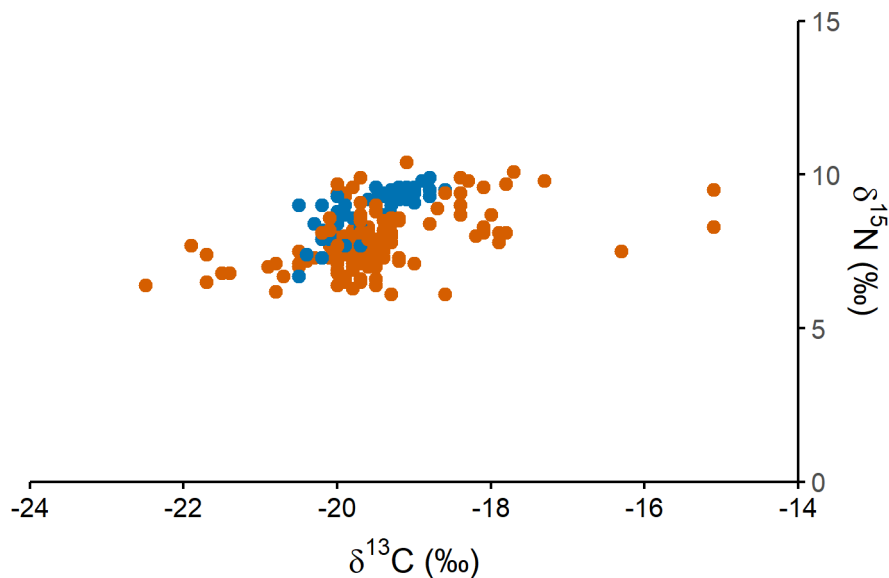


Figure 59. Bulk isotope data of LBA humans from northern Greece. Blue and orange points represent coastal and inland individuals respectively (Data from Petroutsa *et al.* 2009; Petroutsa and Manolis 2010; Triantaphyllou 2015).

Evidence for *P. miliaceum* in Bulgaria

Frequent but sparse observations of *P. miliaceum* are reported at Neolithic sites in Bulgaria, including Kovačevo, Yabalkovo, and Drenkovo-Ploshteko (Popova and Marinova

2006). The nearest early direct radiocarbon dates are from Romania, ca. 1350 cal BCE, and Greece, ca. 1340 cal BCE, neither of which enables an accurate interpretation of either the direction or timing of *P. miliaceum* introduction to Bulgaria (Motuzaitė-Matuzevičiute *et al.* 2013; Wardle *et al.* 2014; Filipovic *et al.* 2020). Carbonised caryopses are also scarce in the Chalcolithic, appearing as single finds at Durankulak (Marinova and Antanassova 2006) and Provadia (Marinova and Valamoti 2014). There is no isotopic evidence to unambiguously suggest significant consumption of *P. miliaceum* in either period (Honch *et al.* 2006; Lightfoot *et al.* 2013), although it is important to reiterate that small scale consumption would not influence isotopic data.

Archaeobotanical evidence indicates that *P. miliaceum* was not well established in Bulgaria until the LBA, as is demonstrated at Kamenska Chuka, Koprivlen, Nebet Tepe, Adata, Okrazna Bolinitza, and Goljama Detelina (Popova and Marinova 2006; Stika and Heiss 2013; Marinova and Valamoti 2014). Consecutive occupation, at sites such as Kush Kaya, suggests that *P. miliaceum* was not present before the LBA (Popov *et al.* 2018; Valamoti *et al.* 2019) and that its importance peaked in the IA (Hrisrova *et al.* 2017; Popov *et al.* 2018).

The importance of *P. miliaceum* varies between sites, representing minor, major, and dominant contributions in the archaeobotanical assemblages at Koprivlen, Kamenska Chuka, and Kush Kaya respectively (Popov *et al.* 2018; Valamoti *et al.* 2019). There is also evidence to suggest that the consumption of *P. miliaceum* varied between sites and individuals, as all individuals from Boyanovo demonstrate ¹³C enrichment, as opposed to only one individual from Benkovski (Gerling 2013). The data from Boyanovo and Benkovski indicate minor ¹³C enrichment, potentially suggesting a relatively low importance of the cereal. However, it is not possible to confirm direct consumption of *P. miliaceum*, as no animal remains have been analysed isotopically. Therefore, further analysis is necessary to determine the nature of *P. miliaceum* exploitation in Bulgaria during the LBA. Furthermore, radiocarbon dating is necessary to attribute ¹³C enrichment to either initial introduction or later adoption of the cereal, as observed patterns may relate to either chronological or cultural differences.

Unfortunately, published reports and analytical studies are scarce for BA Bulgaria and few studies have investigated the role of *P. miliaceum* in this period. Therefore, interpretation of its exploitation is limited. The Romanian archaeological record is equally

as poorly published, preventing an assessment of whether *P. miliaceum* was likely introduced from the north and Ukraine.

The archaeological sites

This section provides brief summaries of the archaeological sites examined in this chapter (Table 22, Figure 60). Relevant characteristics of the sites, including floral and faunal assemblages are highlighted where possible. However, detailed records of excavated materials, and analysis thereof, are severely limited.

Table 22. Summary of Greek and Bulgarian sites and ceramic samples discussed in this chapter.

Country	Period	Sub period	Site / Region	Date	Sherds Sampled
Greece	Neolithic	E-MN	Lete I	6000-5500	15
		LN II	Dikili Tash	4300	16
	Bronze Age	EBA	Archondiko	2130-1877	20
		MBA	Leptokarya-Valtos	1930-1695	4
		LBA	Trimpina	1600-1450	4
			Angelochori	1500-1200	20
			Rema Xydias	1350-1130	10
Pigi Artemidos	1350-1090	2			
Bulgaria	Neolithic (Chalcolithic)	E-MC	Petko Karavelovo		10
		MC	Avren		2
	Bronze Age	EBA	Sokol		6
		LBA	Chokoba	1400-1260	4

Lete I (Central Macedonia, Greece)

Lete I is an E-MN settlement, occupied between 6000 and 5500 BCE, located approximately 10 km north of Thessaloniki, Greece. Lete I is partially overlain by the BA settlement, Lete II, and another E-MN settlement, Lete III, is located around two kilometres away (Dimoula 2017). Lete I is characterised by subterranean dwellings and pit features that are typical of Macedonia during the Neolithic. Dense deposits of artefacts, including ceramics, animal remains, and stone and bone tools were recovered between

dwellings. The ceramic assemblage is primarily comprised of domestic wares, yet exceptional and elaborate vessels exist. Generally, materials and methods of ceramic production indicate a utilitarian function, with multiple vessels formed from similar fabrics. There are strong typo-morphological similarities between ceramics at Lete I and III, indicating a close cultural connection, yet chronological separation of the two settlements is poorly resolved and they may have been occupied either concurrently or consecutively (Dimoula *et al.* 2012).

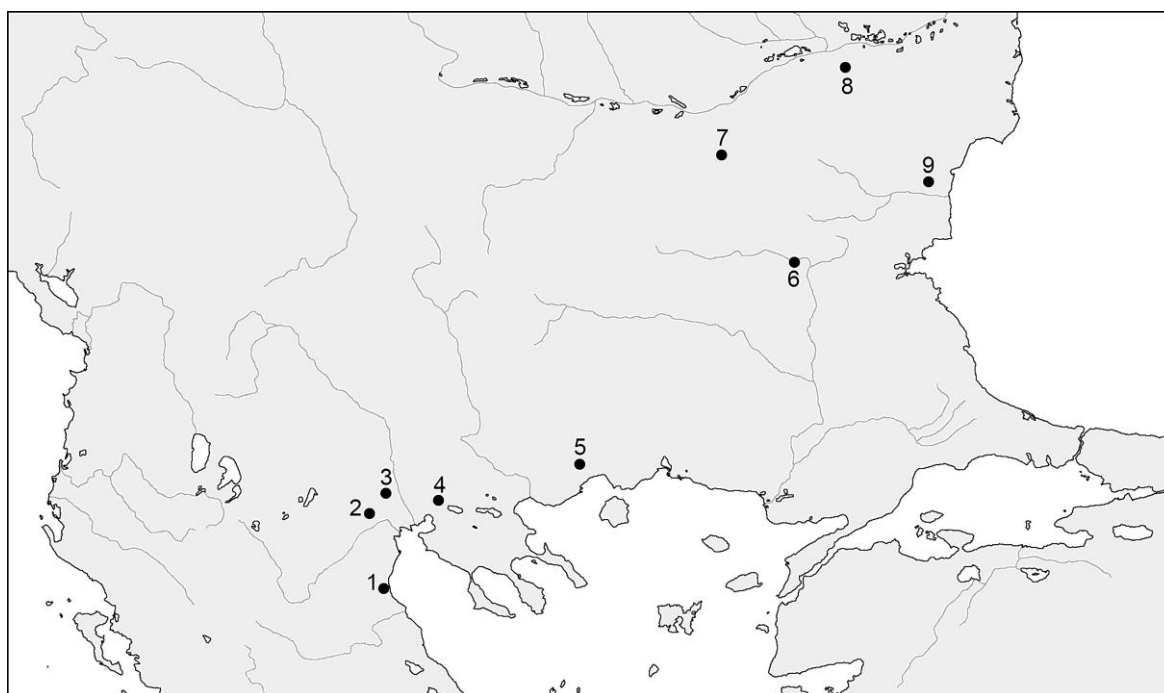


Figure 60. Map of sites examined in this chapter. **1** Olympus sites, **2** Angelochori, **3** Archondiko, **4** Lete I, **5** Dikili Tash, **6** Chokoba, **7** Petko Karavelovo, **8** Sokol, **9** Avren.

Dikili Tash (East Macedonia, Greece)

Dikili Tash is a multiperiod tell site, occupied from the 7th millennium BCE, wherein occupation peaked in the LN and BA (Lespez *et al.* 2013; Tsirtsoni 2016). The tell is located next to a freshwater spring and was previously surrounded by a large lake/swamp area (Lespez *et al.* 2013; Malamidou *et al.* 2018). Material discussed in this chapter was obtained from House 1 in Sector 6 that was destroyed by fire around 4300 cal BCE, corresponding to LNII occupation (Tsirtsoni 2016). The LNII ceramic assemblage includes a variety of storage, processing, serving, and consumption wares. There is no uniformity between house assemblages, potentially demonstrating social differentiation and

individual preference in utility. The assemblage of House 1 is particularly diverse (Tsirtsoni 2016; Urem-Kotsou 2017).

House 1 produced an exceptionally rich and diverse archaeobotanical assemblage incorporating large quantities of wild fruits and nuts, in addition to standard domesticated cereals (Valamoti 2015). Three other houses, also destroyed by fire, contained similarly rich archaeobotanical assemblages (Malamidou *et al.* 2018). The archaeobotanical assemblage of House 1 indicates destruction in either autumn or winter, due to the high abundance of seasonal resources present. Evidence of storage, processing, and preservation indicates that these resources were consumed throughout the year (Valamoti 2015; Garnier and Valamoti 2016). Specifically, the density of grape pips and pressings, preserved during carbonisation, associated with a large coarse ware vessel, wherein tartaric acid was detected, is indicative of large-scale processing of wild grapes, in order to produce juice and potentially wine (Garnier and Valamoti 2016). The exploitation of plant products also extends to Pinaceae *spp.* as resin biomarkers were observed in several samples (Garnier and Valamoti 2016). A single *P. miliaceum* caryopsis was recovered from a Neolithic context at Dikili Tash. However, the presence of BA features near this context likely indicates that the find is intrusive (Valamoti 2016).

Domesticates dominate the zooarchaeological assemblage in the order of pigs, ovicaprids and cattle, with mortality and sex profiles indicate meat production as the primary focus of subsistence. Wild species, including deer, wild boar and aurochs were exploited in relatively low numbers, corresponding to patterns observed at contemporary sites in this region (Jullien 1992; Halstead and Isaakidou 2013). The exploitation of beehive products has been identified in a single sieve type vessel that is relatively common in LNII layers at Dikili Tash (Regert *et al.* 2001).

Archondiko (West Macedonia, Greece)

Archondiko (Archontiko) is a tell settlement occupied in the E-MBA, 2130-1877 cal BCE, and LBA, 1516-1414 cal BCE (Pilali-Papasteriou and Papaefthymiou-Papanthimou 2002; Nitsch *et al.* 2017). The material discussed in this chapter is from EBA occupation phases. The EBA settlement was densely constructed, with households being the basic unit of social organisation and containing storage areas, hearths and platforms indicative of food processing (Petridou 2019). Storage vessels are an important character of the ceramic assemblage, serving wares such as cups and bowls are also present, yet

assessment of the assemblage is ongoing, preventing further discussion (Papaefthymiou-Papanthimou *et al.* 2013). The archaeobotanical assemblage is dominated by wheat and other domesticates, with a lower abundance of wild species, and is typical of the region during this period, except for 40 millet caryopses observed across several EBA floor contexts (Valamoti 2002, 2016; Valamoti *et al.* 2019). There is also potential evidence of specialised cereal processing in the form of bulgur production (Valamoti *et al.* 2019).

Isotopic analysis of faunal remains demonstrates ^{13}C enrichment in collagen from EBA cattle and wild deer, indicating C_4 plant consumption. Environmental landscape studies demonstrate that Archondiko was closer to the coast during the EBA, making the exploitation of wild C_4 plants and ^{13}C enriched environments likely, as similar observations are also made at the Neolithic site of Makriyalos (Nitsch *et al.* 2017; Vaiglova *et al.* 2018). Archondiko was approximately 4 km from the coast and next to a shallow marine/brackish lagoon that developed into a freshwater lake at the beginning of the 2nd millennium BCE (Ghilardi *et al.* 2008; Petridou 2019). The high abundance of shellfish remains at the site demonstrates exploitation of coastal environments. A single EBA human demonstrated no corresponding ^{13}C enrichment (Nitsch *et al.* 2017). However, it is important to note that ^{13}C enriched animals are a minority in the faunal assemblage and it is questionable as to whether estuarine/marsh shellfish would be sufficiently enriched to be distinguished in C_3 environments (Triantaphyllou 2015; Nitsch *et al.* 2017).

Angelochori (West Macedonia, Greece)

Angelochori is a LBA settlement, occupied between 1500-1200 BCE, on the Macedonia Plane (Stefani 2010). The settlement was situated in a swampy area, near a freshwater lake, close to the coast, forming a brackish environment (Pavlopoulos and Kouli 2010). The archaeobotanical assemblage is dominated by wheat, with rare yet consistent barley and millet finds, though preservation is generally poor across the site. One rich and pure deposit of millet, totalling 251 caryopses, potentially indicates the cultivation, harvesting, and processing of cereals separately (Valamoti and Jones 2010). However, mixed deposits are also observed in refuse areas, such as hearths (Valamoti 2016). The faunal assemblage is typical of the period and region, primarily comprising ovicaprids (31%), pigs (23%) and cattle (10%). There is an approximate 70/30 split of domestic to wild species, with deer and boar being dominant (Konstantinidou 2010).

Mortality and sex profiles indicate a meat-oriented subsistence strategy, with little to no exploitation of dairy products (Konstantinidou 2010).

Olympus sites: Valtos-Leptokarya, Trimpina, Pigi Artemidos and Rema Xydias (Northern Greece)

The Olympus sites are situated in the eastern foothills of Mount Olympus, on the western shore of the Thermaic Gulf. They have access to diverse aquatic and terrestrial environments, incorporating freshwater, marine, lowland and upland resources. Archaeobotanical and zooarchaeological analyses are currently in pre-publication phases. Valtos-Leptokarya is a MBA site, occupied between 1930-1695 cal BCE, with both domestic and funerary spaces. Trimpina is a LBA settlement, occupied between 1600-1450 BCE, underlying a Mycenaean cemetery. Pigi Artemidos is a LBA settlement, occupied between 1350-1090, overlying a cemetery. Rema Xydias is a complex LBA settlement, occupied in two phases between 1350-1130 BCE (Dimoula *et al.* 2021).

Mycenaean (southern) influence is common in the ceramic assemblages of the three LBA sites investigated. Three groups of cooking vessel types (A, B and C) are identified across contemporary domestic structures at Rema Xydias and Pigi Artemidos, in addition to early features at Trimpina. Group B is represented at all sites, A is not present at Trimpina, and C is not present at Pigi Artemidos. Rema Xydias produced each type group, although this is potentially a result of increased sampling at the site. Valtos-Leptokarya pre-dates the Mycenaean civilisation and its influence, therefore, it displays no such characteristics in its ceramic assemblage (Dimoula *et al.* 2021).

Petko Karavelovo (North Bulgaria)

Petko Karavelovo is an E-MC tell settlement, on the Yantra River, comprised of complex building architecture that was continually rebuilt and modified, following a series of destruction events. The site has produced a rich assemblage of clay, bone, flint, shell and stone artefacts (Gurova and Chohadzhiev 2019). The abundance of wild species in the faunal assemblage at Petko Karavelovo, and other Bulgarian sites, is greater, around 50%, than is observed at contemporary sites in Northern Greece. Cattle and deer are the dominant domestic and wild species respectively, with ovicaprids and pigs present in an equal abundance, and wild boar a significant contributor to the assemblage (Karastoyanova and Chohadzhiev 2017).

Avren (North East Bulgaria)

Avren-Bobata is a Middle-Late Chalcolithic fortified settlement in the Varna District of NE Bulgaria. Excavations have only recently been undertaken at the site, yet there is evidence of a fortified centre and domestic periphery, house structures and craft areas. Ceramics, stone, bone and metal tools, faunal remains and charred plants have been recovered from the site, yet these have not presently been published (Ivanova and Leshtakov 2016).

Sokol (Central Bulgaria)

Sokol is a tell site, occupied from the Chalcolithic to historic periods, in the Nova Zagora Region of Bulgaria (Semmoto *et al.* 2018). Ceramics analysed in this study are limited to a well stratified EBA1-2 context. The settlement contains domestic structures and craft areas, with evidence for the local production of ceramics (FASTIONLINE 2021). Both utilitarian and fine ware vessels are present in the ceramic assemblage, including the notable observation of a bowl containing the carbonised remains of bread (Leshtakov *et al.* 2016). The archaeobotanical assemblage is dominated by wheat and includes barley, rye and lentils, among other domesticates. These species are observed in varying abundance across contexts, yet wheat generally dominates (FASTIONLINE 2021).

Chokoba (Central Bulgaria)

Chokoba 18a is a flat settlement in Central Bulgaria occupied during the LBA. The site contains several shallow dug-out structures, that are typical of the period, and a varied ceramic typology, including those with Assenovets type handles (Leshtakov 2019).

Sampling and ORA strategy

This study examined organic residues from cooking vessels, with a preference for the sampling of rim sherds. The primary aim of sampling was to obtain around 1 g of ceramic powder for AM extraction, with extra material being obtained, where possible, for solvent extraction. The AM extraction method was favoured due to limited preservation in samples previously analysed in this region (Whelton *et al.* 2018) and the low extraction efficiency of SE. In addition, AM extraction provided the opportunity for compound specific carbon isotope analysis and greater interpretation of residues. Sherds were generally selected from well stratified and securely dated archaeological contexts. However, as sherds were accessed from archaeological stores, museums, and university

collections, with individual sampling constraints, optimal sample collection was not always achievable. Therefore, in total, 40 base, 49 wall, and 39 rim sherds were sampled in this study. The distribution of sherd types is generally even across sites, except for Lete I and Dikili Tash that are predominantly lower-vessel base and mid-vessel wall sherds respectively. Extraction and analytical methods applied to these samples are outlined in Appendix 1. Vessel types sampled are listed in Table 23.

Table 23. Vessel types analysed from Greek and Bulgarian sites studied in this chapter.

Site	Convex bowl	Wide mouthed vessel	Globular vessel	Ovoid jar	Amphora	Pithoid jar	Pyraunos	Large open jar	Wide mouth jar	Biconical bowl	Globular bowl	Hemispherical bowl	Closed pot	Bowl	Small jug	Carinated bowl	Closed high-neck pot
Lete I	9	7															
Dikili Tash			14	1	1												
Archondiko				4	3	13											
Angelochori							16	2	2								
Olympus							4	5	11								
Petko Karavelovo										6	2	1	1				
Sokol				3										2	1		
Avren																1	1
Chokoba				4													

Results and discussion

Lipid recovery rates and yields

Acid methanol extraction produced appreciable lipid yields (> 5 µg g⁻¹) from all but one Greek sample and all Bulgarian samples (Table 24). The lipid recovery rate in this study (> 99%) far exceeds the average recovery rate reported from other Neolithic sites in Northern Greece (approximately 23%, Whelton *et al.* 2018). Increased preservation may reflect the younger age of many of the samples analysed in this study, although contemporary samples from Lete I (E-MN) and Dikili Tash (LN) also produced appreciable lipid yields. Therefore, disparity between these datasets likely relates to either variation in vessel use and preservation conditions between sites or more focused ceramic sample

selection during this study. Despite a substantial difference in recovery rates, average TLE yields from sites investigated in this study are comparable to others in the region (Whelton *et al.* 2018). An increased recovery rate among Bulgarian samples may also reflect preferential preservation conditions in the more northerly region, as seasonal variation in temperature and precipitation are reduced. Indeed, higher average TLE yields from Bulgarian samples potentially support this hypothesis (Table 25). However, as there is no published contemporary material from Bulgaria available for comparison, and the sample size analysed here is small, it is difficult to confidently interpret any difference with Greek datasets. A high proportion of AM extracts from Greek samples, and all Bulgarian samples, produced sufficient yields of palmitic and stearic acid for compound specific carbon isotope analysis (Table 24).

Table 24. Number of samples that produced appreciable lipid yields, by AM and solvent extraction, in addition to number of AM extracts comprising sufficient quantities of palmitic and stearic acid for GC-C-IRMS analysis.

Site / Region	Lipid Yield >5 $\mu\text{g g}^{-1}$		GC-C-IRMS
	AE	SE	
Lete I	15	1 of 7	9
Dikili Tash	16	13 of 16	16
Archondiko	19	0 of 16	18
Angelochori	20	2 of 16	20
Olympus	20	2 of 15	19
Petko Karavelovo	10	0 of 3	10
Avren	2	NA	2
Sokol	6	0 of 2	6
Chokoba	4	0 of 2	4

Solvent extraction was of limited effectiveness at most Greek sites, except for Dikili Tash, and ineffective at all Bulgarian sites, although this is likely influenced by the limited quantity of material available for additional extraction (Table 24). These recovery rates are not unexpected given the low extraction efficiency of solvent extraction (Correa-Ascencio and Evershed 2014).

Table 25. Acid methanol extraction yield and summarised compound specific carbon isotope values of material presented in this chapter.

Site	Mean/Range	TLE Yield $\mu\text{g g}^{-1}$	$\delta^{13}\text{C}_{16:0}$ ‰	$\delta^{13}\text{C}_{18:0}$ ‰
Lete I	M.	24 ± 31	-29.4 ± 1.2	-30.0 ± 0.8
	R.	5 to 133	-30.5 to -27.1	-31.0 to -28.0
Dikili Tash	M.	40 ± 18	-27.8 ± 0.8	-29.3 ± 0.4
	R.	17 to 73	-29.0 to -26.0	-29.8 to -28.2
Archondiko	M.	23 ± 16	-28.1 ± 0.8	-29.0 ± 0.7
	R.	4 to 72	-29.9 to -26.6	-30.1 to -26.9
Angelochori	M.	70 ± 172	-29.4 ± 1.3	-28.5 ± 1.4
	R.	5 to 800	-30.9 to -26.7	-30.8 to -26.3
Olympus Sites	M.	27 ± 17	-27.3 ± 1.4	-28.5 ± 1.4
	R.	12 to 83	-28.9 to -22.1	-31.6 to -21.0
Petko Karavelovo	M.	33 ± 12	-29.7 ± 1.0	-29.1 ± 0.6
	R.	12 to 49	-31.5 to -28.5	-30.3 to -28.2
Avren	M.	20	-29.6 ± 0.3	-29.0 ± 0.3
	R.	20	-29.9 to -29.3	-29.3 to -28.7
Sokol	M.	95 ± 53	-28.0 ± 0.7	-28.5 ± 1.4
	R.	34 to 165	-28.9 to -26.8	-30.5 to -26.7
Chokoba	M.	260 ± 177	-26.3 ± 1.1	-28.8 ± 2.6
	R.	22 to 508	-27.2 to -24.4	-30.7 to -24.4

Contamination

Samples are generally dominated by palmitic and stearic acid, with lesser contributions of unsaturated, branched and dimethyl- fatty acids, cholesterol and phytosterol derivatives, alkanes, and ketones. However, the interpretation of these less abundant compounds, in sherds from Archondiko, Angelochori, and all Bulgarian sites, is complicated by the observation of octocrylene in every sample (Figure 61). Octocrylene is a UVB (Ultraviolet B) absorbing compound and a primary constituent of many modern sunscreens and topical products providing UVB protection (Schakel *et al.* 2004; Baker *et al.* 2016). Surprisingly, neither this nor other sunscreen derived compounds are discussed

in organic residue publications, although several authors have noted the potential for such contamination (Reber 2014; Yates *et al.* 2015). The occurrence of octocrylene only at these sites may relate to specific post-excavation cleaning processes that were not conducted elsewhere. For instance, it is common in Greece for sherd cleaning to be a communal process, conducted outdoors during the summer, with site members sat round a large bowl of water. The solubility of octocrylene is well attested in marine environments (Amine *et al.* 2012; Gago-Ferrero *et al.* 2013), and it is easy to envisage large quantities of sunscreen contaminating waters, and all sherds, as hands are repeatedly dipped in during the cleaning process. It is important to consider that the preference for conducting excavations during the summer, in addition to environmental conditions around the Mediterranean and adjoining regions, increases the probability of sunscreens being worn by most excavation team members. Therefore, the likelihood of contamination from these products is extremely high. As such, it is perplexing that sunscreen contamination has not previously been reported and discussed in ORA publications.

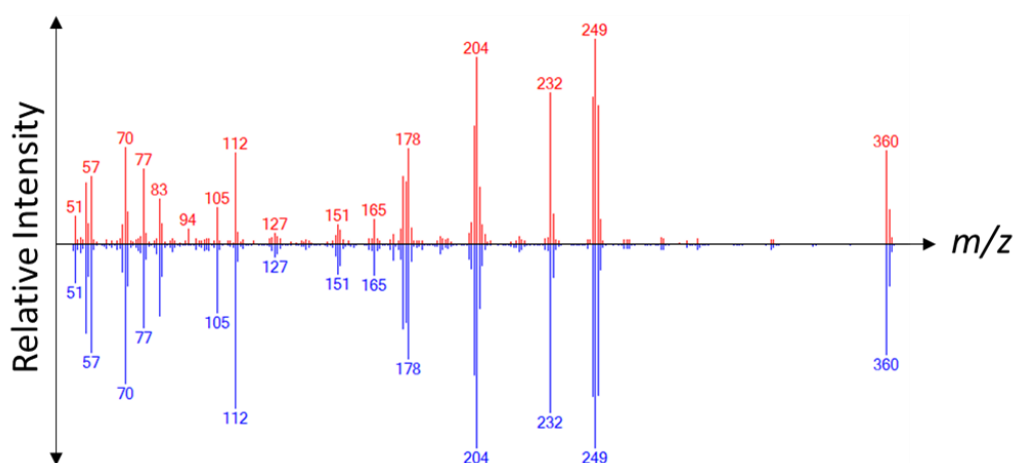


Figure 61. Mass spectra comparison between compound identified as octocrylene in archaeological samples (top) and octocrylene in the NIST 17 MSD (bottom).

It is important to note that sunscreens may comprise a variety of active ingredients that provide UV protection, including both chemical and mineral compounds, in addition to inactive ingredients that increase protection and aid application (Wahie *et al.* 2007). One wonders whether active components of chemical sunscreens, e.g.

octocrylene, are routinely and extensively searched for and identified in archaeological material, as they have not been discussed in previous ORA studies. The extent of sunscreen contamination in this region is presently unknown but is presumed to be high. Increased awareness of the negative effects that chemical sunscreens have on the environment has resulted in increased use of mineral sunscreens (Amine et al. 2012; Gago-Ferrero *et al.* 2013). These products are less likely to be identified as contaminants in archaeological residues, as their distinctive active components (e.g. TiO₂ and ZnO) are not amenable to detection by GC-MS. Therefore, the absence of distinctive chemical components of sunscreens should not be presumed to discount contamination of archaeological materials, especially in regions such as the Mediterranean.

Inactive ingredients in topical products may include alkyl compounds, fatty acids, and corn starch. Natural additives, e.g. beeswax, may also be present for fragrance and colour. Therefore, it is difficult to confidently attribute the presence of these compounds to past activity. As such, molecular evidence presented in this study is done so only when compounds are presumed unlikely to derive from contamination. It is important to note that neither miliacin nor other compounds derived from millets are understood to be used in the production of sunscreens and other topical products.

A more complex issue is the effect that fatty acid contamination may have on compound specific $\delta^{13}\text{C}$ values. Palmitic acid is a known component of some sunscreens and stearic acid may be present as a substituent of other compounds, e.g. benzophenone-3 (Luppi *et al.* 2004). While these compounds are perhaps minor constituents of sunscreens, and additional research is necessary to demonstrate whether fatty acid substituents are released during extraction, there is no method of quantifying the extent of their contamination in archaeological residues. The $\delta^{13}\text{C}$ value of these modern compounds is presently unknown. As such, $\delta^{13}\text{C}$ values of samples that contain octocrylene are treated with caution and subject to revision pending future experiments assessing the impact of sunscreen contamination on ceramic-absorbed residues.

Presently, the only method of approximately understanding the extent of sunscreen contamination in organic residues is via the abundance of octocrylene. However, the relative concentration of octocrylene in sunscreens would influence the extent of contamination by other constituents. Furthermore, the lipophilic nature of octocrylene could overemphasise the extent of contamination in lipid-rich ceramic

fabrics. Therefore, it is imperative that future researchers conduct experiments that attempt to understand the nature of sunscreen contamination in ceramic-absorbed residues, whether this may be avoided, and if there are methods to quantify and account for contamination. It is evident that contaminants penetrate beyond the surface layer of the ceramic fabric, which is removed during sampling (Appendix 1), and that contamination by modern topical products should be of greater concern to archaeologists studying organic residues.

All Bulgarian samples contained octocrylene, comprising on average 0.7% of TLEs, ranging between 0.1 - 1.8%, perhaps suggesting low level contamination. However, molecular and isotopic data from these samples is treated with caution. Octocrylene contamination in samples from Archondiko and Angelochori are discussed and considered in the context of results from each site. Tables detailing the compounds identified in all samples are presented in Appendix 4.

Lete I

Ceramics from Lete I produced lipids in greater frequency and marginally greater abundance than material from Lete III (Whelton *et al.* 2018), potentially demonstrating more widespread and utilitarian vessel use at Lete I. Compound specific isotope analysis demonstrates predominantly ^{13}C depleted sources of carbon. Indeed, most samples plot within the range of C_3 plants, producing relatively high, non-ruminant, $\Delta^{13}\text{C}$ values (Figure 62). A plant contribution is further supported by the observation of 16-hentriacontanone in 10/16 samples, that in most instances corresponds to lower $\delta^{13}\text{C}$ values. However, low P/S (average 1.14) values suggest mixed product processing, most likely of plants and domestic ruminant adipose given the distribution of compound specific isotope values. One sample produced a $\Delta^{13}\text{C}$ value of -2.6‰ that may relate to processing either domestic/wild ruminant adipose or perhaps a combination of products including dairy, as this value is within the maximum range of dairy products. These results correspond well to those observed at Lete III, where ruminant adipose and a single dairy residue were observed from the analysis of seven vessels (Figure 62, Whelton *et al.* 2018). However, the results from Lete I potentially demonstrate a greater importance of plant products to this community.

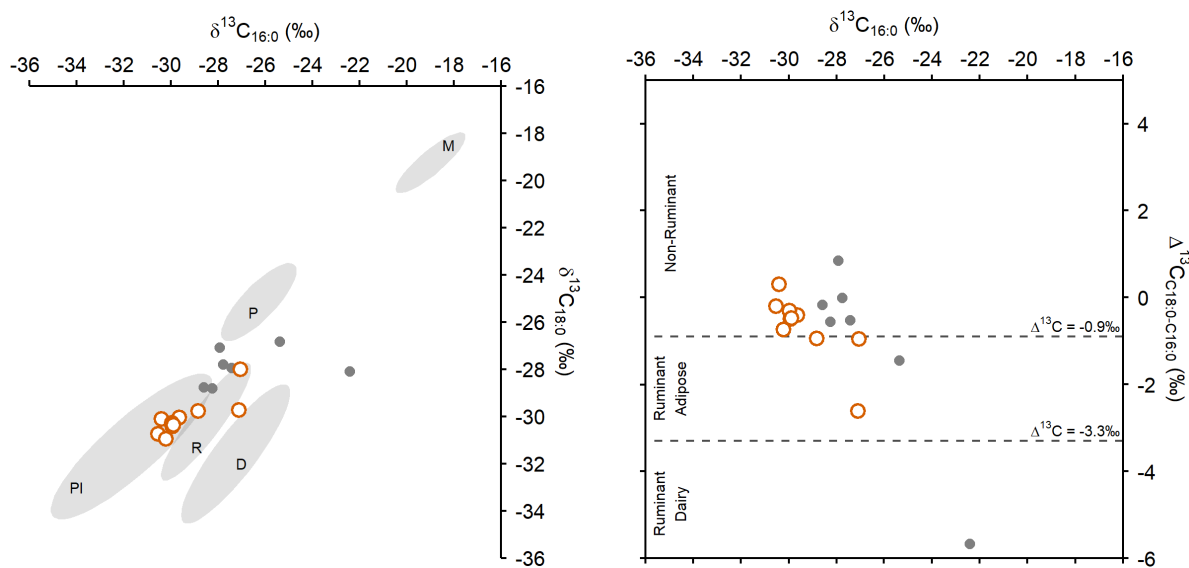


Figure 62. Compound specific carbon isotope data from Lete I (orange circles) and Lete III (grey dots, Whelton *et al.* 2018). **Left:** Plot of $\delta^{13}\text{C}_{16:0}$ and $\delta^{13}\text{C}_{18:0}$ values against reference ellipses (1σ) of modern-carbon corrected foodstuffs. **D** = dairy, **P** = porcine, **PI** = C3 plant, **R** = domesticated ruminant adipose, **M** = *P. miliaceum*. Reference data is presented in Appendix 5. **Right:** Plot of $\delta^{13}\text{C}_{16:0}$ and $\Delta^{13}\text{C}$ ($\delta^{13}\text{C}_{18:0} - \delta^{13}\text{C}_{16:0}$) values.

Dikili Tash

The preservation of lipids at Dikili Tash is high, relative to other Neolithic sites in Greece (Whelton *et al.* 2018), with samples producing increased yields and comprising an extended range of unsaturated fatty acids ($\text{C}_{20:1}$, $\text{C}_{24:1}$, and $\text{C}_{20:2}$) over Lete I. Indeed, SE was exceptionally effective at Dikili Tash in terms of recovery rate and TLE yield, yet interpretation of SEs is limited, as only degraded fats (FFAs and cholesterol derivatives) were observed. The presence of unsaturated LCFAs in several samples may indicate aquatic product processing, potentially of freshwater resources near the site, yet neither APAAs nor isoprenoid fatty acids were observed in any sample. Therefore, these unsaturated LCFAs may also derive from plant products. Pinaceae resin markers, methyl dehydroabietate acid and 7-oxodehydroabietic acid, have been identified in ceramics from Dikili Tash previously (Garnier and Valamoti 2016) and were observed in many of the samples analysed in this study, potentially demonstrating resin exploitation. However, the low abundance of these compounds and absence of retene suggest that contamination by either woodsmoke or the burial environment is a more probable source. No compounds related to beeswax were observed in any of the samples analysed, suggesting that beehive products were either not widely exploited or restricted to the

perforated vessel type analysed previously (Regert *et al.* 2001), as this vessel type was not sampled in the present study.

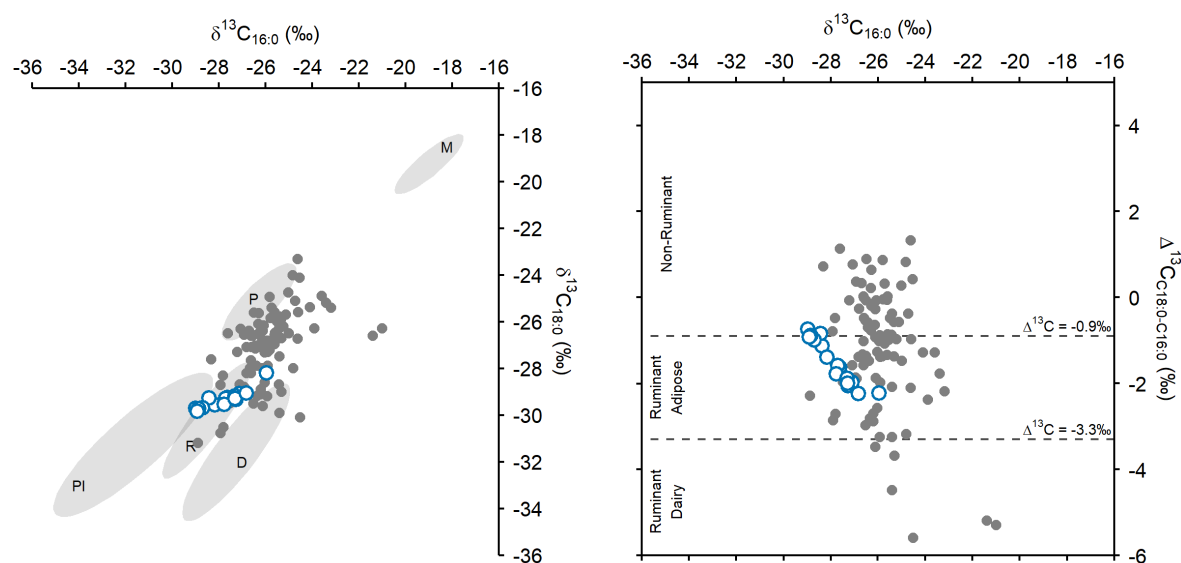


Figure 63. Compound specific carbon isotope data from Dikili Tash (blue circles) and Neolithic sites in Northern Greece (grey dots, Whelton *et al.* 2018). **Left:** Plot of $\delta^{13}\text{C}_{16:0}$ and $\delta^{13}\text{C}_{18:0}$ values against reference ellipses (1 σ) of modern-carbon corrected foodstuffs. **D** = dairy, **P** = porcine, **PI** = C3 plant, **R** = domesticated ruminant adipose, **M** = *P. miliaceum*. Reference data is presented in Appendix 5. **Right:** Plot of $\delta^{13}\text{C}_{16:0}$ and $\Delta^{13}\text{C}$ ($\delta^{13}\text{C}_{18:0} - \delta^{13}\text{C}_{16:0}$) values.

Compound specific isotope analysis indicates a ^{13}C depleted carbon source of these residues. Most samples plot within the reference range of domestic ruminant adipose fats, although $\Delta^{13}\text{C}$ values of several samples also indicate mixtures of ruminant adipose and non-ruminant products (Figure 63). A significant strong correlation between $\Delta^{13}\text{C}$ and P/S values ($r(14) = .850$, $p < .001$) potentially demonstrates a proportional contribution of plant resources to residues, as plants contain a high abundance of ^{13}C depleted $\text{C}_{16:0}$, relative to $\text{C}_{18:0}$. Therefore, a greater contribution of plant products would simultaneously increase the palmitic acid contribution and lower $\delta^{13}\text{C}_{16:0}$ values. Unfortunately, no C_{18} APAAs were present in samples from Dikili Tash, which may have provided additional evidence for the processing of plant products. There is no evidence to suggest that porcine products were processed in the ceramic vessels analysed in this study, despite the abundance of porcine remains in the zooarchaeological assemblage and the prevalence of porcine product processing in the region during the Neolithic

(Whelton *et al.* 2018). This may indicate that porcine products were not processed in either the vessel types analysed or ceramics in general, i.e. aceramic processing.

Archondiko

The average TLE yield of samples from Archondiko is not especially high but is comparable to contemporary sites (Whelton *et al.* 2018). On average, TLEs contain 1.7% octocrylene, ranging between 0.3 - 3.6%, potentially demonstrating low level modern contamination. Many samples contain a low abundance of compounds that may be associated with plant product processing, such as unsaturated fatty acids, 16-hentriacontane, and long chain alkanes, yet these cannot be reliably distinguished from potential contaminants. Sample Ar 14 contains a high abundance of plasticisers and long chain alkanes, indicating contamination from post excavation processes (Figure 64).

Either the processing or use of Pinaceae resin products at Archondiko is likely demonstrated by the observation of retene, methyl dehydroabietate, and 7-oxodehydroabietic acid, at a high abundance, in sample Ar 18. However, additional evidence is necessary to support deliberate production of resinous products, as recent research has demonstrated that a high abundance of these compounds may be transferred to ceramics during firing (Reber *et al.* 2019).

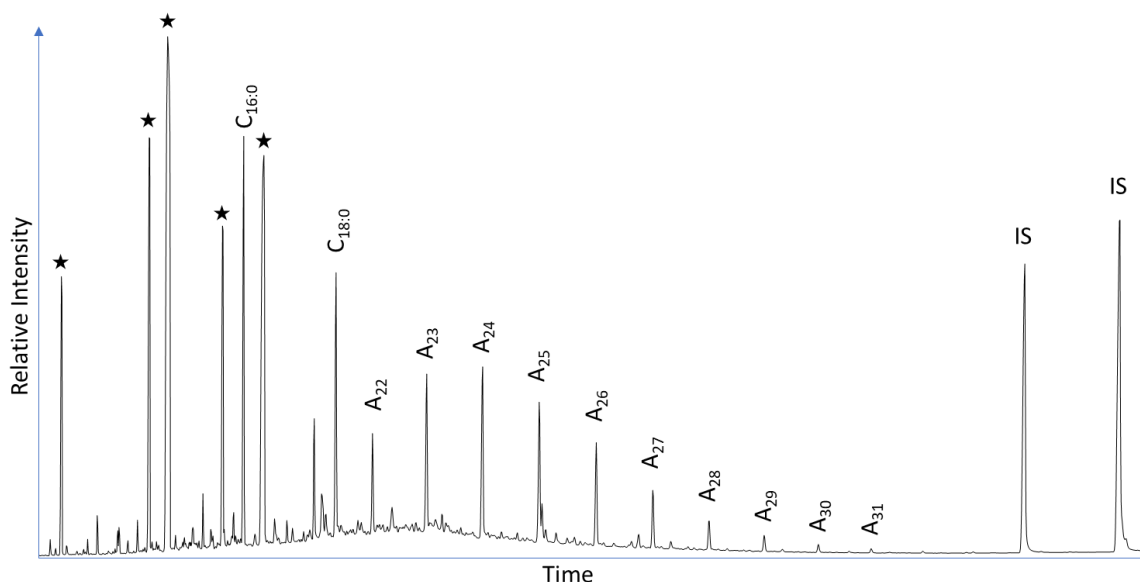


Figure 64. Partial TIC of Ar 14 demonstrating high long chain alkane abundance and plasticiser contamination (★).

A low yet substantial abundance of miliacin (0.5% of the TLE, including all three isomers) was observed in the ceramic-absorbed residue of one pithoid jar sherd (Ar 16) from Archondiko (Figure 65). The sherd is a lower base fragment of a pithoid jar type dating to around 2000 BCE, corresponding to the end of the EBA and transition to the MBA. A substantial number of individual *P. miliaceum* caryopses are observed across floor levels at Archondiko, yet their origin is questionable due to overlying LBA activity (Valamoti 2016). Indeed, current radiocarbon dating programmes indicate that *P. miliaceum* was introduced to Europe in the 16th century BCE (Motuzaite-Matuzeviciute *et al.*, 2013; Filipović *et al.*, 2020). However, the observation of miliacin in a confidently dated and secure ceramic sherd from Archondiko challenges both the direction and timing of the current translocation chronology of *P. miliaceum*.

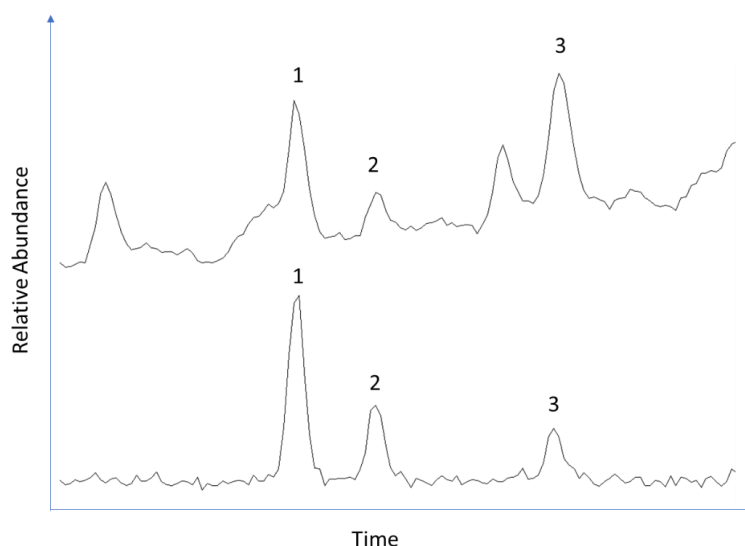


Figure 65. Partial TIC (top) and *m/z* 189 EIC (bottom) of Ar 16, demonstrating the three distinct AM alteration products of miliacin. **1** δ -Amyrin ME, **2** Miliacin, **3** β -Amyrin ME.

The only known miliacin producing species present in Greece, during prehistory, are *P. miliaceum* and *D. sanguinalis* (Valamoti 2016; Kotzamani and Livarda 2018). However, there is no evidence to suggest that either *D. sanguinalis* or any unknown miliacin-producing plant were either harvested, processed, or consumed, in a sufficient quantity that would result in the observation of miliacin in ceramic-absorbed residues. If such species were processed, evidence would surely be present in either archaeobotanical, molecular, or isotopic analysis previously conducted in Greece.

Isomerisation of either β -Amyrin ME or δ -Amyrin ME, derived from another plant source, could also result in the observation of miliacin in Ar 16. However, as these isomers have not been identified in previously analysed residues, examined in this study and other research, it is perhaps unlikely that such alternate products either exist or were processed in this region and period. Therefore, it may be tentatively concluded that miliacin in Ar 16 is derived from the processing of *P. miliaceum*, representing the earliest evidence for the cereal in Europe.

Compound specific $\delta^{13}\text{C}$ values of samples from Archondiko indicate a predominantly ^{13}C depleted carbon source (Figure 66), with no significant difference in the range of $\delta^{13}\text{C}$ values from Lete I and Dikili Tash (paired t-test, $t = 1.5986$, $df = 17$, $p = .1283$). This data corresponds to a low prevalence of *P. miliaceum* in the archaeobotanical assemblage and previous isotopic studies conducted at Archondiko (Nitsch *et al.* 2017). Furthermore, experimental observations (Chapter 5) and archaeological analysis (Chapter 6) indicate that there is little correspondence between miliacin abundance and increased $\delta^{13}\text{C}$ values. In addition, this data, in conjunction with an absence of aquatic biomarkers, demonstrates that marine resources were processed either infrequently in these vessels, in other vessels, or not in vessels at all during the EBA. This is despite the close proximity of Archondiko to the coast and increasing trend of marine resource exploitation during the BA. However, this observation is in agreement with limited human isotope data that suggests marine resources were infrequently consumed at Archondiko (Nitsch *et al.* 2017).

Comparison of ceramic-absorbed residues from Archondiko to modern reference materials indicate that they are primarily formed from ruminant adipose and C_3 plant lipids (Figure 66), with $\Delta^{13}\text{C}$ values around -0.9‰ indicating the mixing of both products. A contribution of lipids from wild ruminants is perhaps likely, given that these species are common in the zooarchaeological assemblage and several samples produced relatively low $\Delta^{13}\text{C}$ values (Craig *et al.* 2012). However, low $\Delta^{13}\text{C}$ values may also relate to the mixing of C_4 plant and C_3 -fed ruminant adipose fats, as is demonstrated by a theoretical mixing model of these products (Figure 67). As the persistence and preservation of miliacin is not presently understood, it is possible that other samples from Archondiko, which demonstrate no ^{13}C enrichment and have low $\Delta^{13}\text{C}$ values, may also comprise a mixture of C_4 plant and C_3 -fed ruminant adipose lipids.

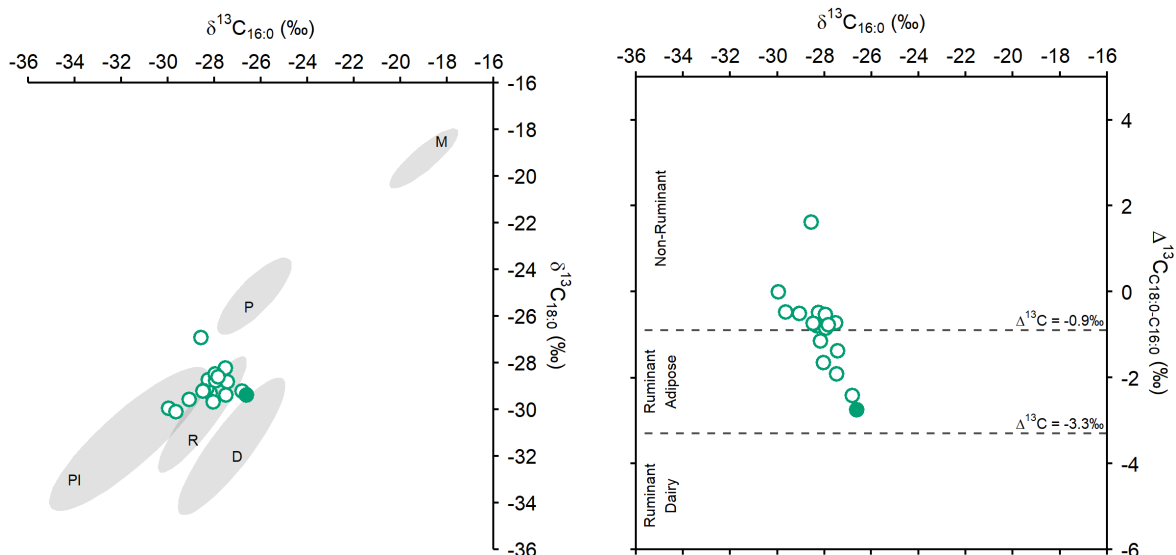


Figure 66. Compound specific carbon isotope data from Archondiko. Filled circle represents sample Ar 16 that contains miliacin. **Left:** Plot of $\delta^{13}\text{C}_{16:0}$ and $\delta^{13}\text{C}_{18:0}$ values against reference ellipses (1σ) of modern-carbon corrected foodstuffs. **D** = dairy, **P** = porcine, **PI** = C₃ plant, **R** = domesticated ruminant adipose, **M** = *P. miliaceum*. Reference data is presented in Appendix 5. **Right:** Plot of $\delta^{13}\text{C}_{16:0}$ and $\Delta^{13}\text{C}$ ($\delta^{13}\text{C}_{18:0} - \delta^{13}\text{C}_{16:0}$) values.

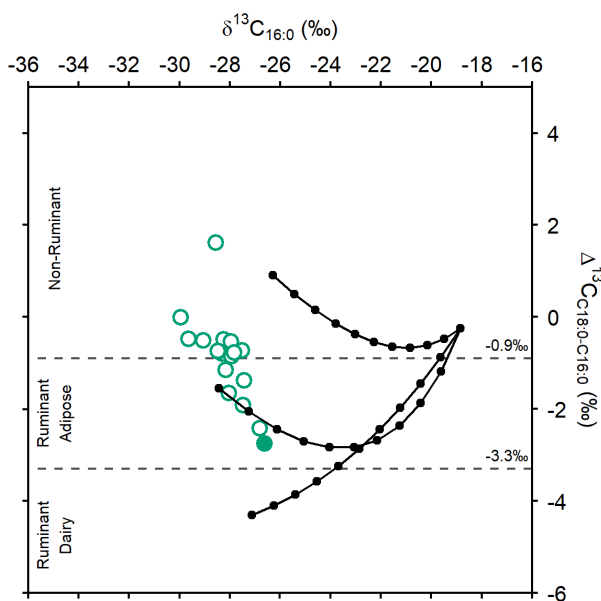


Figure 67. Plot of $\delta^{13}\text{C}_{16:0}$ and $\Delta^{13}\text{C}$ ($\delta^{13}\text{C}_{18:0} - \delta^{13}\text{C}_{16:0}$) values of samples from Archondiko against theoretical mixing lines of modern-carbon corrected foodstuffs, at 10% increments, including *P. miliaceum* mixed with C₃-fed porcine, domesticated ruminant adipose, and dairy products. Filled circle represents sample Ar 16 that contains miliacin. Reference and mixing model data are presented in Appendix 5.

There is little evidence for a contribution of dairy lipids to the residues analysed, although Ar 16 does plot near the reference range of dairy products and a mixture of C₄ plant and C₃-derived dairy products could result in elevated $\Delta^{13}\text{C}$ values that are not indicative of a dairy contribution (Figure 67). However, there is no evidence to suggest that C₄ plant products were processed on such a scale as to influence isotopic results in this way. One sample (Ar 14) plots above the 1 σ range of plant products, towards the porcine product range. This residue may be derived from either a C₃ plant and porcine mixture or a particularly ¹³C enriched C₃ plant. However, as discussed previously, a high abundance of contaminants in this sample prevents accurate characterisation of these results (Figure 64).

There is an interesting potential difference observed between samples from different house contexts at Archondiko (Figure 68). There is a significant difference in the $\delta^{13}\text{C}_{16:0}$ and $\Delta^{13}\text{C}$ values of samples from House E and ΣT (paired t-test, $t = 4.8724$, $df = 6$, $p = .0028$ and $t = 3.2708$, $df = 6$, $p = .017$ respectively). Ceramic absorbed residues from House E comprise non-ruminant products, with a greater proportion of C₃ plant lipids and potentially a contribution of porcine lipids. However, several samples from House ΣT demonstrate significantly lower $\delta^{13}\text{C}_{16:0}$ and $\Delta^{13}\text{C}$ values that may relate to the processing of mixtures comprising either C₃ plants and ruminant meat or ruminant meat with C₄ plants. These differences are not related to vessel type, potentially indicating a household specific cultural element in culinary activities. Indeed, the production, control, and consumption of foodstuffs becomes increasingly hierarchical between the Neolithic and BA in Greece, with household units becoming more distinct (Halstead 2012). Nonetheless, TLE yields of amphora and ovoid jars are significantly different to pithoid jars (paired t-test, $t = 3.9442$, $df = 8$, $p = .0043$), with the latter vessel type generally containing low yields, potentially indicating the use of different vessels for specific activities among all households in this community. However, further analysis at Archondiko is necessary to examine whether this data and interpretation is either a reliable or accurate reflection of differences in culinary activities between households.

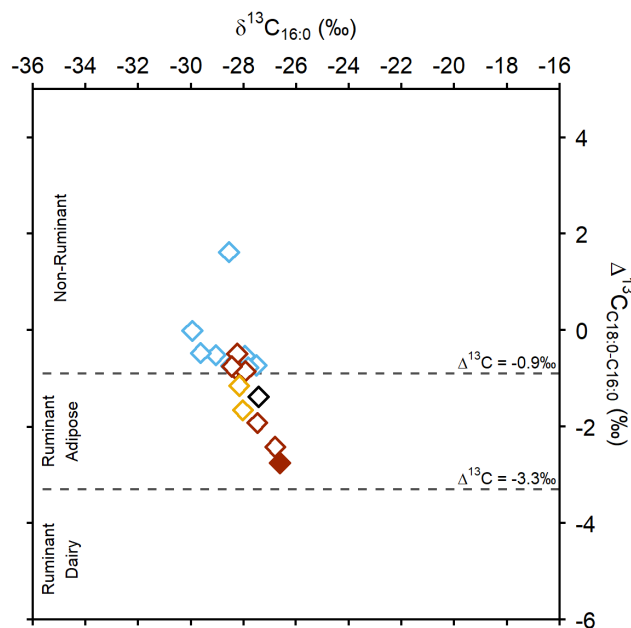


Figure 68. Plot of $\delta^{13}\text{C}_{16:0}$ and $\Delta^{13}\text{C}$ ($\delta^{13}\text{C}_{18:0} - \delta^{13}\text{C}_{16:0}$) values of samples from Archondiko highlighting the difference between houses. **Yellow** = House B, **Blue** = House E, **Black** = House Z, and **Red** = House ΣT .

Angelochori

The recovery rate and average TLE yield of ceramic-absorbed residues from Angelochori are comparable to other sites in the region (Table 24 and 25). On average, TLEs contain 0.3% octocrylene, ranging between 0.05 - 0.87%, demonstrating substantially lower contamination than is observed at Archondiko and Bulgarian sites. There are no distinct compounds that are ubiquitous in this dataset that would suggest contamination from a common source. Therefore, exceptional preservation observed in Ang 1 and Ang 14, which comprise acyl lipids and wax esters, is likely derived from the initial contents of the vessel (Figure 69, 70 and 71). A high abundance of LCFAs, LC alkanes and C_{40-48} palmitic wax esters in samples Ang 1, 2 and 8 (Figure 70 and 71), likely demonstrates either the processing of beehive products in vessels or application of beeswax to vessels as a sealant (Regert *et al.* 2001). Interestingly, Ang 14 does not contain compounds related to beehive products yet produced the highest yield of all samples ($800 \mu\text{g g}^{-1}$), suggesting either the processing or storage of a lipid rich product(s), potentially over a long period.

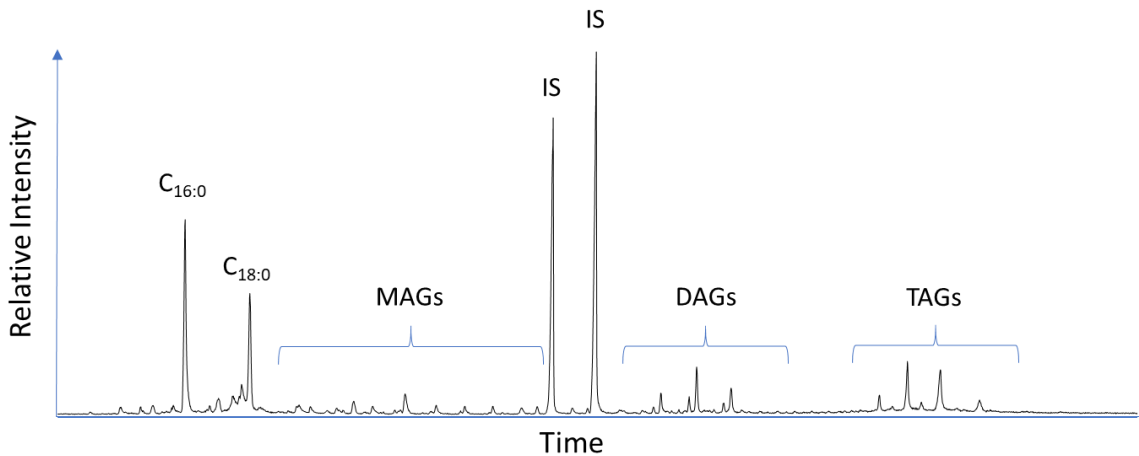


Figure 69. Partial TIC of Ang 14 SE demonstrating the extent of lipid preservation.

A low abundance of miliacin was observed in seven of twenty ceramic-absorbed residues analysed, potentially indicating substantial processing of *P. miliaceum* in ceramic vessels at Angellochori. While the abundance of *P. miliaceum* caryopses in the archaeobotanical assemblage does not indicate substantial use of the cereal, it is important to note that archaeobotanical assemblages are not necessarily an accurate representation of subsistence and culinary practices, due to various biases in the formation and preservation of macro remains. However, experimental research is also necessary to demonstrate the persistence of miliacin, in ceramic-absorbed residues, following additional cooking events with different products, as molecular data may overemphasise the use of *P. miliaceum* in culinary contexts.

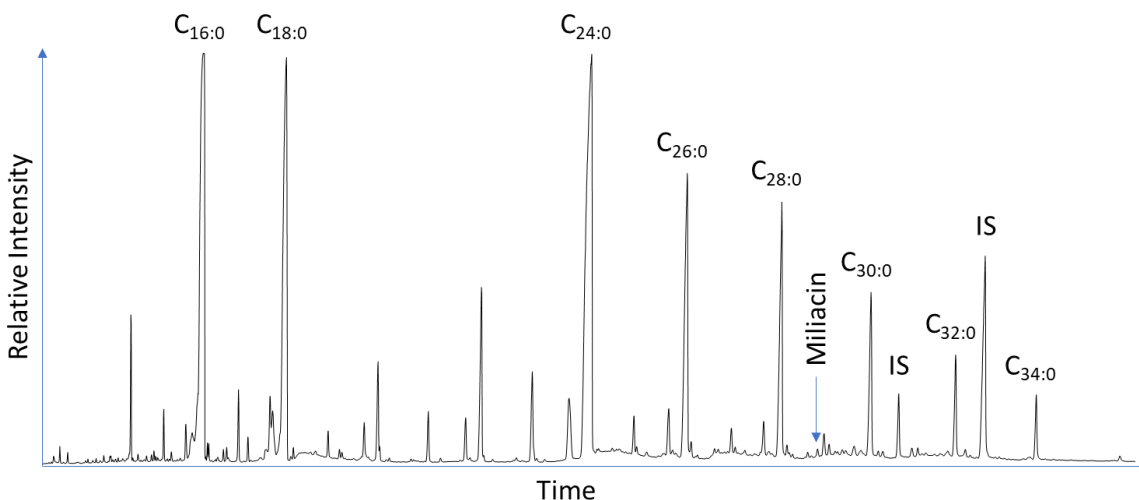


Figure 70. Partial TIC of Ang 1 AE highlighting abundant long chain fatty acids, indicative of beeswax and miliacin.

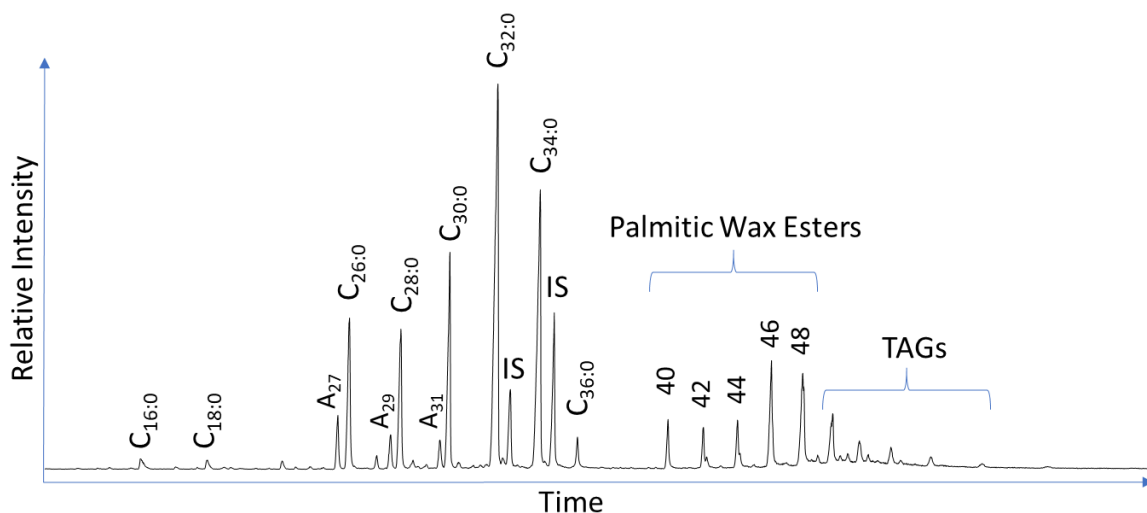


Figure 71. Partial TIC of Ang 1 SE highlighting the presence of compounds derived from beeswax.

Miliacin is observed with compounds derived from plant and animal products, including 16-hentriacontanone and palmitic wax esters, indicating either sequential or concurrent processing of *P. miliaceum* and other products in multi-use vessels (Figure 70 and 71). Indeed, compound specific carbon isotope data indicates that residues containing miliacin are primarily formed from C₃ plant lipids and, to a lesser extent, ruminant and non-ruminant adipose, and potentially dairy lipids (Figure 72). This data suggests that *P. miliaceum* was processed as a staple product, as LBA archaeobotanical records indicate, in utilitarian vessel types, which may indicate limited significance of the cereal in cultural, e.g. religious and ceremonial, activities.

Ceramic-absorbed residues from Angelochori primarily plot within the reference range of C₃ plants and produce $\Delta^{13}\text{C}$ values indicative of non-ruminant, i.e. plant, products (Figure 72). However, miliacin is observed in four of these samples, demonstrating a contribution of ¹³C enriched lipids. Failure to recognise a contribution of lipids from *P. miliaceum* was demonstrated at Bruszczewo (Chapter 6) and may relate to limited absorption of lipids when processing this cereal (Chapter 5). In addition, other factors, such as the type and order of product mixing, may also contribute to *P. miliaceum* lipids being overwhelmed. Therefore, this data does not necessarily demonstrate that *P. miliaceum* was a minor component of subsistence.

Several samples from Angelochori plot within the reference ranges of both C₃ plant and C₃-fed ruminant adipose lipids, producing intermediate $\Delta^{13}\text{C}$ values around -

0.9‰, potentially demonstrating either concurrent or sequential mixing of these products. In addition, three samples demonstrate ^{13}C enrichment that is likely derived from C_3 plants and porcine products processed in the same vessel. Miliacin is observed in one of these samples, yet the samples produced an extremely high TLE yield ($800 \mu\text{g g}^{-1}$) and low P/S value (0.65), likely indicating that the residue is primarily formed from porcine lipids.

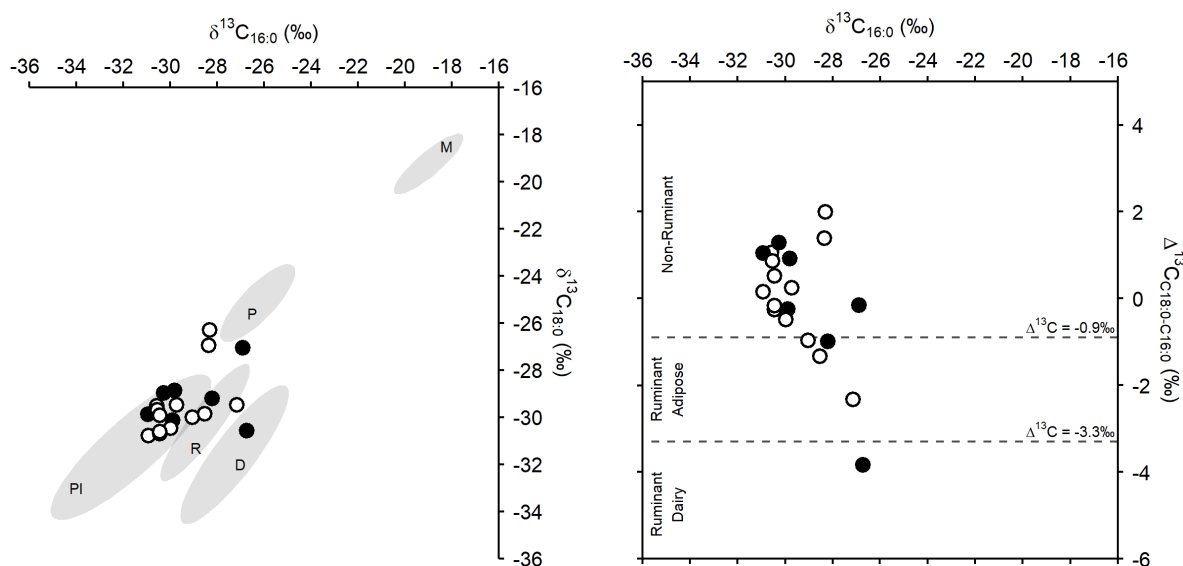


Figure 72. Compound specific carbon isotope data from Angelochori. Filled circles represent samples that contain miliacin. **Left:** $\delta^{13}\text{C}_{16:0}$ and $\delta^{13}\text{C}_{18:0}$ values plotted against 1σ reference ellipses of modern-carbon corrected foodstuffs. **P** = porcine, **PI** = C_3 plants, **R** = domestic ruminant adipose, **D** = dairy and **M** = *P. miliaceum*. **Right:** $\delta^{13}\text{C}_{16:0}$ and $\Delta^{13}\text{C}$ ($\delta^{13}\text{C}_{18:0} - \delta^{13}\text{C}_{16:0}$) values. Reference data is presented in Appendix 5.

One ceramic-absorbed residue, Ang 1, produced a $\Delta^{13}\text{C}$ value of -3.8‰ and plots within the reference range of wild ruminant adipose and dairy lipids (Craig *et al.* 2012). However, a contribution of lipids from dairy products is unlikely, given that dairying is not well attested at the site and the sample contains miliacin and palmitic wax esters. Palmitic wax esters and *P. miliaceum* contribute ^{13}C enriched $\text{C}_{16:0}$ to the residue, relative to $\text{C}_{18:0}$ from other sources, lowering the $\Delta^{13}\text{C}$ value of this sample. Therefore, this residue is likely derived from either wild or even domesticated ruminant adipose products.

There is evidence to propose that *P. miliaceum* may have been restricted socially at Angelochori. Six of fourteen samples from the interior of House A contain miliacin, whereas none ($n = 3$) from the interior of House D contain miliacin (Figure 73). One of four

samples from the exterior of these houses, found closest to House D, also contained miliacin, yet the spatial organisation of these samples requires refinement before being attributed to either structure. While the sample size for House D is small and requires additional analysis, it may be hypothesised that the occupants of House D did not consume *P. miliaceum*, but the occupants of House A did. One may question how and why certain members of the Angelochori community either controlled, were restricted to, or excluded from, its consumption. This may relate to the motives for *P. miliaceum* introduction to the site and region, yet it is important to consider that if the species was introduced during the EBA, as has been eluded to at Archondiko, a more complex social and cultural framework, lasting half a millennia, must be explored. The present sample size, specifically of House D, is small and additional analysis is necessary to investigate this observation in greater detail across all houses. Furthermore, greater integration of this data with archaeological characteristics associated with status and subsistence, in the LBA, is required to attribute the consumption of *P. miliaceum* to social factors. Nevertheless, this data potentially poses interesting questions as to the nature of *P. miliaceum* introduction, adoption, and use in the second millennium BCE.

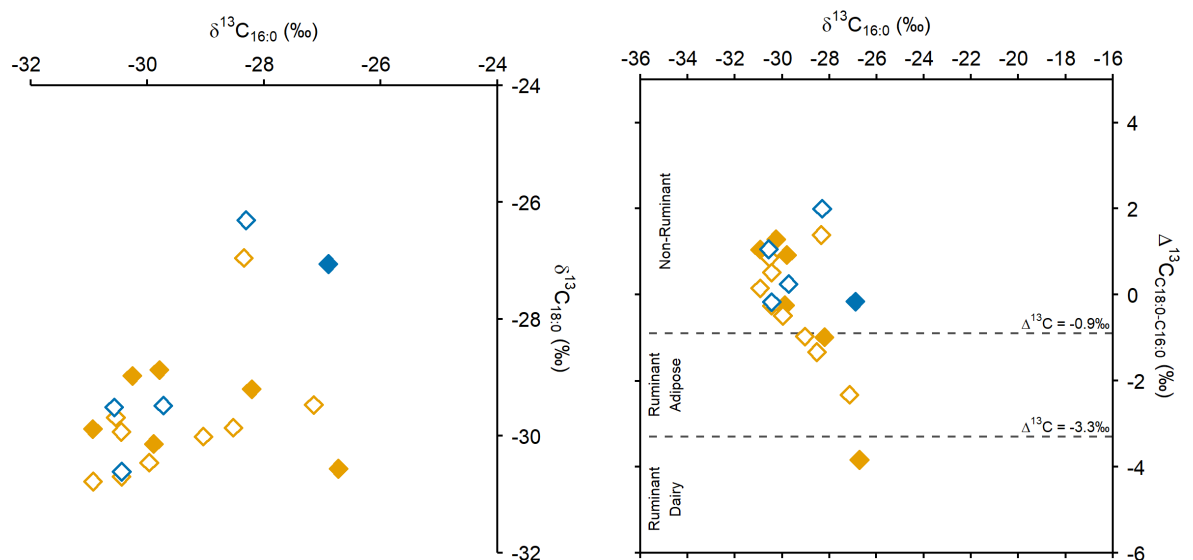


Figure 73. Compound specific isotope data from Angelochori highlighting difference between houses. **Yellow** = House A and **Blue** = House D. Filled diamonds contain miliacin. **Left:** $\delta^{13}\text{C}_{16:0}$ and $\delta^{13}\text{C}_{18:0}$ values. **Right:** $\delta^{13}\text{C}_{16:0}$ and $\Delta^{13}\text{C}$ ($\delta^{13}\text{C}_{18:0} - \delta^{13}\text{C}_{16:0}$) values.

Statistical analysis cannot be used to accurately determine a difference between the $\delta^{13}\text{C}_{16:0}$ and $\delta^{13}\text{C}_{18:0}$ values of samples, from House A and D, as the sample size is too small. However, plotting this data clearly demonstrates that ceramic-absorbed residues from sherds in (n= 14) and around (n= 1) House A are derived from ruminant adipose and non-ruminant products, whereas residues from sherds in (n= 3) and around (n= 2) House D are primarily derived from non-ruminant products (Figure 73). Three samples containing beeswax all originate from House A, potentially negatively impacting the observed difference in $\Delta^{13}\text{C}$ values, although not to the extent of removing the processing of ruminant adipose products from contention, as the abundance of palmitic wax esters in the solvent extracts, and LC alkanes in the AM extracts, indicate a low abundance of beeswax, relative to other compounds present in the residues. Therefore, a difference in the presence of miliacin and palmitic wax esters, in addition to $\delta^{13}\text{C}$ values, provides compelling evidence to propose a potential difference in culinary activities, and perhaps subsistence strategies, between House A and D. This observation is perhaps indicative of increased household autonomy during the BA, as was outlined previously for Archondiko (Halstead 2012). However, as with the Archondiko dataset, additional sampling is necessary to assess the accuracy and reliability of any perceived pattern in culinary activities between households.

Miliacin was exclusively identified in pyraunos vessels from Angelochori. This vessel type (Figure 74) has been tentatively associated with the adoption of *P. miliaceum*, during the LBA, in Greece. This association has not previously been extensively explored and is dependent on both the vessel and cereal having been introduced at the same time. However, co-introduction is not supported by EBA evidence for *P. miliaceum* from Archondiko, presented in this study, and Skala Sotiros (Valamoti 2016). Greater emphasis is not placed on the exclusive observation of miliacin in pyraunos vessels, from Angelochori, for two reasons. Firstly, 16/20 sherds sampled were from pyraunos vessels, making the dataset heavily biased. Secondly, 9/16 pyraunos samples did not contain miliacin. Therefore, neither an exclusive nor dominant relationship may be drawn between vessel and product. However, additional research is necessary to investigate whether *P. miliaceum* was processed in any other vessel type, and confirm that pyraunos use was utilitarian, as a relationship between the two, albeit different from co-introduction, may still exist.



Figure 74. Reconstruction diagram of a pyraunos vessel (Deliopoulos 2007, See Valamoti 2016 55).

Olympus

The recovery rate and average TLE yield of ceramic-absorbed residues from Olympus are comparable to contemporary Greek sites (Table 24 and 25). Residues generally contained only ubiquitous fatty acids, with ambiguous cholesterol and stigmasterol derivatives observed in a minority of samples. Miliacin was not observed in any of the ceramic-absorbed residues analysed, including those from pyraunos vessel sherds (n= 4). This indicates that *P. miliaceum* was not processed in any of the vessels analysed and further discounts an association between the cereal and pyraunos vessels. Archaeobotanical and isotopic datasets from the Olympus sites are reported to provide evidence for *P. miliaceum* and ^{13}C enrichment respectively, although this data has not been satisfactorily published (Dimoula *et al.* 2021). Furthermore, the quantity of evidence has not been reported, there are no direct dates, and *P. miliaceum* caryopses are notoriously intrusive. Therefore, these observations are presently unreliable and potentially overemphasise evidence for *P. miliaceum* at Olympus. Nonetheless, if *P. miliaceum* was present at the site during the LBA, the absence of miliacin in ceramic-absorbed residues may indicate that the cereal fulfilled a different role in subsistence, e.g. animal fodder.

The absence of miliacin in ceramic-absorbed residues at Olympus is interesting, given its prevalence at Angelochori, which is nearby, and the abundance of *P. miliaceum* caryopses identified at sites across Northern Greece (Valamoti 2016). Olympus is situated in Northern Greece, yet it is the most southerly site examined in this study. Therefore, it is potentially more susceptible to cultural influence from the south, i.e. the Mycenaeans. Archaeobotanical and isotopic evidence for *P. miliaceum* in South Greece during the LBA is extremely scarce but potentially indicates an aversion, among most individuals, to the crop (Valamoti 2016). Therefore, one may question whether such cultural ideas impacted subsistence practices at Olympus. Indeed, the analysis of ceramics from the Olympus sites discussed in this study indicate a Mycenaean influence beginning in the LBA with the merging of ceramic styles (Dimoula *et al.* 2021).

Ceramic-absorbed residues from Olympus are formed from both ^{13}C enriched and depleted lipids (Table 25, Figure 75). Sample Oly 10 plots within the reference range of marine lipids, with a weighted average $\delta^{13}\text{C}$ value of -21.5‰ , but does not contain either isoprenoid fatty acids or C_{20+} APAAs. Indeed, molecular evidence for aquatic products are not observed in any ceramic-absorbed residue from Olympus. These markers are prone to degradation and are inconsistently observed in archaeological residues. Therefore, it is possible that marine products were processed in these vessels and the biomarkers have degraded. As miliacin is observed in archaeological ceramic-absorbed residues that demonstrate substantial ^{13}C depletion (e.g. Angelochori and Bruszczewo), it is unlikely that ^{13}C enrichment in samples from Olympus is derived from the processing of *P. miliaceum* caryopses. However, enrichment may be derived from the processing of terrestrial animals that have consumed ^{13}C enriched products, e.g. *P. miliaceum* and wild resources exploited during seasonal transhumance (Nitsch *et al.* 2017; Vaiglova *et al.* 2018), which would also explain the absence of biomarkers. Isotopic analysis of faunal remains is necessary to resolve the source of ^{13}C enrichment.

Many of the samples from Olympus produce $\Delta^{13}\text{C}$ values around -0.9‰ and plot within the reference range of C_3 plant and C_3 -fed ruminant adipose, likely indicating either sequential or concurrent mixing of these products in vessels. In addition, Oly 18 produced a $\Delta^{13}\text{C}$ value of -4.3‰ and plots within the range of C_3 dairy products, providing the first reliable indication of dairying in this study (Craig *et al.* 2012). Interpretation of the remaining samples that demonstrate varying degrees of ^{13}C enrichment is more

difficult, as the source and quantity of ^{13}C enriched lipids is unknown. The $\Delta^{13}\text{C}$ value of samples provides some interpretive potential, as the degree of isotopic fractionation is maintained from diet (Craig *et al.* 2005), yet they are subject to influence from mixtures of different products (Hendy *et al.* 2018). Most samples with high $\delta^{13}\text{C}_{16:0}$ values also produced high $\Delta^{13}\text{C}$ values indicative of non-ruminant products, yet this may relate to either a C_4 plant, marine, or porcine lipid contribution. The processing of C_4 -fed animal products cannot be excluded, as ^{13}C enrichment is potentially observed in one sample that produced a $\Delta^{13}\text{C}$ value indicative of ruminant adipose lipids. However, greater evidence is necessary to confirm the nature and extent of any potential C_4 plant consumption.

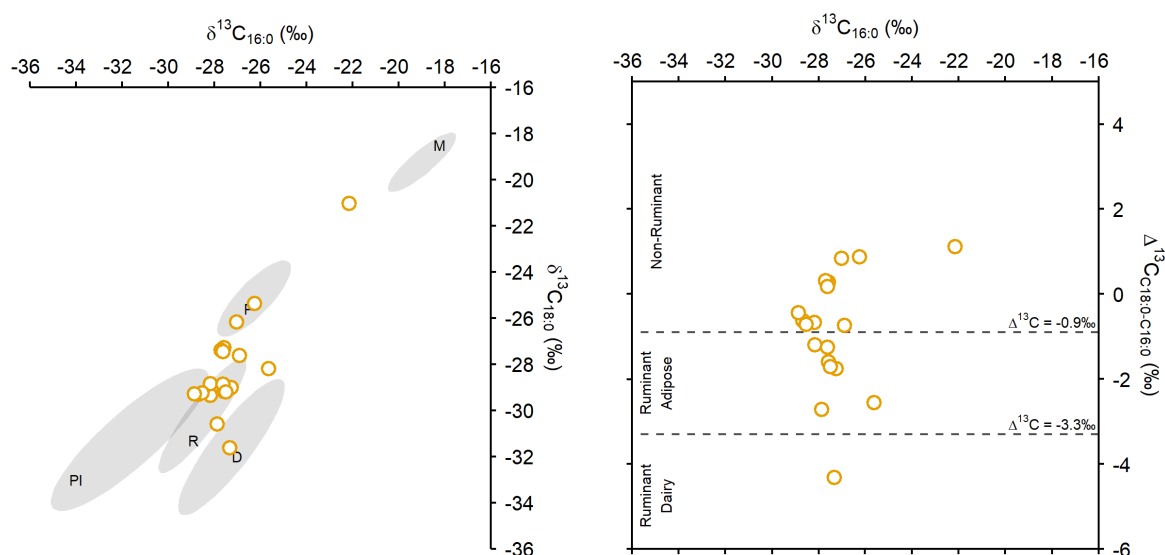


Figure 75. Compound specific isotope data from Olympus. **Left:** $\delta^{13}\text{C}_{16:0}$ and $\delta^{13}\text{C}_{18:0}$ values plotted against 1σ reference ellipses of modern-carbon corrected foodstuffs. **P** = porcine, **PI** = C_3 plants, **R** = domestic ruminant adipose, **D** = dairy, and **M** = *P. miliaceum*. **Right:** $\delta^{13}\text{C}_{16:0}$ and $\Delta^{13}\text{C}$ ($\delta^{13}\text{C}_{18:0} - \delta^{13}\text{C}_{16:0}$) values. Reference data is presented in Appendix 5.

Petko Karavelovo

All samples from Petko Karavelovo produced non-ruminant $\Delta^{13}\text{C}$ values ($> -0.9\text{‰}$) and plot within the reference range of C_3 plant products (Figure 76). This supports the attribution of even over odd LCFAs, LC alkanes, and 16-hentriacontane, which are observed in half of the samples, to plant product processing (Figure 77). These compounds are unlikely derived from sunscreens, as they do not co-occur with octocrylene in all samples. An absence of evidence for the contribution of animal lipids to

ceramic-absorbed residues may demonstrate that animal products were processed in either small quantities, different vessels, or not using ceramics. However, additional analysis is necessary to investigate this theory, as only ten samples, from a limited range of vessel types, were analysed in this study.

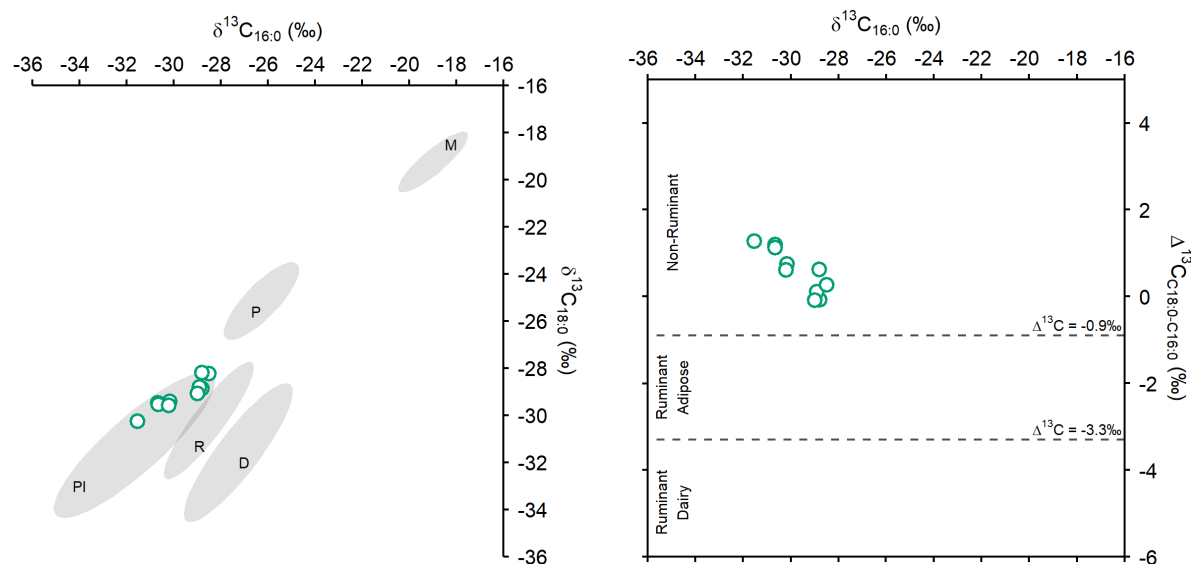


Figure 76. Compound specific isotope data from Petko Karavelovo. **Left:** $\delta^{13}\text{C}_{16:0}$ and $\delta^{13}\text{C}_{18:0}$ values plotted against 1σ reference ellipses of modern-carbon corrected foodstuffs. **P** = porcine, **PI** = C_3 plants, **R** = domestic ruminant adipose, **D** = dairy, and **M** = *P. miliaceum*. **Right:** $\delta^{13}\text{C}_{16:0}$ and $\Delta^{13}\text{C}$ ($\delta^{13}\text{C}_{18:0} - \delta^{13}\text{C}_{16:0}$) values. Reference data is presented in Appendix 5.

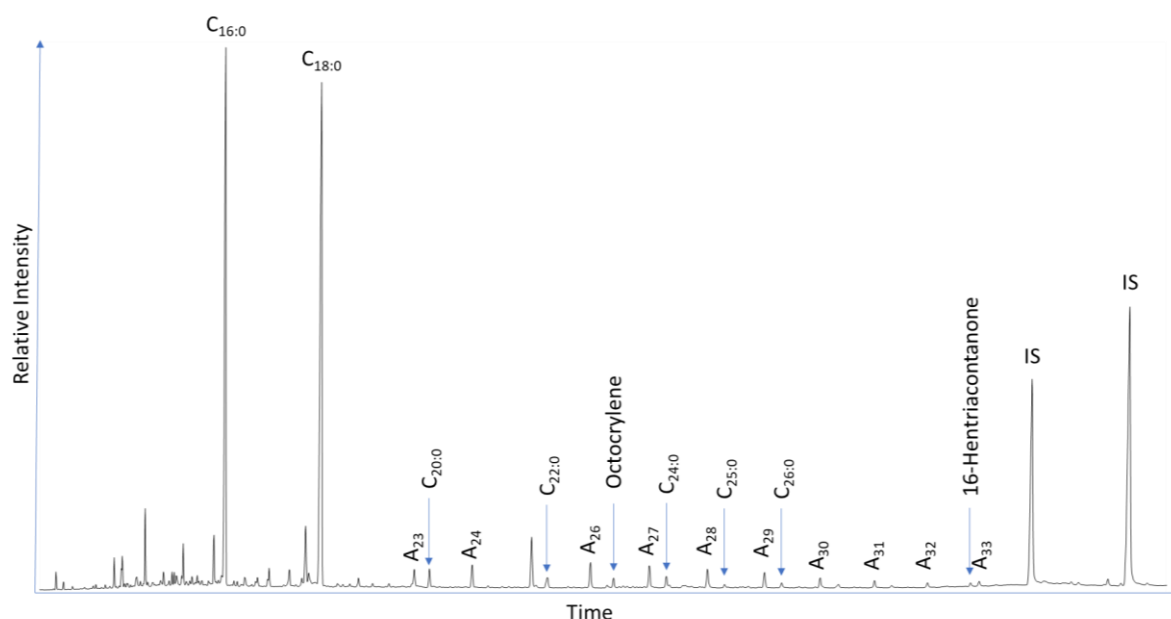


Figure 77. Partial TIC of PK 3 AE highlighting abundant compounds indicative of plant products.

Avren and Sokol

Only two sherds were sampled from Avren, both of which produced remarkably similar residues, in terms of TLE yield, molecular content, and isotopic composition, despite originating from two distinct vessels (Table 25, Figure 78). Long chain fatty acids and alkanes were observed in both samples and 16-hentriacontanone was observed in one sample. Furthermore, an average octocrylene content of 0.7% indicates that contamination is not substantial. Both samples produced non-ruminant $\Delta^{13}\text{C}$ values of 0.6‰ and plot within the range of C_3 plants. This data likely demonstrates that both residues are primarily comprised of C_3 plant lipids.

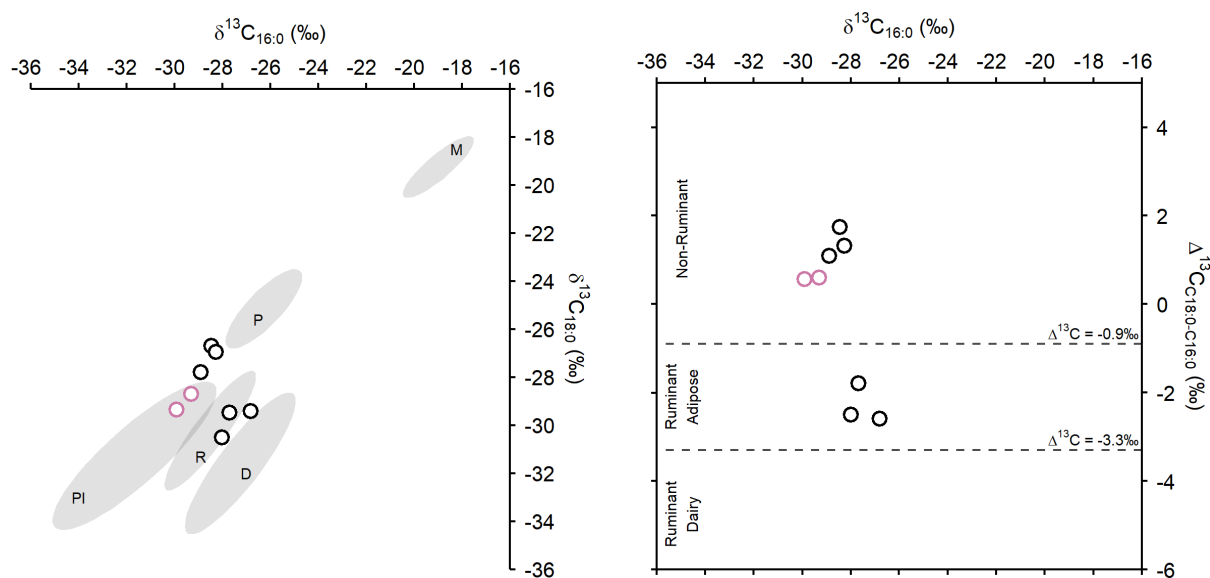


Figure 78. Compound specific isotope data from Avren (pink circles) and Sokol (black circles). **Left:** $\delta^{13}\text{C}_{16:0}$ and $\delta^{13}\text{C}_{18:0}$ values plotted against 1σ reference ellipses of modern-carbon corrected foodstuffs. **P** = porcine, **PI** = C_3 plants, **R** = domestic ruminant adipose, **D** = dairy, and **M** = *P. miliaceum*. **Right:** $\delta^{13}\text{C}_{16:0}$ and $\Delta^{13}\text{C}$ ($\delta^{13}\text{C}_{18:0} - \delta^{13}\text{C}_{16:0}$) values. Reference data is presented in Appendix 5.

Three of six samples from Sokol produced relatively high TLE yields compared to the other three samples, with an average of $143 \mu\text{g g}^{-1}$ compared to $46 \mu\text{g g}^{-1}$. However, increased yields do not correspond to either vessel or sherd type, molecular contents, or isotopic composition. While the dataset is limited, this observation potentially indicates varied and utilitarian use of vessels, with no specific purpose attributed to vessel type. Pinaceae resin markers, dehydroabietate and 7-oxodehydroabietic acid, are observed in low abundance in four samples. Retene is also observed in two of these samples,

potentially demonstrating deliberate application of resinous products to the interior surface of vessels. However, due to the low abundance of these compounds, contamination from either woodsmoke or burial environment cannot be ruled out (Reber *et al.* 2019).

Two distinct groups are apparent when plotting compound specific isotope values of samples from Sokol. However, the sample size is too small to assess their difference statistically. Half of samples produced non-ruminant $\Delta^{13}\text{C}$ values and plot between C_3 plant and porcine products, whereas the other three samples produced ruminant $\Delta^{13}\text{C}$ values and plot in the range of domestic and wild ruminant adipose lipids (Figure 78). These distinct groups do not correspond to either a location at the site or vessel type. Therefore, it may be proposed that, while vessel types may not have had a specific use, they were perhaps not multi-purpose, potentially indicating that the mixing of different products, either concurrently or sequentially, was not an aspect of food culture at Sokol. However, further analysis is necessary to understand the extent and reliability of these observations at the site, as the small sample assessed here limits statistical analysis and correlation between factors.

Chokoba

Three of four samples analysed from Chokoba produced exceptionally high TLE yields of 195, 313 and 508 $\mu\text{g g}^{-1}$. These samples produced $\Delta^{13}\text{C}$ values between -3.5‰ and -5.2‰, potentially indicating a common function related to processing dairy products (Figure 79), although it is important to consider that $\Delta^{13}\text{C}$ values between -3.3‰ and -4.3‰ may also indicate wild ruminant adipose lipids (Craig *et al.* 2012). Nonetheless, these samples are in stark contrast to Cho 4, which produced a low TLE yield (22 $\mu\text{g g}^{-1}$), a $\Delta^{13}\text{C}$ value of 2.4‰, and contained miliacin, providing the first and earliest molecular evidence for *P. miliaceum* in Bulgaria.

Comparison of Cho 4 to theoretical mixing models suggests the residue is formed almost entirely of porcine fats, with *P. miliaceum* likely contributing < 10% of lipids to the residue (Figure 80). Additional analysis is necessary in order to assess the extent and nature of *P. miliaceum* processing at Chokoba. All four sherds derive from similar vessel types, potentially indicating that the cereal was processed in everyday domestic contexts,

yet whether *P. miliaceum* was processed exclusively with porcine products requires additional sampling.

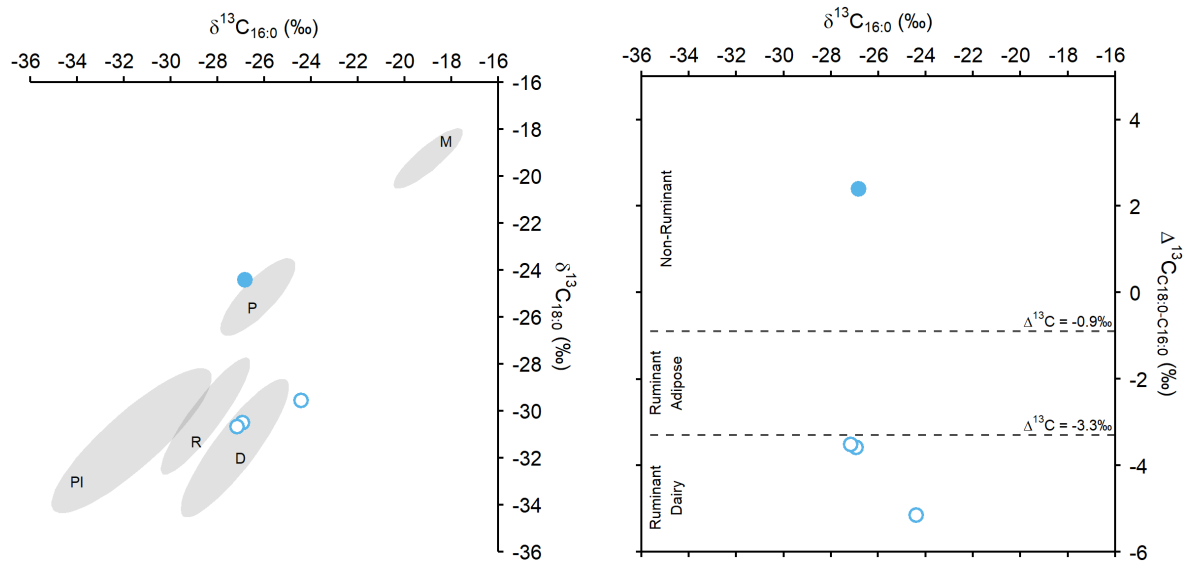


Figure 79. Compound specific isotope data from Chokoba. **Left:** $\delta^{13}\text{C}_{16:0}$ and $\delta^{13}\text{C}_{18:0}$ values plotted against 1σ reference ellipses of modern-carbon corrected foodstuffs. **P** = porcine, **PI** = C_3 plants, **R** = domestic ruminant adipose, **D** = dairy, and **M** = *P. miliaceum*. **Right:** $\delta^{13}\text{C}_{16:0}$ and $\Delta^{13}\text{C}$ ($\delta^{13}\text{C}_{18:0} - \delta^{13}\text{C}_{16:0}$) values. Reference data is presented in Appendix 5.

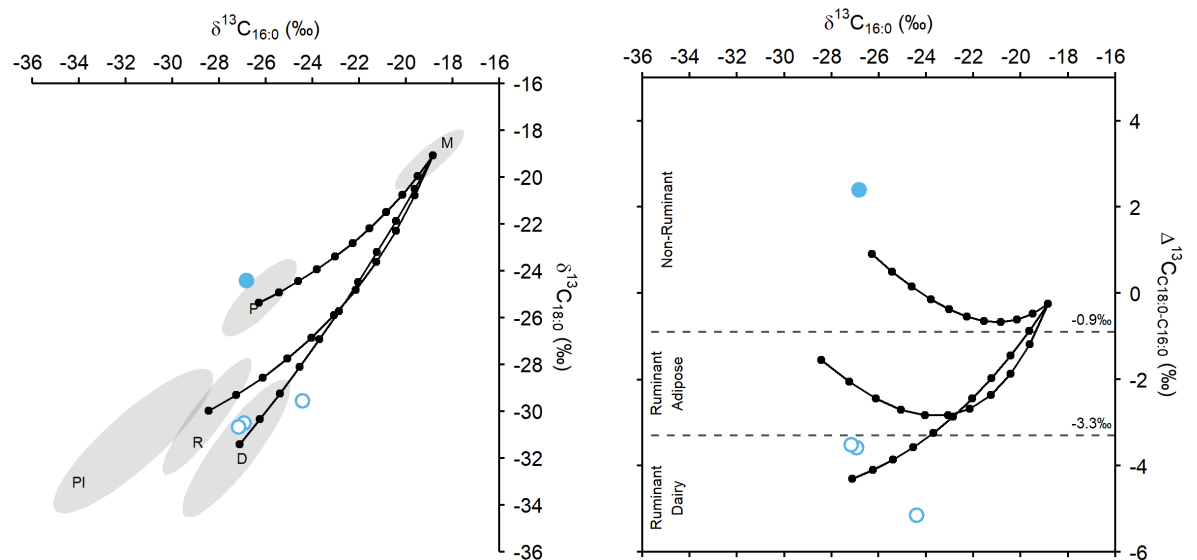


Figure 80. Plots of **Left:** $\delta^{13}\text{C}_{16:0}$ and $\delta^{13}\text{C}_{18:0}$ values and **Right:** $\delta^{13}\text{C}_{16:0}$ and $\Delta^{13}\text{C}$ ($\delta^{13}\text{C}_{18:0} - \delta^{13}\text{C}_{16:0}$) values of samples, from Chokoba, against 1σ reference ellipses and theoretical mixing lines of modern-carbon corrected foodstuffs, at 10% increments, of **P** = porcine, **R** = domestic ruminant adipose, **D** = dairy, with **M** = *P. miliaceum*. **PI** = C_3 plants. Reference and mixing model data are presented in Appendix 5.

Summary and discussion of *P. miliaceum* in SE Europe

Miliacin is not present in the 43 Neolithic and Chalcolithic ceramic-absorbed residues, from Lete I (n= 15), Dikili Tash (n= 16), Petko Karavelovo (n= 10) and Avren (n= 2), analysed in this study. The absence of miliacin at Dikili Tash is most significant in this study, as it is the only site that has produced a carbonised *P. miliaceum* caryopsis in a Neolithic context, even though the caryopsis is presumed to be intrusive. Previously published compound specific carbon isotope data, from hundreds of Greek and Bulgarian Neolithic ceramic-absorbed residues (Ethier *et al.* 2017; Whelton *et al.* 2018), does not indicate ¹³C enrichment attributable to *P. miliaceum*. However, as is demonstrated in samples from Bruszczewo and Angelochori, this technique is of limited effectiveness in identifying a contribution of *P. miliaceum* lipids to ceramic-absorbed residues. Furthermore, previous studies may not have utilised miliacin in the characterisation of archaeological residues. Therefore, while this study indicates that *P. miliaceum* was not present in Northern Greece and Bulgaria during the Neolithic, previous ORA studies cannot be used to support this interpretation. Nonetheless, in combination with archaeobotanical analysis, radiocarbon dating, and human and faunal isotopic analysis (Papathanasiou 2003; Motuzaitė-Matuzevičiūtė *et al.* 2013; Triantaphyllou 2015; Valamoti 2016; Vaiglova *et al.* 2018, 2020; Filipovic *et al.* 2020), it is increasingly unlikely that *P. miliaceum* was present in this region prior to the BA.

Neolithic and Chalcolithic ceramic residues are dominated by C₃ plant and ruminant adipose lipids and mixtures thereof (Figure 81). Furthermore, there is no evidence of secondary product processing and limited evidence to suggest wild species processing, corresponding to previous organic residue and zooarchaeological analysis (Jullien 1992; Halstead and Isaakidou 2011, 2013; Karastoyanov and Chohadjiev 2017; Whelton *et al.* 2018; Dotsika *et al.* 2019). However, evidence for porcine product processing is generally poor, with only limited isotopic data potentially demonstrating its exploitation in Bulgaria, despite the apparent significance of this product in Neolithic and Chalcolithic subsistence (Jullien 1992; Halstead and Isaakidou 2011; 2013).

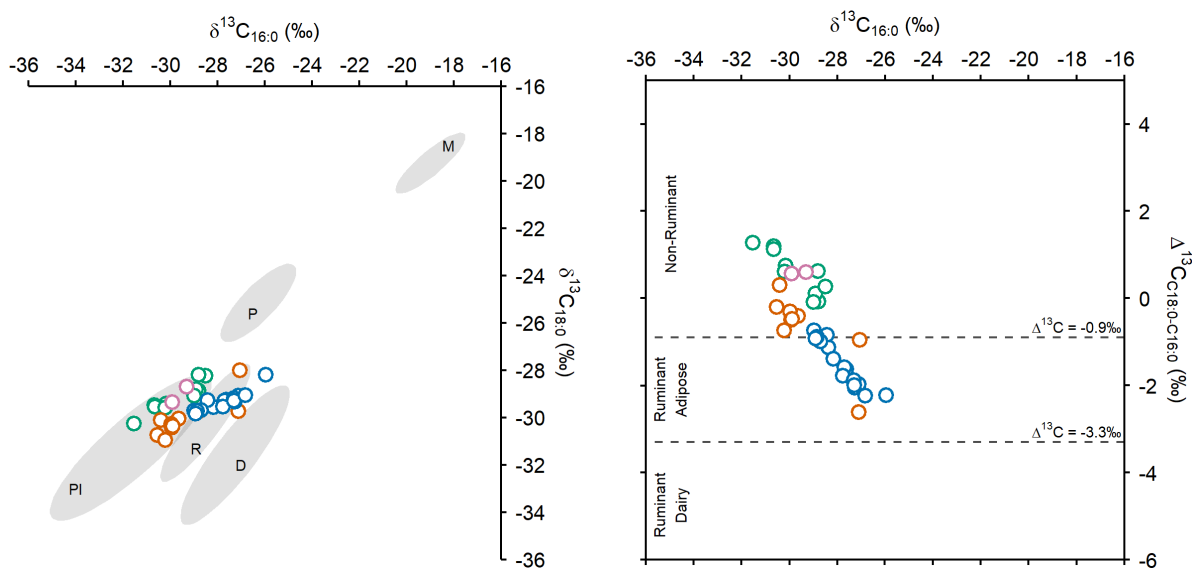


Figure 81. Plots of **Left** $\delta^{13}\text{C}_{16:0}$ and $\delta^{13}\text{C}_{18:0}$ values and **Right** $\delta^{13}\text{C}_{16:0}$ and $\Delta^{13}\text{C}$ ($\delta^{13}\text{C}_{18:0} - \delta^{13}\text{C}_{16:0}$) values of samples from Neolithic Greece and Chalcolithic Bulgaria. **Orange** = Lete I, **blue** = Dikili Tash, **green** = Petko Karavelovo, and **pink** = Avren.

Chapter 3 indicated that *P. miliaceum* was likely translocated for the purpose of subsistence, due to a short time difference between introduction and mass adoption of the cereal. Recent radiocarbon dating programmes suggest that *P. miliaceum* spread rapidly from its initial area of introduction and had dispersed across much of Europe in little over a century, supporting a subsistence-based theory (Motuzaitė-Matuzevičiūtė *et al.* 2013; Filipović *et al.* 2020). However, this hypothesis is based on a limited number of direct radiocarbon dates, from archaeobotanical assemblages that have been subject to various formation, degradation, and selection biases. Therefore, one cannot be confident that either initial or early, small-scale, introduction of *P. miliaceum* would be recognised.

The observation of miliacin, in a single sample from Archondiko, provides the earliest, confidently dated and secure, evidence for *P. miliaceum* processing in Europe, with corroboratory archaeobotanical evidence from Archondiko and other sites in the region (Valamoti 2016). This observation highlights the sensitivity and benefits of ORA, in detecting the use of *P. miliaceum*, relative to human and animal isotope studies that demonstrate no ^{13}C enrichment, prior to the LBA, in Greece (Figure 82). However, confidence in the use of miliacin is somewhat reduced, as there is a remote possibility that the compound originates from another source. Direct radiocarbon dating may provide confirmatory evidence of this observation, although this is not guaranteed given

the possibility of sampling an intrusive caryopsis. This is especially true at Archondiko, where a small number of individual caryopses are scattered across floor levels overlain by LBA activity. Therefore, either multiple radiocarbon dates or increased sampling of ceramic-absorbed residues, and local reference material, may be necessary to detect early and small-scale processing at Archondiko.

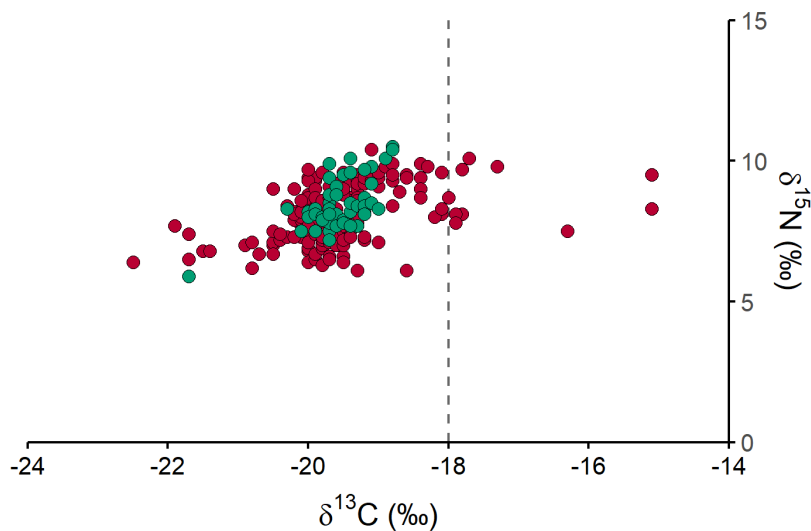


Figure 82. Human bulk isotope values of individuals from E-MBA (green) and LBA (red) Greece, demonstrating no ^{13}C enrichment in the E-MBA and substantial enrichment ($\delta^{13}\text{C}$ values $> -18\text{‰}$) in several LBA individuals.

If *P. miliaceum* was present at Archondiko in the EBA, around 2000 BCE, it would predate the earliest directly dated *P. miliaceum* caryopsis in Greece by at least 600 years and Europe by 500 years. Indeed, it would represent the earliest evidence for this species west of the Murghab Region of Turkmenistan, over 3000 km to the east (Chapter 3). This would require significant reconsideration of the speed, direction, and mode of *P. miliaceum* translocation across western Asia and into Europe. Presently, the earliest evidence for *P. miliaceum* outside of China is from East Kazakhstan, dating to ca. 2700 cal BCE (Hermes *et al.* 2019). This could suggest that the cereal crossed Central and West Asia in perhaps as little as 700 years. Furthermore, given the potentially short time frame between evidence for *P. miliaceum* in Central Asia (Spengler *et al.* 2018) and Greece, one must consider a more direct translocation route than is currently hypothesised (Filipovic *et al.* 2020), i.e. via Turkey. As such, the cereal may not have been translocated to adjacent communities but traded through long distance exchange networks. Indeed, this

method of translocation could provide a potential explanation for limited early evidence in the Caucasus and Turkey, with a small number of *P. miliaceum* producing sites in these regions yet to be discovered. The observation of miliacin at Archondiko also indicates that the chronology and direction of *P. miliaceum* translocation, in European contexts, requires significant revision. For instance, the currently perceived rapid east-west movement of *P. miliaceum*, across Ukraine, Hungary, and Italy, may actually demonstrate contemporary movements that radiated northward, from the south.

The observation of miliacin at Archondiko poses significant and exciting questions regarding the current understanding of *P. miliaceum* translocation across Eurasia, of which there is substantial scope for further investigation in Central and West Asia and Eastern Europe. For instance, the occurrence of *P. miliaceum* in Greece, without mass adoption, may indicate a cultural motive for translocation, e.g. related to either religious, ritual, or prestige activity, and not subsistence. Conversely, low occurrence could demonstrate its importance to the subsistence of the few, yet negatively perception and rejection by the many, thereby presenting juxtaposed subsistence and cultural significance among different communities. Sparse and sporadic early evidence of *P. miliaceum* cultivation and consumption may also indicate false-start introductions that ultimately did not result in adoption. The observation of miliacin in just one ceramic-absorbed residue, in addition to sparse archaeobotanical evidence, prevents detailed interpretation of the uses and significance of *P. miliaceum* in this period. However, this study highlights target material and questions for future analysis that will likely provide evidence of the motives, methods and nuanced uses of *P. miliaceum* introduction to Archondiko, Greece, and Europe.

This study provides the first molecular evidence for *P. miliaceum* processing in LBA Greece and Bulgaria. The observation of miliacin in ceramic residues from Angelochori and Chokoba, in addition to its absence at Olympus, supports archaeobotanical and isotopic analyses that demonstrate sporadic uptake of this cereal among communities of North Greece and Bulgaria during the LBA (Triantaphyllou 2015; Valamoti 2016, Figure 82).

The observation of miliacin in one of four sampled from Chokoba may indicate extensive processing of *P. miliaceum*. Furthermore, a nuanced attitude towards the use of either *P. miliaceum* or ceramic vessels, in cuisine, is potentially demonstrated by the

distinction of samples that do and do not contain miliacin (Figure 83). Fortunately, the preservation of ceramic-absorbed residues at the site is high, enabling further investigation of the prevalence, methods, and significance of *P. miliaceum* processing at Chokoba during the LBA.

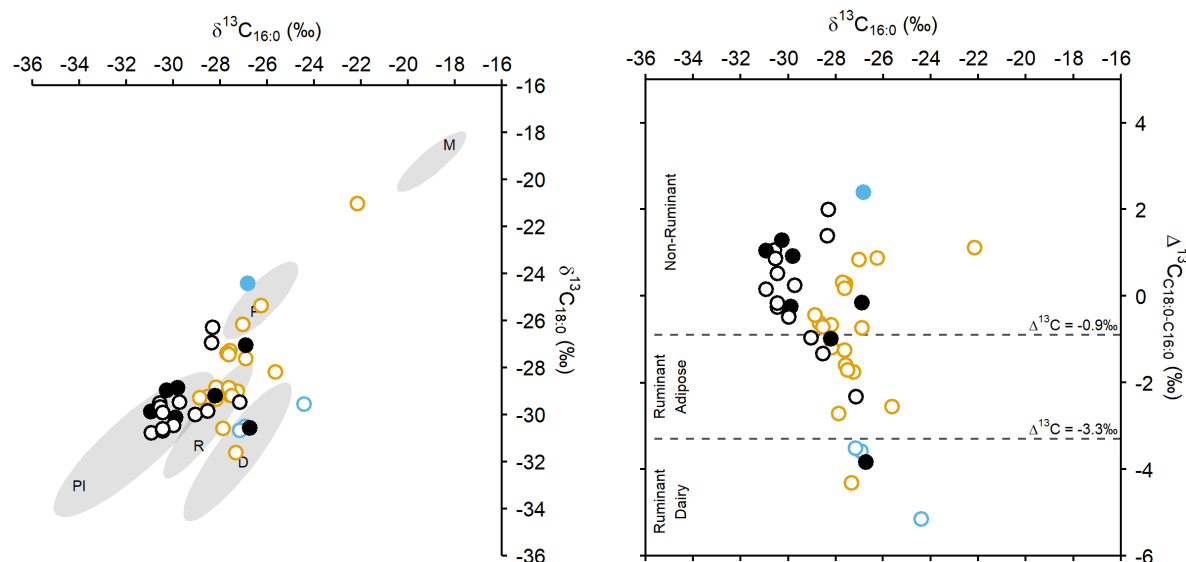


Figure 83. Plots of **Left** $\delta^{13}\text{C}_{16:0}$ and $\delta^{13}\text{C}_{18:0}$ values and **Right** $\delta^{13}\text{C}_{16:0}$ and $\Delta^{13}\text{C}$ ($\delta^{13}\text{C}_{18:0} - \delta^{13}\text{C}_{16:0}$) values of samples from LBA Greece and Bulgaria. **Black** = Angelochori, **yellow** = Olympus, and **blue** = Chokoba. Filled circles contain miliacin.

Substantial processing of *P. miliaceum* at Angelochori is demonstrated by the observation of miliacin in seven of twenty samples analysed, likely indicating its role as a staple. The variety of products that contribute to residues containing miliacin potentially indicate ubiquitous use of the cereal. However, without the analysis of charred crusts, it is not possible to determine whether residues represent either concurrent or sequential processing of different products. Contextual data does not convey the cultural importance of this species, if indeed it had one, although spatial analysis potentially reveals a social significance of *P. miliaceum* that distinguishes households. Additional analysis is required to prove whether these observations are accurate, yet it is interesting to consider their implications. If households truly display different attitudes towards *P. miliaceum*, is this related to either socioeconomic status, cultural affiliation or personal preference. One may question the provenance of these attitudes, whether they developed either internally or externally, and their duration within the community.

There is a significant difference between the weighted average $\delta^{13}\text{C}$ value of samples from Angelochori and Olympus (paired t-test, $t=2.1765$, $df=19$, $p <.05$). While miliacin is observed at Angelochori, and there is no molecular evidence for ^{13}C enriched products at Olympus, ceramic-absorbed residues from the latter site demonstrate ^{13}C enrichment (Figure 83). The data indicates a significant difference in either subsistence methods or the use of ceramic vessels, that may relate to affiliation with Mycenaean culture. However, further analysis of LBA ceramic-absorbed residues is necessary to explore attitudes towards this cereal in Northern Greece.

Conclusion

The results presented in this chapter provide a comprehensive spatial and temporal investigation of ceramic-absorbed organic residues in Greece and Bulgaria, from the Neolithic to Bronze Age, with specific emphasis on the detection of *P. miliaceum* processing. High recovery rates and appreciable lipid yields enabled a thorough investigation of residues, many of which demonstrate potential for future research in the region. Subsequently, this chapter has addressed the four research questions posed at the outset of this chapter.

1. There is no evidence to suggest that *P. miliaceum* was processed in ceramic vessels, in Northern Greece and Bulgaria, prior to the Bronze Age, corresponding to archaeobotanical and isotopic datasets.
2. There is confidently dated and secure evidence for *P. miliaceum* processing in EBA Greece, although the reliability of this evidence is subject to further investigation.
3. While evidence for *P. miliaceum* processing was not observed at all LBA sites investigated, those presenting molecular evidence indicated that the cereal was processed in vessels either frequently or in significant quantities.
4. Potential differences were observed in the use, uses, and significance of *P. miliaceum* at different sites, with apparent rejection at Olympus; socially restricted use as a staple, in utilitarian vessels at Angelochori; and restricted use, with other products, in utilitarian vessels at Chokoba; although all of these observations require extensive additional analysis.

Future lines of inquiry have been detailed throughout this chapter. It is strongly believed that by addressing these issues, specifically at Archondiko and Angelochori, one may be able to ascertain the timing, direction and motives for *P. miliaceum* introduction to this region and perhaps Europe.

Chapter 8: Conclusion

Archaeological interest in *P. miliaceum* has increased substantially in the past decade, with researchers employing a variety of established and novel analytical techniques to understand the presence, uses, and significance of this cereal in the past. Researchers are increasingly employing ORA in the investigation of *P. miliaceum* use in culinary contexts, yet criteria originally used in the identification of residues comprising this cereal (Heron *et al.* 2016) have not been utilised invariably in subsequent studies, with focus placed on the observation of miliacin in archaeological residues (e.g. Ganzarolli *et al.* 2018; Rageot *et al.* 2019a; 2019b; Junno *et al.* 2020). Furthermore, the accuracy and reliability of molecular and isotopic criteria have not been critically assessed.

Research aims and objectives

The primary aim of this thesis was to improve understanding of three criteria employed in the identification and interpretation of organic residues derived from *P. miliaceum*. This aim was addressed by the completion of two objectives, including comprehensive analysis of reference materials (Chapter 4) and the undertaking of thorough experimental research (Chapter 5). The secondary aim of this thesis was to demonstrate and test the application and usefulness of enhanced identification criteria in the characterisation and understanding of archaeological organic residues. This aim was achieved by the completion of two objectives. Firstly, a detailed methodological investigation of charred crust and ceramic-absorbed residues from Bruszczewo, Poland, via GC-MS, GC-C-IRMS, and EA-IRMS (Chapter 6), that assessed, developed, and expanded previous research conducted by Heron *et al.* (2016). Secondly, a comprehensive spatiotemporal study of *P. miliaceum* introduction and exploitation, in Northern Greece and Bulgaria, via GC-MS and GC-C-IRMS analysis of ceramic-absorbed residues from 12 archaeological sites (Chapter 7).

Revised identification criteria

This study provides evidence and gives cause to refine and redefine criteria employed in the identification and characterisation of archaeological food residues comprising *P. miliaceum* (Chapter 1). Doing so achieves the overarching aim of this thesis

and will improve the accuracy, reliability, and interpretive potential of future archaeological research.

1. The identification of miliacin, in solvent extracted samples from either charred crusts or ceramics, can confirm the processing of *P. miliaceum* caryopses if no other miliacin-producing plants are present in an environment. However, plants that produce either β -amyrin ME or δ -amyrin ME must also be considered when miliacin is identified in AM extracted samples.

a. It is important to consider the archaeological and archaeobotanical context of sampled material, including the contemporary presence of *P. miliaceum* in a region and the likelihood that other species, which produce the three PTMEs listed, were used in culinary contexts. As such, a robust archaeological approach may be employed in the attribution of miliacin to *P. miliaceum* without extensive sampling of reference material, although doing so would increase confidence in any interpretation.

2. The observation of ^{13}C enrichment in bulk $\delta^{13}\text{C}$ values of charred crusts demonstrates that *P. miliaceum* likely comprised $\geq 25\%$ of a processed mixture. However, it is important to consider that, depending on the type, quantity, and cooking time(s) of processed products, the $\delta^{13}\text{C}$ value of mixtures comprising *P. miliaceum* may not exceed -22% .

a. A charred crust that produces relatively low $\delta^{13}\text{C}$, high $\delta^{15}\text{N}$, and low C/N values indicates the processing of *P. miliaceum* with animal products.

b. A charred crust that produces relatively high $\delta^{13}\text{C}$, low $\delta^{15}\text{N}$, and high C/N values indicates the processing of *P. miliaceum* either in isolation or with other cereals.

3. The observation of ^{13}C enrichment in $\delta^{13}\text{C}_{16:0}$ and $\delta^{13}\text{C}_{18:0}$ values of charred crusts may demonstrate a contribution of lipids from *P. miliaceum*, to a foodcrust, although significant enrichment is not guaranteed when a charred crust comprises material from C_3 products.

a. It is unlikely that accumulated ceramic-absorbed residues would demonstrate significant ^{13}C enrichment, observed in $\delta^{13}\text{C}_{16:0}$ and $\delta^{13}\text{C}_{18:0}$ values, derived from *P. miliaceum* processing, although vessels repeatedly

used for specific purposes, e.g. processing *P. miliaceum* in isolation, could conceivably demonstrate ^{13}C enrichment.

Archaeological research outcomes

The analysis of archaeological foodcrusts and ceramic-absorbed residues provided an opportunity to enhance understanding of food residues formed from *P. miliaceum* and explore the presence, uses, and significance of this cereal to past populations across Europe. This research demonstrated the interpretive potential of ORA and has significantly advanced the investigation of *P. miliaceum* in this region. The main outcomes of this research include:

1. Identifying the earliest, confidently dated, specific, and secure evidence for *P. miliaceum* in Europe, by the observation of miliacin in one ceramic-absorbed residue from Archondiko, Greece.
2. Understanding differences in regional and local approaches to *P. miliaceum* use, including potential social differentiation of millet consumers, by the comparison of ceramic-absorbed residues from sites in Northern Greece.
3. Demonstrating that *P. miliaceum* was processed concurrently with different ingredients, and processed in multipurpose vessels, by comparison of molecular and isotopic data, from charred crust and ceramic-absorbed residues, from Bruszczewo, Poland.
4. Demonstrating that AM extraction is more effective than solvent extraction in identifying *P. miliaceum* processing, despite distributing the initial miliacin content of residues across three isomers, by comparison of different extraction methodologies applied to ceramic-absorbed residues from Archondiko, Angelochori, and Chokoba.
5. Providing evidence to support the hypothesis that ^{13}C enriched lipids, released from *P. miliaceum* during cooking, have a limited impact on accumulated $\delta^{13}\text{C}_{16:0}$ and $\delta^{13}\text{C}_{18:0}$ values of ceramic-absorbed residues, as was demonstrated in material from Bruszczewo, Archondiko, Angelochori, and Chokoba.

Suggestions for future research

Reference materials and experiments

Chapter 4 highlights the importance and potential benefits of comprehensively analysing reference materials. Chapter 5 examined the extent to which molecular and isotopic datasets may be used to identify and understand *P. miliaceum* residues. However, further research is necessary to improve confidence in the application of molecular and isotopic criteria and further assess their interpretive potential in archaeological contexts. This includes the following investigations:

1. To develop a greater understanding of β -amyrin ME, δ -amyrin ME, and miliacin production, among commonly consumed plants, in targeted regions.
2. To understand whether fermentation of *P. miliaceum* induces isomerisation of miliacin and if traces of fermentation persist during deposition.
3. To understand the preservation potential of miliacin, in different depositional contexts, relative to fatty acids and biomarkers of cereals and aquatic products.
4. To understand the formation of *P. miliaceum* residues when the cereal is processed with multiple ingredients, pre-processed grains, and dairy products.
5. To understand when *P. miliaceum* releases miliacin and other ^{13}C enriched compounds into suspension and whether an early release of compounds is sufficient to influence the accumulated residue of different products if *P. miliaceum* is added during the final stage of cooking.

Archaeological investigations

Chapter 6 and 7 demonstrated the application of ORA in identifying and understanding the use and significance of *P. miliaceum* in various archaeological contexts. Archaeological discoveries presented in these chapters revise the chronology of *P. miliaceum* introduction to Europe, by 500 years, and force reconsideration of the direction from which the cereal was introduced and dispersed. In addition, the motivations for adopting *P. miliaceum* must be reconsidered, with cultural and social factors observed in its use demonstrating that subsistence was neither the only nor main driver of exploitation. Considering these factors, and current gaps in our understanding of *P. miliaceum* use in Northern Eurasia (Chapter 3), necessary and potentially fruitful areas of future archaeological research include the following:

1. To understand where, when, and how *P. miliaceum* was introduced to Europe and whether this occurred with the movement of other cultural traditions, materials, ideas, and people.
 - a. This may be achieved by conducting large-scale ORA investigations, and integrating them with other archaeological datasets, on EBA and MBA material from circum-Pontic regions.
2. To understand whether the uses and significance of *P. miliaceum* changed after its introduction to Europe.
 - a. Presently, investigations should examine the chronological development of *P. miliaceum* use at Archondiko, as the site presents evidence that is far earlier than any other in Europe, although investigations may be expanded as other early sites of early adoption are identified.
3. To understand whether the use of *P. miliaceum* is influenced by either large-scale, cultural affiliation or small-scale, social differentiation, and whether these differences correspond to the use of material culture.
 - a. The expansion of ORA to material from Mycenaean sites would help elucidate cultural factors influencing the adoption of *P. miliaceum* in northern, central, and southern Greece during the BA.
 - b. Targeted ORA of material from households at Angelochori would determine whether the use of *P. miliaceum* was influenced by social factors.
4. To understand differences in the use, i.e. processing methods, of *P. miliaceum* during subsistence-based and other cultural activities, e.g. feasting.
 - a. This may be investigated by targeted ORA investigations, integrated with archaeological datasets, at culturally significant sites with known purposes, e.g. Vix-Mont Lassois, France, and Heuneburg, Germany (Rageot *et al.* 2019a; 2019b).
5. To understand how evidence of *P. miliaceum* processing, in ceramic vessels, compares to isotopic evidence for its consumption by humans and animals.

- a. Expanding ORA to specific sites in regions where large-scale isotopic investigations have already been conducted, e.g. Greece, Northern Italy, and Hungary, would enable rapid comparison of datasets.
- b. Targeted analysis of specific burials that possess ceramic grave goods, i.e. Maciejowice (Isaksson and Nilsson 2018), would provide extremely interesting, individual specific, understanding of *P. miliaceum* consumption, in addition to elucidating the potentially integral role that this species may have occupied in subsistence and culture.

New methods of identifying *P. miliaceum* residues

Future investigation of *P. miliaceum* residues need not rely on ORA and isotopic techniques assessed and employed in this thesis. Researchers are beginning to develop novel, and expand existing, molecular and isotopic techniques that may provide new opportunities to identify and characterise *P. miliaceum* residues. This research is either in its infancy or is yet to be applied to the investigation of *P. miliaceum* residues, yet the potential exists to enhance current ORA studies with new datasets. There are a limited number of published studies available for these novel applications, preventing detailed discussion. However, the potential of these techniques is worth noting, if only briefly.

Microscopy

Microscopic analysis of charred cereal fragments, amorphous food residues, and foodcrusts enables nuanced interpretation of processing methods used to create different cereal products. Researchers have proposed methods to differentiate between “bread-like” and “porridge-like” products, formed from different grades of ground/pounded/boiled cereals (González-Carretero *et al.* 2017; Valamoti *et al.* 2019), although experiments have not focused on the differentiation of *P. miliaceum* products. Understanding how foodstuffs were used enables a greater understanding of culinary characteristics that may differ within and between communities and cultures (e.g. González-Carretero *et al.* 2017). These characteristics are entwined with the selection and combination of different foodstuffs and are susceptible to change over time. This thesis demonstrates that cuisine may be understood by ORA investigations and the application of experimental data to archaeological material. Indeed, the identification of different

(pre-)processing methods would enable targeted application of experimental bulk isotope datasets, improving the identification of products that contributed to the formation of charred food residues. As such, microscopy could enable deeper and more reliable interpretation of past culinary activities.

Pyrolysis

Pyrolysis is a process wherein large organic compounds are thermally degraded (heated) in the absence of oxygen, forming smaller organic compounds (pyrolysis products) that are, in theory, easier to analyse and identify. Pyrolysis products are often separated and identified by coupling analytical pyrolysis (Py) with GC-MS (Py-GC-MS). This technique is commonly employed in the characterisation of organic compounds present in microsamples (50 – 100 µg) taken from artwork (Tamburini 2018), although it has rarely been applied to archaeological food residues (Oudemans and Boon 1991, 1993). If miliacin is either thermally stable or produces distinct pyrolysis products, and the technique is sufficiently sensitive, it may be possible to identify *P. miliaceum* processing in archaeological charred crusts that are either too small or precious to analyse by standard ORA extraction methodologies, which require samples sizes > 10 mg. Indeed, the molecular sensitivity of Py-GC-MS would complement the application of bulk isotope analysis, enabling molecular and isotopic assessment of samples ≤ 1 mg in mass. Furthermore, an additional benefit of Py-GC-MS is that samples do not require time consuming preparation and extraction processes before analysis, enabling higher throughput and requiring lower investment than other ORA methods.

Proteomics

The analysis of proteins enables a greater degree of taxonomic and tissue specific identification than is achievable by the analysis of lipids. While proteins are more susceptible to degradation, they may be preserved over extended timescales depending on deposition conditions, e.g. in the presence of a mineral substrate (Hendy 2021). The investigation of proteins in archaeological culinary contexts is an expanding area of research, with the potential to identify specific foodstuffs and elucidate the methods used to produce them (Yang *et al.* 2014). However, investigations that combine the analysis of proteins and lipids, preserved within ceramics, have been limited, despite demonstrating significant potential (Hendy *et al.* 2018). It is important to consider that

the preservation and extraction of proteins, from ceramic matrices, are currently major limitations in the application of this technique (Hendy 2021), yet the development of new methods may enable more reliable identification of food residues preserved in ceramics.

Tandem analysis of proteins and lipids may enable a more comprehensive assessment of culinary activities, such as identifying products that are either lipid-poor, e.g. cereals, or not identifiable by GC-MS analysis (Hendy *et al.* 2018; Chowdhury *et al.* 2021). The observation of miliacin provides a sensitive and generally specific approach to identifying *P. miliaceum*, limiting the benefits of a proteomic approach, relative to other foodstuffs. However, the identification of cereal-specific proteins may aid the attribution of miliacin to a specific plant source, when either multiple miliacin-producing species are present in a region or there is no additional evidence for *P. miliaceum* in a specific archaeological context, thus removing the need for large-scale analysis of reference materials. Furthermore, the analysis of proteins would likely prove a useful tool in identifying plant and animal products processed with *P. miliaceum*. Finally, different methods of processing *P. miliaceum* may result in the production of characteristic proteins, such as has been identified with the fermentation of milk (Yang *et al.* 2014). However, it is necessary to demonstrate whether proteomic techniques can identify *P. miliaceum*.

Final statement

This thesis has detailed archaeological interest in *P. miliaceum* and provided explanations as to how and why employing ORA may better elucidate the uses and significance of this cereal in archaeological contexts. The analysis of reference and experimental materials has refined understanding of methods used to detect and characterise *P. miliaceum* processing, enabling more specific, secure, and detailed interpretation of different archaeological materials. Limitations in the identification of *P. miliaceum* residues are highlighted throughout this thesis and future experimental research questions are outlined during this conclusion. Furthermore, areas of future archaeological research are proposed along with novel analytical methods that may further elucidate the uses and significance of *P. miliaceum* across different regions and in different contexts.

It is evident from this study that the detection of miliacin is crucial in the identification of *P. miliaceum* residues. Unfortunately, charred foodcrusts are an uncommon find, relative to ceramics, limiting the application of bulk and compound specific carbon isotope analysis to this material. In addition, compound specific carbon isotope analysis of ceramic-absorbed residues appears to be of little, if any, use in the detection of *P. miliaceum* processing. As such, re-examination of GC-MS data-files, from samples analysed prior to Heron *et al.* (2016), would likely enable a rapid re-assessment of *P. miliaceum* processing, via the identification of miliacin, in charred crust and ceramic-absorbed residues. However, a retrospective review of previously published compound specific analyses, of ceramic-absorbed residues, is unlikely to result in a substantial increase in evidence for *P. miliaceum* processing.

When analysed, ceramic-absorbed and charred foodcrust residues can provide either qualitative or quantitative information on the use of *P. miliaceum* that is especially informative when molecular and isotopic datasets are combined and integrated with established typo-functional and spatial investigations of ceramics.

References

- Abe, S. (1960). Chemical Structure of Miliacin. *Chemical Society of Japan*, 33(2), 271-272. [Online]. Available at: doi:10.1246/bcsj.33.271.
- Ackman, R.G. and Hooper, S.N. (1968). Examination of isoprenoid fatty acids as distinguishing characteristics of specific marine oils with particular reference to whale oils. *Comparative Biochemistry and Physiology*, 24(2), 549-565. [Online]. Available at: doi:10.1016/0010-406x(68)91008-6.
- Aliscioni, S.S., Giussani, L.M., Zuloaga, F.O. and Kellogg, E.A. (2003). A molecular phylogeny of *Panicum* (Poaceae: Paniceae): tests of monophyly and phylogenetic placement within the Panicoideae. *American Journal of Botany*, 90(5), 796-821. [Online]. Available at: doi:10.3732/ajb.90.5.796.
- Amine, H., Gomez, E., Halwani, J., Casellas, C. and Fenet, H. (2012). UV filters, ethylhexyl methoxycinnamate, octocrylene and ethylhexyl dimethyl PABA from untreated wastewater in sediment from eastern Mediterranean river transition and coastal zones. *Marine Pollution Bulletin*, 64(11), 2435-2442. [Online]. Available at: doi:10.1016/j.marpolbul.2012.07.051.
- Amundson, R., Austin, A.T., Schuur, E.A.G., Yoo, K., Matzek, V., Kendall, C., Uebersax, A., Brenner, D. and Baisden, W.T. (2003). Global patterns of the isotopic composition of soil and plant nitrogen. *Global Biogeochemical Cycles*, 17(1), 1031. [Online]. Available at: doi:10.1029/2002GB001903.
- An, C-B., Dong, W., Li, H., Zhang, P., Zhao, Y., Zhao, X. and Yu, S.-Y. (2015). Variability of the stable carbon isotope ratio in modern and archaeological millets: evidence from northern China. *Journal of Archaeological Science*, 53, 316-322. [Online]. Available at: doi:10.1016/j.jas.2014.11.001.
- An, T. (2018). *Re-visiting the correlation between movement of Chinese millet and painted pottery before the 2nd millennium BC*. Unpublished: University of Cambridge. PhD. [Online]. Available at: doi:10.17863/CAM.30926.
- An, T., Pashkevich, G. and Jones, M. (2019). Re-examining millet impressions in Usatovo clay materials from NW Black Sea region, Ukraine. *Archaeological and Anthropological Sciences*, 11(7), 3201-3211. [Online]. Available at: doi:10.1007/s12520-018-0718-3.
- Arshadi, M., Backlund, I., Geladi, P. and Bergsten, U. (2013). Comparison of fatty and resin acid composition in boreal lodgepole pine and Scots pine for biorefinery applications. *Industrial Crops and Products*, 49, 535-541. [Online]. Available at: doi:10.1016/j.indcrop.2013.05.038.
- Assimopoulou, A.N. and Papageorgiou, V.P. (2005a). GC-MS analysis of penta- and tetracyclic triterpenes from resins of *Pistacia* species. Part II. *Pistacia terebinthus* var. Chia. *Biomedical Chromatography*, 19(8), 586-605. [Online]. Available at: doi:10.1002/bmc.484.
- Assimopoulou, A.N. and Papageorgiou, V.P. (2005b). GC-MS analysis of penta- and tetracyclic triterpenes from resins of *Pistacia* species. Part I. *Pistacia lentiscus* var. Chia. *Biomedical Chromatography*, 19(4), 285-311. [Online]. Available at: doi:10.1002/bmc.454.

- Aursand, M., Mabon, F. and Martin, G.J. (2000). Characterization of farmed and wild salmon (*Salmo salar*) by a combined use of compositional and isotopic analyses. *Journal of the American Oil Chemists' Society*, 77(6), 659-666. [Online]. Available at: doi:10.1007/s11746-000-0106-5.
- Bakels, C.C. (2003). The contents of ceramic vessels in the Bactria-Margiana Archaeological Complex, Turkmenistan. *Electronic Journal of Vedic Studies*, 9 (1), 49-52. [Online]. Available at: <http://nbn-resolving.de/urn:nbn:de:bsz:16-ejvs-7850>.
- Baker, L.A., Horbury, M.D. and Stavros, V.G. (2016). Ultrafast photoprotective properties of the sunscreens octocrylene. *Optics express*, 24(10), 10700-10709. [Online]. Available at: doi:10.1364/OE.24.010700.
- Ballentine, D.C., Macko, S.A. and Turekian, V.C. (1998). Variability of stable carbon isotopic compositions in individual fatty acids from combustion of C4 and C3 plants: implications for biomass burning. *Chemical Geology*, 152(1), 151-161. [Online]. Available at: doi:10.1016/S0009-2541(98)00103-X.
- Barden, T.J., Croft, M.Y., Murby, E.J. and Wells, R.J. (1997). Gas chromatographic determination of organic acids from fruit juices by combined resin mediated methylation and extraction in supercritical carbon dioxide. *Journal of Chromatography A*, 785(1-2), 251-261. [Online]. Available at: doi:10.1016/S0021-9673(97)00411-1.
- Bari, M.A., Baumbach, G., Kuch, B. and Scheffknecht, G. (2010). Temporal variation and impact of wood smoke pollution on a residential area in southern Germany. *Atmospheric Environment*, 44(31), 3823-3832. [Online]. Available at: doi:10.1016/j.atmosenv.2010.06.031.
- Barnard, H., Dooley, A.N., Areshian, G., Gasparyan, B. and Faull, K.F. (2011). Chemical evidence for wine production around 4000 BCE in the Late Chalcolithic Near Eastern highlands. *Journal of Archaeological Science*, 38(5), 977-984. [Online]. Available at: doi:10.1016/j.jas.2010.11.012.
- Bastos, D.Z.L., Pimentel, I.C., de Jesus, D.A. and de Oliveira, B.H. (2007). Biotransformation of betulonic and betulonic acids by fungi. *Phytochemistry*, 68(6), 834-839. [Online]. Available at: doi:10.1016/j.phytochem.2006.12.007.
- Bernreuther, A., Koziat, J., Brunerie, P., Krammer, G., Christoph, N. and Schreier, P. (1990). Chiroselective capillary gaschromatography (HRGC) and on-line HRGC-isotope ratio mass spectrometry of γ -decalactone from various sources. *Zeitschrift für Lebensmittel-Untersuchung und Forschung*, 191(4), 299-301. [Online]. Available at: doi:10.1007/BF01202430.
- Boardman, S. and Jones, G. (1990). Experiments on the effects of charring on cereal plant components. *Journal of Archaeological Science*, 17 (1), 1-11. [Online]. Available at: doi:10.1016/0305-4403(90)90012-T.
- Bogaard, A., Heaton, T.H.E., Poulton, P. and Merbach, I. (2007). The impact of manuring on nitrogen isotope ratios in cereals: archaeological implications for reconstruction of diet and crop management practices. *Journal of Archaeological Science*, 34(3), 335-343. [Online]. Available at: doi:10.1016/j.jas.2006.04.009.

- Boivin, N., Fuller, D. Q. and Crowther, A. (2012). Old World globalization and the Columbian exchange: comparison and contrast. *World Archaeology*, 44(3), 452-469. [Online]. Available at: doi:10.1080/00438243.2012.729404.
- Bondetti, M., Scott, E., Courel, B., Lucquin, A., Shoda, S., Lundy, J., Labra-Odde, C., Drieu, L. and Craig, O.E. (2021). Investigating the formation and diagnostic value of ω -(*o*-alkylphenyl)alkanoic acids in ancient pottery. *Archaeometry*, 63(3), 594-608. [Online]. Available at: doi:10.1111/arcm.12631.
- Bossard, N., Jacob, J., Le Milbeau, C., Lallier-Vergès, E., Terwilliger, V.J. and Boscardin, R. (2011). Variation in δD values of a single, species-specific molecular biomarker: a study of miliacin throughout a field of broomcorn millet (*Panicum miliaceum* L.). *Rapid communications in Mass Spectrometry*, 25(19), 2732-2740. [Online]. Available at: <https://onlinelibrary.wiley.com/doi/abs/10.1002/rcm.5092>.
- Bossard, N., Jacob, J., Le Milbeau, C., Sauze, J., Terwilliger, V., Poissonnier, B. and Vergès, E. (2013). Distribution of miliacin (olean-18-en-3 β -ol methyl ether) and related compounds in broomcorn millet (*Panicum miliaceum*) and other reputed sources: Implications for the use of sedimentary miliacin as a tracer of millet. *Organic Geochemistry*, 63, 48-55. [Online]. Available at: <https://doi.org/10.1016/j.orggeochem.2013.07.012>.
- Boutard, A. (2012). *Beautiful Corn: America's Original Grain from Seed to Plate*. Gabriola: New Society Publishers.
- Brettell, R.C., Stern, B., Reifarth, N. and Heron, C. (2014). The 'Semblance of Immortality'? Resinous Materials and Mortuary Rites in Roman Britain. *Archaeometry*, 56(3), 444-459. [Online]. Available at: doi:10.1111/arcm.12027.
- Brettell, R.C., Schotsmans, E.M., Rogers, P.W., Reifarth, N., Redfern, R.C., Stern, B. and Heron, C.P. (2015). 'Choicest unguents': molecular evidence for the use of resinous plant exudates in late Roman mortuary rites in Britain. *Journal of Archaeological Science*, 53, 639-648. [Online]. Available at: <https://www.sciencedirect.com/science/article/pii/S0305440314004130>.
- Brinkkemper, O., Braadbaart, F., van Os, B., van Hoesel, A., van Brussel, A.A.N. and Fernandes, R. (2018). Effectiveness of different pre-treatments in recovering pre-burial isotopic ratios of charred plants. *Rapid Communications in Mass Spectrometry*, 32(3), 251-261. [Online]. Available at: doi:10.1002/rcm.8033.
- Brite, E. B., Kidd, F.J., Betts, A. and Cleary, M.N. (2017). Millet cultivation in Central Asia: A response to Miller *et al.* *The Holocene*, 27(1), 1415-1422. [Online]. Available at: doi:10.1177/0959683616687385.
- Burger, P., Charrié-Duhaut, A., Connan, J., Flecker, M. and Albrecht, P. (2009). Archaeological resinous samples from Asian wrecks: Taxonomic characterization by GC-MS. *Analytica Chimica Acta*, 648(1), 85-97. [Online]. Available at: doi:10.1016/j.aca.2009.06.022.
- Burger, P., Charrié-Duhaut, A., Connan, J. and Albrecht, P. (2011). Taxonomic characterisation of fresh Dipterocarpaceae resins by gas chromatography-mass spectrometry (GC-MS): providing clues for identification of unknown archaeological

resins. *Archaeological and Anthropological Sciences*, 3(2), 185-200. [Online]. Available at: doi:10.1007/s12520-010-0050-z.

CABI (2019). *Digitaria sanguinalis*. Invasive Species Compendium, Wallingford, UK, CAB International. [Online]. Available at: <https://www.cabi.org/isc/datasheet/18916>.

Chakraborty, K.S., Slater, G.F., Miller, H.M.L., Shirvalkar, P. and Rawat, Y. (2020). Compound specific isotope analysis of lipid residues provides the earliest direct evidence of dairy product processing in South Asia. *Scientific Reports*, 10(1), 16095. [Online]. Available at: doi:10.1038/s41598-020-72963-y.

Chandler, R.F. and Hooper, S.N. (1979). Friedelin and associated triterpenoids. *Phytochemistry*, 18(5), 711-724. [Online]. Available at: doi:10.1016/0031-9422(79)80002-3.

Charrié-Duhaut, A., Porraz, G., Cartwright, C.R., Igreja, M., Connan, J., Poggenpoel, C. and Texier, P.-J. (2013). First molecular identification of a hafting adhesive in the Late Howiesons Poort at Diepkloof Rock Shelter (Western Cape, South Africa). *Journal of Archaeological Science*, 40(9), 3506-3518. [Online]. Available at: doi:10.1016/j.jas.2012.12.026.

Charters, S. (1996). Chemical analysis of absorbed lipids and laboratory simulation experiments to interpret archaeological pottery vessel contents and use. Unpublished: University of Bristol. PhD.

Charters, S., Evershed, R.P., Goad, L.J., Leyden, A., Blinkhorn, P.W. and Denham, V. (1993a). Quantification and Distribution of Lipid in Archaeological Ceramics: Implications For Sampling Potsherds For Organic Residue Analysis and The Classification of Vessel Use. *Archaeometry*, 35(2), 211-223. [Online]. Available at: doi:10.1111/j.1475-4754.1993.tb01036.x.

Charters, S., Evershed, R.P., Goad, L.J., Heron, C. and Blinkhorn, P. (1993b). Identification of an Adhesive Used to Repair a Roman Jar. *Archaeometry*, 35(1), 91-101. [Online]. Available at: doi:10.1111/j.1475-4754.1993.tb01025.x.

Charters, S., Evershed, R.P., Quye, A., Blinkhorn, P.W. and Reeves, V. (1997). Simulation Experiments for Determining the Use of Ancient Pottery Vessels: The Behaviour of Epicuticular Leaf Wax During Boiling of a Leafy Vegetable. *Journal of Archaeological Science*, 24(1), 1-7. [Online]. Available at: doi:10.1006/jasc.1995.0091.

Colombini, M.P., Modugno, F., Silvano, F. and Onor, M. (2000). Characterization of the Balm of an Egyptian Mummy from the Seventh Century B.C. *Studies in Conservation*, 45(1), 19-29. [Online]. Available at: <http://www.jstor.org/stable/1506680>.

Colombini, M.P., Giachi, G., Modugno, F. and Ribechini, E. (2005). Characterisation of organic residues in pottery vessels of the Roman age from Antinoe (Egypt). *Microchemical Journal*, 79(1), 83-90. [Online]. Available at: doi:10.1016/j.microc.2004.05.004.

Colonese, A.C., Farrell, T., Lucquin, A., Firth, D., Charlton, S., Robson, H.K., Alexander, M. and Craig, O.E. (2015). Archaeological bone lipids as palaeodietary markers. *Rapid Communications in Mass Spectrometry*, 29(7), 611-618. [Online]. Available at: <https://doi.org/10.1002/rcm.7144>.

- Colonese, A.C., Hendy, J., Lucquin, A., Speller, C.F., Collins, M.J., Carrer, F., Gubler, R., Kühn, M., Fischer, R. and Craig, O.E. (2017). New criteria for the molecular identification of cereal grains associated with archaeological artefacts. *Scientific Reports*, 7. [Online]. Available at: <https://doi.org/10.1038/s41598-017-06390-x>.
- Connan, J. and Nissenbaum, A. (2003). Conifer tar on the keel and hull planking of the Ma'agan Mikhael Ship (Israel, 5th century BC): identification and comparison with natural products and artefacts employed in boat construction. *Journal of Archaeological Science*, 30(6), 709-719. [Online]. Available at: [doi:10.1016/S0305-4403\(02\)00243-1](https://doi.org/10.1016/S0305-4403(02)00243-1).
- Connor, H.E. and Purdie, A.W. (1981). Triterpene methyl ethers in *Chionochloa* (Gramineae): Distribution in western South Island, New Zealand. *New Zealand Journal of Botany*, 19(2), 161-170 [Online]. Available at: [doi:10.1080/0028825X.1981.10425116](https://doi.org/10.1080/0028825X.1981.10425116).
- Coplen, T.B. (1995). Discontinuance of SMOW and PDB. *Nature*, 375(6529), 285-285. [Online]. Available at: [doi:10.1038/375285a0](https://doi.org/10.1038/375285a0).
- Copley, M.S., Evershed, R.P., Rose, P.J. and Clapham, A. (2001). Processing palm fruits in the Nile Valley—Biomolecular evidence from Qasr Ibrim. *Antiquity*, 75(289), 538-542. [Online]. Available at: [doi https://doi.org/10.1017/S0003598X00088761](https://doi.org/10.1017/S0003598X00088761).
- Copley, M.S., Berstan, R., Dudd, S.N., Docherty, G., Mukherjee, A.J., Straker, V., Payne, S. and Evershed, R.P. (2003). Direct chemical evidence for widespread dairying in prehistoric Britain. *Proceedings of the National Academy of Sciences of the United States of America*, 100(4), 1524-1529. [Online]. Available at: [doi:10.1073/pnas.0335955100](https://doi.org/10.1073/pnas.0335955100).
- Copley, M.S., Hansel, F.A., Evershed, R.P. and Sadr, K. (2004). Organic residue evidence for the processing of marine animal products in pottery vessels from the pre-colonial archaeological site of Kasteelberg D east, South Africa. *South African Journal of Science*, 100(5), 279-283. [Online]. Available at: <https://journals.co.za/doi/abs/10.10520/EJC96255>.
- Copley, M.S., Berstan, R., Dudd, S.N., Straker, V., Payne, S. and Evershed, R.P. (2005). Dairying in antiquity. I. Evidence from absorbed lipid residues dating to the British Iron Age. *Journal of Archaeological Science*, 32(4), 485-503. [Online]. Available at: [doi:10.1016/j.jas.2004.07.004](https://doi.org/10.1016/j.jas.2004.07.004).
- Correa-Ascencio, M. and Evershed, R. P. (2014). High throughput screening of organic residues in archaeological potsherds using direct acidified methanol extraction. *Analytical Methods*, 6(5), 1330-1340. [Online]. Available at: <https://doi.org/10.1039/c3ay41678j>.
- Correa-Ascencio, M., Robertson, I.G., Cabrera-Cortés, O., Cabrera-Castro, R. and Evershed, R.P. (2014). Pulque production from fermented agave sap as a dietary supplement in Prehispanic Mesoamerica. *Proceedings of the National Academy of Sciences of the United States of America*, 111(39), 14223-14228. [Online]. Available at: [doi:10.1073/pnas.1408339111](https://doi.org/10.1073/pnas.1408339111).
- Courel, N., Schaeffer, P., Adam, P., Motsch, E., Ebert, Q., Moser, E., Féliu, C., Bernasconi, S.M., Hajdas, I., Ertlen, D. and Schwartz, D. (2017). Molecular, isotopic and radiocarbon evidence for broomcorn millet cropping in Northeast France since the Bronze Age. *Organic Geochemistry*, 110, 13-24. [Online]. Available at: [doi:10.1016/j.orggeochem.2017.03.002](https://doi.org/10.1016/j.orggeochem.2017.03.002).

- Courel, B., Schaeffer, P., Féliu, C., Thomas, Y. and Adam, P. (2018). Birch bark tar and jewellery: The case study of a necklace from the Iron Age (Eckwersheim, NE France). *Journal of Archaeological Science: Reports*, 20, 72-79. [Online]. Available at: doi:10.1016/j.jasrep.2018.04.016.
- Craig, O.E., Love, G.D., Isaksson, S., Taylor, G. and Snape, C.E. (2004). Stable carbon isotopic characterisation of free and bound lipid constituents of archaeological ceramic vessels released by solvent extraction, alkaline hydrolysis and catalytic hydrolysis. *Journal of Analytical and Applied Pyrolysis*, 71(2), 613-634. [Online]. Available at: doi:10.1016/j.jaap.2003.09.001.
- Craig, O. E., Taylor, G., Mulville, J., Collins, M.J. and Pearson, M.P. (2005). The identification of prehistoric dairying activities in the Western Isles of Scotland: an integrated biomolecular approach. *Journal of Archaeological Science*, 32 (1), 91-103. [Online]. Available at: doi:10.1016/j.jas.2004.06.009.
- Craig, O.E., Forster, M., Andersen, S.H., Koch, E., Crombé, P., Milner, N.J., Stern, B., Bailey, G.N. and Heron, C.P. (2007). Molecular and Isotopic Demonstration of the Processing of Aquatic Products in Northern European Prehistoric Pottery. *Archaeometry*, 49(1), 135-152 [Online]. Available at: doi:10.1111/j.1475-4754.2007.00292.x.
- Craig, O.E., Steele, V.J., Fischer, A., Hartz, S., Andersen, S.H., Donohoe, P., Glykou, A., Saul, H., Jones, D.M., Koch, E. and Heron, C.P. (2011). Ancient lipids reveal continuity in culinary practices across the transition to agriculture in Northern Europe. *Proceedings of the National Academy of Sciences of the United States of America*, 108(44), 17910-17915. [Online]. Available at: doi:10.1073/pnas.1107202108.
- Craig, O.E., Allen, R.B., Thompson, A., Stevens, R.E., Steele, V.J. and Heron, C. (2012). Distinguishing wild ruminant lipids by gas chromatography/combustion/isotope ratio mass spectrometry. *Rapid Communications in Mass Spectrometry*, 26(19), 2359-2364. [Online]. Available at: doi:10.1002/rcm.6349.
- Cramp, L. and Evershed, R.P. (2014). Reconstructing aquatic resource exploitation in human prehistory using lipid biomarkers and stable isotopes. In Holland, H.D. and Turekian, K.K. (eds.). *Treatise on Geochemistry: Archaeology and Anthropology*, 2 ed., Vol. 12. Amsterdam: Elsevier, pp. 319-339.
- Crowther, A., Veall, M-A., Boivin, N., Horton, M., Kotarba-Morley, A., Fuller, D.Q., Fenn, T., Haji, O. and Matheson, C.D. (2015). Use of Zanzibar copal (*Hymenaea verrucosa* Gaertn.) as incense at Unguja Ukuu, Tanzania in the 7-8th century CE: chemical insights into trade and Indian Ocean interactions. *Journal of Archaeological Science*, 53, 374-390. [Online]. Available at: doi:10.1016/j.jas.2014.10.008.
- Czebreszuk, J., (2013). The Bronze age in the polish lands. In Harding, A. and Fokkens, H. (eds.). *The Oxford Handbook of the European Bronze Age*. Oxford: Oxford University Press, pp. 767-786.
- Czebreszuk, J., (2015). Chapter 4: Únětice culture settlement in the mineralized zone of the site. In Czebreszuk, J. and Müller, J. (eds.). *Bruszczewo III. The settlement and fortification in the mineral zone of the site*. Studien zur Archäologie in Ostmitteleuropa 13. Bonn: Habelt, pp. 53-238.

Czebreszuk, J. and Müller, J. (eds.). (2004). *Bruszczewo I: Ausgrabungen und Forschungen in einer prähistorischen Fundregion Großpolens. Forschungsstand - Erste Ergebnisse - Das östliche Feuchtbodenareal*. Studien zur Archäologie in Ostmitteleuropa 2. Poznan: VML Rahden.

Czebreszuk and Jager (2015). Chapter 2: Stratigraphy of fortifications in the mineralised area of the site. In Czebreszuk, J. and Müller, J. (eds.). *Bruszczewo III. The settlement and fortification in the mineral zone of the site*. Studien zur Archäologie in Ostmitteleuropa 13. Bonn: Habelt, pp. 31-42.

Czebreszuk, J. and Müller, J. (eds.). (2015). *Bruszczewo III. The settlement and fortification in the mineral zone of the site*. Studien zur Archäologie in Ostmitteleuropa 13. Bonn: Habelt.

Czebreszuk, J., Jaeger, M., Stróżyk, M., (2015e). Chapter 5: Únětice culture pottery from the fortifications. In Czebreszuk, J. and Müller, J. (eds.). *Bruszczewo III. The settlement and fortification in the mineral zone of the site*. Studien zur Archäologie in Ostmitteleuropa 13. Bonn: Habelt, pp. 239-284.

Czebreszuk, J., Müller, J., Jaeger, M., Kneisel, J. (2015c). Chapter 2: Absolute chronology of settlement. In Czebreszuk, J., Müller, J., Jaeger, M. and Kneisel, J. (eds.). *Bruszczewo IV: Natural resources and economic activities of the Bronze Age people*. Studien zur Archäologie in Ostmitteleuropa 14. Bonn: Habelt, pp. 39-52.

Czebreszuk, J., Müller, J., Jaeger, M. and Kneisel, J. (eds.). (2015d). *Bruszczewo IV: Natural resources and economic activities of the Bronze Age people*. Studien zur Archäologie in Ostmitteleuropa 14. Bonn: Habelt.

Dal Corso, M., Nicosia, C., Balista, C., Cupitò, M., Longa, E.D. and Kirleis, W. (2017). Bronze Age crop processing evidence in the phytolith assemblages from the ditch and fen around Fondo Paviani, northern Italy. *Vegetation History and Archaeobotany*, 26(1), 5-24. [Online]. Available at: doi:10.1007/s00334-016-0573-z.

Dall'Asta, M., Calani, L., Tedeschi, M., Jechiu, L., Brighenti, F. and Del Rio, D. (2012). Identification of microbial metabolites derived from in vitro fecal fermentation of different polyphenolic food sources. *Nutrition*, 28(2), 197-203. [Online]. Available at: doi:10.1016/j.nut.2011.06.005.

de Laeter, J.R. Böhlke, J.K., De Bièvre, P., Hidaka, H., Peiser, H.S., Rosman, K.J.R. and Taylor, P.D.P. (2003). Atomic weights of the elements. Review 2000 (IUPAC Technical Report). *Pure and Applied Chemistry*, 75(6), 683-800. [Online]. Available at: doi:10.1351/pac200375060683.

DeNiro, M.J. (1987). Stable Isotopy and Archaeology. *American Scientist*, 75(2), 182-191. [Online]. Available at: <http://www.jstor.org/stable/27854539>.

DeNiro, M.J. and Epstein, S. (1978). Influence of diet on the distribution of carbon isotopes in animals. *Geochimica et Cosmochimica Acta*, 42(5), 495-506. [Online]. Available at: doi:10.1016/0016-7037(78)90199-0.

Dimoula, A. (2017). In the trenches: Old sites, new finds and the Early Neolithic Period in Macedonia, Greece. In: Shapland, A. and Stefani, E. (eds). *Archaeology Behind the Battle*

Lines: The Macedonian Campaign (1915-19) and its Legacy. [Online]. Routledge. Available at:

<https://books.google.co.uk/books?hl=en&lr=&id=EpkuDwAAQBAJ&oi=fnd&pg=PA1930&dq=dimoula+2017+lete&ots=xN-vtgXaop&sig=zCainFlvsz5M-RPXssRCsRFpiOE>.

Dimoula, A., Pentedeka, A. and Filis, K. (2012). Lete I. The pottery of a Neolithic site in central Macedonia 100 years after. *A Century of Research in Prehistoric Macedonia*, 491-503. [Online]. Available at: [10.13140/RG.2.1.2324.4002](https://doi.org/10.13140/RG.2.1.2324.4002).

Dimoula, A., Koulidou, S., Tsirtsoni, Z., Standall, E.A., Craig, O. and Valamoti, S.M. (2021). Fusion cuisine in the shadow of Mount Olympus: an integrated study of Mycenaean cooking pots. Unpublished paper presented at 'Archaeological Excavations in Macedonia and Thrace' April 2021, Thessaloniki.

Dong, G., Yang, Y., Han, J., Wang, H. and Chen, F. (2017). Exploring the history of cultural exchange in prehistoric Eurasia from the perspectives of crop diffusion and consumption. *Science China Earth Sciences*, 60(6), 1110-1123. [Online]. Available at: [doi:10.1007/s11430-016-9037-x](https://doi.org/10.1007/s11430-016-9037-x).

Dotsika, E., Diamantopoulos, G., Lykoudis, S., Gougoura, S., Kranioti, E., Karalis, P., Michael, D., Samartzidou, E. and Palaigeorgiou, E. (2019). Establishment of a Greek Food Database for Palaeodiet Reconstruction: Case Study of Human and Fauna Remains from Neolithic to Late Bronze Age from Greece. *Geosciences Journal*, 9(4), 165. [Online]. Available at: <https://doi.org/10.3390/geosciences9040165>.

Dreslerová, D. and Kočár, P. (2013). Trends in cereal cultivation in the Czech Republic from the Neolithic to the Migration period (5500 B.C.-A.D. 580). *Vegetation History and Archaeobotany*, 22(3), 257-268. [Online]. Available at: [doi:10.1007/s00334-012-0377-8](https://doi.org/10.1007/s00334-012-0377-8).

Drieu, L., Horgnies, M., Binder, D., Pétrequin, P., Pétrequin, A-M., Peche-Quilichini, K., Lachenal, T. and Regert, M. (2019). Influence of porosity on lipid preservation in the wall of archaeological pottery. *Archaeometry*, 61(5), 1081-1096. [Online]. Available at: [doi:10.1111/arcm.12479](https://doi.org/10.1111/arcm.12479).

Drieu, L., Rageot, M., Wales, N., Stern, B., Lundy, J., Zerrer, M., Gaffney, I., Bondetti, M., Spiteri, C., Thomas-Oates, J. and Craig, O.E. (2020). Is it possible to identify ancient wine production using biomolecular approaches?. *Science & Technology of Archaeological Research*, 6(1), 1-14. [Online]. Available at: [doi:10.1080/20548923.2020.1738728](https://doi.org/10.1080/20548923.2020.1738728).

Dubois, V., Breton, S., Linder, M., Fanni, J. and Parmentier, M. (2007). Fatty acid profiles of 80 vegetable oils with regard to their nutritional potential. *European Journal of Lipid Science and Technology*, 109(7), 710-732. [Online]. Available at: [doi:10.1002/ejlt.200700040](https://doi.org/10.1002/ejlt.200700040).

Dudd, S.N. (1999). Molecular and isotopic characterisation of animal fats in archaeological pottery. Unpublished: University of Bristol. PhD. [Online]. Available at: <https://research-information.bris.ac.uk/ws/portalfiles/portal/34490556/DX213544.pdf>.

Dudd, S.N., and Evershed, R.P. (1998). Direct demonstration of milk as an element of archaeological economies. *Science*, 282(5393), 1478-1481. [Online]. Available at: [doi:10.1126/science.282.5393.1478](https://doi.org/10.1126/science.282.5393.1478).

Dudd, S.N. and Evershed, R.P. (1999). Unusual triterpenoid fatty acyl ester components of archaeological birch bark tars. *Tetrahedron Letters*, 40(2), 359-362. [Online]. Available at: doi:10.1016/S0040-4039(98)02311-9.

Dudd, S.N., Regert, M. and Evershed, R.P. (1998). Assessing microbial lipid contributions during laboratory degradations of fats and oils and pure triacylglycerols absorbed in ceramic potsherds. *Organic Geochemistry*, 29(5), 1345-1354. [Online]. Available at: doi:10.1016/S0146-6380(98)00093-X.

Dunne, J., Mercuri, A.M., Evershed, R.P., Bruni, S. and Di Lernia, S. (2016). Earliest direct evidence of plant processing in prehistoric Saharan pottery. *Nature Plants*, 3, 16194. [Online]. Available at: doi:10.1038/nplants.2016.194.

Dunne, J., Chapman, A., Blinkhorn, P. and Evershed, R.P. (2019). Reconciling organic residue analysis, faunal, archaeobotanical and historical records: Diet and the medieval peasant at West Cotton, Raunds, Northamptonshire. *Journal of Archaeological Science*, 107, 58-70. [Online]. Available at: doi:10.1016/j.jas.2019.04.004.

Effenberger, H. (2018). The plant economy of the Northern European Bronze Age—more diversity through increased trade with southern regions. *Vegetation History and Archaeobotany*, 27(1), 65-74. [Online]. Available at: doi:10.1007/s00334-017-0621-3.

Ethier, J., Bánffy, E., Vuković, J., Leshtakov, K., Bacvarov, K., Roffet-Salque, M., Evershed, R.P. and Ivanova, M. (2017). Earliest expansion of animal husbandry beyond the Mediterranean zone in the sixth millennium BC. *Scientific Reports*, 7(1), 7146. [Online]. Available at: doi:10.1038/s41598-017-07427-x.

Evershed, R.P. (1993). Biomolecular archaeology and lipids. *World Archaeology*, 25(1), 74-93. [Online]. Available at: doi:10.1080/00438243.1993.9980229.

Evershed, R.P. (2008a). Experimental approaches to the interpretation of absorbed organic residues in archaeological ceramics. *World Archaeology*, 40(1), 26-47. [Online]. Available at: doi:10.1080/00438240801889373.

Evershed, R.P. (2008b). Organic residue analysis in archaeology: the archaeological biomarker revolution. *Archaeometry*, 50(6), 895-924. [Online]. Available at: <http://onlinelibrary.wiley.com/doi/10.1111/j.1475-4754.2008.00446.x/full>.

Evershed, R.P. (2009). Compound-specific stable isotopes in organic residue analysis in archaeology. In Colombini, M.P. and Modugno, F. (eds.), (2009). *Organic mass spectrometry in art and archaeology*. New York: John Wiley & Sons. pp. 391-432.

Evershed, R.P., Heron, C. and Goad, L.J. (1991). Epicuticular wax components preserved in potsherds as chemical indicators of leafy vegetables in ancient diets. *Antiquity*, 65(248), 540-544. [Online]. Available at: doi:10.1017/S0003598X00080145.

Evershed, R.P., Heron, C., Charters, S. and Goad, L.J. (1992). The survival of food residues: new methods of analysis, interpretation and application. *Proceedings of the British Academy*, 77, 187-208. [Online]. Available at: <http://www.britac.ac.uk/pubs/proc/files/77p187.pdf>.

Evershed, R.P., Arnot, K.I., Collister, J., Eglinton, G. and Charters, S. (1994). Application of isotope ratio monitoring gas chromatography-mass spectrometry to the analysis of

organic residues of archaeological origin. *The Analyst*, 119(5), 909-914. [Online]. Available at: doi:10.1039/AN9941900909.

Evershed, R.P., Stott, A.W., Raven, A., Dudd, S.N., Charters, S. and Leyden, A. (1995). Formation of long-chain ketones in ancient pottery vessels by pyrolysis of acyl lipids. *Tetrahedron Letters*, 36(48), 8875-8878. [Online]. Available at: doi:10.1016/0040-4039(95)01844-8.

Evershed, R.P., Vaughan, S.J., Dudd, S.N. and Soles, J.S. (1997). Fuel for thought? Beeswax in lamps and conical cups from Late Minoan Crete. *Antiquity*, 71(274), 979-985. [Online]. Available at: <https://doi.org/10.1017/S0003598X00085860>.

Evershed, R.P., Dudd, S.N., Charters, S., Mottram, H., Stott, A.W., Raven, A., van Bergen, P.F. and Bland, H.A. (1999). Lipids as carriers of anthropogenic signals from prehistory. *Philosophical Transactions of the Royal Society B, Biological Sciences*, 354(1379), 19-31. [Online]. Available at: <https://royalsocietypublishing.org/doi/abs/10.1098/rstb.1999.0357>.

Evershed, R.P., Dudd, S.N., Anderson-Stojanovic, V.R. and Gebhard, E.R. (2003). New Chemical Evidence for the Use of Combed Ware Pottery Vessels as Beehives in Ancient Greece. *Journal of Archaeological Science*, 30(1), 1-12. [Online]. Available at: doi:10.1006/jasc.2001.0827.

Evershed, R.P., Copley, M.S., Dickson, L. and Hansel, F.A. (2008a). Experimental evidence for the processing of marine animal products and other commodities containing polyunsaturated fatty acids in pottery vessels. *Archaeometry*, 50(1), 101-113. [Online]. Available at: doi:10.1111/j.1475-4754.2007.00368.x.

Evershed, R.P., Payne, S., Sherratt, A.G., Copley, M.S., Coolidge, J., Urem-Kotsu, D., Kotsakis, K., Özdoğan, M., Özdoğan, A.E., Nieuwenhuys, O., Akkermans, P.M.M.G., Bailey, D., Andeescu, R-R., Campbell, S., Farid, S., Hodder, I., Yalman, N., Özbaşaran, M., Bıçakçı, E., Garfinkel, Y., Levy, T. and Burton, M.M. (2008b). Earliest date for milk use in the Near East and southeastern Europe linked to cattle herding. *Nature*, 455(7212), 528-531. [Online]. Available at: doi:10.1038/nature07180.

Fahy, E., Subramaniam, S., Brown, H.A., Glass, C.K., Merrill, A.H., Jr, Murphy, R.C., Raetz, C.R.H., Russell, D.W., Seyama, Y., Shaw, W., Shimizu, T., Spener, F., van Meer, G., VanNieuwenhze, M.S., White, S.H., Witztum, J.L. and Dennis, E.A. (2005). A comprehensive classification system for lipids. *Journal of Lipid Research*, 46(5), 839-861. [Online]. Available at: doi:10.1194/jlr.E400004-JLR200.

FAOSTAT (2019). [Online]. Rome: Food and Agriculture Organization of the United Nations (FAO). Available at: <http://www.fao.org/faostat/en/#data/QCL>.

Farquhar, G.D., Ehleringer, J.R. and Hubick, K.T. (1989). Carbon Isotope Discrimination and Photosynthesis. *Annual Review of Plant Physiology and Plant Molecular Biology*, 40(1), 503-537. [Online]. Available at: doi:10.1146/annurev.pp.40.060189.002443.

FASTIONLINE. (2021). *Himitliyata Settlement Mound*. [Online]. FASTIONLINE. http://www.fastionline.org/excavation/site/AIAC_765. [Accessed 29 August 2021].

Filipović, D., Meadows, J. Corso, M.D., Kirleis, W., Alsleben, A., Akeret, Ö., Bittmann, F., Bosi, G., Ciută, B., Dreslerová, D., Effenberger, H., Gyulai, F., Heiss, A.G., Hellmund, M., Jahns, S., Jakobsch, T., Kapcia, M., Kloöß, S., Kohler-Schneider, M., Kroll, H., Makarowicz, P., Marinova, E., Märkle, T., Medović, A., Mercuri, A.M., Mueller-Bieniek, A., Nisbet, R., Pashkevich, G., Perego, R., Pokorný, P., Pospieszny, Ł., Przybyła, M., Reed, K., Rennwanz, J., Stika, H.-P., Stobbe, A., Tolar, T., Wasylkova, K., Wiethold, J. and Zerl, T. (2020). New AMS ¹⁴C dates track the arrival and spread of broomcorn millet cultivation and agricultural change in prehistoric Europe. *Scientific Reports*, 10(1), 1-18. [Online]. Available at: <https://doi.org/10.1038/s41598-020-70495-z>.

Flad, R., Schuicheng, L., Xiaohong, W. and Zhijun, Z. (2010). Early wheat in China: Results from new studies at Donghuishan in the Hexi Corridor. *Holocene*, 20(6), 955-965. [Online]. Available at: <https://doi.org/10.1177/0959683609358914>.

Frachetti, M.D., Spengler, R.N., Fritz, G.J. and Mar'yashev, A.N. (2010). Earliest direct evidence for broomcorn millet and wheat in the central Eurasian steppe region. *Antiquity*, 84(326), 993-1010. [Online]. Available at: <https://doi.org/10.1017/S0003598X0006703X>.

Fraser, R.A., Bogaard, A., Heaton, T., Charles, M., Jones, G., Christensen, B.T., Halstead, P., Merbach, I., Poulton, P.R., Sparkes, D. and Styring, A.K. (2011). Manuring and stable nitrogen isotope ratios in cereals and pulses: towards a new archaeobotanical approach to the inference of land use and dietary practices. *Journal of Archaeological Science*, 38(10), 2790-2804. [Online]. Available at: [doi:10.1016/j.jas.2011.06.024](https://doi.org/10.1016/j.jas.2011.06.024).

Fraser, R.A., Bogaard, A., Charles, M., Styring, A.K., Wallace, M., Jones, G., Ditchfield, P. and Heaton, T.H.E. (2013). Assessing natural variation and the effects of charring, burial and pre-treatment on the stable carbon and nitrogen isotope values of archaeobotanical cereals and pulses. *Journal of Archaeological Science*, 40(12), 4754-4766 [Online]. Available at: [doi:10.1016/j.jas.2013.01.032](https://doi.org/10.1016/j.jas.2013.01.032).

Friedli, H., Löttscher, H., Oeschger, H., Siegenthaler, U. and Stauffer, B. (1986). Ice core record of the ¹³C/¹²C ratio of atmospheric CO₂ in the past two centuries. *Nature*, 324(6094), 237-238. [Online]. Available at: <https://link.springer.com/content/pdf/10.1038/324237a0.pdf>.

Gago-Ferrero, P., Alonso, M.B., Bertozzi, C.P., Marigo, J., Barbosa, L., Cremer, M., Secchi, E.R., Azevedo, A., Lailson-Brito Jr, J., Torres, J.P. and Malm, O. (2013). First determination of UV filters in marine mammals. Octocrylene levels in Franciscana dolphins. *Environmental Science & Technology*, 47(11), 5619–5625. [Online]. Available at: [doi:10.1021/es400675y](https://doi.org/10.1021/es400675y).

Gamarra, B., Howcroft, R., McCall, A., Dani, J., Hajdú, Z., Nagy, E.G., Szabó, L.D. and Domboróczki, L. (2018). 5000 years of dietary variations of prehistoric farmers in the Great Hungarian Plain. *PLOS ONE*, 13(5), 1-20. [Online]. Available at: <https://doi.org/10.1371/journal.pone.0197214>.

Gamba, C. Jones, E.R., Teasdale, M.D., McLaughlin, R.L., Gonzalez-Fortes, G., Mattiangeli, V., Domboróczki, L., Kóvári, I., Pap, I., Anders, A., Whittle, A., Dani, J., Raczky, P., Higham, T.F.G., Hofreiter, M., Bradley, D.G. and Pinhasi, R. (2014). Genome flux and stasis in a five millennium transect of European prehistory. *Nature Communications*, 5, 5257-5256. [Online]. Available at: [doi:10.1038/ncomms6257](https://doi.org/10.1038/ncomms6257).

- Ganzarolli, G., Alexander, M., Arnau, A.C. and Craig, O.E., (2018). Direct evidence from lipid residue analysis for the routine consumption of millet in Early Medieval Italy. *Journal of Archaeological Science*, 96, 124-130. [Online]. Available at: doi:10.1016/j.jas.2018.06.007.
- García-Granero, J.J., Urem-Kotsou, D., Bogaard, A. and Kotos, S., (2018). Cooking plant foods in the northern Aegean: Microbotanical evidence from Neolithic Stavroupoli (Thessaloniki, Greece). *Quaternary International*, 496, 140-151. [Online]. Available at: doi:10.1016/j.quaint.2017.04.007.
- Garnier, N. and Valamoti, S.M. (2016). Prehistoric wine-making at Dikili Tash (Northern Greece): Integrating residue analysis and archaeobotany. *Journal of Archaeological Science*, 74, 195-206. [Online]. Available at: doi:10.1016/j.jas.2016.03.003.
- Garnier, N., Richardin, P., Cheynier, V. and Regert, M. (2003). Characterization of thermally assisted hydrolysis and methylation products of polyphenols from modern and archaeological vine derivatives using gas chromatography-mass spectrometry. *Analytica Chimica Acta*, 493(2), 137-157. [Online]. Available at: doi:10.1016/S0003-2670(03)00869-9.
- Gerling, C. (2013). A multi-isotopic approach to the reconstruction of prehistoric mobility and economic patterns in the West Eurasian steppes 3500 to 300 BC. *Journal for Ancient Studies*, (3), 1-21. [Online]. Available at: <https://refubium.fu-berlin.de/handle/fub188/19673>.
- Gershenzon, J. (1984). Changes in the Levels of Plant Secondary Metabolites Under Water and Nutrient Stress. In B. N. Timmermann, C. Steelink, and F. A. Loewus (Eds.) *Phytochemical Adaptations to Stress*. Boston, MA: Springer US, pp. 273-320. [Online]. Available at: doi:10.1007/978-1-4684-1206-2_10.
- Ghilardi, M., Fouache, F., Queyrel, F., Syrides, G., Vouvalidis, K., Kunesch, S., Styllas, M. and Stiros, S. (2008). Human occupation and geomorphological evolution of the Thessaloniki Plain (Greece) since mid Holocene. *Journal of Archaeological Science*, 35(1), 111-125. [Online]. Available at: doi:10.1016/j.jas.2007.02.017.
- Giblin, J.I. and Yerkes, R.W. (2016). Diet, dispersal and social differentiation during the Copper Age in eastern Hungary. *Antiquity*, 90(349), 81-94. [Online] Available at <http://doi:10.15184/aqy.2016.3>.
- González-Carretero, L., Wollstonecroft, M. and Fuller, D.Q. (2017). A methodological approach to the study of archaeological cereal meals: a case study at Çatalhöyük East (Turkey). *Vegetation History and Archaeobotany*, 26(4), 415-432. [Online]. Available at: doi:10.1007/s00334-017-0602-6.
- Goslar, T., Jankowski, M., Koško, A. and Lityńska-Zajac, M. (2017). Builders and Users of Ritual Centres, Yampil Barrow Complex: Studies of Diet Based on Stable Carbon and Nitrogen Isotope Composition. *Baltic-Pontic Studies*, 22(1), 91-125. [Online]. Available at: <https://doi.org/10.1515/bps-2017-0023>.
- Guasch-Jané, M.R., Ibern-Gómez, M., Andrés-Lacueva, C., Jáuregui, O. and Lamuela-Raventós, R.M. (2004). Liquid chromatography with mass spectrometry in tandem mode

- applied for the identification of wine markers in residues from ancient Egyptian vessels. *Analytical Chemistry*, 76(6), 1672-1677 [Online]. Available at: doi:10.1021/ac035082z.
- Gurova, M. and Chohadzhiev, A. (2019). Enigmatic artefacts from the Chalcolithic tell Petko Karavelovo (Veliko Tarnovo district). *Българско е-Списание за Археология*. 9. 119-129. [Online]. Available at: <https://www.cceol.com/content-files/document-871465.pdf>.
- Gyulai, F. (2014). The history of broomcorn millet (*Panicum miliaceum* L.) In the Carpathian-basin in the mirror of archaeobotanical remains II. From the roman age until the late medieval age. *Columella*, 1(1), 39-48. [Online]. Available at: doi:10.18380/SZIE.COLUM.2014.1.1.39..
- Halstead, P. and Isaakidou, V. (2011). Revolutionary secondary products: the development and significance of milking, animal-traction and wool-gathering in later prehistoric Europe and the Near East. In Wilkinson, T.C., Sherratt, S. and Bennet. J., (eds.). *Interweaving worlds: systemic interactions in Eurasia, 7th to 1st millennia BC*. Oxford: Oxbow, pp. 61-76.
- Halstead, P. (2012). *Feast, food and fodder in Neolithic-Bronze Age Greece: Commensality and the construction of value*. *eTopoi*, 2, 21-51. [Online]. Available at: doi:10.17169/REFUBIUM-22386 [Accessed 4 August 2021].
- Halstead, P. and Isaakidou, V. (2013). Early stock-keeping in Greece. In S. College, J. Conolly, K. Dobney, K Manning and S. Shennan (Eds). *The Origins and Spread of Stock-keeping in the Near East and Europe*. New York: Routledge, pp. 129-144.
- Hammann, S. and Cramp, L.J.E. (2018). Towards the detection of dietary cereal processing through absorbed lipid biomarkers in archaeological pottery. *Journal of Archaeological Science*, 93, 74-81. [Online]. Available at: doi:10.1016/j.jas.2018.02.017.
- Hammer, B.T., Fogel, M.L. and Hoering, T.C. (1998). Stable carbon isotope ratios of fatty I acids in seagrass and redhead ducks. *Chemical Geology*, 152(1), 29-41. [Online]. Available at: doi:10.1016/S0009-2541(98)00094-1.
- Handley, L.L., Austin, A.T., Stewart, G.R., Robinson, D., Scrimgeour, C.M., Raven, J.A., Heaton, T.H.E. and Schmidt, S. (1999). The $\delta^{15}\text{N}$ natural abundance ($\delta^{15}\text{N}$) of ecosystem samples reflects measures of water availability. *Functional plant biology*, 26(2), 185-199. [Online]. Available at: doi:10.1071/PP98146.
- Hansel, F.A., Copley, M.S., Madureira, L.A. and Evershed, R.P. (2004). Thermally produced ω -(o-alkylphenyl) alkanic acids provide evidence for the processing of marine products in archaeological pottery vessels. *Tetrahedron Letters*, 45(14), 2999-3002. [Online]. Available at: doi:10.1016/j.tetlet.2004.01.111.
- Hart, J.P., Lovis, W.A., Schulenberg, J.K. and Urquhart, G.R. (2007). Paleodietary implications from stable carbon isotope analysis of experimental cooking residues. *Journal of Archaeological Science*, 34(5), 804-813. [Online]. Available at: doi:10.1016/j.jas.2006.08.006.
- Hart, J.P., Urquhart, G.R., Feranec, R.S. and Lovis, W.A. (2009). Non-linear relationship between bulk $\delta^{13}\text{C}$ and percent maize in carbonized cooking residues and the potential

- of false-negatives in detecting maize. *Journal of Archaeological Science*, 36(10), 2206-2212 [Online]. Available at: doi:10.1016/j.jas.2009.06.005.
- Heaton, T.H.E., Jones, G., Halstead, P. and Tsipopoulos, T. (2009). Variations in the $^{13}\text{C}/^{12}\text{C}$ ratios of modern wheat grain, and implications for interpreting data from Bronze Age Assiros Toumba, Greece. *Journal of Archaeological Science*, 36(10), 2224-2233. [Online]. Available at: doi:10.1016/j.jas.2009.06.007.
- Heiss, A. G. (2014). Ceremonial foodstuffs from prehistoric burnt-offering places in the Alpine region. In A. Chevalier, E. Marinova, and L. Peña-Chocarro (eds). *Plants and People: Choices and Diversity through Time*. Oxford: Oxbow Books, pp. 343-353.
- Helwig, K., Monahan, V., Poulin, J. and Andrews, T.D. (2014). Ancient projectile weapons from ice patches in northwestern Canada: identification of resin and compound resin-ochre hafting adhesives. *Journal of Archaeological Science*, 41, 655-665. [Online]. Available at: doi:10.1016/j.jas.2013.09.010.
- Hendy, J. (2021). Ancient protein analysis in archaeology. *Science Advances*, 7(3), [Online]. Available at: doi:10.1126/sciadv.abb9314.
- Hendy, J., Colonese, A.C., Franz, I., Fernandes, R., Fischer, R., Orton, D., Lucquin, A., Spindler, L., Anvari, J., Stroud, E., Biehl, P.F., Speller, C., Boivin, N., Mackie, M., Jersie-Christensen, R.R., Olsen, J.V., Collins, M.J., Craig O.E. and Rosenstock E. (2018). Ancient proteins from ceramic vessels at Çatalhöyük West reveal the hidden cuisine of early farmers. *Nature Communications*, 9(1), 1-10. [Online]. Available at: DOI: 10.1038/s41467-018-06335-6.
- Hermes, T.R., Frachetti, M.D., Dupuy, P.N.D., Mar'yashev, A., Nebel, A. and Makarewicz, C.A. (2019). Early integration of pastoralism and millet cultivation in Bronze Age Eurasia. *Proceedings of the Royal Society B*, 286(1910), 1-9. [Online]. Available at: <https://doi.org/10.1098/rspb.2019.1273>.
- Heron, C. and Evershed, R.P. (1993). The Analysis of Organic Residues and the Study of Pottery Use. *Archaeological Method and Theory*, 5, 247-284. [Online]. Available at: <http://www.jstor.org/stable/20170233>.
- Heron, C. and Craig, O.E. (2015). Aquatic Resources in Foodcrusts: Identification and Implication. *Radiocarbon*, 57(4), 707-719. [Online]. Available at: doi:10.2458/azu_rc.57.18454.
- Heron, C., Evershed, R.P. and Goad, L.J. (1991). Effects of migration of soil lipids on organic residues associated with buried potsherds. *Journal of Archaeological Science*, 18(6), 641-659. [Online]. Available at: doi:10.1016/0305-4403(91)90027-M.
- Heron, C., Craig, O.E., Luquin, A., Steele, V.J., Thompson, A. and Piličiauskas, G. (2015). Cooking fish and drinking milk? Patterns in pottery use in the southeastern Baltic, 3300-2400 cal BC. *Journal of Archaeological Science*, 63, 33-43. [Online]. Available at: doi:10.1016/j.jas.2015.08.002.
- Heron, C., Shoda, S., Barcons, A.B., Czebreszuk, J., Eley, Y., Gorton, M., Kirleis, W., Kneisel, J., Lucquin, A., Müller, J. and Nishida, Y. (2016). First molecular and isotopic evidence of

millet processing in prehistoric pottery vessels. *Scientific Reports*, 6, 38767 -38776. [Online]. Available at: doi:10.1038/srep38767.

Herrscher, E., Poulmarc'h, M., Pecqueur, L., Jovenet, E., Benecke, N., Decaix, A., Lyonnet, B., Guliyev, F. and André, G. (2018a). Dietary inferences through stable isotope analysis at the Neolithic and Bronze Age in the southern Caucasus (sixth to first millennium BC, Azerbaijan): From environmental adaptation to social impacts. *American Journal of Physical Anthropology*, 167(4), 856-875. [Online]. Available at: <http://journals.openedition.org/pm/1367>.

Higham, T., Warren, R., Belinskij, A., Härke, H. and Wood, R. (2010). Radiocarbon Dating, Stable Isotope Analysis, and Diet-Derived Offsets in 14C Ages from the Klin-Yar Site, Russian North Caucasus. *Radiocarbon*, 52(2), 653-670. [Online]. Available at: doi:10.1017/S0033822200045689.

Hjulström, B., Isaksson, S. and Hennius, A. (2006). Organic Geochemical Evidence for Pine Tar Production in Middle Eastern Sweden During the Roman Iron Age. *Journal of archaeological Science*, 33(2), 283-294. [Online]. Available at: doi:10.1016/j.jas.2005.06.017.

Hollund, H. I., Higham, T., Belinskij, A. and Korenevskij, S. (2010). Investigation of palaeodiet in the North Caucasus (South Russia) Bronze Age using stable isotope analysis and AMS dating of human and animal bones. *Journal of Archaeological Science*, 37(12), 2971-2983. [Online]. Available at: doi:10.1016/j.jas.2010.08.009.

Honch, N. V., Higham, T.F., Chapman, J., Gaydarska, B. and Hedges, R.E. (2006). A palaeodietary investigation of carbon (13C/12C) and nitrogen (15N/14N) in human and faunal bones from the Copper Age cemeteries of Varna I and Durankulak, Bulgaria. *Journal of Archaeological Science*, 33(11), 1493-1504. [Online]. Available at: doi:10.1016/j.jas.2006.02.002.

Horiuchi, A., Miyata, Y., Kamijo, N., Cramp, L. and Evershed, R.P. (2015). A Dietary Study of the Kamegaoka Culture Population during the Final Jomon Period, Japan, Using Stable Isotope and Lipid Analyses of Ceramic Residues. *Radiocarbon*, 57(4), 721-736. [Online]. Available at: doi:10.2458/azu_rc.57.18455.

Hrisrova, I., Atanassova, J. and Marinova, E. (2017). Plant economy and vegetation of the Iron Age in Bulgaria: archaeobotanical evidence from pit deposits. *Archaeological and Anthropological Sciences*, 9(7), 1481-1494. [Online]. Available at: doi:10.1007/s12520-016-0328-x.

Huang, W-Y., Liu, Y.-M., Wang, J., Wang, X-N. and Li, C-Y. (2014). Anti-inflammatory effect of the blueberry anthocyanins malvidin-3-glucoside and malvidin-3-galactoside in endothelial cells. *Molecules*, 19(8), 12827-12841. [Online]. Available at: doi:10.3390/molecules190812827.

Hunt, H.V., Vander Linden, M., Liu, X., Motuzaitė-Matuzevičiūtė, G., Colledge, S. and Jones, M.K. (2008). Millets across Eurasia: chronology and context of early records of the genera *Panicum* and *Setaria* from archaeological sites in the Old World. *Vegetation History and Archaeobotany*, 17(Suppl 1), 5-18. [Online]. Available at: doi:10.1007/s00334-008-0187-1.

- Hunt, H. V., Campana, M.G., Lawes, M.C., PARK, Y.J., Bower, M.A., Howe, C.J. and Jones, M.K. (2011). Genetic diversity and phylogeography of broomcorn millet (*Panicum miliaceum* L.) across Eurasia. *Molecular Ecology*, 20(22), 4756-4771. [Online]. Available at: doi:10.1111/j.1365-294X.2011.05318.x.
- Hunt, H. V., Badakshi, F., Romanova, O., Howe, C.J., Jones, M.K. and Heslop-Harrison, J.P. (2014). Reticulate evolution in *Panicum* (Poaceae): the origin of tetraploid broomcorn millet, *P. miliaceum*. *Journal of Experimental Botany*, 65(12), 3165-3175. [Online]. Available at: doi:10.1093/jxb/eru161.
- Hunt, H. V., Rudzinski, A., Jiang, H., Wang, R., Thomas, M.G. and Jones, M.K. (2018). Genetic evidence for a western Chinese origin of broomcorn millet (*Panicum miliaceum*). *Holocene*, 28(12), 1968-1978. [Online]. Available at: doi:10.1177/0959683618798116.
- Ignaczak, M., (2015). Chapter 7: Lusatian Urnfields pottery assemblages from the site centre. In Czebreszuk, J. and Müller, J. (eds.). *Bruszczewo III. The settlement and fortification in the mineral zone of the site*. Studien zur Archäologie in Ostmitteleuropa 13. Bonn: Habelt, pp. 299-352.
- Isaksson, S. and Nilsson, C. (2018). Analyses of lipid residues in Lusatian pottery from Maciejowice, Poland. *Uppdragsrapport*, 327. [Online]. Available from: <http://urn.kb.se/resolve?urn=urn:nbn:se:su:diva-158652>.
- Ito, H. (1934). The chemical investigation of some gramineae oils. *Journal of the Faculty of Agriculture, Hokkaido Imperial University*, 37(1), 1-40. [Online]. Available at: [https://eprints.lib.hokudai.ac.jp/dspace/bitstream/2115/12704/1/37\(1\)_p1-40.pdf](https://eprints.lib.hokudai.ac.jp/dspace/bitstream/2115/12704/1/37(1)_p1-40.pdf).
- Irvine, B.T. (2017). An Isotopic Analysis of Dietary Habits in Early Bronze Age Anatolia. Unpublished: Freie Universität Berlin. PhD. [Online]. Available at: doi:10.17169/REFUBIUM-11531.
- Irvine, B., Erdal, Y.S. and Richards, M.P. (2019). Dietary habits in the Early Bronze Age (3rd millennium BC) of Anatolia: A multi-isotopic approach. *Journal of Archaeological Science: Reports*, 24, 253-263. [Online]. Available at: doi:10.1016/j.jasrep.2019.01.015.
- Ivanova, M.B. and Leshtakov, P. (2016). Avren-Bobata: A late chalcolithic fortified settlement on the Avren Plateau, Varna District, Northeast Bulgaria. In Bacvarov, K. and Gleser, R. (eds). *Southeast Europe and Anatolia in Prehistory. Essays in Honor of Vassil Nikolov on His 65th Anniversary* (293). Bonn: Habelt, pp. 327–336.
- Jacob, J., Disnar, J-R., Boussafir, M., Spadano Albuquerque, A.L., Sifeddine, A. and Turcq, B. (2005). Pentacyclic triterpene methyl ethers in recent lacustrine sediments (Lagoa do Caçó, Brazil). *Organic Geochemistry*, 36(3), 449-461. [Online]. Available at: doi:10.1016/j.orggeochem.2004.09.005.
- Jacob, J., Disnar, J.R., Arnaud, F., Chapron, E., Debret, M., Lallier-Vergès, E., Desmet, M. and Revel-Rolland, M. (2008a). Millet cultivation history in the French Alps as evidenced by a sedimentary molecule. *Journal of Archaeological Science*, 35(3), 814-820. [Online]. Available at: doi:10.1016/j.jas.2007.06.006.
- Jacob, J., Disnar, J-R. and Bardoux, G. (2008b). Carbon isotope evidence for sedimentary miliacin as a tracer of *Panicum miliaceum* (broomcorn millet) in the sediments of Lake le

- Bourget (French Alps). *Organic Geochemistry*, 39(8), 1077-1080. [Online]. Available at: doi:10.1016/j.orggeochem.2008.04.003.
- Jacob, J., Disnar, J.R., Arnaud, F., Gauthier, E., Billaud, Y., Chapron, E. and Bardoux, G. (2009). Impacts of new agricultural practices on soil erosion during the Bronze Age in the French Prealps. *Holocene*, 19(2), 241-249. [Online]. Available at: doi:10.1177/0959683608100568.
- Jaeger, M., (2016). *Bronze Age Fortified Settlements in Central Europe*. Studien zur Archäologie in Ostmitteleuropa 17. Bonn: Habelt.
- Jaeger, M. and Czebreszuk, J., (2011). Does a periphery look like that. The cultural landscape of the Unetice culture's Kościan group. In Kiel Graduate School (eds.). *Landscapes and Human Development: The Contribution of European Archaeology. Proceedings of the International Workshop "Socio-Environmental Dynamics over the Last 12,000 Years: The Creation of Landscapes (1st-4th April 2009)*. Bonn: Habelt, pp. 217-235.
- Jaeger, M., and Strózyk, M., (2015). Chapter 6. Remains of buildings inside the settlement and daub finds in the mineral zone. In Czebreszuk, J., Müller, J., (eds.). *Bruszczewo III. The settlement and fortification in the mineral zone of the site*. Studien zur Archäologie in Ostmitteleuropa 13. Bonn: Habelt, pp. 285-298.
- Jaybhaye, R.V., Pardeshi, I.L., Vengaiah, P.C. and Srivastav, P.P. (2014). Processing and technology for millet based food products: A review. *Journal of Ready to Eat Food*, 1(2), 32-48. [Online]. Available at: http://jakraya.com/journal/pdf/2-jrefarticle_1.pdf [Accessed 1 July 2021].
- Johnson, J.S., Clark, J., Miller-Antonio, S., Robins, D., Schiffer, M.B. and Skibo, J.M. (1988). Effects of firing temperature on the fate of naturally occurring organic matter in clays. *Journal of Archaeological Science*, 15(4), 403-414. [Online]. Available at: doi:10.1016/0305-4403(88)90038-6.
- Jones, M., Hunt, H., Lightfoot, E., Lister, D., Liu, X. and Motuzaitė-Matuzevičiūtė, G. (2011). Food globalization in prehistory. *World Archaeology*, 43(4), 665-675. [Online]. Available at: doi:10.1080/00438243.2011.624764.
- Jones, M. K., Hunt, H., Kneale, C., Lightfoot, E., Lister, D., Liu, X. and Motuzaitė-Matuzevičiūtė, G. (2016). Food globalisation in prehistory: The agrarian foundations of an interconnected continent. *Journal of the British Academy*, (4), 73-87. [Online]. Available at: doi: 10.5871/jba/004.073.
- Jullien, R. (1992). Les faunes domestique et sauvage, les moyens de subsistence. In Treuil R (ed.). *Dikili Tash, village préhistorique de Macédoine orientale, I. Fouilles de Jean Deshayes (1961-1975), vol. 1*, BCH Suppl. 24. École Française d'Athènes: Athènes, pp. 147-153.
- Junno, A., Isaksson, S., Hirasawa, Y., Kato, H. and Jordan, P.D. (2020). Evidence of increasing functional differentiation in pottery use among Late Holocene maritime foragers in northern Japan. *Archaeological Research in Asia*, 22, 100194. [Online]. Available at: doi:10.1016/j.ara.2020.100194.

- Kanstrup, M., Thomsen, I.K., Andersen, A.J., Bogaard, A. and Christensen, B.T. (2011). Abundance of ¹³C and ¹⁵N in emmer, spelt and naked barley grown on differently manured soils: towards a method for identifying past manuring practice. *Rapid Communications in Mass Spectrometry*, 25(19), 2879-2887. [Online]. Available at: doi:10.1002/rcm.5176.
- Kapcia, M. and Mueller-Bieniek, A. (2019). An insight into Bronze Age subsistence strategy in forested Carpathian foothills, based on plant macro-remains. *Archaeological and Anthropological Sciences*, 11(6), 2879-2895. [Online]. Available at: doi:10.1007/s12520-018-0720-9.
- Karakaya, D. (2019). Botanical Aspects of the Environment and Economy at Tell Tayinat from the Bronze to Iron Ages (ca. 2.200-600 BCE), in south-central Turkey. Unpublished: Universität Tübingen. PhD. [Online]. Available at: <https://d-nb.info/1206172924/34>.
- Karastoyanova, N., and Chohadziev, A., (2017). Hunting and stock-breeding in the early chalcolith: osteological analysis of mammalian remains in Petko Karavelovo tell, Veliko Tarnovo region. *Annual of Natural Sciences Department*, 5(2017), 96-108. [Online]. Available at: https://www.academia.edu/39635138/Hunting_and_stock_breeding_in_the_early_chalcolith_osteological_analysis_of_mammalian_remains_in_Petko_Karavelovo_tell_Veliko_Tarnovo_region.
- Keeling, C.D., Piper, S.C. and Heimann, M. (2013). A three-dimensional model of atmospheric CO₂ transport based on observed winds: 4. Mean annual gradients and interannual variations. In: *Aspects of Climate Variability in the Pacific and the Western Americas*. Washington D.C.: American Geophysical Union. pp. 305-363. [Online]. Available at: doi:10.1029/gm055p0305.
- Kimpe, K., Jacobs, P.A. and Waelkens, M. (2002). Mass spectrometric methods prove the use of beeswax and ruminant fat in late Roman cooking pots. *Journal of Chromatography A*, 968(1-2), 151-160. [Online]. Available at: doi:10.1016/s0021-9673(02)00825-7.
- Kneisel, J., Czebreszuk, J., Müller, J., and Jaeger, M. (2015). Chapter 1: Excavations in season 2007-2008. In Czebreszuk, J. and Müller, J. (eds.). *Bruszczewo III. The settlement and fortification in the mineral zone of the site*. Studien zur Archäologie in Ostmitteleuropa 13. Bonn: Habelt, pp. 11-30.
- Konstantinidou, A. (2010). Chapter 6: Preliminary analysis and interpretation of the archaeological material. In Stefani, E. (ed.). *Angelochori, Imathia. Late Bronze Age settlement. Angelochori: A Late Bronze Age Settlement in Emathia, Macedonia, Greece*. Vol 1. Thessaloniki: Kyriakidis Brothers, pp. 199-220.
- Kotzamani, G. and Livarda, A. (2018). People and plant entanglements at the dawn of agricultural practice in Greece. An analysis of the Mesolithic and early Neolithic archaeobotanical remains. *Quaternary International*, 496, 80-101. [Online]. Available at: doi:10.1016/j.quaint.2018.04.044.
- Krentscher, C., Dubois, N., Camperio, G., Prebble, M. and Ladd, S.N. (2019). Palmitone as a potential species-specific biomarker for the crop plant taro (*Colocasia esculenta* Schott)

on remote Pacific islands. *Organic Geochemistry*, 132, 1-10. [Online]. Available at: doi:10.1016/j.orggeochem.2019.03.006.

Kroll, H., (2010). Die Archäobotanik von Bruszczewo - Darstellung und Interpretation der Ergebnisse. In Müller, J., Czebreszuk, J. and Kneisel, J. (eds.). *Bruszczewo II: Ausgrabungen und Forschungen in einer prähistorischen Siedlungskammer Großpolens*. Studien zur Archäologie in Ostmitteleuropa 6. Bonn: Habelt, pp. 251-288.

Kučera, L., Peška, J., Fojtík, P., Barták, P., Kučerová, P., Pavelka, J., Komárková, V., Beneš, J., Polcerová, L., Králík, M. and Bednář, P. (2019). First direct evidence of broomcorn millet (*Panicum miliaceum*) in Central Europe. *Archaeological and Anthropological Sciences*, 11(8), 4221-4227. [Online]. Available at: doi:10.1007/s12520-019-00798-4.

Kulkova, M., Kashuba, M., Gavrylyuk, N., Kulkov, A., Kaiser, E., Vetrova, M., Zanoci, A., Platonova, N., Hellström, K. and Winger, K. (2020). Composition of white paste inlay on the pottery from sites of the 10th–8th centuries bce in the northern Pontic region. *Archaeometry*, 62(5), 917-934. [Online]. Available at: doi:10.1111/arcm.12567.

Lee-Thorp, J.A. (2008). On Isotopes and Old Bones. *Archaeometry*, 50(6), 925-950. [Online]. Available at: doi:10.1111/j.1475-4754.2008.00441.x.

Leipe, C., Long, T., Sergusheva, E.A., Wagner, M. and Tarasov, P.E. (2019). Discontinuous spread of millet agriculture in eastern Asia and prehistoric population dynamics. *Science Advances*, 5(9), 1-9. [Online]. Available at: doi:10.1126/sciadv.aax6225.

Leshtakov, L. (2019). Some LBA pyraunoi and vessels with internal lugs from Eastern Bulgaria. In Sîrbu, V., Comşa, A. and Hortopan, D. (eds.). *Digging in the Past of Old Europe: Studies in Honor of Christian Schuster at his 60th Anniversary*. Brăila: Editura Istros a Muzeului Brăilei, pp. 173-188.

Leshtakov, K., Illieva, D., Petrova, V. and Popova, T. (2016). Excavations at the Himitliyata Tell, the Village of Sokol, Nova Zagora Municipality. In Aladzhov, A. (ed). *Archaeological Discoveries & Excavations in 2015*. Sofia: National Institute and Museum of Archaeology, pp. 139-142.

Lespez, L., Tsirtsoni, Z., Darcque, P., Koukouli-Chryssanthaki, H., Malamidou, D., Treuil, R., Davidson, R., Kourtessi-Philippakis, G. and Oberlin, C. (2013). The lowest levels at Dikili Tash, northern Greece: a missing link in the Early Neolithic of Europe. *Antiquity*, 87(335), 30-45. [Online]. Available at: https://www.academia.edu/download/33861995/Lespez-et-al_Antiquity2013.pdf.

Lightfoot, E., Liu, X. and Jones, M.K. (2013). Why move starchy cereals? A review of the isotopic evidence for prehistoric millet consumption across Eurasia. *World Archaeology*, 45(4), 574-623. [Online]. Available at: doi:10.1080/00438243.2013.852070.

Lightfoot, E., Slaus, M. and O'Connell, T.C. (2012). Changing cultures, changing cuisines: Cultural transitions and dietary change in Iron Age, Roman, and Early Medieval Croatia. *American Journal of Physical Anthropology*, 148(4), 543-556. [Online]. Available at: doi:10.1002/ajpa.22070.

Lightfoot, E., Motuzaitė-Matuzevičiute, G., O'Connell, T.C., Kukushkin, I.A., Loman, V., Varfolomeev, V., Liu, X. and Jones, M.K. (2015a). How 'Pastoral' is Pastoralism? Dietary

Diversity in Bronze Age Communities in the Central Kazakhstan Steppes: Dietary diversity in Bronze Age communities, Kazakhstan steppes. *Archaeometry*, 57(51), 232-249. [Online]. Available at: doi:10.1111/arcm.12123.

Lightfoot, E., Šlaus, M., Šikanjić, P.R. and O'Connell, T.C. (2015b). Metals and millets: Bronze and Iron Age diet in inland and coastal Croatia seen through stable isotope analysis. *Archaeological and Anthropological Sciences*, 7(3), 375-386. [Online]. Available at: <https://doi.org/10.1007/s12520-014-0194-3>.

Lillie, M.C. and Richards, M. (2000). Stable Isotope Analysis and Dental Evidence of Diet at the Mesolithic-Neolithic Transition in Ukraine. *Journal of Archaeological Science*, 27(10), 965-972. [Online]. Available at: doi:10.1006/jasc.1999.0544.

Lillie, M.C., Budd, C.E., Potekhina, I., Price, T.D., Sokhatsky, M.P. and Nikitin, A.G. (2017). First isotope analysis and new radiocarbon dating of Trypillia (Tripolye) farmers from Vertebe Cave, Bilche Zolote, Ukraine. *Documenta Praehistorica*, 44(2017), 306-324. [Online]. Available at: http://www.academia.edu/download/55460397/Lillie_et_al_2017_First_isotope_analysis_and_new_dating_of_Vertebe_Cave.pdf.

Lityńska-Zajac, M., Czekaj-Zastawny, A. and Rauba-Bukowska, A. (2017). Utilisation of cultivated and wild plants in the economy of the Linear Pottery Culture in the Upper Vistula basin. *Sprawozdania Archeologiczne*, 69(2017), 271-295. [Online]. Available at: 10.23858/SA69.2017.011.

Liu, X. and Jones, M.K. (2014). Food globalisation in prehistory: top down or bottom up? *Antiquity*, 88(341), 956-963. [Online]. Available at: doi:10.1017/S0003598X00050912.

Liu, X., Jones, P.J., Matuzeviciute, G.M., Hunt, H.V., Lister, D.L., An, T., Przelomska, N., Kneale, C.J., Zhao, Z. and Jones, M.K. (2019). From ecological opportunism to multi-cropping: Mapping food globalisation in prehistory. *Quaternary Science Reviews*, 206, 21-28. [Online]. Available at: doi:10.1016/j.quascirev.2018.12.017.

Long, T., Leipe, C., Jin, G., Wagner, M., Guo, R., Schröder, O. and Tarasov, P.E. (2018). The early history of wheat in China from 14C dating and Bayesian chronological modelling. *Nature Plants*, 4(5), 272-279. [Online]. Available at: doi:10.1038/s41477-018-0141-x.

Lu, H., Zhang, J., Liu, K-B., Wu, N., Li, Y., Zhou, K., Ye, M., Zhang, T., Zhang, H., Yang, X., Shen, L., Xu, D. and Li, Q. (2009a). Earliest domestication of common millet (*Panicum miliaceum*) in East Asia extended to 10,000 years ago. *Proceedings of the National Academy of Sciences of the United States of America*, 106(18), 7367-7372. [Online]. Available at: doi:10.1073/pnas.0900158106.

Lu, H., Zhang, J., Wu, N., Liu, K-B., Xu, D. and Li, Q. (2009b). Phytoliths analysis for the discrimination of Foxtail millet (*Setaria italica*) and Common millet (*Panicum miliaceum*). *PLOS ONE*, 4(2), 1-15. [Online]. Available at: <https://doi.org/10.1371/journal.pone.0004448>.

Lu, T.L-D. (1998). Some botanical characteristics of green foxtail (*Setaria viridis*) and harvesting experiments on the grass. *Antiquity*, 72(278), pp.902-907. [Online]. Available at: doi:10.1017/s0003598x00087548.

Lucejko, J.J., La Nasa, J., Porta, F., Vanzetti, A., Tanda, G., Mangiaracina, C.F., Corretti, A., Colombini, M.P. and Ribechini, E. (2018). Long-lasting ergot lipids as new biomarkers for assessing the presence of cereals and cereal products in archaeological vessels. *Scientific Reports*, 8(1), 1-6. [Online]. Available at: <https://doi.org/10.1038/s41598-018-22140-z>.

Lucquin, A., Colonese, A.C., Farrell, T.F.G. and Craig, O.E. (2016a). Utilising phytanic acid diastereomers for the characterisation of archaeological lipid residues in pottery samples. *Tetrahedron Letters*, 57(6), 703-707. [Online]. Available at: doi: 10.1016/j.tetlet.2016.01.011.

Lucquin, A., Gibbs, K. and Uchiyama, J. (2016b). Ancient lipids document continuity in the use of early hunter-gatherer pottery through 9,000 years of Japanese prehistory. *Proceedings of the National Academy of Science of the United States of America*, 113(15), 3991-3996. [Online]. Available at: <https://www.pnas.org/content/113/15/3991.short>.

Makowiecki, D., (2015). Chapter 3: Animal husbandry and natural environment of the multicultural settlement at Bruszczewo, site 5. A study of faunal remains recovered in 1995-2008. Czebreszuk, J., Müller, J., Jaeger, M., Kneisel, J., (eds.). *Bruszczewo IV: Natural resources and economic activities of the Bronze Age people*. Studien zur Archäologie in Ostmitteleuropa 14. Bonn: Habelt.

Marekovic, S., Karavanic, S., Kudelic, A. and Sostaric, R. (2015). The botanical macroremains from the prehistoric settlement Kalnik-Igrisce (NW Croatia) in the context of current knowledge about cultivation and plant consumption in Croatia and neighboring countries during the Bronze Age. *Acta Societatis Botanicorum Poloniae*, 84(2), 227-235. [Online]. Available at: <http://yadda.icm.edu.pl/yadda/element/bwmeta1.element.agro-e62ba55c-2083-4980-a77c-56d5d22b3b00>.

Malamidou, D., Ntinou, M., Valamoti, S-M., Tsirtsoni, Z., Koukouli-Chryssanthaki, H. and Darcque, P. (2018). An investigation of Neolithic settlement pattern and plant exploitation at Dikili Tash: Reconsidering old and new data from the late 5th millennium BC settlement. In Kalogeropoulou, E., Kalayci, T., Karimali, E. and Sarris, A. (eds.). *Communities, Landscapes and Interaction in Neolithic Greece. Proceedings of the International Conference, 29-30 May 2015*. International Monographs in Prehistory: Archaeological Series. Rethymno: Berghahn Books, pp. 60-80. [Online]. Available at: doi: 10.2307/j.ctvw049k3.11.

March, R.J. (2013). Searching for the functions of fire structures in Eynan (Mallaha) and their formation processes: a geochemical approach. In Bar-Yosef, O. and Valla, F.R. (eds.). *Natufian foragers in the Levant: Terminal Pleistocene social changes in Western Asia*, Vol. 19. Berghahn Books. Ann Arbor: International Monographs in Prehistory, pp. 227-283.

Marinova, E. and Atanassova, J. (2006). Anthropogenic impact on vegetation and environment during the Bronze Age in the area of Lake Durankulak, NE Bulgaria: Pollen, microscopic charcoal, non-pollen palynomorphs and plant macrofossils. *Review of Palaeobotany and Palynology*, 141(1), 165-178. [Online]. Available at: doi:10.1016/j.revpalbo.2006.03.011.

Marinova, E. and Valamoti, S. M. (2014). 3.2. *Crop diversity and choices in the prehistory of SE Europe: the archaeobotanical evidence from Greece and Bulgaria*. [Online]. Oxbow Books. Available at: <https://lirias.kuleuven.be/1705697?limo=0>.

- Märkle, T. and Rösch, M. (2008). Experiments on the effects of carbonization on some cultivated plant seeds. *Vegetation History and Archaeobotany*, 17(1), 257-263. [Online]. Available at: doi:10.1007/s00334-008-0165-7.
- Marston, J.M. (2011). Archaeological markers of agricultural risk management. *Journal of Anthropological Archaeology*, 30(2), 190-205. [Online]. Available at: doi:10.1016/j.jaa.2011.01.002.
- Masotti, S., Varalli, A., Goude, G., Moggi-Cecchi, J. and Gualdi-Russo, E. (2019). A combined analysis of dietary habits in the Bronze Age site of Ballabio (northern Italy). *Archaeological and Anthropological Sciences*, 11(3), 1029-1047. [Online]. Available at: doi:10.1007/s12520-017-0588-0.
- Mathe, C., Connan, J., Archier, P. and Mouton, M. (2007). Analysis of frankincense in archaeological samples by gas chromatography-mass spectrometry. *Annali di Chimica*, 97(7), 433-445. [Online]. Available at: <https://onlinelibrary.wiley.com/doi/abs/10.1002/adic.200790029>.
- Mathe, C., Culioli, G., Archier, P. and Vieillescazes, C. (2004). Characterization of archaeological frankincense by gas chromatography-mass spectrometry. *Journal of Chromatography A*, 1023(2), 277-285. [Online]. Available at: doi:10.1016/j.chroma.2003.10.016.
- May, P. and Tuckson, M. (2000). *The Traditional Pottery of Papua New Guinea*. Sydney: Bay Books.
- McGovern, P.E. and Hall, G.R. (2016). Charting a Future Course for Organic Residue Analysis in Archaeology. *Journal of Archaeological Method and Theory*, 23(2), 592-622. [Online]. Available at: doi:10.1007/s10816-015-9253-z.
- McGovern, P.E., Zhang, J., Tang, J., Zhang, Z., Hall, G.R., Moreau, R.A., Nuñez, A., Butrym, E.D., Richards, M.P., Wang, C.-S., Cheng, G., Zhao, Z. and Wang, C. (2004). Fermented beverages of pre- and proto-historic China. *Proceedings of the National Academy of Sciences of the United States of America*, 101(51), 17593-17598. [Online]. Available at: doi:10.1073/pnas.0407921102.
- McGovern, P.E., Underhill, A.P., Fang, H., Luan, F., Hall, G.R., Yu, H., Wang, C.-S., Cai, F., Zhao, Z. and Feinman, G.M. (2005). Chemical Identification and Cultural Implications of a Mixed Fermented Beverage from Late Prehistoric China. *Asian Perspectives*, 44(2), 249-275. [Online]. Available at: doi:10.1353/asi.2005.0026.
- McGovern, P., Jalabadze, M., Batiuk, S., Callahan, M.P., Smith, K.E., Hall, G.R., Kvavadze, E., Maghradze, D., Rusishvili, N., Bouby, L., Failla, O., Cola, G., Mariani, L., Boaretto, E., Bacilieri, R., This, P., Wales, N. and Lordkipanidze, D. (2017). Early Neolithic wine of Georgia in the South Caucasus. *Proceedings of the National Academy of Sciences*, 114(48), pp.E10309-E10318. [Online]. Available at: doi:10.1073/pnas.1714728114.
- Meier-Augenstein, W. (1999). Applied gas chromatography coupled to isotope ratio mass spectrometry. *Journal of Chromatography A*, 842(1-2), 351-371. [Online]. Available at: doi:10.1016/s0021-9673(98)01057-7.

Meier-Augenstein, W. (2002). Stable isotope analysis of fatty acids by gas chromatography-isotope ratio mass spectrometry. *Analytica Chimica Acta*, 465(1), 63-79. [Online]. Available at: doi:10.1016/S0003-2670(02)00194-0.

Michel, R.H., McGovern, P.E. and Badler, V.R. (1993). The First Wine & Beer: Chemical detection of ancient fermented beverages. *Analytical Chemistry*, 65(8), 408A-413A. [Online]. Available at: doi:10.1021/ac00056a734.

Mikołaj, L. and Marciniak, A. (2015). Chapter 4: Taphonomy of animal bones from Únětice settlement at Bruszczewo, Kościan district. In Czebreszuk, J., Müller, J., Jaeger, M. and Kneisel, J. (eds.). *Bruszczewo IV: Natural resources and economic activities of the Bronze Age people*. Studien zur Archäologie in Ostmitteleuropa 14. Bonn: Habelt, pp. 189-220.

Miller, M.J., Whelton, H.L., Swift, J.A., Maline, S., Hammann, S., Cramp, L.J.E., McCleary, A., Taylor, G., Vacca, K., Becks, F., Evershed, R.P. and Hastorf, C.A. (2020). Interpreting ancient food practices: stable isotope and molecular analyses of visible and absorbed residues from a year-long cooking experiment. *Scientific Reports*, 10(1), 1-16. [Online]. Available at: doi:10.1038/s41598-020-70109-8.

Miller, N.F. (2015). Rainfall seasonality and the spread of millet cultivation in Eurasia. *Iranian Journal of Archaeological Studies*, 5(1), 1-10. [Online]. Available at: http://ijas.usb.ac.ir/article_3015_0.html.

Miller, N.F., Spengler, R.N. and Frachetti, M. (2016). Millet cultivation across Eurasia: Origins, spread, and the influence of seasonal climate. *Holocene*, 26(10), 1566-1575. [Online]. Available at: doi:10.1177/0959683616641742.

Minagawa, M. and Wada, E. (1984). Stepwise enrichment of ^{15}N along food chains: Further evidence and the relation between $\delta^{15}\text{N}$ and animal age. *Geochimica et Cosmochimica Acta*, 48(5), 1135-1140. [Online]. Available at: doi:10.1016/0016-7037(84)90204-7.

Mnich, B. *et al.* (2020). Terrestrial diet in prehistoric human groups from southern Poland based on human, faunal and botanical stable isotope evidence. *Journal of Archaeological Science: Reports*, 32, 102382-102382. [Online]. Available at: doi:10.1016/j.jasrep.2020.102382.

Modugno, F., Ribechini, E. and Colombini, M.P. (2006). Aromatic resin characterisation by gas chromatography-mass spectrometry. Raw and archaeological materials. *Journal of Chromatography A*, 1134(1-2), 298-304. [Online]. Available at: doi:10.1016/j.chroma.2006.09.010.

Moore, J.H. and Christie, W.W. (1981). Lipid metabolism in the mammary gland of ruminant animals. In: Christie, W.W. (ed). *Lipid Metabolism in Ruminant Animals*. Oxford: Pergamon. pp. 227-277. [Online]. Available at: doi:10.1016/B978-0-08-023789-3.50010-6.

Moskal-del Hoyo, M., Lityńska-Zajac, M., Korczyńska, M., Cywa, K., Kienlin, T.L. and Cappenberg, K. (2015). Plants and environment: results of archaeobotanical research of the Bronze Age settlements in the Carpathian Foothills in Poland. *Journal of Archaeological Science*, 53, 426-444. [Online]. Available at: doi:10.1016/j.jas.2014.10.024.

- Moskal-del Hoyo, M., Rauba-Bukowska, A., Lityńska-Zajęc, M., Mueller-Bieniek, A. and Czekaj-Zastawny, A. (2017). Plant materials used as temper in the oldest Neolithic pottery from south-eastern Poland. *Vegetation History and Archaeobotany*, 26(3), 329-344. [Online]. Available at: doi:10.1007/s00334-016-0595-6.
- Mottram, H.R., Dudd, S.N., Lawrence, G.J., Stott, A.W. and Evershed, R.P. (1999). New chromatographic, mass spectrometric and stable isotope approaches to the classification of degraded animal fats preserved in archaeological pottery. *Journal of Chromatography*, A, 833(2), 209-221. [Online]. Available at: doi:10.1016/S0021-9673(98)01041-3.
- Motuzaitė-Matuzevičiute, G. (2012). The earliest appearance of domesticated plant species and their origins on the western fringes of the Eurasian Steppe. *Documenta Praehistorica*, 39, 1-21 [Online]. Available at: <https://revije.ff.uni-lj.si/DocumentaPraehistorica/article/view/39.1>.
- Motuzaitė-Matuzevičiute, G., Hunt, H. V. and Jones, M. K. (2012). Experimental approaches to understanding variation in grain size in *Panicum miliaceum* (broomcorn millet) and its relevance for interpreting archaeobotanical assemblages. *Vegetation History and Archaeobotany*, 21(1), 69-77. [Online]. Available at: doi:10.1007/s00334-011-0322-2.
- Motuzaitė-Matuzevičiute, G., Staff, R.A., Hunt, H.V., Liu, X. and Jones, M.K. (2013). The early chronology of broomcorn millet (*Panicum miliaceum*) in Europe. *Antiquity*, 87(338), 1073-1085. [Online]. Available at: doi:10.1017/S0003598X00049875.
- Motuzaitė-Matuzevičiute, G., Lightfoot, E., O'Connell, T.C., Voyakin, D., Liu, X., Loman, V., Svyatko, S., Usmanova, E. and Jones, M.K. (2015). The extent of cereal cultivation among the Bronze Age to Turkic period societies of Kazakhstan determined using stable isotope analysis of bone collagen. *Journal of Archaeological Science*, 59, 23-34. [Online]. Available at: doi:10.1016/j.jas.2015.03.029.
- Motuzaitė-Matuzevičiute, G., Jacob, J., Telizhenko, S. and Jones, M.K. (2016). Miliacin in palaeosols from an Early Iron Age in Ukraine reveal in situ cultivation of broomcorn millet. *Archaeological and Anthropological Sciences*, 8(1), 43-50. Available at: doi:10.1007/s12520-013-0142-7.
- Muccio, Z. and Jackson, G.P. (2009). Isotope Ratio Mass Spectrometry. *The Analyst*, 134(2), 213-222. [Online]. Available at: doi:10.1039/b808232d.
- Mueller-Bieniek, A., Kittel, P., Muzolf, B. and Muzolf, P. (2015). Useful plants from the site Lutomiersk-Koziówki near Łódź (central Poland) with special reference to the earliest find of *Xanthium strumarium* L. seeds in Europe. *Journal of Archaeological Science: Reports*, 3, 275-284.
- Mueller-Bieniek, A., Nowak, M., Styring, A., Lityńska-Zajęc, M., Moskal-del Hoyo, M., Sojka, A., Paszko, B., Tunia, K. and Bogaard, A. (2019). Spatial and temporal patterns in Neolithic and Bronze Age agriculture in Poland based on the stable carbon and nitrogen isotopic composition of cereal grains. *Journal of Archaeological Science: Reports*, 27, 101993-102007. [Online]. Available at: doi:10.1016/j.jasrep.2019.101993.

Muffler, K., Leipold, D., Scheller, M.-C., Haas, C., Steingroewer, J., Bley, T., Neuhaus, H.E., Mirata, M.A., Schrader, J. and Ulber, R. (2011). Biotransformation of triterpenes. *Process Biochemistry*, 46(1), 1-15. [Online]. Available at: doi:10.1016/j.procbio.2010.07.015.

Mukherjee, A.J., Gibson, A.M. and Evershed, R.P. (2008). Trends in pig product processing at British Neolithic Grooved Ware sites traced through organic residues in potsherds. *Journal of Archaeological Science*, 35(7), 2059-2073. [Online]. Available at: doi:10.1016/j.jas.2008.01.010.

Müller, J. and Knisel, J., (2010). Bruszczewo 5. Production, distribution, consumption, and the formation of social differences. In Müller, J., Czebreszuk, J., and Kneisel, J. (eds.). *Bruszczewo II: Ausgrabungen und Forschungen in einer prähistorischen Siedlungskammer Großpolens*. Studien zur Archäologie in Ostmitteleuropa 6. Bonn: Habelt, pp. 756-850.

Müller, J., Czebreszuk, J., and Kneisel, J. (eds.). (2010). *Bruszczewo II: Ausgrabungen und Forschungen in einer prähistorischen Siedlungskammer Großpolens*. Studien zur Archäologie in Ostmitteleuropa 6. Bonn: Habelt.

Narasimhan, V.M., Patterson, N., Moorjani, P., Rohland, N., Bernardos, R., Mallick, S., Lazaridis, I., Nakatsuka, N., Olalde, I., Lipson, M., Kim, A.M., Olivieri, L.M., Coppa, A., Vidale, M., Mallory, J., Moiseyev, V., Kitov, E., Monge, J., Adamski, N., Alex, N., Broomandkhashbacht, N., Candilio, F., Callan, K., Cheronet, O., Culleton, B.J., Ferry, M., Fernandes, D., Freilich, S., Gamarra, B., Gaudio, D., Hajdinjak, M., Harney, É., Harper, T.K., Keating, D., Lawson, A.M., Mah, M., Mandl, K., Michel, M., Noval, M., Oppenheimer, J., Rai, N., Sirak, K., Slon, V., Stewardson, K., Zalzal, F., Zhang, Z., Akhatov, G., Bagashev, A.N., Bagnera, A., Baitanayev, B., Bendezu-Sarmiento, J., Bissembaev, A.A., Bonora, G.L., Chargynov, T.T., Chikisheva, T., Dashkovskiy, P.K., Derevianko, A., Dobeš, M., Douka, K., Dubova, N., Duisengali, M.N., Enshin, D., Epimakhov, A., Fribus, A.V., Fuller, D., Goryachev, A., Gromov, A., Grushin, S.P., Hanks, B., Judd, M., Kazizov, E., Khokhlov, A., Krygin, A.P., Kupriyanova, E., Kuznetsov, P., Luiselli, D., Maksudov, F., Mamedov, A.M., Mamirov, T.B., Meiklejohn, C., Merrett, D.C., Micheli, R., Mochalov, O., Mustafokulov, S., Nayak, A., Pettener, D., Potts, R., Razhev, D., Rykun, M., Sarno, A., Savenkova, T.M., Sikhymbaeva, K., Slepchenko, S.M., Soltobaev, O.A., Stepanova, N., Svyatko, S., Tabaldiev, K., Teschler-Nicola, M., Tishkin, A.A., Tkachev, V.V., Vasilyev, S., Velemínský, P., Voyakin, D., Yermolayeva, A., Zahir, M., Zubkov, V.S., Zubova, A., Shinde, V.S., Lalueza-Fox, C., Meyer, M., Anthony, D., Boivin, N., Thangaraj, K., Kennett, D.J., Frachetti, M., Pinhasi, R. and Reich, D. (2019). The formation of human populations in South and Central Asia. *Science*, 365(6457). [Online]. Available at: doi:10.1126/science.aat7487.

Nesbitt, M. and Summers, G. D. (1988). Some recent discoveries of millet (*Panicum miliaceum* L. and *Setaria italica* (L.) P. Beauv.) at Excavations in Turkey and Iran. *Anatolian Studies*, 38, 85-97. [Online]. Available at: doi:10.2307/3642844.

Nguyen, T.T., Nguyen, D.H., Zhao, B.T., Le, D.D., Min, B.S., Kim, Y.H. and Woo, M.H. (2017). Triterpenoids and sterols from the grains of *Echinochloa utilis* Ohwi & Yabuno and their cytotoxic activity. *Biomedicine & Pharmacotherapy*, 93, 202-207. [Online]. Available at: doi:10.1016/j.biopha.2017.06.042.

Nikitina, A.G., Sokhatsky, M., Kovaliukh, M. and Videiko, M.Y. (2010). Comprehensive Site Chronology and Ancient Mitochondrial DNA Analysis from Verteba Cave -a Trypillian

Culture Site of Eneolithic Ukraine. *Interdisciplinaria Archaeologica - Natural Sciences in Archaeology*, 1(1-2), 9-18. [Online]. Available at: <http://dx.doi.org/10.24916/iansa.2010.1-2.1>.

Nitsch, E., Andreou, S., Creuzieux, A., Gardeisen, A., Halstead, P., Isaakidou, V., Karathanou, A., Kotsachristou, D., Nikolaidou, D., Papanthimou, A., Petridou, C., Triantaphyllou, S., Valamoti, S.M., Vasileiadou, A. and Bogaard, A. (2017). A bottom-up view of food surplus: using stable carbon and nitrogen isotope analysis to investigate agricultural strategies and diet at Bronze Age Archontiko and Thessaloniki Toumba, northern Greece. *World Archaeology*, 49(1), 105-137. [Online]. Available at: https://www.tandfonline.com/doi/abs/10.1080/00438243.2016.1271745?casa_token=WtAdUAuJCLQAAAAA:G4d6-csXTuEQPKky7cfyX5uxXOq8ysPWz2uqDvJpMOHA1UFNwyfdVh6P_4-7ss8X3H4AEi-eCIY.

O'Leary, M.H. (1988). Carbon Isotopes in Photosynthesis. *Bioscience*, 38(5), 328-336. [Online]. Available at: doi:10.2307/1310735.

Obara, T. and Abe, S. (1957). Structure of Sawamilletin from Sawamillet Oil. *Bulletin of the Agricultural Chemical Society of Japan*, 21(6), 388-389. [Online]. Available at: doi:10.1080/03758397.1957.10857419.

Ohmoto, T., Ikuse, M. and Natori, S. (1970). Triterpenoids of the Gramineae. *Phytochemistry*, 9(10), 2137-2148. [Online]. Available at: [https://doi.org/10.1016/S0031-9422\(00\)85379-0](https://doi.org/10.1016/S0031-9422(00)85379-0).

Oras, E., Lucquin, A., Lõugas, L., Tõrv, M., Kriiska, A. and Craig, O.E. (2017). The adoption of pottery by north-east European hunter-gatherers: Evidence from lipid residue analysis. *Journal of Archaeological Science*, 78, 112-119. [Online]. Available at: doi:10.1016/j.jas.2016.11.010.

Oudemans, T.F.M. and Boon, J.J. (1991). Molecular archaeology: Analysis of charred (food) remains from prehistoric pottery by pyrolysis—gas chromatography/mass spectrometry. *Journal of Analytical and Applied Pyrolysis*, 20, 197-227. [Online]. Available at: https://openaccess.leidenuniv.nl/bitstream/handle/1887/27993/Analecta-praehistorica-leidensia-26-1993_017.pdf?sequence=1.

Oudemans, T.F.M. and Boon, J.J. (1993). Traces of ancient vessel use: investigating prehistoric usage of four pot types by organic residue analysis using pyrolysis mass spectrometry. In Vermeeren, C. (ed). *Analecta Praehistorica Leidensia 26: The end of our third decade: Papers written on the occasion of the 30th anniversary of the Institute of prehistory*. Leiden: Leiden University Press, pp. 221-234.

Oudemans, T.F. and Boon, J.J. (2007). A Comparative Study of Extractable Lipids in the Sherds and Surface Residual Crusts of Charred Vessels from Neolithic and Roman Iron Age Settlements in the Netherlands. In Barnard, H. and Eerkens, J.W. (eds). *Theory and Practice of Archaeological Residue Analysis*. Oxford: Archaeopress, pp. 99-124.

Ourisson, G. and Albrecht, P. (1992). Hopanoids. 1. Geohopanoids: the most abundant natural products on Earth? *Accounts of Chemical Research*, 25(9), 398-402. [Online]. Available at: doi:10.1021/ar00021a003.

Out, W.A. and Madella, M. (2016). Morphometric distinction between bilobate phytoliths from *Panicum miliaceum* and *Setaria italica* leaves. *Archaeological and Anthropological Sciences*, 8(3), 505-521. [Online]. Available at: doi:10.1007/s12520-015-0235-6.

Oyo-Ita, O.E., Ekpo, B.O., Oros, D.R. and Simoneit, B.R. (2010). Occurrence and sources of triterpenoid methyl ethers and acetates in sediments of the cross-river system, southeast Nigeria. *International Journal of Analytical Chemistry*, 2010, 502076. [Online]. Available at: doi:10.1155/2010/502076.

Pääkkönen, M., Evershed, R.P. and Asplund, H. (2020). Compound-specific stable carbon isotope values of fatty acids in modern aquatic and terrestrial animals from the Baltic Sea and Finland as an aid to interpretations of the origins of organic residues preserved in archaeological pottery. *Journal of Nordic Archaeological Science*, 19, 3-19. [Online]. Available at: <https://www.archaeology.su.se/english/publications/publication-series/jonas/jonas-19>.

Papaefthymiou-Papanthimou, A., Valamoti, S., Papadopoulou, E., Tsagkaraki, E. and Voulgari, E. (2013). Food storage in the context of an Early Bronze Age household economy: new evidence from Archontiko Giannitson. *Αριστοτέλειο Πανεπιστήμιο Θεσσαλονίκης*, 103-111. [Online]. Available at: <http://ikee.lib.auth.gr/record/310994>.

Papakosta, V., Smittenberg, R.H., Gibbs, K., Jordan, P. and Isaksson, S. (2015). Extraction and derivatization of absorbed lipid residues from very small and very old samples of ceramic potsherds for molecular analysis by gas chromatography–mass spectrometry (GC–MS) and single compound stable carbon isotope analysis by gas chromatography–combustion–isotope ratio mass spectrometry (GC–C–IRMS). *Microchemical Journal*, 123, 196-200. [Online]. Available at: doi:10.1016/j.microc.2015.06.013.

Papathanasiou, A. (2003). Stable isotope analysis in Neolithic Greece and possible implications on human health. *International Journal of Osteoarchaeology*, 13(5), 314-324. [Online]. Available at: doi:10.1002/oa.705.

Parras, D.J., Sánchez, A., Tuñón, J.A., Rueda, C., Ramos, N. and García-Reyes, J.F. (2015). Sulphur, fats and beeswax in the Iberian rites of the sanctuary of the oppidum of Puente Tablas (Jaén, Spain). *Journal of Archaeological Science: Reports*, 4(2015), 510-524. [Online]. Available at: doi:10.1016/j.jasrep.2015.10.010.

Pavlopoulos, K. and Kouli, K. (2010). Chapter 2: Paleogeography, climate and vegetation in the plain of Western Macedonia. In Stefani, E. (ed.). *Angelochori, Imathia. Late Bronze Age settlement. Angelochori: A Late Bronze Age Settlement in Emathia, Macedonia, Greece*. Vol 1. Thessaloniki: Kyriakidis Brothers, pp. 33-78.

Pearson, J.A. and Hedges, R.E.M. (2007). Stable carbon and nitrogen analysis and the evidence for diet at Ecsegfalva and beyond. In Whittle, A.W.R. (ed.). *The Early Neolithic on the Great Hungarian Plain: investigations of the Körös culture site of Ecsegfalva 23, County Békés*. *Varia archaeologica Hungarica*, vol. 21. Budapest: Institute of Archaeology, Hungarian Academy of Sciences, pp. 413-419.

Pecci, A., Giorgi, G., Salvini, L. and Cau Ontiveros, M.Á. (2013). Identifying wine markers in ceramics and plasters using gas chromatography-mass spectrometry. *Experimental and*

archaeological materials. *Journal of Archaeological Science*, 40(1), 109-115. [Online]. Available at: doi:10.1016/j.jas.2012.05.001.

Pecci, A., Gabrieli, R.S., Inserra, F., Cau, M.A. and Waksman, S.Y. (2015). Preliminary results of the organic residue analysis of 13th century cooking wares from a household in Frankish Paphos (Cyprus). *Science & Technology of Archaeological Research*, 1(2), 99-105. [Online]. Available at: doi:10.1080/20548923.2016.1183960.

Pecci, A., Degl'Innocenti, E., Giorgi, G., Cau Ontiveros, M.Á., Cantini, F., Solanes Potrony, E., Alós, C. and Miriello, D. (2016). Organic residue analysis of experimental, medieval, and post-medieval glazed ceramics. *Archaeological and Anthropological Sciences*, 8(4), 879-890. [Online]. Available at: doi:10.1007/s12520-015-0262-3.

Perego, R. (2015). *Contribution to the development of the Bronze Age plant economy in the surrounding of the Alps: an archaeobotanical case study of two Early and Middle Bronze Age sites in northern Italy (Lake Garda region)*. Unpublished: University of Basel. PhD. [Online]. Available at: doi:10.5451/unibas-006737816.

Petridou, C. (2019). Plant food remains from prehistoric Greece: first insights from Archondiko. *Bulgarian e-Journal of Archaeology Supplements*, 7, 211-220. [Online]. Available at: <https://be-ja.org/index.php/supplements/article/view/203>.

Petroutsas, E.I., Richards, M.P., Kolonas, L. and Manolis, S.K. (2009). Isotope Paleodietary Analysis of Humans and Fauna from the Late Bronze Age Site of Voudeni. *Hesperia Supplements*, 43, 237–243. [Online]. Available at: <http://www.jstor.org/stable/27759967>.

Petroutsas, E. I. and Manolis, S. K. (2010). Reconstructing Late Bronze Age diet in mainland Greece using stable isotope analysis. *Journal of Archaeological Science*, 37(3), 614-620. [Online]. Available at: doi:10.1016/j.jas.2009.10.026.

Pilali-Papasteriou, A. and Papaefthymiou-Papanthimou, A. (2002). Die Ausgrabungen auf der Toumba von Archontiko. *De Gruyter*, 77 (2), 137-147. [Online]. Available at: doi:10.1515/prhz.2002.77.2.137.

Pokutta, D.A. (2014). Food and cooking in the Unětice Culture. *Apulum*, 51(1), 135-159. [Online]. Available at: <http://www.diva-portal.org/smash/record.jsf?pid=diva2:922585>.

Pokutta, D.A. and Howcroft, R. (2015). Children, Childhood and Food : The Diets of Subadults in the Unetice Culture of Southwestern Poland. In Suchowska-Ducke, P., Reiter, S.S. and Vandkilde, H. (eds). *12th Nordic Bronze Age Symposium, International Conference: Cultural Mobility in Bronze Age Europe, Aarhus, Denmark, June 6-9, 2012*, Vol 1. Oxford: British Archaeological Reports. pp.245-252. [Online]. Available at: <https://www.diva-portal.org/smash/record.jsf?pid=diva2%3A610644&dswid=6061>.

Pokutta, D.A., Baron, J., Dąbrowski, P. and Karlsson, C. (2015). Bioarchaeology of Social Inequality in the Unetice Culture: A Case Study. In Suchowska-Ducke, P., Reiter, S.S. and Vandkilde, H. (eds). *12th Nordic Bronze Age Symposium, International Conference: Cultural Mobility in Bronze Age Europe, Aarhus, Denmark, June 6-9, 2012*. 1. 2015. Oxford: British Archaeological Reports. pp.111-119. [Online]. Available at: doi:10.13140/RG.2.1.2390.0247.

Popov, H., Marinova, E., Hristova, I. and Iliev, S. (2018). Plant food from the Late Bronze Age and Early Iron Age hilltop site Kush Kaya, Eastern Rhodope Mountains, Bulgaria: insights on the cooking practices. In Ivanova, M., Athanassov, B., Petrova, V., Takorova, D. and Stockhammer, P.W. (eds). *Social dimensions of food in the Prehistoric Balkans*. Oxford: Oxbow Books, pp. 263-277. [Online]. Available at: <http://www.diva-portal.org/smash/record.jsf?pid=diva2:1273417>.

Popova, T. and Marinova, E. (2006). Palaeobotanical data in south-western region of Bulgaria. In: Stefanovic, M. and Todorova, H. (eds). *The Struma/Strymon river valley in prehistory*. In the steps of James Harvey Gaul 2, Museum of History Kyustendil. Sofia: Gerda Henkel Stiftung, pp. 523-532. [Online]. Available at: https://www.academia.edu/download/46712030/Popova_Marinova2007.pdf.

Pospieszny, Ł., Makarowicz, P., Lewis, J., Górski, J., Taras, H., Włodarczyk, P., Szczepanek, A., Ilchysyn, V., Jagodinska, M.O., Czebreszuk, J. and Muzolf, P. (2021). Isotopic evidence of millet consumption in the Middle Bronze Age of East-Central Europe. *Journal of Archaeological Science*, 126, 105292. [Online]. Available at: [doi:10.1016/j.jas.2020.105292](https://doi.org/10.1016/j.jas.2020.105292).

Quirk, M.M., Wardroper, A.M., Wheatley, R.E. and Maxwell, J.R. (1984). Extended hopanoids in peat environments. *Chemical Geology*, 42(1-4), 25-43. [Online]. Available at: [doi:10.1016/0009-2541\(84\)90003-2](https://doi.org/10.1016/0009-2541(84)90003-2).

Rageot, M., Pêche-Quilichini, K., Py, V., Filippi, J.-J., Fernandez, X. and Regert, M. (2016). Exploitation of Beehive Products, Plant Exudates and Tars in Corsica During the Early Iron Age: Beehive products, plant exudates and tars in Corsica. *Archaeometry*, 58(2), 315-332. [Online]. Available at: [doi:10.1111/arcm.12172](https://doi.org/10.1111/arcm.12172).

Rageot, M., Mötsch, A., Schorer, B., Bardel, D., Winkler, A., Sacchetti, F., Chaume, B., Della Casa, P., Buckley, S., Cafisso, S. and Fries-Knoblach, J. (2019a). New insights into Early Celtic consumption practices: Organic residue analyses of local and imported pottery from Vix-Mont Lassois. *PLOS ONE*, 14(6). [Online]. Available at: <https://doi.org/10.1371/journal.pone.0218001>.

Rageot, M., Mötsch, A., Schorer, B., Gutekunst, A., Patrizi, G., Zerrer, M., Cafisso, S., Fries-Knoblach, J., Hansen, L., Tarpini, R. and Krausse, D. (2019b). The dynamics of Early Celtic consumption practices: A case study of the pottery from the Heuneburg. *PLOS ONE*, 14(10). [Online]. Available at: <https://doi.org/10.1371/journal.pone.0222991>.

Rageot, M., Théry-Parisot, I., Beyries, S., Lepère, C., Carré, A., Mazuy, A., Filippi, J.J., Fernandez, X., Binder, D. and Regert, M. (2019c). Birch bark tar production: Experimental and biomolecular approaches to the study of a common and widely used prehistoric adhesive. *Journal of Archaeological Method and Theory*, 26(1), 276-312. [Online]. Available at: <https://doi.org/10.1007/s10816-018-9372-4>.

Ramaroli, V., Hamilton, J., Ditchfield, P., Fazeli, H., Aali, A., Conningham, R.A.E. and Pollard, A.M. (2010). The Chehr Abad 'Salt men' and the isotopic ecology of humans in ancient Iran. *American Journal of Physical Anthropology*, 143(3), 343-354. [Online]. Available at: [doi:10.1002/ajpa.21314](https://doi.org/10.1002/ajpa.21314).

- Raven, A.M., van Bergen, P.F., Stott, A.W., Dudd, S.N. and Evershed, R.P. (1997). Formation of long-chain ketones in archaeological pottery vessels by pyrolysis of acyl lipids. *Journal of Analytical and Applied Pyrolysis*, 40-41, 267-285. [Online]. Available at: doi:10.1016/S0165-2370(97)00036-3.
- Reber, E.A., (2014). Gas Chromatography-Mass Spectrometry (GC-MS): Applications in Archaeology. In: Smith, C. (ed). *Encyclopedia of Global Archaeology*. New York: Springer, 2953-2959. [Online]. Available at: doi:10.1007/978-1-4419-0465-2_340.
- Reber, E.A., (2021). Comparison of Neutral Compound Extraction from Archaeological Residues in Pottery Using Two Methodologies: A Preliminary Study. *Separations Technology*, 8(6), 1-17. [Online]. Available at: doi:10.3390/separations8010006.
- Reber, E.A. and Evershed, R.P. (2004). How Did Mississippians Prepare Maize? The Application of Compound-Specific Carbon Isotope Analysis to Absorbed Pottery Residues from Several Mississippi Valley Sites. *Archaeometry*, 46(1), 19-33. [Online]. Available at: doi:10.1111/j.1475-4754.2004.00141.x.
- Reber, E.A. and Hart, J.P. (2008). Pine resins and pottery sealing: analysis of absorbed and visible pottery residues from central New York State. *Archaeometry*, 50(6), 999-1017. [Online]. Available at: doi:10.1111/j.1475-4754.2008.00387.x.
- Reber, E.A., Dudd, S.N., van der Merwe, N.J. and Evershed, R.P. (2004). Direct detection of maize in pottery residues via compound specific stable carbon isotope analysis. *Antiquity*, 78(301), 682-691. [Online]. Available at: doi:10.1017/S0003598X00113316.
- Reber, E.A., Kerr, M.T., Whelton, H.L. and Evershed, R.P. (2019). Lipid Residues from Low-Fired Pottery. *Archaeometry*, 61(1), 131-144. [Online]. Available at: doi:10.1111/arc.12403.
- Reed, K.E., (2013). *Farmers in transition: the archaeobotanical analysis of the Carpathian Basin from the Late Neolithic to the Late Bronze Age (5000-900 BC)*. [Online]. Unpublished: University of Leicester. PhD. Available at: <https://www.semanticscholar.org/paper/43ecde56c26580d9e050a3ef66fe13304e0b02e7>
- Regert, M. (2004). Investigating the history of prehistoric glues by gas chromatography-mass spectrometry. *Journal of Separation Science*, 27(3), 244-254. [Online]. Available at: <https://onlinelibrary.wiley.com/doi/abs/10.1002/jssc.200301608>.
- Regert, M. (2011). Analytical strategies for discriminating archaeological fatty substances from animal origin. *Mass Spectrometry Reviews*, 30(2), 177-220. [Online]. Available at: doi:10.1002/mas.20271.
- Regert, M. and Rolando, C. (2002). Identification of archaeological adhesives using direct inlet electron ionization mass spectrometry. *Analytical Chemistry*, 74(5), 965-975. [Online]. Available at: doi:10.1021/ac0155862.
- Regert, M., Bland, H.A., Dudd, S.N., van Bergen, P.F. and Evershed, R.P. (1998). Free and bound fatty acid oxidation products in archaeological ceramic vessels. *Proceedings of the Royal Society B: Biological Sciences*, 265(1409), 2027-2032. [Online]. Available at: <https://dx.doi.org/10.1098%2Frspb.1998.0536>.

- Regert, M., Colinart, S., Degrand, L. and Decavallas, O. (2001). Chemical Alteration and Use of Beeswax Through Time: Accelerated Ageing Tests and Analysis of Archaeological Samples from Various Environmental Contexts. *Archaeometry*, 43(4), 549-569. [Online]. Available at: doi:10.1111/1475-4754.00036.
- Regert, M., Devière, T., Le Hô, A.S. and Rougeulle, A. (2008). Reconstructing ancient Yemeni commercial routes during the Middle Ages using structural characterization of terpenoid resins. *Archaeometry*, 50(4), 668-695. [Online]. Available at: <https://onlinelibrary.wiley.com/doi/abs/10.1111/j.1475-4754.2007.00372.x>.
- Rembisz, A., Gackowski, J., Makowiecki, D., Markiewicz, M. and Polcyn, M. (2009). Ślady gospodarki roślinno-zwierzęcej ludności kultury łuzycyckich pól popielnicowych z osady w Rudzie, gmina Grudziadz, północna Polska. *Środowisko - Człowiek - Cywilizacja*, 2, 109-122. [Online]. Available at: <https://www.scopus.com/record/display.uri?eid=2-s2.0-85030424411&origin=inward>.
- Ribéreau-Gayon, P., Glories, Y., Maujean, A. and Dubourdiou, D. (2006). *Handbook of Enology, Volume 2: The Chemistry of Wine Stabilization and Treatments, 2nd edition*. Chichester: John Wiley & Sons.
- Ripley, B.S., Gilbert, M.E., Ibrahim, D.G. and Osborne, C.P. (2007). Drought constraints on C₄ photosynthesis: stomatal and metabolic limitations in C₃ and C₄ subspecies of *Alloterosis semialata*. *Journal of Experimental Botany*, 58(6), 1351-1363. [Online]. Available at: doi:10.1093/jxb/erl302.
- Robert, T., Khalfallah, N., Martel, E., Lamy, F., Poncet, V., Allinne, C., Remigereau, M-S., Rekima, S., Leveugle, M., Lakis, G., Siljak-Yakovlev, S. and Sarr, A. (2011). Pennisetum. In Kole, C. (ed). *Wild Crop Relatives: Genomic and Breeding Resources: Millets and Grasses*. Berlin: Springer, pp. 217-255. [Online]. Available at: doi:10.1007/978-3-642-14255-0_13.
- Roberts, P., Fernandes, R., Craig, O.E., Larsen, T., Lucquin, A., Swift, J. and Zech, J. (2018). Calling all archaeologists: guidelines for terminology, methodology, data handling, and reporting when undertaking and reviewing stable isotope applications in archaeology. *Rapid Communications in Mass Spectrometry*, 32(5), 361-372. [Online]. Available at: <https://onlinelibrary.wiley.com/doi/abs/10.1002/rcm.8044>.
- Roffet-Salque, M., Dunne, J., Altoft, D.T., Casanova, E., Cramp, L.J.E., Smyth, J., Whelton, H.L. and Evershed, R.P. (2017a). From the inside out: Upscaling organic residue analyses of archaeological ceramics. *Journal of Archaeological Science: Reports*, 16, 627-640. [Online]. Available at: doi:10.1016/j.jasrep.2016.04.005.
- Roffet-Salque, M., Lee, M.R.F., Timpson, A. and Evershed, R.P. (2017b). Impact of modern cattle feeding practices on milk fatty acid stable carbon isotope compositions emphasise the need for caution in selecting reference animal tissues and products for archaeological investigations. *Archaeological and Anthropological Sciences*, 9(7), 1343-1348. [Online]. Available at: doi:10.1007/s12520-016-0357-5.
- Romanus, K., Baeten, J., Poblome, J., Accardo, S., Degryse, P., Jacobs, P., De Vos, D. and Waelkens, M. (2009). Wine and olive oil permeation in pitched and non-pitched ceramics: relation with results from archaeological amphorae from Sagalassos, Turkey. *Journal of*

Archaeological Science, 36(3), 900-909. [Online]. Available at:
doi:10.1016/j.jas.2008.11.024.

Rottoli, M. and Castiglioni, E. (2009). Prehistory of plant growing and collecting in northern Italy, based on seed remains from the early Neolithic to the Chalcolithic (c. 5600-2100 cal B.C.). *Vegetation History and Archaeobotany*, 18(1), 91-103. [Online]. Available at: doi:10.1007/s00334-007-0139-1.

Rullkötter, J., Peakman, T.M. and Haven, L.O.T. (1994). Early diagenesis of terrigenous triterpenoids and its implications for petroleum geochemistry. *Organic Geochemistry*, 21(3-4), 215-233. [Online]. Available at: doi:10.1016/0146-6380(94)90186-4.

Salque, M., Bogucki, P.I., Pyzel, J., Sobkowiak-Tabaka, I., Grygiel, R., Szmyt, M. and Evershed, R.P. (2013). Earliest evidence for cheese making in the sixth millennium BC in northern Europe. *Nature*, 493(7433), 522-525. [Online]. Available at:
doi:10.1038/nature11698.

Samuel, D. (1996). Approaches to the archaeology of food. *Petits Propos Pulinaires*, 54, 12-21. [Online]. Available at: <http://www.ancientgrains.org/samuel1996food.pdf>.

Schakel, D.J., Kalsbeek, D. and Boer, K. (2004). Determination of sixteen UV filters in suncare formulations by high-performance liquid chromatography. *Journal of Chromatography A*, 1049(1-2), 127-130. [Online]. Available at:
<https://www.ncbi.nlm.nih.gov/pubmed/15499924>.

Schieber, A., Keller, P. and Carle, R. (2001). Determination of phenolic acids and flavonoids of apple and pear by high-performance liquid chromatography. *Journal of Chromatography. A*, 910(2), 265-273. [Online]. Available at: doi:10.1016/s0021-9673(00)01217-6.

Schwab, V.F., Garcin, Y., Sachse, D., Todou, G., Séné, O., Onana, J.M., Achoundong, G. and Gleixner, G. (2015). Effect of aridity on $\delta^{13}\text{C}$ and δD values of C3 plant- and C4 graminoid-derived leaf wax lipids from soils along an environmental gradient in Cameroon (Western Central Africa). *Organic Geochemistry*, 78, 99-109. [Online]. Available at:
doi:10.1016/j.orggeochem.2014.09.007.

Semmoto, M., Kannari, T., Shibata, T., Kamuro, H. and Leshtakov, K. (2018). Petrographic and chemical characterization of Early Bronze Age pottery from Sokol-Himitliyata in Nova Zagora region: An interim report. In Popnedelev (ed). *Studia Archaeologica Universitatis Serdicensis: Tome 6 / 2016*. Sofia: St. Kliment Ohridski University Press, pp. 153-167.

Serpico, M. and White, R. (2000). Oil, fat and wax. In Nicholson, P.T. and Shaw, I. (eds.), *Ancient Egyptian Materials and Technologies*. Cambridge: Cambridge University Press, pp. 390-429.

Sherratt, A. (1991). Sacred and profane substances: the ritual use of narcotics in later Neolithic Europe. In Garwood, P., Jennings, D., Skeates, R. and Toms, J., (eds). *Sacred and Profane: proceedings of a conference on archaeology, ritual and religion 1989*. Oxford: University Committee for Archaeology Monographs, pp. 50-64.

Silaska, P. (ed) (2012). *Wczesnobrązowa osada obronna w Bruszczewie : badania 1964-1968*. Poznań: Muzeum Archeologiczne.

- Simoneit, B.R.T., Rogge, W.F., Lang, Q. and Jaffé, R. (2000). Molecular characterization of smoke from campfire burning of pine wood (*Pinus elliottii*). *Chemosphere-Global Change Science*, 2(1), 107-122. [Online]. Available at: doi:10.1016/S1465-9972(99)00048-3.
- Smith, R.J., Hobson, K.A., Koopman, H.N. and Lavigne, D.M. (1996). Distinguishing between populations of fresh- and salt-water harbour seals (*Phoca vitulina*) using stable-isotope ratios and fatty acid profiles. *Canadian Journal of Fisheries and Aquatic Sciences*, 53, 272-279. [Online]. Available at: doi:10.1139/cjfas-53-2-272.
- Song, J., Zhao, Z. and Fuller, D.Q. (2013). The archaeobotanical significance of immature millet grains: an experimental case study of Chinese millet crop processing. *Vegetation History and Archaeobotany*, 22(2), 141-152. [Online]. Available at: doi:10.1007/s00334-012-0366-y.
- Sorkina, T.I., Segal, G.M., Belova, S.M., Chernogubova, I.P. and Torgov, I.V. (1968). The structure of miliacin. *Russian Chemical Bulletin*, 17(5), 1072-1073. [Online]. Available at: doi:10.1007/BF00910849.
- Sőkand, R., Pieroni, A., Biró, M., Dénes, A., Dogan, Y., Hajdari, A., Kalle, R., Reade, B., Mustafa, B., Nedelcheva, A. and Quave, C.L. (2015). An ethnobotanical perspective on traditional fermented plant foods and beverages in Eastern Europe. *Journal of Ethnopharmacology*, 170, 284-296. [Online]. Available at: doi:10.1016/j.jep.2015.05.018.
- Spangenberg, J.E. and Ogrinc, N. (2001). Authentication of vegetable oils by bulk and molecular carbon isotope analyses with emphasis on olive oil and pumpkin seed oil. *Journal of Agricultural and Food Chemistry*, 49(3), 1534-1540. [Online]. Available at: <https://doi.org/10.1021/jf001291y>.
- Spangenberg, J.E., Jacomet, S. and Schibler, J. (2006). Chemical analyses of organic residues in archaeological pottery from Arbon Bleiche 3, Switzerland—evidence for dairying in the late Neolithic. *Journal of Archaeological Science*, 33(1), 1-13. [Online]. Available at: <https://doi.org/10.1016/j.jas.2005.05.013>.
- Spangenberg, J.E., Ferrer, M., Tschudin, P., Volken, M. and Hafner, A. (2010). Microstructural, chemical and isotopic evidence for the origin of late neolithic leather recovered from an ice field in the Swiss Alps. *Journal of Archaeological Science*, 37(8), 1851-1865. [Online]. Available at: <https://doi.org/10.1016/j.jas.2010.02.003>.
- Spengler, R.N., Frachetti, M.D. and Doumani, P.N. (2014a). Late Bronze Age agriculture at Tasbas in the Dzhungar Mountains of eastern Kazakhstan. *Quaternary International*, 348, 147-157. [Online]. Available at: doi:10.1016/j.quaint.2014.03.039.
- Spengler, R.N., Cerasetti, B., Tengberg, M., Cattani, M. and Rouse, L.M. (2014b). Agriculturalists and pastoralists: Bronze Age economy of the Murghab alluvial fan, southern Central Asia. *Vegetation History and Archaeobotany*, 23(6), 805-820. [Online]. Available at: doi:10.1007/s00334-014-0448-0.
- Spengler, R.N., Ryabogina, N., Tarasov, P.E. and Wagner, M. (2016). The spread of agriculture into northern Central Asia: Timing, pathways, and environmental feedbacks. *Holocene*, 26(10), 1527-1540. [Online]. Available at: doi:10.1177/0959683616641739.

Spengler, R.N., de Nigris, I., Cerasetti, B., Carra, M. and Rouse, L.M. (2018). The breadth of dietary economy in Bronze Age Central Asia: Case study from Adji Kui 1 in the Murghab region of Turkmenistan. *Journal of Archaeological Science: Reports*, 22, 372-381. [Online]. Available at: doi:10.1016/j.jasrep.2016.03.029.

Spiteri, C.D. (2012). Pottery use at the transition to agriculture in the western Mediterranean: evidence from biomolecular and isotopic characterisation of organic residues in Impressed/Cardial Ware vessels. Unpublished: University of York. PhD. [Online]. Available at: https://etheses.whiterose.ac.uk/3391/1/CDS_PhD_2012.pdf.

Srinivasulu, C., Ramgopal, M., Ramanjaneyulu, G., Anuradha, C.M. and Suresh Kumar, C. (2018). Syringic acid (SA) – A Review of Its Occurrence, Biosynthesis, Pharmacological and Industrial Importance. *Biomedicine & Pharmacotherapy*, 108, 547-557. [Online]. Available at: doi:10.1016/j.biopha.2018.09.069.

Stefani, E. (ed.) (2010). *Angelochori, Imathia. Late Bronze Age settlement. Angelochori: A Late Bronze Age Settlement in Emathia, Macedonia, Greece*. Vol 1. Thessaloniki: Kyriakidis Brothers.

Stern, B., Heron, C., Serpico, M. and Bourriau, J. (2000). A Comparison of Methods for Establishing Fatty Acid Concentration Gradients Across Potsherds: A Case Study Using Late Bronze Age Canaanite Amphorae. *Archaeometry*, 42(2), 399-414. [Online]. Available at: doi:10.1111/j.1475-4754.2000.tb00890.x.

Stern, B., Heron, C., Corr, L., Serpico, M. and Bourriau, J. (2003). Compositional variations in aged and heated Pistacia resin found in Late Bronze Age Canaanite amphorae and bowls from Amarna, Egypt. *Archaeometry*, 45(3), 457-469. [Online]. Available at: <https://onlinelibrary.wiley.com/doi/abs/10.1111/1475-4754.00121>.

Stern, B., Heron, C., Tellefsen, T. and Serpico, M. (2008). New investigations into the Uluburun resin cargo. *Journal of Archaeological Science*, 35(8), 2188-2203. [Online]. Available at: doi:10.1016/j.jas.2008.02.004.

Stika, H-P. and Heiss, A.G. (2013). Seeds from the Fire. Charred Plant Remains from Kristian Kristiansen's excavations in Sweden, Denmark, Hungary and Sicily. In Bergerbrant, S. and Sabatini, S. (eds). *Counterpoint: Essays in Archaeology and Heritage Studies in Honour of Professor Kristian Kristiansen*. Oxford: Archaeopress, pp. 77-86. [Online]. Available at: <https://pdfs.semanticscholar.org/83c4/647915b60474c80ca8c3150582f98e9317be.pdf>.

Stott, A.W., Davies, E. and Evershed, R.P. (1997). Monitoring the Routing of Dietary and Biosynthesised Lipids Through Compound - Specific Stable Isotope (d13C) Measurements at Natural Abundance. *Naturwissenschaften*, 84(2), 82-86. [Online]. Available at: <https://doi.org/10.1007/s001140050354>.

Styring, A.K., Ater, M., Hmimsa, Y., Fraser, R., Miller, H., Neef, R., Pearson, J.A. and Bogaard, A. (2016). Disentangling the effect of farming practice from aridity on crop stable isotope values: A present-day model from Morocco and its application to early farming sites in the eastern Mediterranean. *The Anthropocene Review*, 3(1), 2-22. [Online]. Available at: doi:10.1177/2053019616630762.

Styring, A.K., Diop, A.M., Bogaard, A., Champion, L., Fuller, D.Q., Gestrich, N., Macdonald, K.C. and Neumann, K. (2019). Nitrogen isotope values of *Pennisetum glaucum* (pearl millet) grains: towards a reconstruction of past cultivation conditions in the Sahel, West Africa. *Vegetation History and Archaeobotany*, 28(6), 663-678. [Online]. Available at: doi:10.1007/s00334-019-00722-9.

Suryanarayan, A., Cubas, M., Craig, O.E., Heron, C.P., Shinde, V.S., Singh, R.N., O'Connell, T.C. and Petrie, C.A. (2021). Lipid residues in pottery from the Indus Civilisation in northwest India. *Journal of Archaeological Science*, 125, 105291. [Online]. Available at: doi:10.1016/j.jas.2020.105291.

Szpak, P. (2014). Complexities of nitrogen isotope biogeochemistry in plant-soil systems: implications for the study of ancient agricultural and animal management practices. *Frontiers in Plant Science*, 5(288). [Online]. Available at: <https://dx.doi.org/10.3389%2Ffpls.2014.00288>.

Taché, K., Jaffe, Y., Craig, O.E., Lucquin, A., Zhou, J., Wang, H., Jiang, S., Standall, E.A. and Flad, R.K. (2021). What do “barbarians” eat? Integrating ceramic use-wear and residue analysis in the study of food and society at the margins of Bronze Age China. *PLOS ONE*, 16(4). [Online]. Available at: <https://doi.org/10.1371/journal.pone.0250819>.

Tafuri, M.A., Craig, O.E. and Canci, A. (2009). Stable isotope evidence for the consumption of millet and other plants in Bronze Age Italy. *American Journal of Physical Anthropology*, 139(2), 146-153. [Online]. Available at: doi:10.1002/ajpa.20955.

Tafuri, M.A., Rottoli, M., Cupitò, M., Pulcini, M.L., Tasca, G., Carrara, N., Bonfanti, F., Salzani, L., and Canci, I. A. (2018). Estimating C4 plant consumption in Bronze Age Northeastern Italy through stable carbon and nitrogen isotopes in bone collagen. *International Journal of Osteoarchaeology*, 28(2), 131-142. [Online]. Available at: doi:10.1002/oa.2639.

Tamburini, D. (2018). Analytical pyrolysis in cultural heritage. *Analytical Methods*, 10(46), 5463-5467. [Online]. Available at: doi: 10.1039/c8ay90151a.

ten Haven, H.L., Peakman, T.M. and Rullkötter, J. (1992). Early diagenetic transformation of higher-plant triterpenoids in deep-sea sediments from Baffin Bay. *Geochimica et Cosmochimica Acta*, 56(5), 2001-2024. [Online]. Available at: doi:10.1016/0016-7037(92)90326-E.

Tenberge, K.B. (1999). Biology and life strategy of the ergot fungi. In V. Kerb, and L. Cvak, (Eds). *Ergot*. London: CRC Press, pp. 40-71.

Tieszen, L.L. (1991). Natural variations in the carbon isotope values of plants: Implications for archaeology, ecology, and paleoecology. *Journal of Archaeological Science*, 18(3), 227-248. [Online]. Available at: doi:10.1016/0305-4403(91)90063-U.

Triantaphyllou, S. (2015). Stable Isotope Analysis of Skeletal Assemblages from Prehistoric Northern Greece. *Hesperia Supplements*, 49(2015), 57-75. [Online]. Available at: <http://www.jstor.org/stable/24637311>.

Trias, M.C., Van Strydonck, M., Picornell-Gelabert, L., Boudin, M., Santacreu, D.A., Sabater, M.C. and Rosselló, J.G. (2020). Dying in the Hallstatt Plateau: the case of wooden

coffins from Iron Age necropolises in Mallorca (Balearic Islands, Western Mediterranean) and the difficulties in defining their chronology. *Archaeological and Anthropological Sciences*, 12(10), 1-19. [Online]. Available at: doi:10.1007/s12520-020-01206-y.

Trifonov, V.A. Shishlina, N.I., Lebedeva, E.Y., van der Plicht, J. and Rishko, S.A. (2017). Directly dated broomcorn millet from the northwestern Caucasus: Tracing the Late Bronze Age route into the Russian steppe. *Journal of Archaeological Science: Reports*, 12, 288-294. [Online]. Available at: doi:10.1016/j.jasrep.2017.02.004.

Tsirtsoni, Z. (2016). The Late Neolithic II (Chalcolithic)-Early Bronze Age Transition at the Tell of Dikili Tash. In Tsirtsoni, Z. (ed). *The Human Face of Radiocarbon*. MOM Éditions. [Online]. Available at: <https://hal.archives-ouvertes.fr/hal-02556175/>.

Tutin, T.G. 2000. *Flora Europaea*. Cambridge: Cambridge University Press.

Urem-Kotsou, D. (2017). Storage of food in the Neolithic communities of northern Greece. *World Archaeology*, 49(1), 73-89. [Online]. Available at: doi:10.1080/00438243.2016.1276853.

Urem-Kotsou, D., Stern, B., Heron, C. and Kotsakis, K. (2002). Birch-bark tar at Neolithic Makriyalos, Greece. *Antiquity*, 76(294), 962-967. [Online]. Available at: doi:10.1017/S0003598X00091766.

Vaiglova, P., Snoeck, C., Nitsch, E., Bogaard, A. and Lee-Thorp, J. (2014). Impact of contamination and pre-treatment on stable carbon and nitrogen isotopic composition of charred plant remains. *Rapid Communications in Mass Spectrometry*, 28(23), 2497-2510. [Online]. Available at: doi:10.1002/rcm.7044.

Vaiglova, P., Halstead, P., Pappa, M., Triantaphyllou, S., Valamoti, S.M., Evans, J., Fraser, R., Karkanas, P., Kay, A., Lee-Thorp, J. and Bogaard, A. (2018). Of cattle and feasts: Multi-isotope investigation of animal husbandry and communal feasting at Neolithic Makriyalos, northern Greece. *PLOS ONE*, 13(6), 1-30. [Online]. Available at: <https://doi.org/10.1371/journal.pone.0194474>.

Vaiglova, P., Gardeisen, A., Buckley, M., Cavanagh, W., Renard, J., Lee-Thorp, J. and Bogaard, A. (2020). Further insight into Neolithic agricultural management at Kouphovouno, southern Greece: expanding the isotopic approach. *Archaeological and Anthropological Sciences*, 12(2), 43. [Online]. Available at: doi:10.1007/s12520-019-00960-y.

Valamoti, S.M. (2002). Food remains from Bronze Age-Archondiko and Mesimeriani Toumba in northern Greece?. *Vegetation History and Archaeobotany*, 11(1), 17-22. [Online]. Available at: doi:10.1007/s003340200002.

Valamoti, S.M. (2015). Harvesting the 'wild'? Exploring the context of fruit and nut exploitation at Neolithic Dikili Tash, with special reference to wine. *Vegetation History and Archaeobotany*, 24(1), 35-46. [Online]. Available at: <https://link.springer.com/article/10.1007/s00334-014-0487-6>.

Valamoti, S.M. (2016). Millet, the late comer: on the tracks of *Panicum miliaceum* in prehistoric Greece. *Archaeological and Anthropological Sciences*, 8(1), 51-63. [Online]. Available at: doi:10.1007/s12520-013-0152-5.

- Valamoti, S.M. and Jones, G. (2010). Bronze and Oil: A Possible Link between the Introduction of Tin and *Lallemantia* to Northern Greece. *Annual of the British School at Athens*, 105, 83-96. [Online]. Available at: <https://doi.org/10.1017/S006824540000037X>.
- Valamoti, S.M., Marinova, E., Heiss, A.G., Hristova, I., Petridou, C., Popova, T., Michou, S., Papadopoulou, L., Chrysostomou, P., Darcque, D., Grammenos, D., Iliev, S., Kotsos, S., Koukouli-Chrysanthaki, C., Leshtakov, K., Malamidou, D., Merousis, N., Nikolov, V. and Ruseva, T.K. (2019). Prehistoric cereal foods of southeastern Europe: An archaeobotanical exploration. *Journal of Archaeological Science*, 104, 97-113. [Online]. Available at: [doi:10.1016/j.jas.2018.11.004](https://doi.org/10.1016/j.jas.2018.11.004).
- Van de Wouw, M., Jorge, M.A., Bierwirth, J. and Hanson, J. (2008). Characterisation of a collection of perennial *Panicum* species. *Tropical Grasslands*, 42(1), 40-53. [Online]. Available at: [https://cgspace.cgiar.org/bitstream/handle/10568/27921/Vol42\(40_53\).pdf?sequence=1](https://cgspace.cgiar.org/bitstream/handle/10568/27921/Vol42(40_53).pdf?sequence=1).
- Varalli, A., Moggi-Cecchi, M., Dori, I., Boccone, S., Bortoluzzi, S., Salzani, P. and Tafurid, M.A. (2016a). Dietary continuity vs. discontinuity in Bronze Age Italy. The isotopic evidence from Arano di Cellore (Illasi, Verona, Italy). *Journal of Archaeological Science: Reports*, 7, 104-113. [Online]. Available at: [doi:10.1016/j.jasrep.2016.03.047](https://doi.org/10.1016/j.jasrep.2016.03.047).
- Varalli, A., Moggi-Cecchi, J., Moroni, A. and Goude, G. (2016b). Dietary Variability During Bronze Age in Central Italy: First Results. *International Journal of Osteoarchaeology*, 26(3), 431-446. [Online]. Available at: [doi:10.1002/oa.2434](https://doi.org/10.1002/oa.2434).
- Veberic, R., Colaric, M. and Stampar, F. (2008). Phenolic acids and flavonoids of fig fruit (*Ficus carica* L.) in the northern Mediterranean region. *Food Chemistry*, 106(1), 153-157. [Online]. Available at: [doi:10.1016/j.foodchem.2007.05.061](https://doi.org/10.1016/j.foodchem.2007.05.061).
- Ventresca-Miller, A., Usmanova, E., Logvin, V., Kalieva, S., Shevnina, I., Logvin, A., Kolbina, K., Suslov, A., Privat, K., Haas, K. and Rosenmeier, M. (2014). Subsistence and social change in central Eurasia: stable isotope analysis of populations spanning the Bronze Age transition. *Journal of Archaeological Science*, 42, 525-538. [Online]. Available at: [doi:10.1016/j.jas.2013.11.012](https://doi.org/10.1016/j.jas.2013.11.012).
- Ventresca-Miller, A.R. and Makarewicz, C.A. (2019). Intensification in pastoralist cereal use coincides with the expansion of trans-regional networks in the Eurasian Steppe. *Scientific Reports*, 9(1), 1-12. [Online]. Available at: <https://doi.org/10.1038/s41598-018-35758-w>.
- Vernon, R.G. (1980). Lipid metabolism in the adipose tissue of ruminant animals. *Progress in Lipid Research*, 19(1-2), 23-106. [Online]. Available at: [doi:10.1016/0163-7827\(80\)90007-7](https://doi.org/10.1016/0163-7827(80)90007-7).
- Vika, E. (2011). Diachronic dietary reconstructions in ancient Thebes, Greece: results from stable isotope analyses. *Journal of Archaeological Science*, 38(5), 1157-1163. [Online]. Available at: [doi:10.1016/j.jas.2010.12.019](https://doi.org/10.1016/j.jas.2010.12.019).
- Wahie, S., Lloyd, J.J. and Farr, P.M. (2007). Sunscreen ingredients and labelling: a survey of products available in the UK. *Clinical and Experimental Dermatology*, 32(4), 359-364. [Online]. Available at: [doi:10.1111/j.1365-2230.2007.02404.x](https://doi.org/10.1111/j.1365-2230.2007.02404.x).

- Wallace, M., Jones, G., Charles, M., Fraser, R., Halstead, P., Heaton, T.H.E. and Bogaard, A. (2013). Stable carbon isotope analysis as a direct means of inferring crop water status and water management practices. *World Archaeology*, 45(3), 388-409. [Online]. Available at: doi:10.1080/00438243.2013.821671.
- Wallace, M.P., Jones, G., Charles, M., Fraser, R., Heaton, T.H.E. and Bogaard, A. (2015). Stable Carbon Isotope Evidence for Neolithic and Bronze Age Crop Water Management in the Eastern Mediterranean and Southwest Asia. *PLOS ONE*, 10(6), 1-19. [Online]. Available at: <https://doi.org/10.1371/journal.pone.0127085>.
- Walsh, R. (2017). Experiments on the effects of charring on *Setaria italica* (foxtail millet). *Vegetation History and Archaeobotany*, 26(4), 447-453. [Online]. Available at: doi:10.1007/s00334-016-0600-0.
- Wang, T., Wei, D., Chang, X., Yu, Z., Zhang, X., Wang, C., Hu, Y. and Fuller, B.T. (2017). Tianshanbeilu and the Isotopic Millet Road: reviewing the late Neolithic/Bronze Age radiation of human millet consumption from north China to Europe. *National Science Review*, 6(5), 1024-1039. [Online]. Available at: <https://doi.org/10.1093/nsr/nwx015>.
- Wang, X., Fuller, B.T., Zhang, P., Hu, S., Hu, Y. and Shang, X. (2018). Millet manuring as a driving force for the Late Neolithic agricultural expansion of north China. *Scientific Reports*, 8(1). [Online]. Available at: <https://doi.org/10.1038/s41598-018-23315-4>.
- Wardle, K., Higham, T. and Kromer, B. (2014). Dating the end of the Greek Bronze Age: a robust radiocarbon-based chronology from Assiros Toumba. *PLOS ONE*, 9(9), 1-9. [Online]. Available at: <https://doi.org/10.1371/journal.pone.0106672>.
- Weber, S.A. and Fuller, D.Q. (2008). Millets and their role in early agriculture. *Pragdhara*, 18 (69), 69-90. [Online]. Available at: <http://dx.doi.org/>.
- Weete, J.D., Abril, M. and Blackwell, M., (2010). Phylogenetic distribution of fungal sterols. *PLOS ONE*, 5(5), 1-6. [Online]. Available at: <https://doi.org/10.1371/journal.pone.0010899>.
- Weisskopf, A. R. and Lee, G.-A. (2016). Phytolith identification criteria for foxtail and broomcorn millets: a new approach to calculating crop ratios. *Archaeological and Anthropological Sciences*, 8(1), 29-42. [Online]. Available at: doi:10.1007/s12520-014-0190-7.
- Whelton, H.L., Roffet-Salque, M., Kotsakis, K., Urem-Kotsou, D. and Evershed, R.P. (2018). Strong bias towards carcass product processing at Neolithic settlements in northern Greece revealed through absorbed lipid residues of archaeological pottery. *Quaternary International*, 496, 127-139. [Online]. Available at: <https://doi.org/10.1016/j.quaint.2017.12.018>.
- Woodbury, S.E., Evershed, R.P., Rossell, J.B., Griffith, R.E. and Farnell, P. (1995). Detection of Vegetable Oil Adulteration Using Gas Chromatography Combustion/Isotope Ratio Mass Spectrometry. *Analytical Chemistry*, 67(15), 2685-2690. [Online]. Available at: doi:10.1021/ac00111a029.
- Xu, Y., Liu, M., Li, C., Sun, F., Li, P., Meng, F., Zhao, X., He, M., Wang, Z., Shu, X., Zhao, X. and Shou, H. (2019). Domestication and Spread of Broomcorn Millet (*Panicum miliaceum*

- L.) Revealed by Phylogeography of Cultivated and Weedy Populations. *Agronomy*, 9(12), 1-17. [Online] Available at: <https://doi.org/10.3390/agronomy9120835>.
- Yang, Q., Li, X., Liu, W., Zhou, X., Zhao, K. and Sun, N. (2011). Carbon isotope fractionation during low temperature carbonization of foxtail and common millets. *Organic Geochemistry*, 42(7), 713-719. [Online]. Available at: doi:10.1016/j.orggeochem.2011.06.012.
- Yang, X., Wan, Z., Perry, L., Lu, H., Wang, Q., Zhao, C., Li, J., Xie, F., Yu, J., Cui, T., Li, M. and Ge, Q. (2012a). Early millet use in northern China. *Proceedings of the National Academy of Sciences of the United States of America*, 109(10), 3726-3730. [Online]. Available at: doi:10.1073/pnas.1115430109.
- Yang, X., Zhang, J., Perry, L., Ma, Z., Wan, Z., Li, M., Diao, X. and Lu, H. (2012b). From the modern to the archaeological: starch grains from millets and their wild relatives in China. *Journal of Archaeological Science*, 39(2), 247-254. [Online]. Available at: doi:10.1016/j.jas.2011.09.001.
- Yang, Y., Shevchenko, A., Knaust, A., Abuduresule, I., Li, W., Hu, X., Wang, C. and Shevchenko, A. (2014). Proteomics evidence for kefir dairy in Early Bronze Age China. *Journal of Archaeological Science*, 45, 178-186. [Online]. Available at: doi:10.1016/j.jas.2014.02.005.
- Yates, A.B., Smith, A.M. and Bertuch, F. (2015). Residue radiocarbon AMS dating review and preliminary sampling protocol suggestions. *Journal of Archaeological Science*, 61(C), 223-234. [Online]. Available at: doi:10.1016/j.jas.2015.06.011.
- Yoneda, M., Kisida, K., Gakuhari, T., Omori, T. and Abe, Y. (2019). Interpretation of bulk nitrogen and carbon isotopes in archaeological foodcrusts on potsherds. *Rapid Communications in Mass Spectrometry*, 33(12), 1097-1106. [Online]. Available at: doi:10.1002/rcm.8446.
- Zadernowski, R., Naczek, M. and Nesterowicz, J. (2005). Phenolic acid profiles in some small berries. *Journal of agricultural and food chemistry*, 53(6), 2118-2124. [Online]. Available at: doi:10.1021/jf040411p.
- Zavodny, E., McClure, S.B., Welker, M.H., Culleton, B.J., Balen, J. and Kennett, D.J. (2019). Scaling up: Stable isotope evidence for the intensification of animal husbandry in Bronze-Iron Age Lika, Croatia. *Journal of Archaeological Science: Reports*, 23, 1055-1065. [Online]. Available at: doi:10.1016/j.jasrep.2018.10.008.
- Zhang, J., Lu, H., Wu, N., Yand, X. and Diao, X. (2011). Phytolith analysis for differentiating between foxtail millet (*Setaria italica*) and green foxtail (*Setaria viridis*). *PLOS ONE*, 6(5), 1-11. [Online]. Available at: <https://doi.org/10.1371/journal.pone.0019726>.
- Zhao, Z. (2011). New Archaeobotanic Data for the Study of the Origins of Agriculture in China. *Current Anthropology*, 52(S4), S295-S306. [Online]. Available at: doi:10.1086/659308.
- Zohary, D., Hopf, M. and Weiss, W. (2012). *Domestication of plants in the old world: the origin and spread of domesticated plants in south-west Asia, Europe, and the Mediterranean basin*, 4th ed. Oxford: Oxford University Press.

Appendix One: Methods

Cleaning

The equipment used during this project is divided into two categories, glassware and other. Glassware was either purchased 'clean' or re-used within the lab, all of which was subject to heating in a furnace, at 400°C, prior to use. In addition, re-used glassware was physically cleaned of visible debris, using water and a pipe cleaner, before chemical cleaning in a dishwasher. Other equipment was cleaned using a combination of physical cleaning with water, followed by rinsing sequentially with methanol (x2), and DCM (x3).

Sampling

Ceramics

Samples of ceramics were primarily obtained, in a powdered form, using a model drill. The sampling area was cleaned, using the drill, by removing the top surface layer of the sherd. A clean drill bit was used for taking the sample. Samples of archaeological sherds were obtained from an approximately 2 x 2 cm area on the internal surface, away from the sherd edge, up to a depth of 0.5 cm. Several archaeological sherds were too small to sample with a drill, although they could be cleaned by this method. After cleaning, these sherds were crushed, by hand, using a clean agate pestle and mortar. Experimental ceramic samples utilised the entire ceramic sherd, as lipids were absorbed from all directions. Therefore, the entire external surface was removed, and the entire height and depth of the sherd used as a sample.

Foodcrusts

Samples of foodcrusts were taken from ceramics and, in one case, an amorphous charred food deposit, using a scalpel. Samples were crushed and homogenised in an agate pestle and mortar prior to analysis.

Millet

Small quantities of millet seeds were obtained from the UCL (University College London) archaeobotanical reference collection. Subsamples of the seeds were crushed and homogenised by hand, using an agate pestle and mortar, and stored in glass vials, prior to extraction and analysis.

Cooking liquids

Cooking liquid samples were freeze dried prior to bulk carbon and nitrogen isotope analysis.

Lipid Extraction

Acid methanol

Simultaneous extraction and derivatisation of lipids was achieved using an adapted acid methanol methodology (Correa-Ascencio and Evershed 2014). Methanol was added to homogenised samples of ceramic powders (4 mL to 1 g), charred foodcrusts (1 mL to 20 mg), raw millets (4 mL to < 50 mg). Mixtures were ultrasonicated for 15 minutes, before adding concentrated (98%) sulphuric acid (H₂SO₄), and heating, at 70°C, for four hours. The volume of H₂SO₄ used was proportional to the volume of methanol, with 800 µL used for ceramic powder and raw millet samples and 200 µL for charred foodcrust samples. Following centrifugation, at 3000 rpm for five minutes, extracts were transferred to a separate vial. Lipids were extracted from the acidified mixture using n-hexane (3 x 2 mL) and dried under a gentle stream of nitrogen. Samples were resuspended in 100 µL of n-hexane and transferred to a conical insert, in a GC vial, with 10 µL of a C₃₆ alkane standard that was agitated, before analysis, to ensure homogenisation. A C_{16:0} and C_{18:0} fatty acid standard was processed with each batch of around 10 samples, in addition to a method blank.

Solvent

Lipids were extracted from ceramic and millet samples, by ultrasonication for 15 minutes, with a 2:1 v:v mixture of DCM:MeOH (3 x 2 mL). The supernatant was separated from the ceramic powder, between each sonication stage, by centrifugation at 3000 rpm for 5 minutes. Extracts were dried under a gentle stream of nitrogen before derivatisation. Before analysis, samples were silylated, requiring the heating of extracts for an hour, at 70°C, with 100 µL of N,O-bis(trimethylsilyl)trifluoroacetamide (BSTFA) with 1% trimethylchlorosilane (TMCS). Samples were resuspended in 100 µL of n-hexane and transferred to a conical insert, in a GC vial, with 10 µL of a C₃₆ alkane standard that was agitated, before analysis, to ensure homogenisation. A C_{16:0} and C_{18:0} fatty acid standard was processed with each batch of around 10 samples, in addition to a method blank.

Bulk Isotope Sample Preparation

Pre-treatment was not applied to archaeological foodcrust samples subjected to EA-IRMS analysis, due to inconsistent results and sample loss reported elsewhere (Brinkkemper *et al.* 2018). As such, sample preparation was consistent with Heron *et al.* (2016).

Analysis

EA-IRMS

Bulk carbon and nitrogen isotope analysis was undertaken on samples (1 mg duplicate) of reference materials, freeze-dried experimental cooking liquids, and archaeological charred foodcrusts. Samples were combusted, to obtain CO₂ and N₂, with a Sercon (Crewe, UK) continuous flow 20-22 Isotope Ratio Mass Spectrometer with universal Faraday triple collectors (C,N,S,O) and additional single Faraday collector for *m/z* 3 (H). This was coupled to an EA-GSL preparation unit with a 66 place open carousel autosampler. Uncertainties of each measurement were calculated according to Kragten (1994), combining uncertainty values of international standards and repeat measurements of samples and reference materials. Data was corrected with international standards, IAEA 600 caffeine, IAEA N2 ammonium sulphate, and IA R006 cane sugar (IsoAnalytical). Results were reported in per mil (‰) relative to standards. The precision of experimental cooking liquid samples was 0.7 (1σ) for δ¹³C and δ¹⁵N. The precision of charred crust samples from Bruszczewo was 0.05 (1σ) for δ¹³C and 0.18 (1σ) for δ¹⁵N.

Gas Chromatography - Mass Spectrometry

GC-MS analysis of solvent and AM extracted Polish, Greek, and Bulgarian archaeological samples, experimental ceramic samples, and reference millet samples, was undertaken using an Agilent 7890A Series Gas Chromatograph coupled to an Agilent 5977B Mass-selective detector equipped with a quadrupole mass analyser (Agilent technologies, Cheshire, UK). A split/splitless injector, operated in splitless mode with a purge flow of 50 mL min⁻¹, was maintained at 300°C and a DB-5MS column was used (30 m x 250 μm x 0.25 μm, Agilent technologies, Cheshire, UK). Helium was the carrier gas (2 mL min⁻¹). For acid methanol extracts, the oven temperature was set to 50°C for 2 minutes, then increased at 10°C min⁻¹ to 200°C before increasing at 4°C min⁻¹ to 320°C and held for 5 minutes. For solvent extracts, the oven temperature was set to 50°C

for 2 minutes, then increased at $10^{\circ}\text{C min}^{-1}$ to 325°C and held for 15 minutes. The ionization energy of the mass spectrometer was 70 eV and spectra were obtained in scanning mode between m/z 50 and 800. The transfer line temperature was held at 280°C .

Selective ion monitoring (SIM) of solvent extracts was undertaken using an Agilent 7890A Series Gas Chromatograph coupled to an Agilent 5977B Mass-selective detector equipped with a quadrupole mass analyser (Agilent Technologies, Cheshire, UK). A split/splitless injector, operated in splitless mode with a purge flow of 50 mL min^{-1} , was maintained at 300°C and a (50%-cyanopropyl)-methylpolysiloxane DB-23 column was used (PN 122-2362; $60\text{ m} \times 250\text{ }\mu\text{m} \times 0.25\text{ }\mu\text{m}$; J&W Scientific technologies, Folsom, CA, USA). Helium was the carrier gas (1.5 mL min^{-1}). The oven was set to 50°C for 2 minutes, increased at $10^{\circ}\text{C min}^{-1}$ to 100°C , increased at $4^{\circ}\text{C min}^{-1}$ to 140°C , increased at $0.5^{\circ}\text{C min}^{-1}$ to 160°C , then increased at $20^{\circ}\text{C min}^{-1}$ to 250°C and held for 10 minutes. SIM mode was used in order to target the specific markers of aquatic resources using characteristic ion groups: m/z 74, 87, 213, 270 for 4,8,12-trimethyltridecanoic acid (4,8,12-TMTD), m/z 74, 88, 101, 312 for pristanic acid, m/z 74, 101, 171, 326 for phytanic acid, and m/z 74, 105, 262, 290, 318, 346 for the detection of ω -(*o*-alkylphenyl)alkanoic acids of carbon lengths C16 to C22 (APAA16-22). The transfer line temperature was held at 280°C .

MassHunter software (Agilent Technologies) and the NIST 17 mass spectra database was used for quantitative and qualitative analysis of extracts.

Gas Chromatography - Combustion - Isotope Ratio Mass Spectrometry

Compound specific carbon isotope (GC-C-IRMS) analysis of methyl palmitate and methyl stearate was undertaken, for AM extracts, using an Isoprime 100 (Isoprime, Cheshire, UK) IRMS detector coupled to an Agilent 7890B Series Gas Chromatograph with an Isoprime GC5 interface. An 5975C inert XL mass-selective detector (MSD) equipped with a quadrupole mass analyser was also coupled to the GC. A split/splitless injector, operated in splitless mode with a purge flow of 50 mL min^{-1} , was maintained at 300°C and a DB-5MS UI column was used (PN 122-5562UI; $60\text{ m} \times 250\text{ }\mu\text{m} \times 0.25\text{ }\mu\text{m}$; J&W Scientific technologies, Folsom, CA, USA). Helium (ultra-high purity grade) was the carrier gas (2 mL min^{-1}). The oven temperature was set to 50°C for 0.5 minutes, increased at $25^{\circ}\text{C min}^{-1}$ to 175°C , then increased at $8^{\circ}\text{C min}^{-1}$ to 325°C and held for 20 minutes. Gases eluted from the column were split into two streams, that entered the MSD and GC5 interface. The

ionization energy of the mass spectrometer was 70 eV and spectra were obtained in scanning mode between m/z 50 and 800. The GC5 furnace tube (CuO) was maintained at 850°C to oxidise carbon species to CO₂. Clear resolution and baseline separation of analysed peaks was achieved. Products eluted from the furnace were ionised in the IRMS by electron impact. Ion intensities of m/z 44, 45 and 46 were recorded for automatic computing of the ¹³C/¹²C ratio of each peak in the extracts.

Computation was made with IonVantage and IonOS softwares (Isoprime, Cheadle, UK). The results of the analysis were expressed in per mill (‰) relative to an international standard, V-PDB. The accuracy and precision of the instrument was determined on *n*-alkanoic acid ester standards of known isotopic composition (Indiana standard F8-3). The mean ± S.D. values of these were: -29.96 ± 0.11‰ (Bruszczewo); -29.96 ± 0.08‰ (Lete I, Olympus, Archondiko); and -29.96 ± 0.11‰ (Dikili Tash) for the methyl ester of C_{16:0} (reported mean value vs. VPDB -29.90 ± 0.03‰), and -23.31 ± 0.08‰ (Bruszczewo); -23.27 ± 0.07‰ (Lete I, Olympus, Archondiko); -23.79 ± 0.48‰ (Dikili Tash) for C_{18:0} (reported mean value vs. VPDB -23.24 ± 0.01‰). Each sample was measured in duplicate (mean of S.D. 0.30‰ (Bruszczewo), 0.13‰ (Lete I, Olympus, Archondiko), and 0.01‰ (Dikili Tash) for C_{16:0} and 0.26‰ (Bruszczewo), 0.10‰ (Lete I, Olympus, Archondiko), and 0.01‰ (Dikili Tash) for C_{18:0}). Values were also corrected after analysis to account for the methylation of the carboxyl group that occurs during acid extraction. Corrections were based on comparisons with a standard mixture of C_{16:0} and C_{18:0} fatty acids of known isotopic composition processed in each batch under identical conditions. The results from the analysis are reported in parts per mil (‰) relative to an international standard (V-PDB). Each batch of samples was calibrated using a calibration curve (average R² = 0.998 (Bruszczewo) in 1 batch; 0.999 ± 0.011 (Lete I, Olympus, Archondiko) in 4 batches; 0.995 (Dikili Tash) in 1 batch) based on expected vs. measured δ¹³C values of *n*-alkanes and *n*-alkanoic acid esters international standards (Indiana A6 and F8-3 mixture). More precisely, the accuracy of the instrument was determined on *n*-alkanoic acid ester standards of known isotopic composition (Indiana standard F8-3, 4 (Bruszczewo); 12 (Lete I, Olympus, Archondiko); 4 (Dikili Tash) measurements).

Appendix Two: Triterpene Identification (Chapter 4)

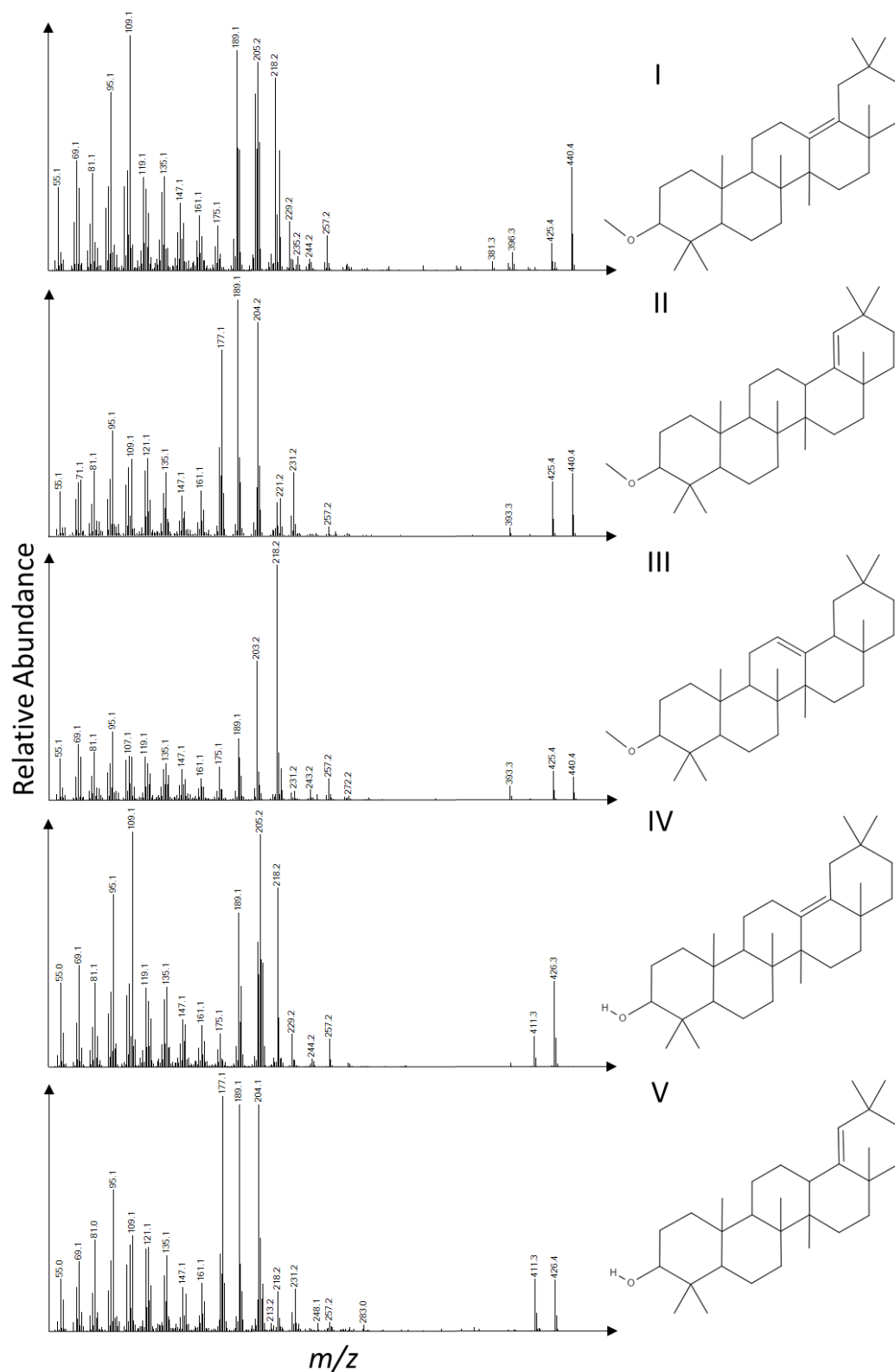


Figure A2. 1. Mass spectra and identified/proposed structure of compounds observed in solvent and acid methanol extracts of millets discussed in Chapter 4. **I** δ -amyirin ME, **II** miliacin, **III** β -amyirin ME, **IV** δ -amyirin, **V** germanicol.

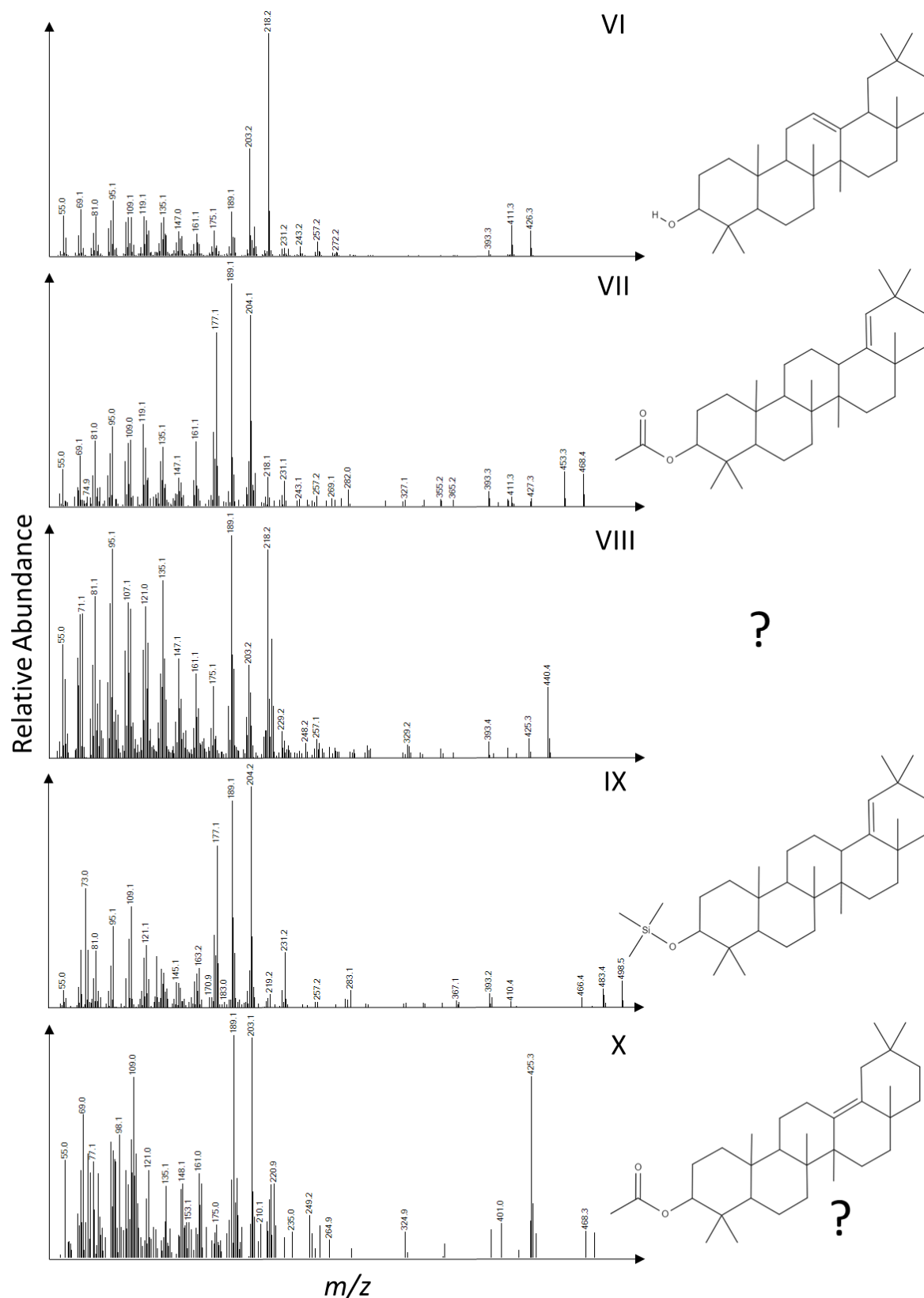


Figure A2. 2. Mass spectra and identified/proposed structure of compounds observed in solvent and acid methanol extracts of millets discussed in Chapter 4. **VI** β -amyrin, **VII** germanicol acetate, **VIII** compound unknown, **IX** germanicol TMS, **X** δ -amyrin acetate?.

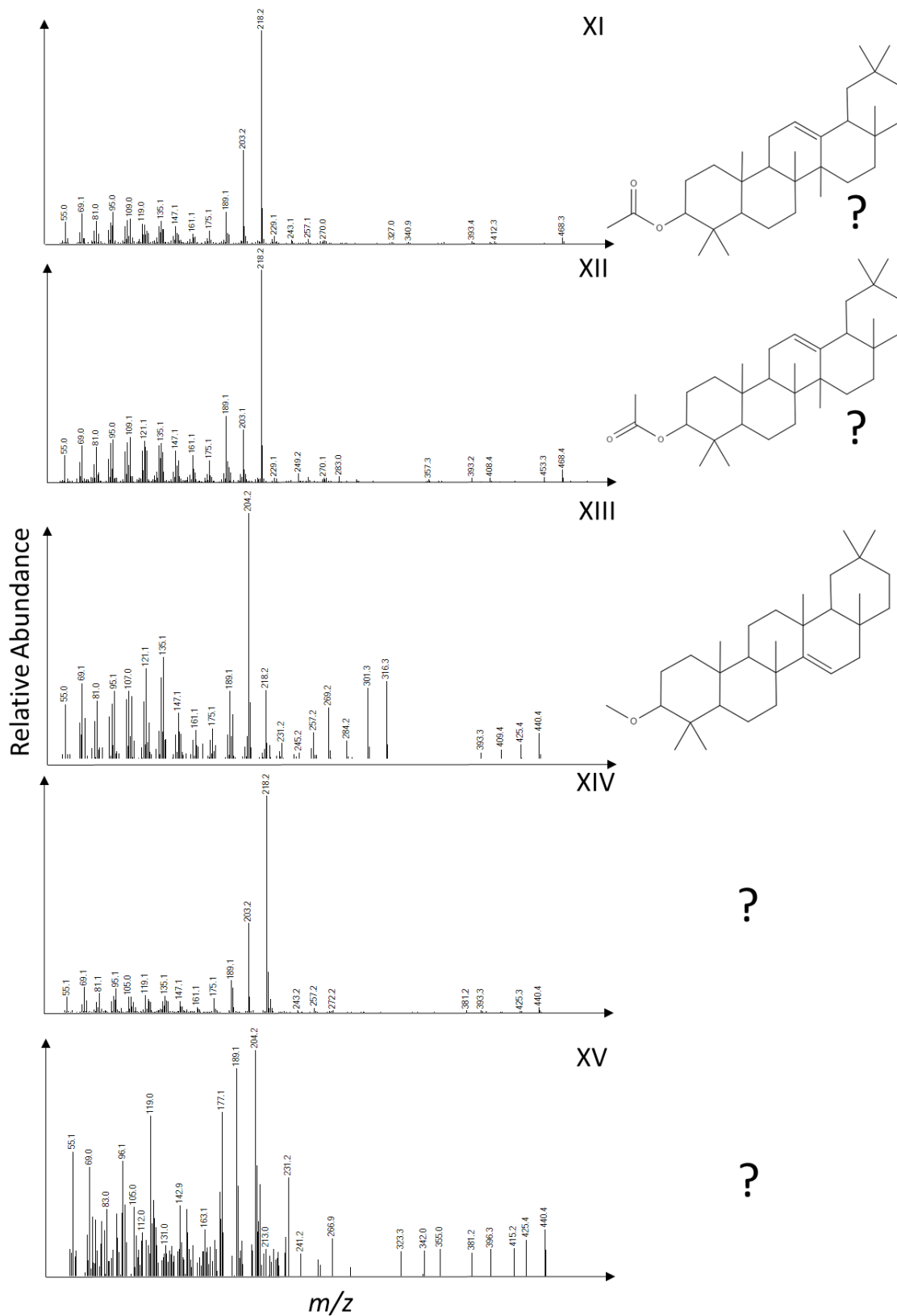


Figure A2. 3. Mass spectra and identified/proposed structure of compounds observed in solvent and acid methanol extracts of millets discussed in Chapter 4. **XI** β -amyrin acetate?, **XII** β -amyrin acetate?, **XIII** sawamilletin, **XIV** compound unknown, **XV** compound unknown.

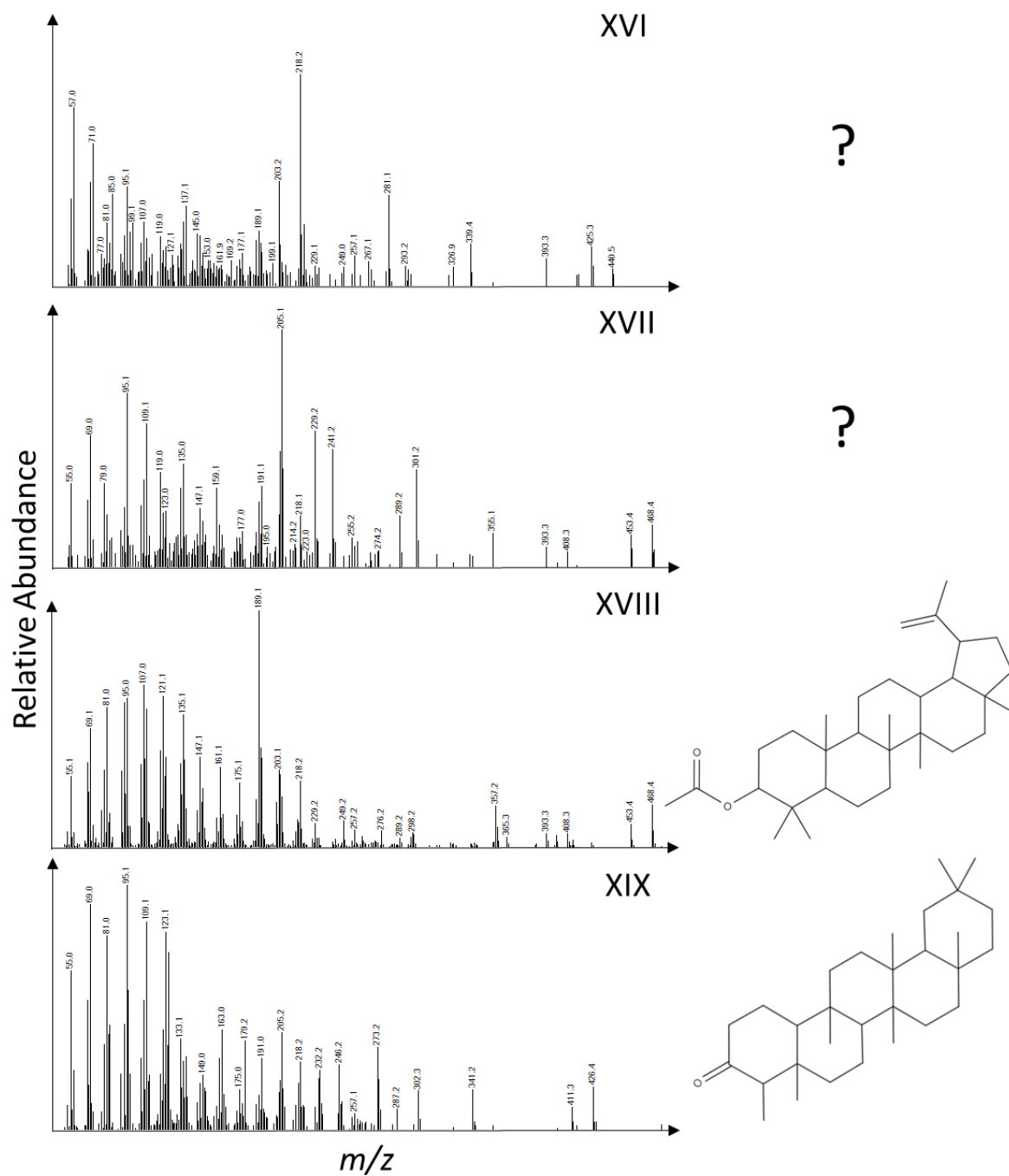


Figure A2. 4. Mass spectra and identified/proposed structure of compounds observed in solvent and acid methanol extracts of millets discussed in Chapter 4. **XVI** compound unknown, **XVII** compound unknown, **XVIII** lupeol acetate, **XIX** friedelin.

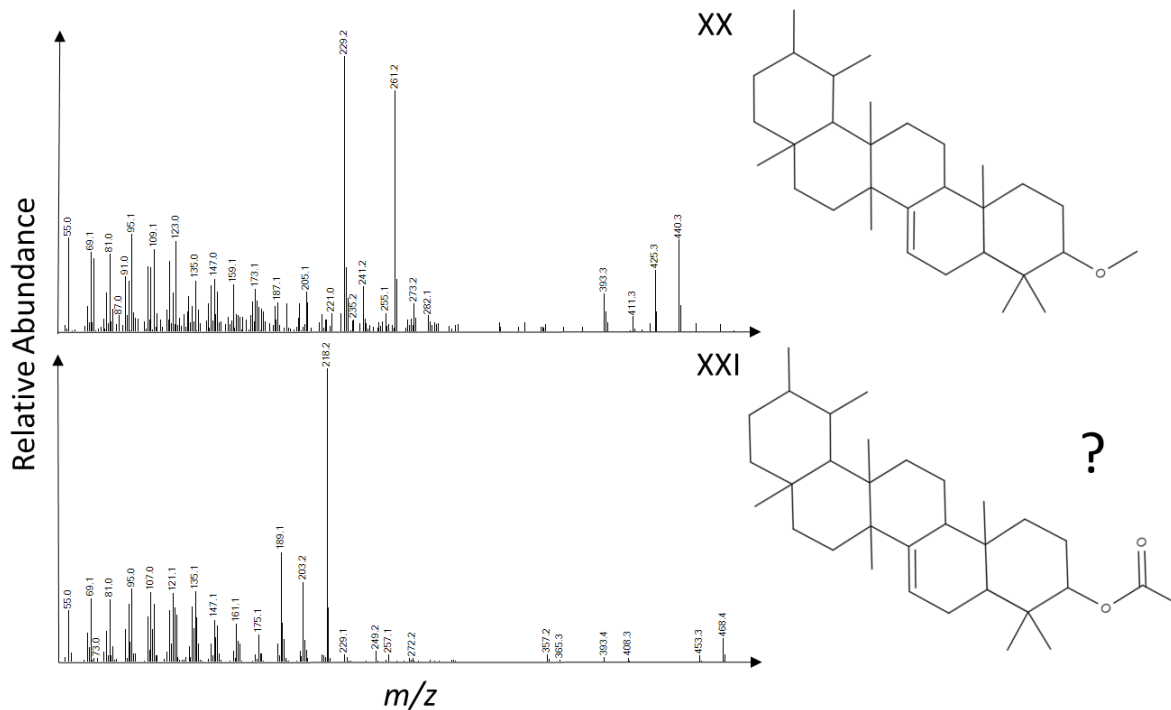


Figure A2. 5. Mass spectra and identified/proposed structure of compounds observed in solvent and acid methanol extracts of millets discussed in Chapter 4. **XX** bauerenol ME and **XXI** compound unknown.

Appendix Three: Bruszczewo Dataset (Chapter 6)

Table A3. 1. Contextual information for samples from Bruszczewo.

Personal ID	Find No.	ID No.	Trench	Area	X	Y	Z	Horizon	Feature No.	Feature Description	Additional Finds						Description (Additional to Ceramic)	
											Bone (H)	Bone (A)	Ceramic	Botanical	Daub	Other		
B1	F4088	3699	30	4	55.5	-95.5	0	6	BEF4006	Sand tor mixture	X	X	X					Charred Crust
B2	F7164	2985	31	7	60.5	-67	0	5	BEF7007	Transgression layer in lake	X	X						Charred Crust
B3	F1428	1810	30	1	49.7	-87.3	69.4	6-7	BEF1003, 1006							X		Charred Crust
B4	F11806	12385	52	11	53.5	-89.5	0	2-3	BEF11616	Part of a small post			X					Charred Crust
B5	F11806	12385	52	11	53.5	-89.5	0	2-3	BEF11616	Part of a small post			X					Charred Crust
Br 001	F4311	4409	30	4	45.5	-93.5	0	4	BEF4014	Cultural layers around the wattle fences							X	Amorphous Charred Material
Br 002	F4361	4329	30	4	54.3	-93.5	0	3	BEF4013	Cultural layer over wattle fence								
Br 003	F6122	7932	31	6	63.5	-91.5	0	4	BEF6006	Accumulation on wattle fence, cultural deposits								
Br 004	F8659	6646	31	8	59.5	-70.5	0	1	BEF8015	Cultural layers around the wattle fences	X						X	
Br 005	F18236	21403	52	12/14	0	0	0	3-4	BEF11078 D	Older cultural layer								
Br 006	F18320	20634	52	12/14	59	-68.5	0	4b	BEF12034	Cultural layer								
Br 007	F18236	21224?	52	12/14	58	-70.5	0	3-4	BEF11078 D									
Br 008	F12516	18161	52	12	50.5	-88.5	0	4b	BEF12034	Cultural layer	X							Silver coating, charred crust inside
Br 009	F18321	21001	52	12/14	60.5	-72.5	0	4b	BEF12034	Cultural layer								
Br 010	F18325	20814	52	12/14	62.5	-70.5	0	4b	BEF12034	Cultural layer								
Br 011	F7308	3590	31	7	63.5	-71.5	0	0	BEF7010	Occupation layer								
Br 012	F11786	12454	52	11	63.5	-72.5	0	2-3	BEF11530	Lower layer path between houses	X	X						
Br 013	F14200	14074	52	14	64.5	-72.5	0	3-4	BEF11078	House remains rubble, house 4C								
Br 014	F14211	13510	52	14	62.1	-67.4	68.9	3-4	BEF11100	House 4C								
Br 015	F14236	13704	52	14	63.5	-63.5	0	3-4	BEF11078	House remains rubble, house 4C								
Br 016	F14625	14700	52	14	0	0	0	3-4	BEF14042a	Collapsed daub wall House 4C								
Br 017	F18116	21283	52	12/14	59	-69.5	0	4b	BEF12034	Cultural layer							X	
Br 018	F18275	21217	52	12/14	58	-68.5	0	4b	BEF12034	Cultural layer							X	
Br 019	F18304	20714	52	12/14	59	-69.5	0	3-4	BEF11078D								X	
Br 020	F18414	20140	52	12/14	57.5	-94.5	0	2-3	BEF14010	Wattle fence (nr. 2)								X

Table A3. 1. Continued.

Personal ID	Find No.	ID No.	Trench	Area	X	Y	Z	Horizon	Feature No.	Feature Description	Additional Finds					Description (Additional to Ceramic)	
											Bone (H)	Bone (A)	Ceramic	Botanical	Daub		Other
Br-101	F1082	2680	30	1				6	BEF1007	Peat sand mixture, lake shore							Peat or Charred Crust
Br-102	F1082	2680	30	1	49.5	-90.5	0.0	6	BEF1006	Peat sand mixture, lake shore			X				Peat or Charred Crust
Br-103	F2344	1523	30	2	44.5	-90.5	0.0	6	BEF2031	Peat sand mixture disturbed layer			X				
Br-104	F4071	3796	30	4	49.5	-87.5	0.0	6b	BEF4005	Dung layer			X				
Br-105	F4148	3889	30	4	49.5	-87.5	0.0	6b	BEF4005	Dung layer			X				
Br-106	F7062	4657	31	7	48.5	-88.5	0.0	7	BEF7004	Brown peat			X				
Br-107	F7073	4200	31	7	48.5	-93.5	0.0	7	BEF7004	Brown peat			X				
Br-108	F7308	3590	31	7	0.0	0.0	0.0	0	BEF7010	Occupation layer			X				
Br-109	F8140	6403	31	8	0.0	0.0	0.0	6	BEF8004	Dung layer			X				
Br-110	F9089	7244	31	9	61.5	-91.5	0.0	7	BEF9005	Carr peat, lake shore with trees			X				Black inner coating
Br-111	F12352	18447	52	12	62.1	-67.4	68.9	8	BEF12021	Dislocated cultural layer			X				Bright inner crust
Br-112	F12384	18300	52	12	62.1	-67.4	68.9	7-8	BEF12030	Peat sand mixed layer maybe already Horizon 6, lake shore			X				
Br-113	F1428	1810	30	1	50.0	-90.5	0.0	6-7	BEF1003, 1006								X
Br-114	F3102	4632	30	3	43.8	-93.3	0.0						X				
Br-115	F4088	3697	30	4	0.0	0.0	0.0	6	BEF4006	Sand for mixture			X		X		
Br-116	F4096	3693	30	4	0.0	0.0	0.0	6b	BEF4005	Dung layer			X				
Br-117	F4217	4494	30	4				6b	BEF4009	detritus layer with rubbish along lake shore							X
Br-118	F5042	5444	31	5	0.0	0.0	0.0	6	BEF5003	Peat sand mixture, lake shore			X				
Br-119	F6080	7671-77	31	6	50.5	-91.5	0.0						X				X
Br-120	F7063	4713	31	7	44.9	-88.9	69.7	7	BEF7004	Brown peat			X				
Br-121	F7063	4713	31	7				7	BEF7004	Brown peat			X				
Br-122	F8104	6388	31	8	57.5	-67.6	69.1	6	BEF8004	Dung layer			X				

Table A3. 2. Details of ceramic sherds sampled from Bruszczewo.

Personal ID	Fragments		Weight	Wall thickness (min)	Wall thickness (max)	Ceramic Style				Surface Treatment	Temper	Temper/Inclusion Type				Sherd Type	Storage Vessel
	1	2				go - type	gt - type	gu - type	gb - type			Ornamentation	Feldspar	Mica	Limestone		
B1	1	12	6	8								X					
B2	1	10	12	13					Partial silver coat	0.65- 1 mm			X		Wall		
B3	1	78	11	13								X					X
B4	1	45	6	7					Smoothed	0.65- 1 mm		X	X		Wall		
B5	1	45	6	7					Smoothed	0.65- 1 mm		X	X		Wall		
Br 6152	1									0.3 mm					Wall		
Br-001	1	28	9	12									X				
Br-002	1	22	10	11								X	X				
Br-003	1	12	8	8						0.3- 0.63 mm		X	X		Wall		
Br-004	1	36	5	5						> 1 mm		X			Wall		
Br-005	2	118	5	8					Slop Coat	0.3- 0.63 mm			X		Wall		
Br-006	1	15	6	8					Slop Coat	0.65- 1 mm		X	X		Wall		
Br-007	10	58	11	14													
Br-008	1	48	9	10						> 1 mm			X		Wall		
Br-009	1	13	7	9					Polished	> 1 mm			X		Wall		
Br-010	1	16	8	9					slop coat	0.65- 1 mm					Wall		
Br-011	1	44	11	12									X	X			
Br-012	1	13	7	7					Slop Coat	0.65- 1 mm		X	X		Wall		
Br-013	1	18	8	8					Slop Coat	> 1 mm		X	X		Wall		
Br-014	1	5	4	5					Smoother	0.65- 1 mm		X	X		Wall		
Br-015	2	36	5	12					Slop Coat	> 1 mm		X	X		Wall		
Br-016	1	64	10	11								X	X		Wall		X
Br-017	1	11	7	8					Smoothed	> 1 mm			X		Wall		
Br-018	4	52	10	11					Slop Coat	> 1 mm			X		Wall		
Br-019			4	7					Smoothed	0.65- 1 mm					Wall		
Br-020	1	6	6	7					Slop Coat	0.65- 1 mm			X		Wall		X

Table A3. 2. Continued.

Personal ID	Fragments	Weight	Wall thickness (min)	Wall thickness (max)	Ceramic Style					Surface Treatment	Temper	Temper/Inclusion Type				Sherd Type	Storage Vessel
					go - type	gt - type	gu - type	gb - type	Ornamentation			Feldspar	Mica	Limestone	Quartz		
Br-101	1	43	10	13						Partial Silver Coating	> 1 mm		X				
Br-102	1	50	10	12			GU 01 C			Rough	> 1 mm			X			
Br-103	1	41	5	6			GU 01 B	GB 08		Rough	0.3- 0.63 mm	X	X	X			
Br-104	1	16	6	8						Smoothed	> 1 mm	X			X		
Br-105	1	64	9	10						Smoothed	0.55- 1 mm		X		X		Wall
Br-106	2	18	9	9						Smoothed	> 1 mm	X	X				
Br-107	1	44	11	12						Smoothed	> 1 mm			X			
Br-108	1	90	12	12						Smoothed	0.55- 1 mm	X	X		X		Wall
Br-109	1	12	7	7						Silt Cover	~ 0.3 mm				X		Wall
Br-110	1	22	3	6						Smoothed	0.55- 1 mm		X		X		Wall
Br-111	1	36	6	11	GO 04 D	Steep walled			VZ 04 Plastic Molding A	Smoothed	> 1 mm		X		X		Rim and Wall
Br-112	1	78	11	13						Silt Cover	0.55- 1 mm	X			X		
Br-113	1	215	0	0					Miller Impression	Rough	> 1 mm	X					Base
Br-114	1	11	11	12	GO 04 C	Steep walled			VZ 05 Finger Pin B	Smoothed	0.55- 1 mm	X	X		X		Rim and Wall
Br-115	1	17	6	7						Silt Cover	0.55- 1 mm	X	X		X		
Br-116	1	87	9	11					Other unknown	Smoothed	0.55- 1 mm	X	X		X		Wall
Br-117	1	8	9	12						Smoothed	0.3- 0.63 mm			X			Wall
Br-118	1	40	9	11	GO 04 D				VZ 05 Finger Pin B	Smoothed	0.55- 1 mm			X			Wall
Br-119	3	67	10	12						Silt Cover	0.55- 1 mm	X					Wall
Br-120	2	67	10	12						Silt Cover	0.55- 1 mm	X					Wall
Br-121	2	67	10	12						Silt Cover	0.55- 1 mm	X					Wall
Br-122	2	67	10	12						Silt Cover	0.55- 1 mm	X					Wall

Figure A3. 3. TLE yield and compound identification of samples from Bruszczewo.

Personal I.D.	Sample Mass (mg)	Lipid Concentration (µg/g)	Free Fatty Acids				Diacids	APAA	Miltac in	Cholesterol Derivatives	Sterols	Pine Diterpenes		
			S - FFA	U - FFA	PU - FFA	Br - FFA						Retene	Dehydrated	7-Oxo-
B1	21	3227	10-30	16, 18	18	14,15,16	8,10,12	18	Yes	Yes	Sitosterol	Yes	Yes	Yes
B2	10	-	-	-	-	-	-	-	-	-	-	-	-	-
B3	20	857	14-30	18, 22		14	9	18	Yes		Sitosterol			
B4	32	883	12-31	18, 22		14	8	18	No		Stigmasterol	Yes		
B5	14	491												
Br 001 I	1014	139	12-28,30,32	18, 22		14,16,18		18	No	Yes				
Br 001 F	18	814	14-26,28	16,18,20, 22		14-16		18	No	Yes	Sitosterol			
Br 002 I	1129	26	16,18,20, 22,24,25, 26,27,28, 28,30,32, 34	22					No			Yes	Yes	
Br 002 F	26	152	16-18,20,22, 24-30,32	18,22		15,16			No					
Br 003 I	1132	65	12-28,30	18, 22		24	9		No	Yes			Yes	Yes
Br 003 F	17	732	14-28	18, 22		14-18	12-14	18	No	Yes			Yes	Yes
Br 004 I	1040	16	16-26 Even	22					No					
Br 004 F	-	-	-	-	-	-	-	-	-	-	-	-	-	-
Br 005 I	1010	21	14-28,30,32	16,18,22			13	18	No					
Br 005 F	29	767	14-30,32,34	16,18,20, 22, 24			14-17,23,25	18	No	Yes	Stigmasterol, Ergosterol			
Br 006 I	1017	94	10-32,34	18		13,15,16, 17	8-11,13	18	No		Sitosterol			
Br 006 F	-	-	-	-	-	-	-	-	-	-	-	-	-	-
Br 007 I	1073	267	10-30,32	16,17,18, 22		12-26	8,10,11,1 2	18	No	Yes			Yes	Yes
Br 008 I	1149	17	15-18,20,22, 24-26,28,30, 32	18, 22		14,16			No					
Br 009 I	929	39	14-28,30	18, 22					No	Yes			Yes	
Br 009 F	-	-	-	-	-	-	-	-	-	-	-	-	-	-
Br 010 I	1067	39	14-30,32	16,18,22	18	14-16			No					
Br 010 F	20	518	14-32	16, 18, 22		14-17	13	18	No					
Br 011 I	1016	37	14-30,32	18, 22		14			No					
Br 012 I	1092	66	14-30	18, 22		14-16			No				Yes	Yes
Br 013 I	988	24	12-16,18,20, 22-24,26,28	18, 22		14-16			No			Yes	Yes	Yes
Br 013 F	-	-	-	-	-	-	-	-	-	-	-	-	-	-
Br 014 I	1056	268	11-30	16,18,20, 22		13-18	8-14		No	Yes				
Br 015 I	1058	303	14-18	18		14-16			No			Yes	Yes	Yes
Br 016 I	1000	18	15-18,20,22-26,28	18		14,16			No				Yes	
Br 016 F	20	87	16-30	18, 22					No					
Br 017 I	1076	637	9-30	16,17,18, 20	18	14-17	7-12	18+	No	Yes				
Br 017 F	15	1202	14-28,30	16,18,22		14-18	11-14		No					
Br 018 I	1017	35	14-28,30,32	18, 22		14-16	13		No				Yes	
Br 019 I	1025	134	12-28,30	16,18,22		13-18	10-16	18	No	Yes				
Br 020 I	1065	20	12-18,20,22-28	16,18,22		14-16			No					
Br 020 F	25	113	16-26,28	18, 22		15,16		18	No					

Figure A3. 3. Continued

Personal ID.	Sample Mass (mg)	Lipid Concentration (µg/g)	Free Fatty Acids				Diacids	APAA	Miliacin	Cholesterol Derivatives	Sterols	Pine Diterpenes			
			S - FFA	U - FFA	PU - FFA	Br - FFA						Retene	Dehydric	7-Oxo-	
Br 101 I	1039	23	14-26,28	18,22		14-16			Yes						
Br 101 F	23	433	14-26,28,30	18,22		14-17		18	Yes						
Br 102 I	1102	627	9-28,30,32	16-18,20	18	12,14-18,21	7-14		Yes	Yes	Ergosterol	Yes	Yes	Yes	
Br 102 F	33	2187	12-28,30	14-18,20,22	18	13-18,25	9-13		Yes	Yes	Sitosterol		Yes	Yes	
Br 103 I	1087	14	14-20,22,24,26	18,22		14-16			No				Yes		
Br 103 F	20	70	16-28 Even	22					No						
Br 104 I	1065	393	10-24,26	16-18		14-18	8-14	18	No				Yes	Yes	Yes
Br 105 I	1021	24	14-26,28,30	16,18,22		14-16		18	Yes				Yes		
Br 106 I	1016	2469	9-26	16,18		13-16	7-11	18	Yes				Yes	Yes	Yes
Br 107 I	1067	23	12-20,22,24,26	22		12-17			No						
Br 107 F	20	30	16,18,22	22					No						
Br 108 I	1046	610	9-26,28	17,18	18	10-18,20,21,23,25	7-12		No	Yes			Yes		
Br 109 I	1098	23	14-26,28	18,22		14-17			Yes				Yes		
Br 109 F	21	41	16-18,20,22,24,26,28	18,22					No						
Br 110 I	1053	42	13-30	16-18,22		13-19	13,16,18		Yes	Yes	Stigmastanol		Yes		
Br 111 I	1075	28	14-26,28,30	16,18,22		14-17			Yes	Yes			Yes		
Br 112 I	1142	20	14-26	16,18		14-18	13		No				Yes	Yes	
Br 112 F	-	-	-	-	-	-	-	-	-	-	-	-	-	-	
Br 113 I	1095	23	14-26,28,30	18,22		14-17	16	18	Yes				Yes	Yes	
Br 113 F	23	1773	12-30,32,34,36	16,18,22	18	14-16	9-13	18	Yes		Sitosterol, Campesterol, Stigmasterol		Yes	Yes	
Br 114 I	1070	29	13-26,28,30	16,18		13-16			Yes				Yes		
Br 115 I	1082	20	14-28	18,22		13-16			Yes				Yes		
Br 115 F	-	-	-	-	-	-	-	-	-	-	-	-	-	-	
Br 116 I	1029	152	11-30	16,18,20,22		13-19	8-14	18	No				Yes	Yes	
Br 117 I	1073	591	10-30,32,34	10,15-18,24	18	13-19	7-14		Yes	Yes	Ergosterol, Stigmastanol				
Br 117 F	-	-	-	-	-	-	-	-	-	-	-	-	-	-	
Br 118 I	1073	30	13-26,28,30	18,22		13-17		18	Yes				Yes		
Br 118 F	-	-	-	-	-	-	-	-	-	-	-	-	-	-	
Br 119 I	1033	195	11-26,28,30	16,18		14-18	9-13	18	Yes				Yes		
Br 120 I	1052	277	11-26,28,30	16-18	18	13-18	8-14	18	Yes						
Br 120 F	-	-	-	-	-	-	-	-	-	-	-	-	-	-	
Br 121 I	1039	137	12-26,28,30	16-18,22	18	13-17	8-14	18	Yes	Yes	Ergosterol				
Br 121 F	18	1509	14-28,30	16,18,20,22	18	14-16	10-13	18	Yes	Yes	Ergosterol, Sitosterol				
Br 122 I	1159	287	11-28,30	16-18,20,22		13-18,20	8-14	18	Yes		Ergosterol				
Br 6152	24	3524	12-30,32	16,18,20,22,24	18	14,15	9-13	18	No		Stigmasterol, Campesterol				

Table A3. 4. List of compound specific carbon and bulk carbon and nitrogen isotope values of all samples from Bruszczewo analysed in this study.

Personal ID	Compound Specific				Bulk			
	Ceramic		Charred Crust		$\delta^{13}\text{C}$	C %	$\delta^{15}\text{N}$	N %
	$\delta^{13}\text{C}_{16:0}$	$\delta^{13}\text{C}_{18:0}$	$\delta^{13}\text{C}_{16:0}$	$\delta^{13}\text{C}_{18:0}$				
B1			-19.7	-19.1	-16.6	49.3	4.8	1.6
B2					-26.6	33.6	3.9	1.2
B3			-23.5	-21.3	-18.9	44.7	2.9	2.3
B4			-30.3	-30.5	-26.4	27.2	4.8	1.6
Br 001 I	-29.1	-30.9	-29.9	-30.6	-24.0	45.8	5.2	4.6
Br 002 I			-31.1	-30.1	-24.8	25.1	2.2	1.5
Br 003 I	-29.1	-30.2	-28.5	-30.0	-27.8	34.3	6.4	3.7
Br 004 I								
Br 005 I	-28.8	-29.6	-31.5	-30.8	-24.4	30.2	4.5	2.4
Br 006 I	-28.2	-27.3			-25.4	19.8	4.5	1.9
Br 007 I	-30.4	-32.5						
Br 008 I								
Br 009 I	-30.4	-30.3			-25.5	18.4	2.4	1.0
Br 010 I	-29.7	-29.9						
Br 011 I	-30.9	-30.6						
Br 012 I	-28.3	-31.9						
Br 013 I					-24.8	29.1	6.1	1.0
Br 014 I	-29.7	-30.6						
Br 015 I								
Br 016 I								
Br 017 I	-26.1	-26.8	-27.2	-26.6				
Br 018 I	-31.1	-30.6						
Br 019 I	-28.6	-30.1						
Br 020 I								
Br 101 I	-28.6	-28.8						
Br 102 I	-26.5	-27.2	-27.3	-28.0				
Br 103 I					-24.9	12.9	1.7	2.3
Br 104 I	-26.8	-26.5						
Br 105 I	-30.0	-29.1						
Br 106 I	-27.4	-29.8						
Br 107 I								
Br 108 I	-27.4	-28.8						
Br 109 I	-28.9	-29.3						
Br 110 I	-31.6	-30.4						
Br 111 I	-29.4	-29.8						
Br 112 I	-30.3	-29.6			-26.5	23.8	4.7	1.0
Br 113 I	-28.1	-28.0	-22.5	-19.1	-18.3	43.6	0.9	2.3
Br 114 I	-28.8	-30.6						
Br 115 I								
Br 116 I	-28.4	-29.2			-25.5	50.1	5.8	5.1
Br 117 I	-28.8	-30.1						
Br 118 I								
Br 119 I	-29.7	-31.5						
Br 120 I	-26.8	-27.6						
Br 121 I	-28.6	-29.4	-22.3	-22.7	-15.4	59.8	1.2	3.0
Br 122 I	-27.7	-28.7						
Br 6152			-33.6	-33.6	-25.0	51.0	3.8	3.0

Appendix Four: Greece and Bulgaria Dataset (Chapter 7)

Table A4. 1. Bulgarian sherd type and contextual information.

Personal ID	Location in Site	Context	Vessel Type	Sherd Type
Sok 1	Trench L9	Area of a large sized closed circular hearth	Ovoid necked jar, holes below rim	Upper vessel-neck
Sok 2	Trench M9	Area with open and closed hearths	Medium sized bowl	Lower vessel-base
Sok 3	Trench L6	Area with open and closed hearths	Large sized ovoid open jar, impressions on and below rim	Upper vessel-rim
Sok 4	Trench M9	Area with open and closed hearths	Large sized bowl, vertical ridges on rim	Lower vessel-base
Sok 5	Trench M8	Area with open and closed hearths	Large sized ovoid jar	Lower vessel-base
Sok 6	Trench M6	S of hearth 4b	Small sized jug	Lower vessel-base
Cho 1		Pit feature	Large sized ovoid open jar, arched handle below rim, interior double lug	Upper vessel-rim
Cho 2		Pit feature	Ovoid necked jar, band with oblique incisions below rim	Upper vessel-rim
Cho 3		Pit feature	Large sized ovoid open jar, band with oblique impressions below rim	Upper vessel-rim
Cho 4		Pit feature	Large sized ovoid open jar, band with impressions below rim	Upper vessel
Av 1	Sector V, Square 20M31, Structure 2	Area of a large sized closed hearth in a room	Carinated bowl with flat base	Lower vessel-base
Av 2	Sector V, Square 20M31, Structure 2	Area of a large sized closed hearth in a room	Closed pot with high neck, small vertical roll handles on the upper part, lugs on the middle	Mid vessel
PK 1	Trench B2, Square 88, Feature 154	House/Feature 154	Small sized spouted hemispherical bowl	Upper vessel-rim
PK 2	Trench B2, Square 88, Feature 50	Northern part of burnt House 10	Biconical bowl with impressions below rim	Upper vessel-rim
PK 3	Trench B2, Square 88, Feature 50	Northern part of burnt House 10	Biconical bowl	Lower vessel-base
PK 4	Trench B2, Square 98, Feature 155	House/Feature 155	Small sized globular bowl with twin lugs	Upper vessel-rim
PK 5	Trench B2, Square 88, Feature 154	House/Feature 154	Biconical bowl	Mid vessel
PK 6	Trench B2, Square 88, Feature 50	Northern part of burnt House 10	Biconical bowl, incisions below rim	Upper vessel-rim
PK 7	Trench B2, Square 88, Feature 50	Northern part of burnt House 10	Small sized globular bowl with twin lug	Mid vessel
PK 8	Trench B2, Square 88, Feature 154	House/Feature 154	Closed pot	Upper vessel-rim
PK 9	Trench B2, Square 88, Feature 50	Northern part of burnt House 10	Biconical bowl	Mid vessel
PK 10	Trench B2, Square 88, Feature 50	Northern part of burnt House 10	Biconical bowl	Mid vessel

Table A4. 2. Greek sherd type and contextual information.

Personal I.D	Location in Site	Context	Vessel Type	Sherd Type
Ang 1	Trench D, #04005	House A-interior	Pyraunos	Mid vessel
Ang 2	Trench D, #04003	House A-interior	Pyraunos	Mid vessel
Ang 3	Trench D, #04013	House A-interior	Wide mouthed jar	Upper vessel-rim
Ang 4	Trench D, #04007	House A-interior	Pyraunos	Lower vessel-base
Ang 5	Trench D, #04009	House A-interior	Pyraunos	Lower vessel-base
Ang 6	Trench E, #05009	House A-interior	Pyraunos	Mid vessel
Ang 7	Trench E, #05009	House A-interior	Pyraunos	Mid vessel
Ang 8	Trench E, #05005	House A-interior	Large open jar	Mid vessel
Ang 12	Bulk D-E, #7	House A-interior	Wide mouthed jar	Upper vessel-rim
Ang 13	Trench Z, #07007	House D-exterior	Pyraunos	Lower vessel-base
Ang 14	Trench Z, #07020	House D-exterior	Pyraunos	Mid vessel
Ang 15	Trench ̒, #14006	House D-interior	Pyraunos	Mid vessel
Ang 16	Trench ̒, #14004	House D-interior	Pyraunos	Lower vessel-base
Ang 17	Trench ̒, #14002	House D-interior	Large open jar	Mid vessel
Ang 19	Trench L, #11007	House A-exterior	Pyraunos	Mid vessel
Ang 21	Trench D, #04007	House A-interior	Pyraunos	Upper vessel-rim
Ang 22	Trench D, #04009	House A-interior	Pyraunos	Lower vessel-base
Ang 23	Trench D, #04009	House A-interior	Pyraunos	Mid vessel
Ang 24	Trench E, #05005	House A-interior	Pyraunos	Mid vessel
Ang 25	Trench E, #05009	House A-interior	Pyraunos	Mid vessel
L 1	Georgantas Plot, Pit	Pit House	Wide mouthed vessel, convex base, tubular handles	Lower vessel-base
L 2	Georgantas Plot, Pit	Pit House	Wide mouthed vessel, convex base, tubular handles	Lower vessel-base
L 3	Georgantas Plot, Pit	Pit House	Wide mouthed vessel, convex base, tubular handles	Lower vessel-base
L 4	Georgantas Plot, Pit	Pit House	Bowl, convex base	Lower vessel-base
L 5	Georgantas Plot, Pit	Pit House	Bowl, convex base	Lower vessel-base
L 6	Georgantas Plot, Pit, layer 2, #4	Pit House	Bowl, convex base	Lower vessel-base
L 7	Georgantas Plot, Pit, layer 2, #3	Pit House	Bowl, convex base	Lower vessel-base
L 8	Georgantas Plot, Pit, layer 2, #4	Pit House	Bowl, convex base	Lower vessel-base
L 9	Georgantas Plot, Pit, layer 2, #4	Pit House	Bowl, convex base	Lower vessel-base
L 10	Georgantas Plot, Pit, layer 2, #3	Pit House	Bowl, convex base	Lower vessel-base
L 11	Georgantas Plot, Pit, layer 2, #4	Pit House	Wide mouthed vessel, convex base, tubular handles	Lower vessel-base
L 12	Georgantas Plot, Pit, layer 3, #1	Pit House	Wide mouthed vessel, convex base, tubular handles	Lower vessel-base
L 13	Georgantas Plot, Pit, layer 2, #3	Pit House	Wide mouthed vessel, convex base, tubular handles	Lower vessel-base
L 14	Georgantas Plot, Pit, layer 2, #4	Pit House	Wide mouthed vessel, convex base, tubular handles	Lower vessel-base
L 15	Georgantas Plot, Pit, layer 2, #3	Pit House	Bowl, convex base	Upper vessel-rim
L 16	Georgantas Plot, Pit	Pit House	Bowl, convex base	Upper vessel

Table A4. 2. Continued.

Personal ID	Location in Site	Context	Vessel Type	Sherd Type
DT 1	Sector 6, locus 6-032, Layer 6-5	House I	Amphora, piriform, with vertical handles	Upper vessel-rim
DT 2	Sector 6, locus 6-022, Layer 6-5	House I	Globular vessel with flat base and handles-lugs on the periphery	Mid vessel
DT 3	Sector 6, locus 6-015, Layer 6-5	House I	Globular vessel with flat base and lugs on the periphery	Mid vessel
DT 4	Sector 6, locus 6-067, Layer 6-5	House I	Globular vessel with flat base	Mid vessel
DT 5	Sector 6, locus 6-125, Layer 6-5	House I	Globular vessel with flat base and lugs on the periphery	Mid vessel
DT 6	Sector 6, locus 6-048, Layer 6-5	House I	Globular vessel with flat base and lugs on the periphery	Mid vessel
DT 7	Sector VIIr (603), Layer 6-5	House I	Globular vessel with flat base and lugs on the periphery	Mid vessel
DT 8	Sector 6, locus 6-091, Layer 6-5	House I	Globular vessel with flat base	Mid vessel
DT 9	Sector 6, locus 6-038, Layer 6-5	House I	Globular vessel with flat base	Mid vessel
DT 10	Sector 6, locus 6-126, Layer 6-5	House I	Globular vessel with flat base and lugs on the periphery	Mid vessel
DT 11	Sector 6, locus 6-091, Layer 6-5	House I	Globular vessel with flat base	Mid vessel
DT 12	Sector 6, locus 6-022, Layer 6-5	House I	Globular vessel with flat base	Mid vessel
DT 13	Sector 6, behind locus 6-015, Layer 6-5 or 6-4	House I	Globular vessel with flat base	Upper vessel-rim
DT 14	Sector 6, locus 6-047, Layer 6-5	House I	Globular vessel with flat base	Mid vessel
DT 15	Sector 6, locus 6-047, Layer 6-5	House I	Globular vessel with flat base	Mid vessel
DT 16	Sector 6, layer 6-2		Ovoid jar	Mid vessel
Ar 1	Bulk Ψ -Q, #23033	House E	Pithoid jar with impressed cordon and lugs under rim	Lower vessel
Ar 2		House B	Ovoid jar with tongue lugs	Upper vessel-rim
Ar 3		House ST	Pithoid jar with impressed cordon and lugs under rim	Mid vessel
Ar 4	Trench Λ , bulk Λ -M, #29026	House ST	Pithoid jar with impressed cordon and lugs under rim	Mid vessel
Ar 5		House ST	Pithoid jar with impressed cordon and lugs under rim	Mid vessel
Ar 6	Bulk Λ A-IB, #5016	House Z	Ovoid jar with tongue lugs	Upper vessel
Ar 7	Bulk Λ A-M	House ST	Pithoid jar with incised cordon and lugs under rim	Upper vessel
Ar 8	Trench M, #30028	House ST	Ovoid jar with tongue lugs	Mid vessel
Ar 9	Trench Ψ , #2311-2312	House E	Pithoid jar	Lower vessel-base
Ar 10	Trench M	House E	Amphora	Mid vessel
Ar 11		House E	Pithoid jar with impressed cordon and lugs under rim	Upper vessel-rim
Ar 12		House E	Pithoid jar with impressed cordon and lugs under rim	Mid vessel
Ar 13	Trench P, #16018	House E	Pithoid jar with impressed cordon and lugs under rim	Upper vessel-rim
Ar 14	Trench P, #6019	House E	Ovoid jar with tongue lugs	Upper vessel
Ar 15	Bulk Ψ -Q, #23035	House E	Pithoid jar with impressed cordon and lugs under rim	Upper vessel
Ar 16	Trench Λ , #29009	House ST	Pithoid jar	Lower vessel-base
Ar 17	Trench Ψ , #23101	House E	Amphora	Mid vessel
Ar 18	Trench Π , #16017	House B	Amphora	Mid vessel
Ar 19	Trench Λ , #29009	House ST	Pithoid jar	Lower vessel-base
Ar 20	Trench Λ , #29007	House ST	Pithoid jar	Lower vessel-base

Table A4. 2. Continued.

Personal I.D	Location in Site	Context	Vessel Type	Sherd Type
Oly 1	Sector IX, Sub-Sector 7, Square B,	Apsidal building interior	Two handled large open jar with pointed base	Mid vessel
Oly 2	Sector IX, Sub-Sector 7, Square B,	Apsidal building interior	Two handled large open jar with pointed base	Mid vessel
Oly 3	Sector IX, Sub-Sector 29, Square Γ	Enclosure walls	Pyraunos	Mid vessel
Oly 4	Sector IX, Sub-Sector 18, Square A	South of the apsidal building complex	Pyraunos	Lower vessel
Oly 5	Sector IX, Sub-Sector 7, Square B	Apsidal building interior	Two handled large open jar with pointed base	Mid vessel
Oly 6	Sector IX, Sub-Sector 18, Square Γ	Apsidal building interior	Wide mouthed jar with handle - tripod	Upper vessel
Oly 7	Sector IX, Sub-Sector 8, Square A	East of the apsidal building complex	Wide mouthed jar with handle - tripod	Lower vessel
Oly 8	Sector IX, Sub-Sector 28, Square Γ	Enclosure walls	Pyraunos	Upper vessel
Oly 9	Sector IX, Sub-Sector 7, Square B	Apsidal building interior	Wide mouthed tripod jar with handle	Upper vessel
Oly 10	Sector IX, Sub-Sector 18, Square A	Building 2, room B interior	Open jar	Lower vessel
Oly 11	Sector VII, Sub-Sector 80, Square B	Pit 15	Pyraunos	Mid vessel
Oly 12	Sector VII, Sub-Sector 70, Square Δ	Pit 12	Wide mouthed jar with handle - tripod	Mid vessel
Oly 13	Sector VI	Pit	Wide mouthed jar	Lower vessel
Oly 14	Sector VII, Sub-Sector 80, Square B	Pit 15	Wide mouthed jar	Mid vessel
Oly 15	Sector III, Sub-Sector 29, Square B	Ceramic kiln area	Wide mouthed jar with handle - tripod	Upper vessel
Oly 16	Sector III, Sub-Sector 39, Square Γ	Ceramic kiln area	Wide mouthed jar with handle - tripod	Upper vessel
Oly 17	Sector IV, Sub-Sector 16, Square A	Mudbrick destruction layer of a house	Wide mouthed jar with handle - tripod	Mid vessel
Oly 18	Sector IV, Sub-Sector 16, Square A	Mudbrick destruction layer of a house	Wide mouthed jar	Mid vessel
Oly 19	Sector IV, Sub-Sector 16, Square B	Mudbrick destruction layer of a house	Wide mouthed jar with handle	Mid vessel
Oly 20	Sector III, Sub-Sector 29, Square B	House floor	Open jar with handle	Mid vessel

Table A4. 3. TLE yield and compound identification of AM extracts from Bulgarian samples.

Personal I.D.	Sample Mass (mg)	Lipid Concentration (ug/g)	Contamination	Free Fatty Acids					Diacids	APAA	Miltiacin	Cholesterol Derivatives	Phytosterols	16-Hentriacontanone	Pine Diterpenes		
				S - FFA	U - FFA	PU - FFA	Br - FFA	Retene							Dehydro	7-Oxo-	
Sok 1	958	34	Octocrylene	11-33	16-18, 22	18	15, 16	1-11			Yes				Yes		
Sok 2	756	165	Octocrylene	10-28	14-19, 22		13-16	9, 13, 16			Yes						
Sok 3	524	107	Octocrylene	12-28	14, 16, 18, 22		13-16	9, 13, 15									
Sok 4	802	159	Octocrylene	11-28	14-18, 20, 22	18	12	8-13			Yes				Yes	Yes	Yes
Sok 5	641	61	Octocrylene	12-28	14, 16, 18, 22		14-16	9-13			Yes				Yes	Yes	Yes
Sok 6	575	43	Octocrylene	6-32	14, 16, 18, 22		14-16	9-13									Yes
Cho 1	690	508	Octocrylene	8, 12-30	14, 16-18, 20, 22		12-16, 18	8, 13-16			Yes						
Cho 2	1128	313	Octocrylene	11-30	14, 16, 18, 22	18	13-18	8, 13, 14		Trace?	Yes						
Cho 3	964	195	Octocrylene	12-30	16, 18, 22	18	14-16, 21-26	8-13		Trace?	Yes	Stig					
Cho 4	924	22	Octocrylene	13-30	16, 18, 22		13-17	9, 13		Yes							Yes
Av 1	1151	20	Octocrylene	12-30	14-18	18	13-16	9-16			Yes						Yes
Av 2	1066	20	Octocrylene	12-30	16-18, 22	19	13-16, 18	9-16			Yes				Yes		
PK 1	1086	49	Octocrylene	10-28	16-18		14, 15	8-13			Yes						
PK 2	716	12	Octocrylene	12-26	16, 18, 22	18	14, 15	9-13			Yes						
PK 3	1109	34	Octocrylene	12-28	16, 18, 22	18	13-16	9-13			Yes				Yes		
PK 4	785	28	Octocrylene	12-28	16-18, 22	18, 22	13-16, 18	9-13			Yes				Yes		
PK 5	556	14	Octocrylene	12-26	16-18, 22	18	14-16	10			Yes						
PK 6	561	46	Octocrylene	12-20	16, 18, 22	18	14, 16	10-13									
PK 7	808	35	Octocrylene	12-30	16-18	18	14, 16	9-13			Yes				Yes		
PK 8	1085	42	Octocrylene	12-30	16, 18, 22	18	13, 14, 16				Yes				Yes		
PK 9	726	48	Octocrylene	12-28	15-18	18	14-16	9-13			Yes				Yes		
PK 10	729	26	Octocrylene	12-26	16-18	18	14-16	9			Yes						

Table A4. 4. TLE yield and compound identification of AM extracts from Greek samples.

Personal I.D.	Sample Mass (mg)	Lipid Concentration (µg/g)	Contamination	Free Fatty Acids				Diacids	APAA	Miliacin	Cholesterol Derivatives	Phytosterols	16-Hentriacontanone	Pine Diterpenes		
				S - FFA	U - FFA	PU - FFA	Br - FFA							Retene	Dehydro	7-Oxo-
L1	672	29		11-28	16, 18, 22	18	12-19	8			Yes					
L2	1050	18		12-26	16, 18, 22		13-18	8-13						Yes	Yes	
L3	823	34		10-28	14, 16, 17, 18, 22	18	13-18	8-13			Yes			Yes		
L4	1062	18		11-30	16, 18, 20, 22		13, 16	8-13								
L5	1093	36		10-30	16, 18, 22	18	11-16	7-13				Yes				
L6	933	8		12-30	14, 16, 18, 22	18	13-16	9-13			Yes		Yes			
L7	1249	9		12-28	16, 18	18	9, 12-15	9-13			Yes		Yes			
L8	1251	8		11-26	16, 18, 22	18	13-16	9-13				Yes				
L9	1151	7		12-26	16, 18, 22		14	13			Yes			Yes		
L10	648	11		12-28	14, 16, 18, 22	18	14, 16	9-13			Yes		Yes			
L11	667	5		12-26	14, 16, 18, 22		13-16	13			Yes		Yes			
L12	686	5		12-26	14, 15, 16, 18		13-15	10-13								
L13	-	-	-	-	-	-	-	-	-	-	-	-	-	-	-	-
L14	813	13		9-26	14, 16, 18	18	13-16	9-13			Yes		Yes			
L15	698	19		12-26	16, 18, 22		14	10, 13				Yes				
L16	1167	133		12-30	14, 16, 18, 22		13, 14	8						Yes	Yes	
DT1	1014	19		12-28	14, 15, 16, 18, 20, 22	18	13-15	9-13			Yes		Yes			
DT2	1060	19		12-26	14, 16, 18, 20, 22	18	13-16	9-13			Yes		Yes			
DT3	1062	20		10-26	14-18, 20, 22	18, 20	13-15	9-13			Yes					
DT4	440	73		9-28	14, 15, 16, 18, 20, 22	18	16	9-13			Yes		Yes			
DT5	764	67		9-28	14-18, 20, 22	18, 20	12-16	8-13			Yes	Stig	Yes			
DT6	667	59		8-28	14-16, 18, 20, 22, 24	18	13, 15, 16	8-13			Yes		Yes			
DT7	775	28		8-26	14, 16, 18, 20	18	15, 16	6-13					Yes	Yes		
DT8	891	56	Octocrylene (high)	8-28	14-18, 22	18	12-16	6-13			Yes	Stig	Yes			
DT9	1007	33		9-26	16, 18, 20, 22	18	12, 13, 16	6-13			Yes		Yes			
DT10	898	43		12-28	16-18, 20, 22	18	14, 15	9-13			Yes		Yes			
DT11	663	17		12-26	14, 16-18, 20, 22	18	14, 16	9-13								
DT12	704	52		12-28	14, 16, 18, 20, 22	18	14, 16	10-13						Yes		
DT13	664	60		12-30	14-16, 18, 20, 22	18	14, 16	13			Yes					
DT14	663	32		12-30	14-18, 20, 22	18	12-16	9-13			Yes	Stig				
DT15	960	27		12-30	14-18, 20, 22	18	15, 16	9-13			Yes	Stig				
DT16	397	32		11-30	14, 16, 18, 20, 22	18	14, 16	9-13			Yes	Stig				

Table A4. 4. Continued.

Personal I.D.	Sample Mass (mg)	Lipid Concentration (ug/g)	Contamination	Free Fatty Acids				Diacids	APAA	Milliacin	Cholesterol Derivatives	Phytosterols	16-Hentriacontanone	Pine Diterpenes			
				S - FFA	U - FFA	PU - FFA	Br - FFA							Retene	Dehydro	7-Oxo-	
Ar 1	702	20	Octocrylene	12-24	16-18	18	13, 14	10, 13			Yes						Yes
Ar 2	1030	28	Octocrylene	12-30	15-18, 22	18	13-17	9-13			Yes						Yes
Ar 3	795	21	Octocrylene	13-28	15-18, 22		13-16	10, 13			Yes						
Ar 4	786	17	Octocrylene	12-28	16, 18, 22		13	13									
Ar 5	1158	15	Octocrylene	13-26	16-18, 22	18	13-16, 18	10-13			Yes		Yes				Yes
Ar 6	972	19	Octocrylene	12-28	14, 16-18, 22	18	13-18	9, 13, 16	18								Yes
Ar 7	1057	14	Octocrylene	12-24	15-18, 22	18	13, 15-18	13			Yes		Yes				
Ar 8	1018	24	Octocrylene	12-28	14, 16-18, 22	18	12-16	9, 13									
Ar 9	718	15	Octocrylene	13-26	16, 18, 22		13-16	10, 13					Yes				Yes
Ar 10	873	22	Octocrylene	13-26	16-18, 20, 22	18	14, 16	13									
Ar 11	1034	19	Octocrylene	13-26	15, 16, 18, 22	18	13-16	10	20?		Yes						
Ar 12	1084	20	Octocrylene	13-28	15-18, 20, 22	18	14-16	10			Yes						
Ar 13	962	8	Octocrylene	15-26	16-18, 22	18	15-17	13			Yes						
Ar 14	1102	72	Octocrylene	9-24	16, 18		14-16	10-13									
Ar 15	1084	4	Octocrylene	-	-	-	-	-	-	-	-	-	-	-	-	-	-
Ar 16	721	24	Octocrylene	13-26	15-18, 20, 22	18	13-16	13		Yes	Yes						
Ar 17	930	29	Octocrylene	13-26	16-18, 22	18	14-16	10-13			Yes						
Ar 18	712	59	Octocrylene	12-26	14, 18		14	9-13						Yes			Yes
Ar 19	1169	8	Octocrylene	14-26	16-18, 20, 22	18, 20?	14-18	10-13			Yes						Yes
Ar 20	726	22	Octocrylene	14-28	16-18, 22		13-18	10, 13			Yes						

Table A4. 4. Continued.

Personal I.D.	Sample Mass (mg)	Lipid Concentration (ug/g)	Contamination	Free Fatty Acids				Diacids	APAA	Miliacin	Cholesterol Derivatives	Phytosterols	16-Hentriacontanone	Pine Diterpenes		
				S - FFA	U - FFA	PU - FFA	Br - FFA							Retene	Dehydro	7-Oxo-
Ang 1	1024	188	Octocrylene	7-36	16, 18, 24		14, 16, 18	8, 16, 18, 22	Yes							
Ang 2	1030	21	Octocrylene	12-30	14-18, 22		13-18	9, 13, 16			Yes	Yes			Yes	
Ang 3	830	22	Octocrylene	12-32	14, 16, 18, 22		13-18, 20	9, 14			Yes	Yes			Yes	Yes
Ang 4	1211	48	Octocrylene	12-33	18, 20, 22	18	14-18	9, 13, 14, 16, 18		Yes		Yes				
Ang 5	1014	14	Octocrylene	14-32	14, 16, 18, 22	18	14, 16, 18	13		Yes		Yes				
Ang 6	1153	5	Octocrylene	14-28	16, 18, 22	18	14-16	13								
Ang 7	1051	51	Octocrylene	12-30	18, 22	18	14-16	9-13				Yes				
Ang 8	980	70	Octocrylene	12-38	16, 18		13-18	9, 14, 20				Yes				
Ang 12	1021	9	Octocrylene	14-26	16, 18, 22	18	14-18	13								
Ang 13	1047	14	Octocrylene	13-30	16, 18, 22		13, 14, 16, 18, 13	9, 13		Yes		Yes				
Ang 14	931	800	Octocrylene	10-30	16-18		13-18	7-13	18	Yes		Yes				
Ang 15	1004	11	Octocrylene	13-26	16, 18, 22		13-15	10, 13		Yes		Yes				
Ang 16	1044	17	Octocrylene	12-30	16, 18, 22		13-16	10, 13		Yes		Yes				
Ang 17	977	8	Octocrylene	12-24	16, 18, 22		14, 15	9-13				Yes				
Ang 19	847	13	Octocrylene	12-28	16, 18, 22		14-16	9-13								
Ang 21	1205	9	Octocrylene	14-30	16, 18, 22		13-18, 21	10		Yes					Yes	Yes
Ang 22	971	30	Octocrylene	12-30	16, 18, 22		13, 16	9								
Ang 23	1355	38	Octocrylene	12-30	16, 18, 22		14	9-13		Yes						
Ang 24	880	16	Octocrylene	12-30	16, 18, 22		13-16	10-13		Yes					Yes	
Ang 25	1268	14	Octocrylene	12-28	16, 18		13-16	9								

Table A4. 4. Continued.

Personal I.D.	Sample Mass (mg)	Lipid Concentration (ug/g)	Contamination	Free Fatty Acids					Diacids	APAA	Miltacin	Cholesterol Derivatives	Phytosterols	16-Hentriacontanone	Pine Diterpenes		
				S - FFA	U - FFA	PU - FFA	Br - FFA	Retene							Dehydro	7-Oxo-	
Oly 1	1061	20		12-28	14-16, 18, 22	18	12-16	9-13			Yes						
Oly 2	774	25		12-28	14, 16, 18, 22	18	15-16	9-13			Yes						
Oly 3	523	48		12-30	14-16, 18, 22	18	14, 16	8-13			Yes						
Oly 4	1070	38		9-26	15, 16, 18	18	13-15	8-13			Yes						
Oly 5	901	25		12-30	14-16, 18, 22	18	12-14	9-13			Yes	Stig					
Oly 6	1202	83	High plastic	10-30	14-16, 18, 22	18	12-15	6-10									
Oly 7	983	31		10-30	14-16, 18, 22	18	13, 14	8-13									
Oly 8	698	25		12-30	14-16, 18	18	13-16	9									
Oly 9	1112	34		12-28	14-16, 18, 20, 22	18	13, 16, 20	9-13			Yes						
Oly 10	970	47		10-26	16, 18	18	13, 14, 16	8-13, 16	18					Yes			
Oly 11	1134	13		14-28	14-16, 18, 22	18	14-6, 18	13									
Oly 12	1028	19		12-28	14-16, 18, 22	18	14-16	9, 13			Yes						
Oly 13	1072	17		12-28	14, 16, 18	18	14-16	9, 13									
Oly 14	1162	13		14-30	14, 16, 18, 22	18	14-16	10-13									
Oly 15	699	13		14-28	16, 18, 22	18	14, 15										
Oly 16	1192	16		12-30	14, 16, 18, 22	18	14-16	9-13				Stig					
Oly 17	1173	34		12-30	16, 18, 20, 22		14-16	9-14									
Oly 18	981	12		14-26	14, 16, 18, 22		14-16	9-13									
Oly 19	1159	16		12-28	16, 18, 22	18											
Oly 20	1271	18		12-30	14, 16, 18, 22	18	14-16	9			Stig					Yes	

Table A4. 5. TLE yield and compound identification of solvent extracts from Greek samples.

Personal I.D.	Sample Mass (mg)	Lipid Concentration (ug/g)	FFAs	Long chain alkanes	Miliacin	Cholesterol + derivatives	Phytosterols + derivatives	MAG	DAG	TAG	Wax esters
Ang 1	1218	133	X	X					X	X	X
Ang 14	1010	25	X		X			X	X	X	
L 16	1101	50	X								
DT 1	864	7	X			X					
DT 3	1140	10	X			X					
DT 4	414	15	X			X					
DT 5	646	9	X			X	X				
DT 7	769	7	X								
DT 8	833	10	X								
DT 10	878	7	X			X					
DT 11	553	7	X								
DT 12	671	20	X								
DT 13	541	29	X								
DT 14	702	22	X								
DT 15	751	14	X								
DT 16	282	29	X								
Oly 17	1173	20	X								
Oly 18	1101	13	X								

Table A4. 6. Compound specific carbon isotope values of Bulgarian samples.

Personal ID	$\delta^{13}\text{C}_{16:0}$	$\delta^{13}\text{C}_{18:0}$	$\Delta^{13}\text{C}$
Sok 1	-28.9	-27.8	1.1
Sok 2	-28.0	-30.5	-2.5
Sok 3	-26.8	-29.4	-2.6
Sok 4	-28.5	-26.7	1.7
Sok 5	-28.3	-27.0	1.3
Sok 6	-27.7	-29.5	-1.8
Cho 1	-24.4	-29.6	-5.2
Cho 2	-26.9	-30.5	-3.6
Cho 3	-27.2	-30.7	-3.5
Cho 4	-26.8	-24.4	2.4
Av 1	-29.3	-28.7	0.6
Av 2	-29.9	-29.3	0.6
PK 1	-28.8	-28.9	-0.1
PK 2	-28.9	-28.8	0.1
PK 3	-30.7	-29.5	1.2
PK 4	-30.2	-29.4	0.7
PK 5	-28.5	-28.2	0.3
PK 6	-31.5	-30.3	1.3
PK 7	-29.0	-29.1	-0.1
PK 8	-30.6	-29.5	1.1
PK 9	-30.2	-29.6	0.6
PK 10	-28.8	-28.2	0.6

Table A4. 7. Compound specific carbon isotope values of Greek samples.

Personal ID	$\delta^{13}\text{C}_{16:0}$	$\delta^{13}\text{C}_{18:0}$	$\Delta^{13}\text{C}$
Ang 1	-26.7	-30.6	-3.8
Ang 2	-29.0	-30.0	-1.0
Ang 3	-28.5	-29.9	-1.3
Ang 4	-28.2	-29.2	-1.0
Ang 5	-29.9	-30.1	-0.2
Ang 6	-30.0	-30.5	-0.5
Ang 7	-30.9	-30.8	0.1
Ang 8	-27.1	-29.5	-2.3
Ang 12	-30.4	-30.7	-0.3
Ang 13	-30.4	-30.6	-0.2
Ang 14	-26.9	-27.1	-0.2
Ang 15	-29.7	-29.5	0.2
Ang 16	-30.6	-29.5	1.1
Ang 17	-28.3	-26.3	2.0
Ang 19	-28.3	-27.0	1.4
Ang 21	-29.8	-28.9	0.9
Ang 22	-30.3	-29.0	1.3
Ang 23	-30.9	-29.9	1.1
Ang 24	-30.5	-29.7	0.9
Ang 25	-30.4	-29.9	0.5
L 1	-28.8	-29.8	-0.9
L 2	-29.9	-30.4	-0.5
L 3	-30.4	-30.1	0.3
L 4	-30.5	-30.7	-0.2
L 5	-29.6	-30.1	-0.4
L 7	-30.0	-30.3	-0.3
L 8	-29.9	-30.4	-0.5
L 14	-30.2	-31.0	-0.7
L 15	-27.1	-29.7	-2.6
L 16	-27.1	-28.0	-1.0
DT 1	-27.6	-29.2	-1.6
DT 2	-28.4	-29.5	-1.1
DT 3	-28.2	-29.6	-1.4
DT 4	-28.4	-29.3	-0.8
DT 5	-27.3	-29.3	-2.1
DT 6	-29.0	-29.7	-0.7
DT 7	-26.0	-28.2	-2.2
DT 8	-27.7	-29.3	-1.6
DT 9	-27.8	-29.5	-1.8
DT 10	-28.7	-29.7	-1.0
DT 11	-27.1	-29.1	-2.0
DT 12	-28.9	-29.7	-0.9
DT 13	-28.9	-29.8	-0.9
DT 14	-27.3	-29.2	-1.9
DT 15	-27.3	-29.3	-2.0
DT 16	-26.8	-29.1	-2.2

Table A4. 7. Continued.

Personal ID	$\delta^{13}\text{C}_{16:0}$	$\delta^{13}\text{C}_{18:0}$	$\Delta^{13}\text{C}$
Ar 1	-27.5	-28.2	-0.7
Ar 2	-28.2	-29.3	-1.2
Ar 3	-28.3	-29.1	-0.8
Ar 4	-28.2	-28.7	-0.5
Ar 5	-27.9	-28.8	-0.8
Ar 6	-27.4	-28.8	-1.4
Ar 8	-28.4	-29.2	-0.8
Ar 9	-27.9	-28.5	-0.5
Ar 10	-29.9	-30.0	0.0
Ar 11	-28.5	-29.2	-0.7
Ar 12	-29.1	-29.6	-0.5
Ar 13	-29.6	-30.1	-0.5
Ar 14	-28.6	-26.9	1.6
Ar 16	-26.6	-29.4	-2.8
Ar 17	-27.8	-28.6	-0.8
Ar 18	-28.0	-29.7	-1.7
Ar 19	-26.8	-29.2	-2.4
Ar 20	-27.5	-29.4	-1.9
Oly 1	-28.2	-29.4	-1.2
Oly 2	-28.7	-29.3	-0.6
Oly 3	-27.6	-27.3	0.3
Oly 4	-27.3	-29.0	-1.8
Oly 5	-28.2	-28.8	-0.7
Oly 6	-26.2	-25.4	0.9
Oly 7	-27.6	-29.2	-1.6
Oly 8	-27.9	-30.6	-2.7
Oly 9	-26.9	-27.6	-0.7
Oly 10	-22.1	-21.0	1.1
Oly 11	-27.6	-28.9	-1.3
Oly 12	-27.7	-27.4	0.3
Oly 13	-28.5	-29.2	-0.7
Oly 14	-27.5	-29.2	-1.7
Oly 16	-27.0	-26.2	0.8
Oly 17	-28.9	-29.3	-0.4
Oly 18	-27.3	-31.6	-4.3
Oly 19	-25.6	-28.2	-2.6
Oly 20	-27.6	-27.4	0.2

Appendix Five: Modern Reference and Mixing Model Data

Table A5. 1. Modern reference $\delta^{13}\text{C}_{16}$ and $\delta^{13}\text{C}_{18}$ values.

Category	Product Source (Common name)	Product Source (Binomial name)	$\delta^{13}\text{C}_{16:0}$	$\delta^{13}\text{C}_{18:0}$	Reference
DP	Pig	<i>Sus scrofa</i>	-27.4	-27.7	March (2013)
DP	Pig	<i>Sus scrofa domesticus</i>	-25.1	-23.8	Dudd (1999)
DP	Pig	<i>Sus scrofa domesticus</i>	-24.8	-24	Dudd (1999)
DP	Pig	<i>Sus scrofa domesticus</i>	-25.4	-24.1	Dudd (1999)
DP	Pig	<i>Sus scrofa domesticus</i>	-25.5	-24.4	Dudd (1999)
DP	Pig	<i>Sus scrofa domesticus</i>	-25.7	-24.4	Dudd (1999)
DP	Pig	<i>Sus scrofa domesticus</i>	-26.4	-24.8	Dudd (1999)
DP	Pig	<i>Sus scrofa domesticus</i>	-26.5	-24.8	Dudd (1999)
DP	Pig	<i>Sus scrofa domesticus</i>	-26	-24.9	Dudd (1999)
DP	Pig	<i>Sus scrofa domesticus</i>	-24.4	-25.3	Dudd (1999)
DP	Pig	<i>Sus scrofa domesticus</i>	-26.9	-25.4	Pääkkönen <i>et al.</i> (2020)
DP	Pig	<i>Sus scrofa domesticus</i>	-27.1	-25.5	Pääkkönen <i>et al.</i> (2020)
DP	Pig	<i>Sus scrofa domesticus</i>	-27.9	-26.4	Pääkkönen <i>et al.</i> (2020)
DP	Pig	<i>Sus scrofa domesticus</i>	-27.2	-26.6	Pääkkönen <i>et al.</i> (2020)
DP	Pig	<i>Sus scrofa domesticus</i>	-25.6	-26.5	Spangenberg <i>et al.</i> (2006)
DP	Pig	<i>Sus scrofa domesticus</i>	-28.7	-27.4	Spangenberg <i>et al.</i> (2006)
DRA	Cattle	<i>bos taurus</i>	-26.7	-28.5	March (2013)
DRA	Lamb	<i>Ovis aries</i>	-29.6	-32.7	March (2013)
DRA	Sheep	<i>Ovis aries</i>	-28.2	-30	Dudd (1999)
DRA	Sheep	<i>Ovis aries</i>	-28.4	-30.1	Dudd (1999)
DRA	Sheep	<i>Ovis aries</i>	-28.8	-30.1	Dudd (1999)
DRA	Sheep	<i>Ovis aries</i>	-28.7	-30.4	Dudd (1999)
DRA	Sheep	<i>Ovis aries</i>	-29	-30.4	Dudd (1999)
DRA	Sheep	<i>Ovis aries</i>	-29.2	-31.1	Dudd (1999)
DRA	Sheep	<i>Ovis aries</i>	-29.3	-31.1	Dudd (1999)
DRA	Sheep	<i>Ovis aries</i>	-29.4	-31.2	Dudd (1999)
DRA	Sheep	<i>Ovis aries</i>	-28.4	-31.3	Dudd (1999)
DRA	Cow	<i>Bos taurus</i>	-28.7	-31.5	Dudd (1999)
DRA	Cow	<i>Bos taurus</i>	-29.9	-31.6	Dudd (1999)
DRA	Cow	<i>Bos taurus</i>	-28.9	-31.8	Dudd (1999)
DRA	Sheep	<i>Ovis aries</i>	-29.4	-31.8	Dudd (1999)
DRA	Sheep	<i>Ovis aries</i>	-30.4	-32.2	Dudd (1999)
DRA	Cow	<i>Bos taurus</i>	-29.8	-32.3	Dudd (1999)
DRA	Sheep	<i>Ovis aries</i>	-30.2	-32.3	Dudd (1999)
DRA	Sheep	<i>Ovis aries</i>	-30.5	-32.5	Dudd (1999)
DRA	Cattle	<i>Bos taurus</i>	-27	-28.5	Pääkkönen <i>et al.</i> (2020)
DRA	Cattle	<i>Bos taurus</i>	-27.4	-28.8	Pääkkönen <i>et al.</i> (2020)
DRA	Cattle	<i>Bos taurus</i>	-26.7	-29.2	Pääkkönen <i>et al.</i> (2020)
DRA	Cattle	<i>Bos taurus</i>	-27.5	-29.5	Pääkkönen <i>et al.</i> (2020)

DRA	Sheep	<i>Ovis aries</i>	-27.7	-26.4	Spangenberg <i>et al.</i> (2006)
DRA	Cattle	<i>Bos taurus</i>	-30	-30.2	Spangenberg <i>et al.</i> (2006)
DRA	Cattle	<i>Bos taurus</i>	-31.4	-31.3	Spangenberg <i>et al.</i> (2006)
DRA	Cattle	<i>Bos taurus</i>	-27.1	-28.6	Spangenberg <i>et al.</i> (2006)
DRA	Cattle	<i>Bos taurus</i>	-27.8	-28.3	Spangenberg <i>et al.</i> (2006)
DRA	Cow	<i>Bos taurus</i>	-26.1	-25.3	Spangenberg <i>et al.</i> (2010)
DRA	Cow	<i>Bos taurus</i>	-25.4	-26.1	Spangenberg <i>et al.</i> (2010)
DRA	Calf leather	<i>Bos taurus</i>	-25.3	-26.3	Spangenberg <i>et al.</i> (2010)
DRA	Sheep	<i>Ovis aries</i>	-27.2	-28.3	Spangenberg <i>et al.</i> (2010)
DRA	Young goat-treat	<i>Capra hircus</i>	-28.3	-30	Spangenberg <i>et al.</i> (2010)
DRA	Young goat-raw	<i>Capra hircus</i>	-28.4	-30	Spangenberg <i>et al.</i> (2010)
DRM	Cow	<i>Bos taurus</i>	-27.8	-32.1	Dudd (1999)
DRM	Cow	<i>Bos taurus</i>	-27.4	-32.2	Dudd (1999)
DRM	Cow	<i>Bos taurus</i>	-27.9	-33.1	Dudd (1999)
DRM	Sheep	<i>Ovis aries</i>	-29	-33.4	Dudd (1999)
DRM	Cow	<i>Bos taurus</i>	-28.9	-33.7	Dudd (1999)
DRM	Sheep	<i>Ovis aries</i>	-29.4	-33.8	Dudd (1999)
DRM	Cow	<i>Bos taurus</i>	-28.1	-34	Dudd (1999)
DRM	Cow	<i>Bos taurus</i>	-28.6	-34.1	Dudd (1999)
DRM	Cow	<i>Bos taurus</i>	-30.8	-34.4	Dudd (1999)
DRM	Cow	<i>Bos taurus</i>	-29.6	-34.9	Dudd (1999)
DRM	Milk (goat, <i>Capra hircus</i>)	<i>Capra hircus</i>	-25.4	-29.6	Pääkkönen <i>et al.</i> (2020)
DRM	Milk (Northern Finncattle)	<i>Bos taurus</i>	-26.8	-30.7	Pääkkönen <i>et al.</i> (2020)
DRM	Milk (Northern Finncattle)	<i>Bos taurus</i>	-27.1	-30.7	Pääkkönen <i>et al.</i> (2020)
DRM	Milk (goat, <i>Capra hircus</i>)	<i>Capra hircus</i>	-27.2	-30.9	Pääkkönen <i>et al.</i> (2020)
DRM	Milk (Northern Finncattle)	<i>Bos taurus</i>	-26.6	-31.2	Pääkkönen <i>et al.</i> (2020)
DRM	Milk (Northern Finncattle)	<i>Bos taurus</i>	-26.8	-31.5	Pääkkönen <i>et al.</i> (2020)
DRM	Milk (goat, <i>Capra hircus</i>)	<i>Capra hircus</i>	-27.6	-31.5	Pääkkönen <i>et al.</i> (2020)
DRM	Milk (Northern Finncattle)	<i>Bos taurus</i>	-27.5	-31.6	Pääkkönen <i>et al.</i> (2020)
DRM	Milk (goat, <i>Capra hircus</i>)	<i>Capra hircus</i>	-27.2	-32.3	Pääkkönen <i>et al.</i> (2020)
DRM	Goat	<i>Capra hircus</i>	-24.9	-27.6	Spangenberg <i>et al.</i> (2006)
DRM	Goat	<i>Capra hircus</i>	-24.8	-28.7	Spangenberg <i>et al.</i> (2006)
DRM	Goat	<i>Capra hircus</i>	-28.2	-31.1	Spangenberg <i>et al.</i> (2006)
DRM	Goat	<i>Capra hircus</i>	-25.5	-32.4	Spangenberg <i>et al.</i> (2006)
DRM	Sheep	<i>Ovis aries</i>	-30.8	-33.2	Spangenberg <i>et al.</i> (2006)
DRM	Goat	<i>Capra hircus</i>	-26.2	-33.3	Spangenberg <i>et al.</i> (2006)
DRM	Sheep	<i>Ovis aries</i>	-28	-33.4	Spangenberg <i>et al.</i> (2006)
DRM	Sheep	<i>Ovis aries</i>	-29	-33.9	Spangenberg <i>et al.</i> (2006)
DRM	Cattle	<i>Bos taurus</i>	-27.1	-29.9	Spangenberg <i>et al.</i> (2006)
DRM	Cattle	<i>Bos taurus</i>	-27.5	-30.7	Spangenberg <i>et al.</i> (2006)
DRM	Cattle	<i>Bos taurus</i>	-26.9	-31	Spangenberg <i>et al.</i> (2006)
DRM	Cattle	<i>Bos taurus</i>	-28.5	-31	Spangenberg <i>et al.</i> (2006)

DRM	Cattle	<i>Bos taurus</i>	-27.8	-31.7	Spangenberg <i>et al.</i> (2006)
DRM	Cattle	<i>Bos taurus</i>	-27.3	-31.9	Spangenberg <i>et al.</i> (2006)
DRM	Cattle	<i>Bos taurus</i>	-25.6	-32.2	Spangenberg <i>et al.</i> (2006)
DRM	Cattle	<i>Bos taurus</i>	-27.5	-32.9	Spangenberg <i>et al.</i> (2006)
DRM	Cattle	<i>Bos taurus</i>	-28.1	-32.9	Spangenberg <i>et al.</i> (2006)
DRM	Cattle	<i>Bos taurus</i>	-28.5	-33.5	Spangenberg <i>et al.</i> (2006)
DRM	Cow milk	<i>Bos taurus</i>	-27	-30.8	Spiteri (2012)
DRM	Cow milk	<i>Bos taurus</i>	-23.9	-26.3	Spiteri (2012)
DRM	Goat milk	<i>Capra hircus</i>	-23.4	-26.4	Spiteri (2012)
DRM	Cow milk	<i>Bos taurus</i>	-23.3	-26.5	Spiteri (2012)
DRM	Goat milk	<i>Capra hircus</i>	-24.9	-28.1	Spiteri (2012)
DRM	Sheep milk	<i>Ovis aries</i>	-24.2	-28.5	Spiteri (2012)
DRM	Sheep milk	<i>Ovis aries</i>	-24.4	-29	Spiteri (2012)
F	Tench	<i>Tinca tinca</i>	-24.4	-26.5	Craig <i>et al.</i> (2011)
F	European eel	<i>Anguilla anguilla</i>	-28.4	-28.6	Craig <i>et al.</i> (2011)
F	Tench	<i>Tinca tinca</i>	-27.9	-29	Craig <i>et al.</i> (2011)
F	Northern pike	<i>Esox lucius</i>	-35	-35.2	Craig <i>et al.</i> (2011)
F	Tench	<i>Tinca tinca</i>	-37.4	-36.7	Craig <i>et al.</i> (2011)
F	Roach	<i>Rutilus rutilus</i>	-32.2	-32.5	Cramp <i>et al.</i> (2014)
F	European perch	<i>Perca fluviatilis</i>	-32.2	-32.8	Cramp <i>et al.</i> (2014)
F	European perch	<i>Perca fluviatilis</i>	-33.4	-33.2	Cramp <i>et al.</i> (2014)
F	Roach	<i>Rutilus rutilus</i>	-32.8	-33.3	Cramp <i>et al.</i> (2014)
F	European perch	<i>Perca fluviatilis</i>	-33.6	-33.6	Cramp <i>et al.</i> (2014)
F	Roach	<i>Rutilus rutilus</i>	-32.7	-33.7	Cramp <i>et al.</i> (2014)
F	European perch	<i>Perca fluviatilis</i>	-34	-33.7	Cramp <i>et al.</i> (2014)
F	Roach	<i>Rutilus rutilus</i>	-32.8	-33.9	Cramp <i>et al.</i> (2014)
F	European perch	<i>Perca fluviatilis</i>	-32.9	-33.9	Cramp <i>et al.</i> (2014)
F	European perch	<i>Perca fluviatilis</i>	-32.6	-34.1	Cramp <i>et al.</i> (2014)
F	Roach	<i>Rutilus rutilus</i>	-34.1	-34.3	Cramp <i>et al.</i> (2014)
F	Roach	<i>Rutilus rutilus</i>	-33.6	-34.8	Cramp <i>et al.</i> (2014)
F	European perch	<i>Perca fluviatilis</i>	-34.8	-34.9	Cramp <i>et al.</i> (2014)
F	European perch	<i>Perca fluviatilis</i>	-35.7	-35.1	Cramp <i>et al.</i> (2014)
F	European perch	<i>Perca fluviatilis</i>	-34.5	-35.5	Cramp <i>et al.</i> (2014)
F	European perch	<i>Perca fluviatilis</i>	-34.5	-35.5	Cramp <i>et al.</i> (2014)
F	European perch	<i>Perca fluviatilis</i>	-34.3	-35.6	Cramp <i>et al.</i> (2014)
F	European perch	<i>Perca fluviatilis</i>	-35.2	-35.8	Cramp <i>et al.</i> (2014)
F	Northern pike	<i>Esox lucius</i>	-28.2	-25.8	Lucquin <i>et al.</i> (2016a)
F	Crucian carp	<i>Carassius carassius</i>	-30.2	-28.2	Lucquin <i>et al.</i> (2016a)
F	European perch	<i>Perca fluviatilis</i>	-31	-28.4	Lucquin <i>et al.</i> (2016a)
F	Bleak	<i>Alburnus alburnus</i>	-26.6	-25.9	Pääkkönen <i>et al.</i> (2020)
F	Vendace	<i>Coregonus albula</i>	-28.2	-26.8	Pääkkönen <i>et al.</i> (2020)
F	Vendace	<i>Coregonus albula</i>	-29.1	-27.8	Pääkkönen <i>et al.</i> (2020)
F	Vendace	<i>Coregonus albula</i>	-27.9	-29.5	Pääkkönen <i>et al.</i> (2020)
F	Pike-perch	<i>Sander lucioperca</i>	-30.2	-29.9	Pääkkönen <i>et al.</i> (2020)
F	Ide	<i>Leuciscus idus</i>	-32.8	-31.2	Pääkkönen <i>et al.</i> (2020)

F	Northern pike	<i>Esox lucius</i>	-31.7	-31.3	Pääkkönen <i>et al.</i> (2020)
F	Ide	<i>Leuciscus idus</i>	-33.4	-31.8	Pääkkönen <i>et al.</i> (2020)
F	Roach	<i>Rutilus rutilus</i>	-29.4	-31.9	Pääkkönen <i>et al.</i> (2020)
F	Northern pike	<i>Esox lucius</i>	-33.4	-32.2	Pääkkönen <i>et al.</i> (2020)
F	European perch	<i>Perca fluviatilis</i>	-32	-32.3	Pääkkönen <i>et al.</i> (2020)
F	European perch	<i>Perca fluviatilis</i>	-32.9	-32.3	Pääkkönen <i>et al.</i> (2020)
F	Bleak	<i>Alburnus alburnus</i>	-33.8	-32.3	Pääkkönen <i>et al.</i> (2020)
F	Burbot	<i>Lota lota</i>	-34.3	-32.3	Pääkkönen <i>et al.</i> (2020)
F	European perch	<i>Perca fluviatilis</i>	-33.3	-32.5	Pääkkönen <i>et al.</i> (2020)
F	European perch	<i>Perca fluviatilis</i>	-32	-32.6	Pääkkönen <i>et al.</i> (2020)
F	Northern pike	<i>Esox lucius</i>	-33.2	-32.9	Pääkkönen <i>et al.</i> (2020)
F	Roach	<i>Rutilus rutilus</i>	-34	-32.9	Pääkkönen <i>et al.</i> (2020)
F	European perch	<i>Perca fluviatilis</i>	-34.3	-33.2	Pääkkönen <i>et al.</i> (2020)
F	European perch	<i>Perca fluviatilis</i>	-34.9	-33.3	Pääkkönen <i>et al.</i> (2020)
F	Pike-perch	<i>Sander lucioperca</i>	-34.5	-33.7	Pääkkönen <i>et al.</i> (2020)
F	Bleak	<i>Alburnus alburnus</i>	-34.1	-34.5	Pääkkönen <i>et al.</i> (2020)
F	Bleak	<i>Alburnus alburnus</i>	-36	-34.5	Pääkkönen <i>et al.</i> (2020)
F	European perch	<i>Perca fluviatilis</i>	-35.1	-34.6	Pääkkönen <i>et al.</i> (2020)
F	European perch	<i>Perca fluviatilis</i>	-35.2	-34.7	Pääkkönen <i>et al.</i> (2020)
F	Bleak	<i>Alburnus alburnus</i>	-35.6	-35.1	Pääkkönen <i>et al.</i> (2020)
F	European perch	<i>Perca fluviatilis</i>	-35.3	-36.8	Pääkkönen <i>et al.</i> (2020)
F	Vendace	<i>Coregonus albula</i>	-36.8	-37.8	Pääkkönen <i>et al.</i> (2020)
M	Millet	<i>Panicum miliaceum</i>	-19.8	-19.7	Taché <i>et al.</i> (2021)
M	Millet	<i>Panicum miliaceum</i>	-19.8	-19.4	Taché <i>et al.</i> (2021)
M	Millet	<i>Panicum miliaceum</i>	-19.4	-19.5	Taché <i>et al.</i> (2021)
M	Millet	<i>Panicum miliaceum</i>	-19.5	-20	Taché <i>et al.</i> (2021)
M	Millet	<i>Panicum miliaceum</i>	-17.8	-17.4	Taché <i>et al.</i> (2021)
M	Millet	<i>Panicum miliaceum</i>	-19.3	-20	Taché <i>et al.</i> (2021)
M	Millet	<i>Panicum miliaceum</i>	-17.8	-18.5	Taché <i>et al.</i> (2021)
M	Millet	<i>Panicum miliaceum</i>	-17.3	-18.2	Taché <i>et al.</i> (2021)
P	Manioc	<i>Manihot esculenta</i>	-37.6	-35.9	March (2013)
P	Cabbage	<i>Brassica oleracea capitata</i>	-27.1	-25.2	March (2013)
P	Kohlrabi	<i>Brassica oleracea var. gongylodes</i>	-28.6	-27.7	March (2013)
P	Spinach	<i>Spinacia oleracea</i>	-33.2	-28	March (2013)
P	Hazelnut	<i>Corylus avellana</i>	-29.9	-30.7	March (2013)
P	Wild carrot	<i>Daucus carotta</i>	-32.8	-31	March (2013)
P	Hazelnut	<i>Corylus avellana</i>	-29.3	-31.4	March (2013)
P	Nettle	<i>Urtica sp.</i>	-34.5	-33.6	March (2013)
P	Oat	<i>Avena sativa</i>	-34.2	-33.7	March (2013)
P	Oat	<i>Avena sativa</i>	-33.7	-33.9	March (2013)
P	Wheat	<i>Triticum sp.</i>	-33	-34.1	March (2013)
P	Parsnip	<i>Pastinaca sativa</i>	-38	-35.4	March (2013)
P	Olive	<i>Olea europaea</i>	-30.9	-29.6	Spangenberg and Ogrinc (2001)
P	Olive	<i>Olea europaea</i>	-29	-29.9	Spangenberg and Ogrinc (2001)

P	Olive	<i>Olea europaea</i>	-30.3	-30.5	Spangenberg and Ogrinc (2001)
P	Olive	<i>Olea europaea</i>	-31.4	-30.9	Spangenberg and Ogrinc (2001)
P	Olive	<i>Olea europaea</i>	-31.9	-31.2	Spangenberg and Ogrinc (2001)
P	Olive	<i>Olea europaea</i>	-29.8	-29.7	Spangenberg and Ogrinc (2001)
P	Olive	<i>Olea europaea</i>	-30.6	-30.7	Spangenberg and Ogrinc (2001)
P	Olive	<i>Olea europaea</i>	-31.3	-30.7	Spangenberg and Ogrinc (2001)
P	Olive	<i>Olea europaea</i>	-30.9	-31.3	Spangenberg and Ogrinc (2001)
P	Olive	<i>Olea europaea</i>	-33	-31.9	Spangenberg and Ogrinc (2001)
WP	Wild boar	<i>Sus scrofa</i>	-26.9	-24.4	March (2013)
WP	Wild boar	<i>Sus scrofa</i>	-26.6	-25.5	March (2013)
WP	Wild boar	<i>Sus scrofa</i>	-28	-28.3	Colonese <i>et al.</i> (2015)
WP	Wild boar	<i>Sus scrofa ferus</i>	-26.4	-25.5	Pääkkönen <i>et al.</i> (2020)
WP	Wild boar	<i>Sus scrofa ferus</i>	-26.8	-26.8	Pääkkönen <i>et al.</i> (2020)
WP	Wild boar adipose	<i>Sus scrofa</i>	-25.1	-24.8	Spiteri (2012)
WP	Wild boar adipose	<i>Sus scrofa</i>	-28.1	-28	Spiteri (2012)
WR	Reindeer	<i>Rangifer tarandus</i>	-28.2	-32.9	March (2013)
WR	Reindeer	<i>Rangifer tarandus</i>	-28.1	-33	March (2013)
WR	Roe deer	<i>Capreolus capreolus</i>	-29.2	-29.7	Colonese <i>et al.</i> (2015)
WR	Red deer	<i>Cervus elaphus</i>	-27.4	-31.1	Craig <i>et al.</i> (2012)
WR	Red deer	<i>Cervus elaphus</i>	-27.7	-31.5	Craig <i>et al.</i> (2012)
WR	Red deer	<i>Cervus elaphus</i>	-28.9	-32.3	Craig <i>et al.</i> (2012)
WR	Red deer	<i>Cervus elaphus</i>	-28.4	-32.6	Craig <i>et al.</i> (2012)
WR	Red deer	<i>Cervus elaphus</i>	-29.1	-32.7	Craig <i>et al.</i> (2012)
WR	Red deer	<i>Cervus elaphus</i>	-28.8	-33	Craig <i>et al.</i> (2012)
WR	Red deer	<i>Cervus elaphus</i>	-29.4	-33	Craig <i>et al.</i> (2012)
WR	Red deer	<i>Cervus elaphus</i>	-30.4	-33	Craig <i>et al.</i> (2012)
WR	Red deer	<i>Cervus elaphus</i>	-29.5	-33.1	Craig <i>et al.</i> (2012)
WR	Red deer	<i>Cervus elaphus</i>	-30	-33.7	Craig <i>et al.</i> (2012)
WR	Red deer	<i>Cervus elaphus</i>	-28.3	-29.7	Dudd (1999)
WR	Red deer	<i>Cervus elaphus</i>	-29.4	-29.7	Dudd (1999)
WR	Red deer	<i>Cervus elaphus</i>	-28.8	-30.5	Dudd (1999)
WR	Red deer	<i>Cervus elaphus</i>	-28.8	-32.1	Dudd (1999)
WR	Red deer	<i>Cervus elaphus</i>	-28	-33.2	Dudd (1999)
WR	Red deer	<i>Cervus elaphus</i>	-30.8	-33.6	Dudd (1999)
WR	Red deer	<i>Cervus elaphus</i>	-30.7	-33.8	Dudd (1999)
WR	Red deer	<i>Cervus elaphus</i>	-31.5	-33.2	Lucquin <i>et al.</i> (2016a)
WR	Red deer	<i>Cervus elaphus</i>	-31.4	-33.6	Lucquin <i>et al.</i> (2016a)
WR	Wild forest reindeer	<i>Rangifer tarandus fennicus</i>	-24.4	-26.2	Pääkkönen <i>et al.</i> (2020)
WR	Wild forest reindeer	<i>Rangifer tarandus fennicus</i>	-25.3	-26.5	Pääkkönen <i>et al.</i> (2020)
WR	Reindeer	<i>Rangifer tarandus</i>	-24	-26.9	Pääkkönen <i>et al.</i> (2020)
WR	Reindeer	<i>Rangifer tarandus</i>	-24.1	-26.9	Pääkkönen <i>et al.</i> (2020)
WR	Wild forest reindeer	<i>Rangifer tarandus fennicus</i>	-24.7	-27.8	Pääkkönen <i>et al.</i> (2020)
WR	Eurasian elk	<i>Alces alces</i>	-28.6	-30.2	Pääkkönen <i>et al.</i> (2020)
WR	Eurasian elk	<i>Alces alces</i>	-28.6	-30.8	Pääkkönen <i>et al.</i> (2020)

WR	Eurasian elk	<i>Alces alces</i>	-29.4	-31.8	Pääkkönen <i>et al.</i> (2020)
WR	Eurasian elk	<i>Alces alces</i>	-30.8	-32.7	Pääkkönen <i>et al.</i> (2020)
WR	Red deer	<i>Cervus elaphus</i>	-31	-33.1	Spangenberg <i>et al.</i> (2006)
WR	Deer	<i>Cervus sp.</i>	-24	-24.9	Spangenberg <i>et al.</i> (2010)
WR	Chamois	<i>Rupicapra rupicapra</i>	-26.3	-25.7	Spangenberg <i>et al.</i> (2010)
WR	Red deer	<i>Cervus elaphus</i>	-29.7	-32.2	Spangenberg <i>et al.</i> (2010)
WR	Red deer adipose	<i>Cervus elaphus</i>	-24.9	-26.1	Spiteri (2012)
WR	Roe deer adipose	<i>Capreolus capreolus</i>	-24.5	-30.5	Spiteri (2012)

Table A5. 2. Theoretical mixing model data of *P. miliaceum* (millet) with average DRA, DRM, and DP $\delta^{13}\text{C}_{16}$ and $\delta^{13}\text{C}_{18}$ values (Table A5. 1.).

Domestic Ruminant Adipose + <i>P. miliaceum</i>								
Foodstuff		C16_conc	C18_conc			d13C16	d13C18	BigD
A	DRA	60.00%	40.00%			-28.4	-30.0	-1.6
B	Millet	76%	24.00%			-18.8	-19.1	-0.3
%A	%B	A C16 contribution	A C18 contribution	B C16 contribution	B C18 contribution	d13C16	d13C18	BigD
100%	0%	100%	100%	0%	0%	-28.4	-30.0	-1.6
90%	10%	88%	94%	12%	6%	-27.3	-29.3	-2.1
80%	20%	76%	87%	24%	13%	-26.1	-28.6	-2.4
70%	30%	65%	80%	35%	20%	-25.1	-27.8	-2.7
60%	40%	54%	71%	46%	29%	-24.0	-26.9	-2.8
50%	50%	44%	63%	56%	38%	-23.1	-25.9	-2.8
40%	60%	34%	53%	66%	47%	-22.1	-24.8	-2.7
30%	70%	25%	42%	75%	58%	-21.3	-23.6	-2.4
20%	80%	16%	29%	84%	71%	-20.4	-22.3	-1.9
10%	90%	8%	16%	92%	84%	-19.6	-20.8	-1.2
0%	100%	0%	0%	100%	100%	-18.8	-19.1	-0.3
Domestic Ruminant Milk + <i>P. miliaceum</i>								
Foodstuff		C16_conc	C18_conc			d13C16	d13C18	BigD
A	DRM	72.00%	28.00%			-27.1	-31.4	-4.3
B	Millet	76%	24.00%			-18.8	-19.1	-0.3
%A	%B	A C16 contribution	A C18 contribution	B C16 contribution	B C18 contribution	d13C16	d13C18	BigD
100%	0%	100%	100%	0%	0%	-27.1	-31.4	-4.3
90%	10%	90%	91%	10%	9%	-26.2	-30.4	-4.1
80%	20%	79%	82%	21%	18%	-25.4	-29.2	-3.9
70%	30%	69%	73%	31%	27%	-24.5	-28.1	-3.6
60%	40%	59%	64%	41%	36%	-23.7	-26.9	-3.2
50%	50%	49%	54%	51%	46%	-22.9	-25.7	-2.9

40%	60%	39%	44%	61%	56%	-22.0	-24.5	-2.4
30%	70%	29%	33%	71%	67%	-21.2	-23.2	-2.0
20%	80%	19%	23%	81%	77%	-20.4	-21.9	-1.5
10%	90%	10%	11%	90%	89%	-19.6	-20.5	-0.9
0%	100%	0%	0%	100%	100%	-18.8	-19.1	-0.3
Domestic Porcine + <i>P. miliaceum</i>								
Foodstuff		C16_conc	C18_conc			d13C16	d13C18	BigD
A	DP	65.00%	35.00%			-26.3	-25.4	0.9
B	Millet	76%	24.00%			-18.8	-19.1	-0.3
Contribution Analysis								
%A	%B	A C16 contribution	A C18 contribution	B C16 contribution	B C18 contribution	d13C16	d13C18	BigD
100%	0%	100%	100%	0%	0%	-26.3	-25.4	0.9
90%	10%	89%	93%	11%	7%	-25.4	-24.9	0.5
80%	20%	77%	85%	23%	15%	-24.6	-24.5	0.1
70%	30%	67%	77%	33%	23%	-23.8	-23.9	-0.1
60%	40%	56%	69%	44%	31%	-23.0	-23.4	-0.4
50%	50%	46%	59%	54%	41%	-22.3	-22.8	-0.5
40%	60%	36%	49%	64%	51%	-21.5	-22.2	-0.6
30%	70%	27%	38%	73%	62%	-20.8	-21.5	-0.7
20%	80%	18%	27%	82%	73%	-20.1	-20.8	-0.6
10%	90%	9%	14%	91%	86%	-19.5	-20.0	-0.5
0%	100%	0%	0%	100%	100%	-18.8	-19.1	-0.3